AD_____

Award Number: DAMD17-99-1-9264

TITLE: Training Program in Breast Cancer Research at the University of Texas M.D. Anderson Cancer Center

PRINCIPAL INVESTIGATOR: Mien-Chie Hung, Ph.D.

CONTRACTING ORGANIZATION: The University if Texas M.D. Anderson Cancer Center
Houston, Texas 77030

REPORT DATE: September 2001

TYPE OF REPORT: Annual Summary

PREPARED FOR: U.S. Army Medical Research and Materiel Command
Fort Detrick, Maryland 21702-5012

DISTRIBUTION STATEMENT: Approved for Public Release;
Distribution Unlimited

The views, opinions and/or findings contained in this report are those of the author(s) and should not be construed as an official Department of the Army position, policy or decision unless so designated by other documentation.

20020719 099

REPORT DOCUMENTATION PAGE

Form Approved
OMB No. 074-0188

Public reporting burden for this collection of information is estimated to average 1 hour per response, including the time for reviewing instructions, searching existing data sources, gathering and maintaining the data needed, and completing and reviewing this collection of information. Send comments regarding this burden estimate or any other aspect of this collection of information, including suggestions for reducing this burden to Washington Headquarters Services, Directorate for Information Operations and Reports, 1215 Jefferson Davis Highway, Suite 1204, Arlington, VA 22202-4302, and to the Office of Management and Budget, Paperwork Reduction Project (0704-0188), Washington, DC 20503

1. AGENCY USE ONLY (Leave blank)	2. REPORT DATE	3. REPORT TYPE AND DATES COVERED
	September 2001	Annual Summary (1 Sep 00 - 31 Aug 01)

4. TITLE AND SUBTITLE
Training Program in Breast Cancer Research at the University of Texas M.D. Anderson Cancer Center

5. FUNDING NUMBERS
DAMD17-99-1-9264

6. AUTHOR(S)
Mien-Chie Hung, Ph.D.

7. PERFORMING ORGANIZATION NAME(S) AND ADDRESS(ES)
The University if Texas M.D. Anderson Cancer Center
Houston, Texas 77030

E-Mail: mhung@mdanderson.org

8. PERFORMING ORGANIZATION REPORT NUMBER

9. SPONSORING / MONITORING AGENCY NAME(S) AND ADDRESS(ES)
U.S. Army Medical Research and Materiel Command
Fort Detrick, Maryland 21702-5012

10. SPONSORING / MONITORING AGENCY REPORT NUMBER

11. SUPPLEMENTARY NOTES
Report contains color

12a. DISTRIBUTION / AVAILABILITY STATEMENT
Approved for Public Release; Distribution Unlimited

12b. DISTRIBUTION CODE

13. Abstract ***(Maximum 200 Words)*** *(abstract should contain no proprietary or confidential information)*

Under support from the US Army/DOD the training program in breast cancer research at University of Texas at M. D. Anderson Cancer Center has had a successful second year. The training program has supported four predoctoral and five postdoctoral fellows. As reported last year, the extra postdoctoral trainees are funded by Breast Cancer Research Program at UT-MDACC. Each trainee has made notable progress as evidenced by publications and presentations at national meetings. Some of trainees have completed his or her work before this progress report. Significant strides have been made within the scope of the original specific aims in the following research areas: 1) Therapeutic approaches for breast cancer through regulation of oncogene and tumor suppressor gene expression, and control of signal transduction, apoptosis, and DNA repair; 2) Use of animals to understand the biology of breast cancer and to provide models for preclinical therapeutic and preventive studies; 3) Novel preventive strategies for breast cancer; 4) Population-based studies on breast cancer; 5) Molecular diagnostic/prognostic factors for breast cancer; and 6) The basis biology of breast cancer. In addition to laboratory pursuits each trainee has participated in departmental group meetings, journal clubs, and retreats. The goal of the training program is to further the successful training of fellows who will develop research programs of their own which continue to tackle problems of breast cancer.

14. SUBJECT TERMS
Breast Cancer

15. NUMBER OF PAGES
386

16. PRICE CODE

17. SECURITY CLASSIFICATION OF REPORT	18. SECURITY CLASSIFICATION OF THIS PAGE	19. SECURITY CLASSIFICATION OF ABSTRACT	20. LIMITATION OF ABSTRACT
Unclassified	Unclassified	Unclassified	Unlimited

Table of Contents

Cover	1
SF 298	2
Table of Contents	3
Introduction	4
Body	5
Key Research Accomplishments	10
Reportable Outcomes	11
Conclusions	15
Appendices	16

Introduction

The breast cancer training program at the University of Texas M. D. Anderson Cancer Center is a multidisciplinary research program comprising students and faculty from twenty different departments. The ultimate goal of this training program is to provide support to aid the development of exceptional scientists in the field of breast cancer research. The predoctoral and postdoctoral trainees for the U. S. army/Department of Defense (DOD) training grant are chosen from the laboratories of all faculty involved in the entire Breast Cancer Research Program at MDACC which includes over seventy faculty members and twenty departments. The scope of the research conducted by the trainees includes a variety of topics related to breast cancer research. Some trainees are conducting research aimed at developing novel therapeutic approaches for breast cancer through regulation of oncogenes and tumor suppressor genes and control of signal transduction, apoptosis and DNA repair. Others are using animals to understand the biology of breast cancer and to develop models for pre-clinical therapeutic and preventive studies. Still others are studying molecular diagnostic/prognostic factors for breast cancer and developing novel preventive strategies for this disease. The trainees are involved in many departmental and interdepartmental events including journal clubs, group meetings, retreats, and seminars. Theses activities outside of the laboratory provide opportunities for the trainees to gain a truly multi-disciplinary perspective on their own research projects by communicating and collaborating with researchers from each department at MDACC involved in breast cancer research. The breast cancer training program at MDACC is well on its way to producing superior investigators who will continue to explore the problems of breast cancer well into the future.

Body

Support from the U.S. Army/DOD to develop the Breast Cancer Training Program at the University of Texas M. D. Anderson Cancer Center (UT-MDACC) has led to another successful year in breast cancer research for several predoctoral and postdoctoral fellows. The Breast Cancer Training Program at UT-MDACC was developed to provide support for exceptional young scientist training in laboratories that are part of the Breast Cancer Research Program (BCRP) at UT-MDACC. The program provides comprehensive interdisciplinary research training to each fellow. The program faculty is comprised of members who cover a full spectrum of breast cancer research, including investigators involved in basic, translation, clinical and population-based studies related to breast cancer. The strength of the training programs at UT-MDACC stem from the strong interactions that take place between basic science researchers and clinicians in the exciting environment, which allows for swift transfer of scientific discoveries from the laboratory to the clinic. Predoctoral and postdoctoral trainees at MDACC benefit from this unique environment and are able to gain unparalleled experience in multidisciplinary studies. The ultimate goal of this training program is to train predoctoral and postdoctoral fellows to become highly qualified breast cancer researchers who will develop programs of merit in breast cancer research.

The training program was instigated after approval of the U.S. Army/DOD training grant awarded to UT-MADCC. This program consists of over seventy faculty members from more than twenty departments at UT-MDACC involved breast cancer research. The program developed a nomination process that involved the participation of each faculty member in nominating individuals to serve on the U. S. Army Breast Cancer Training Grant Steering Committee. Following the nomination process each BCRP faculty member voted for his or her choices for members to serve the steering committee. This committee was formed to serve in the selection of U. S. Army Training Grant recipients, the mentoring of the selected fellows, and the monitoring of each fellow's research progress. This process resulted in the election of the following six faculty members to serve on the committee:

Mien-Chie Hung, Ph.D., Principal Investigator of U.S. Army/DOD Training Grant, Professor & Director, Breast Cancer Basic Research Program, and Chair, Department of Molecular and Cellular Oncology

Melissa Bondy, Ph.D., Associate Professor, Department of Epidemiology

Gabriel Hortobagyi, M. D., Professor & Chair, Department of Breast Medical Oncology

Rakesh Kumar, Ph. D., Professor, Department of Molecular and Cellular Oncology

Janet Price, Ph. D., Associate Professor, Department of Cancer Biology

Di-Hua Yu, M.D., Ph.D., Associate Professor, Department of Surgical Oncology-Research

The steering committee commenced its activities by accepting proposals for the U. S. Army/DOD Breast Cancer Training Program Fellowships. It is well expected that some trainees will complete his or her training by the end of their second year on the training grant (Fall 2001). When the U.S./Army/DOD training grant initiated two years ago, the steering committee has chosen four predoctoral and four postdoctoral trainees out of eighteen candidates. Due to their exceptional qualifications, the U.S. Army Training Grant Steering Committee awarded an additional two postdoctoral trainees fellowships, and although designated as U. S. Army/DOD Training Grant Fellows, these individuals are supported by BRCP at UT-MDACC funding as reported last year. Recently, the committee has received sixteen applications from six predoctoral and ten postdoctoral trainees involved in breast cancer research at MDACC. The general impression from each member of the steering committee was that those recent applicants are consisted of highly qualified candidates with many intriguing proposals (Appendix 2.0-Biographical sketches and abstracts). Eventually, after careful review, eight individuals were selected to join the U.S. Army/DOD Breast Cancer Training Program. The awardees include four predoctoral trainees and two postdoctoral trainees who are supported by funds from the U. S. Army/DOD Training Grant. **Again, due to candidates' superior qualifications, the U.S. Army Training Grant Steering Committee awarded**

another two postdoctoral trainees fellowships, and although designated as U. S. Army/DOD Training Grant Fellows, these individuals are supported by BRCP at UT-MDACC funding. The superlative applicant pool truly impressed the steering committee. Their overall consensus is that the U. S. Army/DOD Training Grants in combination with the BCRP at UT-MDACC will not only provide each fellow with a excellent orientation to the various aspects of breast cancer research, but will also serve as a solid foundation in their careers.

Not only do trainees participate regular monthly journal clubs and seminars which are organized by BCPR at UT-MDACC, and the Women's Cancer Research Group, respectively, but also they attend weekly laboratory meetings and seminars in their own individual departments. Furthermore, the BCRP held annual retreat as reported last year which was held at Four Seasons Hotel, on August 5, 2000. This year was at the Crowne Plaza Hotel in Houston, Texas, on September 22. (Appendix 1.0-Agenda). This retreat served as a forum for the U.S. Army/DOD Breast Cancer Training Grant fellows to discuss and collaborate with BCRP faculty and other trainees in the various areas of breast cancer research. It is required that each U.S. Army/DOD Training Grant fellow gave a ten-minute oral presentation outlining both their research accomplishments and future goals. The presentation was then followed by open and helpful discussions among the trainees and faculty. In attendance were members of the BCRP-including each fellow, the steering committee and other BCRP faculty members. The overall feeling among participants was that it was a rewarding and exciting opportunity to hear all U.S. Army/DOD Training Grant fellows to give excellent and impressive presentations. Each faculty member agreed that the trainees were making significant progress with their projects as well as in developing critical thinking skills. Over and above the oral presentations, each trainee was asked to submit a description of their research accomplishments. The achievements of this group of trainees is exceptional and includes publication in several highly reputable journals such as *Nature Cell Biology, Oncogene, Cancer Research, and Molecular Cell Biology* (Appendix 3-Cited publications). A summary of the accomplishments of trainee is described below:

Yong Liao, M. D., Ph. D. - Postdoctoral fellow

In our current investigation, we established that E1A sensitizes human breast cancer cell lines (MDA-MB-231 and MCF-7) to Taxol-induced apoptosis. Moreover, by inoculating female nude mice with MDA-MB-231, we showed that E1A could enhance Taxol-induced antitumor effect and chemosensitivity. To further examine whether apoptosis-related molecules such as MAPK p38, Akt and JNK, were involved in E1A-mediated sensitization to Taxol. We detected enhanced p38 MAPK activity and repressed Akt activity in E1A expressing cells . However, phosphorylation of JNK remains unaffected. The upregulation of p38 phosphorylation and downregulation of Akt phosphorylation have correlated with Taxol-induced apoptosis. The same mechanism for E1A-mediated sensitization to Taxol is also applied for other anticancer drugs (doxorubicin, cis-platin, methotrexate and gemcitabine) which are currently used in clinical treatment of cancer patients. Therefore, inactivation of Akt and activation of p38 are required for E1A-mediated chemosensitization. We further identified a serine/threonine phosphatase PP2A, which the expression of catalytic subunit (PP2A/C) is upregulated in E1A-expressing cells, participates in E1A-mediated chemosensitization. Since PP2A directly dephosphorylates Akt, upregulation of PP2A/C in E1A-expressing cells could repess Akt activity, in turn, which would result in p38 activation. The "feed forward" mechanism may account for E1A-mediated chemosensitization.

Soo-Jeong Kim#, Ph. D.- Postdoctoral fellow

We have previously reported that Grb2 (growth factor receptor protein-2) is required for the proliferation of Erb-2overexpressing breast cancer cells. We investigated whether Grb2 protein plays a role in heregulin-stimulated proliferation. We have found that Grb2 protein inhibition led to growth inhibition of heregulin-stimulated breast cells, but not Erk1 and 2 activation. Since Akt can also be activated by heregulin,, we have shown that Akt was inactivated by heregulin. We then examined the effects of Grb2 downregulation on Akt in Erb2-overexpressing cells in the absence of heregulin. Similar to heregulin-stimulated cells, Grb2 inhibition also led to Akt inactivation in Erb2-overexpressing breast cancer cells. In summary, our data indicated that activation of Erb2 by heregulin or by its overexpression requires Grb2 to stimulate the Akt pathway to propagate mitogenic signals.

Keishi Makino#, M. D., Ph. D. - Postdoctoral fellow

Previously, we have demonstrated that Taxol could induce p55Cdc mRNA expression through activation of the p55Cdc promoter, which led to increase p55Cdc protein expression. In addition, Taxol activated p55Cdc-associated kinase. In this progress report, we have successfully identified that overexpressing of p55Cdc resulted in decreaed expression of cyclin B1 and in cell death in Hela cells and NIH3T3 cells in a dose-dependent manner. Moreover, a dominant-negative mutant of $p34^{cdc2}$ inhibited p55Cdc-induced and Taxol-induced apoptosis, but not in serum-starved cells.

Rui-An Wang#, M. D., Ph. D. - Postdoctoral fellow

Activation of heregulin signaling in the estrogen receptor-positive breast cancer cells leads to the suppression of estrogen receptor element (ERE)-driven transcription, the disruption of estradiol responsiveness, the acquisition of the hormone-independent phenotype and thus, contributes in breast cancer tumor progression to more invasive phenotype. Steroid receptors have been shown to control gene transcription in conjunction with histone acetylation modifying complexes. Here we report the identification of a metastatic-associated protein 1 (MTA 1), a component of histone deacetylase and nucleosome remodeling complexes, as a gene product induced by heregulin-1. Stimulation of cells with heregulin-1 was accompanied by a suppression of histone-4 acetylation, and an enhancement of deacetylase activity. In addition, MTA 1 was discovered to be a potent corepressor of ERE-transcription as it blocked the ability of estradiol to stimulate the ERE-transcription. Histone deacetylase inhibitor trichostatin A blocked the MTA 1-mediated repression of ERE transcription. *In vivo*, MTA 1associates with several components of the NuRD complex, including histone deacetylases 1, 2 and 3, chromodomain proteins 3 and 4, and Sin3. Furthermore, the MTA 1 directly interacted with the histone deacetylase 1 and 2, and also with the activation domain AF2 of the estrogen receptor α. These results identify ERE-mediated transcription as a nuclear target of MTA 1 and suggest that histone deacetylase complexes associated with the MTA 1 corepressor mediates estrogen receptor transcriptional repression by heregulin-1.

Binhua Peter Zhou#, Ph. D.-Postdoctoral fellow

Cellular localization of $p21^{Cip1/WAF1}$ has been proposed to be pivotal in either promoting cell survival or inhibiting cell growth. In our previously study, we have shown that HER-2/neu-mediated cell growth required the activation of Akt, which associated with $p21^{Cip1/WAF1}$ and phosphorylated it at threonine 145, then resulted in cytoplasmic localization of $p21^{Cip1/WAF1}$. Furthermore, blocking the Akt pathway with a dominant-negative mutant of Akt restored the nuclear localization and the cell growth inhibition activity of $p21^{Cip1/WAF1}$. Our study indicated that HER-2/neu induces in cytoplasmic localization of $p21^{Cip1/WAF1}$ via the activation of Akt to promote cell growth, which may have implications in oncogenic activity of HER-2/neu and Akt.

In our present investigation, we showed that HER-2/neu-mediated resistance to DNA damaging agents (etoposide and doxorubincin) required the activation of Akt, which enhanced MDM2-mediated ubiquitination and degradation of p53. Akt physically associated with MDM2 and then, in turn, phosphorylates it at serine 166 and 168 residues. The phosphorylation of MDM2 resulted in the enhancement of nuclear localization of MDM2 and its interaction with a transcriptional coactivator CBP/p300 and inhibited its interaction with $p19^{ARF}$, thus increasing p53 degradation. In summary, our study indicated that blocking the Akt pathway mediated by Her-2/neu would increase the cytotoxic effect of DNA damaging drugs in tumor cells with wild type p53.

Kristine Klos - Predoctoral fellow

The primary objective of this study is to define the downstream effectors of Erb2 receptor-induced angiogenic responses which may lead to enhanced metastatic potential. By establishing stable transfectants in human breast cell line MDA-MB-435 with various Erb2 mutants (such as constitutive-activating, dominant negative, autophosphorylayion site defective, and c-terminal deleted mutants), we may determine the structural requirements of the Erb2 receptor for mediating Erb2 signals leading to angiogenic responses. We have observed that in Erb2-overexpressing and constitutive active mutant cell lines, Erb2 can activate Akt, Src and Erk. To further investigate the critical Erb2 motif for signaling to prime the metastasis, we have injected SCID mice with different established Erb2 mutant cell lines. The Erb2 oevrexpressing, constitutively active Erb2 and C-terminal truncated cell lines can

cause lower survival due to metastases in mice. We also identified that VEGF secretion was higher in overexpressing, constitutively active , and c-terminal truncated Erb2 mutant cell lines in vitro. In order to pursue the angiogenic–related properties, we are currently experimenting the HUVEC migration assay, HUVEC differentiation assay and MMP-2 and MMP-9 zymography for the optimal conditions.

Christopher Neal - Predoctoral fellow

Western blot analysis of 14-3-3zeta (29 kda protein) in pairs of pathologist-dissected breast tumors and normal autologous tissues revealed that 14-3-3zeta expression in >70% tumors. Recently, by using IHC to study 240 parafin-embedded sections of breast samples to determine 14-3-3zeta expression, we have determined that the percentage of 14-3-3zeta overexpression to be >70% in breast cancer samples and >80% in invasive carcinoma. In addition, patients whose tumors had highest expression were found to have significantly lower disease-free and survival rates. To study the role of 14-3-3 overexpression in breast cancer, we stably transfected the human breast cancer cell line, MDA-MB-435 with 14-3-3FL (constitutively active mutant) and vector control. The 14-3-3FL transfectants were notably more resistant to gamma irradiation induced apoptosis and had three fold increased in colony formation than vector alone. Therefore, we consider the 14-3-3zeta protein as a potential novel marker for breast cancer.

Yong Wen# - Predoctoal fellow

We have demonstrated that p202 (52 kda protein) has the ability of tumor suppression and sensitization to tumor necrosis factor-α-induced apoptosis in human breast caner cell lines. To examine the potential gene therapy application for p202, we inoculated human breast cancer cell line MDA-MB-468 into female nude mice to form about 5mm in diameter of tumor size. Then, p202 DNA which was conjugated with SN2 liposome delivery system was injected intravenously into tumor-bearing mice. Compared to the control treatment with luciferase/SN2 complex, the tumor growth was significantly suppressed in mice with p202/SN2 treatment. The result strongly suggests that the p202 gene could be a potential therapeutic application in human breast cancer. We also identified the mechanism which p202 nay be involved in suppressing angiogensis. By analyzing the immunohistochemical staining, in tumor samples which has received p202/SN2 injection, we have shown that the expression of angiogenic factors (VEFG and IL-8) were inhibited.

Zhenming Yu – Predoctoral fellow

We have shown that PEA3, a transcription factor of *ets* family, can suppress HER2/heu transforming phenotype *in vitro* and inhibit tumor growth *in vivo*. To further elucidate the mechanism of tumor suppress functionality of PEA3, we established a panel of tetracycline inducible PEA3 stable transfectants. With the availability of those cell lines, we could further examine effects of various level of PEA3 expression.

 # Previous trainee has completed his or her training.

Again, after careful review, the U. S. Army/DOD Breast Cancer Training Program Steering Committee was impressed with the excellent progress made each by training grant recipient in array areas of laboratory research, development of ideas, and critical thinking. These predoctoral and postdoctoral trainees have taken full advantage of the opportunities provided to them as a result of the U.S. Army/DOD Training Grant awarded to UT-MDACC. All the trainees make significant strides in their research. In addition, the U.S. Army/DOD Breast Cancer Training Program provides trainees a unique opportunity which allows themselves to develop crucial skills that are essential to become competitive investigators in the field of breast cancer research. Moreover, each U.S. Army/DOD Training Grant fellow's progress has been monitored by the steering committee over the entire two-year period for which grants were awarded. In the first two-year training period, trainees are extremely successful in their research as evidenced by their productive publications in peer-reviewed journals. Last year (2000) trainees had ten papers in publication as reported in the last year progress report. This year (2001) the steering committee members are greatly impressed by trainees' highly regarded and prolific publications. Trainees have nineteen

published papers in a collection of solid and reputable journals.(Reportable outcomes, page 11) Recently, the steering committee posted an announcement for additional applications for the U.S. Army/DOD Training Grant as well as the selection process completed to choose the most qualified candidates. Once again, four predoctoral and four postdoctoral trainees have been selected (including two additional postdoctoral trainees fellowships who are supported by BRCP at UT-MDACC funding). Additionally, the progress of U.S. Army/DOD Training Grant recipients continuing studies at UT-MADCC after two years on the grant will be reviewed by the steering committee and decisions will be made regarding whether or not to continue funding.

In sum, the U.S. Army/DOD Breast Cancer Training Program at the University of Texas M. D. Anderson Cancer Center has served as an unprecedented opportunity for bright young scientists. Not only have these trainees benefited from the support and multidisciplinary activities offered by the program, but also the program has served as an unique attraction for young scientists from around the world to devote their energy to breast cancer research at UT-MDACC.

Key Research Accomplishments
(see Reportable Outcomes for details)

- Completed studies of the wild type E1A and E1A functional domain mutants anti-tumor effect *in vivo.*
- Evaluated the chemosensitization effect of E1A by systemic E1A gene therapy approach.
- Identified the causal relationships between E1A-mediated regulation of p38 activity and Akt activity and E1A chemosensitization.
- Identified a protein phosphatase PP2A participate in E1A-mediated chemosensitization and the feed forward regulation among PP2A, Akt and p38.
- Discover that Grb2 downregulation leads to Akt inactivation in heregulin-stimulated and Erb2-overexpressing breast cancer cells
- Identified over-expression of p55Cdc resulted in decreased expression of cyclin B1.
- Identified over-expression of p55Cdc gene resulted in cell death in Hela cells and NIH3T3 cells in a dose-dependent manner.
- A dominant–negative mutant of $p34^{cdc2}$ inhibited p55Cdc-induced and taxol-induced cell death, but not in serum-starved cell death.
- Discover that Metastasis-Associated Protein 1 represses estrogen receptor transcription via recruiting histone deacetylase complexes.
- Identified novel Akt substrates, $p21^{Cip1/WAF1}$ and MDM2.
- Established a panel of transfectant cell lines with Erb2 mutants.
- Over-expression of Erb2 can activate Akt, Src and Erk.
- Discover that over-expression of Erb2 cell lines have higher level of VEGF secretion which may promote cell invasion *in vivo.*
- Discover that 14-3-3zeta protein could be a potential marker for breast cancer.
- Over-expression of active mutant of 14-3-3zeta demonstrated that transfectants have more resistance to gamma irradiation and increased anchorage independent.
- Discover that p202/SN2 intravenous injection significantly suppressed tumor growth in an orthotopic breast cancer animal model.
- P202/SN2 delivery system as a potential gene therapy for treatment of breast cancer.
- Discover that p202 can suppress angiogensis by inhibiting expression of angiogenic factors VEGF and IL-8.
- Established the tetracycline inducible PEA3 stable transfectants of *HER-2/neu* over-expressing breast cell lines (MDA-MB-453 and MDA-MB-361T2) and *HER-2/neu* non-overexpressing cell lines (MDA-MB-435 and MVF7) by two-step stable transfection.

Reportable Outcomes

Peer reviewed Journals:

Zhou, B. P.[*#]**., Liao, Y.**[*], Xia, W. Y., Zou, Y. Y., Spohn, B. and Hung, M.-C. HER-2/neu induced p53 ubiquitination via Akt-mediated MDM2 phosphorylation. *Nature Cell Biology*, 2001. *In Press* (* equal contribution)

Liao, Y.[*], Funda, M.[*], Lee, W. P., Pollock, R. E. and Hung, M.-C. Adenovirus 5 early region 1A does not induce expression of the Ewing sarcoma fusion products EWS-FLI1 in breast and ovarian cancer cells lines. *Clinical Cancer Research* 6, 3832-3836, 2000. (* equal contribution)

Zhou, B. P.[#]**, Liao. Y.**, Xia, W. Y., Spohn, B., Lee, M.-H. and Hung, M.-C. Cytoplasmic localization of $p21^{cip1/waf1}$ by Akt-mediated phosphorylation in HER-2/neu-overexpressing cells. *Nature Cell Biology* 3, 245-252, 2001. *

*Accompanied by ***News and Views*** by El-Deiry, W.S. Akt takes centre stage in cell-cycle deregulation. ***Nature Cell Biol.*** 3:E1-E3, 2001.

Liao, Y., Zou, Y., Xia, W. and Hung, M.-C. Enhancement of chemosentivity and antitumor effects by Adenovirua E1A-mediated regulation of Akt and p38 activities. *Submitted.*

Lim, S. J.[#]**,** Lepez-Berestein, G., Hung, M.-C., Lupu, R. and Tari, A. M. Grb2 downregulation leads to Akt inactivation in heregulin-stimulated and Erb2-overexpressing breast cells. *Oncogene*, 19, 6271-6276, 2001.

Tari, A. M., **Lim, S. J.**[#], Hung, M.-C., Esteva, F. J. and Lopez-Berestein, G. A novel mechanism to induce ATRA resistance in breast cancer cells: the HER2/neu-Grb2-Akt pathway. *Submitted*

Vadlamudi, R., **Wang, R.-A.**[#], Talukder, A.H., Adam, L., Johnson, R. and Kumar, R. Evidence of Rab3 expression, regulation of vesicle trafficking, and cellular secretion in response to heregulin in mammary epithelial cells. *Molecular Cell Biology* 20, 9092-9101, 2000.

Vadlamudi, R., **Wang, R.-A.**[#], Mazumdar, A. and Kumar, R. PELP1, a novel human protein that acts as a bifunctional regulator of steroid receptors. *J. Biological Chemistry*, 2001. *In Press*

Kumar, R. and **Wang, R.-A.**[#] Protein kinases in mammary gland development and cancer. Microscopy Research and Technique, 2001. *In Press*

Mazmudar, A., **Wang, R.-A.**[#], Mishra, S., Adam, L., Yarmand, R., Mabdal, A., Vadlamudi, R. and Kumar, R. Transcriptional repression of estrogen receptor by metastasis-associated protein 1, a compoenet of histone deacetylase and nucleosome remodeling complexes.
Nature Cell Biology, 3, 32-37, 2001.

Makino, K.[#], Yu, D. and Hung, M.-C. Transcriptional upregulation and activation of p55Cdc via $p34^{cdc2}$ in Taxol induced apoptosis. *Oncogene* 20, 2537-2543, 2001.

Wang, S. C., **Makino, K.**[#], Su, L. K., Pao, A., Kim, J. S. and Hung, M.-C. Ultraviolet irradiation induces depletion of BRCA 2 protein through a p53-independent proteosome-independent pathway. *Cancer Research* 61, 2838-2842, 2001.

Lin, S.-Y., **Makino, K**[#]., Xia, W. Y., Matin, A., **Wen, Y.**, Kwong, K. Y., Bourguignon, L. and Hung, M.-C. Nuclear localization of EGF receptor and its potential new role as a transcription factor. *Nature Cell Biology* 3, 802-808, 2001. *

*Accompanied by ***News and Views*** by Waugh, M.G., and Hsuan, J.J. EGF receptor as transcription factors: ridiculous or sublime? ***Nature Cell Biol.*** 3:E209-E11, 2001.

Wang, S. C., **Makino, K.**[#], Xia, W., Kim, J. S., Im, S. A., Peng, H., Mok, S. C., Singletary, S. E. and Hung, M.-C. DOC-2 inhibits ILK activity and induces anoikis in breast cancer cells. *Oncogene*, 2001. *In press.*

Yao, J., Xiong, S., **Klos, K.**, Nguyen, N., Grijalva, R., Li, P. and Yu, D. Multiple signaling pathways involved in activation of matrix metalloptrpteinase-9 (MMP-9) by heregulin-β1 in human breast cancer cells. *Oncogene*, 2001. *In press.*

Lee, S., Yang, W., Sellappan, S., **Klos, K.**, Silwkowski, M., Hortobagyi G., Hung, M.-C. and Yu, D. Enhanced sensitization to Taxol-induced by Herceptin pretreatment cells apoptosis in HER-2- overexpressing breast cancer cells. *Cancer Research*, 2001. *Submitted.*

Wen, Y.[#], Hu, M. C., Makino, K., Spohn, B., Bartholomeusz, Z., Yan, D. H. and Hung, M.-C. HER-2/neu promotes androgen-independent survival and growth of prostate cancer through the Akt pathway. *Cancer Research*, 60, 6841-6845, 2000.

Wen, Y.[#], Yan, D. H., Wang, B., Spohn, B., Ding, Y., Shao, R. Zou, Y., Xie and Hung, M.-C. p202, an interferon-inducible protein, mediates multiple anti-tumor activities in human pancreatic cancer xenograft models. *Cancer Research*, 2001. *In press.*

Ding, Y., Wang, L., Spohn, B., Kwong, K. Y., Shao R., **Wen, Y.**[#], Li, Z., Hortobagyi, G., Hung, M.-C. and Yan, D. H. Pro-apoptotic effect of adenovirus-mediated p202 gene transfer on breast cancer cells. *Cancer Research*, 2001. *In revision.*

 # Previous trainee has completed his or her training.

Meeting Abstracts:

Liao, Y., Zou, Y. Y., Xia, W. Y., Lee, W. P. and Hung, M.-C. Modulation of apaototic theshold: enhanced anti-tumor therapy through downregulation Akt and upregulating p38 by adenovirus E1A in human breast cancer cells. *Proceedings of the Ninety-Second Annual Meeting of the American Association for Cancer Research*, 42, 658-659, 2001.

Tan, M., **Klos, K.**, Grijalva, R. and Yu, D. Heregulin β1-activated Erb2 receptor signaling and human breast cancer cell aggregation, invasion and metastasis. *Keystone Symposia on Molecular and Cellular Biology*, 2000.

Presentation:

Zhou, B. P.[#] and Hung, M.-C. Activation of Akt is required for HER-2/neu-mediated anchorage independent cell growth. Oral presentation. *Annual Meeting of American Association for Cancer Research*, New Orleans, LA, U. S. A., 2001.

 # Previous trainee has completed his or her training.

Patent:

U. S. Patent Application No. 60/277, 788, People Republic of China No. 011117869 and Taiwan Counterpart Patent No. 90106723. Entitled "Composition and Methods for Inactivation the Akt Oncogene and Activating the p38 Pro-apoptotic Gene" by **Liao, Y. et al.** Filing date: March 21, 2001.

Degree obtained:

Yong Wen obtained her Ph. D. degree in August, 2001.

Funding applied:

Yong Liao is the recipient of a postdoctoral fellowship from the US Army Breast Cancer Research Program. Award No. DAMD 17-01-1-0300.

Employment or Research Opportunities for previous trainees:

Soo-Jeong Lim, Ph. D. became a postdoctoral fellow at College of Pharmacy, Seoul National University, South Korea.

Keishi Makino, M. D. and Ph. D. became a junior faculty member at Kumamoto University, Japan, effective in May, 2001.

Rui-An Wang, M. D. and Ph. D. became an instructor at University of Texas M. D. Anderson Cancer Center, effective in May 2001

Binhua Peter Zhou, Ph. D. became an instructor at University of Texas M. D. Anderson Cancer Center, effective in September, 2001.

Conclusions

In conclusion, the U.S. Army/DOD Breast Cancer Research Training Program at the University of Texas M. D. Anderson Cancer Center has had a continuing successful second year. Each U.S. Army/DOD Training Grant recipient has benefited from the multidisciplinary program as evidenced by significant progress in their respective research projects and an outstanding publication record. Additionally, each trainee has gained invaluable knowledge and critical thinking skills as a result of departmental and inter-departmental seminars and group meetings. With continued support from the U.S. Army/DOD Breast Cancer Research Program, UT-MDACC will prosper in trainin scientists in the field of breast cancer research. We are expecting the newly awarded trainees will continue to do well in the coming year.

Appendices

Appendix 1.0	page 17	Agenda-Breast Cancer Retreat 2001
Appendix 2.0	page 20	US Army/DOD Breast Cancer Research Training Grar Applicants-2001: Biographical Sketches and Abstracts
Appendix 3.0	page 21	Cited Manuscripts and Abstracts

Appendix 1.0

Breast Cancer Research Program Retreat-2001

Agenda

MD ANDERSON CANCER CENTER

BREAST CANCER RESEARCH GROUP

FALL RETREAT

Crowne Plaza Medical Center
6701 Main Street
713-797-1110

SATURDAY, SEPTMEBER 22, 2001

Breast Imaging

8:00 - 8:25 am	Registration and Breakfast, Room: Houston II
8:25 - 8:30 am	Gabriel Hortobagyi, MD: Welcome & Introduction
8:30 - 8:35am	Peter Dempsey, MD: Overview of Program

A) Screening (Moderator: Tanya Stephens, MD)

8:35 - 8:45 am	Carol Stelling, MD: Overview: Benefits and Limitations of Screening
8:45 - 8:55 am	Chris Shaw, Ph.D: Resolution Studies - FFDM
8:55 - 9:05 am	Gary Whitman, MD: Advanced Applications – Clinical - FFDM -Angio/Tomo/CAD/Subtraction
9:05 - 9:15 am	Carol Stelling, MD: Screening High Risk Women/Screening High Risk Women with MRI -BR CA 1-2, h/o atypia, h/o LCIS, FH, pXRT
9:15 - 9:25 am	Peter Dempsey, MD: US – Screening – Pro/Con
9:25 - 9:45 am	Tanya Stephens, MD: Discussion
9:45 - 10:00 am	BREAK

B) Imaging Angiogenesis (Moderator: Gary Whitman)

10:00 - 10:10 am	Michael O'Reilly, MD: Intro – Angiogenesis
10:10 - 10:20 am	Xiaohong Joe Zhou, Ph.D.: Intro – Small Animal Lab
10:20 - 10:45 am	Anthony Purchio, Ph.D.: In vivo biophotonic imaging -applications in oncology -gene expression in transgenic mice

10:45 - 10:55 am	Chusilp Charnsangavej, MD: CT – Angiogenesis
10:55 - 11:05 am	Edward Jackson, Ph.D.: MRI – Angiogenesis
11:05 - 11:20 am	Gary Whitman, MD: Discussion
11:20 – 11:30 pm	BREAK

C) PET (Moderator: Anne Chmielewshi Kushwaha)

11:30 – 11:45 pm	Ebrahim Delpassand, MD: Introduction and PET in the evaluation of breast cancer
11:45 - 11:55 pm	Wai-Hoi (Gary) Wong, Ph.D.: New PET Cameras
11:55 - 12:10 pm	Anne Chmielewshi Kushwaha, MD: Discussion
12:10- 12:20 pm	BREAK

Ablation (Moderator: Peter Dempsey)

12:20 – 12:40 pm	Henry Kuerer, MD & Nour Sneige, M.D.: Ablation Overview and MDACC RF Ablation
12:40- 1:00pm	Peter Dempsey, M.D.: Discussion
1:30pm-3:30pm	DOD Breast Cancer Training Grant Trainees: Oral Presentations

Appendix 2.0

U.S. Army /DOD Breast Cancer Research Training Grant Applicants-2001

Biographical Sketches and Abstracts*

Predoctoral applicants:

Chi-Ping Day, M.S.•

Kristine Sue Klos, B.S.

Keng-Hseueh Lan, M.D. •

Yan Li, M.D.•

Christopher L. Neal, B.S.

Xiaoyan Sunny Wang, M.D.•

Postdoctoral Applicants:

Geoffrey A. Bartholomeusz, Ph.D.

Yi Ding, M.D., Ph.D.

Jaw-Ching Liu, Ph.D.

Yoichi Nagata, M.D., Ph.D.✧

Chenyi Zhou, Ph.D.•

Seyed Mahmoud Arab Najafi, Ph.D.•

Snehalata A. Pawar Nee Bhosale, Ph.D.

Lin Qiu, Ph.D.

Zhibo Yang, M.D., Ph.D.

Jijiang Zhu, M.D., Ph.D.✧

*The applicants' proposals contain applicant's biographical sketch and transcript, mentor's biographical sketch and active support, letter of support from the mentor, and proposal for application to the U.S Army Breast Cancer Research Program Training Grant (including abstract, research proposal, and figures and legends). Only Applicant'sBiographical sketches and Abstracts are attached in Appendix 2.0.

• The recent awardees started from September 1, 2001.

✧The awardees are funded by BCRP and started from September 1, 2001.

Biographical Sketches

Provide the following information for the key personnel listed on page 1 of the Detailed Cost Estimate form for the initial budget period.

NAME CHI-PING DAY	POSITION TITLE PREDOCTORAL FELLOW

EDUCATION/TRAINING (Begin with baccalaureate or other initial professional education, such as nursing, and include postdoctoral training.)

INSTITUTION AND LOCATION	DEGREE (IF APPLICABLE)	YEAR(S)	FIELD OF STUDY
National Cheng-Kung University, Taiwan.	B.S.	1992	Chemistry
National Yang-Ming University, Taiwan.	M.S.	1996	Biochemistry

RESEARCH AND PROFESSIONAL EXPERIENCE: Concluding with present position, list, in chronological order, previous employment, experience, and honors. Include present membership on any Federal Government public advisory committee. List, in chronological order, the titles, all authors, and complete references to all publications during the past 3 years and representative earlier publications pertinent to this application. PAGE LIMITATIONS APPLY. DO NOT EXCEED THREE PAGES FOR THE ENTIRE BIOGRAPHICAL SKETCH PER INVESTIGATOR.

Research and Professional Experience:

1992-1994 Lieutenant Lecturer, Department of Chemical Protection, Army Chemical School, Taiwan.
1996-1997 Research Assistant, Institute of Immunology & Microbiology, National Yang-Ming University, Taiwan.
1997-1998 Technician, Institute of Neurology, Veterans General Hospital-Taipei, Taiwan.
1998-1999 Chemist, Drug Abuse Urinalysis Lab-Taipei., SGS Taiwan Ltd., Taiwan.
1999-2000 Senior Auditor, Quality Assurance Unit, Protech Pharmaservices Corporation, Taiwan.
2000-present Graduate Research Assistant, Department of Molecular and Cellular Oncology, U.T.-M.D. Anderson Cancer Center.

Honors and Awards

1. Exchange Student, Department of Chemistry, University of Delaware, U.S.A., 92/01 – 92/02
2. First Place Award, Chinese Institute of Engineers (CIE) 1992 Student Scientific Paper Contest. Thesis title: *Optimization of Ionic Composition in Protein Analysis with Capillary Zone Electrophoresis*
3. Dr. Li-Yang Shen's Graduate Student Scholarship in 1995, National Yang-Ming University

Publication

1. Lin CT, Day CP, Kuei CH. Application of on-line SFC/SFE in environmental analysis. *J. Chi. Chem. Soc.*, 1993, 40, 121-129
2. Lin YJ, Hu JY, Day CP, Ho YH, Lin WC, Wu PL, Kuei CH. The analysis of conjugated bile acids with micellar eletrokinetic chromatography. *J. Microcolumn Separations*, 1998, 10, 625-632

Transcriptional Activation of IKKα/IKKβ by Integrin Linked Kinase in HER2/neu-mediated NF-kB activation Pathway

Abstract

Activation of nuclear transcription factor NF-kappaB by tyrosine kinase receptors induces resistance to apoptotic stimuli. Akt is involved in HER2/neu- or PDGF-mediated NF-kappaB activation[1,2]. In this proposal, we ask: (1) How does HER2/neu regulate integrin-linked kinase (ILK), which is known to involved in integrin signaling, and the NF-kB pathway in breast tumor cells? (2) May the activation of ILK and IKK correlate with the pathogenesis of breast cancer? First, we will examine the interaction between HER2/neu and ILK. Second, we will investigate the effect of blocking the ILK pathway on HER2/neu-induced resistance to apoptosis. The preliminary data showed that HER2/neu activated ILK. Blocking the ILK pathway with a dominant-negative ILK (ILK-KD) sensitized the HER2/neu-overexpressing cells to TNF-induced apoptosis, and inhibit the activation of NF-kB. We will continue to study the mechanism of ILK-mediated regulation of NF-kB pathway in HER2/neu-overexpressing cells by treating the cells with tyrosine kinase inhibitor and PI-3K inhibitor. The effects of ILK inactivation on the expression of IKKα and IKKβ will also be examined. The immunohistochemical analysis of HER2/neu, ILK, IKKα and IKKβ will also be performed to determine pathological significance and correlation.

Curriculum Vitae

Kristine Sue Klos
MD Anderson Cancer Center
Department of Surgical Oncology Box 107
1515 Holcombe Blvd.
Houston, TX 77030
713-794-1233
kklos@gsbs3.gs.uth.tmc.edu

Education:

University of Minnesota B.S. Biology 1990-1995

University of Texas-Houston Health Science Center 1998-
Graduate School of Biomedical Sciences
Advisor: Dihua Yu, M.D., Ph.D.
(M.S.)Ph.D. Program

Training:

University of Minnesota

Directed Research 1994-1995
Advisor: Robert G. McKinnell, Ph.D.
Thesis: Heart Primordia Transplants in Amphibian Embryos
Presentations: Poster at the "College of Biological Sciences Undergraduate Research Symposium"

Junior Scientist 1996-1998
Genetics and Cell Biology Department
R.G. McKinnell Laboratory
enucleated amphibian oocytes for nuclear transplantation of *R. pipiens* renal carcinoma cells, transplanted frog embryo tissues, tissue culture, autopsied frogs with physical deformities, fieldwork in MN frog population studies
Presentations: *Frog Deformities* 1997
Blessed Trinity Middle School Richfield, MN
Hot Topics in Science: Cloning and Frog Deformities 1997
Valley View Middle School Edina, MN

University of Texas - GSBS

Tutorials 1998-1999

Advisors: Dr. Elizabeth Grimm – Cancer Biology
Immunohistochemistry on melanoma cells
Dr. Dihua Yu – Surgical Oncology
ErbB2 expression in breast cancer cells
Dr. Sharon Roth – Biochemistry and Molecular Biology
Histone mutations and the cell cycle in yeast

Other Experience:

University of Minnesota

Teaching Assistant 1997-1998
Undergraduate Cancer Biology Course

Administrative Assistant 1997-1998
International Society of Differentiation

Abstracts:

McKinnell, R.G., **Klos, K.**, Christ, C., Rollins-Smith, L.A., and Kowles, R. "Functional hearts derived from mitotic progeny of a renal carcinoma genome." *Proceedings of the American Association for Cancer Research.* Volume 37 March 1996

Tan, M., **Klos, K.**, Grijalva, R., and Yu, D. "Heregulin β1-activated ErbB2 Receptor Signaling and Human Breast Cancer Cell Aggregation, Invasion, and Metastasis." *Keystone Symposia on Molecular and Cellular Biology*, 2000

Publications:

Yao, J., Xiong, S., **Klos, K.**, Nguyen, N., Grijalva, R., and Yu, D. "Multiple signaling pathways involved in activation of matrix metalloproteinase-9 (MMP-9) by heregulin-β1 in human breast cancer cells". *Oncogene*, In press, 2001.

Lee, S., Sellappan, S., **Klos, K.**, Sliwkowski, M., Hortobagyi, G., Hung, M.-C., and Yu, D. "Superior sensitization of HER2-overexpressing breast cancer cells to Taxol by Herceptin pretreatment priming cells to apoptosis". *Cancer Research*, Submitted, 2001

Honors and Awards:

Predoctoral Fellow – US Army Breast Cancer Research Training Grant 1999-2001

ABSTRACT

The *erb*B2 (or HER2, *neu*) gene-encoded receptor tyrosine kinase (RTK) belongs to the EGF receptor family. ErbB2 overexpression correlates with poor prognosis and the number of lymph node metastases in breast cancer patients. Previously, our laboratory found that stable transfection of the human *erb*B2 gene into the low *erb*B2-expressing MDA-MB-435 human breast cancer cells (named 435.eB transfectants) enhanced the intrinsic metastatic potential of these cells. Furthermore, erbB2 overexpression in breast cancer cells has now been shown to upregulate VEGF, a biological marker for angiogenesis. Despite the well-established notion that *erb*B2 enhances metastasis of breast cancer cells, and the acceptance that erbB2 overexpression mediates angiogenesis, little is known about the underlying molecular mechanisms. Since erbB2 overexpression has been found in ~ 30% of breast tumors, it is very important to examine the molecular mechanisms underlying erbB2-mediated angiogenesis, and thus, metastasis.

Our laboratory has found that erbB2 overexpression in 435.eB transfectants led to increased cell invasion, matrix metalloprotease (MMP)-2/MMP-9 activities, vascular endothelial growth factor (VEGF) secretion, and apoptosis resistance. Furthermore, we have found that by using various mutants of the erbB2 receptor, we see various amounts of metastasis and VEGF secretion. We hypothesize that erbB2 overexpression can enhance the RTK signaling capacity that elicits these effects, which all can contribute to enhanced metastatic potential. Recent studies indicate that angiogenic responses are very important in promoting cancer metastasis. This fellowship application focuses on experimental approaches to elucidate the requirement of the erbB2 receptor signaling leading to the angiogenic effect of erbB2. Using these various mutants of the erbB2 receptor, I will determine the structural requirements of the tyrosine kinase domain and tyrosine autophosphorylation sites in the erbB2 receptor for mediating signals leading to cell invasion, MMP-9 activity, (MMP-9 is known to facilitate angiogenesis), angiogenesis, and ultimately, metastasis in an animal model (mammary fat pad injection of various erbB2 mutant transfected MDA-MB-435 cells) of breast cancer metastasis. I will also investigate the involvement of erbB2 downstream signaling in the angiogenic effects of erbB2 by biochemical and genetic manipulations of the signaling molecules in breast cancer cells.

The completion of the experiments outlined in this application will provide the first detailed analysis of the relationship between erbB2 signal transduction and angiogenic effects in human breast cancer cells, and ultimately will identify critical points in the signaling pathways for future intervention of erbB2-mediated metastasis.

BIOGRAPHICAL SKETCH

Provide the following information for the key personnel listed on the budget page for the initial budget period

NAME	POSITION TITLE
Keng-hsueh Lan, M.D.	Graduate Student (Ph.D. program)

EDUCATION/TRAINING *(Begin with baccalaureate or other initial professional education, such as nursing, and include postdoctoral training.)*

INSTITUTION AND LOCATION	DEGREE (if applicable)	YEAR(s)	FIELD OF STUDY
National Taiwan University, Taipei, Taiwan	M.D.	09/90 – 06/97	Medicine
Univ. of Texas Health Science Center, Houston,		08/99 - now	Molecular and Cellular Oncology

RESEARCH AND PROFESSIONAL EXPERIENCE: Concluding with present position, list, in chronological order, previous employment, experience, and honors. Include present membership on any Federal Government public advisory committee. List, in chronological order, the titles, all authors, and complete references to all publications during the past three years and to representative earlier publications pertinent to this application. If the list of publications in the last 3 years exceeds two pages, select the most pertinent publications. PAGE LIMITATIONS APPLY. DO NOT EXCEED 3 PAGES FOR THE ENTIRE BIBLIOGRAPHICAL SKETCH PER INVESSTIGATOR.

Education

09/90-07/97: National Taiwan University, College of Medicine, Taipei, Taiwan; M.D. degree
06/97: passed Taiwan Medical License Examination
10/98: took TOEFL; Score: 643 (Sec.1: 64, Sec.2: 65, Sec.3: 64)
11/98: took GRE General Test; Score: 2060 (V: 550/73%, Q: 800/99%, A: 710/88%)
12/98: took GRE Subject Test; Subject: Biochemistry, Cell and Molecular Biology; Score: 620/80%
08/99-now: Graduate Student, Graduate School of Biomedical Sciences, University of Texas-Health Science Center at Houston

Personal Position

09/90-06/92: Social Chairperson of the class 97, Department of Medicine, National Taiwan University
06/96-06/97: Intern doctor, National Taiwan University Hospital, Taipei, Taiwan
07/97-09/98: Medical officer, Air Force, Republic of China, Taiwan

RESEARCH AND PROFESSIONAL EXPERIENCE (continued). PAGE LIMITATIONS APPLY. DO NOT EXCEED THREE PAGES FOR THE ENTIRE BIBLIOGRAPHICAL SKETCH PER INVESTIGATOR.

Research Experience

Summer/95: Summer student in Dr. Chia-Li Yu's laboratory at National Yang-Ming University, Taipei, Taiwan

12/98-02/99: Research assistant in Professor Omata's laboratory at Tokyo University, Tokyo, Japan

04/99-06/99: Summer student in Professor Pei-Jer Chen's laboratory at National Taiwan University, Taipei, Taiwan

08/99-12/99: Tutorial student in Dr. Sue-Hwa Lin's laboratory at the University of Texas, M.D. Anderson Cancer Center; Project: The Expression Profile Study of CEA-CAM Transfectants using Subtractive Hybridization Techniques

12/99-03/00: Tutorial student in Dr. Mien-Chie Hung's laboratory at the University of Texas, M.D. Anderson Cancer Center; Project: Activation of Akt by ErbB2

03/00-now: Tutorial student in Dr. Dihua Yu's laboratory at the University of Texas, M.D. Anderson Cancer Center; Project: Mechanisms of p34Cdc2 Inhibition by ErbB2 that Confer Taxol Resistance in Breast Cancers

Publication

Jing, T., Tan, M., Lee, S., **Lan, K.-H.**, Nagata, Y., Li, P., Liu, J., Arlinghaus, R., Hung, M.-C., Yu, D. Direct Phosphorylation on Tyrosine-15 of $p34^{Cdc2}$ by erbB2 Receptor Tyrosine Kinase Inhibits $p34^{Cdc2}$ Activation, (*Nature Cell Biol,* under review), 2001

Lan, Keng-hsueh

Proposal Abstract

Title of the proposal: Peptide Therapeutics for Breast Cancers

It has been recognized that the next frontier in molecular medicine is the delivery of therapeutics. Among the biological therapeutics, peptide/protein is especially challenging to deliver. Interestingly, a peptide sequence localized within a 13-amino acid domain of Tat (named "penetratin"), when linked to other peptides/proteins, was able to carry attached peptide/protein into the cells when they were added to cell culture medium. The penetratin system is very powerful in that more than 1,000,000 molecules can be delivered inside one single cell. We hypothesize that the unique property of penetratin can be utilized for delivery of therapeutic peptides/proteins. The major goal of this proposal is to develop a penetratin-based peptide delivery system that specifically targets erbB2-overexpressing breast cancer cells.

Overexpression of erbB2-encoded receptor tyrosine kinase (p185) was found in ~ 30% of breast cancers. Many studies (including our own) demonstrated that *erb*B2 overexpression in breast cancer cells can enhance their metastatic potential and confer upon them increased chemoresistance, thereby leading to poor clinical outcome. Hence *erb*B2 is an excellent target for the development of novel breast cancers therapies. However, despite exciting progress in the biology underlying the role of erbB2 overexpression in breast cancer metastasis and chemoresistance, development of new therapies for breast cancers is still lagging behind. This application will employ a novel approach of using an erbB2 extracellular domain (ECD)-binding peptide to achieve targeted delivery of therapeutic peptides specifically into erbB2-overexpressing breast cancer cells.

The therapeutic peptide used in this proposal will be tyrosine-phosphorylated peptides that correspond to Shc binding sites in the C-terminal domain of erbB2. The peptides should specifically interfere with the association between tyrosine phosphorylated erbB2 and Shc. Since erbB2-Shc association leads to subsequent activation of the Shc-->ERK pathway that contributes to increased invasion/metastasis and chemoresistance in the erbB2-overexpressing breast cancer cells, interference with this association should block the activation of the erbB2-Shc downstream pathway and provide therapeutic benefits for erbB2-overexpressing breast cancer cells. Alternatively, our lab has recently found that 14-3-3zeta is a critical downstream mediator required for erbB2-mediated transformation. Therefore, we can deliver R18 peptide, a 14-3-3 inhibitor, to block erbB2 transformation signal and inhibit erbB2-mediated breast cancer progression/metastasis. The specific aims of the proposal are:

1. To develop penetratin-based delivery system specifically targeting erbB2-overexpressing breast cancer cells. We will use the anti-Her2/neu peptide mimetic (AHNP), which was developed based on a humanized anti-erbB2 monoclonal antibody, Herceptin. AHNP will be synthesized in conjunction with penetratin (penetratin-AHNP). The resultant peptides will be tested for increased delivery specificity to erbB2-overexpressing breast cancer cells.

2. To test the effect of erbB2 signal-blocking peptides using penetratin delivery. Phospho-peptides derived from the C-terminal domain of erbB2 that correspond to the binding sites for Shc will be conjugated to the penetratin delivery system developed in Aim 1. The resultant peptides will be tested for their ability to translocate inside breast cancer cells and to block erbB2 signaling. If these tests demonstrate positive results, we will further test the inhibitory effects of these peptides on invasion and chemoresistance of erbB2-overexpressing breast cancer cells. In addition, R18 peptides will be conjugated to the penetratin-AHNP and tested for translocation and inhibition of ErbB2-overexpressing breast cancer cells.

We hope that the innovative approaches of this proposal will bring original and important contributions to targeted delivery of therapeutic peptides.

Biographical Sketches

Provide the following information for the key personnel listed on page 1 of the Detailed Cost Estimate form (see Appendix F) for the initial budget period.

NAME YAN LI	POSITION TITLE GRADUATE RESEARCH ASSISTANT

EDUCATION/TRAINING (Begin with baccalaureate or other initial professional education, such as nursing, and include postdoctoral training.)

INSTITUTION AND LOCATION	DEGREE (IF APPLICABLE)	YEAR(S)	FIELD OF STUDY
Zhejiang University, China	Bachelor of Medicine	1990-1995	Medicine
Peking Union Medical College, China	Doctor of Medicine	1995-1998	Medicine
Peking Union Medical College Hospital, China	Resident	1998-1999	Surgery
Univ. of Texas, MD Anderson Cancer Center and Houston Health Science Center, Texas	Ph.D. Student	1999-Present	Cancer Biology and Gene Therapy

RESEARCH AND PROFESSIONAL EXPERIENCE: Concluding with present position, list, in chronological order, previous employment, experience, and honors. Include present membership on any Federal Government public advisory committee. List, in chronological order, the titles, all authors, and complete references to all publications during the past 3 years and representative earlier publications pertinent to this application. PAGE LIMITATIONS APPLY. DO NOT EXCEED THREE PAGES FOR THE ENTIRE BIOGRAPHICAL SKETCH PER INVESTIGATOR.

Winbow V.M., **Li Y.**, O'Brien, J. Phosphorylation of connexins 35 and 34.7 by PKA. Annual ARVO Meeting Abstract, Miami, Florida, 2001.

Li W, He Z, **Li Y,** Yanoff M. "Vascular endothelial growth factor regulates both apoptosis and angiogenesis of choriocapillaris endothelial cells." Microvasc Res. 2000 Mar;59(2):286-9.

Li W, Yanoff M, **Li Y,** He Z. "Artificial senescence of bovine retinal pigment epithelial cells induced by near-ultraviolet in vitro." Mech Ageing Dev. 1999 Oct 22;110(3):137-55.

Li Y, Pang GX, Zhan SH, Li W et al. "The Apoptosis and Proliferation after Photorefractive Keratectomy" .Chinese Journal of Ophthalmology,1999, 35(1),

Qin M, Duan SM, **Li Y,** Zhang WH , Li W et al. "Application of polymerase chain reaction in the rapid diagnosis of herpesvirus infection". Acta Academiae Medicinae Sinicae, 1999, 21(1).

Fellowship,
Prevent Blindness America--Fight For Sight Research Awards, 1999 – 2000

Excellent Student Scholarships,
Zhejiang University and Peking Union Medical College, P.R.China, 1991--1997

ABSTRACT

Targeting Breast Cancer by Cancer-Specific Recombinase-Mediated Transgene Expression
Yan Li., DOD Predoctoral Traineeship Applicant

Background: With one million new cases in the world each year, breast cancer is the most common malignancy in woman and accounts for about 30% of all cancer diagnosed in U.S. Gene therapy is one of the novel and promising approaches to treat breast cancer based on molecular mechanism and pathophysiology. One of the most important difficulties facing breast cancer gene therapy is to generate tumor-specific treatment to achieve greater anti-tumor activity with less toxicity. However, many tumor specific promoters are too weak to achieve sufficient therapeutic effect. The current proposal will aim at this weakness by developing cancer-specific recombinase-mediated gene therapy methods. Success of this proposal may provide an efficient therapeutic approach to benefit breast cancer patients.

Objective/Hypothesis: The goal of this research project is to apply a recombinase system FLP/FRT to achieve sufficient cancer-specific transgenic expression in breast cancer, which is switched by Human telomerase reverse transcriptase promoter (hTERTP). We can also modify this system by combining it with either inducible heat shock protein 70 promoter (HSP70P) to achieve heat–directed cancer-specific transgene expression in the site of primer breast cancer or metastasis lesions or HER-2/neu promoter to further restrict transgene expression in HER-2/neu overexpressing breast cancer, which depends on the therapeutic purpose.

Specific Aims: (1) To test the efficiency of the FLP/FRT recombinase-mediated transgene expression in breast cancer cells switched by cancer specific hTERT promoter. (2) To develop heat-inducible cancer-specific transgene expression driven by HSP70 switched by the hTERTP-controlled FLP/FRT system. (3) To develop the specific transgene expression in HER2/neu overexpressing breast cancer cells driven by HER-2/neu promoter switched by the hTERTP-controlled FLP/FRT system. (4) To test the above cancer-specific FLPe-mediated transgene expression systems in breast tumor model in vivo.

Study Design: We will construct the single vector containing promoter and switch system: hTERT promoter will induce FLPe-mediated excision of an FRT-flanked stop cassette in a silenced expression vector. This will result in amplified levels of CMV promoter-driven expression of exogenous reporter gene and the pre-apoptotic *bik* gene. At first we will test the recombination efficiency of our system. Then we will study the cancer-specific reporter gene expression and *bik* therapeutic effect in vitro and in vivo delivered by cationic liposome. According to the therapeutic purpose, we will replace the CMV promoter with either inducible heat shock protein 70 (HSP70) promoter, to achieve heat–directed cancer-specific transgene expression, or HER-2/neu promoter, to further restrict transgene expression in HER-2/neu overexpressing breast cancer.

Relevance: Common tumor specific promoters are too weak to drive sufficient and specific therapeutic effects in breast cancer. Our proposal aims at the common weakness by developing a cancer-specific recombinase-mediated gene therapy approach. The outcome of the tumor specific promoters operating FLP/FRT system proposal will provide important ground work for further exploring the possibility of targeting cancer therapy: specific and sufficient therapeutic effects in cancer cells with minimal side effects and toxic effects to normal cells.

Curriculum Vitae

Christopher L. Neal

Work Address: M D Anderson Cancer Center
Department of Surgical Oncology, Box 107
1515 Holcombe Blvd.
Houston, TX 77030

Work Phone: (713) 794-1233

E-mail Address: cneal@gsbs3.gs.uth.tmc.edu

Education:

1997-present — Ph.D. (M.S.), University of Texas-Houston Health Science Center, Graduate School Of Biomedical Sciences,
Houston, TX 77054
Program: Cancer Biology
Advisor: Dihua Yu, M.D., Ph.D.

1991-1996 — B.S., East Tennessee State University,
Johnson City, TN 37614
Major: Biology Minor: Philosophy
GPA in Major: 3.37 Cumulative GPA: 3.17

Tutorials at UTH-GSBS:

Aug. 1997-Dec. 1997 — Role of p16 promoter methylation in senescence
Department of Carcinogenesis,
Science Park Research Division
Advisor: Marcelo Aldaz, Ph.D.

Jan. 1998-Mar. 1998 — Development of a novel gene therapy delivery system
Department of Surgical Oncology
Advisor: Dihua Yu, M.D., Ph.D.

Mar. 1998-May 1998 — Role of 14-3-3 sigma (HMe1) in cell cycle regulation
Department of Surgical Oncology
Advisor: Mong-Hong Lee, Ph.D.

Research Honors at UTH-GSBS: Pre-doctoral Fellow, US Army Breast Cancer Research Training Grant 1999-2001,
Grant No. DAMD17-99-1-9264

Research Honors at ETSU: Ronald McNair Research Program
Intern 1993-1994

James H. Quillen School of Medicine
Research Forum
2nd place Undergraduate Poster Division, 1994

Honor Societies at ETSU: Tri-Beta Biological Society

Research and Work Experience at ETSU:

Sept. 1995-Aug.1997	Research Technician, NIH funded project Department of Internal Medicine, ETSU College of Medicine Advisor: Elaine Walker, Ph.D.
May 1995-April 1997	Research Technician, NIH funded project Department of Biological Science, ETSU Advisor: Foster Levy, Ph.D.
Aug. 1992-April 1997	Undergraduate research, projects funded by Ronald McNair Research Program and student worker program Department of Biological Sciences, ETSU Advisor: Foster Levy, Ph.D.

Scientific Publications at UTH-GSBS:

Abstracts:

Larango C, Neal CL, Lee MH. HMe1, a p53 inducible protein, plays a key role in cell cycle regulation. *Society of Surgical Oncology*, March 1999.

Larango C, Neal CL, Lee MH. HMe1, a 14-3-3 family member, is a regulator of the cell cycle. *Proc. Amer. Assoc. Cancer Res.*, April 1999.

Papers:

Larango C, Yang HY, Neal CL, Lee MH. Association of the cyclin-dependent kinases and 14-3-3 Sigma negatively regulates cell cycle progression. *J. Biol. Chem.* **275**,23106-12 (2000).

Scientific Publications at ETSU:

Abstracts:

Neal C, Berk S, Holtzclaw-Berk S, Laffan E, Kalbfleisch JH and Walker ES. Temporal trends in antimicrobial resistance in a local population of Moraxella catarrhailis. *American Society of Microbioloby* **97**, 321 (1997).

Papers:

Levy F and Neal CL. Spatial and temporal genetic structure in chloroplast and allozyme markers in Phacelia dubia implicate genetic drift. *Heredity* **82** (Pt 4), 422-31 (1999).

Walker ES, Neal CL, Berk S, Holtzclaw-Berk S, Laffan E, Kalbfleisch JH. Trends in Susceptibility of Moraxella catarrhailis. *J. Antimicrobial Chemotherapy* **45**, 175-182 (2000).

US Army Breast Cancer Training Grant
Predoctoral Fellowship Proposal

Role of 14-3-3zeta in human breast cancer metastasis

GSBS student: Christopher L. Neal

Advisor: Dihua Yu, M.D., Ph.D.

Department of Surgical Oncology

The University of Texas, M.D. Anderson Cancer Center
1515 Holcombe Blvd., Houston, Texas 77030

Phone: (713) 794-1233
Fax: (713) 794-4830
E-mail: cneal@gsbs3.gs.uth.tmc.edu

Proposal Abstract

A. Specific Aims

The 14-3-3 proteins are a family of ubiquitously expressed acidic proteins which are highly conserved through evolution. Currently, there are nine 14-3-3 isoforms in human. 14-3-3 can bind to various proteins involved in many important cellular processes in a phospho-serine-dependent manner. 14-3-3 has been implicated to function in the cell cycle G2/M DNA damage checkpoint, cell growth, differentiation, transformation, and apoptosis. Furthermore, 14-3-3 proteins can interact with tumor suppressors and oncoproteins such as p53, Bcr, and the middle T antigen of the polyoma virus suggesting certain roles for 14-3-3 in oncogenesis. Recently, our new findings indicate that (a) 14-3-3zeta is overexpressed in >70% human primary breast tumors and in most breast cancer cell lines; (b) overexpression of 14-3-3zeta increased colony formation in soft agar, suppressed apoptosis and increased foci formation in combination with activated Ras; and (c) the 14-3-3ΔN dominant negative mutant impacted transformation and metastasis-related properties. **Thus, we hypothesize that 14-3-3zeta facilitates breast cancer progression/metastasis by regulating specific metastasis-related properties.** Overexpression of 14-3-3 may promote metastasis by increased colonization in target organ sites, resistance to stress-induced apoptosis during tumor cell dissemination, and decreased aggregation (increased dissemination). On the other hand, 14-3-3 dominant negative mutants may interfere with wt 14-3-3 function and inhibit metastasis. The specific aims of this proposal are:

1. **To investigate the biological role of 14-3-3 in breast cancer cells *in vitro*.**
First, we will transfect into MDA-MB-435 breast cancer cells HA-tagged 14-3-3FL, 14-3-3ΔN, 14-3-3ΔC, 14-3-3K49E, 14-3-3R56,60A constructs and empty vectors in a neomycin resistant system to establish stable transfectants. We will then examine these transfectants for cell growth, apoptosis, aggregation, and their growth in hard agar, which has previously been shown to correlate well with *in vivo* metastatic potential.
2. **To identify effective blocking reagents of 14-3-3 to inhibit breast cancer tumorigenicity/metastasis.**
Since our studies have demonstrated that 14-3-3 indeed plays an important role in promoting breast cancer tumorigenicity/metastasis, we will develop various reagents that block 14-3-3 functions. To this end, we will make 14-3-3 dominant negative mutants (ΔN, ΔC, K49E, R56,60A) and a blocking peptide, R18. We will then test these mutants and blocking peptide for transformation/metastasis inhibitory effects in MDA-MB-435 breast cancer cells.
3. **To determine the tumorigenic and metastatic potential of 14-3-3 transfectants in vivo.**
We will compare the ability of the 14-3-3FL, 14-3-3ΔN, 14-3-3ΔC, 14-3-3K49E, 14-3-3R56,60A transfectants to induce tumors and metastases in ICR-SCID mice. We will perform (a) experimental metastasis assays by injecting cells into the tail vein of the mice, and (b) tumorgenicity/spontaneous metastasis assays by injecting cells to the mammary fat pad of the mice.

To the best of our knowledge, there is no previous report on 14-3-3 overexpression in breast cancers. Moreover, the *consequence of 14-3-3 overexpression in human breast cancers, especially in breast cancer metastasis, has never been investigated.* 14-3-3 is overexpressed in >70% of breast tumors, whereas the currently intensively studied genes in breast cancers, such as p53, erbB2, BRCA1 and BRCA2, do not affect breast cancers at this high rate. Thus, it is imperative to investigate the unexplored area of the role of 14-3-3 in breast cancer tumorigenicity/metastasis. The pursuance of this proposal will bring original and important contributions to this unexplored area. It will bring timely findings regarding the role of 14-3-3 in breast cancers and ways to block the function of overexpressed 14-3-3 in breast cancers.

BIOGRAPHICAL SKETCH

NAME	POSITION TITLE
Xiaoyan (Sunny) Wang, M.D.	Graduate Research Assistant

EDUCATION/TRAINING (*Begin with baccalaureate or other initial professional education, such as nursing. Include postdoctoral training.*)

INSTITUTION AND LOCATION	DEGREE (*if applicable*)	YEAR(s)	FIELD OF STUDY
Dalian Medical University	M.D.	1996	Medicine

RESEARCH AND PROFESSIONAL EXPERIENCE: Concluding with present position, list, in chronological order, previous employment, experience, and honors. Include present membership on any Federal Government public advisory committee. List, in chronological order, the titles, all authors, and complete references to all publications during the past three years and representative earlier publications pertinent to this application. If the list of publications in the last three years exceeds two pages, select the most pertinent publications. DO NOT EXCEED TWO PAGES.

Postgraduate Training:

1999-present — Ph.D. student – Department of Bioimmunotherapy
University of texas Houston Health Science Center
Houston, Texas

1996-1999 — Resident - Internal Medicine
Shenyang 202 Hospital
Shenyang, Liaoning, P.R.China

Honors and Awards:

1997 -1998 — Guofan Wang, M.D. Award for Excellence in Residency

Memberships:

1996-1999 — China Red Cross Society

Abstract

HER2/*neu* expression in a breast cancer biopsy indicates poor prognosis due to likely metastasis. A vaccine targeting HER2/*neu* could have significant therapeutic and preventative application by controlling the growth and spread of the highly aggressive HER2/*neu*+ cells. The most recent findings for DNA vaccines indicate that maximum effectiveness is achieved using a Prime-Boost strategy in which a plasmid containing the gene of interest is used as the priming vaccine and a crippled virus, also containing the gene, is use for the boosting vaccination. We are trying to test here if a primary vaccination with the plasmid ELVIS-*neu* and secondary vaccination with VPR-*neu* (Viral Particle Replicon of Sindbis Virus) or Adeno-*neu* (replication deficient adenovirus) can be used as a therapeutic vaccine for women with HER2/*neu*+ breast cancer.

Specific Aims: 1) To test in mice the hypothesis that vaccination with ELVIS-*neu* will be non-toxic and generate measurable humoral and cellular immunity 2) To test in mice the hypothesis that vaccination with either VPR-*neu* or Adeno-*neu* will be non-toxic and generate measurable humoral and cellular immunity 3) To test in mice the hypothesis that primary vaccination with ELVIS-*neu* followed by secondary vaccination with either VPR-*neu* or Adeno-*neu* will be more effective than any of these three agents used alone for both primary and secondary vaccination 4) To test the hypothesis that vaccination with ELVIS-*neu* will be non-toxic and generate measurable humoral and cellular immunity in breast cancer patients with responding disease and at high risk for disease recurrence. If the phase Ib clinical trial in Specific Aim 4 show that ELVIS2-*neu* is effective as a therapeutic vaccine for women with breast cancer and animal testing supports the hypothesis described in Specific Aim 3, we would propose another Phase Ib clinical trial to test primary vaccination with ELVIS2-*neu* and secondary vaccination with VPR-*neu* or Adeno-*neu* as a therapeutic vaccine for women with HER2/*neu*$^{+}$ breast cancer.

Study design: ELVIS-*neu* DNA plasmid or VPR-*neu* or Adeno-*neu* or ELVIS-*neu* DNA plasmid followed by VPR-*neu* or Adeno-*neu* will be given to the mice weeks before the mice are challenged with the highly aggressive A2L2 tumor cell, which is a mouse breast cancer cell line that has been transfected with *neu* and highly expresses *neu* antigen on its surface. A2L2 cells would be injected intravenously or into mammary fat pad to test the value of the vaccine for tumor prevention. ELVIS-*neu* DNA plasmid or VPR-*neu* or Adeno-*neu* or ELVIS2-*neu* DNA plasmid followed by VPR-*neu* or Adeno-*neu* will also be given to the mice whose tumor are surgically removed three weeks after the mice are injected with A2L2 cells in the mammary fat pad to test the therapeutic value of the vaccine. Flow cytometry and IFN-γ releasing assay will be used to test the humoral and CTL response induced by the vaccines. Our final goal is a phase Ib clinical trial using a two stage vaccine approach in which primary vaccination with plasmid is followed by "booster" injections of either Adeno-*neu* or VPR-*neu* depending on the preclinical studies.

Biographical Sketch – Applicant

NAME	POSITION TITLE
Geoffrey A. Bartholomeusz	Postdoctoral Fellow

EDUCATION/TRAINING (Begin with baccalaureate or other initial professional education, such as nursing, and include post-doctoral training.)

INSTITUTION AND LOCATION	DEGREE (IF APPLICABLE)	YEAR(S)	FIELD OF STUDY
University of Zambia, Lusaka. Zambia	Bsc	1984	Human Biology
University of Zambia, Lusaka. Zambia	Msc	1988	Medical. Microbiol
Rochester Institute of Technology, Rochester, N.Y.	Msc	1990	Clinical Chemistry
University of Oklahoma , Norman, Oklahoma	Ph.D.	1998	Microbiol
University of Texas M.D.Anderson Cancer Center Houston TX.	Predoctoral.	1997-1998	Molecular Genetics
University of Texas M.D.Anderson Cancer Center Houston TX.	Postdoctoral	1998-1999	Molecular Genetics
University of Texas M.D.Anderson Cancer Center Houston TX	Postdoctoral	1999-present	Oncogene

RESEARCH AND PROFESSIONAL EXPERIENCE: Concluding with present position, list, in chronological order, previous employment, experience, and honors. Include present membership on any Federal Government public advisory committee. List, in chronological order, the titles, all authors, and complete references to all publications during the past 3 years and to representative earlier publications pertinent to this application. If the list of publications in the last 3 years exceeds two pages, select the most pertinent publications. PAGE LIMITATIONS APPLY. DO NOT EXCEED THREE PAGES FOR THE ENTIRE BIOGRAPHICAL SKETCH PER INVESTIGATOR.

Professional Experience

1981-1983	Undergraduate Research Assaitant, University of Zambia, Department of Biological Sciences.
1984-1985	Medical Student Assistant, University of Zambia Teaching Hospital.
1988-1989	Research Assistant Rochester General Hospital, Department of Surgery.
1988-1990	Research Assistant Rochester Institute of Technology, Department of Clinical Chemistry.
1989-1990	Lab Technician, University of Rochester Department of Biology.
1994-1996	Graduate Research Assistant University of Oklahoma Depertment of Microbiology.
1997-1998	Predoctoral fellow,Department of Molecular Genetics, U.T. M.D.Anderson Cancer Center, Houston,TX.
1989-1999	Postdoctoral fellow, Department of Molecular Genetics, U.T. M.D.Andercon Cancer Center, Houston TX.
1999-present	Postdoctoral felow Department of Molecular and Cellular Oncology, M.D.Anderson Cancer Center, Houston, TX.

Scholarships

1988-1989 Rochester General Hospital Fellowship.
1989-1990 RIT Graduate Scholarship.
1992-1996 OU Graduate College Fee Waiver Scholarship

Memberships

1994-1995 University of Oklahoma Student Senator and Ways and Means Committee.
1996-1998 University of Oklahoma School of Arts and Science, Budget Committee.
1998-present American Association for the Advancement of Science (AAAS)
1999-present American Society for Gene therapy (ASGT)

Publications and Presentations

- Bao,S., Qyang,T., Yang,P., Kim,HW., Bartholomeusz,G. Henkel,J., Pimental,R., Verdc,F.,and Marcus,S. "The Highly Conserved Protein Methyltransferase,Skb1 ,is a Mediator of Hyperosmotic Stress in the Fission Yeast Schizosaccharomyces pombe" J.Biol..Chem. 276:14549-14552 (2001)
- Wen,Y., Hu,M.C.T., Makino,K., Spohn,B., Bartholomeusz,G. Yan,DH. and Hung MC, "HER-2/neu Promotes Androgen-independent Survival and Growth of Prostate Cancer through the AKT Pathway" Cancer Research 60:6841-6845 (2000)
- (equal first author) Bartholomeusz,G. , E.Chang , R.Pimental, J.Chen, H.Lai, Li-hua, L.Wang. P.Yang and S.Marcus. Direct Binding and in-vivo regulation of the fission yeast PAK Shk1 by the SH3 domain protein Scd2. Mol.Cel. Biol. (1999) 19:8066-74
- (equal first author) Bartholomeusz G, M.Gilbert, p.Yang,R.A.Pimental, S.Kansara, R.Gadiraju and S.Marcus. Negative regulation of mitosis in fission yeast by the Shk1 interacting protein Skb1 and its human homolog Skb1Hs. (1998) Proc.Natl.Acad.Sci USA. 95:14781-6
- Bartholomeusz,G. Y.Zhu and J.Downard. Growth medium-dependent regulation of Myxococcus xanthus fatty acid content is controlled by the esg locus (1998) J.Bacteriol. 180:5269-72
- Presented a talk titled "Direct binding and in-vivo regulation of the fission yeast Ste20/PAK homolog Shk1 by the Bem-1 related SH3 domain protein Scd2 at the Yeast Cell Biology meeting at Cold Spring Harbor held on August 17 – 22 1999
- Presented evidence that a SH3 domain protein Scd2 directly binds to the fission yeast PAK Shk1 and is in turn phosphorylated by Shk1 at the Genes and Development Spring Retreat 1999, at Mustang Island Texas.
- Presented a poster at the Myxococcus xanthus International Conference in June 1966 titled Brancehed Chain Amino Acids are substrates for Myxococcus xanthus lipid synthesis by an esg-dependent pathway.
- Presented: Evidence that Branched-chain fatty acids are the esg signal of Myxococcus xanthus, at the meeting of the American Society of Microbiology in March 1995.
- Presented Analysis of the role of the E-locus (esg) in Myxococcus xanthus, at the Myxococcus xanthus International Conference in June 1995.
- Co-authored the paper on : Reproducible Stapbylococcus aureus infection model in rats, presented by Dr. Francine Cantor at the 33rd World Congress of Surgery, Totonto, Canada in September 1989

ABSTRACT

Proposal Title: **A Novel Apoptotic Molecule Bok for the Treatment of Breast Cancer**

Geoffrey A. Bartholomeusz - Applicant for the US Army Breast Cancer Research Program Postdoctoral Training Grant

Background Breast cancer remains the major cause of death among women in the United States. The formation of homodimers or heterodimers between members of the Bcl-2 family or their phosphorylation by kinases is an important component of their regulation. Human Bok (hBok), a pro-apoptotic Bcl-2 protein, is a potent inducer of apoptosis when ectopically expressed in cancer cells including breast cancer cells. The apoptotic function of hBok is caspase dependent and is not inhibited by the strong antiapoptotic protein Bcl-2. The above properties of hBok makes it a potential anti-cancer agent.

Objective/hypothesis **Utilization of hBok Induced Apoptosis to Cure Breast Cancer in a Telomerase Dependent Manner** We have demonstrated that hBok inhibits survival of breast cancer cells and that this function of hBok is independent of p53 and is not affected by high Her-2 levels reported to correlate with poor survival for patients with breast cancer. Phosphorylation of hBok may be required for its proapoptotic function. The promoter activity and expression of the catalytic subunit of the human telomerase(hTERT) are significantly up regulated in cancer tissue and cancer cell lines but stringently repressed in normal somatic cells. The hTERT promoter may therefore serve as a tumor specific promoter to direct the expression of hBok by systemic delivery.

Specific Aims (1). To investigate hBok-induced apoptosis and confirm hBok-mediated transformation suppression in breast cancer cells. (2) To investigate the mechanisms of hBok-induced apoptosis. (3) To develop a tumor specific promoter using hTERT promoter driven hBok to examine the pre-clinical effect of hBok for breast cancer gene therapy

Study Design We have shown that hBok inhibits survival of breast cancer cells and will continue our investigation on the therapeutic potential of hBok by determining if this effect is by induction of apoptosis and/or reduction of cell growth. A non-viral delivery system will be utilized to determine if the expression of hBok in cancer cells affects their cell growth rate (anchorage-dependent growth rate) and colony formation in soft agarose (anchorage-independent growth rate). To realize hBok's potential as a therapeutic agent, an understanding of the unique mechanism regulating its apoptotic activity is important. We have shown that hBok induced apoptosis is caspase-3-independent and will continue to study the role of caspases in hBok-induced apoptotsis. Our preliminary results indicate that a hBok mutant with a disrupted MAP kinase substrate motif is somewhat more active than wildtype. We will identify the hBok associated MAP kinase and determine its role in the regulation of hBok activity. It is probable that nuclear localization of hBok may be important for its apoptotic function (please see preliminary results). We will continue to address this issue and determine if phosphorylation of hBok will influence its nuclear translocation and hence its apoptotic function. Finally, we will use the non-viral delivery system to deliver hBok into breast cancer cells in tumor-bearing mice. We will use the hTERT promoter to drive the expression of hBok with the objective of expressing hBok in a tumor specific manner.

Relevance. By utilizing our knowledge on the mechanisms involved in hBok regulation and apoptotic function we propose to genetically alter hBok into a very potent proapoptotic molecule. We will optimize its therapeutic efficiency by targeting it expression specifically to breast cancer cells with the goal of killing breast cancer cells. The long term goal of this proposal is to develop hBok gene therapy as an effective treatment for breast cancer by using it to sensitize breast cancer cells that are resistant to the routinely prescribed chemotherapeutic agents in order to develop an effective protocol using acombination of gene therapy and chemotherapy to treat breast cancer. Our eventual goal is to take this pre-clinical animal model into clinical trials to treat human breast cancer.

Appendix E

Biographical Sketches

Provide the following information for the key personnel listed on page 1 of the Detailed Cost Estimate form (see Appendix F) for the initial budget period.

NAME YI DING	POSITION TITLE POSTDOCTORAL FELLOW

EDUCATION/TRAINING (Begin with baccalaureate or other initial professional education, such as nursing, and include postdoctoral training.)

INSTITUTION AND LOCATION	DEGREE (IF APPLICABLE)	YEAR(S)	FIELD OF STUDY
Department of Molecular and Cellular Oncology, The University of Texas, M. D. Anderson Cancer center.		2000-present	Cell Biology Tumor Biology Experimental Therapeutics
Department of Preventive Medicine, Kyoto Prefectural University of Medicine, Japan.	Ph. D.	1996-2000	Cell&Molecular Biology
Department of Medicine, Kyoto Prefectural University of Medicine, Japan.		1994-1996	Cell & Molecular Biology
Attached Hospital of East China, Science and Technological University, China.		1985-1994	Alternative Medicine
Zhejang College of Traditional Chinese Medicine, China	M. D.	1980-1985	Medical student

Professional Experience:

Vov.1985-Feb.1994: physician, Attached Hospital of East China Science and Technological University, China.

Apr. 1994- Mar.1996: Research student in First Department of Medicine, Kyoto Prefectural University of Medicine, Japan.

Apr. 1996- Mar.2000: Graduate student (Ph.D.), department of Preventive medicine, Kyoto Prefectural University of Medicine, Japan.

Jan. 2000- present: Postdoctoral Fellow, Department of Molecular and Cellular Oncology, The University of Texas, M. D. Anderson Cancer Center.

Publications:

Fulu Bai, Takayoshi Matsui, Naoko Ohtani-Fujita, Yoshizumi Matsukawa, **Yi Ding,** and Toshiyuki Sakai. Promoter activation and following induction of the p21/WAF1 gene by flavone is involved in G1 phase arrest in A549 lung adenocarcinoma cells. FEBS Lett., 437:61-64, 1998.

Yi Ding, Yoshizumi Matsukawa, Naoko Ohtani-Fujita, Daishiro Kato, Su Dao, Takaaki Fujii, Yuji Naito, Toshikazu Yoshikawa, Toshiyuki Sakai, and Gerald A. Rosenthal. Growth inhibition of A549 human lung adenocarcinoma cells by L-Canavanine is associated with p21/WAF1 induction.Jan. J. Cancer Res., 90:69-74, 1999.

Yi Ding, Toshiaki Inoue, Jun Kamiyama, Yutaka Tamura, Naoko Ohtani-Fujita, Eiji Igata, and Toshiyuki Sakai. Molecular cloning and functional characterization of the upstream promoter region of the human p73 gene. DNA Res., 6: 347-351, 1999.

Yong Wen, Duen-Hwa Yan, Bailiang Wang, Bill Sphon, **Yi Ding**, Ruping Shao, Yiyu Zou, Keping Xie, and Mien-Chie Hung. p202, an interferon-inducible protein, mediates multiple anti-tumor activities in human pancreatic cancer xenograft models. Cancer Res., (in press).

Yi Ding, Li Wang, Bill Spohn, Ka yin Kwong, Ruping Shao, Yong Wen, Zheng Li, Gabriel N. Hortobagyi, Mien-Chie Hung, and Duen-Hwa Yan. Submitted to Cancer Res.,

Abstract

Adenovirus-mediated p202 Gene Transfer in Breast Cancer Gene Therapy
Yi Ding, M.D., Ph.D. Post-doctoral Fellowship Award Applicant

Background: p202, an IFN-inducible, chromatin-associated protein, belongs to a murine 200-amino acid repeat family. Enforced expression of p202 in stable murine fibroblasts and human cancer cell lines leads to retardation of cell growth and suppression of transformation phenotype. Furthermore, we showed that p202 stable breast cancer cells are sensitized to TNF-α-induced apoptosis, and that is associated with inactivation of the TNF-α-induced NF-κB via p202/NF-κB interaction. To generate a p202-based therapeutic agent for efficacy study in animal model and a tool to study the biological function of p202, we constructed Ad-p202 (andenoviral vector expressing p202 cDNA driven by a CMV promoter), and demonstrated that Ad-p202 infection in breast cancer cells not only inhibits cell growth and sensitizes cells to TNF-α-induced apoptosis, but also induce apoptosis.
Objective/Hypothesis: 1. Ad-p202 infection results in growth inhibition, apoptosis, and sensitization to TNF-α (or chemo- drugs, or γ-irradiation)-induced apoptosis in breast cancer cells, and that the p202 region(s) responsible for these effects can be identified. 2. Systemic delivery of Ad-p202 may results in multiple anti-tumor activities in an orthotopic breast cancer xenograft model, and that anti-tumor effects may be enhanced by a combined Ad-p202 and TNF-α (or chemo-drugs or γ-irradiation) treatment.
Specific Aims: 1. Determine the Ad-p202-mediated anti-tumor activities *in vitro*. 2. Determine the Ad-p202-mediated anti-tumor activities *in vivo*.
Study Design: We will identify the p202 domain responsible for growth inhibition and confirm the *in vitro* pro-apoptosis activity of p202 in other breast cancer cell lines. Likewise, we will identify the p202 domain responsible for the sensitization to TNF-α-induced apoptosis and also determine the Ad-p202-mediated sensitization to chemo-drugs or γ-irradiation induced apoptosis. Moreover, we will determine the tumor-specific anti-tumor activity of Ad-hTERT-p202 (adenoviral vector carrying human terlomerase gene promoter-driven p202 cDNA) *in vitro*. Importantly, we will determination of the anti-tumor activity by systemic delivery of Ad-p202 in an orthotopic breast cancer animal model. Furthermore, the anti-metastasis and anti-angiogenesis activities by systemic delivery of Ad-p202 in an orthotopic breast cancer animal model will be examined. Likewise, we will determine the efficacy of a combined treatment of Ad-p202 with TNF-α in an orthotopic breast cancer animal model as well as the efficacy of a combined treatment of Ad-p202 with chemo-drugs (or γ-irradiation) in the same xenograft model. Finally, we will determine the tumor-specific anti-tumor activity of Ad-hTERT-p202 in an orthotopic breast cancer animal model.
Relevance: Approximately 180,000 women are diagnosed with breast cancer in the United States each year. Despite recent therapeutic advances, metastatic breast cancer remains a significant cause of morbidity and mortality. Novel treatment modalities are clearly needed. Using systemic delivery of Ad-p202 in the proof-of-concept experiments detailed in this proposal, we will examine the treatment efficacy of p202 gene therapy in breast cancer orthotopic xenograft model. In addition, the proposed experiments should lead to a better understanding how p202 exerts multiple anti-tumor activities in vitro and in vivo. Success of the proposed experiments will provide a scientific basis for developing p202-based gene therapy against metastatic breast cancer.
Training Plan: The current proposal will help me to elucidate the mechanisms by which Ad-p202 mediates anti-tumor activities in breast cancer cells and to test the treatment efficacy of Ad-p202 in orthotopic breast cancer xenograft model. The success of the proposal will certainly set the stage for future clinical trials using p202-based gene therapy in breast cancer treatment. During the past one and half years in Dr. Yan's lab, I have enjoyed what I have been doing. After my post-doc training, if possible, I would like to continue working in the field of breast cancer research in an academic setting. With my training in medicine and molecular biology, and now in gene therapy, I have found that I can best contribute my expertise in breast cancer gene therapy. Thus, the DoD breast cancer research post-doctoral fellowship, if funded, will certainly provide me a significant impetus to move toward my career goals.

Biographical Sketches

Provide the following information for the key personnel listed on page 1 of the Detailed Cost Estimate form for the initial budget period.

NAME JAW-CHING LIU	POSITION TITLE POSTDOCTORAL FELLOW

EDUCATION/TRAINING (Begin with baccalaureate or other initial professional education, such as nursing, and include postdoctoral training.)

INSTITUTION AND LOCATION	DEGREE (IF APPLICABLE)	YEAR(S)	FIELD OF STUDY
Natl' Chung-Hsing Univ. Taichung, Taiwan	B.S.	1984-1988	Entomology
Natl' Chung-Hsing Univ. Taichung, Taiwan	M.S.	1988-1993	Entomology
Univ. of Florida, Gainesville, Florida	Ph.D.	1993-1997	Entomology
Univ. of Texas, HSC-Houston, Texas	postdoctoral	1997-1998	Human Genetic
Univ. of Texas, HSC-Houston, Texas	postdoctoral	1999-2001	Pharmacology
Univ. of Texas, MD Anderson cancer Center	postdoctoral	2001-	Cancer

RESEARCH AND PROFESSIONAL EXPERIENCE: Concluding with present position, list, in chronological order, previous employment, experience, and honors. Include present membership on any Federal Government public advisory committee. List, in chronological order, the titles, all authors, and complete references to all publications during the past 3 years and representative earlier publications pertinent to this application. PAGE LIMITATIONS APPLY. DO NOT EXCEED THREE PAGES FOR THE ENTIRE BIOGRAPHICAL SKETCH PER INVESTIGATOR.

Employment:

1989-1991: Research Assistant. Cancer and Virus Research Group. Institute of Biomedical Sciences, Academia Sinica. Taipei, Taiwan.

1996: Teaching Assistant. ENY6905: Molecular Biology Techniques. Department of Entomology and Nematology, University of Florida.

1997-1998: Postdoctoral Fellow. Human Genetic Center. School of Public Health. University of Texas-Houston Health Science Center, Houston, Texas.

1999-2001: Postdoctoral Fellow. Department of Integrative of Biology and Pharmacology. Medical School. University of Texas-Houston Health Science center, Houston, Texas.

2001-: Postdoctoral Fellow: Department of Molecular and Cellular Oncology. University of Texas M.D. Anderson Cancer Center, Houston, Texas

RESEARCH AND PROFESSIONAL EXPERIENCE (CONTINUED). PAGE LIMITATIONS APPLY. DO NOT EXCEED THREE PAGES FOR THE ENTIRE BIOGRAPHICAL SKETCH PER INVESTIGATOR.

Publication

Liu, J.-C., Makova, K. D., Adkins, R. M., Gibson, S., and Li, W.-H. (2001) Episodic evolution of growth hormone in primates and emergence of the species of human growth hormone receptor. Molecular Biology and Evolution 18,945-953.

Liu, J.-C., and Maruniak, J. E. (1999) Molecular characterization of genes in the gp41 region of baculoviruses and phylogenetic analysis based upon gp41 and polyhedrin genes. Virus Research 64,187-196.

Liu, J.-C., Boucias, D. G., Pendland, J. C., Liu, W. Z., and Maruniak, J. (1996) The mode of action of Hirsutellin A on eukaryotic cells. Journal of Invertebrate Pathology 67,224-228.

Liu, J.-C., and Maruniak, J. E. (1995) Nucelotide sequence and transcriptional analysis of the gp41 gene of *Spodoptera furgiperda* nuclear polyhedrosis virus. Journal of General Virology 76,1443-1450.

Yeh, K.-W., Yahng, W.-K., Huang, H.-C., Feng, Y.-N., Liu, J.-C., Wu, F.-Y., and Wu, C.-W., (1995) Cloning and characterization of the endogenous retrovirus-tRNA(Glu) multigene family from human genomes of different racial background. Gene 155,247-252.

Hung, C.-F., Kao, C.-H., Liu, J.-C., Lin, J.-G., and Sun, C.-N. (1990) Detoxifying enzyme of selected insect species with chewing and sucking habits. Journal of Economic Entomology 83,361-365.

ABSTRACT

Proposal Title: Oncogenicity of β-catenin in Breast Cancer

Applicant: Jaw-Ching Liu, Ph.D.

Background: β-catenin is an important regulator of cell-cell adhesion and embryonic development that associates with the LEF/TCF family of transcription factors. β-catenin has been shown to be an oncogene that transactivated the proto-oncogene c-*myc* and the cell cycle regulator cyclin D1 genes in several cancers including breast cancer, ovarian cancer, and colon cancer. The immunohistochemical examining showed that β-catenin is negatively correlated to patient survival rates in breast cancer and correlated to breast cancer metastasis.

Objective/Hypothesis: I propose to study the use of β-catenin as a strong and independent prognostic marker for early breast cancer. By demonstrating β-catenin either directly involves in the oncogenicity or indirectly transactives targets genes in downstream signaling pathway that involves in oncogenicity, we could define the potential mechanism preventing breast cancer invasion and metastasis.

Specific Aims: (1) Identify the β-catenin downstream transactivated target genes and determines their roles in oncogenicity, cancer cell invasion and metastasis (2) determine the role of β-catenin in breast cancer invasion and metastasis in genetically defined human breast cancer cell lines *in vitro* and *in vivo* (3) evaluate whether β-catenin is a strong and independent prognostic factor that could be useful for early breast cancer diagnosis.

Study Design: To further study the role of β-catenin in tumorgenicity, cancer cell invasion and metastasis, we develop an inducible β-catenin overexpression breast cancer cell line. By using this system combining with cDNA microarry technique, we will be able to identify β-catenin trasacivated target genes. Subsequently, we will determine the biological function of these identified target genes by dominant negative mutant method. Finally an immunohistochemical examining of breast cancer tissues for β-catenin expression and a mutlivariate statistical analysis will be performed to ascertain β-catenin is a strong and independent prognostic marker.

Relevance: β-catenin has been implicated in breast cancer development and metastasis. It transactivates downstream target genes involving in oncogenicity. Blocking β-catenin was shown to inhibit invasion in a variety of tumor cell lines. Immunohistochemical examining also showed that β-catenin is correlated to breast cancer metastasis. β-catenin thus serves as a promising prognostic marker for breast cancer adjuvant therapy.

BIOGRAPHICAL SKETCH

Name: Yoichi Nagata
Birth Date: June 8, 1964
Birth Place: Tokyo,Japan
Citizenship: Japan
Marital Status: Married, 1993 ; no child
Education:
1999 PhD. Kurume/Kumamoto University School of Medicine
1990 M.D. Hokkaido University School of Medicine,.
1984 Graduated from High School

Professional Training:

1999-present Post-doc fellow in the Department of surgical oncology, MD Anderson Cancer Cntr.,USA
1999 Instructor, Kurume University, Fukuoka, Japan
1995-1999 MD-PhD student in the Department of Tumor Genetics and Biology, Kumamoto University , Kumamoto, Japan
1994-1995 Research Assistant in the Department of Pediatrics and Child Health, Kurume University Hospital, Japan
1990-1994 Residency in Pediatrics, Kurume University Hospital, Fukuoka, Japan
1990 Passed the Examination of National Board

Memberships:

Japanese Society of Pediatrics
Japanese Cancer Association
Japanese Society of Molecular Biology
American Association for Cancer Research (associate member)

Publications:

1. Jing, T., Tan, M., Lee, S., Lan, K-S., **Nagata, Y.**, Li, P., Liu, J., Yu, D. (2001) Direct phosphorylation of tyrosine-15 of p34cdc2 by erbB2 receptor tyrosine kinase inhibits p34cdc2 activation. *Nature Cell Biology*, under review.

2. **Nagata, Y.**, Anan, T., Yoshida, T., Mizukami, T., Taya, Y., Fujiwara, T., Kato, H., Saya, H., & Nakao, M. (1999) The stabilization mechanism of mutant-type p53 by impaired ubiquitination: the loss of wild-type p53 function and the hsp90 association. *Oncogene* 18(44):6037-49

3.Anan, T., **Nagata, Y.**, Koga, H., Yabuki, N., Miyamoto, C., Kuwano, A., Matsuda, I., Endo, F., Saya, H., & Nakao, M. (1998) Human ubiquitin-protein ligase Nedd4: expresssion, subcellular localization and selective interaction with ubiquitin-conjugating enzymes. *Genes to Cells* 3, 751-763

4.Nakao, M., **Nagata, Y.**, Honda, Y., & Anan, T. (1998) How the amount of p53 regulated by its degradation and stabilization? *BioReview* (Japanese), Tokyo: Shujunsha, 59-72

5.Shimizu, T., Eguchi, H., **Nagata, Y.**, Takahashi, T., Inada, H., Ando, S., & Suenobu, S. (1995) Multiple peripheral blood stem cell autografts in the treatment of pediatric progressive rhabdomyosarcoma. *The Japanese journal of pediatric hematology* (Japanese) 9, 404-408

6.Komori H. Matsuishi T. Abe T. **Nagata Y.** Ohtaki E. Kojima K. Yukizane S.(1993) Turner syndrome and occlusion of the internal carotid artery. *Journal of Child Neurology*. 8(4):412-415.

7.Matsuoka, K., Hayashi, K., Eto, K., Eguchi, H., **Nagata, Y.**, & Yamashita, F. (1991) A case of testicular relapse in childhood acute lymphoblastic leukemia. *Rinsho Hinyokika* (Japanese) 45(5):418-420

Yoichi Nagata

PTEN and Herceptin Responsiveness in Breast Cancers

Abstract

Overexpression of ErbB2, a 185kDa membrane receptor tyrosine kinase, can be found in approximately 30% of human breast cancers and is known to play an important role in breast cancer development and progression. Numerous efforts have been directed at developing ErbB2-targeting cancer therapies. One successful example of this is the recombinant humanized anti-ErbB2 antibody Herceptin (Trastuzumab) that specifically binds to the extracellular domain of ErbB2 and down-regulates $p185^{erbB2}$. Herceptin has demonstrated impressive therapeutic efficacy in phase II and phase III clinical trials, and is the first FDA approved antibody therapeutics for breast cancer. However, less than 20% of patients respond to Herceptin. Herceptin treatment can have severe side effects (e.g., cardiomyopathy) in some patients. Thus, there is an urgent need to identify patients who are unlikely to respond to Herceptin treatment to spare them from the potential side effects and unnecessary cost. More importantly, it is imperative to identify molecular alterations that confer Herceptin resistance, which can be used to predict patients' responses to Herceptin and may serve as molecular targets for overcoming Herceptin resistance. Unfortunately, mechanisms underlying Herceptin resistance are poorly understood.

Recently, we have found that Herceptin treatment leads to rapid Akt dephosphorylation before PI3K inhibition or ErbB2-down-regulation. Additionally, we found that Herceptin treatment rapidly activated PTEN phosphatase which corresponded to Akt dephosphorylation. This suggests PTEN activation may contribute to growth inhibition of breast cancer by Herceptin via dephosphorylation of Akt, a critical down-stream signal for ErbB2-mediated breast cancer progression. These data introduces a new concept that activation of PTEN as well as down-regulation of ErbB2 contribute to the growth inhibition by Hereptin, which challenges the existing paradigm that Herceptin elicits its growth inhibition via down-regulation of ErbB2. Furthermore, we and others have identified PTEN deficiencies in ~40% of breast cancers by LOH analyses and IHC studies, thus, we hypothesize that PTEN deficiency may render breast cancer cells resistant to Herceptin. The purpose of this proposed study is to test this novel hypothesis by pursuing the following three Specific Aims:

1. **To inhibit PTEN expression in breast cancer cells and determine if this impairs Herceptin-mediated Akt dephosphorylation.** First, we will inhibit PTEN expression in breast cancer cells containing wt PTEN (SKBr3, BT474) using PTEN antisense oligonucleotides, and by transfecting BT474 cells with HA-tagged-tet inducible, PTEN sense, antisense, and empty vectors to establish stable transfectants. We will treat these cells with or without Herceptin and investigate if Herceptin-mediated PTEN phosphatase activation and Akt dephosphorylation will be impaired by PTEN antisense. We will also determine the impact of PTEN antisense on Herceptin regulated signaling events, including ErbB2 down-regulation, ErbB2 phosphorylation, p85/ErbB2 association, and PI3K activity.
2. **To determine whether PTEN deficiency leads to resistance to Herceptin-mediated inhibition of breast cancer *in vitro* and *in vivo*.** We will first examine cells containing PTEN antisense for their responses to Herceptin treatment *in vitro*, including cell cycle profile, cell growth, apoptosis, and growth in soft agar. We will then use BT474 stable transfectants (sense, anti-sense, and vectors) to determine if PTEN deficiency will confer resistance to Herceptin-mediated tumor growth inhibition in ICR-SCID mice.
3. **To identify the mechanisms of PTEN activation by Herceptin in breast cancer cells.** We will compare phosphorylation status of PTEN in Herceptin treated and untreated SKBr3 and BT474 cells. If there is a difference, we will further compare the PTEN kinase CK2 expression level, CK2 binding to PTEN, CK2 association with ErbB2, and CK2 kinase activity. We will also examine whether Herceptin may induce PTEN translocation.

This proposal represents a new paradigm in the study of breast cancer. To the best of our knowledge, there is no previous report on Herceptin activation of PTEN. Moreover, predictive factor(s) have never been identified for breast tumor response to Herceptin. PTEN deficiencies have been found in ~40% of breast tumors. Thus, it is imperative to investigate the contribution of PTEN in Herceptin-mediated inhibition of breast cancer and explore the potential of using PTEN status as a predictive factor for Herceptin responsiveness. The pursuance of this proposal will bring original findings and important new insights into this unexplored area.

BIOGRAPHICAL SKETCH

Provide the following information for the key personnel in the order listed for Form Page 2.
Follow the sample format for each person. **DO NOT EXCEED FOUR PAGES.**

NAME	POSITION TITLE
Chenyi Zhou, Ph.D.	Postdoctoral Fellow

EDUCATION/TRAINING *(Begin with baccalaureate or other initial professional education, such as nursing, and include postdoctoral training.)*

INSTITUTION AND LOCATION	DEGREE *(if applicable)*	YEAR(s)	FIELD OF STUDY
East China University of Chemical Technology, China	B.S.	1986	Engineering
The City College of The City University of New York, NY	M.A.	1993	Biochemistry
The City College of The City University of New York, NY	Ph.D.	1998	Biochemistry

PROFESSIONAL EXPERIENCE AND POSTGRADUATE TRAINING

1986-1991	Biochemical Engineer, Department of Tetracycline, Pharmaceutical of Guilin, Guilin, China
1991-1998	Graduate Doctoral Fellow, Division of Biohemistry, The City College of the City University of New York, NY
1998-1999	Research Scientist, Department of Research and Development, Lifecodes Corporation, Stamford, CT
1999-present	Postdoctoral Fellow, Department of Pathology, Division of Pathology and Laboratory Medicine, The University of Texas MD Anderson Cancer Center, Houston, TX

HONORS AND AWARDS

1991-1996	The City College of the City University of New York Fellowship
1993	Helen Rubinstein Award
1997	Monthly Employee
2000-2001	Career Development Award from SPORE in Ovarian Cancer

PUBLICATIONS

1. Zhou, C., Huang, F., and Calhoun, D.H. Participation of Ribonucleases and Rho in the Formation, Processing and Stability of the *ilvGMEDA* Coded Transcripts of *Escherichia coli* K-12. Journal of Bacteriology, 1998 (submitted).
2. Zhou, C., Kay, S., Zhou, L., and Calhoun, D.H. The ilv Gene Cluster in *ESHERICHIA COLI.* THE 1995 NIGMS MINORITY PROGRAMS RESEARCH SYMPOSIUM, 1995.
3. Zhou, C., Zhou, L., and Calhoun, D.H. *ESHERICHIA COLI*: mRNA produced from *ilvGMEDA*. The First Annual Science Poster Session, GSCU, NY, 1994.
4. Zhou, C. and Liu, J. Regulation of human Telomerase expression in ovarian cell lines. (Manuscript in preparation.)
5. Zhou, C., Smith, J.L., and Liu, J. The last 49 amino acids of BRCA1 are required for the transcriptional activation and subnuclear assembly of BRCA1 in an ovarian cancer cell line. (Manuscript in preparation.)
6. Zhou, C., Huang, P., and Liu, J. The subnuclear assembly of RAD51 requires a functional BRCA1 protein after treatment with cisplatin but not ionizing radiation. (Manuscript in preparation.)

RESEARCH SUPPORT (during the last three years)

Chenyi Zhou, Ph.D.

ONGOING

Project: (Post-doctoral Research Fellow, Sponsor: Jinsong Liu, M.D., Ph.D.) Dates of Project: 9/30/2000-8/31/2001 Effort: 100%

Source: Career Development Award, SPORE in Ovarian Cancer Annual Direct Costs: $50,000

Title of Project: BRCA1 Protein Mediated Killing of Human Ovarian Cancer Cells by Carboplatin and Paclitaxel

The major goals of this project is to study how BRCA1 affects the drug resistance of ovarian cancer to cisplatin and taxel.

Abstract: Breast cancer progression is caused by multiple molecular and genetic changes. Invasive breast cancer is though to arise from pre-existing benign breast lesions. The biologic mechanisms involved in the progression of intraductal carcinoma to invasive cancer are not fully understood. BRCA1, a gene responsible for approximately half of all hereditary breast cancer, may play important role in breast cancer progression. In addition, it may coordinately regulated with another gene, hTERT, a gene involved in human cellular immortalization to control the breast tumor progression. We hypothesize that coordinated expression of BRCA1 and telomerase plays a critical role in breast cancer progression and expression level can be used to predict the clinical behavior of breast cancer such as recurrence or metastasis. We plan to test this hypothesis by using in situ hybridization and immunohistochemistry and examine the level of BRCA1 and telomerase expression at the single cell level. If this proves to be the case, then quantitation of BRCA1 and hTERT expression could be used to help to 1) classify preneoplastic lesions with potential to progress to carcinoma and 2) predict aggressive behavior of intraductal carcinoma and 3) predict responsiveness of invasive carcinoma to hormonal therapy. We propose to develop an immunohistochemically based assay to determine the level of BRCA1 and hTERT protein in the archived breast tumor and correlate their with patients' survival, tumor stage, histological grade, sensitivity to chemotherapy agents and radiation, and disease-free survival. If the proposed experiments work, we will have novel diagnostic and prognostic markers to predict the behavior of breast tumor and can individualize the best chemotherapy for that particular patient.

Appendix E

Biographical Sketches

Provide the following information for the key personnel listed on page 1 of the Detailed Cost Estimate form (see Appendix F) for the initial budget period.

NAME SEYED MAHMOUD ARAB NAJAFI	POSITION TITLE POSTDOCTORAL FELLOW

EDUCATION/TRAINING (Begin with baccalaureate or other initial professional education, such as nursing, and include postdoctoral training.)

INSTITUTION AND LOCATION	DEGREE (IF APPLICABLE)	YEAR(S)	FIELD OF STUDY
University of Tehran - Iran	B.Sc.	1988	Sciences
University of Tehran School of Medicine – Iran	M.Sc.	1990	Microbiology
University of Oxford – England	Ph.D.	1996	Biochemistry
University of Pennsylvania	Postdoc	1997-99	

RESEARCH AND PROFESSIONAL EXPERIENCE: Concluding with present position, list, in chronological order, previous employment, experience, and honors. Include present membership on any Federal Government public advisory committee. List, in chronological order, the titles, all authors, and complete references to all publications during the past 3 years and representative earlier publications pertinent to this application. PAGE LIMITATIONS APPLY. DO NOT EXCEED THREE PAGES FOR THE ENTIRE BIOGRAPHICAL SKETCH PER INVESTIGATOR.

Research and Professional Experience:

1988 – 1990 Graduate Student, School of Medical Sciences, University of Tehran - Iran

1991 - 1992 Instructor, School of Medicine, Shahid Beheshti University – Tehran, Iran

1992 – 1993 Research Associate, National Research Center for Genetic Engineering and Biotechnology, Shahid Beheshti University – Tehran, Iran

1993 – 1996 Ph.D. Student, Department of Biochemistry, University of Oxford – England

1997 – 1999 Research Scholar, School of Medicine, Howard Hughes Medical Institute, University of Pennsylvania – Philadelphia, PA

1999-present Assistant Professor, National Research Center for Genetic Engineering and Biotechnology – Tehran, Iran

2001-present Post-doctoral Fellow, Department of Molecular and Cellular Oncology, U. T. M. D. Anderson Cancer Center – Houston, Texas

RESEARCH AND PROFESSIONAL EXPERIENCE (CONTINUED). PAGE LIMITATIONS APPLY. DO NOT EXCEED THREE PAGES FOR THE ENTIRE BIOGRAPHICAL SKETCH PER INVESTIGATOR.

Publications:

Diederich B, Wilkinson JF, Magnin T, **Najafi SMA**, Errington J, and Yudkin M. Role of interaction between SpoIIAA and SpoIIAB in regulating cell-specific transcription factor σF of *Bacillus subtilis*. *Genes & Development* 8:2653-63, 1994.

Najafi SMA, Willis AC and Yudkin MD. Site of phosphorylation of SpoIIAA, the anti-anti-sigma factor for sporulation-specific σF of *Bacillus subtilis*. *Journal of Bacteriology* 177:2912-13, 1995.

Najafi SMA, Harris DA and Yudkin MD. The SpoIIAA protein of *Bacillus subtilis* has GTP-binding properties. *Journal of Bacteriology* 178:6632-34, 1996.

Errington J, Feucht A, Lewis PJ, Lord M, Magnin T, **Najafi SMA**, Wilkinson JF and Yudkin MD. Control of the cell-specificityof σF activity in *Bacillus subtilis*. *Phil Trans Royal Soc.* 351:537-42, 1996.

Najafi SMA, Harris DA and Yudkin MD. Properties of the phosphorylation reaction catalysed by SpoIIAB that help to regulate sporulation of *Bacillus subtilis*. *Journal of Bacteriology* 179:5628-31, 1997.

Najafi SMA. What is the best anti-cancer diet? *Hamshahri* 8:2035, 2000.

Najafi SMA and Klein PS. The Gq class of G proteins inhibits GSK-3β and stabilizes β-catenin: A possible role for Gq in the regulation of Wnt/Fz signal transduction. (In preparation)

Abstract:

The adenoviral early gene product, E1A, functions as a potent stimulator of cell cycle progression in quiescent rodent cells. The oncogenic effect of E1A is thought to be due to its ability to bind and inactivate some cellular proteins like the tumor suppressor protein, Rb, and the transcriptional co-activator p300/CBP. The E1A protein can be found as two forms (243 a.a and 289 a.a) that these two products are the result of splicing of a single E1A message.

Despite extensive studies, the oncogenic feature of E1A has not been clearly shown in human cells. In fact there are many studies indicating that E1A functions as a general tumor suppressor protein in human cancers. E1A is currently in clinical trials for the treatment of head and neck, breast, and ovarian cancers. However its mechanism is not very well understood. In this study we are going to investigate the relationship between E1A and cell cycle. Our preliminary data in MDA-MB-231 breast cancer cells and SKOV3-ip1 ovarian cancer cells show that E1A can increase expression of the Cyclin-dependent kinase inhibitor, p21/Cip1 at the RNA and protein levels. E1A and the induced p21 were mainly found in the nucleus. Reporter assay experiments using p21 promoter show that only the full length E1A (13S) can activate p21 expression. Interestingly E1A had no effect on expression of another member of the p21 family, p27. Our data also show that E1A can decrease expression of Cyclin D1 at the RNA and protein levels. Although the cDNA mircroarray data showed that E1A decreases the expression levels of Cyclins A, A1, and B1, the protein levels of these Cyclins were similar in the E1A stable transfectant cells and in the parental cells transfected with the empty vectors. These data suggest that E1A might decrease the activity of some cyclin dependent kinase inhibitors to inhibit cell proliferation in cancer cells. Our further experiments, described below, are designed to find out more about the molecular mechanism of the effect of E1A on cell cycle molecules.

Appendix E

Biographical Sketches

Provide the following information for the key personnel listed on page 1 of the Detailed Cost Estimate form (see Appendix F) for the initial budget period.

NAME SNEHALATA A. PAWAR NEE BHOSALE	POSITION TITLE POSTDOCTORAL FELLOW

EDUCATION/TRAINING (Begin with baccalaureate or other initial professional education, such as nursing, and include postdoctoral training.)

INSTITUTION AND LOCATION	DEGREE (IF APPLICABLE)	YEAR(S)	FIELD OF STUDY
University of Bombay, Mumbai, India	B.S	1990	Microbiol.
M. S. University, Baroda, India	M.S	1992	Biochem
University of Pune, India	Ph.D.	1999	Biochem.
The Univ. of Texas, M.D.Anderson Cancer Center, Houston, TX	Postdoc.	2000-present	Molecular Genetics

RESEARCH AND PROFESSIONAL EXPERIENCE: Concluding with present position, list, in chronological order, previous employment, experience, and honors. Include present membership on any Federal Government public advisory committee. List, in chronological order, the titles, all authors, and complete references to all publications during the past 3 years and representative earlier publications pertinent to this application. PAGE LIMITATIONS APPLY. DO NOT EXCEED THREE PAGES FOR THE ENTIRE BIOGRAPHICAL SKETCH PER INVESTIGATOR.

AWARDS & HONORS:

1. Recipient of the CSIR-UGC-NET Fellowship awarded by the Council of Scientific & Industrial Research, New Delhi, India:
   a. Junior Research Fellowship, 1993-1995
   b. Senior Research Fellowship, 1995-1998

2. Recipient of Welch Foundation Fellowship, March 2000 - present

ABSTRACTS & POSTER PRESENTATIONS:

1. Pawar , S. A. and Deshpande V.V. (1998) Abstract entitled "Characterization of acid-induced unfolded intermediates of glucose/xylose isomerase from Streptomyces sp. NCIM 2730 " accepted for the Annual Meeting of Society of Biological Chemists, India, held at New Delhi, during Dec17-21, 1998

2. Pawar, S. A. and Sawadogo, M. (2001) Poster entitled, "E-box dependent transactivation of CDK4 promoter by Upstream Stimulatory Factor," presented at the Genes & Development Retreat 2001, held at Corpus Christi, Texas, during March 27- 31, 2001

3. Pawar, S. A. and Sawadogo, M. (2001) Poster entitled, "E-box dependent transactivation of CDK4 promoter by Upstream Stimulatory Factor," presented at the Trainee Recogneetion Day event, held at M. D.Anderson Cancer Center, Houston, Texas, on April 26,2001.

PARTICIPATION IN TRAINING COURSES:

Participated in annual workshop on Protein/peptides sequencing and analysis, held at Indian Institute of Technology, Mumbai, June 20-22, 1996.

PUBLICATIONS:

1. Gupta, S., Bhosale, S., Pandya, K. (1994) Effect of low level exposure of Lead and Cadmium on delta-ALAD and Acetylcholinesterase in rats. Indian. J. Exp. Biol. 32, 819-821.

2. Bhosale, S. H., Rao, M. B., Srinivasan, M. C. and Deshpande, V. V. (1995) Thermostability of high activity alkaline protease from Conidiobolus coronatus (NCL 86.8.20) Enz. Microb. Technol.17, 136-139.

3. Bhosale, S. H., Rao, M. B. and Deshpande, V. V. (1996) Molecular and industrial aspects of glucose isomerase. Microbiol.Rev. 60, 281-290.

4. Bhosale, S. H., Ghatge, M. S. and Deshpande, V. V. (1996) Molecular cloning and expression of glucose/xylose isomerase from Streptomyces sp. NCIM 2730 in E.coli. FEMS. Microbiol. Lett. 145, 95-100.

5. Paul, A., Bhosale, S. H., Maity, T. K., and Deshpande, V. V. (1998) Effect of coordinated addition of specific amino acids on the synthesis of recombinant glucose isomerase. Enz. Microbe. Technol. 23,

   506-510

6. Pawar , S. A. and Deshpande, V. V. (2000) Characterization of acid-induced unfolded intermediates of glucose/xylose isomerase from Streptomyces sp. NCIM 2730. Eur. J. Biochem. 267, 6331-38

ABSTRACT

Proposal Title: **Role of USF in the regulation of the *CDK4* promoter in breast epithelial cells**

Investigator: **Snehalata A. Pawar**

Breast cancer, one of the most common cancers in women accounts for nearly 30% of cancer incidence and 15% of cancer mortality in the United States. Abnormal gene expression is common including increased oncogene activity (c-ErbB-2, c-Ras, c-Myc) and loss of tumor suppressor function (p53, pRb). In addition, the aberrant expression of cell cycle mediators such as Cdk4, cyclin D1 contributes to the transformation of normal mammary cells.

USF is a cellular transcription factor, which shares with c-Myc structural similarity and DNA-binding specificity to elements called E-boxes, which contain a central CACGTG sequence. c-Myc belongs to the basic helix-loop-helix leucine zipper family of transcription factors that display sequence-specific binding to the CACGTG sequence. c-Myc is a protooncogene involved in cellular proliferation, differentiation and apoptosis. Genetic alteration of *c-myc* is a frequent event in tumor progression. Despite the similarities, USF and c-Myc have opposite functions in growth control. USF overexpression inhibits cellular proliferation and *Ras* and *c-myc*-induced transformation. Recent studies in our laboratory in breast cancer cell lines demonstrated a loss in the transcriptional activity of USF, suggesting its involvement in a tumor suppressor pathway. In cancer cells, overexpression of c-Myc causes cellular proliferation and loss of USF function in cancer cells confers a selective growth advantage to cells. USF is involved in regulating genes that control growth and cell cycle such as *p53*, *TGF-β2*, *cdc2*, *cyclin B1, MKP-1* and *BRCA2*.

CDK4 is an important regulator of the *Rb* pathway, and is active in early to late G1. Deregulation of the *CDK4* gene has been implicated in several cancers including breast cancers. Recent studies using serial analysis of gene expression to examine the transcripts regulated by exogenous expression of c-Myc revealed *CDK4* as one of the target genes. The transactivation of the *CDK4* promoter by c-Myc was mediated through four highly conserved CACGTG motifs present upstream to the transcription start site.

Discrimination between USF and Myc binding can be achieved through the sequences, which flank the core sequence of the E-box. Binding studies indicated a strong preference for thymidine residue on the 5' flank of the core sequence for recognition by USF as opposed to Myc, which prefers a cytosine residue. Analysis of the flanks of the CACGTG motifs of the *CDK4* promoter suggested these to be potential USF-binding sites.

In context of the effect of USF on growth regulation and loss of USF transcriptional activity in cancer cells, I hypothesize that USF is involved in the regulation of *CDK4* in normal cells. I, therefore, propose to: a) elucidate the role of USF in the regulation of the *CDK4* promoter in normal breast epithelial cells which contain active endogenous USF and low levels of c-Myc and b) investigate the differential regulation of the *CDK4* promoter in breast cancer cell lines containing high levels of c-Myc and transcriptionally inactive USF. To achieve this proposed goal, binding of USF to the *CDK4* promoter will be confirmed by DNase I footprinting, Electromobility Shift Assays (EMSA) and Chromatin Immunoprecipitation (ChIP) assays. Transcriptional regulation and mapping of the domains of USF involved in regulation will be monitored by transient transfection assays in normal breast epithelial cells and in breast cancer cell lines. The transcription initiation sites on the *CDK4* promoter will be mapped in normal and breast cancer cell lines.

Thus the proposed studies will unfold the functional relationship between two transcription factors that share common downstream targets, but have opposite effects on cellular proliferation. The long-range hope is to understand the basis of normal and abnormal growth at the molecular and cellular levels in order to develop strategies to selectively block the growth and division of cancer cells.

Biographical Sketches

Provide the following information for the key personnel listed on page 1 of the Detailed Cost Estimate form for the initial budget period.

NAME LIN QIU	POSITION TITLE POSTDOCTORAL FELLOW

EDUCATION/TRAINING (Begin with baccalaureate or other initial professional education, such as nursing, and include postdoctoral training.)

INSTITUTION AND LOCATION	DEGREE (IF APPLICABLE)	YEAR(S)	FIELD OF STUDY
Norman Bethune Univ. of Medical Science. ChangChun, China	B.S.	1979-1984	Medicine
Norman Bethune Univ. of Medical Science. ChangChun, China	M.S.	1984-1987	Hematology
Medical School of Tokyo Univ. Tokyo, Japan	Ph.D.	1991-1995	Immunology
Univ. of Texas, MD Anderson Cancer Center, Houston, Texas	postdoctoral	1999-2001	Molecular Hematology
Univ. of Texas, MD Anderson Cancer Center, Houston, Texas	postdoctoral	2001-now	Molecular Oncology

RESEARCH AND PROFESSIONAL EXPERIENCE: Concluding with present position, list, in chronological order, previous employment, experience, and honors. Include present membership on any Federal Government public advisory committee. List, in chronological order, the titles, all authors, and complete references to all publications during the past 3 years and representative earlier publications pertinent to this application. PAGE LIMITATIONS APPLY. DO NOT EXCEED THREE PAGES FOR THE ENTIRE BIOGRAPHICAL SKETCH PER INVESTIGATOR.

Research and Professional Experience:

1987-1989: Research Assistant. Department of Cell Biology. Institute of Traditional Chinese Medical Science, Academy of Chinese Traditional Medical Science. Beijing, China

1996-1999: Investigator Department of Immunology. The Institute of Clinical Medical Science, China-Japan Friendship Hospital. Beijing, China

1999-2001: Postdoctoral Fellow Department of Blood and Marrow transplantation, M.D. Anderson Cancer Center, The University of Texas

2001- now: Postdoctoral Fellow Department of Molecular and Cellular Oncology. Anderson Cancer Center, The University of Texas

RESEARCH AND PROFESSIONAL EXPERIENCE (CONTINUED). PAGE LIMITATIONS APPLY. DO NOT EXCEED THREE PAGES FOR THE ENTIRE BIOGRAPHICAL SKETCH PER INVESTIGATOR.

Publication

1. **Qiu L** Cong X Tan and Yiwei. (2000) Application of Microsatellite Alteration of the Urine sediment in the early diagnosis of Bladder Cancer. *Chinese J of Oncology*. 22:483-486.

2. Wang, ZY, and **Qiu L**. (2000) Application of Microsatellite analysis in lung cancer. *J. China- Japan Friendship Hospital.* 14:172-174.

3. **Qiu L** Cong X, Zhao WS. (2000) Detection of lung cancer micrometastases in bone marrow by Keratin 19 mRNA RT-PCR method. *Chinese J of Oncology*.22:32-35.

4. **Qiu L** Cong X, Zhao WS. (1998) Development of RT-PCR method to detect keratin 19 mRNA expression. *J. China-Japan Friendship Hospital.* 12:103-107.

5. **Qiu L** Nishmura M, Juji T. (1996) Enhancement of the expression of progesterone receptor on progesterone treated lymphocyte after immunotherapy in recurrent spontaneous abortion. *Am J Report Immunol.* 35:552-557.

6. Li FW, Zhang LSH and **Qiu L** (1996) Effect of TongMaining, a Chinese Medicine on Rabbit Microcirculation. *Chinese J of Basic Medicine in Traditional Chinese Medicine*. 12:30-31.

7. Yamamoto JY, Fujino Y, **Qiu L**. (1994) S-antigen specific T cell clones from a patient with Behcet's disease. British J. Ophthalmology. 78:927-932.

8. **Qiu L** Ma J, Liu J. (1989) Study on the differential regulation of hemopoietic progenitor in chronic myelogenic leukemia. *Chinese J. Hematology*. 10:307-308.

9. **Qiu L** Ma J, Liu J. (1988) A modified culture method of human pluripotent hemopoietic Progenitor (CFU-Mix) in vitro. J. Norman Bethune Uni. Med. Sci. 14:389-341.

10. **Qiu L** Ma J, Liu J. (1988) The effect of chronic renal failure plasma on hemopoietic progenitor. Chinese J. Nephrophathy. 1:8-11.

11. **Qiu L** Liu J. (1987) The effect of CFU-GEMM in human hemopoietic process. *Chinese Med. Sci. Abroad*, 4:261-265.

12. **Qiu L** Wang G. The relationship between gerontal sex hormone change and heart, lung and blood vessel diseases with radio-immunoassay. *Chinese J. Gereology* 2:357-359, 1985

Abstract

Proposal title: $p21^{Cip1/WAF1}$ Gene Therapy in Breast Cancer

Applicant: Lin Qiu

Background: Amplification/overexpression of *Her2/neu* in cancer cells confers resistance to apoptosis and promotes cell growth. The PI-3K/Akt pathway, one of downstream signaling pathways of *Her2/neu*, plays an important role in preventing cells from undergoing apoptosis and contributes to the pathogenesis of malignancy. Cellular localization of $p21^{Cip1/WAF1}$ has been proposed to be critical in either promoting cell survival or inhibiting cell growth. In our recent study, we found that *Her2/neu*-mediated cell growth required the activation of Akt, which associated with $p21^{Cip1/WAF1}$ and phosphorylated it at threonine 145, and then resulted in cytoplasmic localization of $p21^{Cip1/WAF1}$. Furthermore, blocking the Akt pathway with a dominant-negative mutant of Akt restored the nuclear localization and the cell growth inhibition activity of $p21^{Cip1/WAF1}$. Our results indicated that *Her2/neu* induces cytoplasmic localization of $p21^{Cip1/WAF1}$ via the activation of Akt to promote cell growth, which may have implications that nuclear $p21^{Cip1/WAF1}$ may be as a therapeutic agent in gene therapy against *Her2/neu* overexpressing breast cancer.

Hypothesis/Purpose: Based on the background described above, we propose that nuclear $p21^{Cip1/WAF1}$ (T145A) may be used as a therapeutic agent in gene therapy against *Her2/neu* overexpressing breast cancer.

Specific Aims: (1) To examine tumor suppressor function of nuclear $p21^{Cip1/WAF1}$ (T145A) in different breast cancer cell lines. (2) To test the anti-tumor activity of nuclear $p21^{Cip1/WAF1}$ using preclinical gene therapy strategies in several orthotopic breast cancer animal models. (3) To evaluate the relationship between the efficacy of therapies and *Her2/neu* expression, Akt activity and localizations of $p21^{Cip1/WAF1}$.

Study design: In this study, we choose to use MDA-MB231, MDA-MB-468, MDA-MB-361 and BT-474 breast cancer cell lines for colony forming assay *in intro* and inducing tumor in the mammary fat pad of female nude mice. At first we will examine the anti-growth activity of nuclear $p21^{Cip1/WAF1}$(T145A) and compare the activity with wild type $p21^{Cip1/WAF1}$ and cytoplasmic $p21^{Cip1/WAF1}$ (T145D) by colony forming assay. NIH3T3 and *Her2/neu*-3T3 cell lines will be selected as negative and positive cell lines. Then, we will generate orthotopic breast tumors by mammary fat pads inoculation of breast cancer cells in nude mice. The tumor-bearing mice then will be treated with wild type $p21^{Cip1/WAF1}$, cytoplasmic $p21^{Cip1/WAF1}$ and nuclear $p21^{Cip1/WAF1}$ mutant gene plus the gene delivery system, in which the non-viral delivery systems, such as SN (liposome), will be used. Therapeutic efficacy will be evaluated by examining tumor volume, metastasis and survival. In addition, two injection types, intravenous injection and subcutaneously introtumoral injection will be compared in therapy. In order to confirm the relationship between treatment efficacy and *Her/neu* expression Akt activity and localizations of $p21^{Cip1/WAF1}$ in four breast cancer cell lines, tumor samples will be analyzed by immunohistochemical staining and western blot as described in our precious study.

Relevance: The techniques involved in this proposal, such as transfection, biological assays, animal models and so on are well established in the P.I.'s laboratory as evident from the preliminary results sections and the previous publications. We, therefore, do not expect too much technical difficulty. We expect to find anti-tumor activity of nuclear $p21^{Cip1/WAF1}$ (T145A) in this gene therapy study.

BIOGRAPHICAL SKETCH

Provide the following information for the key personnel in the order listed for Form Page 2.
Follow the sample format for each person. **DO NOT EXCEED FOUR PAGES.**

NAME	POSITION TITLE
Zhibo Yang, M.D., Ph.D.	Postdoctoral Fellow

EDUCATION/TRAINING *(Begin with baccalaureate or other initial professional education, such as nursing, and include postdoctoral training.)*

INSTITUTION AND LOCATION	DEGREE *(if applicable)*	YEAR(s)	FIELD OF STUDY
China Medical University, Shenyang P.R. China	M.D.	1995	Clinical Medicine
Cancer Institute China Medical University, Shenyang P.R. China	Ph.D.	2000	Molecular Oncology

PROFESSIONAL EXPERIENCE AND POSTGRADUATE TRAINING

1995-1997	Research Assistant, Cancer Institute, China Medical University, Shenyang P.R. China
2000-2001	Special Exchange Student, Department of Microbiology and Immunology, Hamamatsu University School of Medicine, Hamamatsu, Japan
2001-present	Postdoctoral Fellow, Department of Pathology, Division of Pathology and Laboratory Medicine, The University of Texas MD Anderson Cancer Center, Houston, TX

PUBLICATIONS

1. Z. Yang, Qian Liu, Changshan Ren. Detection on the mutations of von Hippel-Linda (VHL) tumor suppressor gene in paraffin-embedded kidney neoplasm. Journal of China Medical University 28(5):366-367 (cited by Biological Abstracts 2000vol.107(4), NO.47517), 1999.
2. Z. Yang, Qian Liu, Changshan Ren. Microsatellite instability and hMSH2 gene mutation in bladder carcinoma. Journal of China Medical University 28(6):415-416, 1999.
3. Z. Yang, Qian Liu, Changshan Ren. Study on the relationship of cyclin-dependent kinase inhibitor p27kip1 with Robson stage for renal carcinoma. Journal of China Medical University 28(5):364-365 (cited by Biological Abstracts 2000 vol.107 (4), NO.57433), 1999.
4. Z. Yang, Qian Liu, Changshan Ren. Expression of p21WAF1/CIP1 and its correlation with clinicopathological features in human bladder transitional carcinoma. Journal of China Medical University 28(6):453-454, 1999.

Role of BRCA2 in Cellular Immortalization of Genetically Defined Breast Epithelial Cells (Abstract)

Background: Recent studies suggest that *BRCA2* and *BRCA1*, two genes responsible for approximately 90% of hereditary breast cancers, acts in concert with DNA-repair enzymes to maintain the integrity of the genome during a period of rapid growth. The gene product of ataxia-telangiectasia-mutated (ATM) controls the overall phosphorylation of *BRCA1* in response to ionizing radiation. Heterozygous carriers of a dysfunctional ATM gene have been reported to be highly sensitive to ionizing radiation and predisposed to the development of breast cancer. It is not clear whether patients with heterozygous *BRCA2* mutation have a similar phenotype as the ATM heterozygote.

Objective/Hypothesis: We hypothesize that $BRCA2^{+/-}$ human mammary epithelial cells (HMECs) are haplo-insufficient in their function for DNA repair and cell cycle regulation. This defect can be significantly magnified when the breast epithelial cells are under stressed conditions or in the presence of a defective p53 gene product. Defective *BRCA2* and p53 genes will increase genetic instability and predispose the cells to immortalization. We will evaluate the biologic differences between $BRCA2^{+/-}$ HMECs and $BRCA2^{+/+}$ HMECs upon treatment with ionizing radiation.

Specific Aims: (1) to examine the biologic differences between $BRCA2^{+/-}$ HMECs and $BRCA2^{+/+}$ HMECs, and (2) to test whether inactivation of the p53 gene promotes genetic instability and increase the frequency of immortalization in $BRCA2^{+/-}$ HMECs.

Research Design: We will collect and culture breast epithelial cells from prophylactic mastectomy specimens from patients with a family history of breast and ovarian cancer who have tested positive for the *BRCA2* mutation. We will compare the *BRCA2* mRNA and protein levels in these cells with those from $BRCA2^{+/+}$ HMECs. We will examine the cell response to ionizing radiation. If there is no difference, we will introduce a vector expressing transdominant negative protein or human papillomavirus (HPV) E6 gene to inactivate the endogenous p53 protein and examine the frequency of immortalization, genetic instability, and changes in cell cycle.

Relevance: Understanding of the role of *BRCA2* in breast cancer has been hampered by a lack of genetically well-defined cell lines representing different stages of progression. This propose will create model systems to study the genetic instability and critical events required for hereditary breast cancer development. These *in vitro* models not only should facilitate the understanding of the biology of *BRCA2* but also may provide useful premalignant model systems to select potential chemopreventive and therapeutic agents.

BIOGRAPHICAL SKETCH

Name	Position Title
Jijiang Zhu, M.D., Ph.D.	**Postdoctor**

EDUCATION/TRAINING

INSTITUTION AND LOCATION	DEGREE *(if applicable)*	YEAR(s)	FIELD OF STUDY
Jinzhou Medical College, Jinzhou, China	B.S.	1981-1986	Medicine
China Medical University, Shenyang, China	M.S.	1986-1989	Medicine (Pathology)
China Medical University, Shenyang, China	Ph.D.	1992-1995	Medicine (Pathology)
University of Tokyo, Tokyo, Japan	Visiting Scientist	1995-1996	Molecular Biology
University of Texas, Texas, USA	Visiting Scientist	2000-2001	Molecular Epidemiology

Research and Professional Experience

1986-1989: Postgraduate for Master's Degree, Department of Pathology,
China Medical University, Shenyang, P. R. China
1989-1992: Teaching Assistant, Department of Pathology,
Medical University, Shenyang, P. R. China
1992-1995: Postgraduate for Ph.D. Degree, Lung Cancer Laboratory, Cancer Research Institute,
China Medical University, Shenyang, P. R. China
1995-1996: Visiting Scholar, Department of Pathology
University of Tokyo Faculty of Medicine, Tokyo, Japan
1992-1998: Instructor, Department of Pathology,
China Medical University, Shenyang, P. R. China
1998-2000: Associate Professor, Department of Pathology,
China Medical University, Shenyang, P. R. China
2000-2001: Visiting Scientist, Department of Gastrointestinal Oncology and Digestive Diseases
University of Texas MD Anderson Cancer Center

Publications

1. **ZHU J,** HE M. Flow cytometric analysis of cellular DNA content and cytokinetic study on experimental lung squamous cell carcinomas of Wistar rats. Chinese Journal of Pathology, 1991, 20(1): 31-4.
2. **ZHU J,** HE M. Application of flow cytometry to lung cancer research. Foreign Medical Sciences: Physiology, Pathology and Clinics, 1991, 12(2): 76-8(21 ref.).
3. **ZHU J,** HE M. Angiomatoid malignant fibrous histiocytoma. Journal of Clinical and Experimental Pathology, 1993, 9(1): 67-8(6 ref.).
4. **ZHU J,** HE M. Malignant rhabdoid tumor: Research and Progress. Foreign Medical Sciences: Physiology, Pathology and Clinics, 1993, 14(2): 93-9(13 ref.).
5. **ZHU J,** HE A. The significance of ras oncogene point mutation and its product p21 protein expression in lung cancer. Foreign Medical Sciences: Physiology, Pathology and Clinics, 1995, 16(2): 101-3(14 ref.).
6. **ZHU J,** HE A. The detection of seral ras oncogene product p21 protein and its significance in lung cancer diagnosis. Foreign Medical Sciences: Oncology. 1995, 16(Suppl.): 55-7(16 ref.).

7. **ZHU J,** LIU K, HE A, QU H. The expression and significance of cell proliferating nuclear antigen in non-small cell lung carcinomas. Chinese Journal of Oncology, 1995, 16(Suppl.): 51-3.
8. **ZHU J,** JIANG Y, HE A, ZHOU B. Flow cytometric analysis of p53 protein expression and its significance in non-small cell lung carcinomas. Chinese Journal of Physical Medicine, 1996, 18(1): 24-6.
9. **ZHU J,** DAI X, HE A, LIU K. The expression and significance of oncogene product p21 protein in lung carcinomas. Journal of China Medical University, 1996, 25(4): 343-5.
10. MA J, **ZHU J,** LI L, ZHOU B, WANG Y. Analysis of the prognostic factors of the patients with early ovarian epithelial carcinomas by Cox model. Journal of Practical Oncology, 1997, 11(4): 281-3.
11. Xie C, **ZHU J,** Liu X, Li J. The detection of HBV-DNA in gallbladders of the patients with chronic hepatitis by polymerase chain reaction. Journal of China Medical University, 1998, 27(2): 218.
12. Li J, **ZHU J,** Zhou B. Analysis of the prognostic factors of the patients with lung squamous cell carcinomas by Cox model. Chinese Journal of Health Statistics, 1998, 15(3): 20-1.
13. Zhou B, **ZHU J,** Dai X, He A, Yang C. Molecular markers (ras p21, p53, PCNA) as indicators in evaluating the prognosis of the patients with lung adenocarcinomas. Chinese Journal of Epidemiology, 1998, 19(4): 231-3.
14. Shimizu Y, **ZHU J,** Han F, Ishikawa T, Oda H. Different frequencies of p53 codon-249 hot-spot mutations in hepatocellular carcinomas in Jiang-Su province of China. International Journal of Cancer, 1999, 82:187-90.
15. Yu H, Shi C, **ZHU J**, Li Z, Qiu X, Wang E. Cyclin A Expression in Non-small Cell Lung Carcinoma is Related to Proloferative Activity and Prognosis. Chinese Journal of Cancer, 2001, 20(1):38-40.
16. Firozi FF, **ZHU J**, Sen SS, Kuang J, Abbruzzese JL, Evans DB, LI D. STK15 amplification and overexpression in human pancreatic cancer. Proceedings of American Association of Cancer Research, Volume 42: #2659, 2001.

Jijiang Zhu

Abstract

Analysis of MtDNA Mutation in Relation to Oxidative Stress in Breast Cancer

Background

Though highly suspected in causality, the contribution of DNA damage in breast carcinogenesis has been difficult to demonstrate in humans, in part, because of the suspected mixed nature of exposures (i.e., hormonal, dietary, environmental), the general transient nature of exposure related endpoints and low levels and severely limited access to the target tissue. The level of DNA damage (i.e., DNA adducts) is affected by numerous factors most notably the extent of exposure, the rate of cell turn-over and rate of repair (often hours). Thus, as determinants of subsequent risk, measures of DNA damage via adduct formation have proven highly variable and difficult to assess in human tissues. On the other hand, DNA mutations arising through damage and lack of repair can be viewed as more stable indicators of exposure from reactive oxygen species and chemical carcinogens, however their relative abundance in nuclear DNA is low even with exposure and distributed throughout the genome. On the other hand, mitochondrial DNA (mtDNA) is subject to more oxidative damage than nuclear DNA, in part, because of the lack of protective proteins and less sufficient DNA repair. Recent observations from aged tissues suggest that focally located and amplified mutations (hotspots) in mtDNA may accumulate with age and serve as novel biological markers (biomarkers) of age-related events (i.e., prolonged exposure to oxidative damage, chemical exposures) or a so-called marker of biological versus chronological age. Each cell contains hundreds to thousands of copies of mtDNA. In several studies, age-dependent and tissue-specific accumulations of mutation in hot spots have been identified in the hypervariable control regions of the mtDNA. Given that for most sporadic cancers, including breast, that advancing age is the most reliable risk factor, we argue that these same mtDNA hotspot mutations may be useful in population-based cancer risk assessment studies for evaluating the extent of permanent damage in a particular tissue relative to an individual's chronological age. This project will explore whether or not the mtDNA mutations in breast tissues can be used as novel quantitative markers for oxidative DNA damage in breast cancer.

Hypothesis

There may be mammary epithelial cell-specific mtDNA mutation hot spots in the control region of mtDNA and these mtDNA mutations may be associated with oxidative DNA damage in breast cancer.

Objectives and Study Design

1. *To Identify the mtDNA mutation hot spots in human mammary epithelial cells and in human breast tumors.* The control region of mtDNA from mammary carcinoma and non-malignant cell lines will be amplified and sequenced. Sequence and frequency will be also determined from tumor and normal tissue samples from 30 women with breast cancers. Matched peripheral blood lymphocytes will also be used to eliminate the contribution of genetic polymorphisms in areas of apparent sequence heterogeneity. The mutation profiles will be compared between different cell lines and tissues from different individuals to identify any mutation hot spots present in breast tissues.
2. *To quantitatively analyze the fraction of mtDNA mutations by allele-specific termination of primer extension method.* We will develop allele-specific termination of primer extension method for the rapid quantitative assessment of mtDNA mutations for each of the candidate hotspot mutations.
3. *To demonstrate whether the mtDNA mutation profile is related to oxidative DNA damage in breast tumor.* The level of 8-OH-dG (8-hydroxydeoxyguanosine), an oxidized DNA base, will be measured by using the HPLC-EC method in DNA samples from the same cell lines and breast tissues used above. The levels of oxidative DNA damage will be expressed as 8-OH-dG/10^5 dG. Three parameters of mtDNA mutation will be analyzed in relation to the level of 8-OH-dG, i.e. the frequency, the fraction, and the types of mutations. The correlation analysis will demonstrate whether there is any association between the mtDNA mutation and level of oxidative DNA damage.

Relevance.

Given that DNA damage may play an important role in breast cancer etiology, establishing a reliable and quantitative method to measure cumulative genetic damage as opposed to a simple measure of chronological age may provide new tools for risk assessment and improve the selection criteria for high-risk individuals for prevention-based strategies.

Appendix 3.0

Cited Manuscripts and Abstracts

HER-2/neu induces p53 ubiquitination via Akt-mediated MDM2 phosphorylation

Binhua P. Zhou*, Yong Liao*, Weiya Xia, Yiyu Zou, Bill Spohn and Mien-Chie Hung†

Department of Molecular and Cellular Oncology, Breast Cancer Basic Research Program, The University of Texas M. D. Anderson Cancer Center, Houston, Texas 77030, USA

**These authors contributed equally to this work*

†e-mail: mhung@notes.mdacc.tmc.edu

***HER-2/neu* amplification or overexpression can make cancer cells resistant to apoptosis and promotes their growth. p53 is crucial in regulating cell growth and apoptosis, and is often mutated or deleted in many types of tumour. Moreover, many tumours with a wild-type gene for p53 do not have normal p53 function, suggesting that some oncogenic signals suppress the function of p53. In this study, we show that *HER-2/neu*-mediated resistance to DNA-damaging agents requires the activation of Akt, which enhances MDM2-mediated ubiquitination and degradation of p53. Akt physically associates with MDM2 and phosphorylates it at Ser166 and Ser186. Phosphorylation of MDM2 enhances its nuclear localization and its interaction with p300, and inhibits its interaction with $p19^{ARF}$, thus increasing p53 degradation. Our study indicates that blocking the Akt pathway mediated by *HER-2/neu* would increase the cytotoxic effect of DNA-damaging drugs in tumour cells with wild-type p53.**

The *HER-2/neu* gene (also known as *c-erbB2*) encodes a 185-kDa transmembrane receptor tyrosine kinase that has partial homology with other members of the epidermal growth factor receptor family. Amplification or overexpression of *HER-2/neu* has been found in various cancer types and has been associated with poor clinical outcome, including short survival and short time to relapse[1–3]. We have previously showed that HER-2/*neu* activates the Akt pathway and so confers resistance to tumour necrosis factor (TNF)-induced {AUTHOR—OK?} apoptosis[4], and increases cell proliferation by inducing cytoplasmic localization of $p21^{Cip1/WAF1}$ (ref. 5). The phosphatidylinositol-3 kinase (PI(3)K)–Akt pathway plays an important role in preventing cells from undergoing apoptosis and contributes to the pathogenesis of malignancy[6,7]. Several targets of the PI(3)K–Akt signalling pathway have recently been identified that might underlie the ability of this regulatory cascade to promote cell survival and cell growth. These substrates include two components of the intrinsic cell death machinery (Bad and caspase 9; refs 8,9), transcription factors of the forkhead family[10,11], Ikk-α (a kinase that regulates NF-κB activation[12]) and $p21^{Cip1/WAF1}$ (a cell-cycle inhibitor that controls cell growth[5]). The PI(3)K–Akt pathway has also been reported to delay p53-mediated apoptosis[13], suggesting that there is a link between the PI(3)K–Akt signalling pathway and p53-mediated apoptosis.

The tumour-suppresser protein p53 is a transcription factor that can induce either growth arrest or apoptosis and is frequently mutated or deleted in many types of tumour[14–21]. In addition, many tumours with a wild-type gene for p53 do not have functional p53 protein, suggesting that some oncogenic signals suppress the function of p53 (refs 14,17). The levels and activity of p53 are controlled largely by MDM2, which is amplified or overexpressed in a variety of human tumours and can function as an oncogene in tissue culture systems[14,17,20]. MDM2 can bind directly to p53 and promote its ubiquitination and subsequently its degradation by the proteasome[20,21]. The ability of MDM2 to degrade p53 depends on its ubiquitin E3 ligase activity and its nuclear localization signal (NLS) and nuclear export signal (NES), which are required for MDM2 to shuttle between the nucleus and the cytoplasm[14,20]. The nucleus–cytoplasm shuttling of MDM2 presumably mediates p53 degradation by cytoplasmic proteasomes.

In addition to MDM2, the transcriptional co-activator CBP/p300 has also been shown to play a role in efficient degradation of p53 (refs 22,23). CBP/p300 forms a complex with MDM2 *in vitro* and *in vivo*, and provides a platform to allow the assembly of the protein complex necessary for MDM2-mediated ubiquitination and degradation of p53 (ref. 23). MDM2 is feedback regulated by p53 and by the expression of ARF protein (p14 in humans and p19 in mice), which is encoded by the *Ink4A* locus[15,24–26]. Loss of ARF increases tumour susceptibility in mice, and mutations in *Ink4A* are often detected in human cancers[26]. The ARF protein binds directly to MDM2 to block p53 degradation by inhibiting the ubiquitin E3 ligase activity associated with MDM2 (ref. 27) and by sequestering MDM2 in nucleoli to prevent its export to the cytoplasm[28,29]. Interestingly, the regions that control MDM2 nucleus–cytoplasm shuttling (amino acids 181–185 of the NLS and amino acids 191–205 of the NES)[20] and the regions required for p300 binding (amino acids 102–222)[22,23] and $p19^{ARF}$ binding (amino acids 154–221)[24] overlap, suggesting that p300, $p19^{ARF}$ and other cellular proteins interact to control the function of MDM2.

In this study, we show that *HER-2/neu*-mediated resistance to DNA-damaging agents requires the activation of Akt, which enhances MDM2-mediated ubiquitination and degradation of p53. Akt interacts physically with MDM2 and phosphorylates it at Ser166 and Ser186, and so increases the nuclear localization of MDM2. Furthermore, phosphorylation of MDM2 increases its interaction with p300 and inhibits its interaction with $p19^{ARF}$ and so increases p53 degradation. Our study indicates that blocking the Akt pathway mediated by *HER-2/neu* would increase the cytotoxic effect of DNA-damaging drugs in tumour cells with wild-type p53.

RESULTS

Blocking the Akt pathway sensitizes *HER-2/neu*-transformed cells to DNA-damaging agents. Because overexpression of *HER-2/neu* induces resistance to apoptosis mediated by chemotherapeutic drugs[3,4,30,31] and the Akt pathway is known to increase cell survival, we examined whether blocking the Akt pathway would sensitize

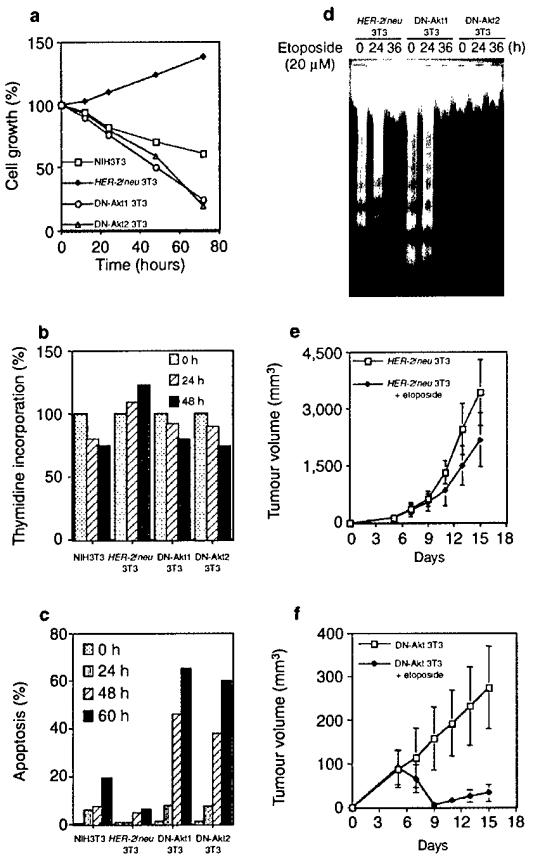

Figure 1 **The Akt pathway is required for *HER-2/neu*-mediated chemoresistance to etoposide. a**, Blocking the Akt pathway reduces the growth of DN-Akt 3T3 cells in the presence of etoposide. The cells (3×10^3) were seeded in 96-well plates and grown in Dulbecco's modified Eagle's medium/F12 medium plus 5% foetal bovine serum in presence of 20 μM etoposide. The growth rate was monitored by the MTT assay. The results are presented as the mean ± standard error **{AUTHOR—OK? (was "average" and "SE")}** of three independent experiments performed in quadruplicate. **b**, Cells (3×10^3) were grown as described in (**a**) with 1 μCi of [^{3}H]-thymidine for 12 h. The cell replication rate was determined by measuring [^{3}H]-thymidine incorporation. The results are presented as the mean ± standard error **{AUTHOR—OK? (was "average" and "SE")}** of three independent experiments performed in quadruplicate. **c**, Blocking the Akt pathway significantly induced apoptosis in DN-Akt 3T3 cells. The cells were grown in 5% serum plus 20 μM etoposide, and the percentage of cells in apoptosis was measured by fluorescence-activated cell sorting as described previously[4]. The results are presented as the mean ± standard error **{AUTHOR—OK? (was "average" and "SE")}** of three independent experiments. **d**, Blocking the Akt pathway induced etoposide-mediated apoptosis in DN-Akt 3T3 cells, as measured by the DNA fragmentation assay[4]. The cells were grown in 100-mm plates as described in (**a**) with 20 μM etoposide. **e**,**f**, Tumours induced by DN-Akt 3T3 cells were much more sensitive to etoposide treatment. *HER-2/neu* 3T3 cells (**e**) and DN-Akt 3T3 cells (**f**) were inoculated subcutaneously in nude mice. One group of five mice from each cell line was treated with intravenous injections of etoposide on days 5 and 7 after the inoculation (solid symbols). The control groups (open symbols) were injected with the same volume of saline. The tumour volume was measured every two days, and the data represent the mean ± standard deviation **{AUTHOR—OK? (was "SD")}** from five mice.

cells to DNA-damaging drugs in our model system. This system consists of NIH3T3 cells, *HER-2/neu* 3T3 cells (*HER-2/neu*-transformed NIH3T3 cells) and DN-Akt 3T3 cells (*HER-2/neu* 3T3 cells transfected with *DN-Akt*, a mutant *Akt* gene that produces a protein with no kinase activity)[4]. As expected, the *HER-2/neu* 3T3 cells were not affected by the DNA-damaging agent etoposide (Fig. 1). The Akt pathway is known to be constitutively activated in *HER-2/neu* 3T3 cells[4] and, when this pathway was blocked by DN-Akt in DN-Akt 3T3 cells, the cells grew much more slowly (Fig. 1a). When the DNA synthesis rate was determined by measuring [^{3}H]-thymidine incorporation, *HER-2/neu* 3T3 cells did not synthesize more DNA than the parental NIH3T3 cells or DN-Akt 3T3 cells (Fig. 1b).

The net cell growth rate depends on a fine balance between the cell proliferation rate and the cell death rate, and so we next examined whether apoptosis contributes to the difference in growth in these cells. There was significant difference in apoptosis among these cells as measured by fluorescence-activated cell sorting (FACS) analysis (Fig. 1c). The DN-Akt 3T3 cells underwent more apoptosis than did the *HER-2/neu* 3T3 cells after treatment with etoposide. The apoptosis in these cells was further confirmed by the DNA fragmentation in these cells (Fig. 1d). Therefore, the reduction in cell growth in DN-Akt 3T3 cells after treatment with etoposide was probably due to the increased apoptosis in these cells. Similarly, we treated these cells with another DNA-damaging agent, doxorubicin, and found that DN-Akt 3T3 cells were also more sensitive to apoptosis than *HER-2/neu* 3T3 cells (data not shown).

To examine whether the phenomenon can be observed *in vivo*, we inoculated *HER-2/neu* 3T3 cells and DN-Akt 3T3 cells into nude mice to generate mammary tumours, and tested the susceptibility of these tumours to DNA-damaging agents. Tumours from *HER-2/neu* 3T3 cells were not sensitive to etoposide (Fig. 1e), supporting the notion that *HER-2/neu*-overexpressing tumours are resistant to chemotherapeutic drugs, including DNA-damaging agents[3,30]. However, when the Akt pathway was blocked by DN-Akt, the tumours induced by DN-Akt 3T3 cells became very sensitive to etoposide (Fig. 1f). The dramatic tumour shrinkage after etoposide treatment is probably due to sensitization to apoptosis because massive apoptosis in these tumours was detected by the TUNEL assay (data not shown). Together, our results indicate that the Akt pathway is required for *HER-2/neu*-mediated drug resistance to DNA-damaging agents. Blocking this pathway sensitized *HER-2/neu*-overexpressing cells to DNA-damaging agents both *in vitro* and *in vivo*.

Activation of Akt-induced p53 ubiquitination and degradation. Because etoposide inhibits DNA topoisomerase II and causes DNA breaks, and because p53 is a sensor for damaged DNA and is induced by DNA damage[21,32], we tested whether p53 is involved in this sensitization effect mediated by the blockage of Akt pathway. We treated two pairs of cell lines ($p53^{-/-}$ and wild-type MEF cells, and p53-mutated MDA-MB453 and its DN-Akt/MDA453 transfectants) with etoposide. The p53-wild-type MEF cells were very sensitive to etoposide treatment (Fig. 2a). Blocking the Akt pathway using Wortmannin alone did not affect cell survival, but it dramatically enhanced the sensitization to etoposide treatment in p53-wild-type MEF cells (Fig. 2a). However, no effect was observed in the $p53^{-/-}$ cells (Fig. 2a). Similarly, blocking the Akt pathway with DN-Akt in p53-mutated DN-Akt/MDA453 cells could not sensitize the cells to etoposide treatment (Fig. 2b), although they did respond to TNF-induced apoptosis, as shown previously[4]. When similar experiments were performed in $p53^{-/-}$ and p53-wild-type cells, and apoptosis was measured by FACS analysis, we observed the same results (data not shown). Thus, these results suggest that p53 is crucial for etoposide-induced apoptosis.

To examine whether blockage of the Akt pathway would further sensitize p53-wild-type cells to etoposide-induced apoptosis in other cell types, we treated another two p53-wild-type (HBL-100 and MCF-7) and two p53-mutated (MDA-MB231 and SKOV3-ip1) cancer cell lines with etoposide. We found that the two p53-wild-

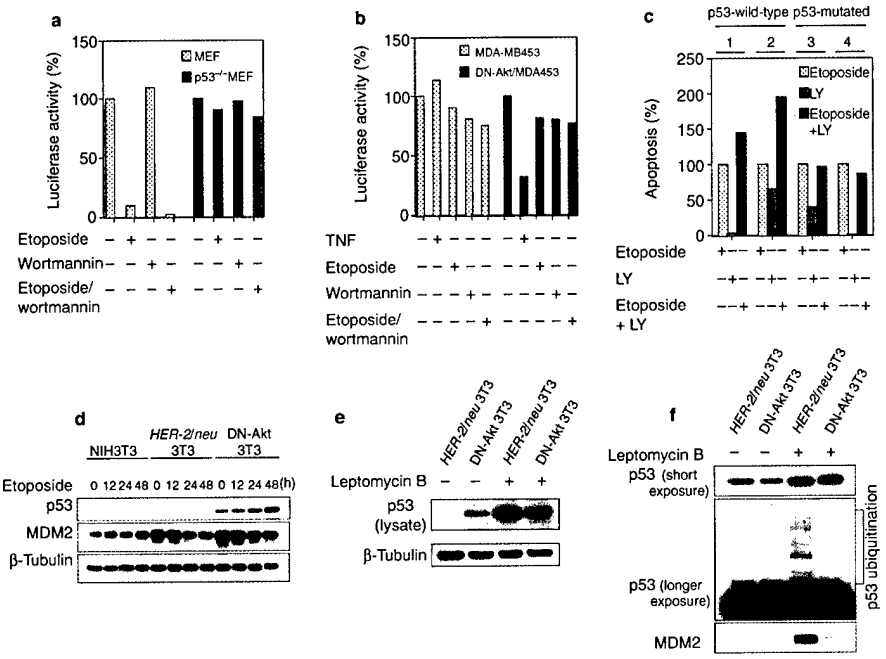

Figure 2 **Activation of Akt induced p53 ubiquitination and degradation. a**, The presence of p53 protein was required for sensitization to etoposide treatment. The p53-wild-type MEF and $p53^{-/-}$ MEF cells were transfected with 2 μg of a plasmid that contains actin-promoter-driven luciferase. After 12 h of transfection, cells were treated with 20 μM etoposide, 100 nM Wortmannin or 100 nM of Wortmannin plus 20 μM of etoposide and incubated for another 36 h. The cell lysates were prepared and the luciferase activity in each sample was measured. The sensitization to etoposide treatment was presented by the luciferase activity (mean ± standard error **{AUTHOR—OK? (was "SE")}** in two separate experiments) over the control without any treatment. **b**, Blockage of the Akt pathway did not sensitize p53-mutated MDA-MB453 cells to etoposide treatment. Breast cancer cell line MDA-MB453 and its DN-Akt transfectants (DN-Akt/MDA453) cells were transfected with 2 μg of a plasmid that contains actin-promoter-driven luciferase. After 12 h of transfection, the cells were treated with 40 ng ml^{-1} of tumour necrosis factor **{AUTHOR—OK?}**, 20 μM etoposide, 100 nM of Wortmannin or 100 nM of Wortmannin plus 20 μM of etoposide as described in (**a**). The cell lysates were prepared and luciferase activity in each sample was measured. The sensitization to etoposide treatment was presented by the luciferase activity (mean ± standard error **{AUTHOR—OK? (was "SE")}** in two separate experiments) over the control without any treatment. **c**, Blocking the Akt pathway sensitized p53-wild-type but not p53-mutated cells to etoposide-induced apoptosis. Two p53-wild-type (HBL-100 and MCF-7) and two p53-mutated (MDA-MB231 and SKOV3-ip1) cancer cell lines were treated with 20 μM etoposide in the presence or absence of the PI(3)K inhibitors LY294002 (50 μM) and Wortmannin (0.1 μM) (LY). Apoptotic cells in each sample were measured by flow cytometry using a fluorescence-activated cell sorter with propidium iodide staining. The two p53-wild-type cell lines were treated with etoposide and/or PI(3)K inhibitors for 24 h and harvested for analysis. Because few cells were found undergoing apoptosis in 24 h for the two p53-mutated cell lines, these two lines were treated with etoposide for 48 h to observe the apoptotic effect mediated by VP16. Apoptotic cells treated with etoposide alone in each sample were defined as 100%. Cell lines 1–4 were HBL-100, MCF-7, MDA-MB231 and SKOV3-ip1, respectively. **d**, Blockage of the Akt pathway led to production of p53. NIH3T3, *HER-2/neu* 3T3 and DN-Akt 3T3 cells were treated with 20 μM etoposide, for the indicated times. Whole cell lysates (50 μg) were prepared and subjected to western blot analyses with antibodies specific for p53 (Ab-7), MDM2 and β-tubulin. **e**, Blocking nuclear export induced p53 stabilization in *HER-2/neu* 3T3 and DN-Akt 3T3 cells. *HER-2/neu* 3T3 and DN-Akt 3T3 cells were treated with 5 ng ml^{-1} leptomycin B for 7 h or not treated, and the p53 and β-tubulin levels were analysed by western blotting. **f**, Activation of Akt induced the ubiquitination of p53 and increased the binding of MDM2 to p53. *HER-2/neu* 3T3 and DN-Akt 3T3 cells were treated with leptomycin B as in (**e**) or left alone. The cell lysates (1.2 mg of *HER-2/neu* 3T3 protein and 0.4 mg of DN-Akt 3T3 protein) were immunoprecipitated with monoclonal anti-p53 antibody (Ab-1) and the precipitates were then subjected to western blotting with polyclonal anti-p53 antibody (Ab-7) for a short (10 sec) or a longer (1 min) exposure. The same membrane was used again for western blotting against MDM2.

type cell lines (HBL-100 and MCF-7) were more sensitive to apoptosis (as measured by FACS analysis) when the Akt pathway was blocked by a PI(3)K inhibitor (LY294002). However, in the two p53-mutated cells, the PI(3)K inhibitor could not sensitize the cells to etoposide-induced apoptosis (Fig. 2c). Similar results were also obtained when we used another PI(3)K inhibitor, Wortmannin (data not shown). Therefore, sensitization to etoposide-induced apoptosis occurred only in p53-wild-type cells, not in p53-mutated or $p53^{-/-}$ cells, suggesting the involvement of p53 and Akt in the etoposide-induced apoptosis.

We next examined the expression of p53 in NIH3T3, *HER-2/neu* 3T3 and DN-Akt 3T3 cells before and after treatment with etoposide. We did not observe the induction of p53 expression in NIH3T3 and *HER-2/neu* 3T3 cells, but did find time-dependent induction of p53 in DN-Akt 3T3 cells (Fig. 2d). Surprisingly, basal expression of p53 in DN-Akt 3T3 cells was dramatically elevated (Fig. 2d), indicating that blocking the Akt pathway increases the p53 protein level. The half-life of p53 is ~15 min, and p53 is present at low levels in cells and only increases in response to physiological stress such as DNA damage[21,32]. The p53 protein level increases as a result of post-translational modification, which stabilizes the protein and is largely controlled by MDM2. MDM2 can bind to p53, promote its ubiquitination and shuttle it to cytoplasm, where it is subsequently degraded by the proteasome. Leptomycin

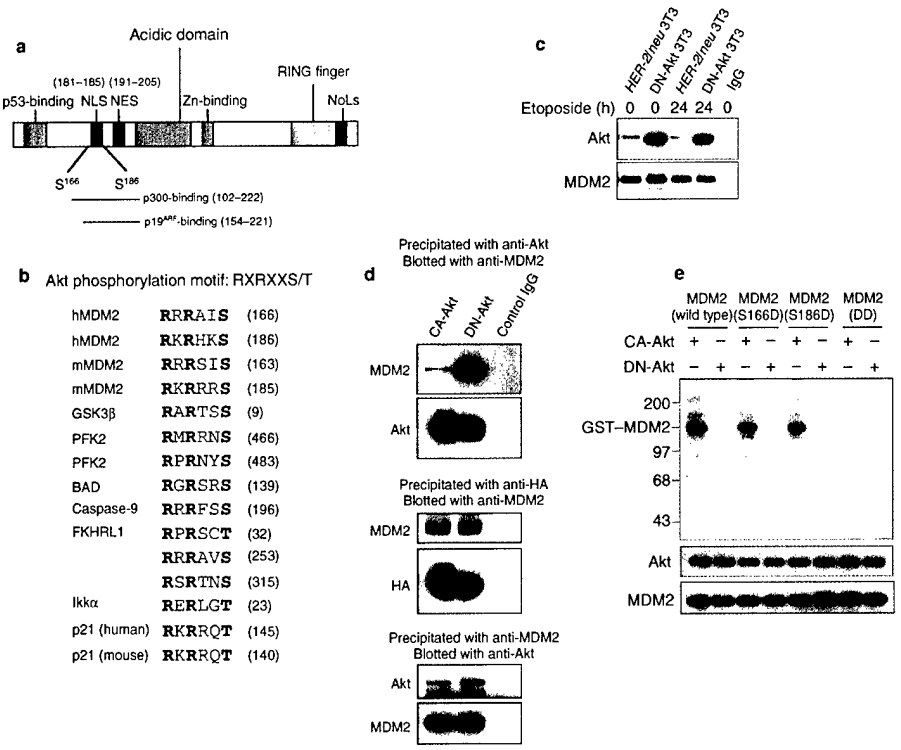

Figure 3 **Akt interacts with MDM2 and phosphorylates Ser166 and Ser186.** **a**, Structure of the MDM2 protein, showing the positions of the nuclear-localization signal (NLS), the nuclear-export signal (NES) and domains that interact with p300 and $p19^{ARF}$. **b**, The consensus Akt phosphorylation motif is highlighted. Sequences of MDM2 and other known Akt substrates are shown for comparison. **c**, Immunoprecipitation of endogenous MDM2 and detection of endogenous Akt. Endogenous MDM2 was immunoprecipitated from 1000 μg of *HER-2* 3T3 or DN-Akt 3T3 cell lysates with an MDM2-specific antibody (SMP14) or control IgG. After transfer to a nitrocellulose membrane, endogenous Akt was detected with an Akt-specific antibody (Upstate Biotechnology). **d**, Association between Akt and MDM2. HA-tagged DN-Akt or CA-Akt (10 μg) was transfected into 293T cells by the calcium phosphate method. The cells were lysed in RIPA buffer after 48 h and Akt was immunoprecipitated with anti-Akt (Upstate Biotechnology) or ani-HA (HA.11; Babco) antibody. After transfer to a nitrocellulose membrane, MDM2 was detected with MDM2-specific antibody. Alternatively, the cell lysates were immunoprecipitated with MDM2-specific antibody. After transfer to a nitrocellulose membrane, the bound Akt was detected with Akt-specific antibody. **e**, Akt phosphorylated MDM2 at Ser166 and Ser186. HA-tagged CA-Akt or DN-Akt (20 μg) was transiently transfected into 293T cells as described in Methods. After 48 h of incubation, CA-Akt and DN-Akt were immunopricipitated with an anti-HA antibody and incubated with 5 μg of either GST–wild-type MDM2 or GST–mutant MDM2 (S166D, S186D and S166,186DD) in a kinase buffer containing 5 μCi of [γ^{32}P]ATP for 30 min at 30 °C. The kinase reaction was stopped by the addition of SDS-PAGE buffer and the samples were assayed by autoradiography. The lower two panels show western blots for Akt and GST–MDM2 used in the phosphorylation reaction, detected with antibodies against Akt and MDM2, respectively.

B (LMB), a cytotoxin produced by streptomycetes, can block nuclear export and stabilize p53 accumulated in the nucleus of LMB-treated cells[33]. To rule out the possibility that the lack of expression of p53 in *HER-2/neu* 3T3 cells was due to a genetic defect in these cells, we treated the cells with LMB. The concentration of p53 increased in *HER-2/neu* 3T3 cells {AUTHOR—OK? Was *HER-3/neu*} after treatment with LMB (Fig. 2e). These results indicate that the absence of p53 in *HER-2/neu* 3T3 cells was not caused by a genetic defect but rather by the destabilization of p53 in these cells.

To compare the ubiquitination of p53 in these cells, we used more cell lysate from *HER-2/neu* 3T3 cells than from DN-Akt 3T3 cells to produce equal amounts of immunoprecipitated p53 before and after treatment with LMB. Surprisingly, there was dramatically more ubiquitination of p53 in *HER-2/neu* 3T3 cells than in DN-Akt 3T3 cells (Fig. 2f). The difference in ubiquitination of p53 was not due to a difference in p53 levels, because nearly equal amounts of p53 were immunoprecipitated from *HER-2/neu* 3T3 and DN-Akt 3T3 cells (short exposure in Fig. 2f). When the same membrane was analysed by western blot using MDM2-specific antibody, we found more MDM2 binding to p53 immunoprecipitated from *HER-2/neu* 3T3 cells (Fig. 2f). Thus, the increased ubiquitination of p53 observed in *HER-2/neu* 3T3 cells resulted largely from increased binding of MDM2 to p53 in these cells (Fig. 2f). These results indicate that the activation of Akt could increase the binding of MDM2 to p53 and induce the ubiquitination of p53. Blocking the Akt pathway stabilized the p53 protein by inhibiting the binding of MDM2 to p53, consequently suppressing the ubiquitination and degradation of p53.

Akt interacts with and phosphorylates MDM2. The inability of MDM2 to bind and ubiquitinate p53 in DN-Akt 3T3 cells seems to be responsible for the cell's increased p53 level and sensitization to DNA-damaging agents. Recently, MDM2 was found to be phosphorylated by ATM {AUTHOR—what is this?}, disrupting its binding to p53 and leading to the stabilization of p53 (ref. 34). We noticed that there were two potential Akt phosphorylation sites

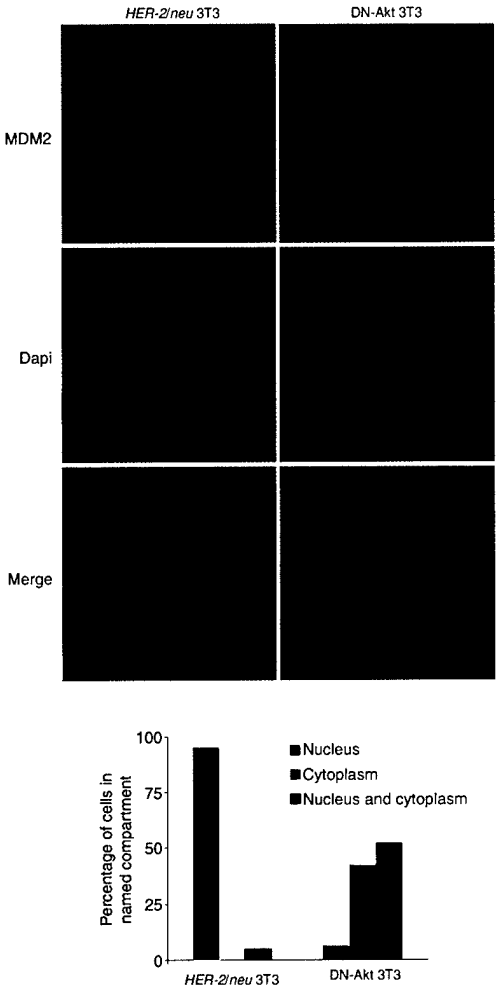

Figure 4 **Akt affects the cellular localization of endogenous MDM2. a,** ~2×10⁴ *HER-2* 3T3 and DN-Akt 3T3 cells were plated into chamber slides for 16 h. After fixation of the samples in 4% paraformaldehyde for 1 h and permeabilization with 0.2% Triton X-100 for 30 min, the cellular localization of MDM2 was detected using a monoclonal antibody against MDM2 (SMP14). After extensive washing in PBS, the samples were further incubated with Texas-Red-conjugated goat anti-mouse IgG plus Dapi and examined under a fluorescent microscope (Zeiss). **b,** Quantification of subcellular MDM2 staining. The subcellular localizations of MDM2 in *HER-2* 3T3 and DN-Akt 3T3 cells were assessed in 100 cells in several different views. The graph shows the percentages of cells with the indicated MDM2 subcellular localization.

(Ser166 and Ser186) in the MDM2 protein (Fig. 3a), and that these two sites were highly conserved across species (Fig. 3b). These two potential phosphorylation sites were in the regions crucial for MDM2 nuclear import and export, and required for p300 and $p19^{ARF}$ binding. To determine whether Akt interacts with and phosphorylates MDM2, and so regulates its function, we performed immunoprecipitation experiments to detect the association between Akt and MDM2. In an immunoprecipitation of endogenous MDM2, we detected the presence of endogenous Akt (Fig. 3c) {AUTHOR—this sentence was not clear. Is my version correct?}. The binding of Akt to MDM2 was increased in DN-Akt 3T3 cells (Fig. 3c). Treatment with etoposide does not seem to affect the interaction between MDM2 and Akt. We also transfected 293T cells with haemagglutinin (HA)-tagged {AUTHOR—OK?} constitutively active Akt (CA-Akt) or DN-Akt. After immunoprecipitating Akt or HA, we detected MDM2, and vice versa (Fig. 3d), indicating that these two molecules are associated. MDM2 seems to associate more strongly with DN-Akt than with CA-Akt.

To examine whether Akt can phosphorylate MDM2, we transfected CA-Akt and DN-Akt into 293T cells and immunoprecipitated Akt from cell lysates. After incubation with glutathione-*S*-transferase (GST)–MDM2 {AUTHOR—OK?} (wild-type), GST–MDM2 (S166D), GST–MDM2 (S186D) or GST–MDM2 (S166, 186DD) in a kinase reaction mixture, we found that Akt phosphorylated MDM2 at Ser166 and Ser186 with equal efficiency, whereas DN-Akt could not (Fig. 3e). When both Ser166 and Ser186 were mutated to aspartic acid, CA-Akt could not phosphorylate this double mutant of MDM2, suggesting that Ser166 and Ser186 in MDM2 were specific for Akt phosphorylation (Fig. 3e). The fact that no phosphorylation was observed in the double mutant of MDM2 (S166,186DD) was not due to the lack of Akt kinase or MDM2 proteins, because nearly equal amount of kinase and protein were used (Fig. 3e, bottom two panels). These results indicate that Akt physically interacted with MDM2 and phosphorylated MDM2 at Ser166 and Ser186.

Akt induces nuclear localization of MDM2. Because the Akt phosphorylation sites in MDM2 are close to the NLS and NES, we examined whether the activation of Akt affects the cellular localization of MDM2. We performed immunofluorescence staining to analyse the cellular localization of endogenous MDM2 in *HER-2/neu* 3T3 and DN-Akt 3T3 cells. In the parental *HER-2/neu* 3T3 cells, MDM2 was usually found in the nucleus (95% of cells), with little in the cytoplasm (Fig. 4a). However, in DN-Akt-transfected cells, MDM2 was either in the cytoplasm (42%) or distributed evenly between the cytoplasm and nucleus (50%) (Fig. 4b). MDM2 has been previously reported to localize mainly to the nucleus. The inability of MDM2 to localize to the nucleus in DN-Akt 3T3 cells suggests that phosphorylation of MDM2 by Akt is required for its nuclear translocation. Blocking the Akt pathway in DN-Akt 3T3 cells would inhibit the nuclear import of MDM2, and so result in the stabilization of p53.

We next tested whether the phosphorylation of MDM2 by Akt affects the cellular localization of MDM2. We transfected $p53^{-/-}$ and $MDM2^{-/-}$ MEF cells with CA-Akt or DN-Akt together with wild-type or mutant MDM2 and examined the cellular localization of MDM2 by immunofluorescence analysis. As shown in Fig. 5, wild-type MDM2 was found predominantly in the nucleus in the presence of CA-Akt but was localized to both the cytoplasm and the nucleus when DN-Akt was introduced. Mutants of MDM2 (S166D, S186D or S166,186DD, in which serine 166 or/and serine 186 were replaced with aspartic acid to mimic the phosphorylation of MDM2 by Akt) were found predominantly in the nucleus even in the presence of DN-Akt. These results strongly indicate that Ser166 and Ser186 of MDM2 are crucial in determining the cellular localization of MDM2, and that the phosphorylation of Ser166 and Ser186 of MDM2 by Akt resulted in the nuclear localization of MDM2. Taken together, our results indicate that Akt can interact with MDM2 and phosphorylate the Ser166 and Ser186 residues in MDM2, leading to the nuclear localization of MDM2.

These results establish the regulation of MDM2 by the HER-2/*neu*–Akt pathway in cell culture. To examine whether this phenomenon also existed in tumour tissues, we compared the levels of activated (phosphorylated) Akt and the cellular localization of MDM2 in 33 cases of human breast tumours that are either HER-2/*neu* and Akt positive or HER-2/*neu* and Akt negative by immunostaining. In 21 HER-2/*neu* and Akt positive breast tumour tissues, we found that MDM2 was mainly present in the nucleus. By

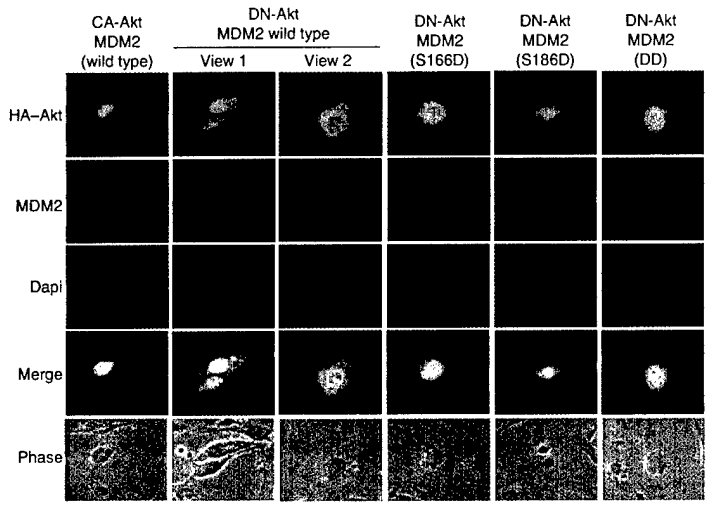

Figure 5 **Akt affects the subcellular localization of MDM2.** A 1:1 ratio of CA-Akt or DN-Akt (2 μg) and the wild-type or mutant MDM2 (2 μg) were transfected into $p53^{-/-}$ and $MDM2^{-/-}$ MEF cells. After 36 h of incubation, the cells were trypsinized and plated into chamber slides for another 12 h. After fixation, the cellular locations of CA-Akt, DN-Akt and MDM2 were detected using antibodies against HA (HA.11, Babco) and MDM2 (Ab-2, Oncogene Research). After extensive washing in PBS, the samples were further incubated with Texas-Red-conjugated goat anti-mouse IgG and FITC-conjugated goat anti-rabbit IgG plus Dapi, and examined under a fluorescent microscope (Zeiss). When wild-type MDM2 was transfected with CA-Akt, MDM2 were found in the nucleus in ~95% of the transfected cells. However, when MDM2 was transfected with DN-Akt, 25% of the transfected cells had MDM2 staining only in the nucleus and 75% of the cells had MDM2 staining in both the nucleus and the cytoplasm. When the S166D, S186D or S166,186DD mutant of MDM2 was transfected with DN-Akt, ~90% of the cells had MDM2 staining only in the nucleus.

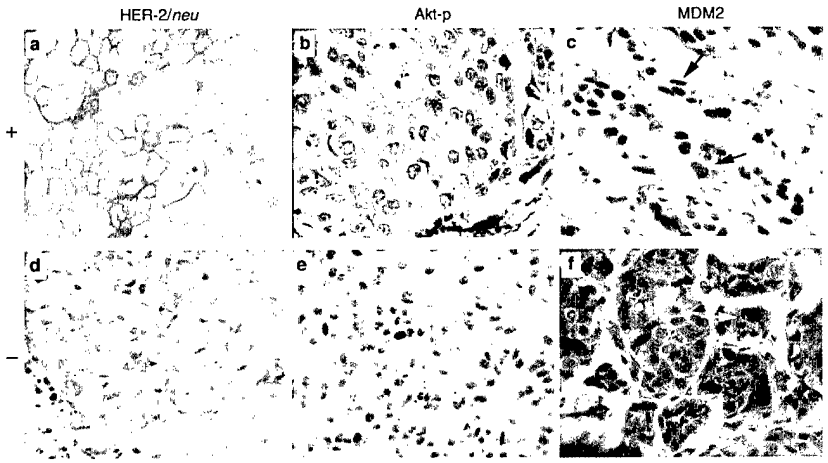

Figure 6 **HER-2/*neu* activates Akt and induces nuclear localization of MDM2 in breast tumour tissues.** Tissue sections from the HER-2/*neu*- and Akt-positive adenocarcinomas (**a–c**) and HER-2/*neu*- and Akt-negative adenocarcinomas (**d–f**) were stained with antibodies specific to HER-2/*neu* (**a** and **d**), phosphorylated Akt (**b** and **e**), MDM2 (**c** and **f**) or normal rabbit serum (data not shown). The immunostaining was visualized with peroxidase-conjugated secondary antibody. The arrows indicate the nuclear and cytoplasmic localization of MDM2 in **c** and **f**, respectively.

contrast, in all 12 HER-2/*neu* and Akt negative breast tumour tissues examined, MDM2 was localized in both the nucleus and cytoplasm (Fig. 6). Similar results were obtained when we used another MDM2 antibody (NCL-MDM2; Novocastra Laboratory {AUTHOR—location?}) (data not shown). The subcellular localization of MDM2 and the activation of Akt were significantly correlated based on the analysis using Fisher's exact test (Table 1). Thus, the correlation between these two molecules in primary tumour samples was consistent with our *in vitro* data from cell lines and transfection studies (Figs 4, 5). The tumour staining data agree

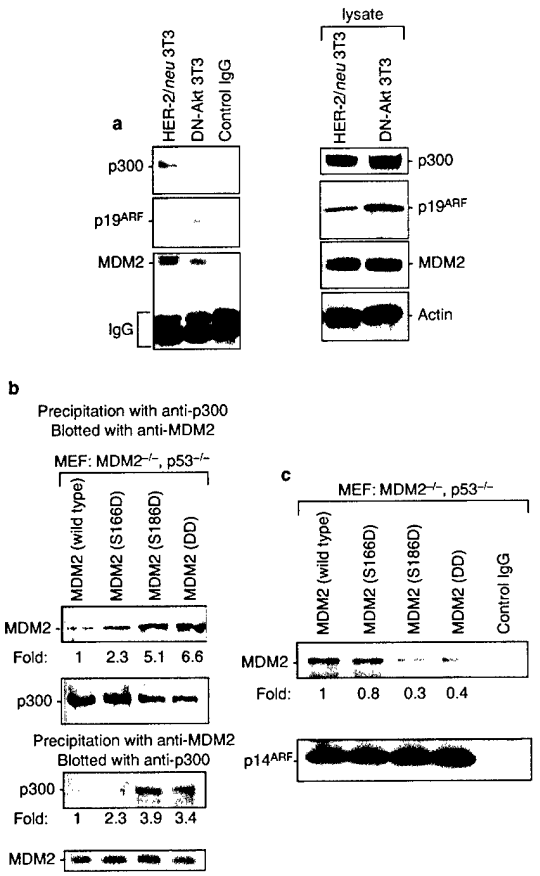

Figure 7 **Phosphorylated MDM2 binds differently to p300 and p19^{ARF}. a**, MDM2 from *HER-2/neu* 3T3 and DN-Akt 3T3 cells had different binding affinities to p300 and p19^{ARF}. Cell lysates from *HER-2/neu* 3T3 or DN-Akt 3T3 cells were immunoprecipitated with monoclonal anti-MDM2 antibody (SMP14) and the precipitates were then subjected to western blotting analysis for the binding of p300 and p19^{ARF}. The same lysates were used for western blotting analysis for the expression of p300, p19^{ARF}, MDM2 and actin. **b**, Preferential binding of the phosphorylated form of MDM2 to p300. The wild-type and phosphorylated forms of MDM2 mutants were transfected into p53$^{-/-}$ and MDM2$^{-/-}$ cells. After 48 h of culture, the cell lysates were immunoprecipitated with anti-p300 and anti-MDM2 antibodies, and the precipitates were subjected to western blot analysis for the binding of MDM2 and p300. The intensities of the bands were quantified by densitometry using NIHimage and are shown under the western blots. **c**, Weaker binding of phosphorylated form of MDM2 to p14^{ARF}. The wild-type and phosphorylated forms of MDM2 were transfected with p14^{ARF} into p53$^{-/-}$ and MDM2$^{-/-}$ cells. After 48 h of culture, the cell lysates were immunoprecipitated with antibodies against p14^{ARF} and the precipitates were subjected to western blot analysis for the binding of MDM2. The intensity of the bands was quantified by densitometry using NIHimage and are shown under the western blot.

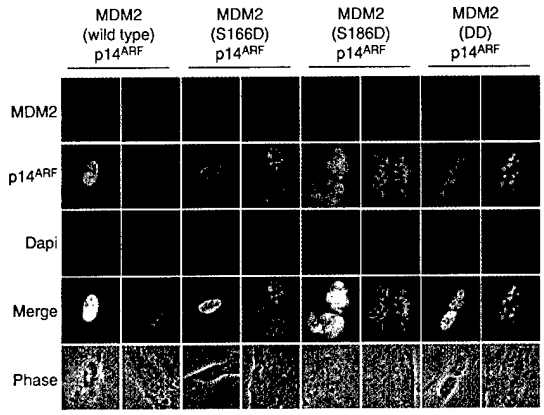

Figure 8 **Nuclear localization of wild-type and mutant MDM2 is not affected by the presence of p14^{ARF}.** A 1:1 ratio of wild-type or mutant MDM2 (2 μg) and p14^{ARF} (2 μg) were transfected into p53$^{-/-}$ and MDM2$^{-/-}$ MEF cells. After 36 h of incubation, the cells were trypsinized and plated into chamber slides for another 12 h. After fixation, the cellular localization of MDM2 and p14^{ARF} were detected by using antibodies against MDM2 (SMP14) and p14^{ARF} (Ab-1; Neomarkers **{AUTHOR—location?}**), respectively. After extensive washing in PBS, the samples were further incubated with Texas-Red-conjugated goat anti-mouse IgG and FITC-conjugated goat anti-rabbit plus Dapi and examined under a fluorescent microscope (Zeiss). For each transfection staining, cells producing both MDM2 and p14^{ARF} are shown on the left-hand side and cells expressed only p14^{ARF} are shown on the right-hand side.

with the observation in cell culture and further strengthen the hypothesis that overexpression of *HER-2/neu* can regulate the cellular distribution of MDM2 via the activation of Akt.

Phosphorylated MDM2 induces preferential binding to p300 but not to p19^{ARF}. Because the Akt phosphorylation sites Ser166 and Ser186 in MDM2 were also within the region required for MDM2 to bind p300 and p19^{ARF}, we investigated whether the loss of p53 ubiquitination in DN-Akt 3T3 cells was due to changed binding of MDM2 to p300 and p19^{ARF}. We immunoprecipitated MDM2 from *HER-2/neu* 3T3 or DN-Akt 3T3 cells and examined MDM2's association with p300 and p19^{ARF}. We found that MDM2 from *HER-2/neu* 3T3 cells bound much more strongly to p300 than in DN-Akt 3T3 cells (Fig. 7a). However, p19^{ARF} binding to MDM2 was dramatically lower in *HER-2/neu* 3T3 cells than in DN-Akt 3T3 cells (Fig. 7a). The differences in p300 and p19^{ARF} bound by MDM2 between *HER-2/neu* 3T3 and DN-Akt 3T3 cells were not due to a difference in protein levels, because equal amounts of MDM2 were immunoprecipitated from these cells and the expression of p300 and p19^{ARF} in these cells was the same (Fig. 7A). We also transfected wild-type MDM2 and phosphorylated forms of MDM2 (S166D, S186D or S166,186DD) into MDM2$^{-/-}$ and p53$^{-/-}$ cells, and analysed the binding of these phosphorylated forms of MDM2 with p300. As seen in Fig. 7b, after immunoprecipitating the p300, the association of phosphorylated forms of MDM2 to p300 was stronger than that of wild-type MDM2. Similarly, when we immunoprecipitated the wild-type and phosphorylated forms of MDM2, we found that more p300 bound to the phosphorylated forms of MDM2. These results indicate that Akt can phosphorylate MDM2 at Ser166 and Ser186, and that the phosphorylated MDM2 has a stronger binding with p300 than the unphosphorylated form {AUTHOR—OK?}.

We also transfected wild-type MDM2 and phosphorylated forms of MDM2 (S166D, S186D or S166,186DD) into MDM2$^{-/-}$ and p53$^{-/-}$ cells with p14^{ARF}, and analysed the binding of these phosphorylated forms of MDM2 with p14^{ARF}. As shown in Fig. 7c, slightly less of the associated phosphorylated forms of MDM2 were present after immunoprecipitating the p14^{ARF} than of wild-type MDM2. The ARF protein binds directly to MDM2 to block p53 degradation by inhibiting the ubiquitin E3 ligase activity associat-

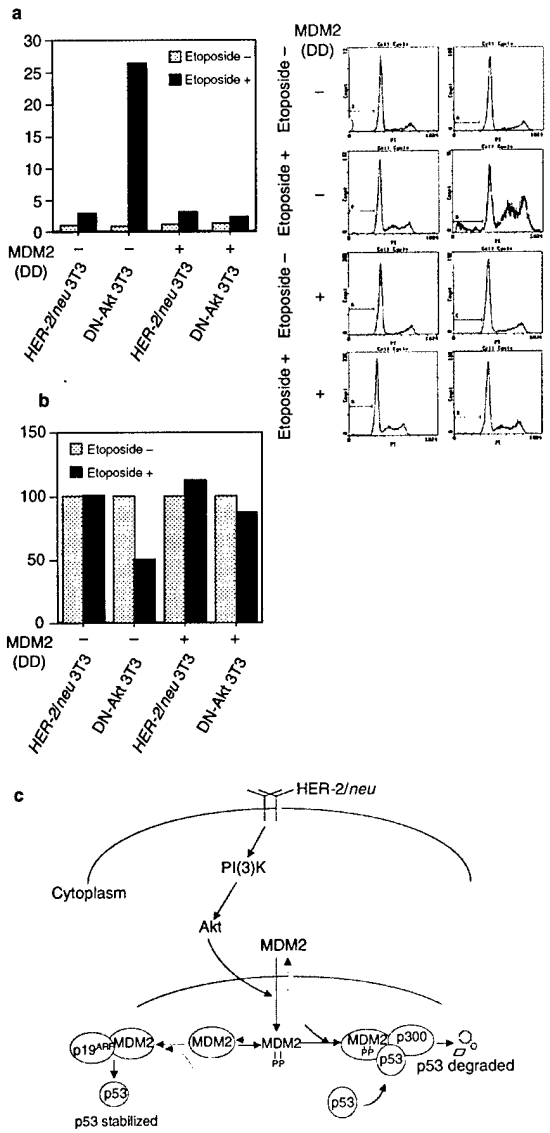

Figure 9 **Sensitization of etoposide-induced apoptosis by DN-Akt can be suppressed by nuclear MDM2 (S166,186DD). a**, Nuclear MDM2 blocks DN-Akt-mediated sensitization to etoposide-induced apoptosis. *HER-2/neu* 3T3 and DN-Akt 3T3 cells were transfected with a mimic phosphorylation form of MDM2 (S166,186DD) and then treated with etoposide (20 μM) for 48 h or left untreated. The apoptotic cells in each sample were analyaed by fluorescence-activated cell sorting as described in Fig. 1c. **b**, *HER-2/neu* 3T3 and DN-Akt 3T3 cells were transfected with MDM2 S166,186DD and a luciferase plasmid. After 12 h of transfection, cells were treated with 20 μM etoposide and incubated for another 36 h. The cell lysates were prepared and the luciferase activity in each sample was measured. **c**, A model showing how HER-2/*neu* induces the nuclear localization and altered binding of MDM2 with p300 and $p19^{ARF}$ via Akt.

ed with MDM2 (ref. 27) and by sequestering MDM2 in nucleoli to prevent its export to the cytoplasm. There is persuasive evidence that ARF can inhibit the ubiquitin ligase activity of MDM2 *in vitro*, but exactly how ARF affects the nucleus–cytoplasm shuttling of MDM2 remains a matter of debate[15]. Current models propose that ARF function depends on its ability to sequester MDM2 in the nucleolus[15]. We examined whether the nucleoplasmic or nucleolus localization was different in wild-type and mutant MDM2 proteins. We transfected $p53^{-/-}$ and $MDM2^{-/-}$ MEF cells with $p14^{ARF}$ together with wild-type or mutants of MDM2, and examined the nucleus and nucleolus localization of MDM2 by immunofluorescence analysis. As shown in Fig. 8, wild-type MDM2 was found uniformly in nucleoplasm in the presence or absence of $p14^{ARF}$. In the absence of MDM2, $p14^{ARF}$ was predominantly found in the nucleolus. Interestingly, MDM2 protein was not sequestered in nucleolus by $p14^{ARF}$, but rather brought the $p14^{ARF}$ out of nucleolus to the nucleoplasm. Our findings agree with recent studies that demonstrated that $p14^{ARF}$ can inhibit MDM2 function without relocalizing MDM2 to the nucleolus[35]. The cellular and subnuclear localization of MDM2 and ARF might depend on dynamic or static complex formation among MDM2, p53, ARF, Akt and some other proteins. Future systemic studies are required to clarify these issues. Taken together, our results indicate that Akt phosphorylates MDM2 at Ser166 and Ser186, and that the phosphorylated MDM2, which has a stronger binding with p300 and weaker association with $p19^{ARF}$, increases its nuclear localization and so leads to p53 degradation.

Sensitization of etoposide-induced apoptosis by DN-Akt can be suppressed by nuclear MDM2 (S166,186DD). As shown in Fig. 2, blocking the Akt pathway stabilizes p53 and therefore sensitizes cells to etoposide-induced apoptosis. MDM2 protein from the nuclear MDM2 mutant is found in the nucleus and is constitutively active without phosphorylation by Akt (Figs 5, 7). Thus, the nuclear MDM2 mutant should be able to suppress etoposide-induced apoptosis to which the cell is sensitized by blocking the Akt pathway. To address this issue, we transfected *HER-2/neu* 3T3 and DN-Akt 3T3 cells with the double mutant of MDM2 (S166,186DD) and measured their apoptosis after treatment with etoposide. As shown in Fig. 9a, the *HER-2/neu* 3T3 cells are resistant to etoposide-induced apoptosis, but blockage of the Akt pathway in DN-Akt 3T3 cells sensitizes the cells to apoptosis. However, when the S166,186DD mutant of MDM2 was transfected into DN-Akt 3T3 cells, the apoptosis induced by etoposide in DN-Akt 3T3 cells was dramatically suppressed. Similar results were obtained when we transfected with a luciferase reporter gene along with the double mutant of MDM2 and measured the luciferase activity after treatment with etoposide (Fig. 9b). Together, our results indicate that the sensitization of etoposide-induced apoptosis by the blockage of Akt pathway can be suppressed by a nuclear MDM2 mutant (S166,186DD).

Discussion

The tumour suppresser p53 plays a crucial role in controlling cell proliferation and apoptosis. In unstressed cells, p53 is latent and is maintained at low levels by targeted degradation mediated by its negative regulator, MDM2 (refs 14,17,20). The ability of MDM2 to ubiquitinate and degrade p53 depends on its E3 ligase activity and its ability to shuttle between the nucleus and the cytoplasm, which is regulated by its NLS and NES[20]. The transcriptional coactivator p300 has also been shown to form a ternary complex with MDM2 to facilitate the degradation of p53 (refs 22,23). However, the activity of MDM2 is negatively regulated by $p19^{ARF}$, which inhibits its E3 ligase activity[15]. Because the regions that control MDM2 cellular localization and binding with p300 and $p19^{ARF}$ overlap, the issues of when, where and how MDM2 is localized and interacts with functionally opposite molecules such as p300 and $p19^{ARF}$ are crucial to understanding the function of MDM2 and its regulation of p53.

In this study, we have identified a novel mechanism that controls the cellular localization of MDM2 and its interaction with p300 and $p19^{ARF}$. We show that Akt physically associates with

Table 1 Immunoreactivity of MDM2, Akt-p and HER-2/*neu* in surgical specimens of breast cancer

	HER-2/*neu* and Akt-p staining		
MDM2 staining	Negative (n = 12)	Positive (n = 21)	Total
Mainly nucleus	1 (3%)	16 (49%)	17 (51%)
Mainly cytoplasm	11 (33%)	5 (15%)	16 (49%)
Total	12 (36%)	21 (64%)	33 (100%)

The 33 surgical specimens of breast cancer were stained for *HER-2/neu*, phosphorylation form of Akt and MDM2 as shownin Fig. 6. The expression patterns of these three molecules in the samples from each patient was determined and summarized. Correlation of subcellular localization of MDM2 and the expression of phosphorylation of Akt was analysed by using Fisher's exact test ($P > 0.001$). A P value of less than 0.05 was set as the criterion for statistical significance.

MDM2 and phosphorylates it at Ser166 and Ser186. Our results, together with previous findings[14–29], lead us to propose a model for how Akt affects the ubiquitination and degradation of p53 (Fig. 9c). Akt phosphorylates MDM2 and induces its nuclear translocation, and the phosphorylated MDM2 binds p300 but not to $p19^{ARF}$. Binding to p300 provides a platform to facilitate the assembly of the phosphorylated MDM2–p300–p53 complex and leads to the ubiquitination and degradation of p53. Blocking the Akt pathway with DN-Akt prevents the nuclear translocation of MDM2. The unphosphorylated MDM2 in the nucleus only binds $p19^{ARF}$ but not to p300. Binding to $p19^{ARF}$ inhibits MDM2's ubiquitin E3 ligase activity and consequently stabilizes the p53 protein.

It is evident that many of the tumours with wild-type p53 show defects in the ability to induce a p53 response. Overexpression of MDM2 is found in many types of tumour[16]. In addition, $p19^{ARF}$, the negative regulator of MDM2, is also often deleted or mutated in a wide spectrum of cancers[15]. Thus, overexpression of *MDM2* and the lack of $p19^{ARF}$ in cancers greatly increase the ability of MDM2 to degrade p53, and cause a problem for gene therapy using p53 constructs. Overexpression of *HER-2/neu* is known to activate the Akt pathway and to confer resistance to the apoptosis induced by many chemotherupeutic drugs[30]. We show that blocking the Akt pathway inhibits the nuclear translocation of MDM2 and the binding of p300, and allows the binding of $p19^{ARF}$, so sensitizing the *HER-2/neu*-overexpressing cells to DNA-damaging agents. Our results might open an avenue for developing novel anticancer therapies for *HER-2/neu*-overexpressing or Akt-activating cancers.

Methods

Materials.

The DNA-damaging agents etoposide and doxorubicin were purchased from Calbiochem. The DNA dye Dapi and anti-HA (12C5) antibody were purchased from Roche Molecular Biochemicals. The anti-p53 antibodies Ab-1 and Ab-7, the anti-MDM2 antibodies SMP 14 and 2A10, and the anti-p300 and anti-$p19^{ARF}$ antibodies were obtained from Oncogene Research and Santa Cruz Biotechnology, respectively. {AUTHOR—which antibody was from which company?} Female nude mice (*Nu/Nu*, 6 weeks old) were purchased from Harland {AUTHOR—location?}.

MDM2 constructs.

A *Bam*HI and an *Eco*RI site were generated near the start and termination codons, respectively, in human *MDM2* by PCR and subcloned into the expression vector pcDNA3. Site-directed mutagenesis was performed as described previously[6]. Ser166 and Ser186 in MDM2 were replaced by Asp by using the following primers: for S166D, 5′-CTAGAAGGAGAGCAATTGATGAGACAGAAGAAAATTC-3′; and for S186D, 5′-GAAAACGCCACAAAGATGATAGTATTTCCC-3′. The sequences of the wild-type and mutant *MDM2* constructs were verified by automated sequencing. To generate wild-type and mutant *MDM2* GST-tagged bacterial expression constructs, the same fragments containing the wild-type and mutant *MDM2* were subcloned into the bacterial expression vector pGEX4T-3 (Pharmacia). Expression of wild-type and mutant MDM2 proteins was induced in *Escherichia coli* strain BL21 and purified by glutathione–Sepharose chromatography (Pharmacia).

Cell culture.

NIH3T3, *HER-2/neu* 3T3, p53 and MDM2-deficient MEF, and 293T cells were cultured in Dulbecco's modified Eagle's medium/F12 medium supplemented with 10% foetal bovine serum. The DN-Akt transfectants of *HER-2/neu* 3T3 cells were grown under the same conditions except that 200 μg ml^{-1} G418 was added to the culture medium[4]. The 293T cells were transfected by the calcium phosphate technique and p53- and MDM2-deficient cells by the liposome method.

In vitro growth rate analysis.

The *in vitro* growth rates of the cell lines were assessed by the MTT assay as described previously[5].

[^{3}H]-Thymidine incorporation assay.

The proliferation rates of the cell lines were analysed by measuring [^{3}H]-thymidine incorporation as described previously[5].

In vivo tumour growth analysis.

The nude mice were randomly divided into four groups of five mice each. Two groups of mice were subcutaneously inoculated with 5×10^5 cells of *HER-2/neu* 3T3 or DN-Akt 3T3 cells per mouse. The tumour taking rate {AUTHOR—what is this?} was 100% for both cell types. On days 5 and 7 after inoculation, one group from each cell line was giving two intravenous injections of etoposide (20 mg kg^{-1}) via the tail vein. Another two groups of mice were injected with the same volume of normal saline (the solvent for etoposide) as a control. The tumour volume (V) was measured every 2 days and calculated as $V = 0.5 \times ab^2$, where a and b are the longest and shortest diameters of the tumour, respectively. {AUTHOR—do you mean $a\times(b^2)$ or $(a\times b)^2$?} The experiment was stopped 15 days after inoculation and the results were tested statistically using two-sided log-rank analysis.

In vitro kinase assay.

293T cells (2×10^5) were transfected with 20 μg of HA-tagged CA-Akt or DN-Akt. 48 h after transfection, Akt was immunoprecipitated from cell extracts and incubated with 5 μg of purified GST–MDM2 (wild-type or mutant) in the presence of 5 μCi of [γ-^{32}P]ATP and 50 mM cold ATP in a kinase buffer for 30 min at 30 °C as described previously[5]. The reaction products were resolved by SDS-PAGE and the ^{32}P-labelled proteins were visualized by autoradiography.

Immunoprecipitation and immunoblotting.

Cells were washed twice with PBS and scraped into 500 μl of lysis buffer {AUTHOR—what is this?}. After a brief sonication, the lysate was centrifuged at 14,000 *g* for 5 min at 4 °C to remove the insoluble cell debris. Immunoprecipitation and immunoblotting were performed as described previously[4].

In situ immunofluorescent staining.

~2×10^4 cells of *HER-2/neu* 3T3 or DN-Akt 3T3 cells were plated into chamber slides for 16 h. After fixation in 4% paraformaldehyde for 1 h and permeabilization with 0.2% Triton X-100 for 30 min, the cellular localization of MDM2 was determined by using a monoclonal antibody against MDM2 (SMP14) diluted 1:1000. After extensive washing in PBS, the samples were further incubated with Texas-Red-conjugated goat anti-mouse IgG (diluted 1:500) plus Dapi (0.1 μg ml^{-1}) for 1 h. After extensive washing, the samples were examined under a fluorescent microscope (Zeiss). Nonspecific reaction of the secondary antibody was ruled out by the absence of fluorescence under the microscope.

RECEIVED 2 MAY 2001; REVISED 24 JULY 2001; ACCEPTED 3 SEPTEMBER 2001; PUBLISHED 2001.

1. Slamon, D. J. *et al.* (1987) Human breast cancer: correlation of relapse and survival with amplification of the *HER-2/neu* oncogene. *Science* **235**, 177–182.
2. Slamon, D. J. *et al.* (1989) Studies of the *HER-2/neu* proto-oncogene in human breast and ovarian cancer. *Science* **244**, 707–712.
3. Yu, D. & Hung, M.-C. (2000) in *DNA Alterations in Cancer* (eds Ehrlich, M. and Natick, M.A.), Ch. 21 {AUTHOR—OK? Please also give the publisher's name.}
4. Zhou, B. P. *et al.* (2000) *HER-2/neu* blocks tumor necrosis factor-induced apoptosis via the Akt/NF-κB pathways. *J. Biol. Chem.* **275**, 8027–8031.
5. Zhou, B. P. *et al.* (2001) Cytoplasmic localization of $p21^{Cip1/WAF1}$ by Akt-induced phosphorylation in *HER-2/neu*-overexpressing cells. *Nature Cell. Biol.* **3**, 245–252.
6. Downward, J. (1998) Mechanisms and consequences of activation of protein kinase B/Akt. *Curr. Opin. Cell Biol.* **10**, 262–267.
7. Datta, S. R., Brunet, A. & Greenberg, M. E. (1999) Cellular survival: a play in three Akts. *Genes Dev.* **13**, 2905–2927.
8. Peso, L. D., Gonzalez-Garcia, M., Page, C., Herrera, R. & Nunez, G. (1997) Interleukin-3-induced phosphorylation of bad through the protein kinase Akt. *Science* **278**, 687–689.
9. Cardone, M. H. *et al.* (1998) Regulation of cell death protease caspase-9 by phosphorylation. *Science* **282**, 1318–1321.
10. Brunet, A. *et al.* (1999) Akt promotes cell survival by phosphorylating and inhibiting a forkhead transcription factor. *Cell* **96**, 857–868.
11. Kops, G. J. P. L. *et al.* (1999) Direct control of the forkhead transcription factor AFX by protein kinase B. *Nature* **398**, 630–634.
12. Ozes, O. N. *et al.* (1999) NF-κB activation by tumor necrosis factor requires the Akt serine–threonine kinase. *Nature* **401**, 82–85.
13. Sabbatini, P. & McCormick, F. (1999) Phosphoinositide 3-OH kinase (PI3K) and PKB/Akt delay the onset of p53-mediated, transcriptionally dependent apoptosis. *J. Biol. Chem.* **274**, 24263–24269.
14. Woods, D. B. & Vousden, K. H. (2001) Regulation of p53 function. *Exp. Cell Res.* **264**, 56–66.
15. Sherr, C. J. & Weber, J. D. (2000) The ARF/p53 pathway. *Cur. Opin. Genet. Dev.* **10**, 94–99.
16. Vousden, K. H. (2000) p53: death star. *Cell* **103**, 691–694.
17. Vogelstein, B., Lane, D. & Levine, A. J. (2000) Surfing the p53 network. *Nature* **408**, 307–310.

18. Hupp, T. R., Lane, D. P. & Ball, K. L. (2000) Strategies for manipulating the p53 pathway in the treatment of human cancer. *Biochem. J.* **352**, 1–17.
19. Caspari, T. (2000) Checkpoints: how to activate p53. *Curr. Biol.* **10**, R315–R317.
20. Momand, J., Wu, H.-H. & Dasgupta, G. (2000) MDM2—master regulator of the p53 tumor suppressor protein. *Gene* **242**, 15–29.
21. Colman, M. S., Afshari, C. A. & Barrett, J. C. (2000) Regulation of p53 stability and activity in response to genotoxic stress. *Mut. Res.* **462**, 179–188.
22. Lill, N. L., Grossman, S. R., Ginsberg, D., DeCaprio, J. & Livingston, D. M. (1997) Binding and modulation of p53 by p300/CBP coactivators. *Nature* **387**, 823–827.
23. Grossman, S. R. *et al.* (1998) p300/MDM2 complexes participate in MDM2-mediated p53 degradation. *Mol. Cell* **2**, 405–415.
24. Pomerantz, J. *et al.* (1998) The *Ink4a* tumor suppressor gene product, $p19^{Arf}$, interacts with MDM2 and nuetralizes MDM2's inhibition of p53. *Cell* **92**, 713–723.
25. Zhang, Y., Xiong, Y. & Yarbrough, W. G. (1998) ARF promotes MDM2 degradation and stabilizes p53: *ARF-Ink4a* locus deletion impairs both Rb and p53 tumor suppressor pathways. *Cell* **92**, 725–734.
26. Sherr, C. J. (2000) The Pezcoller lecture: cancer cell cycles revisited. *Cancer Res.* **60**, 3689–3695.
27. Honda, R. & Yasuda, H. (1999) Association of p19ARF with MDM2 inhibits ubiquitin ligase activity of MDM2 for tumor suppressor p53. *EMBO J.* **18**, 22–27.
28. Weber, J. D., Taylor, L. J., Roussel, M. F., Sherr, C. J. & Bar-Sagi, D. (1999) Nucleolar Arf sequesters Mdm2 and activates p53. *Nature Cell Biol.* **1**, 20–26.
29. Zhang, Y. & Xiong, Y. (1999) Mutation in human ARF exon 2 disrupt its nucleolar localization and impair its ability to block nuclear export of MDM2 and p53. *Mol. Cell* **3**, 579–591.
30. Yu, D. & Hung, M.-C. (2000) Role of erbB2 in breast cancer chemosensitivity. *BioEssays* **22**, 673–680.
31. Tsai, C. M. *et al.* (1995) Enhanced chemoresistance by elevation of p185 levels in *HER-2/neu*-transfected human lung cancer cells. *J. Natl. Cancer Inst.* **87**, 682–684.
32. Zhou, B.-B. S. & Elledge, S. J. (2000) The DNA damage response: putting checkings in perspective. *Nature* **408**, 433–439.
33. Freedman, D. A. & Levine, A. J. (1998) Nuclear export is required for degradation of endogenous p53 by MDM2 and human papillomavirus E6. *Mol. Cell. Biol.* **18**, 7288–7293.
34. Khosravi, R. *et al.* (1999) Rapid ATM-dependent phosphorylation of MDM2 precedes p53 accumulation in response to DNA damage. *Proc. Natl. Acad. Sci. USA* **96**, 14973–14977.
35. Lianos, S., Clark, P. A., Rowe, J. & Peters, G. (2001) Stabilization of p53 by $p14^{ARF}$ without relocation of MDM2 to the nucleolus. *Nature Cell. Biol.* **3**, 445–452.

ACKNOWLEDGEMENTS
We thank G. Lozano for kindly providing $p53^{-/-}$ MEF and $p53^{-/-}$, $MDM2^{-/-}$ MEF cells. This work was supported by grants CA 58880, CA 77858 and CA 78633, by a SPORE grant in ovarian cancer (CA 83639) (to M.-C. H.), and by the Nellie Connally Breast Cancer Research Fund at the M. D. Anderson Cancer Center (to M.-C. H.). B. P. Z. and Y. L. are recipients of postdoctoral fellowships from US Department of Defense Breast Cancer Research Training Grant DAMD17-99-1-9264 and US Department of Defense Breast Cancer Research Program (DAMD17-01-0300), respectively.
Correspondence and requests for materials should be addressed to M.-C. H.

Advances in Brief

Adenovirus 5 Early Region 1A Does Not Induce Expression of the Ewing Sarcoma Fusion Product EWS-FLI1 in Breast and Ovarian Cancer Cell Lines[1]

Funda Meric, Yong Liao, Wei-Ping Lee, Raphael E. Pollock, and Mien-Chie Hung[2]

Departments of Surgical Oncology [F. M., R. E. P., M-C. H.] and Molecular and Cellular Oncology [Y. L., W-P. L., M-C. H.], The University of Texas M. D. Anderson Cancer Center, Houston, Texas 77030

Abstract

The adenovirus 5 early region 1A (E1A) can function as a tumor suppressor gene and is being used in clinical trials as a therapeutic agent for advanced breast, ovarian, and head and neck cancer. Recently, there has been a dispute regarding whether transfection with the *E1A* gene can induce expression of the Ewing sarcoma oncogenic fusion transcript EWS-FLI1 (Sanchez-Prieto *et al.*, Nat. Med., *5:* 1076–1079, 1999; Melot and Delattre, Nat. Med., *5:* 1331, 1999; Kovar *et al.*, Cancer Res., *60:* 1557–1560, 2000). In an effort to settle the controversy, we tested several stable E1A transfectants of cell lines MDA-MB-231, MCF-7, MDA-MB-435 (breast cancer), SKOV3-ip1 (ovarian cancer), and PC-3 (prostate cancer), as well as parental and vector-transfected controls, HEK 293 cells, and RD-ES (Ewing sarcoma) cells, for the EWS-FLI1 fusion product. The EWS-FLI1 transcript could not be identified with reverse transcription-PCR in any of the 13 E1A-transfected cell lines analyzed. Furthermore, the EWS-FLI1 fusion protein could not be detected by Western blot analysis in E1A-transfected cell lines. These results suggest that E1A transfection does not necessarily lead to expression of the oncogenic EWS-FLI1 fusion transcript. Thus, the potential induction of this gene rearrangement by E1A gene therapy is unlikely to be clinically significant in the treatment of advanced malignant disease.

Received 4/25/00; revised 7/17/00; accepted 7/17/00.

The costs of publication of this article were defrayed in part by the payment of page charges. This article must therefore be hereby marked *advertisement* in accordance with 18 U.S.C. Section 1734 solely to indicate this fact.

[1] Supported by NIH Grant R0-1 CA58880 and Ovarian SPORE CA 83639 (to M-C. H.). F. M. and Y. L. are supported by NIH Grant 5T32CA09599-11 (to F. M.) and the University of Texas M. D. Anderson Breast Cancer Research Program (Y. L.). F. M. and Y. L. contributed equally to this work.

[2] To whom requests for reprints should be addressed, at Department of Molecular and Cellular Oncology, Box 108, The University of Texas M. D. Anderson Cancer Center, 1515 Holcombe Boulevard, Houston, TX 77030. Phone: (713) 792-3668; Fax: (713) 794-0209; E-mail: mhung@mdacc.org.

Introduction

The adenovirus E1A[3] can function as a tumor suppressor gene (reviewed in Refs. 1 and 2). E1A can down-regulate the *erb*B2 oncogene to suppress tumorigenesis, and it can suppress metastasis by additional molecular mechanisms. Furthermore, E1A sensitizes cells to cellular host immune responses and to apoptotic agents such as anticancer drugs, tumor necrosis factor, and irradiation. The E1A protein is under active investigation as a potential therapeutic agent. A Phase I clinical trial of *EIA* gene therapy for patients with advanced breast and ovarian cancer has recently been completed (3), and Phase II trials are currently in progress.

Ewing sarcoma 11;22 translocation results in a rearrangement between EWS on chromosome 22q12 and FLI1 on chromosome 11q24, leading to a chimeric transcription factor, EWS-FLI1, that has potent transforming activity (4). Sanchez-Prieto *et al.* (5) have recently reported that the adenoviral E1A protein has the ability to induce expression of the EWS-FLI1 fusion protein. However, data from the studies of Melot and Delattre (6) and Kovar *et al.* (7, 8) do not support this concept. De Alava *et al.* (9) have suggested that this discrepancy may be due to the types of subclones and assay conditions used. Because of this controversy and because the induction of the oncogenic EWS-FLI1 transcript by E1A transfection could have significant consequences in the setting of *E1A* gene therapy, we tested stable, E1A-transfected breast and ovarian cancer cell lines for the expression of the EWS-FLI1 fusion product.

Materials and Methods

Cell Cultures, Plasmids, and Retroviral Vectors. The human breast cancer cell lines MCF-7 and MDA-MB-231 and ovarian cancer cell line SKOV3-ip1 with and without transfection of E1A were routinely maintained in DMEM (Life Technologies, Inc.) supplemented with 10% fetal bovine serum (Sigma, St. Louis, MO). Stable cells expressing wild-type E1A or 12S E1A were established by transfecting cells with the E1A-expressing plasmid pE1A-neo or 12S E1A plasmid DNA plus pSV-neo. The transfectants were grown under the same conditions as controls, except that G418 was added to the culture medium. Expression of E1A was verified by Western blot analysis using monoclonal anti-E1A antibody M58 (Oncogene Science, Cambridge, MA). The human Ewing sarcoma cell line RD-ES was obtained from American Type Culture Collection (Manassas, VA) and maintained in RPMI 1640 supplemented with 15% fetal bovine serum.

[3] The abbreviations used are: E1A, 5 early region 1A; RT-PCR, reverse transcription-PCR; GAPDH, glyceraldehyde-3-phosphate dehydrogenase.

RT-PCR. Total RNA was isolated from cell lines with Trizol reagent (Life Technologies, Inc.). One μg of total RNA was reverse transcribed after priming with oligo(dT) primers using the Superscript Preamplification System (Life Technologies, Inc.). The single-stranded cDNA was amplified by 40 PCR cycles of denaturing at 94°C for 45 s, annealing at 58°C for 1 min, and extension at 72°C for 30 s. RNA from the Ewing sarcoma cell line RD-ES was used as a positive control. Primers described previously by Sanchez-Prieto *et al.* (5) were used: (*a*) 11.3 FLI1, 5′-ACTCCCCGTTGTTGGTCCCCTCC-3′; (*b*) 22.3 EWS, 5′-TCCTACAGCCAAGCTCCAAGTC-3′; (*c*) 11.4 FLI1, 5′-CAGGTGATACAGCTGGCG-3′; and (*d*) 22.4 EWS, 5′-CCAACAGAGCAGCAGCTAC-3′. Nested PCR was first performed using the 11.3 FLI1 and 22.3 EWS primers and then performed using the 11.4 FLI1 and 22.4 EWS primers. Expression of the E1A transcripts was confirmed by RT-PCR using primers 5′-GCGCCTGCTATCCTGAGA-3′ and 5′-CCGCTCGAGTTATGGCCTGGGGCGTTTACA-3′. Amplification of GAPDH was performed as a control using primers 5′-AAGGTGAAGGTCGGAGTCAAC-3′ and 5′-CATGAGTCCTTCCACGATACC-3′. Amplified products were analyzed by 1.5% agarose gel electrophoresis.

Cloning and Sequencing. RT-PCR using the 11.4 FLI1 and 22.4 EWS primers (Fig. 1*a*) and the 11.3 FLI1 and 22.4 EWS primers was performed with RNA from the E1A-transfected MDA-MB-231 cell line and the RD-ES sarcoma cell line. The amplified products were subcloned into the pCR 2.1 vector (Invitrogen, Carlsbad, CA). The recombinant plasmids were sequenced and compared with GenBank database sequences from the National Center for Biotechnology Information using the BLAST algorithm.

Southern Blot Analysis. RT-PCR products were separated by 1.5% agarose gel electrophoresis and blotted onto nylon membranes (GeneScreen; New England Nuclear Life Science Products, Boston, MA). The membranes were hybridized in RapidHyb buffer (Amersham Corp, Arlington Heights, IL) and probed with the RD-ES 11.4 FLI1/22.4 EWS fusion fragment subcloned previously. The probe was randomly labeled with [^{32}P]dCTP using the random primers DNA labeling system (Life Technologies, Inc.). The 22.4 EWS oligonucleotide was radiolabeled with [γ-^{32}P]ATP with T4 polynucleotide kinase (New England Biolabs, Beverly, MA).

Western Blot Analysis. Western blot analysis of whole cell extracts was accomplished using standard procedures. Briefly, cells were collected and lysed with buffer A [20 mM Tris (pH 7.5), 10% glycerol, 1% Triton X-100, 0.15 M NaCl, 1 mM β-mercaptoethanol, 1 mM Na_3VO_4, 1 mM aprotinin, 1 mM phenylmethylsulfonyl fluoride, and 0.1% (w/v) bromphenol blue]. Samples were heated at 100°C for 5 min and separated by 10% SDS-PAGE. After transfer, membranes were incubated with either the M73 antibody (Oncogene Sciences, Cambridge, MA) against E1A protein, the antibody against FLI1 (PharMingen, San Diego, CA), or the N-18 antibody against EWS (Santa Cruz Biotechnology, Santa Cruz, CA). As a loading control, membranes were also incubated with an antibody against actin (Boehringer Mannheim, Indianapolis, IN).

Results

E1A-transfected Cell Lines Do Not Express the EWS-FLI1 Fusion Transcript. Stable E1A transfectant of breast cancer cell line MDA-MB-231 (231-E1A), parental and vector-transfected controls, E1A-expressing HEK 293 cells, and RD-ES (Ewing sarcoma) cell lines were tested for the EWS-FLI1 fusion transcript. When RT-PCR was performed using the primer set 11.4 FLI1 and 22.4 EWS (see "Materials and Methods"), two products (130 and 250 bp) were detected in the 231-EIA and HEK 293 cells but not in the parental MDA-MB-231 or vector-transfected control cells. However, the EWS-FLI1 probe did not hybridize to these products on Southern hybridization (Fig. 1*a*), indicating that they do not represent the EWS-FLI1 fusion transcript. The same membrane was then hybridized with the radiolabeled 22.4 EWS oligonucleotide primer, confirming transfer of the DNA visualized on the ethidium-stained gel to the membrane. The amplification pattern obtained when nested PCR was performed using the external 11.3 FLI1 and 22.3 EWS primers followed by the nested internal 11.4 FLI1 and 22.4 EWS primers was the same as that obtained after PCR with 11.4 FLI1 and 22.4 EWS (described above; data not shown). RT-PCR with the 11.3 FLI1 and 22.4 EWS primers amplified a 340-bp product in 231-EIA cells but not in the parental cells or vector controls. Again, Southern blotting was negative for these samples (Fig. 1*b*). Thus, although E1A is able to induce transcripts that can be amplified by primers derived from the *EWS* and *FLI1* genes, the E1A-induced transcripts do not represent the EWS-FLI1 fusion transcripts.

To confirm and understand what may cause false positive RT-PCR results in E1A-transfected cell lines, the RT-PCR products amplified from the 231-E1A cell line and the Ewing sarcoma line RD-ES were subcloned and sequenced. Sequencing of the RT-PCR product amplified from the RD-ES cell line with the 11.4 FLI1 and 22.4 EWS primers confirmed that it was the EWS-FLI1 fusion product (Fig. 1*c*). In contrast, sequencing of the bands from the 231-EIA transfectants (Fig. 1*a*) proved them to be unrelated genes; the 250-bp band corresponded to the mRNA for the human KIAA0477 protein, and the 130-bp band corresponded to the mRNA for the human KIAA0339 protein. The RT-PCR products were homologous to the fusion product EWS-FLI1 only in the primer sequences, with 100% homology in the 3′ ends of the 11.4 FLI1 and 22.4 EWS primers (Fig. 1*d*). The sequence of the 340-bp product amplified from the 231-E1A cell line with 11.3 FLI1 and 22.4 EWS primers (Fig. 1*b*) corresponded to that of human ribosomal protein L4 mRNA. Again, there was sequence homology between the 22.4 EWS primer and the L4 sequence (the L4 3′-untranslated region sequence annealing to the 11.3 primer is not available in GenBank for comparison). Thus, all of the amplified RT-PCR products in cell lines other than RD-ES, represented false positive results. These genes may be up-regulated with E1A transfection and deserve further study.

A total of 13 stable E1A transfectant E1A cell lines including MDA-MB-231, MCF-7, MDA-MB-435 (breast cancer), SKOV3-ip1 (ovarian cancer), and PC-3 (prostate cancer) were tested for the EWS-FLI1 fusion transcript using RT-PCR. The actual EWS-FLI1 fusion transcript could not be detected in any

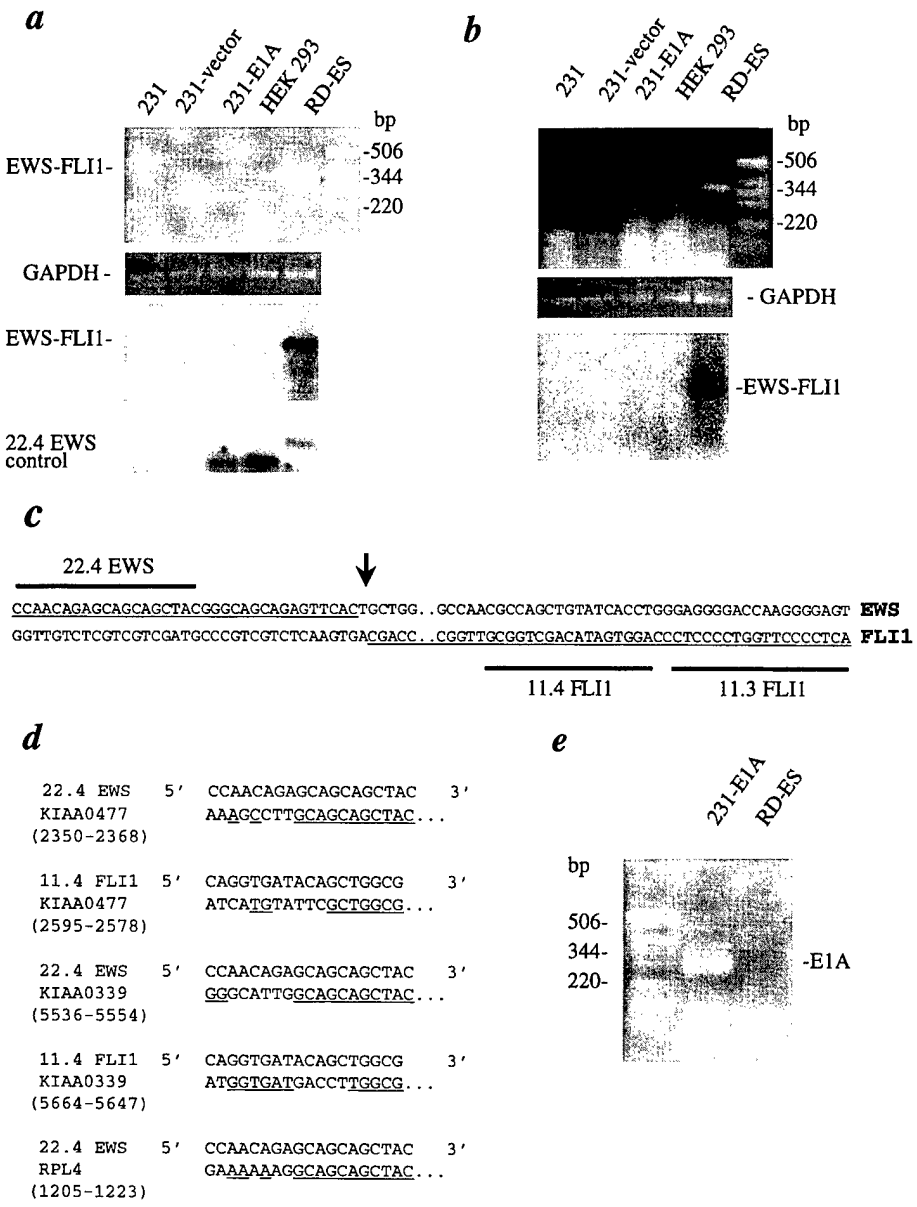

Fig. 1 RT-PCR and Southern blot hybridization of the fusion transcript EWS-FLI1. *a, top panel,* RT-PCR analysis with primers 11.4 FLI1 and 22.4 EWS on total RNA from MDA-MB-231 cells, vector-transfected 231 cells, E1A-transfected 231 cells, HEK 293 cells, and RD-ES Ewing sarcoma cells. *Upper middle panel,* RT-PCR of the same cell lines with primers for GAPDH as a control. *Lower middle panel,* Southern blot analysis of RT-PCR products shown in the *upper panel* with a EWS-FLI1 fusion product probe. *Bottom panel,* Southern blot of the same membrane with radiolabeled 22.4 EWS oligonucleotide probe as transfer control. *b, top panel,* RT-PCR analysis of RNA from the same cell lines with primers 11.3 FLI1 and 22.4 EWS. *Middle panel,* RT-PCR for GAPDH as a control. *Bottom panel,* Southern hybridization of RT-PCR products with the EWS-FLI1 probe. *c*, sequence corresponding to the EWS-FLI1 fusion transcript detected in the RD-ES cell line. The *arrow* indicates the breakpoint. RT-PCR using primers 22.4 EWS and 11.4 FLI1 would be expected to give a 344-bp product as detected in *a*; primers 22.4 EWS and 11.3 FLI1 would be expected to give a 363-bp product as detected in *b*. *d*, sequence alignment of the 22.4 EWS and 11.4 FLI1 primers with human mRNA for KIAA0477 protein (dbj, AB007946.1), human mRNA for KIAA0339 gene (dbj, AB002337), and human ribosomal protein L4 (RPL) mRNA (ref, NM 000986.1). Sequences with homology to the primers are *underlined.* The *numbers* in *parentheses* in the figure represent the location on the reference sequence used for alignment. *e*, RT-PCR analysis of RNA from 231-E1A and RD-ES cell lines with E1A primers.

of the cell lines except the RD-ES Ewing sarcoma line. RT-PCR was also performed with primers specific for E1A, and expression of the E1A transcript was confirmed in the E1A-transfected cell lines (data not shown). The E1A transcript was not detected by RT-PCR in the RD-ES Ewing sarcoma cell line (Fig. 1*e*). Thus, our study does not support the proposal by Sanchez-Prieta *et al.* (5) that E1A induces the Ewing tumor fusion transcript EWS-FLI1.

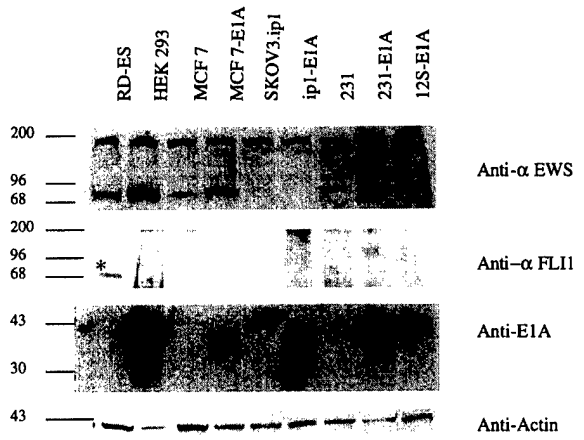

Fig. 2 Western blot analysis of EWS-FLI1 fusion proteins in different E1A stable cell lines. *Top panel*, Western blot analysis of cell lysates with an antibody against EWS protein. *Upper middle panel*, Western blot detection of the expression of EWS-FLI-1 fusion protein with a monoclonal antibody against FLI1. *Lower middle panel*, the same membrane was stripped and reprobed with a monoclonal antibody against E1A. *Bottom panel*, a parallel membrane was probed with a monoclonal anti-actin antibody.

E1A-transfected Cells Do Not Express the EWS-FLI1 Fusion Protein. The human breast cancer cell lines MCF-7 and MDA-MB-231 and ovarian cancer cell line SKOV3-ip1 were studied with and without transfection of E1A to detect the EWS-FLI1 fusion protein. The Ewing sarcoma cell line RD-ES was used as a control for the EWS-FLI-1 fusion protein. After immunoblotting with a polyclonal antibody against EWS; a M_r ~68,000 band was detected in all cell lines studied except SKOV3-ip1 and E1A-transfected ip1-E1A cells (Fig. 2). When a monoclonal anti-FLI1 antibody was used; the expected M_r 68,000 EWS-FLI1 fusion protein was detected only in the RD-ES cell line (Fig. 2). No fusion proteins were detected in any of the E1A-transfected cell lines. Immunoblotting with E1A antibodies confirmed the expression of the E1A protein in the E1A-transfected cell lines. The results indicate that the commercially available anti-EWS polyclonal antibody (Santa Cruz Biotechnology) also cross-reacts with a cellular protein about the same size (M_r ~68,000) as the EWS-FLI1 fusion protein. However, the M_r ~68,000 band detected in HEK 293, MCF-7, MCF-7-E1A, 231, and 231-E1A cells is not the EWS-FLI1 protein because it cannot be detected by the anti-FLI1 antibody.

Discussion

Sanchez-Prieto *et al.* (5) recently reported that adenovirus E1A induces the Ewing sarcoma fusion transcript EWS-FLI1. However, data from the studies of Melot and Delattre (6) and from Kovar *et al.* (7, 8) do not support this hypothesis. In our study, we examined 13 different cell lines stably transfected with E1A to test the hypothesis that expression of the *E1A* gene in human cells could elicit the specific fusion transcript EWS-FLI1. We were unable to find any evidence of the EWS-FLI1 fusion transcript or fusion protein in these E1A transfectants. Interestingly, we found expression of unrelated genes that may be induced by E1A, which can be detected under the PCR assay conditions used (Fig. 1, *a* and *b*). In addition, the commercially available anti-EWS antibody also cross-reacts with a cellular protein about the same size (M_r ~68,000) as the EWS-FLI1 fusion protein (Fig. 2). It is worthwhile to mention that the anti-EWS antibody-detected M_r ~68,000 protein is slightly enhanced in the E1A-transfected cells (compare MCF-7 with MCF7-E1A and 231 with 231-E1A). This phenomenon, without careful further examination with anti-FLI1 antibody to exclude its identity as the EWS-FLI1 fusion protein, could be easily but mistakenly used to support the notion that E1A induces the EWS-FLI1 fusion protein.

Adenovirus E1A has been examined in preclinical studies and found to be a promising therapeutic agent because of its abilities to suppress tumorigenesis and metastasis and to sensitize cells to apoptosis induced by cytotoxic agents (10–16). Extensive preclinical safety studies have been performed with E1A (17–19), and a Phase I clinical trial of *E1A* gene therapy for patients with advanced breast and ovarian cancer has recently been completed (3). Phase II studies of *E1A* gene therapy are currently in progress.

The proposal that E1A may induce EWS-FLI1 expression is revolutionary because it suggests that the Ewing tumor may be of viral etiology and that viral transfections may lead to chromosomal translocations. This hypothesis has implications regarding the safety of the use not only of E1A but also of adenoviral vectors containing E1A, such as Onyx-015 (20) in gene therapy trials. Our findings, however, support those of Melot and Delattre (6), and Kovar *et al.* (7, 8); we found no evidence for an association between E1A expression and expression of the EWS-FLI1 fusion product.

We have not studied the E1A integration site in the genome of our stable E1A transfectants. The integration site may be important for the activation of genes; however, Sanchez-Prieto *et al.* (5) have found that E1A-expressing HEK 293 and IMR 90 cells have multiple gene copies in many chromosomes, with no specific chromosomal site of integration. Thus, the site of gene integration is unlikely to account for differences in our results.

Although we cannot exclude the possibility that some E1A-expressing cell lines may have the EWS-FLI1 fusion as claimed by Sanchez-Prieto *et al.* (5, 9), the presence of such a fusion is not characteristic of E1A-transfected cells. We conclude that the potential for induction of such a gene rearrangement using *E1A* gene therapy is too low to be of clinical significance in the treatment of advanced malignant disease.

Acknowledgments

We thank Kerry Wright (Department of Scientific Publications, The University of Texas M. D. Anderson Cancer Center, Houston, TX) for editorial assistance.

References

1. Yu, D., and Hung, M. C. The *erb*B2 gene as a cancer therapeutic target and tumor- and metastasis-suppressing function of E1A. Cancer Metastasis Rev., *17:* 195–202, 1998.

2. Mymryk, J. S. Tumour suppressive properties of the adenovirus 5 E1A oncogene. Oncogene, *13:* 1581–1589, 1996.

3. Hortobagyi, G. N., Hung, M. C., and Lopez-Berestein, G. A Phase I multicenter study of E1A gene therapy for patients with metastatic breast cancer and epithelial ovarian cancer that overexpresses HER-2/neu or epithelial ovarian cancer. Hum. Gene Ther., *9:* 1775–1798, 1998.

4. May, W. A., Lessnick, S. L., Braun, B. S., Klemsz, M., Lewis, B. C., Lunsford, L. B., Hromas, R., and Denny, C. T. The Ewing's sarcoma EWS-FLI-1 fusion gene encodes a more potent transcriptional activator and is a more powerful transforming gene than FLI-1. Mol. Cell. Biol., *13:* 7393–7398, 1993.

5. Sanchez-Prieto, R., De Alava, E., Palomino, T., Guinea, J., Fernandez, V., Cecrian, S., Lleonart, M., Cabello, P., Martin, P., San Roman, C., Bornstein, R., Pardo, J., Martinez, A., Diaz-Espada, F., Barrios, Y., and Ramon y Cajal, S. An association between viral genes and human oncogenic alterations: the adenovirus E1A induces the Ewing tumor fusion transcript EWS-FLI1. Nat. Med., *5:* 1076–1079, 1999.

6. Melot, T., and Delattre, O. E1A and the Ewing tumor translocation. Nat. Med., *5:* 1331, 1999.

7. Kovar, H. E1A and the Ewing tumor translocation. Nat. Med., *5:* 1331, 1999.

8. Kovar H., Fallaux, F. J., Pridill, I., Jugavic, D., Bartl, S., Ambros, P. F., Aryee, D. N. T., Wiegant, T. C. A. G., and Hoeben, R. C. Adenovirus E1A does not induce the Ewing tumor-associated gene fusion *EWS-FLI1*. Cancer Res., *60:* 1557–1560, 2000.

9. De Alava, E., Sanchez-Prieto, and Ramon y Cajal, S. Adenovirus E1A and Ewing tumors. Nat. Med., *6:* 4, 2000.

10. Yu, D., Wolf, J. K., Scanlon, M., Price, J. E., and Hung, M. C. Enhanced c-erbB-2/neu expression in human ovarian cancer cells correlates with more severe malignancy that can be suppressed by E1A. Cancer Res. *53:* 891–898, 1993.

11. Yu, D., Shi, D., Scanlon, M., and Hung, M. C. Reexpression of neu-encoded oncoprotein counteracts the tumor-suppressing but not the metastasis-suppressing function of E1A. Cancer Res., *53:* 5784–5790, 1993.

12. Zhang, Y., Yu, D., Xia, W., and Hung, M. C. HER-2/neu-targeting cancer therapy via adenovirus-mediated E1A delivery in an animal model. Oncogene, *10:* 1947–1954, 1995.

13. Yu, D., Matin, A., Xia, W., Sorgi, F., Huang, L., and Hung, M. C. Liposome-mediated *in vivo* E1A gene transfer suppressed dissemination of ovarian cancer cells that over express HER-2/neu. Oncogene, *11:* 1383–1388, 1995.

14. Chang, J. Y., Xia, W., Sorgi, F., Hortobagyi, G. N., Huang, L., and Hung, M. C. The tumor suppression activity of E1A in Her-2/neu-overexpressing breast cancer. Oncogene, *14:* 561–568, 1997.

15. Brader, K. R., Wolf, J. K., Hung, M. C., Yu, D., Crispens, M. A., van Golen, K. L., and Price, J. E. Adenoviral E1A expression enhances the sensitivity of an ovarian cancer cell line to multiple cytotoxic agents through an apoptotic mechanism. Clin. Cancer Res., *3:* 2017–2024, 1997.

16. Ueno, N. T., Yu, D., and Hung, M. C. Chemosensitization of Her-2/neu-overexpressing human breast cancer cells to paclitaxel (Taxol) by adenovirus type 5 E1A. Oncogene, *15:* 953–960, 1997.

17. Xing, X., Liu, V., Xia, W., Stephens, L. C., Huang, L., Lopez-Berestein, G., and Hung, M. C. Safety studies of the intraperitoneal injection of E1A-liposome complex in mice. Gene Ther., *4:* 238–243, 1997.

18. Xing, X., Zhang, S., Chang, J. Y., Tucker, S. D., Chen, H., Huang, L., and Hung, M. C. Safety study and characterization of E1A-liposome complex gene-delivery protocol in an ovarian cancer model. Gene Ther., *5:* 1538–1544, 1998.

19. Ueno, N. T., Xia, W., Tucker, S. D., Zhang, S., Lopez-Berestein, G., Huang, L., and Hung, M. C. Issues in the development of gene therapy: preclinical experiments in E1A gene delivery. Oncol. Rep., *6:* 257–262, 1999.

20. Hecht, J. R., Abbruzzese, J. L., Bedford, R., Lahoti, S., Parson, M., and Kirn, D. H. A Phase I study of multiple direct injections of Onyx-015 adenovirus into pancreatic carcinomas under endoscopic ultrasound guidance. Proc. Am. Soc. Clin. Oncol., *18:* 186, 1999.

MOLECULAR AND CELLULAR BIOLOGY, Dec. 1999, p. 8075–8082 Vol. 19, No. 12
0270-7306/99/$04.00+0
Copyright © 1999, American Society for Microbiology. All Rights Reserved.

Axl-Gas6 Interaction Counteracts E1A-Mediated Cell Growth Suppression and Proapoptotic Activity

WEI-PING LEE,[1] YONG LIAO,[1] DAN ROBINSON,[2] HSING-JIEN KUNG,[2] EDISON T. LIU,[3] AND MIEN-CHIE HUNG[1]*

Department of Cancer Biology, Section of Molecular Cell Biology and Breast Cancer Research Program, The University of Texas M. D. Anderson Cancer Center, Houston, Texas 77030[1]; The University of California-Davis Cancer Center, Sacramento, California 95817[2]; and Division of Clinical Sciences, National Cancer Institute, Bethesda, Maryland 20892[3]

Received 20 July 1999/Returned for modification 31 August 1999/Accepted 16 September 1999

The adenovirus type 5 early region 1A gene (*E1A*) has previously been known as an immortalization oncogene because E1A is required for transforming oncogenes, such as *ras* and *E1B*, to transform cells in primary cultures. However, E1A has also been shown to downregulate the overexpression of the *Her-2/neu* oncogene, resulting in suppression of transformation and tumorigenesis induced by that oncogene. In addition, E1A is able to promote apoptosis induced by anticancer drugs, irradiation, and serum deprivation. Many tyrosine kinases, such as the epidermal growth factor receptor, Her-2/Neu, Src, and Axl, are known to play a role in oncogenic signals in transformed cells. To study the mechanism underlying the E1A-mediated tumor-suppressing function, we exploited a modified tyrosine kinase profile assay (D. Robinson, F. Lee, T. Pretlow, and H.-J. Kung, Proc. Natl. Acad. Sci. USA 93:5958–5962, 1996) to identify potential tyrosine kinases regulated by E1A. Reverse transcription (RT)-PCR products were synthesized with two degenerate primers derived from the conserved motifs of various tyrosine kinases. A tyrosine kinase downregulated by E1A was identified by analyzing the *Alu*I-digested RT-PCR products. We isolated the DNA fragment of interest and found that E1A negatively regulated the expression of the transforming receptor tyrosine kinase Axl at the transcriptional level. To study whether downregulation of the Axl receptor is involved in E1A-mediated growth suppression, we transfected *axl* cDNA into E1A-expressing cells (ip1-E1A) to establish cells that overexpressed Axl. The Axl ligand Gas6 triggered a greater mitogenic effect in these ip1-E1A-Axl cells than in ip1-E1A control cells and protected the Axl-expressing cells from serum deprivation-induced apoptosis. These results indicate that downregulation of the Axl receptor by E1A is involved in E1A-mediated growth suppression and E1A-induced apoptosis and thereby contributes to E1A's antitumor activities.

The adenovirus type 5 early region 1A gene (*E1A*), the first viral gene expressed in a cell after adenovirus infection, encodes two major proteins, 243R (12S) and 289R (13S), that are produced by alternative splicing (40). The primary function of these two proteins is to activate viral promoters of early genes, including *E1B*, *E2A*, *E3*, and *E4*, during a permissive viral infection by modifying the host cell transcriptional apparatus, thereby resulting in host cell immortalization or transformation (2). Cellular genes that are transcriptionally activated by the E1A proteins include those encoding β-tubulin (42), heat shock proteins (22), c-Fos (10, 37), c-Jun (10), JunB (10), and c-Myc (37). E1A can also repress several viral and cellular genes at the transcriptional level, such as the simian virus 40 enhancer (3, 50), the polyomavirus enhancer (3, 49), the immunoglobulin heavy-chain gene (21), the cytochrome P450 gene (41), the insulin gene (43), and the *Her-2/neu* gene (57).

Adenovirus type 5 *E1A* is known to be an immortalization oncogene because of the fact that some transforming oncogenes, such as *ras* and *E1B*, although able to induce transformation of immortalized rodent cell lines, require E1A to transform cells in primary cultures. However, adenovirus type 5 E1A alone cannot transform established cell lines (5, 23, 36). Furthermore, there exist many established cell lines that are immortalized but nontumorigenic. As a matter of fact, we have previously shown that E1A could be a tumor suppressor for *Her-2/neu*-transformed cells by transcriptional repression of the oncogene (52, 57). In addition to downregulating Her-2/Neu expression, E1A has multiple antitumor effects on tumor cells that do not overexpress Her-2/Neu, including reversion of transformation (12, 15, 16, 28, 55), inhibition of metastasis (17, 28, 53, 54, 56), and induction of apoptosis (9, 11, 33, 45). To understand the detailed mechanisms underlying E1A's antitumor activities, we examined the E1A-regulated tyrosine kinases and identified Axl, whose expression was suppressed by E1A.

The Axl tyrosine kinase (p140) is the prototype of a family of transmembrane receptors called UFO that include Sky and Eyk. These receptors have a unique extracellular composition of immunoglobin-like and fibronectin type III-like domains (13, 30, 47). Similar domain architectures have been found in adhesion molecules of the cadherin and immunoglobulin superfamily and in receptor tyrosine phosphatases such as PTPμ and PTPκ, suggesting that Axl family members may mediate cell adhesion and intracellular signaling. Increased expression of the Axl receptor can transform NIH 3T3 cells and renders the transformed cells highly tumorigenic in nude mice (30).

All members of the UFO family can transform NIH 3T3 cells. When transfected, the *axl* gene transforms NIH 3T3 cells by overexpression (30). Since no genetic rearrangements or mutations have been found, its transforming ability is most probably a consequence of normal receptor overexpression. The Axl ligand Gas6 is a vitamin K-dependent growth-poten-

* Corresponding author. Mailing address: 1515 Holcombe Blvd., Section of Molecular Cell Biology Box 108, Department of Cancer Biology, The University of Texas M. D. Anderson Cancer Center, Houston, TX 77030. Phone: (713) 792-3668. Fax: (713) 794-0209. E-mail: mchung@notes.mdacc.tmc.edu.

tiating factor (26, 44, 48). The ligand contains a γ-carboxyglutamic acid-rich domain and four epidermal growth factor-like repeats. It is widely secreted by most tissues, particularly those of the lung, intestine, and vascular endothelium (26). Under serum-starved conditions, Gas6 has a mitogenic effect on growth-arrested cells (1, 19, 20). Gas6-Axl signaling also seems to play a critical role in modulating cellular responses to adhesion; in one study, Gas6 stimulated the binding of Axl-expressing monoblast U937 cells to phosphatidylserine, a phospholipid marker used by macrophages to identify dying cells (29). Gas6 also functions as a novel chemoattractant that induces Axl-mediated migration of vascular smooth-muscle cells, suggesting that the Gas6-Axl interaction may enhance cell migration in conditions involving vascular damage (14). In addition, the Axl receptor has been found to be highly expressed in metastatic colon carcinoma (8), melanoma (32), and sarcoma (51) cells, implying that this receptor is involved in cancer invasion and metastasis.

The published data, taken together, suggest that E1A is associated with a tumor suppressor function in human tumor cells and that the Axl receptor behaves as an oncoprotein when it is overexpressed. To study the mechanism underlying E1A's tumor-suppressing activities, we focused on E1A-regulated tyrosine kinases. In the current study, we found that E1A can downregulate the expression of the Axl receptor and that the Gas6-Axl interaction can counteract E1A-mediated growth inhibition and proapoptotic activity, suggesting that downregulation of Axl by E1A may contribute to E1A-mediated antitumor activities.

MATERIALS AND METHODS

Cell lines and cell cultures. SKOV3.ip1 (abbreviated ip1) is a subline of the SKOV3 ovarian cancer cell line. 2774 C-10 (abbreviated 2774) is a human ovarian cancer cell line. The E1A transfectants were designated ip1-E1A and 2774-E1A. The transfectants of the *E1A* frameshift mutant were designated ip1-efs and 2774-efs. Cells were grown in Dulbecco's modified Eagle's medium plus F12 medium (1:1; GIBCO-Bethesda Research Laboratories [BRL]) supplemented with 10% fetal calf serum in a humidified atmosphere of 5% CO_2 at 37°C. ip1-efs, ip1-E1A, 2774-efs, and 2774-E1A cells were maintained in medium containing neomycin at 500 μg/ml (Boehringer Mannheim).

Tyrosine kinase display assay. Total RNA was isolated with the TRIzol reagent (GIBCO-BRL), and the tyrosine kinase display was carried out by a modified form of the method of Robinson et al. (34, 35). Reverse transcription (RT)-PCR was performed with degenerate primers derived from conserved motifs in the activation loop of the catalytic domains of various tyrosine kinases as follows: primer 1 (sense primer), 5′-AARRTTDCNGAYTTYGG encoding the amino acid sequence K[V/I][S/C/G]DFG; primer 2 (antisense primer), 5′-RHAIGMCCAIACRTC encoding the amino acid sequence DVW[S/A][F/Y]. The mixed bases were defined as follows: N = A + C + T + G, D = A + T + G, H = A + T + C, R = A + G, Y = C + T, M = A + C, and I = deoxyinosine. Single-stranded cDNA was synthesized with a kit provided by GIBCO-BRL. Primer 1 was labeled with [γ-^{32}P]ATP (Amersham Life Science) and T4 polynucleotide kinase (New England Biolabs) before PCR (*Taq* DNA polymerase; Fisher Biotech). The RT-PCR products were analyzed by gel electrophoresis with an 8% polyacrylamide gel. DNA was stained with ethidium bromide at 1 μg/ml. The ~150-bp bands were excised from the polyacrylamide gel. DNA was eluted, precipitated, and dissolved in TE buffer (10 mM Tris, 1 mM EDTA, pH 8.0). Equal amounts of radioactive DNA (10^5 cpm) of each cell type were digested with various restriction enzymes recognizing four bases, resolved with a 6% DNA sequencing gel, and then subjected to autoradiography.

Cloning of the band of interest revealed by the tyrosine kinase display assay. In the tyrosine kinase display assay, we found that the E1A proteins downregulated a tyrosine kinase whose catalytic domain sequence possessed the *Alu*I site. This tyrosine kinase was tentatively named TK-Alu I. Because the TK-Alu I band shown in Fig. 1B had been digested by *Alu*I, we could not PCR amplify the TK-Alu I DNA by using the two primers described previously, because the annealing sequence of the TK-Alu I for primer 2 had been separated from the radioactive sequence shown in Fig. 1B by the *Alu*I digestion. To clone TK-Alu I, we established a tyrosine kinase cDNA library from the RT-PCR products of ip1 cells with the TA cloning strategy. At first, all of the RT-PCR products of the 150-bp DNA fragments were ligated into the TA cloning vector PCR2.1 (Invitrogen Inc.) to make a cDNA library of tyrosine kinases. The library was amplified in *Escherichia coli* DH10B. Then, we performed a large-scale preparation of the *Alu*I-digested RT-PCR product. The TK-Alu I band was excised, and the DNA was eluted from the sequencing gel. A TK-Alu I probe was made by synthesizing single-stranded DNA by PCR in a mixture containing primer 1, [α-^{32}P]dCTP, and the eluted TK-Alu I DNA. The radiolabeled probe was used to screen the tyrosine kinase cDNA library described above, the positive clones were picked out, and the plasmid DNA was purified and subjected to PCR as described for the tyrosine kinase display assay. RT-PCR and plasmid-PCR products were digested with *Alu*I and then analyzed by sequencing gel electrophoresis to determine whether the selected clones contained the TK-Alu I insert. Finally, the truly positive TK-Alu I clone was sequenced and that sequence was identified by comparison with the GenBank database sequences of the National Center for Biotechnology Information by using the BLAST algorithm.

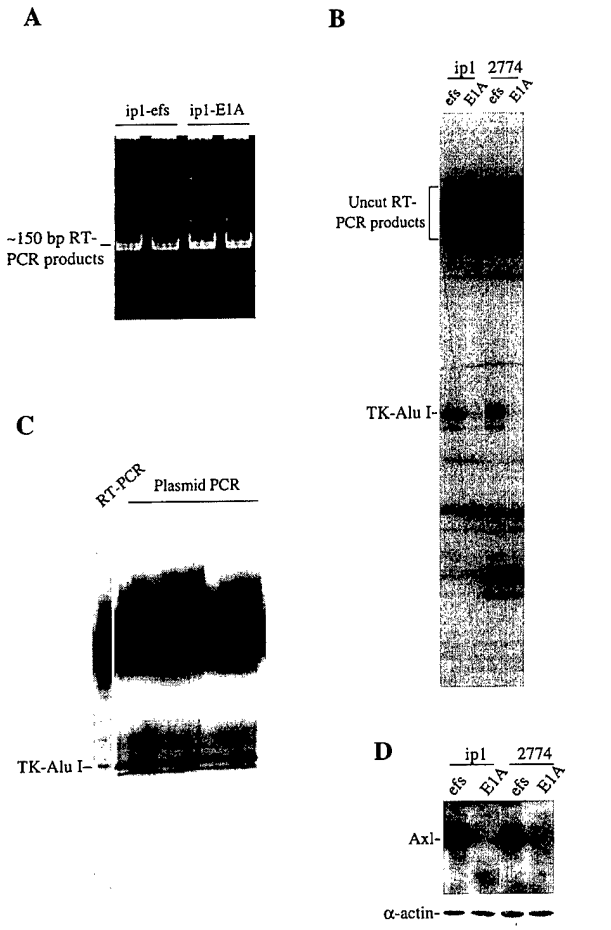

FIG. 1. (A) The 150-bp RT-PCR products representing the activation loop of the catalytic domains of various tyrosine kinases. RNA was isolated by using the TRIzol reagent. Single-stranded cDNA was synthesized with a GIBCO-BRL kit. Primer 1 was labeled with [γ-^{32}P]ATP and T4 polynucleotide kinase before PCR. The RT-PCR products were analyzed by 8% PAGE. DNA was stained with ethidium bromide at 1 μg/ml. SKOV3.ip1 is a subline of the SKOV3 ovarian cancer cell line; ip1-efs is ip1 cells transfected with an E1A frameshift mutant construct. (B) Tyrosine kinase display assay showing downregulation of a tyrosine kinase, designated TK-Alu I, in E1A-transfected cells. The RT-PCR products shown in panel A were excised and eluted from the gel. The eluted DNAs of equal radioactivity were digested with the restriction enzyme *Alu*I and then fractionated with a 6% DNA sequencing gel. 2774 is the ovarian cancer cell line 2774-C10. (C) Tyrosine kinase display assay of bacterial clones obtained from the tyrosine kinase cDNA library screening. The TK-Alu I probe was PCR labeled and used to screen a cDNA library of tyrosine kinases. The positive clones were picked out, and the plasmid DNA was purified and subjected to PCR as described for panel A. The products of both RT-PCR from ip1-efs cells and plasmid PCR from bacterial clones were digested with *Alu*I and then resolved with a 6% DNA sequencing gel. The TK-Alu I band was seen in all of the plasmid PCR clones. (D) Immunoblotting analysis showing decreased level of the Axl receptor protein in E1A-expressing ip1 and 2774 cells. Western blot analysis was performed as described in Materials and Methods, and the Axl receptor was detected by treating the transblot with an anti-Axl antibody. As a gel loading control, the same blot was reprobed with an anti-α-actin antibody.

Nuclear run-on assay. The nuclear run-on assay was performed as described previously (27). Briefly, cells were washed with phosphate-buffered saline (PBS) and lysed in ice-cold buffer (10 mM Tris [pH 7.4], 10 mM NaCl, 3 mM $MgCl_2$, 0.5% Nonidet P-40). The nuclei were then pelleted by centrifugation and suspended in buffer A (50 mM Tris [pH 8.3], 5 mM $MgCl_2$, 0.1 mM EDTA, 40% glycerol). The nascent RNA chains were elongated by mixing the nuclear suspension with an equal volume of the reaction buffer (10 mM Tris [pH 8.0]; 5 mM $MgCl_2$; 0.3 M KCl; 5 mM dithiothreitol; 1 mM each ATP, CTP, and GTP; 0.1 mCi [α-^{32}P]UTP). After incubation at 30°C for 30 min, the ^{32}P-labeled RNA was purified with TRIzol (GIBCO-BRL). Samples (5 μg) of plasmids, pcDNA3, pcDNA3-Axl, and pcDNA3–glyceraldehyde-3-phosphate dehydrogenase (GAPDH) were denatured and immobilized on Hybond N membranes. The membranes were prehybridized in a solution of 50% formamide, 5× SSPE (1× SSPE is 0.18 M NaCl, 10 mM NaH_2PO_4, and 1 mM EDTA), 2× Denhardt's reagent, 0.5% sodium dodecyl sulfate (SDS), and salmon sperm DNA at 100 μg/ml for 2 h at 42°C. Equal amounts of radioactivity (1.0×10^6 cpm) from the test samples were hybridized with the immobilized DNA at 42°C for 24 h. The membranes were then washed for 60 min with 2× SSC (1× SSC is 0.15 M NaCl plus 0.015 M sodium citrate)–0.1% SDS at 55°C and then for 30 min with 0.2× SSC–0.1% SDS at 55°C and finally exposed to X-ray film at −70°C.

Establishment of stable cell lines. The *axl* cDNA was cloned into a pCEP4 vector carrying the hygromycin phosphotransferase gene (*hph*). Expression of the *axl* and *hph* genes was driven by the cytomegalovirus promoter and the thymidine kinase promoter, respectively. The *axl* gene transfection was carried out by using DOTAP liposomes (24). Briefly, 6 μg of plasmid pCEP4-Axl along with the DOTAP liposome mixture was transfected to 1.0×10^6 ip-E1A cells cultured in a 3-cm-diameter tissue culture dish. Approximately 4 h after transfection, the cells were washed with PBS, cultured in fresh medium for 24 h, and then split 1:20. The cells were then grown in a selection medium containing hygromycin B (Boehringer Mannheim) at 20 μg/ml and neomycin at 500 μg/ml for 3 to 5 weeks, after which individual hygromycin-resistant clones were picked out and expanded to mass culture.

Immunoblotting. Immunoblotting analyses were performed as described elsewhere (46). Briefly, cell lysates were resolved by SDS-polyacrylamide gel electrophoresis (PAGE) and then transferred to nitrocellulose membranes. The membranes were treated separately with an anti-Axl (Santa Cruz Biotech), an anti-E1A protein (Oncogene Research), or an anti-α-actin (Amersham Life Science) antibody and then incubated with peroxidase-conjugated secondary antibodies and detected by the enhanced-chemiluminescence method (Amersham Life Science). For the analysis of Gas6 expression, supernatants of cultures were subjected first to SDS-PAGE and then to immunoblotting with an anti-Gas6 polyclonal antibody (Santa Cruz Biotech).

[^{3}H]thymidine incorporation assay. Cells were trypsinized, washed twice with PBS, and then seeded onto 96-well plates at 2,000/well. To the wells was added 10 μCi of [^{3}H]thymidine (Amersham Life Science) at specific times. The cells were then incubated at 37°C for 8 h and then processed by a cell harvester (Cambridge Technology Inc.). Radioactivity was determined with a liquid scintillation counter.

Analysis of [^{3}H]thymidine incorporation after the *gas6* cDNA transfection. The medium used to do the *gas6* cDNA transfection and other studies related to Gas6 contained 4 μM menadione sodium bisulfite, a vitamin K analog (Sigma). The *gas6* cDNA, whose expression was driven by the cytomegalovirus promoter, was cloned in a pcDNA3 vector. Cells (1.0×10^6) were plated in a 3-cm-diameter tissue culture dish and cultured in drug-free medium for 24 h, and then 4 μg of the vector pcDNA3 or plasmid pcDNA3-Gas6 was transfected into ip1-efs, ip1-E1A-pCEP4, and three independent clones of ip1-E1A-Axl cells by using DOTAP liposomes. Cells were exposed to the DNA-liposome composites for 8 h, washed twice with PBS, and cultured in serum-supplemented medium for 24 h. Cell were then trypsinized, washed twice with PBS, and then seeded onto 96-well plates at 2,000/well. At 24, 48, and 72 h thereafter, cells were subjected to [^{3}H]thymidine incorporation. Alternatively, 24 h after being seeded onto 96-well plates, cells were serum deprived for another 24 h and then subjected to [^{3}H]thymidine incorporation.

Analysis of the phosphorylation state of the Axl receptor. Cells for this assay were lysed in a buffer containing 20 mM Tris [pH 7.2], 150 mM NaCl, 50 mM NaF, 2 mM Na_3VO_4, 1 mM phenylmethylsulfonyl fluoride, leupeptin at 25 μg/ml, and aprotinin at 25 μg/ml. The lysates were cleared by centrifugation and immunoprecipitated with 5 μg of anti-Axl polyclonal antibody (Santa Cruz), followed by 20 μl of protein A-agarose (Boehringer Mannheim). The immunocomplexes were washed with lysis buffer, resolved by SDS–10% PAGE, transferred to a nitrocellulose membrane, and then detected with an antiphosphotyrosine antibody (Oncogene Research).

Analysis of apoptosis by flow cytometry. For analysis of apoptosis by flow cytometry, 1.0×10^6 cells were transfected with *gas6* cDNA by using the LPD1 liposome (24). At 24 h after transfection, cells were serum starved for 48 h, harvested by trypsinization, washed twice with PBS, and then fixed in 75% ethanol at 4°C overnight. The fixed cells were washed twice with PBS and suspended in 1 ml of PBS containing 0.5% Tween 20, to which were added 10 μg of RNase and 10 μg of propidium iodide. The propidium iodide-stained cells were analyzed with a FACScan flow cytometer (Becton Dickinson). Apoptotic cells were determined by the percentage of cells in the sub-G_1 region.

RESULTS

Identification of the tyrosine kinase Axl that was downregulated by the E1A proteins. To identify the E1A-regulated tyrosine kinases, we compared the tyrosine kinase expression profiles of cancer cell lines with those of their E1A transfectants by using a novel tyrosine kinase display assay (34), a modification of the tyrosine kinase profile approach (35). Briefly, the entire collection of expressed tyrosine kinases was generated by RT-PCR using degenerate primers corresponding to the highly conserved DFG and DVW motifs. This would yield a relatively homogeneous band of approximately 150 bp for virtually all tyrosine kinases. Different kinases would then be differentiated by digestion with restriction enzymes, based on the characteristic sizes predicted from the GenBank data. To help visualize the restriction products, the 5′ end of the sense primer was radiolabeled with [γ-^{32}P]ATP and the digested products were resolved in a DNA sequencing gel and then autoradiographed. An example of the polyacrylamide gel-resolved and ethidium bromide-stained total RT-PCR products in the range of 150 bp is shown in Fig. 1A. Restriction enzyme digestion of the RT-PCR products would reduce the lengths of certain radiolabeled DNA fragments, which would migrate faster than uncut fragments in a DNA sequencing gel. A tyrosine kinase cDNA fragment, tentatively named TK-AluI, that had been digested with *Alu*I displayed a differential expression pattern in E1A-transfected cells compared with the parental controls (Fig. 1B). This band exhibits a very low radiointensity in both the E1A-expressing ip1 and 2774 ovarian cancer cells compared with the control cells. To confirm that the lower expression of TK-Alu I was due to the expression of E1A, we subjected the breast cancer cell line MDA-MB231 and its E1A stable transfectant (231-E1A) to the same analysis and found downregulation of Axl in 231-E1A cells (data not shown). Thus, it is likely that the mRNA level of the TK-Alu I gene was negatively regulated by E1A. The size of the *Alu*I-digested band predicts that it may be the tyrosine kinase Axl.

To confirm that the TK-Alu I gene encodes Axl but not any fortuitous RT-PCR product, we set out to clone this product. A radioactive probe was prepared by PCR using the TK-Alu I DNA as a template, and that probe was used to screen a tyrosine kinase cDNA library established by ligating the RT-PCR products synthesized from ip1 cells to the TA cloning vector PCR2.1. As expected, the positive clones showed the same TK-Alu I band upon tyrosine kinase display (Fig. 1C). DNA sequencing revealed that TK-Alu I indeed represents the Axl kinase. Once we identified the product of the TK-Alu I gene as Axl, we analyzed Axl protein levels in cancer cell lines and their E1A transfectants. We found that expression of the Axl protein was repressed in E1A transfectants (Fig. 1D). Thus, both protein and mRNA expression findings support the inhibition of Axl expression by E1A.

Repression of *axl* gene expression by E1A at the transcriptional level. The foregoing results suggest that E1A can negatively regulate the expression of both the *axl* transcripts and the Axl protein. We next used a nuclear run-on assay to determine whether E1A represses transcription of the *axl* gene. The radiolabeled transcripts derived from the nuclei of ip1-efs cells hybridized strongly with the *axl* cDNA, but the radiolabeled transcripts derived from ip1-E1A cells gave no hybridization signal (Fig. 2). Hybridization of the same radiolabeled transcripts to GAPDH cDNA, a housekeeping gene, produced equal signals in the ip1-efs and ip1-E1A cells. These results indicate that ip1-E1A cells produced little or no Axl mRNA. To determine whether this phenomenon was caused by transcriptional repression of the *axl* gene or by posttranscriptional

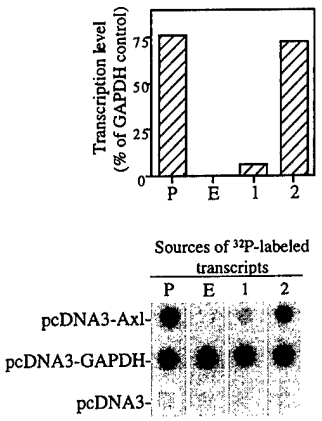

FIG. 2. Nuclear run-on assay showing transcriptional repression of the *axl* gene in ip1-E1A cells. ^{32}P-labeled transcripts were prepared from isolated nuclei by in vitro transcription with [α-^{32}P]UTP. Equal amounts of labeled RNA (10^6 cpm) were hybridized to Hybond N membranes containing the immobilized plasmids pcDNA3-Axl, pcDNA3-GAPDH, and pcDNA3 at 5 μg per blot. P, ip1-efs cells; E, ip1-E1A cells. Lanes: 1, membrane strip hybridized with the in vitro transcription product derived from an equal amount mixture of the nuclear suspensions of ip1-efs and ip1-E1A cells; 2, membrane strip hybridized with the in vitro transcription product derived from the nuclear suspension of ip1-efs cells, to which was added an equal amount of nuclear suspension of ip1-E1A cells after mRNA elongation was completed.

degradation of *axl* mRNA in ip1-E1A cells, we elongated mRNA from ip1-efs cells and then added a nuclear suspension of ip1-E1A cells to the products of in vitro transcription. The hybridization result (Fig. 2, lane 2) was the same as that seen in the lane representing ip1-efs. Thus, the nuclear suspension of ip1-E1A cells did not contain factors that accelerated degradation of the *axl* mRNA. In vitro transcriptional repression was also observed in a mixture of the nuclear suspensions of ip1 cells and ip1-E1A cells (Fig. 2, lane 1), suggesting that some factor in ip1-E1A cells is able to act in *trans* to suppress *axl* transcription in ip1-efs cells. Thus, we conclude that the rate of *axl* gene transcription was greatly inhibited in ip1-E1A cells compared with that in the control ip1-efs cells.

Establishment of Axl-overexpressing ip1-E1A cells. ip1-E1A cells grow more slowly than do the parental ip1 cells (58). To study whether downregulation of the Axl receptor by E1A might be involved in the E1A-mediated reduction of the growth rate of ip1-E1A cells, we established an ip1-E1A cell line that overexpresses Axl (ip1-E1A-Axl). The *axl* cDNA was cloned into the expression vector pCEP4 that carries the hygromycin phosphotransferase gene. The stable cell lines were established by transfection of the pCEP4-Axl plasmid into ip1-E1A cells and selection with hygromycin B. These ip1-E1A-Axl clones overexpressed the Axl receptor; the expression level in clone 2 was comparable to that of the ip1-efs cells (Fig. 3). To verify that E1A was still present in the stable clones, the same blot was reprobed with an anti-E1A antibody. Expression of α-actin was used as a gel loading control.

Promotion of mitogenesis by the Gas6-Axl interaction in ip1-E1A-Axl cells. To determine whether ip1-E1A-Axl cells might recover after growth rate reduction by E1A, we measured mitogenesis by determining [^{3}H]thymidine incorporation. Re-expression of the Axl receptor in ip1-E1A cells (ip1-E1A-Axl) had no significant effect on mitogenesis, compared to ip1-E1A-pCEP4 control cells that were transfected with the vector plasmid (Fig. 4A). Since previous reports had shown that activation of Axl is Gas6 dependent (1, 19, 20), we questioned whether the Axl receptor expressed in ip1-E1A-Axl cells requires the ligand Gas6 for activation.

To determine whether Gas6 could promote mitogenesis in ip1-E1A-Axl clones, cells were transfected with either vector pcDNA3 or plasmid pcDNA3-Gas6 and [^{3}H]thymidine incorporation was performed in the presence of serum at specific times thereafter. Gas6 produced a dose-dependent activation of the Axl receptor in ip1-E1A-Axl cells (Fig. 4B) with transfection of 4 μg of plasmid pcDNA-Gas6 to 10^6 ip1-E1A-Axl-2 cells giving the maximum phosphorylation of the Axl receptor and a plateau incorporation of [^{3}H]thymidine. Gas6 expression in culture supernatants was confirmed by Western blotting. These results indicate that the transfection assay we established can produce enough secreted Gas6 to induce Axl-dependent mitogenesis.

Using the above-described assay, we found that transiently expressed Gas6 had an increased mitogenic effect on ip1-E1A-Axl clones in the absence of serum compared with the same clones without Gas6 stimulation (Fig. 4C). Expression of Gas6 is shown in Fig. 4D-1. This protein had a lesser impact on mitogenesis in ip1-efs cells (1.6-fold increase) than on that in ip1-E1A-Axl cells (10-fold increase). For ip1-E1A-Axl-2 cells, Gas6 induced a 10-fold increase in mitogenesis in the absence of serum (Fig. 4C) but only a 3-fold increase in the presence of serum (4-μg lane in Fig. 4B), suggesting that serum contains other stimulating factors that cover the effect of Gas6.

To confirm the effect of the Gas6-Axl interaction, we analyzed the intrinsic phosphorylation of the Axl receptor in the presence or absence of Gas6 stimulation. Cells were transfected with either the pcDNA3-Gas6 plasmid or the control vector, serum deprived for 24 h, immunoprecipitated with an anti-Axl antibody, and Western blotted with an antiphosphotyrosine antibody. The increased tyrosine phosphorylation of the Axl receptor in the Gas6-stimulated ip1-E1A-Axl cells (Fig. 4D-2) correlates well with the enhanced mitogenic effect in ip1-E1A-Axl cells (Fig. 4C). The same blot was reprobed with an anti-Axl antibody as a control.

Protection of E1A-transfected cells from serum deprivation-induced apoptosis by the Gas6-Axl interaction. E1A-transfected cells are more sensitive to serum deprivation-induced apoptosis than are parental cells (11, 33). We found that Gas6 can induce mitogenesis in ip1-E1A-Axl cells in the absence of serum (Fig. 4C). To examine whether the Gas6-Axl interaction could also protect ip1-E1A-Axl cells from apoptosis triggered by serum deprivation, we transfected cells with plasmid pcDNA3-Gas6, deprived those cells of serum for 48 h, and then processed them for fluorescence-activated cell sorter

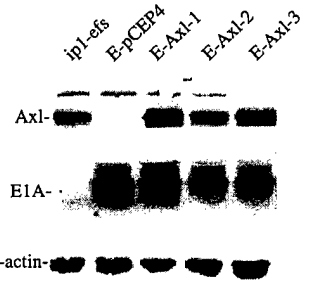

FIG. 3. Immunoblot showing re-expression of the Axl receptor in *axl*-transfected ip1-E1A cells. *axl* cDNA was cloned into the pCEP4 vector, and the DNA was transfected as described in Materials and Methods. Three clones of ip1-E1A-Axl (E-Axl-1, E-Axl-2, and E-Axl-3) showed increased expression of Axl compared to that of ip1-E1A-pCEP4 (E-pCEP4) control cells that were transfected with the pCEP4 vector. An equal amount of cell lysate for each cell type was resolved by SDS–10% PAGE. After electrophoresis, proteins were transferred to a nitrocellulose membrane and then probed with anti-Axl, anti-E1A, and anti-α-actin antibodies.

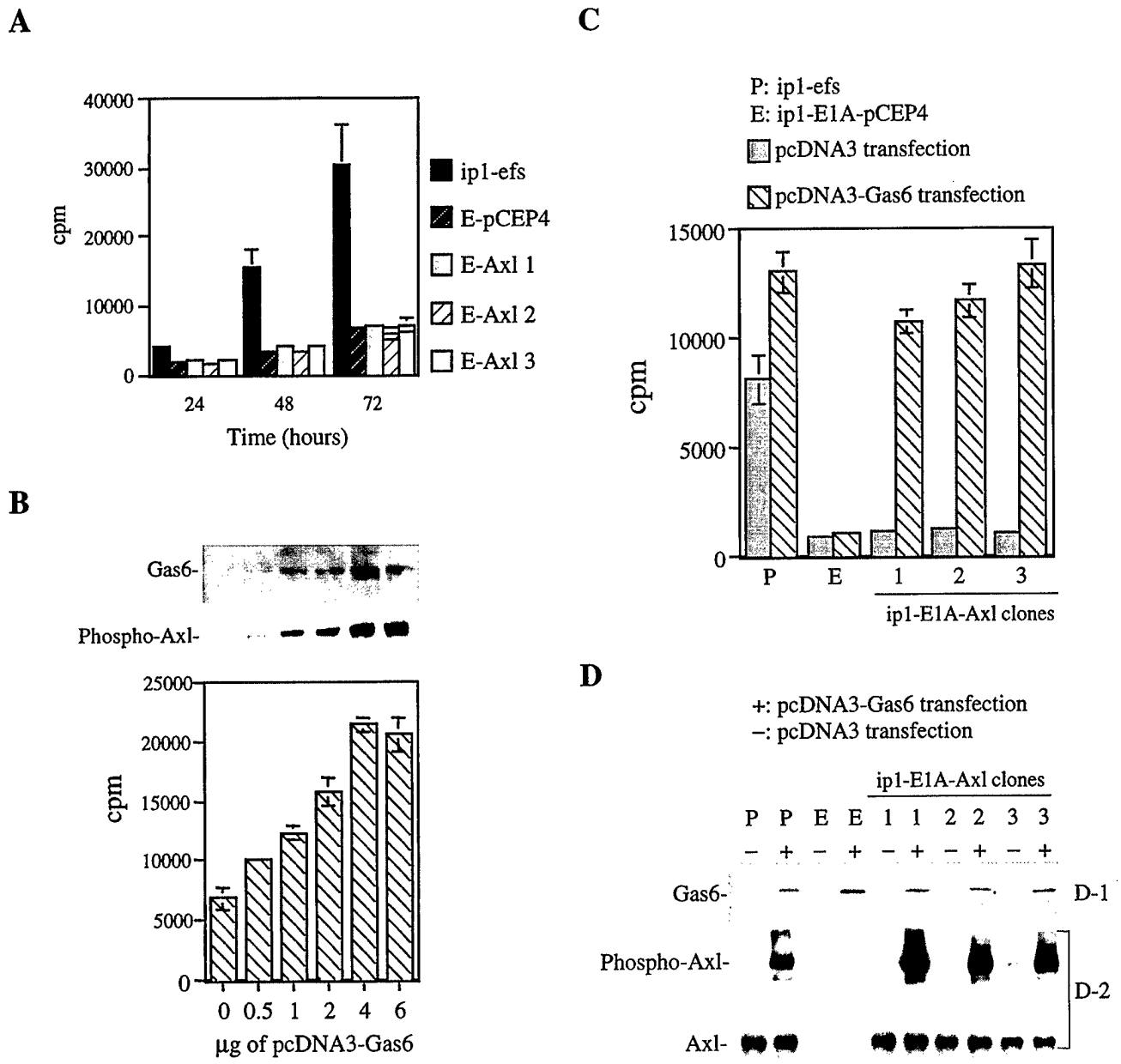

FIG. 4. Mitogenesis in ip1-efs, ip1-E1A, and ip1-E1A-Axl cells. (A) [^{3}H]thymidine incorporation showing no significant difference in mitogenesis between ip1-E1A-pCEP4 (E-pCEP4) cells and ip1-E1A-Axl clones (E-Axl-1, -2, and -3). Cells were seeded onto 96-well plates, [^{3}H]thymidine was added at 24, 48, and 72 h, and cells were incubated at 37°C for 8 h and then processed by a cell harvester. Each bar is the average of four replicates. (B) Dose-dependent activation of the Axl receptor in ip1-E1A-Axl-2 cells by *gas6* cDNA transfection. Various concentrations of pcDNA3-Gas6 plasmid DNA were transfected into 10^6 ip1-E1A-Axl-2 cells as described in Materials and Methods; 4 μg of plasmid pcDNA3-Gas6 was sufficient to cause maximum phosphorylation of the Axl receptor and plateau incorporation of [^{3}H]thymidine. Phosphorylation of the Axl receptor was analyzed by immunoprecipitation with an anti-Axl antibody, followed by Western blotting with an antiphosphotyrosine antibody. Gas6 expression was determined by immunoblotting of culture supernatants. All of the assays were performed 72 h after transfection and under serum-supplemented conditions. (C) The effect of Gas6 on serum-deprived ip1-E1A-Axl cells. Cells (10^6) were transfected with 4 μg of pcDNA3-Gas6 or vector pcDNA3 as described for panel B and seeded onto a 96-well plate at 2,000 cells/well 24 h after transfection. After 24 h of culture in serum-supplemented medium to allow the cells to attach to the wells, the cells were serum deprived for another 24 h and then subjected to [^{3}H]thymidine incorporation. Each bar is the average of triplicate samples. (D-1) Immunoblot showing Gas6 expression in pcDNA3-Gas6-transfected cells. Western blot analysis was performed with supernatants of cell cultures as described for panel B. (D-2) Increased phosphorylation of the Axl receptor in Axl-expressing cells transfected with *gas6* cDNA. Cells were transfected with pcDNA3-Gas6 or vector plasmid pcDNA3 as described for panel C. At 24 h after transfection, cells were serum deprived for 24 h and then lysed, immunoprecipitated with anti-Axl antibody, and subjected to Western blotting with an antiphosphotyrosine antibody. As a control, the same blot was reprobed with an anti-Axl antibody.

(FACS) analysis. Fewer Gas6-stimulated ip1-E1A-Axl cells than unstimulated cells were in the sub-G_1 region (Fig. 5A and B). Gas6 expression is shown in the lower part of Fig. 5B. The ip1-E1A-pCEP4 cells were sensitive to serum deprivation despite the presence of Gas6; the ip1-efs cells were less sensitive to serum withdrawal under the same conditions. These results indicate that Gas6 can protect E1A transfectants from serum deprivation-induced apoptosis if Axl is re-expressed.

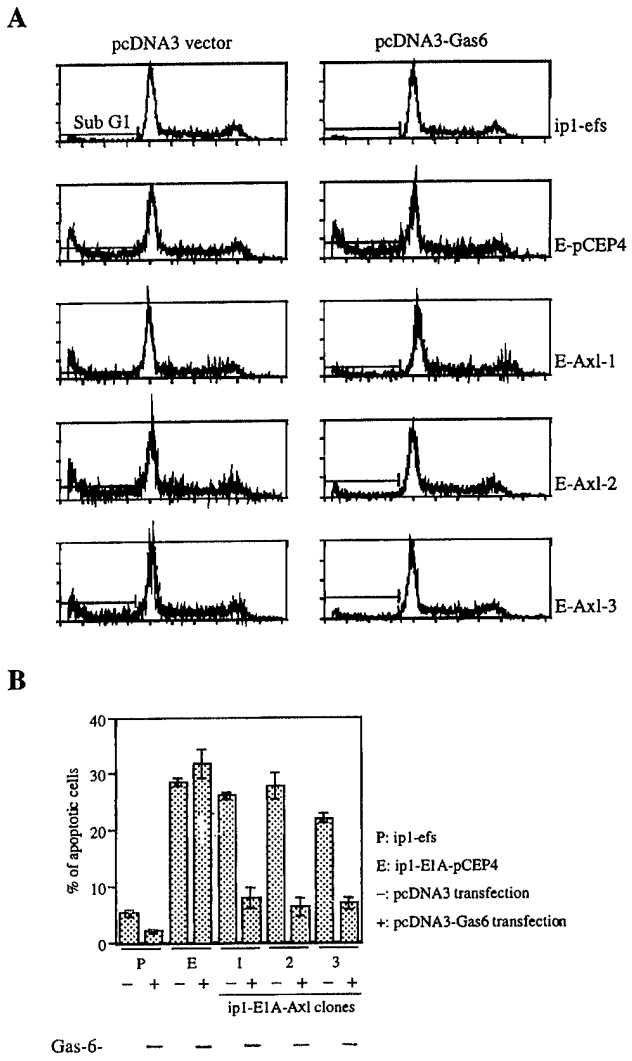

FIG. 5. Protection of Axl-expressing cells from serum deprivation-induced apoptosis by Gas6. (A and B) Decreased apoptosis in ip1-E1A-Axl cells by transiently expressed Gas6. Cells were transfected with *gas6* cDNA or control plasmid pcDNA3 as described for Fig. 4C. At 24 h after transfection, cells were serum deprived for 48 h and then subjected to FACS analysis. The apoptotic cells were determined by measuring the percentage of cells in the sub-G_1 region (A). Each bar in panel B is the average of triplicate samples. Expression of Gas6 in cells transfected with *gas6* cDNA is shown at the bottom of panel B. Supernatants from cells used for FACS analysis were subjected to SDS–10% PAGE. Western blot analysis was performed with an anti-Gas6 polyclonal antibody. Abbreviations for cell types are the same as those in Fig. 3 and 4C and D.

DISCUSSION

E1A has been shown to be associated with multiple antitumor activities, including transcriptional repression of the *Her-2/neu* gene (52, 57), suppression of transformation (12, 15, 16, 28, 55), inhibition of metastasis (17, 28, 53–55), and induction of apoptosis (9, 11, 33, 45). To further understand E1A-mediated tumor suppression, we focused on the tyrosine kinases that are regulated by E1A because tyrosine kinases usually play a pivotal role in the signal pathways that cause cellular transformation. In the current study, we used the tyrosine kinase display and nuclear run-on assays to confirm that the expression of the transforming receptor tyrosine kinase Axl is transcriptionally suppressed by E1A. Our experimental results indicate that the Gas6-Axl interaction counteracts E1A-mediated cell growth suppression and proapoptotic activity.

Multiple molecular mechanisms may account for the tumor- and metastasis-suppressing functions of E1A in different cancer cell types. The tumor-suppressing function has been explained, at least in part, as resulting from the induction of apoptosis through p53-dependent or p53-independent mechanisms (9, 45). E1A may also suppress tumor growth by modulating the response of tumor cells to immune cells, since this protein can sensitize transfected cells to the cytotoxic effects of tumor necrosis factor (TNF) (6, 38) and make target cells susceptible to NK cells and activated macrophages (7). In addition, E1A can abrogate NF-κB activation, resulting in susceptibility of cells to apoptotic stimuli such as TNF and γ irradiation (38, 39). As for the metastasis-suppressing function of E1A, one known mechanism is the transcriptional repression of various proteases that are important for tumor invasion and metastasis, including type IV collagenase (17, 18), interstitial collagenase, urokinase (17), and stromelysin (25, 31). In summary, E1A suppresses tumor growth and metastasis through cumulative changes in cellular gene expression, and many unknown mechanisms remain to be discovered.

Gas6 induced serum-starved NIH 3T3 cells to enter the cell cycle (19, 20); the signaling was shown to be transmitted through the stimulation of Axl tyrosine kinase with subsequent activation of mitogen-activated protein kinase and phosphatidylinositol 3-kinase (19, 20). Adding Gas6 to serum-starved NIH 3T3 cells also prevented cell death induced by complete serum removal and TNF addition, indicating that Gas6 acts as a survival factor for growth-arrested cells (1, 19, 20). In a study of fibroblasts from *axl* knockout mice, the absence of the Axl receptor resulted in higher levels of serum deprivation-induced apoptosis that could not be rescued by the addition of Gas6 (1). Instead of studying normal fibroblasts, we established an ovarian cancer model in which parental ip1 cells, unlike NIH 3T3 cells, were not sensitive to serum deprivation. In this model, downregulation of the Axl receptor by E1A rendered the E1A transfectant ip1-E1A susceptible to serum deprivation-induced apoptosis that was prevented by the Gas6-Axl interaction. In short, abrogation of Gas6-Axl signaling by E1A is involved in E1A-mediated suppression of cell growth and susceptibility to serum deprivation.

The mildly increased rate of [^{3}H]thymidine incorporation in Gas6-stimulated ip1-efs cells (Fig. 4C) is consistent with previous reports that Gas6 is a weaker mitogen than basic fibroblast growth factor and serum (1, 19). In the mitogenesis and apoptosis studies (Fig. 4C and 5), we found that ip1-efs cells were less responsive to Gas6 stimulation than were ip1-E1A-Axl cells, although both expressed Axl. Conversely, the mitogenic effect and resistance to serum withdrawal-induced apoptosis in ip1-E1A-Axl cells were dependent on Gas6 stimulation (Fig. 4C and 5), implicating the role of downregulation of Axl in E1A-mediated tumor suppression and E1A's other activities that render ip1-E1A-Axl cells more dependent than ip1-efs cells on Gas6 during serum depletion. One of these E1A activities may be downregulation of the receptor tyrosine kinase Her-2/Neu (52, 55, 57). Re-expression of Axl did not change the repressed expression of Her-2/Neu in ip1-E1A cells (data not shown). Overexpression of Her-2/Neu in ip1-efs cells (58) may be the reason why ip1-efs cells were less dependent on Gas6 stimulation (Fig. 4C) and more resistant to serum withdrawal-induced apoptosis (Fig. 5) than were ip1-E1A-Axl cells.

Expression of the activated *axl* gene in NIH 3T3 (AF6295) cells can result in cellular transformation (30). However, re-expression of the Axl receptor in ip1-E1A cells (ip1-E1A-Axl)

had no significant effect on mitogenesis as analyzed by [^{3}H]thymidine incorporation, compared to ip1-E1A-pCEP4 control cells that were transfected with the vector plasmid (Fig. 4A). This might be because the level of the Axl receptor in ip1-E1A-Axl clones was not as high as that in the AF6295 cells described by O'Bryan et al. (30). The expression of Axl in AF6295 cells is at least 10-fold more abundant than that in ip1-efs cells (data not shown). The mitogenesis study indicates that the receptor expressed in ip1-E1A-Axl cells requires the Axl ligand Gas6 for activation (Fig. 4B and D-2). Although Gas6 was able to stimulate mitogenesis in ip1-E1A-Axl cells, endogenous Gas6 expression could not be detected in the supernatants of parental ip1 cells or ip1-E1A cells (Fig. 4D-1 and 5B). This finding suggests that repression of the *axl* gene by E1A is not the main mechanism by which growth is suppressed in cultured ip1 cells. However, Gas6 secretion is ubiquitous in the human body (26), so Axl-mediated survival and mitogenic effects may be more important in whole organisms than in cultured cells. It should be mentioned that Axl is overexpressed in approximately 25% of primary breast cancers (4). Given that a tumor cell line can secrete detectable amounts of Gas6 protein, Gas6-Axl signaling may play a supportive role in preventing apoptosis induced by serum deprivation or TNF. On the other hand, Gas6 also can act as a chemoattractant and is involved in cell migration (14); several metastatic cell types have increased expression of the Axl receptor (7, 32, 50). Thus, suppression of the Axl receptor by E1A may partly explain E1A's metastasis-suppressing effect.

In summary, the known characteristics of the Axl receptor and E1A are consistent with our previous findings that E1A functions as a tumor suppressor. Further investigations are required to determine whether negative regulation of Axl by E1A is also involved in the decreased tumorigenicity and decreased metastatic potential observed in ip1-E1A cells. However, the present findings identify a second transforming receptor tyrosine kinase, Axl, that is repressed by E1A.

ACKNOWLEDGMENTS

This work was supported by NIH grants R01-CA58880 and R01-CA77858 (to M.-C.H.).

REFERENCES

1. **Bellosta, P., Q. Zhang, S. P. Goff, and C. Basilico.** 1997. Signaling through the ARK tyrosine kinase receptor protects from apoptosis in the absence of growth stimulation. Oncogene **15:**2387–2397.
2. **Berk, A. J.** 1986. Adenovirus promoters and E1A transactivation. Annu. Rev. Genet. **20:**45–79.
3. **Borrelli, E., R. Hen, and P. Chambon.** 1984. Adenovirus-2 E1A products repress enhancer-induced stimulation of transcription. Nature **312:**608–612.
4. **Burcher, A., E. C. Attar, P. McCloskey, Y.-C. Fridell, and E. T. Liu.** 1998. Determinants for transformation induced by the Axl receptor tyrosine kinase. Oncogene **16:**3177–3187.
5. **Byrd, P. J., R. J. A. Grand, and P. H. Gallimore.** 1988. Differential transformation of primary human embryo retinal cells by adenovirus E1A regions and combinations of E1A + ras. Oncogene **2:**477–484.
6. **Chen, M.-J., B. Holskin, J. Strickler, J. Gorniak, M. A. Clark, P. J. Johnson, M. Mitcho, and D. Shalloway.** 1987. Induction by E1A oncogene expression of cellular susceptibility to lysis by TNF. Nature **330:**581–584.
7. **Cook, J. L., D. L. May, B. A. Wilson, B. Holskin, M.-J. Chen, D. Shalloway, and T. A. Walker.** 1989. Role of tumor necrosis factor-α in E1A oncogene-induced susceptibility of neoplastic cells to lysis by natural killer cells and activated macrophages. J. Immunol. **142:**4527–4534.
8. **Craven, R. J., L. Xu, T. M. Weiner, Y.-W. Fridell, G. A. Dent, S. Srivastava, B. Varnum, E. T. Liu, and W. G. Cance.** 1995. Receptor tyrosine kinases expressed in metastatic colon cancer. Int. J. Cancer **60:**791–797.
9. **Debbas, M., and E. White.** 1993. Wild-type p53 mediates apoptosis by E1A, which is inhibited by E1B. Genes Dev. **7:**546–554.
10. **DeGroot, R., N. Foulkes, M. Mulder, W. Kruijer, and P. Sassone-Corsi.** 1991. Positive regulation of *jun*/Ap-1 by E1A. Mol. Cell. Biol. **11:**192–201.
11. **Deng, J., W. Xia, and M.-C. Hung.** 1998. Adenovirus 5 E1A-mediated tumor suppression associated with E1A-mediated apoptosis *in vivo*. Oncogene **17:**2167–2175.
12. **Douglas, J. L., S. Gopalakrishnan, and M. P. Quinlan.** 1991. Modulation of transformation of primary epithelial cells by the second exon of the Ad5 E1A 12S gene. Oncogene **6:**2093–2103.
13. **Fantl, W. J., D. E. Johnson, and L. T. Williams.** 1993. Signaling by receptor tyrosine kinases. Annu. Rev. Biochem. **62:**453–481.
14. **Fridell, Y.-W. C., J. Villa, Jr., E. C. Attar, and E. T. Liu.** 1998. Gas6 induces Axl-mediated chemotaxis of vascular smooth muscle cells. J. Biol. Chem. **273:**7123–7126.
15. **Frisch, S. M.** 1991. Antioncogenic effect of adenovirus E1A in human tumor cells. Proc. Natl. Acad. Sci. USA **88:**9077–9081.
16. **Frisch, S. M., and K. E. Dolter.** 1995. Adenovirus E1A-mediated tumor suppression by a c-*erbB2/neu*-independent mechanism. Cancer Res. **55:**5551–5555.
17. **Frisch, S. M., R. Reich, I. E. Collier, L. T. Genrich, G. Martin, and G. I. Goldberg.** 1990. Adenovirus E1A represses protease gene expression and inhibits metastasis of human tumor cells. Oncogene **5:**75–83.
18. **Garbisa, S., R. Pozzatti, R. J. Muschel, U. Saffiotti, M. Ballin, R. H. Goldfarb, G. Khoury, and L. A. Liotta.** 1987. Secretion of type IV collagenolytic protease and metastatic phenotype: induction by transfection with c-Ha-ras but not c-Ha-ras plus Ad2-E1a. Cancer Res. **47:**1523–1528.
19. **Goruppi, S., E. Ruaro, and C. Schneider.** 1996. Gas6, the ligand of Axl tyrosine kinase receptor, has mitogenic and survival activities for serum starved NIH3T3 fibroblasts. Oncogene **12:**471–480.
20. **Goruppi, S., E. Ruaro, B. Varnum, and C. Schneider.** 1997. Requirement of phosphatidylinositol 3-kinase-dependent pathway and Src for Gas6-Axl mitogenic and survival activities in NIH 3T3 fibroblasts. Mol. Cell. Biol. **17:**4442–4453.
21. **Hen, R., E. Borrelli, and P. Chambon.** 1985. Repression of the immunoglobulin heavy chain enhancer by the adenovirus-2 E1A products. Science **230:**1391–1394.
22. **Kao, H.-T., and J. R. Nevins.** 1984. Transcriptional activation and subsequent control of the human heat shock gene during adenoviral infection. Mol. Cell. Biol. **4:**2792–2810.
23. **Land, H., L. F. Parada, and R. A. Weinberg.** 1983. Tumorigenic conversion of primary embryo fibroblasts requires at least two cooperating oncogenes. Nature **304:**596–602.
24. **Li, S., M. A. Rizzo, S. Bhattacharya, and L. Huang.** 1998. Characterization of cationic lipid-protamine-DNA (LPD) complexes for intravenous gene delivery. Gene Ther. **5:**930–937.
25. **Linder, S., P. Popowicz, C. Svensson, H. Marshall, M. Bondesson, and G. Akusjarvi.** 1992. Enhanced invasive properties of rat embryo fibroblasts transformed by adenovirus E1A mutants with deletions in the carboxyl-terminal exon. Oncogene **7:**439–443.
26. **Manfioletti, G., C. Brancolini, G. Avanzi, and C. Schneider.** 1993. The protein encoded by a growth arrest-specific gene (*gas6*) is a new member of the vitamin K-dependent proteins related to protein S, a negative coregulator in the blood coagulation cascade. Mol. Cell. Biol. **13:**4976–4985.
27. **Miyazawa, K., A. Mori, H. Miyata, M. Akahane, Y. Ajisawa, and H. Okudaira.** 1998. Regulation of interleukin-1b-induced interleukin-6 gene expression in human fibroblast-synoviocytes by p38 mitogen-activated protein kinase. J. Biol. Chem. **273:**24832–24838.

27a. **Montell, C., G. Courtois, C. Eng, and A. J. Berk.** 1984. Complete transformation by adenovirus 2 requires both E1A proteins. Cell **36:**951–961.

28. **Mymryk, J. S.** 1996. Tumor suppressive properties of the adenovirus 5 E1A oncogene. Oncogene **13:**1581–1589.
29. **Nakano, T., Y. Ishimoto, J. Kishino, M. Umeda, K. Inoue, K. Nagata, K. Ohashi, K. Mizuno, and H. Arita.** 1997. Cell adhesion to phosphatidylserine mediated by a product of growth arrest-specific gene 6. J. Biol. Chem. **272:**29411–29414.
30. **O'Bryan, J. P., R. A. Frye, P. C. Cogswell, A. Neubauer, B. Kitch, C. Prokop, R. Espinosa III, M. M. LeBeau, H. S. Earp, and E. T. Liu.** 1991. *axl*, a transforming gene isolated from primary human myeloid leukemia cells, encodes a novel receptor tyrosine kinase. Mol. Cell. Biol. **11:**5016–5031.
31. **Offringa, R., A. M. Smits, A. Houweling, J. L. Bos, and A. J. van der Eb.** 1988. Similar effects of adenovirus E1A and glucocorticoid hormones on the expression of the metalloprotease stromelysin. Nucleic Acids Res. **16:**10973–10984.
32. **Quong, R. Y. Y., S. T. Bickford, Y. L. Ing, B. Terman, M. Herlyn, and N. J. Lassam.** 1994. Protein kinases in normal and transformed melanocytes. Melanoma Res. **4:**313–319.
33. **Rao, L., M. Debbas, P. Sabbatini, D. Hockenbery, S. Korsmeyer, and E. White.** 1992. The adenovirus E1A proteins induce apoptosis, which is inhibited by the E1B 19-kDa and Bcl-2 proteins. Proc. Natl. Acad. Sci. USA **89:**7742–7746.
34. **Robinson, D., H.-C. Chen, J. T. Yustein, F. He, W.-C. Lin, M. J. Hayman, and H.-J. Kung.** 1998. Tyrosine kinase expression profiles of chicken erythroprogenitor cells and oncogene-transformed erythroblasts. J. Biomed. Sci. **5:**93–100.
35. **Robinson, D., F. Le, T. Pretlow, and H.-J. Kung.** 1996. A tyrosine kinase profile of prostate carcinoma. Proc. Natl. Acad. Sci. USA **93:**5958–5962.
36. **Ruley, H. E.** 1983. Adenovirus early region 1A enables viral and cellular

transforming genes to transform primary cells in culture. Nature **304:**602–606.

37. **Sassone-Corsi, P., and E. Borrelli.** 1987. Promoter transactivation of protooncogenes c-*fos* and c-*myc*, but not c-Ha-*ras*, by products of adenovirus early region 1A. Proc. Natl. Acad. Sci. USA **84:**6430–6433.
38. **Shao, R., M. C.-T. Hu, B. P. Zhou, S.-Y. Lin, P. J. Chiao, R. H. von Lindern, B. Spohn, and M.-C. Hung.** E1A sensitizes cells to tumor necrosis factor-induced apoptosis through inhibition of IκB kinases and nuclear factor κB activities. J. Biol. Chem., in press.
39. **Shao, R., D. Karunagaran, B. P. Zhou, K. Li, S.-S. Lo, J. Deng, P. Chiao, and M.-C. Hung.** 1997. Inhibition of nuclear factor-κB activity is involved in E1A-mediated sensitization of radiation-induced apoptosis. J. Biol. Chem. **272:**32739–32742.
40. **Shenk, T.** 1996. Adenoviridae: the viruses and their replication, p. 2111–2148. *In* B. N. Fields, D. M. Knipe, and P. M. Howley (ed.), Virology. Lippincott-Raven Publishers, Philadelphia, Pa.
41. **Sogawa, K., H. Handa, A. Fujisawa-Sehara, T. Hiromasa, M. Yamane, and Y. Fujii-Kuriyama.** 1989. Repression of cytochrome P450c gene expression by cotransfection with adenovirus E1A DNA. Eur. J. Biochem. **181:**539–544.
42. **Stein, R., and E. Ziff.** 1984. Hela cell β-tubulin gene transcription is stimulated by adenovirus 5 in parallel with viral early genes in an E1A-dependent mechanism. Mol. Cell. Biol. **4:**2792–2801.
43. **Stein, R., and E. B. Ziff.** 1987. Repression of insulin gene expression by adenovirus type 5 E1A proteins. Mol. Cell. Biol. **7:**1164–1170.
44. **Stitt, T. N., G. Conn, M. Gore, C. Lai, J. Bruno, C. Radziejewski, K. Mattsson, J. Fisher, D. R. Gies, P. F. Jones, P. Masiakowski, T. E. Ryan, N. J. Tobkes, D. H. Chen, P. S. DiStefano, G. L. Long, C. Basillico, M. P. Goldfarb, G. Lemke, D. J. Glass, and G. D. Yancopoulos.** 1995. The anticoagulation factor protein S and its relative, GAS6, are ligands for the Tyro 3/Axl family of receptor tyrosine kinase. Cell **80:**661–670.
45. **Teodoro, J. G., G. C. Shore, and P. E. Branton.** 1995. Adenovirus E1A proteins induce apoptosis by both p53-dependent and p53-independent mechanisms. Oncogene **11:**467–474.
46. **Towbin, H., T. Staehelin, and J. Gordon.** 1979. Electrophoretic transfer of proteins from polyacrylamide gels to nitrocellulose sheets: procedure and some applications. Proc. Natl. Acad. Sci. USA **76:**4350–4354.
47. **van der Geer, P., T. Hunter, and R. A. Lindberg.** 1994. Receptor protein-tyrosine kinases and their signal transduction pathways. Annu. Rev. Cell Biol. **10:**251–337.
48. **Varnum, B. C., C. Young, G. Elliott, A. Garcia, T. D. Bartley, Y.-W. Fridell, R. W. Hunt, G. Trail, C. Clogston, R. J. Toso, D. Yanaglhara, L. Bennett, M. Sylber, L. A. Merewether, A. Tseng, E. Escobar, E. T. Liu, and H. K. Yamane.** 1995. Axl receptor tyrosine kinase stimulated by the vitamin K-dependent protein encoded by growth-arrest-specific gene 6. Nature **373:**623–626.
49. **Velich, A., F. G. Kern, C. Basilico, and E. B. Ziff.** 1987. Adenovirus E1A proteins repress expression from polyomavirus early and late promoters. Mol. Cell. Biol. **7:**1164–1170.
50. **Velich, A., and E. B. Ziff.** 1985. Adenovirus E1A proteins repress transcription from the SV40 early promoter. Cell **40:**705–716.
51. **Weiner, T. M., E. T. Liu, R. J. Craven, and W. G. Cance.** 1994. Expression of growth factor receptors, the focal adhesion kinase, and other tyrosine kinases in human soft tissue tumors. Ann. Surg. Oncol. **1:**18–27.
52. **Yan, D.-H., L.-S. Chang, and M.-C. Hung.** 1991. Repressed expression of the *HER-2/c-erb*B-2 proto-oncogene by the adenovirus E1A gene products. Oncogene **6:**343–345.
53. **Yu, D., J.-I. Hamada, H. Zhang, G. L. Nicolson, and M.-C. Hung.** 1992. Mechanisms of *neu* oncogene induced metastasis and abrogation of metastatic properties by the adenovirus 5 E1A gene products. Oncogene **7:**2263–2270.
54. **Yu, D., A. Martin, W. Xia, F. Sorgi, L. Huang, and M.-C. Hung.** 1995. Liposome-mediated *in vivo* E1A gene transfer suppressed dissemination of ovarian cancer cells that overexpress *Her-2/neu*. Oncogene **11:**1383–1388.
55. **Yu, D., K. Scorsone, and M.-C. Hung.** 1991. Adenovirus type 5 E1A gene products act as transformation suppressors of the *neu* oncogene. Mol. Cell. Biol. **11:**1745–1750.
56. **Yu, D., D. Shi, M. Scanlon, and M.-C. Hung.** 1993. Reexpression of *neu*-encoded oncoprotein counteracts the tumor-suppressing but not the metastasis-suppressing function of E1A. Cancer Res. **53:**5784–5790.
57. **Yu, D., T.-C. Suen, D.-H. Yan, L. S. Chang, and M.-C. Hung.** 1990. Transcriptional repression of the *neu* protooncogene by the adenovirus 5 E1A products. Proc. Natl. Acad. Sci. USA **87:**4499–4503.
58. **Yu, D., J. K. Wolf, M. Scanlon, J. E. Price, and M.-C. Hung.** 1993. Enhanced *c-erbB-2/neu* expression in human ovarian cancer cells correlates with more severe malignancy that can be suppressed by E1A. Cancer Res. **53:**891–898.

Cytoplasmic localization of p21$^{Cip1/WAF1}$ by Akt-induced phosphorylation in *HER-2/neu*-overexpressing cells

Binhua P. Zhou, Yong Liao, Weiya Xia, Bill Spohn, Mong-Hong Lee and Mien-Chie Hung*

Department of Molecular and Cellular Oncology, Breast Cancer Basic Research Program, University of Texas M. D. Anderson Cancer Center, Houston, Texas 77030, USA
**e-mail: mhung@notes.mdacc.tmc.edu*

Amplification or overexpression of *HER-2/neu* in cancer cells confers resistance to apoptosis and promotes cell growth. The cellular localization of p21$^{Cip1/WAF1}$ has been proposed to be critical either in promoting cell survival or in inhibiting cell growth. Here we show that *HER-2/neu*-mediated cell growth requires the activation of Akt, which associates with p21$^{Cip1/WAF1}$ and phosphorylates it at threonine 145, resulting in cytoplasmic localization of p21$^{Cip1/WAF1}$. Furthermore, blocking the Akt pathway with a dominant-negative Akt mutant restores the nuclear localization and cell-growth-inhibiting activity of p21$^{Cip1/WAF1}$. Our results indicate that *HER-2/neu* induces cytoplasmic localization of p21$^{Cip1/WAF1}$ through activation of Akt to promote cell growth, which may have implications for the oncogenic activity of *HER-2/neu* and Akt.

The *HER-2/neu* gene (also known as *c-erbB2*) encodes a transmembrane receptor tyrosine kinase of relative molecular mass 185,000 (M_r 185K) that shares partial homology with the other members of the family of epidermal growth-factor receptors. Amplification or overexpression of *HER-2/neu* occurs in ~30% of human breast and ovarian cancers and is a marker of poor prognosis[1–3]. We have previously shown that *HER-2/neu* activates the phosphatidylinositol-3 kinase (PI-3K)/Akt pathway and confers resistance to apoptosis induced by tumour-necrosis factor[4]. The PI-3K/Akt pathway has an important role in preventing cells from undergoing apoptosis and contributes to the pathogenesis of malignancy[5,6]. For example, activated Akt phosphorylates specific targets such as Bad[7], caspase-9 (ref. 8), forkhead transcription factors[9,10] and IKK-α (refs 11, 12), thereby promoting cell survival. However, in addition to its anti-apoptotic function, Akt is also involved in cell proliferation[13–15]. Furthermore, Akt detaches from the inner surface of the plasma membrane, where it is initially activated, and relocalizes to the nucleus within 30 min of activation by growth factors[16,17]. These findings indicate that some critical Akt targets that control cell-cycle progression may be located within the nucleus.

Cell-cycle progression is tightly regulated by the family of cyclin-dependent kinase (CDK) inhibitors. p21$^{Cip1/WAF1}$ was identified through its interaction with Cdk2 (ref. 18), and its expression is induced by activation of wild-type p53 (ref. 19), and during cellular senescence[20]. The cell-growth-inhibiting activity of p21$^{Cip1/WAF1}$ is strongly correlated with its nuclear localization[21,22]. However, recent evidence has shown that p21$^{Cip1/WAF1}$ can also localize in the cytoplasm and has an important role in protecting cells against apoptosis. For instance, nuclear p21$^{Cip1/WAF1}$ translocates to the cytoplasm after differentiation of U937 cells into monocytes, and this translocation event is accompanied by resistance to various apoptotic stimuli[23]. Furthermore, cytoplasmic p21$^{Cip1/WAF1}$ forms a complex with apoptosis-signal-regulating kinase 1 (ASK1) that inhibits the stress-induced mitogen-activated protein (MAP) kinase cascade and therefore results in resistance to apoptosis in these cells[23]. However, the mechanism that regulates the localization of p21$^{Cip1/WAF1}$ is still unknown.

Here we show that blocking the Akt pathway by using a dominant negative Akt mutant (DN-Akt) inhibits cell growth. This growth inhibition is correlated with nuclear localization of p21$^{Cip1/WAF1}$. We demonstrate that Akt can associate with p21$^{Cip1/WAF1}$ and phosphorylates a consensus threonine residue (T145) in the nuclear-localization signal (NLS) of p21$^{Cip1/WAF1}$, leading to the cytoplasmic localization of p21$^{Cip1/WAF1}$. We thus identify a new signalling pathway and show that overexpression of *HER-2/neu* may enhance cell proliferation by inducing cytoplasmic localization of p21$^{Cip1/WAF1}$ through the serine/threonine kinase Akt.

Results

The Akt pathway is required for *HER-2/neu*-mediated cell proliferation. To study the effect of Akt on *HER-2/neu*-mediated cell proliferation, we used a model system that consists of NIH3T3 cells, *HER-2/neu* 3T3 cells (NIH3T3 cells transformed with *HER-2/neu*) and DN-Akt 3T3 cells (*HER-2/neu* 3T3 cells transfected with DN-Akt)[4]. As expected, *HER-2/neu* 3T3 cells grew much faster than the parental NIH3T3 cells (Fig. 1a). The Akt pathway is known to be constitutively activated in *HER-2/neu* 3T3 cells[4], and when this pathway was blocked by DN-Akt, cell growth became slower (Fig. 1a). This was not due to the heterogeneity of the cell clones, because a specific PI-3K inhibitor, wortmannin, also produced a similar slowing of growth in *HER-2/neu* 3T3 cells (Fig. 1a). When the DNA synthesis rate was determined by measuring incorporation of [^{3}H]thymidine, *HER-2/neu* 3T3 cells also exhibited greater amounts of DNA synthesis than the parental NIH3T3 cells (Fig. 1b). *HER-2/neu*-induced DNA synthesis was significantly inhibited by blocking the Akt pathway with either wortmannin or DN-Akt.

As the net rate of cell growth depends on a fine balance between the rates of cell proliferation and cell death, we also investigated whether apoptosis contributes to the difference in growth in these cells. There was no significant difference in apoptosis among these cells, as measured by fluorescence-activated cell sorting (FACS) analysis (Fig. 1c). Therefore, the reduction in cell growth in DN-Akt 3T3 cells was most probably a result of the reduction in cell proliferation. To investigate further, we also carried out the same experiments using another *HER-2/neu*-overexpressing breast-cancer cell line, MDA-MB453, and stable DN-Akt transfectants of it[4]. As in *HER-2/neu* 3T3 and DN-Akt 3T3 cells, three independent clones of DN-Akt transfectants showed reductions in cell growth and DNA synthesis (Fig. 1d, e), but no difference was observed in apoptosis (FACS analysis, data not shown). A revertant that had lost DN-Akt during culture exhibited rates of cell growth and DNA synthesis that were almost identical to those of parental MDA-

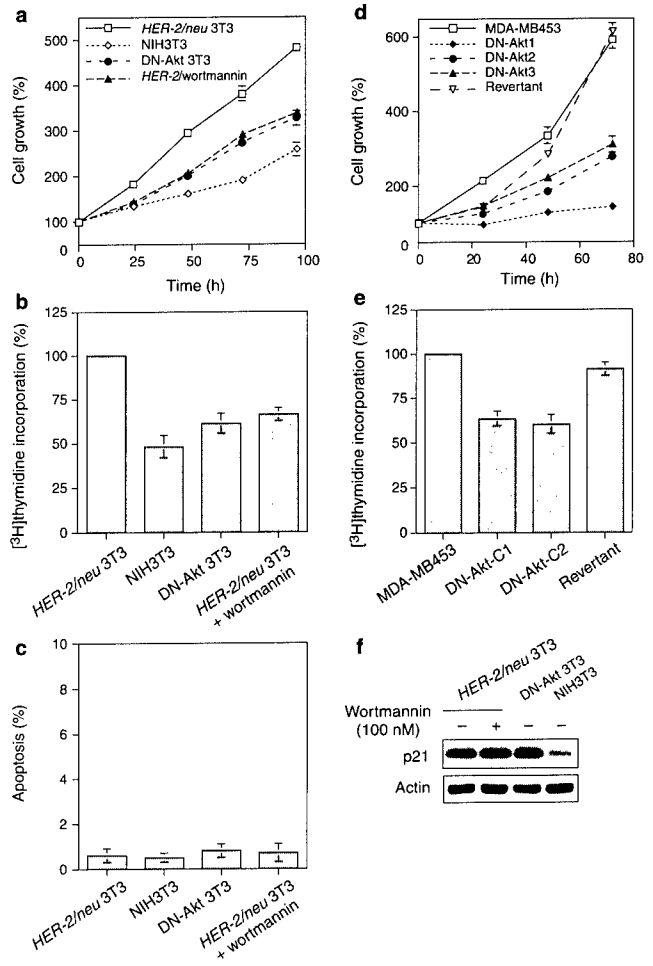

Figure 1 **The Akt pathway is required for *HER-2/neu*-mediated cell proliferation. a**, Blocking the Akt pathway reduces the growth of *HER-2/neu* 3T3 cells. Cells (3×10^3) were seeded in 96-well plates and grown in DMEM/F12 plus 1% FBS. Growth rates were monitored by the MTT assay. Data are means ± s.e.m. from three independent experiments, each carried out in quadruplicate. **b**, Cells (3×10^3) were grown as in **a** with 1 μCi [^{3}H]thymidine for 12 h. Rates of cell replication were determined by measuring [^{3}H]thymidine incorporation. Data are means ± s.e.m. from three independent experiments, each carried out in quadruplicate. **c**, Blocking the Akt pathway does not significantly induce apoptosis in *HER-2/neu* 3T3 cells. Cells were grown in 1% serum, and the percentage of cells in apoptosis was measured by FACS as described[4]. Data are means ± s.e.m. from three independent experiments. **d**, Blocking the Akt pathway reduces cell growth in MDA-MB453 cells. Cells were grown in six-well plates as in **a**, and their growth rates were measured by cell counting (see Methods). Data are means ± s.e.m. from three independent experiments. **e**, Rates of DNA synthesis in each of the cell lines in **d** was determined as in **b**. **f**, Overexpression of *HER-2/neu* induces expression of p21$^{Cip1/WAF1}$. Lysates (50 μg) from the indicated cell lines were analysed by 12% SDS–PAGE. After proteins were transferred to a nitrocellulose membrane, expression of p21$^{Cip1/WAF1}$ was measured using a monoclonal antibody against p21$^{Cip1/WAF1}$ (Pharmingen).

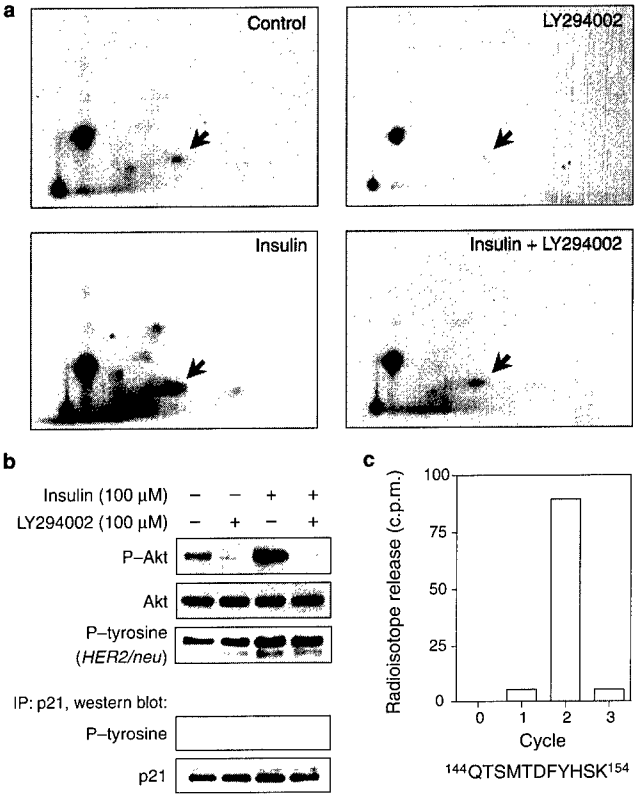

Figure 2 **Threonine 145 of p21$^{Cip1/WAF1}$ is phosphorylated *in vivo*. a**, Endogenous p21$^{Cip1/WAF1}$ is phosphorylated *in vivo* in response to insulin. MDA-MB453 cells were incubated with 1.5 mCi ml^{-1} [^{32}P]orthophosphate for 3.5 h and then stimulated for 30 min with insulin in the presence or absence of LY294002. Cells were then lysed, and the endogenous p21$^{Cip1/WAF1}$ was immunoprecipitated with a specific antibody and subjected to two-dimensional phosphopeptide analysis (see Methods). Arrows indicate the spots induced by insulin and inhibited by PI-3K inhibitor. **b**, Tyrosine residues in p21$^{Cip1/WAF1}$ are not phosphorylated. MDA-MB453 cells were treated as in **a**, and one-third of the lysate was analysed by western blotting for activation of Akt and tyrosine phosphorylation of *HER-2/neu* (exposure to anti-phosphotyrosine antibody clone 4G10 (Upstate Biotechnology) for 2 s). The remaining lysate was subjected to immunoprecipitation (IP) with a specific antibody against p21$^{Cip1/WAF1}$, and to western blotting with specific antibodies against p21$^{Cip1/WAF1}$ and phosphotyrosine (exposure to clone 4G10 for 20 min). P denotes phosphorylation. **c**, p21$^{Cip1/WAF1}$ is phosphorylated at T145. MDA-MB453 cells were treated as in **a**, and p21$^{Cip1/WAF1}$ was immunoprecipitated and subjected to trypsin digestion and to amino-acid sequencing by Edman degradation (the sequence of the relevant peptide is shown at the bottom). The amount of radioisotope released from each cycle of Edman degradation was detected with a Cerenkov counter. Background counts, which were typically 50–60 c.p.m., were subtracted from each measurement.

MB453 cells (Fig. 1d, e). Together, our results indicate that the Akt pathway is required for *HER-2/neu*-mediated cell proliferation and that inhibition of this pathway, either by a PI-3K inhibitor or by DN-Akt, significantly reduces cell proliferation.

Cell proliferation is tightly regulated by the family of CDK inhibitors. For example, p21$^{Cip1/WAF1}$ has been shown to have a critical function in regulating cell proliferation[18–20]. We therefore monitored expression of p21$^{Cip1/WAF1}$ in the cell lines described above. Levels of p21$^{Cip1/WAF1}$ expression were significantly higher in *HER-2/neu* 3T3 cells than in the parental cells (Fig. 1f), which is consistent with previous results[24]. Inhibition of the Akt pathway by DN-Akt did not significantly affect p21$^{Cip1/WAF1}$ expression (Fig. 1f). This result cannot account for the *HER-2/neu*-induced cell proliferation and indicates that there may be an unknown mechanism that overrides that of enhanced expression of p21$^{Cip1/WAF1}$ in *HER-2/neu* 3T3 cells.

Threonine 145 of p21$^{Cip1/WAF1}$ is phosphorylated by Akt. As protein phosphorylation has a significant role in the regulation of protein function, and as p21$^{Cip1/WAF1}$ has been shown to be phosphorylated *in vitro* by protein kinase C (ref. 25), we examined the phosphorylation pattern of endogenous p21$^{Cip1/WAF1}$, using *in vivo* [^{32}P]orthophosphate labelling and two-dimensional phosphopeptide analysis (Fig. 2a). A strong phosphorylated peptide spot was observed after induction by

insulin, which is known to activate PI-3K/Akt; this spot was much weaker in cells that were incubated with the PI-3K inhibitor LY294002. This insulin-induced phosphorylation spot was most probably a result of phosphorylation of serine or threonine, rather than tyrosine, residues in $p21^{Cip1/WAF1}$, because no tyrosine phosphorylation was detected when endogenous $p21^{Cip1/WAF1}$ was immunoprecipitated and examined by western blotting with a specific antibody against phosphorylated tyrosine (Fig. 2b). The fact that no tyrosine-phosphorylated endogenous $p21^{Cip1/WAF1}$ was detected was not due to the quality of the antibody, because the same antibody was able to detect tyrosine phosphorylation of the *HER-2/neu* gene product in the same cell lysate (Fig. 2b). We investigated further the site of insulin-induced phosphorylation in $p21^{Cip1/WAF1}$ by *in vivo* [^{32}P]orthophosphate labelling, and then subjected the trypsin-digested phosphopeptides to amino-acid sequencing by Edman degradation. The activity of radioisotope was released after the second cycle of Edman degradation (Fig. 2c), but was greatly reduced when cells were pretreated with LY294002 (data not shown). Judging from the amino-acid sequence of $p21^{Cip1/WAF1}$, the only trypsin-digested peptide that contains threonine or serine at position 2 in its sequence is ^{144}QTSMTDFYHSK^{154}. Thus, our results indicate that T145 of $p21^{Cip1/WAF1}$ is phosphorylated *in vivo* and that this phosphorylation could be induced by insulin and inhibited by PI-3K inhibitor.

The nuclear localization of $p21^{Cip1/WAF1}$ seems to be responsible for its inhibition of cell growth and is controlled by the NLS at its carboxy terminus[26]. We noticed that there is a putative Akt-phosphorylation motif, containing the phosphorylated T145 residue (Fig. 2) in the NLS of $p21^{Cip1/WAF1}$ and that motif is highly conserved among different species (Fig. 3a). To determine whether Akt interacts with and phosphorylates $p21^{Cip1/WAF1}$ and so regulates its cellular localization, we first carried out co-immunoprecipitation experiments to detect an association between Akt and $p21^{Cip1/WAF1}$. After immunoprecipitating endogenous Akt from MDA-MB453 cells, we detected the presence of endogenous $p21^{Cip1/WAF1}$, whereas no endogenous $p21^{Cip1/WAF1}$ was detected using a non-specfic antibody (Fig. 3b). We also co-transfected 293T cells with constitutively active Akt (CA-Akt) or DN-Akt together with wild-type or mutant $p21^{Cip1/WAF1}$ (the mutant containing a T145A mutation). After immunoprecipitating $p21^{Cip1/WAF1}$, we detected Akt and vice versa (Fig. 3c, d), indicating that these two molecules are associated. This association was dependent on the phosphorylation status of Akt and on the status of $p21^{Cip1/WAF1}$. $p21^{Cip1/WAF1}$ associated more strongly with CA-Akt than with DN-Akt, and un-phosphorylated $p21^{Cip1/WAF1}$(T145A) associated much more weakly with Akt than did wild-type $p21^{Cip1/WAF1}$. Furthermore, Akt could phosphorylate $p21^{Cip1/WAF1}$ both *in vitro* and *in vivo*, whereas DN-Akt could not (Fig. 3e, f). The fact that no phosphorylation was observed on $p21^{Cip1/WAF1}$(T145A) indicates that Akt interacts with $p21^{Cip1/WAF1}$ and phosphorylates it at T145. This is further supported by the fact that phosphorylation at T145 is induced by insulin and inhibited by LY294002 (Fig. 2), as Akt is known to be activated by insulin and inhibited by LY294002.

Activation of Akt induces cytoplasmic localization of $p21^{Cip1/WAF1}$. We next tested whether the activation of Akt affects the cellular localization of $p21^{Cip1/WAF1}$. We co-transfected $p21^{-/-}$ mouse embryonic fibroblasts (MEFs) with CA-Akt or DN-Akt together with wild-type or mutant $p21^{Cip1/WAF1}$ (the mutants containing T145A or T145D mutations) and examined the cellular localization of $p21^{Cip1/WAF1}$ by immunofluorescence analysis. As shown in Fig. 4, wild-type $p21^{Cip1/WAF1}$ was predominantly present in the cytoplasm in the presence of CA-Akt, but was predominantly in the nucleus when DN-Akt was introduced. Mutation at T145A abolished cytoplasmic localization even in the presence of CA-Akt. $p21^{Cip1/WAF1}$(T145D), which mimics $p21^{Cip1/WAF1}$ phosphorylated by Akt, was predominantly present in the cytoplasm, regardless of the activation status of the Akt pathway. These results indicate that T145 in the NLS of $p21^{Cip1/WAF1}$ is critical in determining its cellular localization, and that phosphorylation at this site by Akt results in

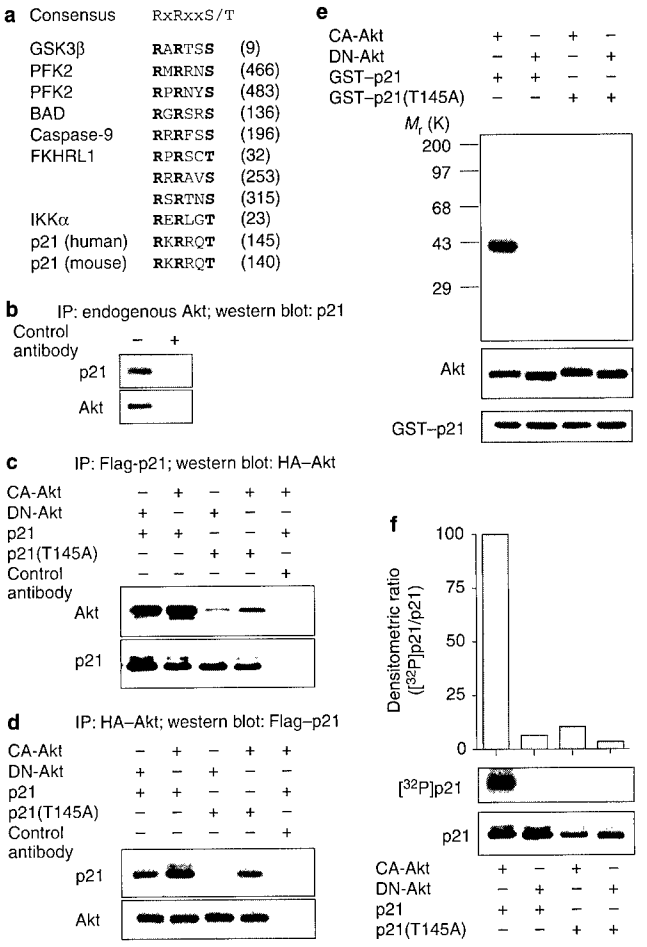

Figure 3 **Akt interacts with $p21^{Cip1/WAF1}$ and phosphorylates it at threonine 145. a**, Comparison of the amino-acid sequences of the Akt-phosphorylation motifs of $p21^{Cip1/WAF1}$ and other known Akt substrates. The consensus sequence is shown at the top. Numbers on the right indicate the positions of the final residues shown in each case. **b**, Immunoprecipitation (IP) of endogenous Akt and detection of endogenous $p21^{Cip1/WAF1}$. Endogenous Akt was immunoprecipitated from 1,000 μg of MDA-MB453 cell lysate with a specific antibody against Akt or with control immunoglobulin G. After transfer to a nitrocellulose membrane, endogenous $p21^{Cip1/WAF1}$ was detected with a specific antibody against $p21^{Cip1/WAF1}$. **c**, Immunoprecipitation of $p21^{Cip1/WAF1}$ and detection of Akt. HA-tagged DN-Akt or CA-Akt (10 μg) and Flag-tagged wild-type or mutant $p21^{Cip1/WAF1}$ (10 μg) were co-transfected into 293T cells. Cells were lysed after 48 h and $p21^{Cip1/WAF1}$ was immunoprecipitated with anti-Flag antibody. After transfer to a nitrocellulose membrane, Akt was detected with anti-HA antibody. **d**, Immunoprecipitation of Akt and western blotting of $p21^{Cip1/WAF1}$. Akt was immunoprecipitated with an anti-HA antibody and $p21^{Cip1/WAF1}$ was detected with an anti-Flag antibody. **e**, Akt phosphorylates $p21^{Cip1/WAF1}$ at T145. HA-tagged CA-Akt or DN-Akt (20 μg) was transiently transfected into 293T cells as described above. After 48 h of incubation, CA-Akt or DN-Akt was immunoprecipitated with an anti-HA antibody and incubated with 5 μg of either GST–$p21^{Cip1/WAF1}$ or GST–$p21^{Cip1/WAF1}$(T145A) in kinase buffer containing 5 μCi [γ-^{32}P]ATP for 30 min at 30 °C. The kinase reaction was terminated with SDS–PAGE buffer, and samples were assayed by autoradiography. The lower two panels show western blots for Akt and the GST-fusion protein used in the phosphorylation reaction, detected with antibodies against Akt and $p21^{Cip1/WAF1}$, respectively. **f**, CA-Akt or DN-Akt (18 μg) and Flag-tagged wild-type or mutant $p21^{Cip1/WAF1}$ (T145A mutation; 2 μg) were co-transfected into 293T cells. After 48 h cells were labelled with 1 mCi ml^{-1} [^{32}P]-orthophosphate for 3 h. $p21^{Cip1/WAF1}$ was immunoprecipitaed from lysates and analysed either by autoradiography, to detect phosphorylation of $p21^{Cip1/WAF1}$ *in vivo* (upper panel), or by western blotting, as a control for equal amounts of $p21^{Cip1/WAF1}$ (lower panel). The histogram shows the amounts of labelled $p21^{Cip1/WAF1}$ relative to the amount of immunoprecipitated $p21^{Cip1/WAF1}$ in western blots.

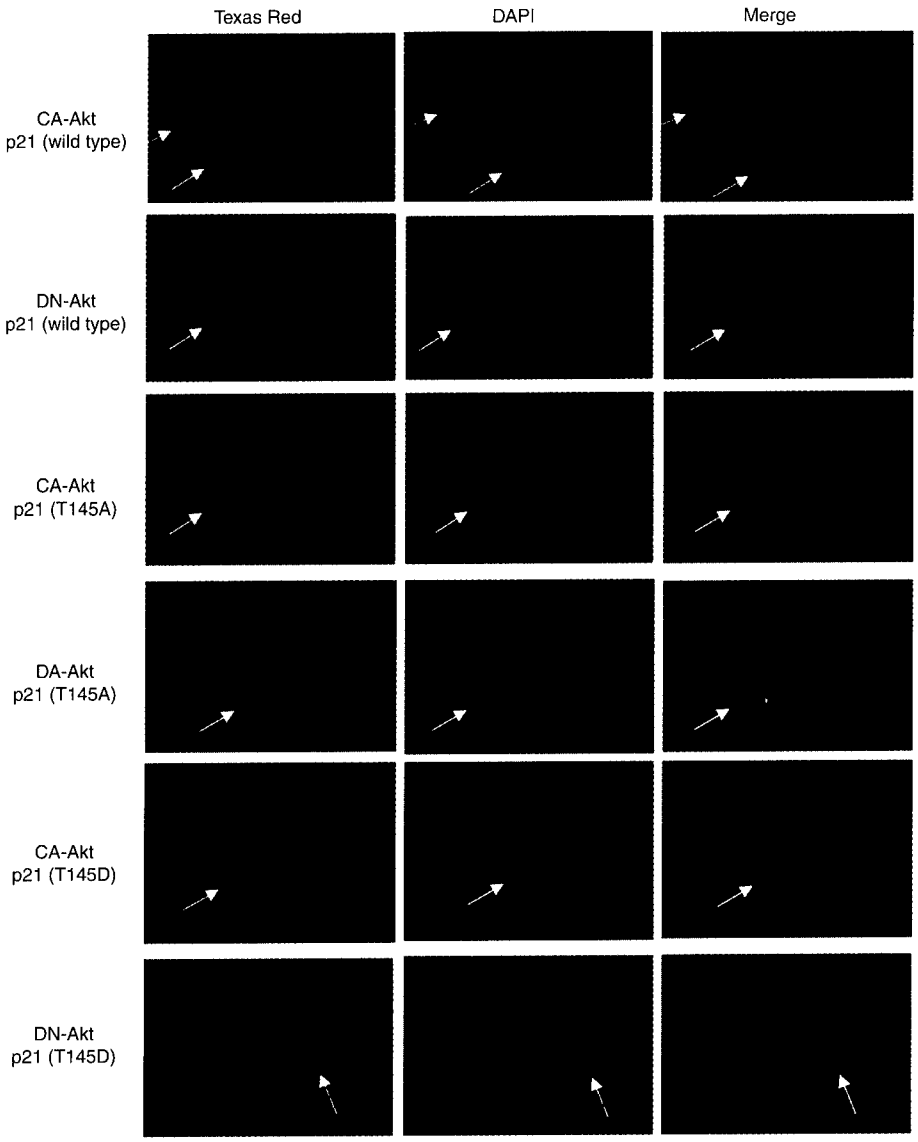

Figure 4 **Akt alters the cellular localization of $p21^{Cip1/WAF1}$.** CA-Akt or DN-Akt (9 μg) and wild-type or mutant $p21^{Cip1/WAF1}$ (1 μg) were co-transfected into $p21^{-/-}$ MEFs. After 36 h of incubation, cells were trypsinized and plated onto chamber slides for a further 12 h. After fixation, the cellular localization of $p21^{Cip1/WAF1}$ was detected using a monoclonal antibody against human $p21^{Cip1/WAF1}$. After extensive washing in PBS, samples were further incubated with Texas Red-conjugated goat anti-mouse immunoglobulin G plus DAPI and examined by fluorescence microscopy. When wild-type $p21^{Cip1/WAF1}$ was co-transfected with CA-Akt, ~75% was localized in the cytoplasm. However, when wild-type $p21^{Cip1/WAF1}$ was co-transfected with DN-Akt, ~90% was detected in the nucleus. When $p21^{Cip1/WAF1}$(T145A) was co-transfected with CA-Akt or DN-Akt, ~80% and ~90%, respectively, was localized in the nucleus. When $p21^{Cip1/WAF1}$(T145D) was cotransfected with CA-Akt or DN-Akt, ~72% and ~78%, respectively, was localized in the cytoplasm.

cytoplasmic localization of $p21^{Cip1/WAF1}$.

We carried out the above experiments in cells that were transiently transfected with exogenous genes. To investigate whether endogenous $p21^{Cip1/WAF1}$ can be regulated in a similar way, we first carried out biochemical cellular fractionation to determine the localization of endogenous $p21^{Cip1/WAF1}$ in *HER-2/neu*-overexpressing cells and their DN-Akt transfectants. $p21^{Cip1/WAF1}$ was predominantly located in the cytoplasm in both *HER-2/neu* 3T3 cells and MDA-MB453 cells, in which Akt was constitutively activated (Fig. 5a). However, when the Akt pathway was blocked by DN-Akt, $p21^{Cip1/WAF1}$ was primarily present in the nucleus in both DN-Akt 3T3 and DN-Akt/MB453 cells (Fig. 5a). As a control, we used actin and proliferating-cell nuclear antigen (PCNA) as cytoplasmic and nuclear markers, respectively, to confirm that the observed cellular localization of $p21^{Cip1/WAF1}$ was not due to contamination. Similar results were obtained when we stained *HER-2/neu* 3T3 cells and their DN-Akt transfectants for endogenous $p21^{Cip1/WAF1}$ using the same techniques as described in Fig. 4 (data not shown). To investigate further whether phosphorylation of endogenous $p21^{Cip1/WAF1}$ by Akt affects its subcellular localization, we treated MDA-MB453 cells with insulin, which is known to be a potent Akt activator (Fig. 2b). Endogenous $p21^{Cip1/WAF1}$ was present in both the nucleus and cytoplasm of MDA-MB453 cells, and the cytoplasmic fraction of $p21^{Cip1/WAF1}$ was significantly increased upon stimulation of insulin (Fig. 5b). Although equal amounts of protein were loaded onto the gel, the ratio of the protein contents of cytoplasm and nucleus was roughly 10:1 in the cellular fraction. In contrast to parental cells, endogenous $p21^{Cip1/WAF1}$ was mainly in the nucleus in DN-Akt

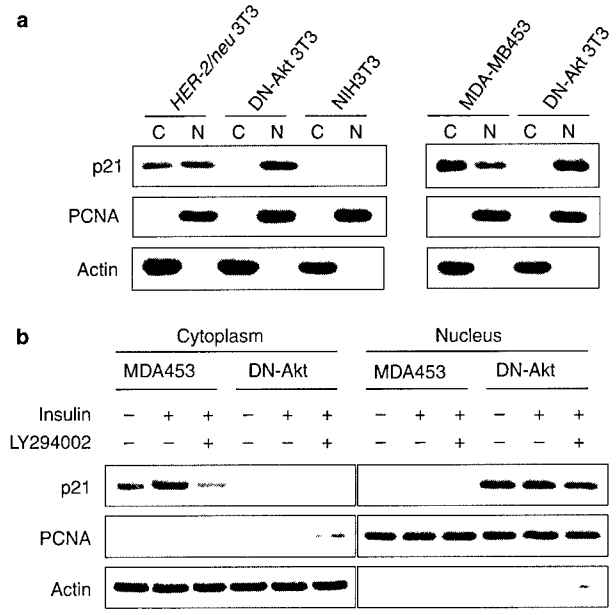

Figure 5 **Cellular localization of endogenous p21$^{Cip1/WAF1}$.** **a**, Cellular fractionation was carried out to determine the cellular localization of p21$^{Cip1/WAF1}$ in *HER-2/neu* 3T3 cells, MDA-MB453 cells, and their DN-Akt transfectants (see Methods). Equal amounts (40 μg) of cytoplasmic fraction (C) and nuclear fraction (N) from each sample were analysed by 12% SDS–PAGE. Actin and proliferating-cell nuclear antigen (PCNA) were used as markers of the cytoplasmic and nuclear fractions, respectively. In each cellular fractionation, ten times as much protein was present in the cytoplasm as in the nucleus. **b**, The cellular location of endogenous p21$^{Cip1/WAF1}$ is regulated by activation of Akt. MDA-MB453 cells were stimulated with insulin in the presence or absence of the PI-3K inhibitor LY294002. Cellular fractionation was carried out (see Methods). Equal amounts of cytoplasmic and nuclear fraction from each sample were analysed by western blotting.

transfectants, and this nuclear localization was not affected by insulin treatment. Together, these results indicate that the distribution of endogenous p21$^{Cip1/WAF1}$ can be regulated by extracellular stimuli, such as insulin, through the PI-3K/Akt pathway.

These results clearly demonstrate that p21$^{Cip1/WAF1}$ is regulated by the *HER-2/neu*–Akt pathway in cell culture. To determine whether this is also the case in tumour tissues, we compared the levels of activated (phosphorylated) Akt and the cellular localization of p21$^{Cip1/WAF1}$ in five *HER-2/neu*-positive and five *HER-2/neu*-negative human breast tumours by immunostaining with specific antibodies against phosphorylated Akt and against p21$^{Cip1/WAF1}$. Consistent with our previous results[4], Akt was activated in all *HER-2/neu*-positive breast tumours. In these tissues, p21$^{Cip1/WAF1}$ was present in both the nucleus and the cytoplasm. In contrast, in all *HER-2/neu*-negative breast tumours examined, Akt was not activated, and p21$^{Cip1/WAF1}$ was primarily localized in the nucleus. A representative experiment is shown in Fig. 6. The tumour-staining data support our findings in cell-culture experiments and further strengthen the hypothesis that overexpression of *HER-2/neu* can regulate the cellular distribution of p21$^{Cip1/WAF1}$ through activation of Akt.

Nuclear p21$^{Cip1/WAF1}$(T145A) preferentially supresses growth of transforming cells. Because Akt can phosphorylate p21$^{Cip1/WAF1}$ and cause it to be localized in the cytoplasm, we next investigated whether the phosphorylation status of p21$^{Cip1/WAF1}$ at T145 affects the cell-growth-inhibiting activity of p21$^{Cip1/WAF1}$. We transfected NIH3T3, HER-2/*neu* 3T3, and DN-Akt 3T3 cells with wild-type p21$^{Cip1/WAF1}$ and its mutants T145A (which cannot be phosphorylated) and T145D (which mimics the phosphorylated wild type), and measured their growth-inhibiting activity using a colony-formation assay. As shown in Fig. 7a, wild-type p21$^{Cip1/WAF1}$ did not effectively inhibit the growth of *HER-2/neu* 3T3 cells, in which Akt is constitutively activated, compared with NIH3T3 and DN-Akt 3T3 cells. However, p21$^{Cip1/WAF1}$(T145A) caused similar inhibition of growth in these three cell lines, and this activity was independent of activation of Akt. In contrast, p21$^{Cip1/WAF1}$(T145D) in all three cell lines behaved similarly to the wild type in *HER-2/neu* 3T3 cells. When the rate of DNA synthesis was measured by incorporation of bromodeoxyuridine (BrdU) (Fig. 7b), inhibition of growth by

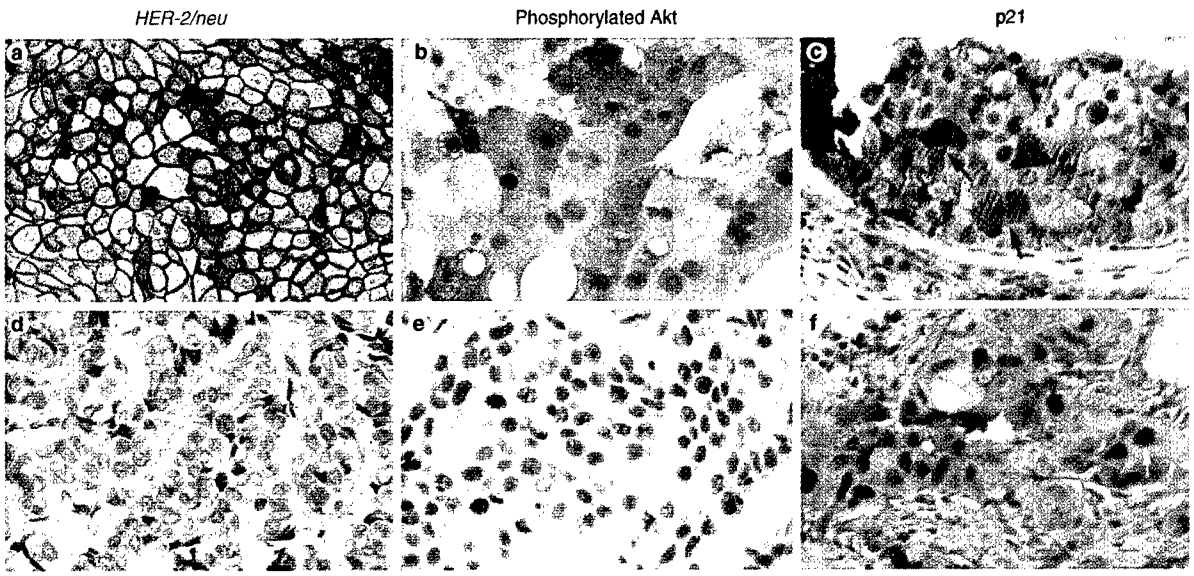

Figure 6 ***HER-2/neu* activates Akt and induces cytoplasmic localization of p21$^{Cip1/WAF1}$ in breast tumours.** Tissue sections from *HER-2/neu*-positive (**a–c**) and HER-2/*neu*-negative (**d–f**) adenocarcinomas were stained with specific antibodies against *HER-2/neu* (**a**, **d**), phosphorylated Akt (**b**, **e**) and p21$^{Cip1/WAF1}$ (**c**, **f**), or with normal rabbit serum (data not shown). Immunostaining was visualized with peroxidase-conjugated secondary antibody. Black and white arrows indicate the cytoplasmic and nuclear localization of p21$^{Cip1/WAF1}$ in **c** and **f**, respectively.

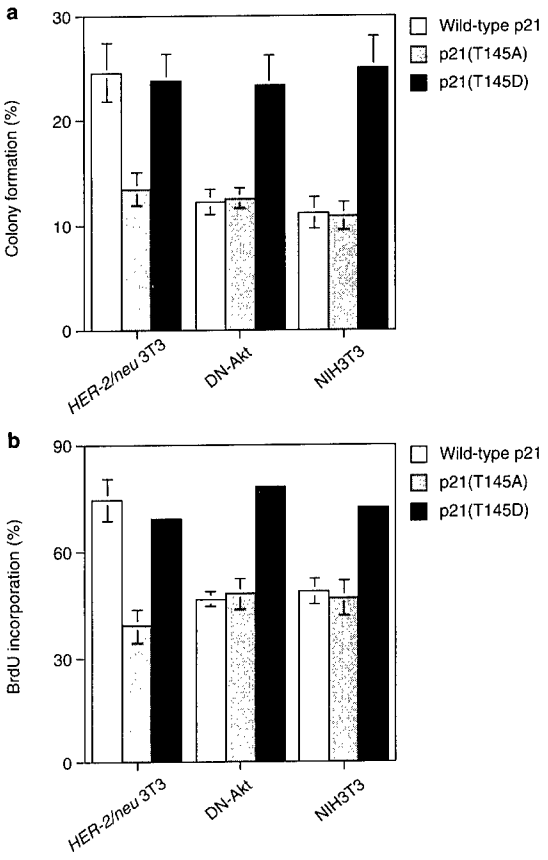

Figure 7 **Growth-inhibiting activities of p21$^{Cip1/WAF1}$ mutants.** p21$^{Cip1/WAF1}$(T145D) has reduced inhibition activity, whereas p21$^{Cip1/WAF1}$(T145A) retains its inhibition activity independently of Akt activation. **a**, The colony-formation assay was used to measure the inhibition activity of p21$^{Cip1/WAF1}$ and its mutants. Wild-type or mutant p21$^{Cip1/WAF1}$ (T145A or T145D mutation) or the vector pcDNA3 (2 μg of each) was transfected into NIH3T3, *HER-2/neu* 3T3, and DN-Akt 3T3 cells. The number of colonies from each transfectant was determined by crystal-violet staining. Percentages of colonies for wild-type and mutant p21$^{Cip1/WAF1}$ were calculated by defining the number obtained from vector transfection alone as 100%. Data are means ± s.e.m. from four independent experiments. **b**, The BrdU-incorporation assay was also used to measure the inhibition activity of p21$^{Cip1/WAF1}$ and its mutants. Vector containing membrane-bound GFP (1 μg) and wild-type or mutant p21$^{Cip1/WAF1}$ or vector pcDNA3 (9 μg each) were co-transfected into NIH3T3, *HER-2/neu* 3T3, and DN-Akt 3T3 cells, using liposome. After 48 h of incubation, cells were labelled with BrdU for 1 h and fixed with 70% ethanol. Cells were then stained with anti-BrdU antibody and incubated with fluorescein-conjugated secondary antibody. After extensive washing, cells were sorted for the presence of GFP signal, and incorporation of BrdU was measured by FACS analysis. Percentages of BrdU incorporation for wild-type and mutant p21$^{Cip1/WAF1}$ were calculated by defining the number obtained from vector (pcDNA3) alone as 100%. Data are means ± s.e.m. from two separate experiments.

wild-type p21$^{Cip1/WAF1}$ was regulated by the activation status of Akt, which is consistent with the results of the colony-formation assay. p21$^{Cip1/WAF1}$(T145A) inhibited growth independently of Akt activation. The activity of p21$^{Cip1/WAF1}$(T145D) was also independent of Akt activation, although its inhibitory effect was weaker in all three cells and was comparable to that of wild-type p21$^{Cip1/WAF1}$ in *HER-2/neu*3T3 cells, in which p21$^{Cip1/WAF1}$ is predominantly located in the cytoplasm. Why p21$^{Cip1/WAF1}$(T145D) only partially lost its ability to inhibit cell growth is not clear. One explanation is that it may still retain its ability to inhibit the function of Cdk2, Cdk4 and cyclin D,

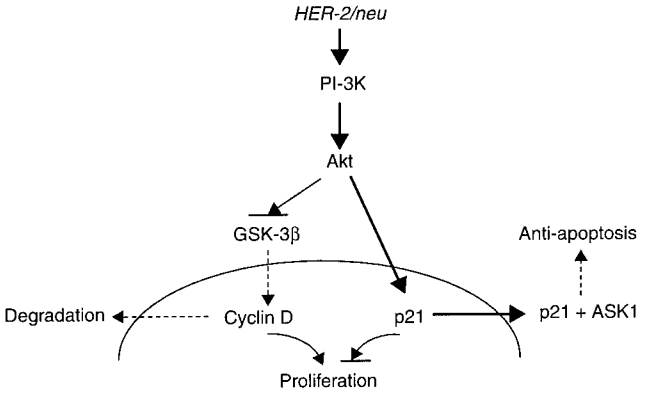

Figure 8 **Model for *HER-2/neu*-induced cytoplasmic localization of p21$^{Cip1/WAF1}$ through activation of Akt.** Dashed lines are derived from previous studies[23,28]. Solid lines are derived from the study reported here.

which shuttle between the nucleus and cytoplasm. Alternatively, cytoplasmic p21$^{Cip1/WAF1}$ may also have effects on cell growth. Further systemic study is required to elucidate the detailed mechanism. Together, our results indicate that phosphorylation at T145 in the NLS of p21$^{Cip1/WAF1}$ by Akt triggers cellular localization and thereby regulates the growth-inhibiting activity of p21$^{Cip1/WAF1}$.

Discussion

The cellular localization of p21$^{Cip1/WAF1}$ was recently proposed to be critical for the regulation of p21$^{Cip1/WAF1}$ function[27]. However, the mechanism by which the cellular localization of p21$^{Cip1/WAF1}$ is controlled was not known. Here we have identified this mechanism as phosphorylation by Akt of p21$^{Cip1/WAF1}$ at T145, which results in cytoplasmic localization and suppression of growth-inhibiting activity. Our results, together with previous findings[28], lead us to propose a plausible model for how Akt simultaneously coordinates two functionally different proteins to achieve a harmonious effect on cell proliferation (Fig. 8). On one hand, activation of Akt inhibits glycogen synthase kinase-3β (GSK-3β) and stabilizes the growth-promoting factor cyclin D in the nucleus to stimulate cell growth[28], whereas on the other hand, Akt can also phosphorylate p21$^{Cip1/WAF1}$ and cause it to localize to the cytoplasm, thereby suppressing its growth-inhibiting activity. Furthermore, our results, together other previous findings[23] also indicate a possible mechanism for the anti-apoptotic effect of p21$^{Cip1/WAF1}$. It has been shown that cytoplasmic p21$^{Cip1/WAF1}$ forms a complex with ASK1 to inhibit the stress-induced MAP kinase cascade, which results in resistance to apoptosis induced by many stimuli[23]. Overexpression of *HER-2/neu* is known to activate the Akt pathway and to confer resistance to apoptosis induced by various stimuli[4,24]. It will be interesting to determine whether this resistance is due to the formation of complexes between cytoplasmic p21$^{Cip1/WAF1}$ and ASK1 in *HER-2/neu*-overexpressing cells. In general, protein translocation is recognized as a crucial mechanism for the regulation of protein function[27]. Our results provide a clear example of regulation by Akt of the cellular location of p21$^{Cip1/WAF1}$ by phosphorylation at T145, and indicate that this process may be involved in *HER-2/neu*- or Akt-mediated cell proliferation. □

Methods

Materials.

The PI-3K inhibitor wortmannin and the DNA dye DAPI were from Roche. Anti-Flag and anti-haemagglutinin (HA; 12C5) antibodies were from Sigma and Roche, respectively. DNA plasmids encoding CA-Akt and DN-Akt were provided by P. Tsichlis (Fox Chase Cancer Center). Antibodies against Akt and p21$^{Cip1/WAF1}$ were from New England Biolabs and Santa Cruz, respectively.

p21$^{Cip1/WAF1}$ constructs.

A *Bam*HI site and an *Eco*RI site were generated by polymerase chain reaction (PCR) near the start and termination codons, respectively, in human wild-type p21$^{Cip1/WAF1}$ and were subcloned into the expression vector pcDNA3. Site-directed mutagenesis was carried out according to the manufacturer's protocol (Clontech). T145 in p21$^{Cip1/WAF1}$ was replaced with either alanine or aspartic acid, using the following primers: T145A, 5′-CGAAAACGGCGGCAGGCCAGCATGAC; T145D, 5′-CGAAAACGGCGG-CAGGACAGCATGAC. For the colony-formation assay in DN-Akt 3T3 cells, a *Bam*HI–*Eco*RI fragment containing wild-type or mutant p21$^{Cip1/WAF1}$ was subcloned into the expression vector pcDNA3–hygromycin. The sequences of the p21$^{Cip1/WAF1}$ constructs were verified by automated sequencing. To generate constructs for bacterial expression of wild-type and mutant p21$^{Cip1/WAF1}$ tagged with glutathione-*S*-transferase (GST), the same fragments were subcloned into the bacterial expression vector pGEX4T-3 (Pharmacia). Wild-type and mutant p21$^{Cip1/WAF1}$ proteins were inducibly expressed in *Escherichia coli* strain BL21 and purified by glutathione–sepharose chromatography (Pharmacia).

Cell culture.

NIH3T3, HER-2/*neu* 3T3 and MDA-MB453 cells, p21$^{Cip1/WAF1}$-deficient MEFs, and 293T cells were cultured in DMEM/F12 supplemented with 10% FBS. DN-Akt transfectants of *HER-2/neu* 3T3 and MDA-MB453 cells were grown under the same conditions, except that 450 μg ml^{-1} G418 was added to the culture medium[4]. 293T cells were transfected using the calcium-phosphate technique and p21$^{Cip1/WAF1}$-deficient cells by the liposome method (Cell and Molecular Technologies, Lavallette, New Jersey).

In vitro growth-rate analysis.

In vitro growth rates of the cell lines were assessed by counting cells with a Coulter counter or by the MTT (3-[4,5-dimethylthiazol-2-yl]2,5-diphenylterazolium bromide) assay as described[29].

[^{3}H]thymidine-incorporation assay.

Proliferation rates of the cell lines were analysed by measuring incorporation of [^{3}H]thymidine as described[29].

Endoproteinase cleavage and two-dimensional phosphopeptide analysis.

Two-dimensional analysis of p21$^{Cip1/WAF1}$ phosphopeptides was carried out using a HTLE-7000 electrophoresis system (CBS Scientific, Del Mar, California) as described[30]. Briefly, MDA-MB453 cells were incubated with 1.5 mCi ml^{-1} [^{32}P]orthophosphate for 3.5 h and then stimulated for 30 min with insulin in the presence or absence of LY294002. Endogenous p21$^{Cip1/WAF1}$ was immunoprecipitated, blotted, and visualized by autoradiography. The ^{32}P-labelled p21$^{Cip1/WAF1}$ protein on the nitrocellulose membrane was excised and digested with Tosyl-L-phenylalanine chloromethyl ketone (TPCK)–trypsin (Sigma). Completely digested phosphopeptides were spotted onto thin-layer cellulose plates (20 × 20 cm) and separated in the first dimension by electrophoresis at 1,000 V for 35 min in buffer (2.2% formic acid and 7.8% acetic acid, pH 1.9). Cellulose plates were then placed in a chromatography tank containing phosphochromatography buffer (38% *N*-butanol, 25% pyridine and 7.5% acetic acid) for 6–8 h to separate the phosphopeptides in the second dimension. Dried cellulose plates were then exposed to Kodak X-AR film.

Edman degradation.

Modified manual Edman degradation was carried out as described[31]. Briefly, phosphopeptides were covalently coupled to Sequelon-AA discs (Perseptive Biosystem Inc., Foster City, California) and subjected to consecutive cycles of Edman degradation. After each cycle, discs were treated with trifluoroacetic acid to cleave and release the amino-terminal amino acid, and the amount of radioisotope released was measured by Cerenkov counting.

In vitro kinase assay.

293T cells (0.2 × 10^6) were transfected with 20 μg of HA-tagged CA-Akt or DN-Akt. After 48 h, Akt was immunoprecipitated from cell extracts and incubated with 5 μg of purified GST–p21$^{Cip1/WAF1}$ (wild-type or mutant) in the presence of 5 μCi [γ-^{32}P]ATP and 50 mM cold ATP in kinase buffer[9] for 30 min at 30 °C. Reaction products were resolved by SDS–PAGE, and ^{32}P-labelled proteins were visualized by autoradiography.

[^{32}P]orthophosphate labelling.

293T cells (0.2 × 10^6) were co-transfected with 18 μg of CA-Akt or DN-Akt and 2 μg of wild-type or mutant p21$^{Cip1/WAF1}$. After 36 h, cells were starved for 12 h and then incubated in phosphate-free medium for 1 h. Cells were then labelled with 1 mCi ml^{-1} [^{32}P]orthophosphate for 3 h. They were then lysed, and p21$^{Cip1/WAF1}$ was immunoprecipitated from cell extracts and separated by 12% SDS–PAGE. Incorporation of ^{32}P-phosphate was measured by autoradiography.

Immunoprecipitation and immunoblotting.

Cells were washed twice with PBS and scraped into 500 μl of lysis buffer. After brief sonication, the lysate was centrifuged at 14,000*g* for 10 min at 4 °C to remove insoluble cell debris. Immunoprecipitation and immunoblotting were carried out as described[4].

In situ immunofluorescent staining.

Roughly 0.2 × 10^6 p21$^{-/-}$ MEFs were plated in 100-mm plates and co-transfected with 9 μg of CA-Akt or DN-Akt and 1 μg of wild-type or mutant p21$^{Cip1/WAF1}$, using liposome. After 36 h of incubation, cells were trypsinized and plated onto chamber slides for a further 12 h. After fixation of samples in acetone for 10 min at 4 °C, the cellular localization of p21$^{Cip1/WAF1}$ was determined using a monoclonal antibody against human p21$^{Cip1/WAF1}$ (1:100; Santa Cruz). After extensive washing in PBS, samples were further incubated with Texas Red-conjugated goat anti-mouse immunoglobulin G (1:400) and DAPI (0.1 μg ml^{-1}) for 1 h. After extensive washing, samples were examined by fluorescence microscopy (Zeiss). The nonspecific reaction of secondary antibody was ruled out by the absence of fluorescence under the microscope.

Cellular fractionation.

Roughly 2 × 10^7 cells were pelleted and resuspended in 800 μl of buffer A (10 mM HEPES pH 7.4, 1 mM EDTA and 1 mM dithiothreitol) containing the protease inhibitors phenylmethylsulphonyl fluoride, leupeptin, aprotinin and pepstatin. After incubation on ice for 10 min, cells were homogenized with ten strokes in a Dounce homogenizer. They were then examined under the microscope to confirm that >98% of cells were lysed. After brief centrifugation at 4 °C, the supernatant (cytoplasmic fraction) was collected and the pellet was washed twice with 400 μl of buffer B[23] and then resuspended in 150 μl of buffer C[23] with gentle rocking for 30 min at 4 °C (ref. 23). After centrifugation, the supernatant (nuclear fraction) was collected. The amounts of protein in the cytoplasmic and nuclear fractions were determined with a protein assay kit (Bio-Rad) and the protein was subjected to immunoblotting.

Colony-formation assay.

The colony-formation assay was used to measure the inhibition activity of p21$^{Cip1/WAF1}$ and its mutants. Wild-type or mutant p21$^{Cip1/WAF1}$ (T145A or T145D mutation) or the vector pcDNA3 (2 μg of each) was transfected into NIH3T3, *HER-2/neu* 3T3 and DN-Akt 3T3 cells in six-well plates, using liposome. After 48 h, cells were trypsinized and evenly distributed into four 100-mm culture plates. Cells were selected with 700 μg ml^{-1} G418 (or 100 μg ml^{-1} hygromycin for DN-Akt 3T3 cells, as they contain the neomycin-resistance gene) for 3 weeks.

Bromodeoxyuridine (BrdU) incorporation.

The BrdU-incorporation assay was also used to measure the inhibition activity of p21$^{Cip1/WAF1}$ and its mutants. Vector containing membrane-bound green fluorescent protein (GFP, 1 μg) and wild-type or mutant p21$^{Cip1/WAF1}$ (T145A or T145D mutation) or the vector pcDNA3 (9 μg of each) were co-transfected into NIH3T3, *HER-2/neu* 3T3 and DN-Akt 3T3 cells, using liposome. After 48 h, cells were labelled with BrdU for 1 h and fixed with 70% ethanol. Cells were then stained with anti-BrdU antibody and incubated with fluorescein-conjugated secondary antibody. After extensive washing, cells were sorted for GFP signal, and incorporation of BrdU was measured by FACS analysis.

RECEIVED 4 MAY 2000; REVISED 5 OCTOBER 2000; ACCEPTED 13 NOVEMBER 2000;
PUBLISHED 5 FEBRUARY 2001.

1. Slamon, D. J. *et al.* Human breast cancer: correlation of relapse and survival with amplification of the HER-2/neu oncogene. *Science* **235,** 177–182 (1987).
2. Slamon, D. J. *et al.* Studies of the HER-2/neu proto-oncogene in human breast and ovarian cancer. *Science* **244,** 707–712 (1989).
3. Yu, D. & Hung, M-C. in *DNA Alterations in Cancer* (ed. Ehrlich, M.) Ch. 21 (Natick, Massachusetts, 2000).
4. Zhou, B. P. *et al.* HER-2/neu blocks tumor necrosis factor-induced apoptosis via the Akt/NF-kB pathways. *J. Biol. Chem.* **275,** 8027–8031 (2000).
5. Downward, J. Mechanisms and consequences of activation of protein kinase B/Akt. *Curr. Opin. Cell Biol.* **10,** 262–267 (1998).
6. Datta, S. R., Brunet, A. & Greenberg, M. E. Cellular survival: a play in three Akts. *Genes Dev.* **13,** 2905–2927 (1999).
7. Peso, L. D., Gonzalez-Garcia, M., Page, C., Herrera, R. & Nunez, G. Interleukin-3-induced phosphorylation of bad through the protein kinase Akt. *Science* **278,** 687–689 (1997).
8. Cardone, M. H. *et al.* Regulation of cell death protease caspase-9 by phosphorylation. *Science* **282,** 1318–1321 (1998).
9. Brunet, A. *et al.* Akt promotes cell survival by phosphorylating and inhibiting a forkhead transcription factor. *Cell* **96,** 857–868 (1999).
10. Kops., G. J. *et al.* Direct control of the forkhead transcription factor AFX by protein kinase B. *Nature* **398,** 630–634 (1999).
11. Ozes, O. N. *et al.* NF-kB activation by tumor necrosis factor requires the Akt serine-threonine kinase. *Nature* **401,** 82–85 (1999).
12. Romashkova, J. A. & Makarov, S. S. NF-kB is a target of Akt in anti-apoptotic PDGF signalling. *Nature* **401,** 86–90 (1999).
13. Ahmed, N. N., Gries, H. L., Bellacosa, A., Chan, T. O. & Tsichlis, P. N. Transduction of interleukin-2 antiapoptotic and proliferative signals via Akt protein kinase. *Proc. Natl Acad. Sci. USA* **94,** 3627–3632 (1997).
14. Brennan, P. *et al.* Phosphatidylinositol 3-kinase couples the interleukin-2 receptor to the cell cycle regulator E2F. *Immunity* **7,** 679–689 (1997).
15. Medema, R. H., Kops, G. J., Bos, J. L. & Burgering, B. M. T. AFX-like forkhead transcription factors mediate cell-cycle regulation by Ras and PKB through p27Kip1. *Nature* **404,** 782–787 (2000).
16. Andjelkovic, M. *et al.* Role of translocation in the activation and function of protein kinase B. *J. Biol. Chem.* **272,** 31515–31524 (1997).
17. Meier, R., Alessi, D. R., Cron, P., Andjelkovic, M. & Hemmings, B. A. Mitogenic activation, phosphorylation and nuclear translocation of protein kinase B. *J. Biol. Chem.* **272,** 30491–30497 (1997).
18. Harper, J. W., Adami, G. R., Wei, N., Keyomarsi, K. & Elledge, S. J. The p21 Cdk-interacting protein Cip is a potent inhibitor of G1 cyclin-dependent kinase. *Cell* **75,** 805–816 (1993).
19. El-Deiry, W. S. *et al.* WAF1, a potential mediator of p53 tumor suppression. *Cell* **75,** 817–825 (1993).
20. Noda, A., Ning, Y., Venable, S. F., Pereira-Smith, O. M. & Smith, J. R. Cloning of senescent cell-derived inhibitors of DNA synthesis using an expression screen. *Exp. Cell Res.* **211,** 90–98 (1994).
21. Sherr, C. J. & Roberts, J. M. Inhibitors of mammalian G1 cyclin-dependent kinases. *Genes Dev.* **9,** 1149–1163 (1995).
22. Goubin, F. & Ducommun, B. Identification of binding domains on the p21Cip1 cyclin-dependent kinase inhibitor. *Oncogene* **10,** 2281–2287 (1995).
23. Asada, M. *et al.* Apoptosis inhibitory activity of cytoplasmic p21$^{Cip1/WAF1}$ in monocytic differentiation. *EMBO J.* **18,** 1223–1234 (1999).
24. Yu, D. *et al.* Overexpression of ErbB2 blocks taxol-induced apoptosis by upregulation of p21Cip1, which inhibits p34Cdc2 kinase. *Mol. Cell* **2,** 581–591 (1998).

25. Scott, M. T., Morrice, N. & Ball, K. L. Reversible phosphorylation at the C-terminal regulatory domain of p21$^{Waf1/Cip1}$ modulates proliferating cell nuclear antigen binding. *J. Biol. Chem.* **275**, 11529–11537 (2000).
26. Chen, J., Jackson, P. K., Kirschner, M. W. & Dutta, A. Separate domains of p21 involved in the inhibition of Cdk kinase and PCNA. *Nature* **374**, 386–388 (1995).
27. Porter, A. G. Protein translocation in apoptosis. *Trends Cell Biol.* **9**, 394–401 (1999).
28. Diehl, J. A., Cheng, M., Roussel, M. F. & Sherr, C. J. Glycogen synthase kinase-3β regulates cyclin D1 proteolysis and subcellular localization. *Genes Dev.* **12**, 3499 (1998).
29. Shao, R. *et al.* Inhibition of nuclear factor-kB activity is involved in E1A-mediated sensitization of radiation-induced apoptosis. *J. Biol. Chem.* **272**, 32739–32742 (1997).
30. Van der Geer, P. & Hunter, T. Phosphopeptide mapping and phosphoamino acid analysis by electrophoresis and chromatography on thin-layer cellulose plates. *Electrophoresis* **15**, 544–554 (1994).
31. Gatti, A. & Traugh, T. A. A two-dimensional peptide gel electrophoresis system for phosphopeptide mapping and amino acid sequencing. *Anal. Biochem.* **266**, 198–204 (1999).

ACKNOWLEDGEMENTS
We thank D. Yu, R. B. Arlinghaus and W. H. Klein for critical comments on the manuscript. This work was supported by grants from the National Institutes of Health (to M-C.H.), by a SPORE grant in ovarian cancer (to M-C.H.), and by the Nellie Connally Breast Cancer Research Fund at the M. D. Anderson Cancer Center (M-C.H.). B.P.Z. is a recipient of a postdoctoral fellowship from the US Department of Defense Breast Cancer Research.
Correspondence and requests for materials should be addressed to M-C.H.

Akt takes centre stage in cell-cycle deregulation

Wafik S. El-Deiry

The universal cell-cycle inhibitor $p21^{Cip1/WAF1}$ is phosphorylated and localized in the cytoplasm in Her2/neu-overexpressing breast cancers as a result of its physical association with the oncogenic Akt protein. Subcellular mislocalization of checkpoint controllers is now surfacing as a mechanism of deregulating cell proliferation in cancer.

Abnormal gene amplification and increased cell-surface expression of the transmembrane Her2/neu oncoprotein receptor (relative molecular mass 185,000; also known as ErbB2) occurs in up to 30% of human breast and other cancers (reviewed in ref. 1). Neu was originally discovered as an oncogene product in chemically-induced neuroblastomas in rats. The Her2/neu receptor, a member of the 'growth factor' glycoprotein family that includes the epidermal growth-factor receptor (EGFR), possesses a cytoplasmic tyrosine-kinase domain that signals cell proliferation and increased cell survival. Moreover, Her2/neu overexpression has been associated with poor patient prognosis and poor response to chemotherapeutic agents such as Taxol. Recent excitement has surrounded the clinical development and remarkable therapeutic effects of Her2/neu-blocking antibodies, such as Herceptin[2]. Meanwhile, the molecular details of how Her2/neu signals enhance growth and survival of cancer cells and induce therapeutic resistance continue to emerge[3]. On page 245 of this issue, Zhou *et al.*[4], describe an elegant mechanism by which Her2/neu and its target oncoprotein Akt subvert the principal negative cell-cycle controller $p21^{Cip1/WAF1}$ to enhance proliferation and survival of cancer cells (Fig. 1).

The cell-survival-promoting oncoprotein Akt (also known as protein kinase B, PKB) is abnormally activated in several human malignancies and can suppress apoptosis[5,6], although data obtained recently from a mouse knockout model indicate, surprisingly, that the p110γ catalytic subunit of phosphoinositide-3-OH kinase (PI(3)K; an upstream activator of Akt) may suppress colon tumorigenesis[7]. Overexpression of the *Drosophila* Akt homologue regulates cell and organ size without significantly affecting cell number or proliferation[8]. The *AKT1* gene encodes a serine/threonine kinase, the activity of which is induced upon recruitment to the plasma membrane and phosphorylation by regulatory kinases[9]. Recruitment and activation of Akt requires the presence of the phosphoinositide triphosphate (PI-3,4,5-P). Increases in PI-3,4,5-P levels (in response to PI(3)K activation) and Akt kinase activity occur in response to a variety of growth and survival signals including insulin, platelet-derived growth factor (PDGF), EGFR, Ras and Her2/neu, and the Akt signalling pathway is negatively regulated by the PTEN tumour-suppressor lipid phosphatase[8,10,11]. Downstream targets of Akt kinase that mediate its proliferative and pro-survival effects include Bad, caspase-9, Forkhead and IκB kinase-α in survival signalling, and p27 and GSK3β/cyclin D1 in pathways that control the cell cycle[9,11].

Remarkable progress has been made in determining how the molecular engine that drives the cell cycle is controlled and in identifying its aberrant function in human cancer. In eukaryotes, carefully orchestrated cell-cycle transitions depend on the ordered assembly, activation and activity of several conserved cyclin-dependent kinase (CDK) complexes, which phosphorylate key substrates such as the retinoblastoma protein family in G1 phase, the origin-recognition complex (ORC) and E2F1 in S phase, and Cdc25C in the G2/M-phase transition. CDK function is regulated at the levels of cyclin synthesis, formation of cyclin–CDK complexes, phosphorylation of activating and inhibitory residues on the CDK kinase, and subcellular localization of cyclin–CDK complexes, and by two families of cell-cycle inhibitory proteins (known as CDK inhibitors or CDKIs; Table 1)[12]. Cyclin–CDK complexes are the ultimate targets of several cell-cycle checkpoints that ensure the maintenance of genomic integrity and cellular good health[13,14]. One hallmark of cancer cells is the failure of such checkpoints, for example in response to improper mitotic-spindle assembly, DNA damage, starvation or oncogene activation; this allows DNA-replication errors and chromosomal abnormalities to be propagated and to accumulate over time because of defective monitoring and repair of the genetic material during cell division. CDKIs were first identified in the early 1990s through a convergence of work in several fields, including cancer biology, cell cycle and the genetics of cellular senescence. $p21^{Cip1/WAF1}$, the first CDKI to be identified, is a transcriptional target of the p53 tumour suppressor during the stress response and seems to be regulated by p53-independent transcription factors during growth arrest associated with cellular differentiation. There is some evidence that loss or haploinsufficiency of $p21^{Cip1/WAF1}$ contributes to checkpoint defects as a result of DNA damage or nucleotide depletion, cellular transformation, tumorigenesis or altered potential for stem-cell repopulation[15–19].

A connection between Her2/neu overexpression, increased $p21^{Cip1/WAF1}$ expression, and resistance of breast cancers to the microtubule-arresting agent Taxol was previously noted by Yu *et al.*[20]. Increased resistance to Taxol was reversed by antisense inhibition of $p21^{Cip1/WAF1}$ expression in cells overexpressing Her2/neu, and Her2/neu failed to sensitize p21-null mouse embryonic fibroblasts to the killing effects of Taxol. The authors proposed that the modest reduction

Table 1 Consequences of CDKI inactivation

CDK inhibitor (CDKI)	Defect in human cancer	Consequences for CDKI
$p16^{INK4A}$	Mutation	Loss of function
	Hypermethylation	Loss of expression
	Deletion	Loss of expression
$p27^{KIP1}$	Mutation	Loss of function
	TGF-β receptor mutation	Reduced function
	Hyperubiquitination	Loss of expression
$p21^{Cip1/WAF1}$	p53 mutation	Reduced expression
	c-Myc overexpression	Transcriptional repression
	Her2/neu overexpression	Cytoplasmic localization
$p57^{KIP2}$	Imprinting	Reduced expression

© 2001 Macmillan Magazines Ltd

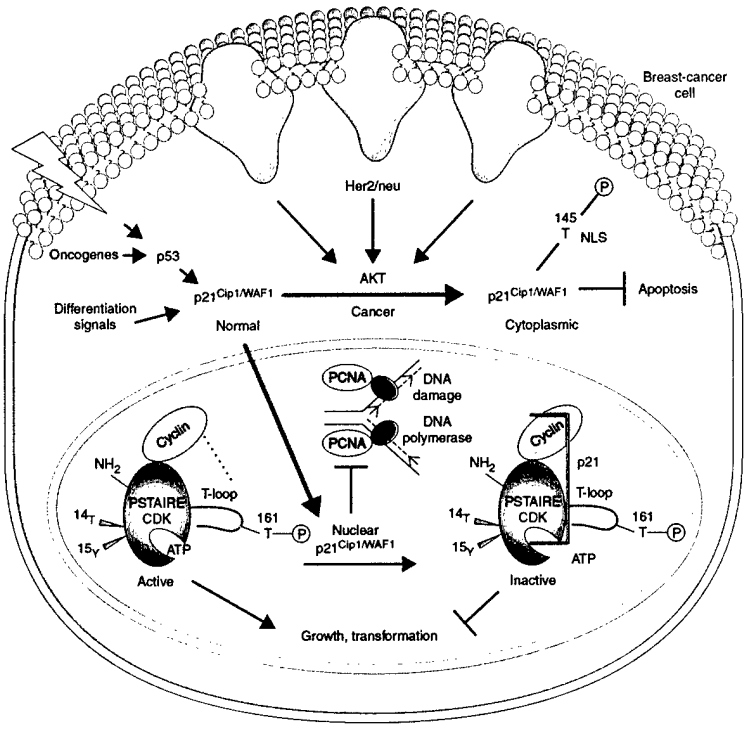

Figure 1 **Oncogene Her2/neu-initiated, Akt-mediated $p21^{Cip1/WAF1}$ inactivation as a suppressor of tumour growth and the cell cycle. During normal cellular growth, the $p21^{Cip1/WAF1}$ CDK inhibitor is expressed at low levels and aids assembly of growth-promoting active cyclin–CDK complexes. Under cellular stress, $p21^{Cip1/WAF1}$ expression is increased through p53-dependent and -independent pathways. Increased $p21^{Cip1/WAF1}$ levels in the nucleus lead to inhibition of CDKs through binding of $p21^{Cip1/WAF1}$ to the complexes. Binding of p21Cip1/WAF1 to cyclin–CDK leads to a conformational change in CDKs, and to steric hindrance of ATP binding to the CDK active site. The C terminus of $p21^{Cip1/WAF1}$, containing its nuclear localization signal (NLS), binds to and inhibits proliferating-cell nuclear antigen (PCNA), thereby blocking DNA replication. In many cancers, the checkpoint function of $p21^{Cip1/WAF1}$ is lost through mutations in its chief regulator during cellular stress, p53. In cancers that overexpress Her2/neu, Akt is also activated. Zhou and colleagues have now identified $p21^{Cip1/WAF1}$ as an Akt-interacting protein and a substrate for phosphorylation in Her2/neu-overexpressing cancers.**

in Cdc2 kinase activity they observed in cells with increased $p21^{Cip1/WAF1}$ levels led in part to the survival of Taxol-treated Her2/neu-overexpressing cells. However, it remained unexplained how $p21^{Cip1/WAF1}$ expression could be greatly increased at the same time as an increase in cell proliferation associated with oncogene Her2/neu overexpression, in the absence of Taxol.

An important clue in the signalling pathway downstream of Her2/neu was uncovered when Zhou and colleagues began investigating the contribution of Akt signalling to Her2/neu-induced cell proliferation. They found that dominant negative Akt or inhibitors of PI(3)-kinases inhibited the proliferation of Her2/neu-overexpressing cells but had no effect on the greatly increased $p21^{Cip1/WAF1}$ expression. These findings indicate that Her2/neu, through Akt, must somehow inactivate the growth-inhibiting effect of $p21^{Cip1/WAF1}$ without altering its expression. As Akt is known to affect the subcellular localization of some proteins, such as the Forkhead transcription factor, through phosphorylation, and as $p21^{Cip1/WAF1}$ contains a potential Akt consensus site, the authors investigated whether $p21^{Cip1/WAF1}$ might be a direct target for Akt phosphorylation. They found that endogenous Akt physically associates with endogenous $p21^{Cip1/WAF1}$ and phosphorylates it at threonine 145, causing $p21^{Cip1/WAF1}$ to be localized in the cytoplasm.

To understand better the role of $p21^{Cip1/WAF1}$ phosphorylation in growth suppression, Zhou and colleagues introduced alanine and aspartate residues at position 145 of human p21. The T145A mutant of $p21^{Cip1/WAF1}$, unlike the wild type, effectively suppressed growth and DNA synthesis in NIH 3T3 cells when Her2/neu was overexpressed, presumably because the mutant was no longer regulated by the kinase activity of Akt. In contrast, the T145D mutant was unable to suppress growth efficiently or to inhibit DNA synthesis under any circumstances, especially in the presence of dominant negative Akt — a condition under which wild-type $p21^{Cip1/WAF1}$ was effective. As the authors predicted, the T145A and T145D mutants of $p21^{Cip1/WAF1}$ were localized predominantly in the nucleus and the cytoplasm, respectively. As an important test of whether the observed phosphorylation of $p21^{Cip1/WAF1}$ might be relevant to tumours derived from breast-cancer patients, the authors obtained convincing evidence by correlating Her2/neu overexpression with Akt phosphorylation and cytoplasmic $p21^{Cip1/WAF1}$ localization in ten different tumours. These *in vivo* results add further support to the idea that activation of Akt kinase downstream of Her2/neu overexpression may be responsible for mislocalization of $p21^{Cip1/WAF1}$ to the cytoplasm and disruption of its potent growth-inhibiting activity.

There are potentially interesting parallels between breast and prostate cancer in terms of the role of Her2/neu and Akt signalling in survival and hormone-independent growth. In breast cancer, there is a well known reciprocal relationship between Her2/neu overexpression, loss of oestrogen-receptor expression and poor prognosis[20]. In prostate cancer, recent work has shown that Akt, acting downstream of overexpressed Her2/neu, binds to and phosphorylates the androgen receptor, leading to androgen-independent growth and survival[21]. It is possible that, in prostate cancer, activated AKT may also deregulate cell-cycle control and enhance survival after cytotoxic exposure through effects on $p21^{Cip1/WAF1}$.

The identification of $p21^{Cip1/WAF1}$ as a target for Akt provides new insights and new avenues for understanding cell-cycle regulation, and indicates potential strategies for therapeutic intervention in cancer. It would be of interest to determine the physiological or pathological circumstances in which $p21^{Cip1/WAF1}$ is phosphorylated and what impact this has on its function. In this regard, animal models in which $p21^{Cip1/WAF1}$ has been found to contribute to differentiation or tumour suppression may prove useful for investigating the effects of knock-in of $p21^{Cip1/WAF1}$ phosphorylation-site mutants. Studying how phosphorylated $p21^{Cip1/WAF1}$ aids cyclin–CDK assembly may

© 2001 Macmillan Magazines Ltd

provide insights into potential functions of $p21^{Cip1/WAF1}$ within the cytoplasm. The interactions of phosphorylated $p21^{Cip1/WAF1}$ may modulate cytoplasmic kinase activities that influence the stress response or cell-death pathways. In this regard, it would be of interest to test $p21^{Cip1/WAF1}$ mutants that are localized to the cytoplasm but that are otherwise impaired in cytoplasmic interactions; that is, is the loss of nuclear localization sufficient for the Her2/neu-overexpression and drug-resistance phenotype, or is there also a gain-of-function in the cytoplasm? It would also be of interest to determine the extent to which $p21^{Cip1/WAF1}$ phosphorylation is required for Akt effects on the cell-cycle, compared with inhibition of cell death, given earlier reports of the effects of Akt on $p27^{KIP1}$ and cyclin D1 in cell-cycle deregulation.

In terms of therapeutic intervention, small peptides may be designed on the basis of the carboxy-terminal structure of $p21^{Cip1/WAF1}$, which may compete with endogenous $p21^{Cip1/WAF1}$ for Akt binding and phosphorylation, thus sending $p21^{Cip1/WAF1}$ back into the nucleus. Such strategies might take advantage of the increased levels of $p21^{Cip1/WAF1}$ in Her2/neu-overexpressing cells to suppress growth. Because increased $p21^{Cip1/WAF1}$ expression might be expected to be lost after treatment with Herceptin, it may be useful to compare the cell-cycle-inhibiting and drug-sensitization effects of blocking the Her2/neu pathway proximally, with effects achieved by blocking specific downstream effectors of Akt signalling. It may also be fruitful to investigate how Her2/neu increases $p21^{Cip1/WAF1}$ expression, with the aim of developing strategies to control the cell cycle while blocking other oncogenic Her2/neu signals. It may be possible to bypass the effect of Akt on $p21^{Cip1/WAF1}$ through the use of small-molecule CDK inhibitors. Knowledge of the Her2/neu-AKT-$p21^{Cip1/WAF1}$ pathway may be of use in designing more effective cytotoxic therapeutic strategies for Her2/neu-overexpressing or PTEN-mutated cancers. For example, agents that induce DNA damage and p53-dependent $p21^{Cip1/WAF1}$ upregulation might be used more effectively to treat wild-type p53-expressing, Her2/neu-overexpressing cancers if $p21^{Cip1/WAF1}$ were re-routed back to the nucleus. Another potential strategy might involve screening for agents that upregulate phosphatases that dephosphorylate $p21^{Cip1/WAF1}$, thus reactivating its nuclear-localization signal. It is clear that Akt is a focal point for deregulation in cancer and can have impact on cell proliferation and survival of cancer cells through a growing list of key targets that now includes $p21^{Cip1/WAF1}$.

Wafik S. El-Deiry is in the Laboratory of Molecular Oncology and Cell Cycle Regulation, Departments of Medicine, Genetics and Pharmacology, Howard Hughes Medical Institute, University of Pennsylvania School of Medicine, 415 Curie Boulevard, Philadelphia, Pennsylvania 19104, USA.
e-mail: wafik@mail.med.upenn.edu

1. Olayioye, M. A., Neve, R. M., Lane, H. A. & Hynes, N. E. *EMBO J.* **19**, 3159–3167 (2000).
2. Dickman, S. *Science* **280**, 1196–1197 (1998).
3. Harari, D. & Yarden, Y. *Oncogene* **19**, 6102–6114 (2000).
4. Zhou, B. P. *et al. Nature Cell Biol.* **3**, 245–252 (2001).
5. Kennedy, S. G. *et al. Genes Dev.* **11**, 701–713 (1997).
6. Kauffman-Zeh, A. *et al. Nature* **385**, 544–548 (1997).
7. Sasaki, T. *et al. Nature* **406**, 897–902 (2000).
8. Verdu, J., Buratovich, M. A., Wilder, E. L. & Birnbaum, M. J. *Nature Cell Biol.* **1**, 500–506 (1999).
9. Datta, S. R., Brunet, A. & Greenberg, M. E. *Genes Dev.* **13**, 2905–2927 (1999).
10. Franke, T. F. *et al. Cell* **81**, 727–736 (1995).
11. Cristofano, A. D. & Pandolfi, P. P. *Cell* **100**, 387–390 (2000).
12. Morgan, D. O. *Nature* **374**, 131–134 (1995).
13. Sherr, C. J. & Roberts, J. M. *Genes Dev.* **13**, 1501–1512 (1999).
14. Chan, T. A., Hermeking, H., Lengauer, C., Kinzler, K. W. & Vogelstein, B. *Nature* **401**, 616–620 (1999).
15. Deng, C. X., Zhang, P. M., Harper, J. W., Elledge, S. J. & Leder, P. *Cell* **82**, 675–684 (1995).
16. Mitchell, K. & El-Deiry, W. S. *Cell Growth Diff.* **10**, 223–230 (1999).
17. Missero, C., DiCunto, F., Kiyokawa, H., Koff, A. & Dotto, G. P. *Genes Dev.* **10**, 3065–3075 (1996).
18. Jones, J. M., Cui, X. S., Medina, D. & Donehower, L. A. *Cell Growth Diff.* **10**, 213–222 (1999).
19. Cheng, T. *et al. Science* **287**, 1804–1808 (2000).
20. Yu, D. *et al. Molecular Cell* **2**, 581–591 (1998).
21. Wen, Y. *et al. Cancer Res.* **60**, 6841–6845 (2000).

© 2001 Macmillan Magazines Ltd

Enhancement of chemosensitivity and antitumor effects by Adenovirus E1A -mediated regulation of Akt and p38 activities*

YONG LIAO, YIYU ZOU, WEIYA XIA & MIEN-CHIE HUNG

Department of Molecular and Cellular Oncology, The University of Texas M. D. Anderson Cancer Center, Houston, TX 77030, USA

Correspondence should be addressed to M.C. H.; email: mchung@odin.mdacc.tmc.edu

Most chemotherapeutic drugs kill cancer cells by inducing apoptosis, and a deficiency in apoptosis often confers drug resistance. Here we show that adenovirus type 5 early region 1A (E1A)-mediated sensitization to paclitaxel (Taxol)-induced apoptosis *in vitro* and *in vivo* through modulation of the apoptotic threshold, by downregulating Akt activity and upregulating p38 activity in breast cancer cells. The same mechanism was observed using other anticancer drugs, including adriamycin (or doxorubicin), *cis*-platin, methotrexate, and gemcitabine. Interestingly, inactivation of Akt results in activation of p38, and vice versa, suggesting that p38 and Akt regulate each other. Moreover, E1A enhances the expression of PP2A/C, a catalytic subunit for an Akt phosphatase complex, PP2A, which may also be involved in E1A-mediated modulation of Akt and p38 activities. Thus, our results support that an interesting "feedforward" regulatory mechanism involving PP2A, Akt, and p38 contributed to E1A-mediated sensitization to chemotherapeutic drug-induced apoptosis.

Apoptosis is a highly conserved and finely regulated process by which cells commit suicide under a variety of internal and external controls. Net increases in apoptosis could result from a decreased apoptotic threshold, enhanced apoptotic stimulation, or a combination of these factors[1-3]. Apoptosis may also be the principle mechanism by which chemotherapy and radiation induce the killing of tumor cells, as deficiencies in apoptosis confer resistance to cytotoxic anticancer drugs and radiation[4]. Therefore, a novel strategy for combating cancer would be to restore the sensitivity of cancer cells to apoptosis[3,5,6].

Mounting evidence suggests that the expression of the adenovirus type 5 early region 1A (E1A) protein sensitizes cells to apoptosis. In primary mouse embryo fibroblasts, E1A-mediated sensitization to apoptosis induced by ionizing radiation and chemotherapeutic drugs has been reported through a p53-dependent and $p19^{ARF}$-dependent pathway[7-9]. Moreover, a p53-independent mechanism for E1A-mediated chemosensitization to the anticancer drugs etoposide and *cis*-plastin has been demonstrated in human cancer cell lines, including Saos-2 osteosarcoma cells[10,11]. So far, E1A has been shown to mediate sensitization to a wide variety of apoptotic stimuli, including serum-starvation, ultraviolet- and γ-radiation, tumor necrosis factor-α, and different categories of anticancer drugs. However, the molecular mechanisms underlying E1A-mediated sensitization to apoptosis have not been completely defined. In addition, E1A gene has been introduced into cancer patients in a few clinical trials[12](Hung M.C., et al., JCO, in press). Coupling with cationic liposome, the E1A gene was delivered in a plasmid form (Hung M.C., et al., JCO, in press). In the clinical trial using Onyx-015 virus in which E1B gene was deleted, the virus introduced into clinical patients also containing the E1A gene. Encouraging therapeutic results were obtained recently by combination of Onyx-015 and chemotherapy in the

clinical trials[13]. Thus, it becomes clinically important to understand the detailed mechanism of the E1A-mediated chemosensitization.

The propensity of cells to trigger apoptosis can be regulated, most notably by the phosphoinositide 3'-kinase (PI3'K)-Akt cell survival pathway and the Jun N-terminal kinase (JNK) and p38 MAP kinase proapoptotic pathways[14 15-19]. Moreover, whether a cell lives or dies is largely dependent on the balance of intrinsic survival signals and preapoptotic signals within the cell[1,2,6,20]. In the present study, we tested E1A transfectants of human breast cancer MDA-MB-231 and MCF-7 cells for their sensitivities to paclitaxel (Taxol), an antimicrotubule anticancer agent, *in vitro* and in an orthotopic breast cancer model *in vivo*. We also evaluated the molecular mechanisms underlying E1A-mediated chemosensitization, with particular emphasis on the roles of the proapoptotic factor p38 and the key cell-survival factor Akt. Our results indicate that E1A-mediated sensitization to drug-induced apoptosis is achieved by modulation of the apoptotic potential, through an interesting "feedforword" mechanism involving regulation of Akt and p38 activities.

E1A sensitizes cells to Taxol-induced apoptosis

Taxol is a promising frontline chemotherapeutic agent for treating breast and ovarian cancers. To test whether E1A could sensitize MDA-MB-231 and MCF-7 cell lines to Taxol-induced killing, we treated E1A-expressing cells with 0.001 μM to 0.1 μM Taxol and performed MTT cytotoxicity assays. Stable expression of wild-type E1A enhanced sensitivity to Taxol-induced killing in MDA-MB-231 cells by more than 10-fold when compared with Taxol-treated parental or vector-transfected control cells (Fig. 1*a*). Stable

expression of E1A also enhanced the sensitivity of MCF-7 cells to Taxol, although to a lesser extent. Interestingly, a revertant of the MCF-7 clone, which lost its E1A expression during cell culture, also lost its sensitivity to Taxol (Fig.1*b*). Three additional independent E1A stable clones from each cell line were analyzed, all of which expressed high levels of E1A protein and showed similar sensitivity to Taxol (data not shown).

To address whether apoptosis was involved in the E1A-mediated sensitization to Taxol, we examined the presence of poly (ADP-ribose) polymerase (PARP) cleavage as an apoptotic cell death marker. We detected PARP cleavage in the E1A-expressing MDA-MB-231 (231-E1A) and MCF-7 (MCF-7-E1A) cells upon treatment with 0.1 μM to 0.001 μM Taxol. In parental and vector-transfected control cells, PARP cleavage was observed only upon treatment with 0.1 μM Taxol; in the revertant MCF-7 cell clone, it was not detected at all (insert, Fig.1*a* and *b*). Flourescence-activated cell sorting (FACS) analysis confirmed that E1A enhanced Taxol-induced apoptosis, demonstrated by an increased proportion of sub-G1 phase cells in E1A-expressing cell lines (Fig. 1*c*). Taxol is well known to induce G2/M arrest (as was observed in parental or vector-transfected cells), but we noticed that the expression of E1A altered Taxol-induced G2/M arrest by an as yet unknown mechanism. Thus, E1A-mediated sensitization to Taxol was correlated with E1A-induced apoptosis.

E1A gene therapy sensitizes cells to Taxol-induced antitumor effect

To test whether E1A also mediated sensitization to Taxol *in vivo*, we used a deoxynucleotide transferase-mediated dUTP-biotin nick end labeling (TUNEL) assay to compare Taxol-induced apoptosis in tumor tissues obtained from animals inoculated with

231-E1A cells with those from animals inoculated with vector-transfected control (231-Vect) cells. Taxol-treated 231-E1A tumor tissues had a significantly higher percentage of TUNEL-positive cells than did Taxol-treated 231-Vect tumor tissues or control saline-treated tumors (Fig. 2*a* and *b*). We then evaluated tumor size. In the absence of Taxol, the mean tumor volume in E1A-inoculated animals was significantly lower than that in the control 231-Vect-inoculated animals ($P < 0.01$). The presence of Taxol, however, produced dramatical tumor regression in 231-E1A tumors, the 231-E1A tumor volume was just 21.7% of that of the control saline-treated 231-E1A group (Fig. 2*c*). When comparing tumors in Taxol treated 231-Vect inoculated animals with those in the Taxol treated 231-E1A group, the 231-E1A group was more sensitive to Taxol ($P < 0.01$).

To explore whether E1A could directly enhance Taxol-induced killing *in vivo*, we designed systemic E1A gene therapy experiments in mice by intravenous (*i.v.*) injection of the E1A gene via the mouse tail vein. We compared the therapeutic effects of E1A gene therapy with and without Taxol chemotherapy in our established orthotopic tumor model of animals inoculated with MDA-MB-231 cells. We used SN-liposome as our gene-delivery system because of its relatively high efficiency *in vivo* (to be addressed somewhere else). Compared with control SN-liposome treatment, six weeks of *i.v.* administration of liposome-E1A or intraperitoneal (*i.p.*) injection of Taxol alone repressed tumor growth during the 12-week observation period ($P < 0.01$). Compared with treatment of E1A-liposome or Taxol alone, a combination of E1A gene therapy and Taxol chemotherapy produced significantly enhanced therapeutic efficacy and dramatically repressed tumor growth ($P < 0.01$) (Fig. 2*d*). Tumors were completely eradicated in four out of seven mice treated with combination therapy. In addition,

survival rates were significantly higher in animals treated with combination therapy than in those treated with SN-liposome alone, liposome-E1A, or Taxol (Fig. 2*e*). Three out of seven animals treated with combination therapy achieved over one year's tumor-free survival. Our data showed that expression of E1A significantly enhanced both chemosensitivity and an antitumor effect induced by Taxol and prolonged animal survival rates in our *in vivo* model.

E1A upregulates p38 activity and downregulates Akt activity

To examine whether apoptosis-related molecules were involved in E1A-mediated sensitization to Taxol, we examined the phosphorylation status of p38, Akt, and JNK in 231-E1A and MCF-7-E1A cells versus vector-transfected cells. We detected phosphorylated p38 in cells stably expressing E1A but not in vector-transfected cells. However, the level of phosphorylated Akt was much higher in vector-transfected cells than in E1A-expressing cells. The levels of total Akt and p38 were similar in both types of cells (Fig. 3*a*). Kinase assays showed that p38 activity was higher and Akt activity was lower in 231-E1A cells than in 231-Vect cells (Fig. 3*b*). We did not detect any differences in the phosphorylation levels of JNK in E1A-expressing cells and vector-transfected cells (data not shown). These results indicated that E1A enhanced p38 activity and repressed Akt activity but did not affect JNK phosphorylation.

Taxol-induced PARP cleavage and Bcl-2 phosphorylation kinetically correlate with decreased Akt phosphorylation and increased p38 phosphorylation

To test whether alteration of the kinase activity of Akt or p38 played a role in E1A-mediated sensititization to Taxol-induced apoptosis, we examined correlations between

levels of phosphorylated Akt and p38 and Taxol-induced apoptosis in 231-E1A cells, using PARP cleavage and Bcl-2 phosphorylation as apoptotic cell death markers. PARP cleavage and Bcl-2 phosphorylation were detected after 4 hours exposure to 0.01 μM Taxol but became more obvious after 12 hours (Fig. 3*c*). Similar kinetics was observed for phosphorylation of p38 and dephosphorylation of Akt, after p38 and Akt protein levels were normalized (Fig. 3*e*). The same concentration of Taxol (0.01 μM) did not trigger PARP cleavage, induce Bcl-2 phosphorylation, or remarkably modulate the levels of phosphorylated p38 and Akt in parental MDA-MB-231 cells; a higher concentration (> 0.1 μM) was required (Fig.3*g*). Thus, PARP cleavage and Bcl-2 phosphorylation correlated well with decreased Akt phosphorylation and increased p38 phosphorylation.

Bax, p53, JNK, and Erk have also been reported to be involved in Taxol-induced apoptosis. We therefore monitored their protein levels in 231-E1A cells after treatment with Taxol. The protein levels of p53, Bax were not significantly changed after treatment (Fig.3*c*), but JNK phosphorylation transiently increased between 30 minutes and 6 hours after exposure to 0.01 μM Taxol and returned to undetectable levels when PARP cleavage and Bcl-2 phosphorylation became obvious (after 12 h) (Fig. 3*d*). A similar pattern was observed for Erk1/2 (Fig. 3*d* and *f*). Our data suggested that downregulation of Akt phosphorylation and upregulation of p38 phosphorylation, but not phosphorylation of JNK and Erk, were involved in E1A-mediated sensitization to Taxol-induced apoptosis.

Inactivating Akt and activating p38 are required for E1A-mediated sensitization to Taxol-induced apoptosis

To test the role that downregulation of Akt activity played in E1A-mediated sensitization to Taxol, an HA-tagged, myristylated, and membrane-targeted constitutively active Akt construct (CA-Akt) and a pcDNA3-luciferase (Luc) reporter construct were cotransfected into 231-E1A cells. Expression of CA-Akt was detected by an anti-HA monoclonal antibody. The level of phosphorylated Akt was increased in CA-Akt-transfected 231-E1A cells, regardless of whether they were exposed to Taxol (Fig. 4*a*). Luciferase activity, which represented viable cells, was significantly higher in cells transfected with CA-Akt than in control 231-E1A cells after exposure to Taxol (Fig. 4*b*). FACS analysis showed that after exposure to 0.01 μM Taxol, less apoptotic cells were detected in CA-Akt-transfected cells (15.9%) than in control 231-E1A cells (25.5%) (bottom, Fig.4*b*). Thus, inhibition of Akt phosphorylation was required for E1A-mediated sensitization to Taxol-induced apoptosis.

To evaluate whether activation of p38 was also required for E1A-mediated sensitization to Taxol, the specific p38 inhibitor SB203580 was used to block p38 activity in 231-E1A cells. Pretreatment with 20 μM SB203580 for 30 minutes prior to and during exposure to 0.01 μM Taxol inhibited the phosphorylation of p38 (Fig. 4*a*). In contrast, in the absence of SB203580, the level of phosphorylated p38 increased after exposure to Taxol for 4 hours (Fig. 4*a* and *b*). We then transfected pcDNA3-luciferase reporter genes into 231-E1A cells. In the absence of SB203580, the luciferase activity in Taxol-treated cells decreased to 38% of that of untreated control cells; when cells were pretreated with SB203580, the luciferase activity increased (Fig. 4*a*). FACS analysis also showed that pretreatment with SB203580 protected 231-E1A cells from apoptosis, whether or not they were exposed to Taxol. (from 4.9% to 1.0% without Taxol and 25.5% to 10.0% in the

presence of Taxol) (bottom, Fig. 4*a*). These data suggested that phosphorylation of p38 was required for E1A-mediated sensitization to Taxol-induced apoptosis.

To further define the role of p38 in E1A-mediated sensitization to Taxol, IPTG-inducible, Flag-tagged, dominant-negative p38 (DN-p38) stable cell clones were established in 231-E1A cells. When cells were switched to medium containing 5 μM IPTG, expression of Flag-tagged DN-p38 was induced (Fig. 4*c*), and the level of phosphorylated Akt increased. When the cells were exposed to either 0.01 μM or 0.1 μM Taxol, the level of phosphorylated Akt remarkably decreased in the absence of IPTG; in the presence of IPTG, neither dose of Taxol noticeably affected the level of phosphorylated Akt. Moreover, this effect was not due to the IPTG itself, because when parental E1A-expressing cells were exposed to the same dose and duration of IPTG, the level of phosphorylated Akt was not affected. FACS analysis showed that the percentage of IPTG-induced DN-p38 expressing cells that were undergoing apoptosis was dramatically lower than in cells without IPTG induction (Fig. 4*c*). Essentially identical results were obtained when two additional stable clones were studied (data not shown). These results further supported that upregulation of p38 activity and downregulation of Akt activity were required for E1A-mediated sensitization to Taxol cytotoxicity and that blocking p38 activity also inhibited this sensitization.

To test whether blocking Akt activity enhanced the sensitivity to Taxol, both biochemical and genetic approaches were employed to block Akt. First, we found that 0.1 μM Wortmannin completely blocked Akt phosphorylation, whether or not cells were exposued to Taxol (Fig. 4*d*). Correspondingly, luciferase activity in the Wortmannin-treated cells decreased more than 20% after exposure to 0.01 μM Taxol, compared with

parental cells that were not treated with Wortmannin (Fig. 4*e*). FACS analysis showed that a higher percentage of Wortmannin-treated cells than of control cells were undergoing apoptosis (bottom, Fig. 4*e*). When a dominant-negative Akt construct (DN-Akt) and a pcDNA3-luciferase reporter were transiently cotransfected into MDA-MB-231 cells, similar results were obtained; both the level of phosphorylated Akt and luciferase activity decreased after exposure to Taxol (Fig. 4*e*). FACS analysis showed that after exxposure to Taxol, the percentage of DN-Akt-transfected cells undergoing apooptosis increased 8.4%, while the percentage of apoptotic parental 231 cells increased only 1.4% (bottom, Fig. 4*e*).

To enhance p38 activity, a hemeaglutamin (HA)-tagged p38 construct (HA-p38) and the pcDNA3-luciferase reporter gene were transiently cotransfected into MDA-MB-231 cells. After exposure to 0.01 μM Taxol for 4 hours, the level of phosphorylated p38 increased, while luciferase activity decreased (Fig. 4*f*). FACS analysis showed that the percentage of apoptotic HA-p38-transfected cells reached nearly 15% after exposure to 0.01 μM Taxol for 24 hours (bottom, Fig. 4*f*). Our results indicated that increasing p38 activity or blocking Akt activity was sufficient to enhance the sensitivity of MDA-MB-231 cells to Taxol-induced apoptosis.

The same mechanism for E1A-mediated sensitization to Taxol-induced apoptosis applies to apoptosis induced by different categories of anticancer drugs

To determine whether the same mechanism for E1A-mediated sensitization to Taxol applied to other anticancer drugs, we tested the effects of four additional drugs that were currently used in clinical treatment of human cancer: doxorubicin (or adriamycin,

topoisomerase II inhibitor), cis-platin (DNA-damaging agent), methotrexate (antimetabolite drug), and gemcitabine (antimetabolite drug). Expression of E1A significantly enhanced each drug's cytotoxicity in MDA-MB-231 cells as determined by MTT assay (Fig. 5*a*). In addition, PARP cleavage was observed in 231-E1A cells but not in 231-Vect control cells treated with each of the drug. Downregulation of Akt phosphorylation and upregulation of p38 phosphorylation were also detected in E1A-expressing cells after 24 hours of exposure to each drug (Fig. 5*b*). Therefore, downregulating Akt activity and upregulating p38 activity may be a general mechanism for E1A-mediated sensitization to chemotherapeutic drug-induced apoptosis.

A "feedforward" mechanism may account for E1A-mediated chemosensitization.

To test whether a physiological association existed between p38 and Akt phosphorylation, MDA-MB-231 or 231-E1A cells were treated with Wortmannin (0.1 μM) or SB203580 (20 μM), respectively. Cells were harvested at 4, 8, 16, and 24 hours. The levels of phosphorylated p38 and Akt were examined in parallel. When the level of phosphorylated p38 decreased, the level of phosphorylated Akt increased (at 8 h). Likewise, when Akt phosphorylation was blocked, the level of phosphorylated p38 dramatically increased (at 4 h) (Fig. 6*a*).

To determine whether Akt physically associated with p38, CA-Akt was transiently transfected into both MDA-MB-231 and 293T cells; and the cells were lysed about 30 hours after transfection. We did not detect p38 in immunoprecipitated Akt samples (Fig. 6*b*) nor Akt in immunoprecipitated p38 samples (data not shown), suggesting Akt and p38 did not directly associate under the conditions we used. Since

ASK1 is an upstream kinase that can phosphorylate p38[21,22], we tested whether it could directly bind Akt and inactivate by Akt (because there is a concensus Akt phosphorylation site in the ASK1 protein sequence). Our result showed ASK1 was immunoprecipitated with Akt (Fig. 6*b*) and an interaction between these two proteins was recently confirmed[23].

We next asked by what mechanism E1A affected Akt or p38 phosphorylation. Since E1A's ability to regulate the expression of certain genes through transcription-dependent or transcription-independent mechanisms has been well documented[24,25] and since the serine/threonine phosphatase PP2A directly dephosphorylates Akt[26], we tested whether PP2A expression was affected by E1A expression. Although the regulatory subunit of PP2A, PP2A/A, showed no significant change in E1A-expressing cells, we did detect a notable enhancement in expression of its catalytic subunit, PP2A/C (Fig. 6c). Therefore, a "feedforward" mechanism may account for E1A-mediated regulation of p38 and Akt activities (Fig. 6*d*). That is, by upregulation of PP2A/C, E1A could repress Akt activity and released ASK1 activity, which would results in p38 activation. Since p38 is know to directly activate PP2A enzyme[27] and transcriptionally activate the expression of Fas ligand (FasL)[28], its activation would further amplify the proapoptotic signals.

Discussion

In the present report, we showed for the first time that E1A sensitizes breast cancer cells to Taxol-induced apoptosis *in vitro* and enhances Taxol-induced anti-tumor effects *in vivo* through modulation of the apoptotic threshold, by downregulating Akt activity and upregulating p38 activity. Blocking p38 activity or introducing constitutively active Akt

into E1A-expressing cells blocked E1A's ability to sensitize cells to Taxol-induced cytotoxicity. Moreover, introducing p38 or blocking Akt activity enhanced sensitivity to Taxol-induced apoptosis in parental cells. The same mechanism was observed for E1A-mediated sensitization to other four different anticancer drugs. Furthermore, the *in vivo* synergistic effect we showed between E1A gene therapy and Taxol treatment suggested that E1A gene therapy might represent a novel and unique strategy for enhancing the chemosensitivity of tumor cells.

Several groups have reported that E1A-mediated chemosensitization can be achieved with various chemotherapeutic agents in other cell lines, although the underlying mechanisms are not very clear[10,29]. One of the well defined mechanisms by which E1A sensitizes cells to undergo apoptosis is by inducing expression of ARF, a protein that is required for p53 induction and stabilization[9,30]. However, this mechanism is not applicable to MDA-MB-231 ($p53^{del}$, ARF+) and MCF-7 ($p53^{wt}$, ARF^{del}) cells. Another mechanism reportedly involved in E1A-mediated chemosensitization is E1A-induced expression of the proapoptotic factor Bax[31]. In our system, E1A expression or treatment with Taxol did not affect the abundance of Bax, although we did not test whether E1A expression affected Bax translocation. Duelli et al.[32] have recently shown that E1A also facilitates cytochrome c release from the mitochondria, which contributes to E1A-mediated sensitization to anticancer drugs. However, the mechanism by which E1A facilitates cytochrome c release is unclear.

Akt is known to play an important role in maintaining mitochondria integrity and inhibiting the release of cytochrome c[18,33]; thus, overexpression of Akt confers resistance to Taxol by inhibiting Taxol-induced cytochrome c release[34]. Akt also negatively

regulates FasL transcription and translation by phosphorylating members of the Forkhead protein family[14]. Therefore, when E1A downregulates Akt activity, it may alter mitochondrial potential, thus facilitating the release of cytochrome c and the transcription of FasL in response to Taxol. In other words, Akt is likely one of the inhibitors of apoptosis that is inactivated by E1A.

E1A may upregulate the PP2A catalytic subunit to inhibit Akt activity by dephosphorylating Akt[35]. Since ASK1, the upstream kinase of p38, can be inactivated through phosphorylation by Akt[23], p38 phosphorylation and activity may also be increased due to PP2A-mediated dephosphorylation of Akt. Moreover, Westermarck et al. [36] have reported that p38 directly enhances PP2A activity. Therefore, we propose a feedforward model for the regulation of the p38 and Akt pathways in E1A-expressing cells (Fig. 6*d*). Through this feedforward regulation, E1A-mediated upregulation of p38 activity and downregulation of Akt activity would be greatly amplified. Since FasL transcriptional activation has been shown to be dependent on p38[28], and p38 is also involved in regulation of cyrochrome c release[37]. By modulating the apoptotic potential of cells through regulation of Akt and p38 activities, E1A expression may facilitate the release of cytochrome c and the expression of FasL upon treatment with chemotherapeutic drugs, such as Taxol. Thus, in E1A-expressing cells, a relatively low concentration of drug would be sufficient to trigger apoptosis, regardless of the drug's primary target.

The synergistic effect we obtained *in vivo* by combining Taxol chemotherapy and E1A gene therapy further suggests that through E1A-mediated modulation of the apoptotic threshold, the therapeutic effect of Taxol is significantly enhanced. A plasma

concentration of 5 μM to 10 μM Taxol can be achieved after bolus infusion of Taxol, but it rapidly falls to a level of several hundred nanomolar or less[38]. Our *in vitro* experiments showed that 10 nM Taxol was also sufficient to induce apoptosis in E1A-expressing cells but not in parental cells. This indicates that clinically relevant concentrations (~200 nM) of Taxol are sufficient to kill most E1A-expressing cells, but parental cells require much higher doses, which may not be clinically achievable[38]. As MDA-MB-231 and MCF-7 cells express low levels of Her-2/neu, they are relatively sensitive to Taxol. However, we have previously shown that E1A can also mediate sensitivity to Taxol-induced apoptosis in Her-2/neu-overexpressing breast and ovarian cancer cells by repressing Her-2/neu expression, although the required doses are much higher than those required for sensitizing MDA-MB-231 and MCF-7 cells[39-41]. Recently, a phase II clinical trial of ONXY-015, an adenovirus mutant that retains wild-type E1A, in combination with chemotherapeutic drugs showed a promising synergistic effect against head and neck cancer[13]. This supports our data that E1A gene therapy may represent a novel and unique way to enhance the chemosensitivity of tumor cells. Thus, E1A provides a promising opportunity to fight human breast cancer and other solid tumors when used as an adjuvant to chemotherapeutic drugs.

Materials & Methods

Cell lines and cultures

HEK-293T cells and human breast cancer MDA-MB-231 and MCF-7 cells were grown in Dulbecco's modified Eagle's medium/F-12 (Life Technologies Inc., Rockville,

Marryland) supplemented with 10% fetal bovine serum. The stable E1A-expressing cell lines were established as previously described[42].

MTT assay

The metabolic conversion of tetrazolium salt (MTT) to formazan was used to indirectly measure the number of viable cells after exposure to Taxol. Cells (3 x 10^3/well) were seeded in triplicate in 96-well culture plates in 0.2 ml of culture medium and allowed to adhere for 24 h. After exposure to Taxol for indicated time periods, 20 μl of MTT was added to each well. Cells were cultured for an additional 2 h, and 100 μl of extraction buffer (20% SDS in 50% *N,N*-dimethyl formamide, pH 4.7) was added to the culture medium. The cells were incubated overnight at 37 °C, and the plate absorbency was measured at 570 nm.

Propidium iodide staining and FACS analysis

Samples of 2 x 10^6 cells were collected, washed once with phosphate-buffered saline (PBS), and fixed with 70% ice-cold ethanol overnight. After fixation, cells were washed with PBS to remove residual ethanol, pelleted, and resuspended in PBS containing 50 μg/ml of propidium iodide (Sigma, St. Louis, Washington). The staining was performed at 4 °C for at least 30 min, and samples were analyzed using a FACScan (Becton-Dickinson, San Jose, California) in the core facility at The University of Texas M. D. Anderson Cancer Center.

Transient transfection and luciferase assay

Expression vectors for HA-p38, CA-Akt or DN-Akt, and cytomegalovirus (CMV)

promoter-luciferase (pCMV-Luc) were used in this study. $1x10^5$ cells in a 60-mm well dish were transfected with 2.2 μg of total DNA using DC-Chol cationic liposome as described previously[40]. After growing for another 48 h, the cells were split into three sets; one set was used for a luciferase assay after exposure with or without Taxol for 24 h, another was for analysis of Akt and p38 protein expression, and the third was sent for FACS analysis. The percentage of Taxol-treated cells that exhibited luciferase activity was normalized using the luciferase activity of untreated cells as base line (100%). Standard deviations were calculated from three independent experiments.

Preparation of cell lysates, western blot analysis, and antibodies

Cells were washed once with PBS and lysed in a lysis buffer containing 20 mM Tris-HCl (pH 7.5), 150 mM NaCl, 5 mM EDTA, 10 mM NaF, 1% Nonidet P-40, 1 mM phenylmethylsulfonyl fluoride (PMSF), 1 mM sodium orthovanadate (NaVO3), and 1.5% aprotinin. The cell extracts were clarified by centrifugation, and protein concentration were determined using a Bio-Rad (Hercules, California) protein assay reagent and analyzed in a spectrophotometer using bovine serum album (Sigma, St. Louis, Washington) as the protein standard. Aliquots of protein were resolved by sodium dodecyl sulfate-polyacrylamide gel electrophoresis (SDS-PAGE) and transferred to nitrocellulose membranes (Millipore Corp., Bedford, Massachusetts) using standard procedures. The membranes were then subjected to western blotting, and the blots were developed with the enhanced chemiluminescence system (Amersham Pharmacia Biotech Inc. Piscataway, New Jersey).

The monoclonal antibody usaed against the E1A proteins was M58 (PharMingen, San Diego, Carlifornia). Rabbit polyclonal anti-Bax antibodies, a hamster antihuman

Bcl-2 monoclonal antibody, mouse antihuman phospho-Erk and phospho-JNK monoclonal antibodies, and rabbit polyclonal anti-ASK1 (H-300) antibodies were purchased from Santa Cruz Biotechnology, Inc. (Santa Cruz, California). Mouse monoclonal antiactin and anti-PARP antibodies were obtained from Amersham Pharmacia Biotech (Piscataway, New Jersey). Rabbit anti-human PP2A/A and PP2A/c were purchased from CalBiochem (La Jolla, California). Rabbit polyclonal antibodies against phospho-p38 (p38-p), phospho-Akt (Akt-p), total p38 and total Akt, and the large fragment of cleaved PARP (ΔPARP) were from New England BioLabs (NEB, Beverly, Massachusetts). To detect HA-tagged p38 and Akt, a monoclonal anti-HA antibody was used (Boerhinger Mannheim, Indianopolis, Indiana). A monoclonal anti-FLAG antibody (M2) was purchased from Sigma (St. Louis, Washington).

Immunoprecipatation

After transient transfection with HA-tagged p38 or CA-Akt, cells were stimulated with 10 μM insulin for 15 min. Cell extracts were prepared by lysing cells in a buffer containing 50 mM HEPES (pH 7.6), 150 mM NaCl, 10 mM EDTA, 2 mM $NaVO_3$, 100 mM NaF, 0.5 mM PMSF, 1 mM aprotinin, and 1% triton X-100 for 15 min at 4 °C. Cell lysates were centrifuged at 14,000 rpm for 30 min. The supernatants were then transferred to a fresh tube. Proteins were cleared by addition of normal mouse or rabbit IgG and immuoprecipitated with anti-p38, anti-Akt, or anti-HA antibodies. Immunoprecipitants were resolved on 10% SDS-PAGE and transferred to nitrocellulose membranes. Akt, p38, and ASK1 were detected by western blotting.

Kinase assay

Nonradioactive kinase assay kits for p38 and Akt were purchased from Cell Signaling of New England BioLabs, Inc. (Beverly, Massachusetts). The p38 and Akt kinase activities were measured according to the manufacturer's protocol, using GST-ATF-2 as the substrate for p38 and GST-GSK-3-β as the substrate for Akt.

Establishment of IPTG-inducible DN-p38 stable cell lines

One of E1A-expressing MDA-MB-231 clones was cotransfected with an IPTG-inducible DN-p38 construct (a kind gift from Philipp E. Schere, Department of Cell Biology, Albert Einstein College of Medicine) and plasmid pCMVLacI (Stratagene, La Jolla, California). Stable clones were selected in the presence of 200 μg/ml hygromycin.

Establishment of orthotopic breast cancer model and systematic E1A gene therapyin nude mice.

MDA-MB-231 cells (1 x 10^6 cells/0.1 ml) or 231-E1A cells (2 x 10^6 cells/0.1 ml) were subcutaneously injected into the mammary fat pad (m.f.p.) of female, athymic, 6-8 weeks old nu/nu mice (Charles River Lab.). Tumors were allowed to develop for 21 days and mice were then randomly grouped and treated with SN-liposome alone (SN, *i.v.*), Taxol alone (*i.p.*, 10 mg/kg/injection, once a week for 6 weeks), E1A alone (*i.v.*, 15 μg/mouse/injection, injection into mouse tail vein twice a week for 6 weeks), or E1A (*i.v.*, 15μg/mouse/injection) plus Taxol (*i.p.*, 10 mg/kg/injection, 24 hours after E1A injection, for 6 weeks). Both maximum and minimum diameters of the resulting tumors were measured twice a week using a slide caliper. Tumor volumes were calculated by

assuming a spherical shape and using the formula, volume = $4/3r^3$, where r = 1/2 of the mean tumor diameter measured in two dimensions. Mice were sacrificed when their tumors were larger than 2 cm in diameter.

In vivo apoptotic (TUNEL) assay

For histological study, tumors were fixed in 10% formalin and embedded in paraffin blocks. Paraffin-embedded sections were then pretreated with dewax and rehydrated. They were washed in xylene and rehydrated through a graded series of ethanol and redistilled water. Tissue sections were incubated with proteinase K (20 μg/ml in 10 mM Tris/HCl, pH 7.4 to 8.0, for 15 min at 37°C), permeabilized in 0.1% Triton-X-100 in 0.1% sodium citrate, and then labeled with the TUNEL reaction mixture (Boehringer Mannheim, Indianopolis, Indiana) according to the manufacturer's protocol.

Acknowledgments

We thank B. Su for providing p38 cDNA and Philipp E. Schere for providing IPTG-inducible DN-p38 constructs. This work was supported by Grant RO1 from the National Cancer Institute of Health (to M.-C. H.). Y. L. is the recipient of a postdoctoral fellowship from the United States Department of Defense Breast Cancer Research Program (DOD-BC-000433).

Reference

Figure Ligands

Fig. 1 E1A sensitization to Taxol-induced apoptosis correlates with PARP cleavage in breast cancer MDA-MB-231 and MCF-7 cells. **a**, Percentage of viable cells after 24 hours exposure to 0.1μM, 0.01 μM, and 0.001 μM of Taxol in MDA-MB-231 (231), vector transfectd cells (Vect.), or E1A expressing cells (E1A) detected by MTT assay. Insert shows cleaved PARP p89 fragment (ΔPARP) detected by a polyclonal antibody against cleaved PARP. **b**, Percentage of viable cells after 24 hours exposure to 0.1μM, 0.01 μM, and 0.001 μM of Taxol in MCF-7, MCF-7 E1A expressing cells (E1A), or revertant of the MCF-7 E1A expressing cells (E1A-R)detected by MTT assay. Insert shows cleaved PARP p89 fragment detected by ploYclonal antibodies against cleaved PARP. **c**., FACS analysis of sub-G1 phase apoptotic cells in cells with or without 0.01 μM Taxol treatment for 24 hours.

Fig. 2 Expression of E1A enhanced Taxol anti-tumor effect in nude mice in vivo and prolonged animal survival rate. TUNEl labelling (**a**) and the percentage (**b**) of apoptotic cells in the tumor tissues with or without treatment of Taxol. The percentage of tumor volume in Taxol treated groups versus control tumors was shown (**c**). Combination of systemic E1A gene therapy with Taxol chemotherapy enhanced Taxol anti-tumor effect in nude mice in vivo (**d**) and prolonged animal survival rate (**e**). Treatment groups included SN-liposome vehicle (■), SN-liposome-E1A (∗), Taxol alone (●), or Taxol plus SN-E1A (+). At least 7 animals were included in each group.

Fig.3 Up-regulation of p38 phosphorylation and down-regulation of Akt phosphorylation by E1A correlate with E1A-mediated sensitization to Taxol-induced apoptosis. **a**,

Phospho-p38 (p38-p) and phospho-Akt (Akt-p) levels in E1A expressing cells versus vector alone transfected MDA-MB-231 or MCF-7 cells. Total p38 (p38-c) and Akt (Akt-c) were used as loading control. **b**.Kinase assay of p38 and Akt and densitomitric analysis of relative p38 activity (GST-ATF-2-p)and Akt activity (GST-GSK-3-β-p) in E1A stable expressing cells versus vector transfected cells. **c**, Kinetics of the protein expression of PARP, Akt, p38, Bcl-2, p53, Bax, and JNK1/2 and Erk1/2 (**d**) in E1A expressing MDA-MB-231 cells before or after exposure to 0.01 μM Taxol. Actin was used as loading control. **e**, Densitometric analysis of the kinetic differences among PARP cleavage, Bcl-2 phosphorylation and the levels of Akt and p38 phosphorylation. Y axe represent the arbitrary unit of each protein obtained from densitometry. **f**. Demsitometric analysis of the kinetic differences between JNK and Erk phosphoryaltion with PARP cleavage and Bcl-2 phosphorylation. **g**. Dose-dependent effect of Taxol on PARP cleavage, Bcl-2, Akt, and p38 phosphorylation in parental MDA-MB-231 cells. Taxol doses are from 0 μM. 0.01 μM, 0.1 μM, to 1 μM.

Fig. 4 Inactivating Akt and activiating p38 are required for E1A-mediated sensitization to Taxol-induced apoptosis. **a**, Western blot analysis of p38 and Akt in E1A expressing MDA-MB-231 cells (insert). CA-Akt and/or pcDNA3-luciferase vector (as control) was transciently transfected into 231-E1A cells by liposome 36 hours before treatment with 0.01 μM Taxol. For SB protection, cells were pretreated with 20 μM of SB for 1 hours before addition of 0.01 μM Taxol. After 4 hours exposure to Taxol, a portion of cells was harvested for protein extraction, the rest cells were grown to 24 hours and then split into two portions, one for luciferase assay (Luc) and the other for FACS analysis. **b**, Dose-dependent effect of SB 203580 on the phosphorylation of p38. **c,** Repression of p38

activity by an IPTG-inducible dominant-negative p38 enhances Akt phosphorylation and abrogates E1A-mediated sensitization to Taxol in E1A expressing MDA-MB-231 cells. Exponential growing, IPTG-inducible, flag-tagged DN-p38 stable clones of 231-E1A cells were shifted to mediums supplemented with or without 5 mM of IPTG for overnight before exposure to Taxol. After exposure to Taxol for 24 hours, cells were then harvested and analyzed for protein expression and for FACS analysis of the apoptotic cells, respectively. **d**, Dose-dependent effect of Wortmannin on the phosphorylation of Akt in MDA-MB-231 cells. **e**, Luciferase assay of cells transciently transfected with DN-Akt and/or pcDNA3-luciferase vector with or without exposure to 0.01 μM of Taxol or 0.1μM of Wortmannin. Insert shows the expression of phospho-Akt and HA-tag in MDA-MB-231 cells. **f**, Luciferase assay of cells transciently transfected with HA-tagged p38 and pcDNA3-luciferase vector with or without exposure to 0.01 μM of Taxol. Insert shows the expression of phospho-p38 and HA-tag in MDA-MB-231 cells. The percentage of apoptosis was obtained by FACS analysis of sub-G1 phase cells after exposure to 0.01 μM of Taxol for 24 hours (bottom).

Fig. 5 E1A-mediated chemosensitization to other anticancer drugs. **a**, Percentage of viable cells in vector-transfected and E1A-transfected MDA-MB-231 cells after exposure to adriamycin (ADR, 1 μM), CDDP (2 μg/ml), gemcitabine (GEM, 2 μg/ml), and methotrexate (MTX, 2 μM) by MTT assay. **b**, Downregulation of Akt phosphorylation and upregulation of p38 phosphorylation correlate with drug-induced PARP cleavage in E1A expressing cells. 231-VECT (V): vector transfected cells, 231-E1A (E): E1A stable cells.

Fig. 6 Regulation of p38 and Akt phosphorylation. Stable E1A-expressing or parental

MDA-MB-231 cells were serum-starved for 24 hours before exposure to 20.0 μM of SB or 0.1 μM of Wartmannin, cells were harvested as times indicated and proteins were extracted for Western analysis (**a**). **b**, Immunoprecipation and western blot analysis of Akt and p38 interactions in 293T cells and MDA-MB-231 cells after transcient transfection of HA-Akt and HA-p38. **c**, Upregulation of PP2A catalytic subunit (PP2A/C) expression by E1A. V: 231-Vect; E: 231-E1A; **C**: control, **T**: cells treated with 0.01 μM of Taxol. **d**. Feedforward model for signal amplification and regulation between p38 and Akt pathways in E1A expressing cells.

Reference:

1. Song, Z., Steller, H. Death by design: mechanism and control of apoptosis. *TIBS* **24**, M49-M52 (1999).
2. Bamford, M., Walkinshaw, G. , Brown, R. Therapeutic applications of apoptosis research. *Exp. Cell Res.* **256**, 1-11 (2000).
3. Kaufmann, S.H., Earnshaw, W.C. Induction of apoptosis by cancer chemotherapy. *Exp. Cell Res.* **256**, 42-49 (2000).
4. Houghton, J.A. Apoptosis and drug response. *Curr. Opin. Oncol.* **11**, 475-481 (1999).
5. Brown, J.M., Wouters, B.G. Apoptosis, p53, and tumor cell sensitivity to anticancer agents. *Cancer Res.* **59**, 1391-1399 (1999).
6. Schmitt, C.A., Lowe, S.W. Apoptosis and therapy. *J. Pathol.* **187**, 127-137 (1999).
7. Lowe, S.W., Ruley, H.E., Jacks, T., and Housman, D.E. p53-dependent apoptosis modulates the cytotoxicity of anticancer agents. *Cell* **74**, 957-967 (1993).
8. Lowe, S.W., Ruley, H.E. Stabilization of the p53 tumor suppressor is induced by

adenovirus 5 E1A and accompanies apoptosis. *Genes & Development* **7**, 535-545 (1993).

9. de Stanchina, E., McCurrach, M.E., Zindy, F., Shieh, S.Y., Ferbeyre, G., Samuelson, A.V., Prives, C., Roussel, M.F., Sherr, C.J., Lowe, S.W. E1A signaling to p53 involves the p19(ARF) tumor suppressor. *Genes & Development* **12**, 2434-2442 (1998).
10. Frisch, S.M., Dolter, K.E. Adenovirus E1a-mediated tumor suppression by a c-erbB-2/neu-independent mechanism. *Cancer Res.* **55**, 5551-5555 (1995).
11. Teodoro, J.G., Shore, G.C. , Branton, P.E. Adenovirus E1A proteins induce apoptosis by both p53-dependent and p53-independent mechanisms. *Oncogene* **11**, 467-474 (1995).
12. Hung, M.C., Hortobagyi, G.N., Ueno, N.T. Development of clinical trial of E1A gene therapy targeting HER-2/neu-overexpressing breast and ovarian cancer. *Adv Exp Med Biol* **465**(2000).
13. Khuri, F.R., Nemunaitis, J., Ganly, I., Arseneau, J., Tannock, I.F., Romel, L., Gore, M., Ironside, J., MacDougall, R.H., Heise, C., Randlev, B., Gillenwater, A.M., Bruso, P., Kaye, S.B., Hong, W.K. & Kirn, D.H. A controlled trial of intratumoral ONYX-015, a selectively-replicating adenovirus, in combination with cisplatin and 5-fluorouracil in patients with recurrent head and neck cancer. *Nat. Med.* **6**, 879-885 (2000).
14. Stambolic, V., Mak, T.K. , Woodgett, J.R. Modulation of cellular apoptotic potential: contributions to oncogenesis. *Oncogene* **18**, 6094-6103 (1999).
15. Toker, A., Newton, AC. Cellular signaling: pivoting around PDK-1. *Cell* **103**, 185-

188 (2000).

16. Chan, T.O., Rittenhouse, S.E. & Tsichlis, P.N. Akt/PKB and other D3 phosphoiositide-regulated kinases: kinase activation by phosphoinositide-dependent phosphorylation.,(1999).
17. Berra, E., Diaz-Meco, M.T. & Moscat, J. The activation of p38 and apoptosis by the inhibition of Erk is antagonized by the phosphoinositide 3-kinase/Akt pathway. *J. Biol. Chem.* **273**, 10792-10797 (1998).
18. Cross, T.G., Toellner, D.S., Henriquez, N.V., Deacon, E., Salmon, M. & Lod, J. Serine/theonine protein kinases and apoptosis. *Exp. Cell Res.* **256**, 34-41 (2000).
19. Nebreda, A.R., Porras, A. p38 MAP kinases: beyond the stress response. *TIBS* **25**, 257-260 (2000).
20. Nicholson, D.W. From bench to clinic with apoptosis-based therapeutic agents. *Nature* **407**, 810-816 (2000).
21. Ichijo, H. et al. Induction of apoptosis by ASK1, a mammalian MAPKKK that activates SAPK/JNK and p38 signaling pathways. *Science* **275**, 90-4. (1997).
22. Tobiume, K., Matsuzawa, A., Takahashi, T., Nishitoh, H., Morita, K., Takeda, K., Minowa, O., Miyazono, K., Noda, T., Ichijo, H. ASK1 is required for sustained activations of JNK/p38 MAP kinases and apoptosis. *EMBO Rep* **2**, 222-228 (2001).
23. Kim, A.H., Khursigara, G., Sun, X., Franke, T.F., Chao, M.V. Akt phosphorylates and negatively regulates apoptosis signal-regulating kinase 1. *Mol. Cell. Biol.* **21**, 893-901 (2001).
24. Hale, T.K., Braithwaite, A.W. The adenovirus oncoprotein E1a stimulates binding of transcription factor ETF to transcriptonally activate the p53 gene. *J. biol. Chem.* **274**,

23777-23786 (1999).

25. Yu, D.H., Hung, M.C. The erbB2 gene as a cancer therapeutic target and the tumor- and metastasis-suppressing function of E1A. *Cancer & Metast. Rev.* **17**, 195-202 (1998).
26. Sato, S., Fujita, N., Tsuruo, T. Modulation of Akt kinase activity by binding to Hsp 90. *Proc. Natl. Acad. Sci. USA* **97**, 10832-10837 (2000).
27. Westermarck, J., Li, SP., Kallunki, T., Han, J.H., Kahari, V.M. p38 mitogen-activated protein kinase-dependent activation of protein phosphatases 1 and 2 A inhibits MEK1 and MEK2 activity and collagenase 1 (MMP-1) gene expression. *Mol. Cell. Biol.* **21**, 2373-2383 (2001).
28. Hsu, S.C., Gavrilin, M.A., Tsai, M.H., Han, J. & Lai, M.Z. p38 mitogen-activated protein kinase is involved in Fas ligand expression. *J. Biol. Chem.* **274**, 25769-25776 (1999).
29. Metcalfe, A., Streuli, C. Epithelial apoptosis. *BioEssays* **19**, 711-720 (1997).
30. Ries, S.J., Brandts, C.H., Chung, A.S., Biederer, C.H., Hann, B.C., lipner, E.M., McCormick, F. & Korn, W.M. Loss of p14ARF in tumor cells facilitates replication of the adenovirus mutant dl1520 (ONYX-015). *Nat. Med.* **6**, 1128-1133 (2000).
31. McCurrach, M.E., Connor, T.M.F., Knudson, C.M., Korsmeyer, S.J., Lowe,S.W. bax-deficiency promotes drug resistance and oncogenic transformation by attenuating p53-dependent apoptosis. *Proc. Natl. Acad. Sci. USA* **94**, 2345-2349 (1997).
32. Duelli, D.M., Lazebnik, Y.A. Primary cells suppress oncogene-dependent apoptosis. *Nat. Cell Biol.* **2**, 859-862 (2000).

33. Kennedy, S.G., Kandel, E.S., Cross, T.K. & Hay, N. Akt/protein kinase B inhibits cell death by preventing the release of cytochrome c from mitochondria. *Mol. Cell. Biol.* **19**, 5800-5810 (1999).

34. Page, C., Lin, H.J., Jin Y., Castle, V.P., Nunez, G., Huang, M. & Lin, J. Overexpression of Akt/AKT can modulate chemotherapy-induced apoptosis. *Anticancer Res.* **20**, 407-416 (2000).

35. Sato, S., Fujita, N. & Tsuruo, T. Modulation of Akt kinase activity by binding to Hsp90. *Proc. Natl. Acad. Sci. USA* **97**, 10832-10837 (2000).

36. Westermarck, J., Li, S.P., Kallunki, T., Han, J. & Kahari, V.M. p38 mitogen-activated protein kinase-dependent activation of protein phosphatases 1 and 2A inhibits MEK1 and MEK2 activity and collagenase 1 (MMP-1) gene expression. *Mol Cell Biol* **21**, 2373-83. (2001).

37. Assefa, Z., Vantieghem, A., Garmyn, M., Declercq, W., Vandenabeele, P., Vandenheede, J.R., Bouillon, R., Merlevede, W., Agostinis, P. p38 mitogen-activated protein kinase regulates a novel, caspase-independent pathway for the mitochondrial cytochrome c release in ultraviolet B radiation-induced apoptosis. *J Biol Chem* **275**, 21416-21421 (2000).

38. Blagosklonny, M.V., Fojo, T. Molecular effects of paclitaxel: myths and reality (a critical review). *Int. J. Cancer* **83**, 151-156 (1999).

39. Ueno, N.T., Yu, D. , Hung, M.C. Chemosensitization of Her-2/neu-overexpressing human breast cancer cells to paclitaxel (Taxol) by adenovirus type 5 E1A. *Oncogene* **15**, 953-960 (1997).

40. Ueno, N.T., Bartholomeusz, C., Herrmann, J.L., Estrov, Z., Saho, R., Andreeff, M.,

Price, J., Paul, R.W., Anklesaria, P., Yu, D. & Hung, M.C. E1A-mediated paclitaxel sensitization in Her-2/neu-overexpressing ovarian cancer SKOV3.ip1 through apoptosis involving the caspase-3 pathway. *Clin. Cancer Res.* **6**, 250-259 (2000).

41. Yu, D., Hung, M.C. Overexpression of ErbB2 in cancer and ErbB2-targeting strategies. *Oncogene* **19**, 6115-21 (2000).

42. Meric, F., Liao, Y., Lee, W.P., Pollock, R.E., Hung, M.C. Adenovirus 5 early region 1A does not induce expression of the Ewing sarcoma fusion product EWS-FLI1 in breast and ovarian cancer cell lines. *Clin. Cancer Res.* **6**, 3832-3836 (2000).

Oncogene (2000) 19, 6271–6276
© 2000 Nature Publishing Group All rights reserved 0950–9232/00 $15.00
www.nature.com/onc

Grb2 downregulation leads to Akt inactivation in heregulin-stimulated and ErbB2-overexpressing breast cancer cells

Soo-Jeong Lim[1], Gabriel Lopez-Berestein[1], Mien-Chie Hung[2], Ruth Lupu[3] and Ana M Tari*,[1]

[1]*Department of Bioimmunotherapy, Section of Immunobiology and Drug Carriers, The University of Texas M.D. Anderson Cancer Center, Houston, Texas, USA;* [2]*Department of Molecular and Cellular Oncology, The University of Texas M.D. Anderson Cancer Center, Houston, Texas, USA;* [3]*Lawrence Berkeley National Laboratories, University of California Berkeley, Berkeley, CA, USA*

ErbB2 can be activated by its own overexpression or be transactivated by the heregulin polypeptide growth factor. Activation of ErbB2 leads to breast cancer cell proliferation, presumably by inducing the activation of extracellular signal-regulated kinases 1,2 (Erk1,2) and Akt. We have previously reported that the growth factor receptor bound protein-2 (Grb2) is required for the proliferation of ErbB2-overexpressing breast cancer cells. We investigated here whether Grb2 protein plays a role in heregulin-stimulated proliferation. Grb2 protein inhibition led to growth inhibition of heregulin-stimulated breast cancer cells, but not Erk1,2 inactivation. These findings are similar to our earlier observations in ErbB2-overexpressing cells. Since Akt can also be activated by heregulin, the effects of Grb2 inhibition on Akt were examined. Akt was inactivated following Grb2 downregulation in heregulin-stimulated breast cancer cells. We then examined the effects of Grb2 downregulation on Akt in ErbB2-overexpressing cells in the absence of heregulin. Similar to heregulin-stimulated cells, Grb2 inhibition also led to Akt inactivation in ErbB2-overexpressing breast cancer cells. Our results indicate that the activation of ErbB2 by heregulin or by its overexpression requires Grb2 to stimulate the Akt pathway to propagate mitogenic signals. *Oncogene* (2000) **19,** 6271–6276.

Keywords: Grb2; heregulin; ErbB2; Akt; breast cancer

Introduction

Amplification of the ErbB2 (also known as Her2/neu) receptor tyrosine kinase gene is found in 20–30% of breast cancer patients and is associated with poor patient prognosis (Slamon *et al.*, 1987, 1989; McCann *et al.*, 1991; Paterson *et al.*, 1991). Unlike its other family members (EGFR, ErbB3 and ErbB4), no ligand has yet been identified for ErbB2. However, ErbB2 can be activated by its own overexpression (Pierce *et al.*, 1991), or be transactivated by heregulin (Holmes *et al.*, 1992; Lupu *et al.*, 1992; Peles *et al.*, 1992). Heregulin is a family of proteins identified as ligands for the ErbB3 and ErbB4 receptor tyrosine kinases. Heregulin induces the formation of heterodimers between ErbB3 and ErbB2 or between ErbB4 and ErbB2, thereby transactivating ErbB2 (Plowman *et al.*, 1993a,b; Sliwkowski *et al.*, 1994; Carraway *et al.*, 1995). In fact, the effects of heregulin are predominantly mediated by ErbB2 since inhibiting the function of ErbB2 can block the cellular transformation and proliferation processes induced by heregulin (Alimandi *et al.*, 1995; Lewis *et al.*, 1996). Heregulin stimulates these cellular processes, probably by activating multiple pathways, including those involving extracellular signal-regulated kinases 1,2 (Erk1,2) and phosphoinositol-3 (PI3) kinase (Fiddes *et al.*, 1995; Marte *et al.*, 1995; Sepp-Lorenzino *et al.*, 1996).

Upon activation by heregulin or its overexpression, ErbB2 becomes phosphorylated (Hazan *et al.*, 1990), and bound to the Src homology 2 (SH2) domain of the growth factor receptor bound protein-2 (Grb2) (Lowenstein *et al.*, 1992). Grb2 then uses its Src homology 3 (SH3) domains to bind to the guanine nucleotide exchange factor, Son of Sevenless (Sos) (Bonfini *et al.*, 1992; Chardin *et al.*, 1993; Li *et al.*, 1993; Simon *et al.*, 1993). Sos stimulates Ras by increasing the amount of guanine nucleotide triphosphate (GTP) on Ras (Downward *et al.*, 1990). GTP-bound Ras then interacts with Raf (Dickson *et al.*, 1992; Vojtek *et al.*, 1993), leading to the stimulation of MEK and Erk1,2 (de Vries-Smits *et al.*, 1992; Howe *et al.*, 1992). Besides binding to Raf, GTP-bound Ras may bind to PI3 kinase (Rodriguez-Viciana *et al.*, 1994), leading to the stimulation of Akt (Burgering and Coffer, 1995; Franke *et al.*, 1995). Thus, Grb2 can potentially link activated ErbB2 to the activation of Erk1,2 and Akt in a Ras-dependent manner. Stimulation of the kinase activities of Erk1,2 and Akt have been shown to be important for mitogenesis (Marais and Marshall, 1996; Treisman, 1996; Alessi and Cohen, 1998). Grb2 may therefore play a vital role in transducing the mitogenic signals of heregulin-activated ErbB2 to Erk1,2 and Akt.

We have previously used liposome-incorporated nuclease-resistant antisense oligodeoxynucelotides specific for the GRB2 mRNA (Tari *et al.*, 1997, 1999) to inhibit Grb2 protein expression. We found that Grb2 downregulation led to growth inhibition of breast cancer cells that have overexpression of ErbB2 (Tari *et al.*, 1999), thus indicating that Grb2 is important for the proliferation of this type of breast cancer cells. Since the effects of heregulin are predominantly mediated by ErbB2 (Alimandi *et al.*, 1995; Lewis *et al.*, 1996), we propose that Grb2 will also be important for the proliferation of heregulin-stimulated breast cancer cells. Here, we provide further evidence that Akt is involved in the mitogenic signaling mediated by Grb2.

*Correspondence: AM Tari, Department of Bioimmunotherapy, Section of Immunobiology and Drug Carriers, Box 60, The University of Texas M.D. Anderson Cancer Center, Houston, Texas, TX 77030, USA
Received 15 May 2000; revised 6 October 2000; accepted 10 October 2000

Results

Liposomal Grb2 antisense oligodeoxynucleotides inhibited the growth of breast cancer cells stimulated by heregulin

Before examining the effects of Grb2 downregulation upon heregulin treatment, the growth-stimulatory effects of heregulin were investigated in two different breast cancer cell lines, T-47D and BT-474. These cells do not express endogenous heregulin but express ErbB3 and/or ErbB4 receptors and thus are able to bind to heregulin (Lewis *et al.*, 1996). These cells also differ in their ErbB2 expression levels (BT-474 > > T-47D) (Lewis *et al.*, 1996). Increasing doses of heregulin stimulated the proliferation of both cell lines even in cell culture medium supplemented with fetal bovine serum (FBS) (Figure 1). At 80 and 100 ng/ml of heregulin, the proliferation of T-47D cells and BT-474 cells were stimulated up to 180 and 160% of untreated cells in mediums supplemented with 5 and 10% FBS, respectively.

We then investigated the effects of liposomal Grb2 antisense oligodeoxynucleotides (L-Grb2) on the growth of T-47D and BT-474 cells in the absence and presence of heregulin. Previously we had reported that Grb2 inhibition induced growth inhibition in breast cancer cells that have high, but not low, expression of ErbB2 (Tari *et al.*, 1999). Therefore, the low ErbB2-expressing T-47D cells were not expected to be growth inhibited by L-Grb2, but the high ErbB2-expressing BT-474 cells were expected to be inhibited by L-Grb2. Indeed, in the absence of heregulin, the growth of T-47D cells was not decreased by L-Grb2 (Figure 2a), but the growth of BT-474 cells was selectively decreased by L-Grb2. BT-474 cell growth was decreased by 50% at 12 μM of L-Grb2 (Figure 2b). Under identical conditions, liposomal control oligodeoxynucleotides (L-control) did not decrease the growth of T-47D and BT-474 cells (Figure 2a and b).

In the presence of heregulin, L-Grb2 selectively decreased the proliferation of T-47D cells. When 12 μM of L-Grb2 was used, the growth of T-47D cells decreased by 75% while the same concentration of L-control decreased growth only by 20% (Figure 2a). A dose-dependent decrease in the proliferation of BT-474 cells was also observed when cells were coincubated with L-Grb2 and heregulin (Figure 2b). At 12 μM of L-Grb2, growth inhibition of BT-474 cells was similar in the absence or presence of heregulin (50% versus 58%). Our data indicate that L-Grb2 can inhibit the heregulin-stimulated proliferation of breast cancer cells regardless of the expression levels of ErbB2.

To further investigate the involvement of Grb2 protein in the heregulin-stimulated proliferation of breast cancer cells, MCF-7 cells transfected with heregulin (MCF-7/T7) were used. MCF-7/T7 cells produce high levels of heregulin and thus have constitutively activated ErbB2 receptors in spite of their low ErbB receptors expression (Tang *et al.*, 1996). A dose-dependent decrease in cell proliferation was observed when MCF-7/T7 cells were incubated with various concentrations of L-Grb2, but not with L-control (Figure 3a). At 12 μM of L-Grb2, the growth of MCF-7/T7 cells was decreased by 40%, while the same concentration of L-control only decreased growth by 4%. MCF-7 cells transfected with the control neomycin vector MCF-7/V were used as a negative

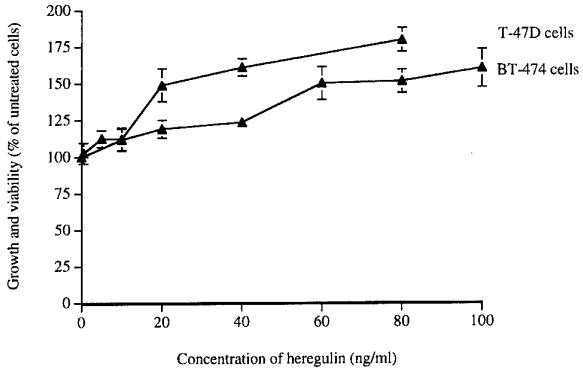

Figure 1 Heregulin induced the proliferation of breast cancer cells. T-47D and BT-474 cells were incubated with different concentrations of heregulin β1 in DMEM/F12 medium supplemented with 5 and 10% FBS, respectively. Cell growth was determined by the MTS proliferation assay. Growth of treated cells was compared with that of untreated cells cultured under the same FBS conditions, and was expressed as per cent of untreated cells

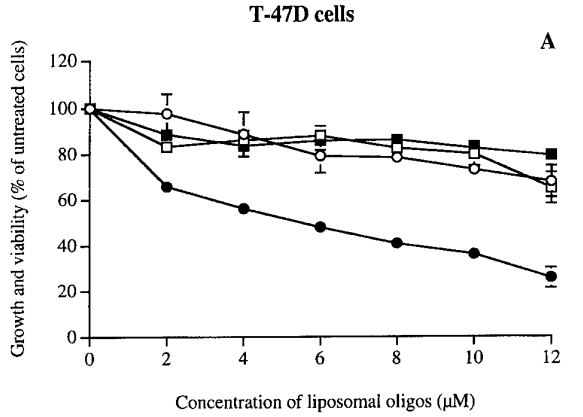

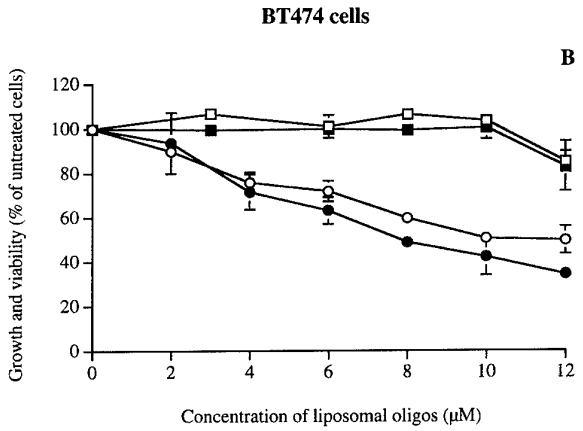

Figure 2 L-Grb2 selectively inhibited the heregulin-stimulated proliferation of breast cancer cells. (**a**) T-47D and (**b**) BT-474 cells were plated in medium supplemented with 5 and 10% FBS, respectively. They were incubated with 0–12 μM of L-Grb2 (○, ●) or L-control (□, ■) for 5–6 days in the absence (○, □) or presence (●, ■) of heregulin. Cell growth was determined by the MTS proliferation assay. Growth of treated cells was compared with that of untreated cells, and was expressed as per cent of untreated cells cultured under the same heregulin conditions

control cell line. These cells have low levels of ErbB2 but do not express any heregulin; therefore ErbB2 is not activated in these cells (Tang *et al*., 1996). As expected, growth inhibitory effects were not observed in MCF-7/V cells incubated with either L-Grb2 or L-control (Figure 3b). These data demonstrate that L-Grb2 can selectively inhibit the proliferation of MCF-7 cells which have activated ErbB2 due to the transfected heregulin gene.

Downregulation of Grb2 protein expression predominantly inhibited Akt activation in heregulin-transfected breast cancer cells

Western blot analysis was carried out to confirm that L-Grb2 could selectively downregulate the expression of Grb2 protein as we had previously reported (Tari *et al*., 1997, 1999). Compared with untreated cells, MCF-7/T7 cells treated with 10 μM of L-Grb2 for 3 days had a 39% decrease in Grb2 protein expression, while cells treated with the same concentrations of L-control had a 9% decrease in Grb2 protein expression (Figure 4). These data indicate that growth inhibition by L-Grb2 (Figure 3) was mediated by specific downregulation of Grb2 protein expression.

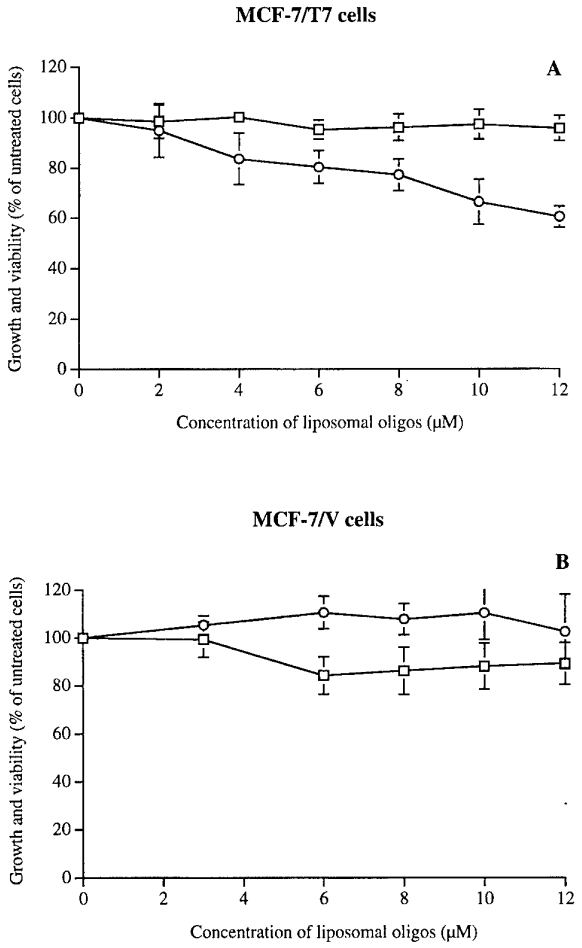

Figure 3 L-Grb2 selectively inhibited the proliferation of breast cancer cells transfected with heregulin. (**a**) MCF-7/T7 and (**b**) MCF-7/V cells were incubated with 0–12 μM final concentration of L-Grb2 (○) or L-control (□) for 5 days. Cell growth was determined by the MTS proliferation assay. Growth of treated cells was compared with that of untreated cells, and was expressed as per cent of untreated cells

We were interested in whether disruption of heregulin-induced growth signaling by Grb2 protein downregulation was due to inactivation of Erk1,2 and Akt, two of the downstream kinases associated with heregulin signaling (Fiddes *et al*., 1995; Marte *et al*., 1995; Sepp-Lorenzino *et al*., 1996; Liu *et al*., 1999). So, we determined the phosphorylation, i.e. activation, levels of Erk1,2 and Akt in the same protein lysates in which Grb2 protein expression was downregulated. The protein levels of Erk1,2 and Akt did not change in MCF-7/T7 cells upon incubation with L-Grb2 or L-control. The phosphorylation levels of Erk1,2 were also not significantly changed after L-Grb2 treatment (Figure 4). Compared with untreated cells, 10 μM of L-Grb2 decreased Erk1,2 activities by 15%, while 10 μM of L-control decreased Erk1,2 activities by 1%. On the other hand, L-Grb2 decreased the phosphorylation levels of Akt (Figure 4). Akt activity was decreased by 62% in cells treated with 10 μM of L-Grb2 but only

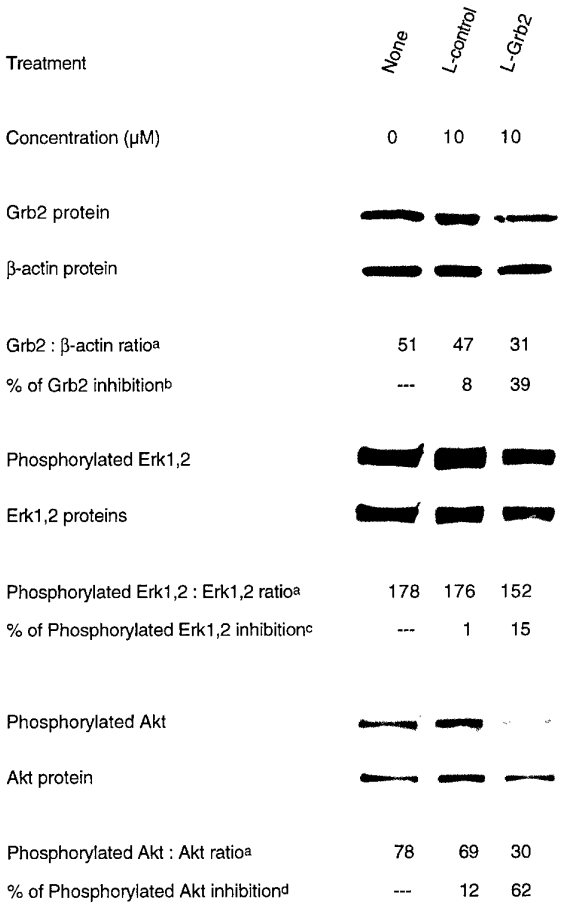

Figure 4 Grb2 downregulation predominantly induced Akt inactivation in heregulin-transfected breast cancer cells. MCF7/T7 cells were incubated with liposomal oligos for 3 days. Protein lysates were obtained and Western blots were performed as described. [a]Densitometric scans were performed on Western blots to measure the ratios of Grb2 to Actin, phosphorylated Erk1,2 to Erk1,2, and phosphorylated Akt to Akt. [b]Grb2 inhibition was obtained by (1-ratio of Grb2:Actin in treated cells/ratio of Grb2:Actin in untreated cells) × 100%. [c]Erk1,2 inactivation was obtained by (1-ratio of phosphorylated Erk1,2:Erk1,2 in treated cells/ratio of phosphorylated Erk1,2:Erk1,2 in untreated cells) × 100%. [d]Akt inactivation was obtained by (1-ratio of phosphorylated Akt:Akt in treated cells/ratio of phosphorylated Akt:Akt in untreated cells) × 100%

12% by L-control. Our data indicate that Grb2 protein downregulation predominantly induces Akt inactivation in heregulin-transfected breast cancer cells.

Grb2 protein downregulation also led to Akt inactivation in ErbB2-overexpressing breast cancer cells

We have demonstrated that Grb2 downregulation could induce growth inhibition but not Erk1,2 inactivation in ErbB2-overexpressing breast cancer cells (Tari *et al.*, 1999). These findings are similar to what we had described above for the heregulin-stimulated cells. Therefore, we speculate that Grb2 downregulation may also lead to Akt inactivation in ErbB2-overexpressing breast cancer cells. We examined the effects of Grb2 downregulation on Akt activities in MDA-MB-453 and BT-474 breast cancer cells, which express high levels of ErbB2 but do not express any heregulin. Similar to what was observed in breast cancer cells stimulated with heregulin, Grb2 inhibition also induced Akt inactivation in ErbB2-overexpressing breast cancer cells (Figure 5). When MDA-MB-453 cells (Figure 5a) and BT-474 cells (Figure 5b) were incubated with 8–12 μM of L-Grb2, Akt activity was inhibited by 34–47%. But Akt activity was inhibited by <4% when same concentration of L-control were used. In all cases, L-Grb2 induced a decrease in Akt activity without decreasing Akt protein expression.

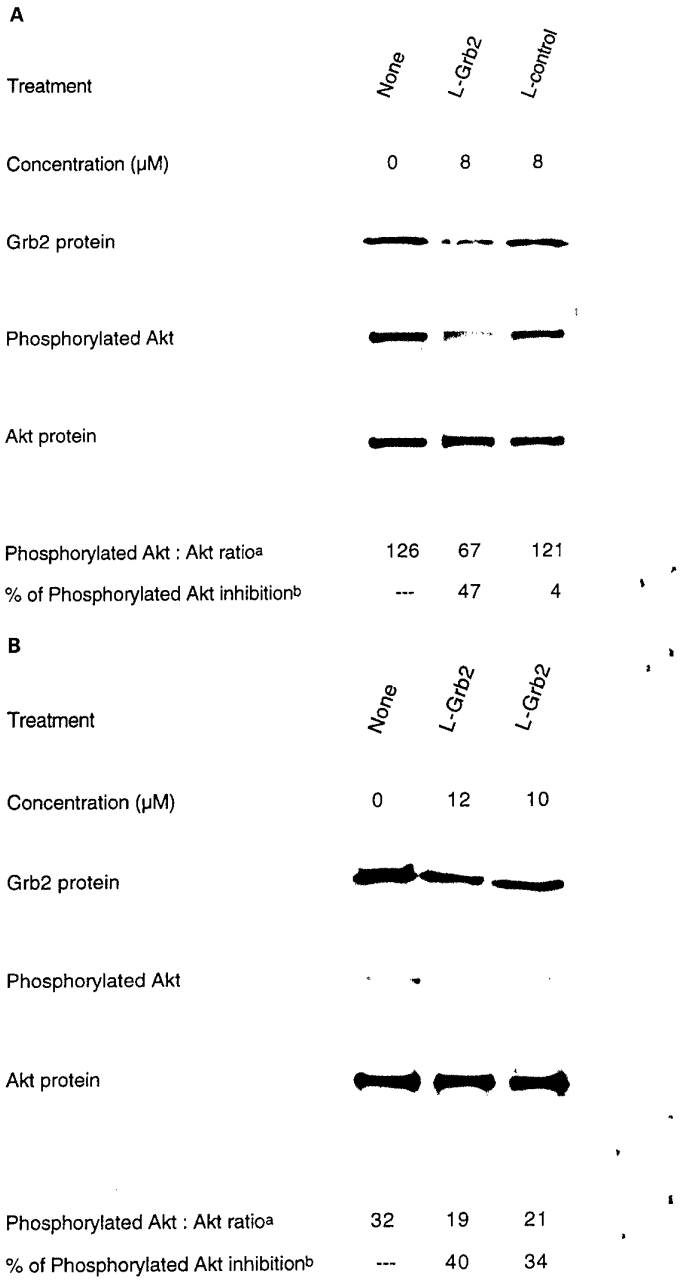

Figure 5 Grb2 downregulation led to Akt inactivation in ErbB2-overexpressing breast cancer cells. (**a**) MDA-MB-453 and (**b**) BT-474 cells were incubated with liposomal oligos for 3 days. Protein lysates were obtained and Western blots were performed as described. [a]Densitometric scans were performed on Western blots to measure the ratios of phosphorylated Akt to Akt. [b]Akt inactivation was obtained by (1-ratio of phosphorylated Akt : Akt in treated cells/ratio of phosphorylated Akt : Akt in untreated cells) × 100%

Discussion

Our results indicate that downregulation of Grb2 protein expression induced growth inhibition and Akt inactivation in ErbB2-overexpressing breast cancer cells as well as in heregulin-stimulated breast cancer cells. It is not surprising that Grb2 downregulation would lead to growth inhibition of heregulin-stimulated cells since there is considerable overlap in signaling between heregulin-stimulated and ErbB2-overexpressing breast cancer cells. Both cell types require the presence and the activation of ErbB2 to induce cellular transformation and mitogenesis (Alimandi *et al.*, 1995; Lewis *et al.*, 1996). The signaling induced by heregulin is initiated mainly from ErbB2 heterodimers while the signaling of ErbB2 overexpression is mainly from ErbB2 homodimers (Muthuswamy *et al.*, 1999).

We postulate that Grb2 regulates Akt activity in a Ras-dependent manner. Grb2 can bind directly to ErbB2 upon ErbB2 activation (Meyer *et al.*, 1994). Alternatively, Grb2 can bind indirectly to ErbB2 via Shc (Meyer *et al.*, 1994; Ravichandran *et al.*, 1995). This is because activation of ErbB2 leads to increased tyrosine phosphorylation on Shc (Segatto *et al.*, 1993), which can bind to Grb2 and ErbB2 simultaneously (Meyer *et al.*, 1994; Segatto *et al.*, 1993). So either directly or indirectly, Grb2 can link activated ErbB2 to Sos, thereby increasing Ras activity (Bonfini *et al.*, 1992; Chardin *et al.*, 1993; Li *et al.*, 1993; Simon *et al.*, 1993). Activated Ras may bind and activate PI3 kinase (Rodriguez-Viciana *et al.*, 1994, 1996), which can in turn stimulate Akt activity (Burgering and Coffer, 1995; Franke *et al.*, 1995). Inhibition of Grb2 expression may therefore disrupt Ras/PI3 kinase/Akt signaling, and induce Akt inactivation. Stimulation of Ras/PI3 kinase activities, for example by expressing constitutively activated forms of Ras/PI3 kianse, should then block the inactivation of Akt by Grb2 downregulation.

On the other hand, Grb2 may also regulate Akt activity in a Ras-independent manner. This is because in addition to binding to Sos, Grb2 can use its SH3 domain to bind to other proline-rich containing proteins, such as PI3 kinase (Wang *et al.*, 1995), and Grb2-associated binder protein-1 (Gab-1) (Holgado-Madruga *et al.*, 1996). Both PI3 kinase and Gab-1 can

stimulate Akt activity (Holgado-Madruga *et al.*, 1997; Wang *et al.*, 1995). The activation of Akt by PI3 kinase or Gab-1 appears to be Ras-independent because the binding of Grb2 to PI3 kinase or Gab-1 can exclude Sos from binding to Grb2, and could potentially stimulate Akt activity without stimulating Erk1,2 activity (Holgado-Madruga *et al.*, 1997; Wang *et al.*, 1995). In that case, inhibition of Grb2 expression may induce Akt inactivation without inducing Erk1,2 inactivation. This postulation is similar to what we have described here for our ErbB2-activated breast cancer systems. However, since Grb2 inhibition was found to decrease Ras activity in fibroblasts transfected with ErbB2 (Xie *et al.*, 1995), we believe that Grb2 inhibition induces Akt inactivation via Ras inactivation.

Even though Akt is known to be activated in response to PI3 kinase activation, some studies have suggested that Akt could be activated by PI3 kinase-independent mechanisms. For example, Filippa's studies suggested that Akt could be activated by protein kinase A (Filippa *et al.*, 1999). When Akt is activated by PI3 kinase, Ser^{473} is always phosphorylated (Franke *et al.*, 1997; Alessi and Cohen, 1998); however in Filippa's studies, protein kinase A activation of Akt did not induce Ser^{473} phosphorylation (Filippa *et al.*, 1999). Since our studies showed that Ser^{473} phosphorylation of Akt was modulated by Grb2, we believe that Grb2 inhibition is followed by PI3 kinase inactivation, and thus Akt inactivation. We are currently investigating whether Ras and/or PI3 kinase is involved in the regulation of Akt activity by Grb2 protein.

Heregulin can stimulate the activation of Erk1,2 and Akt (Fiddes *et al.*, 1995; Marte *et al.*, 1995; Sepp-Lorenzino *et al.*, 1996; Liu *et al.*, 1999); both Erk1,2 and Akt are expected to play major roles in heregulin-induced cellular processes. However, here we report that activation of ErbB2 by heregulin (as well as by ErbB2 overexpression) uses Grb2 to preferentially stimulate Akt, not Erk1,2, activity to effect breast cancer mitogenesis. There have been reports demonstrating that Akt is preferred to Erk1,2 in other heregulin-induced cellular processes, such as cell cycle progression (Daly *et al.*, 1999) and cellular aggregation (Tang *et al.*, 1999). Wortmannin and LY294002, which can inhibit PI3 kinase and therefore Akt activities, can inhibit cell cycle progression and aggregation of breast cancer cells induced by heregulin (Daly *et al.*, 1999; Tang *et al.*, 1999). On the other hand, PD98059, which can inhibit MEK and therefore Erk1,2 activities, cannot inhibit these same breast cancer cellular processes induced by heregulin (Daly *et al.*, 1999; Tang *et al.*, 1999). So, it appears that heregulin may prefer PI3 kinase/Akt pathway to MEK/Erk1,2 pathway in regulating mitogenesis, cell cycle progression, and aggregation of breast cancer cells. It will be very interesting to determine what kinds of cellular processes heregulin will use Erk1,2 for, and the identity of those adaptor proteins that are involved in mediating the activation of Erk1,2 by heregulin.

Materials and methods

Cell lines

T-47D, BT-474, and MDA-MB-453 cells were obtained from ATCC (Manassas, VA, USA). MCF-7 cells transfected with the control neomycin vector (MCF7/V) or the heregulin β-2 gene (MCF7/T7) were obtained from Dr Ruth Lupu (Tang *et al.*, 1996). Cells were cultured in DMEM/F12 medium supplemented with 5 or 10% heat-inactivated FBS at 37°C in a 5% CO_2 humidified incubator.

Antibodies

Monoclonal Grb2 and Actin antibodies were purchased from Transduction Laboratories (Lexington, KY, USA) and Sigma Chemical Co. (St. Louis, MO, USA), respectively. Polyclonal antibodies specific for Erk1,2, phosphorylated Erk1,2 (Thr^{202}/Tyr^{204}), Akt, and phosphorylated Akt (Ser^{473}) were purchased from New England Biolabs (Beverly, MA, USA). These antibodies had been reliably used by us (Tari *et al.*, 1999; Tari and Lopez-Berestein, 2000) and others (Li *et al.*, 1998; Majeti *et al.*, 1998) to measure the phosphorylation, i.e. activation, levels of Erk1,2 and Akt. Antimouse or antirabbit secondary antibodies were obtained from Amersham Life Sciences (Cleveland, OH, USA).

Liposomal oligodeoxynucleotides (oligos)

Nuclease resistant P-ethoxy oligos (18 bases) were purchased from Oligos Etc., Inc. (Willsonville, OR, USA). We have previously reported the sequences of the Grb2 antisense and the control oligos (Tari *et al.*, 1997, 1999). Grb2 antisense: 5′-ATATTTGGCGATGGCTTC-3′; Random control oligo: 5′-GGGCTTTTGAACTCTGCT-3′. Grb2 antisense and control oligos were mixed with dioleoyl-phosphocholine (Avanti Polar Lipids, Alabaster, AL, USA) in the presence of tertiary butanol and prepared as described (Tari *et al.*, 1997, 1999).

Cell growth and viability assay

Breast cancer cells were seeded between $2-8 \times 10^3$ cells/well in 96-well plates in 0.1 ml of DMEM/F12 medium supplemented with 5 or 10% FBS. The next day, heregulin β1 (Neomarkers, Union City, CA, USA) and/or liposomal oligos were added to cells for 5–6 days before cell growth and viability was measured by the CellTiter 96™ AQueous nonradioactive assay (Promega, Madison, WI, USA). This assay measures the conversion of a tetrazolium compound, MTS, into water-soluble MTS-formazan. Each experiment was done in triplicates and repeated at least three times.

Western blots

Breast cancer cells were incubated with liposomal oligos for 3 days. Untreated and treated cells were lysed, and protein lysates were prepared. Proteins were elecrophoresed and electrotransferred as described (Tari *et al.*, 1999; Tari and Lopez-Berestein, 2000). The membranes were incubated with anti-Grb2 antibodies, anti-phosphorylated Erk1,2 antibodies, or anti-phosphorylated Akt antibodies, and protein bands were visualized by enhanced chemiluminescence (Amersham Life Sciences). The membranes were then stripped and reincubated with antibodies specific for Actin, Erk1,2, or Akt. Protein bands were visualized by enhanced chemiluminescence. Images were scanned and quantitated by an Alpha Innotech densitometer using the Alpha Imager application program (Alpha Innotech, San Leandro, CA, USA).

Acknowledgments
We thank Alka Mehta for her excellent technical assistance and Doris Siwak for her critical reading of the manuscript. This work was supported in part by The University of Texas M.D. Anderson Breast Cancer Research Program (to AM Tari), and a postdoctoral fellowship from The Korea Science and Engineering Foundation and from The

University of Texas M.D. Anderson Cancer Center Breast Cancer Research Program/US Army Breast Cancer Research Training Grant Program, Grant No. DAMD 17-94-J-9264 (to S-J Lim).

References

Alessi D and Cohen P. (1998). *Curr. Opin. Genetics Dev.*, **8**, 55–62.

Alimandi M, Romano A, Curia M, Muraro R, Fedi P, Aaronson S, Di Fiore P and Kraus M. (1995). *Oncogene*, **10**, 1813–1821.

Bonfini L, Karlovich C, Dasgupta C and Banerjee U. (1992). *Science*, **255**, 603–606.

Burgering B and Coffer P. (1995). *Nature*, **376**, 599–602.

Carraway K, Soltoff S, Diamonti A and Cantley L. (1995). *J. Biol. Chem.*, **270**, 7111–7116.

Chardin P, Camonis J, Galae N, Van Aelst L, Schlessinger J, Wigler M and Bar-Sagi D. (1993). *Science*, **260**, 1338–1343.

Daly J, Olayioye M, Wong AM-L, Neve R, Lane H, Maurer F and Hynes N. (1999). *Oncogene*, **18**, 3440–3451.

de Vries-Smits A, Burgering B, Leevers S, Marshall C and Bos J. (1992). *Nature*, **357**, 602–604.

Dickson B, Sprenger F, Morrison D and Hafen E. (1992). *Nature*, **360**, 600–603.

Downward J, Graves J, Wame P, Rayter S and Cantrell D. (1990). *Nature*, **346**, 719–721.

Fiddes R, Janes P, Sanderson G, Sivertsen S, Sutherland R and Daly R. (1995). *Cell Growth Differ.*, **6**, 1567–1577.

Filippa N, Sable CL, Filloux C, Hemmings B and Van Obberghen E. (1999). *Mol. Cell. Biol.*, **19**, 4989–5000.

Franke T, Kaplan DR and Cantley LC. (1997). *Cell*, **88**, 435–437.

Franke T, Yang S, Chan T, Datta K, Kazlauskas A, Morrison D, Kaplan D and Tsichlis P. (1995). *Cell*, **81**, 727–736.

Hazan R, Margolis B, Dombalagian M, Ullrich A, Zilberstein A and Schlessinger J. (1990). *Cell Growth Differ.*, **1**, 3–7.

Holgado-Madruga M, Emlet D, Moscatello D, Godwin A and Wong A. (1996). *Nature*, **379**, 560–564.

Holgado-Madruga M, Moscatello D, Emlet D, Dieterich R and Wong A. (1997). *Proc. Natl. Acad. Sci. USA*, **94**, 12419–12424.

Holmes W, Sliwkowski M and Akita R. (1992). *Science*, **256**, 1206–1210.

Howe L, Leeves S, Gomez N, Nakielny S, Cohen P and Marshall C. (1992). *Cell*, **71**, 335–342.

Lewis G, Lofgren J, McMurtrey A, Nuijens A, Fendly B, Bauer K and Sliwkowski M. (1996). *Cancer Res.*, **56**, 1457–1465.

Li J, Simpson L, Takahashi M, Miliaresis C, Myers M, Tonks N and Parsons R. (1998). *Cancer Res.*, **58**, 5667–5672.

Li N, Batzer A, Daly R, Yajnik V, Skolnik E, Chardin P, Bar-Sagi D, Margolis B and Schlessinger J. (1993). *Nature*, **363**, 85–88.

Liu W, Li J and Roth R. (1999). *Biochem. Biophys. Res. Comm.*, **261**, 897–903.

Lowenstein E, Daly R, Batzer A, Li W, Margolis B, Lammers R, Ullrich A, Skolnik E, Bar-Sagi D and Schlessinger J. (1992). *Cell*, **70**, 431–442.

Lupu R, Colomer R, Kannan B and Lippman M. (1992). *Proc. Natl. Acad. Sci. USA*, **89**, 2287–2291.

Majeti R, Bilwes A, Noel J, Hunter T and Weiss A. (1998). *Science*, **279**, 88–91.

Marais R and Marshall C. (1996). *Cell Signalling, Vol. 27: Cancer Surveys*. Parker, P. and Pawson, T. (eds). Cold Spring Harbor Laboratory Press: New York, pp. 101–125.

Marte B, Graus-Porta D, Jeschke M, Fabbro D, Hynes N and Taverna D. (1995). *Oncogene*, **10**, 167–175.

McCann A, Dervan P, O'Regan M, Codd M, Gullick W, Tobin B and Carney D. (1991). *Cancer Res.*, **51**, 3296–3303.

Meyer S, LaBudda K, McGlade J and Hayman M. (1994). *Mol. Cell. Biol.*, **14**, 3253–3262.

Muthuswamy S, Gilman M and Brugge J. (1999). *Mol. Cell. Biol.*, **19**, 6845–6857.

Paterson M, Dietrich KD, Nanyluk J, Paterson A, Lees A, Jamil N, Hanson J, Jenkins H, Krause B, McBlain W, Slamon D and Fourney R. (1991). *Cancer Res.*, **51**, 556–567.

Peles E, Bacus S and Koski R. (1992). *Cell*, **69**, 205–216.

Pierce J, Arnstein P, Di Marco E, Artip J, Kraus M, Lonardo F, Di Fiore P and Aaronson S. (1991). *Oncogene*, **6**, 1189–1194.

Plowman G, Colouscou J, Whitney G, Green J, Carlton G, Foyd L, Neubauer M and Shoyab M. (1993a). *Proc. Natl. Acad. Sci. USA*, **90**, 1746–1750.

Plowman G, Green J, Culouscou J-M, Rothwell V and Buckley S. (1993b). *Nature*, **366**, 473–475.

Ravichandran K, Lorenz U, Shoelson S and Burakoff S. (1995). *Mol. Cell. Biol.*, **15**, 593–600.

Rodriguez-Viciana P, Warne P, Dhand R, Vanhaesebroeck B, Gout I, Fry M, Waterfield M and Downward J. (1994). *Nature*, **370**, 527–532.

Rodriguez-Viciana P, Warne P, Vanhaesebroeck B, Waterfield M and Downward J. (1996). *EMBO J.*, **15**, 2442–2451.

Segatto O, Pelicci G, Giuli S, Digiese G, DiFore P, McGlade J, Pawson T and Pelicci P. (1993). *Oncogene*, **8**, 2105–2112.

Sepp-Lorenzino L, Eberhard I, Ma Z, Cho C, Serve H, Liu F, Rosen N and Lupu R. (1996). *Oncogene*, **128**, 1679–1687.

Simon M, Dodson G and Rubin G. (1993). *Cell*, **73**, 169–177.

Slamon D, Clark M, Wong S, Levin W, Ullrich A and McAuire W. (1987). *Science*, **235**, 177–181.

Slamon D, Godolphin W, Jones L, Holt J, Wong S, Keith D, Levin W, Stuart S, Udove J, Ullrich A and Press M. (1989). *Science*, **244**, 707–712.

Sliwkowski M, Schaefer G, Akita R, Lofgren J, Fitzpatrick V, Nuijens A, Fendly B, Cerione R, Vandlen R and Carraway K.(1994). *J. Biol. Chem.*, **269**, 14661–14665.

Tang C, Perez C, Grunt T, Waibel C, Cho C and Lupu R. (1996). *Cancer Res.*, **1996**, 3350–3358.

Tang M, Grijalva R and Yu D. (1999). *Cancer Res.*, **59**, 1620–1625.

Tari A, Arlinghaus R and Lopez-Berestein G. (1997). *Biochem. Biophys. Res. Comm.*, **235**, 383–388.

Tari A, Hung M-C, Li K and Lopez-Berestein G. (1999). *Oncogene*, **18**, 1325–1332.

Tari A and Lopez-Berestein G. (2000). *Intl. J. Cancer*, **86**, 295–297.

Treisman R. (1996). *Curr. Opin. Cell Biol.*, **8**, 205–215.

Vojtek A, Hollenberg S and Cooper J. (1993). *Cell*, **74**, 205–214.

Wang J, Auger K, Jarvis L, Shi Y and Roberts T. (1995). *J. Biol. Chem.*, **270**, 12774–12780.

Xie Y, Pendergast A and Hung M-C. (1995). *J. Biol. Chem.*, **270**, 30717–30724.

A novel mechanism to induce ATRA resistance in breast cancer cells: the HER2/neu-GRB2-Akt pathway

Ana M. Tari, Soo-Jeong Lim, Mien-Chie Hung, Francisco J. Esteva and Gabriel Lopez-Berestein

Affiliation of authors: A. M. Tari, S.-J. Lim, G. Lopez-Berestein (Department of Bioimmunotherapy, Section of Immunobiology and Drug Carriers), M.-C. Hung (Department of Molecular and Cellular Oncology), F. J. Esteva (Department of Breast Medical Oncology) The University of Texas M. D. Anderson Cancer Center, Houston, Texas

Correspondence to: Ana M. Tari, Department of Bioimmunotherapy, Section of Immunobiology and Drug Carriers, Box 422, The University of Texas M. D. Anderson Cancer Center, 1515 Holcombe Blvd., Houston, TX 77030. Phone: (713) 794-4856. FAX: (713) 796-1731. Email: atari@mdanderson.org

Keywords: HER2/neu, Akt, ATRA, RARα

See "Notes" following "References"

Abstract

BACKGROUND: Amplification of the HER2/neu oncogene has been correlated with poor prognosis in breast cancer patients. Breast cancer cells are often found to be resistant to all-trans retinoic acid (ATRA). We hypothesized that HER2/neu could induce ATRA resistance in breast cancer cells. *METHODS:* Breast cancer cells transfected with HER2/neu or stimulated with the heregulin growth factor, were incubated with ATRA for 5 days. The CellTiter 96 AQueous nonradioactive proliferation assay was used to compare the effects of ATRA on the transfected/stimulated cells and the parental/unstimulated cells. Western blots were used to determine the effects of HER2/neu on RARα expression. The trastuzumab antibody was used to block the expression and function of Her2/neu. Liposome-incorporated GRB2 antisense oligonucleotides were used to downregulate GRB2 protein expression. To inhibit Akt activity, breast cancer cells transfected with a dominant negative Akt mutant were used. *RESULTS:* HER2/neu, when either overexpressed or activated by heregulin, induced ATRA resistance in breast cancer cells by suppressing RARα expression. Conversely, when HER2/neu was blocked by trastuzumab, ATRA sensitivity and RARα expression were reinduced in breast cancer cells. Downregulation of GRB2 protein expression or inhibition of Akt function resensitized HER2/neu-overexpressing breast cancer cells to ATRA by increasing RARα expression. *CONCLUSIONS:* HER2/neu can suppress RARα expression and induce ATRA resistance in breast cancer cells. Furthermore, we demonstrate that HER2/neu utilizes GRB2 and Akt proteins to induce ATRA resistance. This novel pathway of ATRA resistance may have broad implications in the use of ATRA against cancer.

Introduction

All-trans retinoic acid (ATRA) inhibits the growth of various types of cancer cells, including human breast cancer cells (*1*) (*2*) (*3*). However, many breast cancer cell lines are resistant to ATRA. ATRA-resistant breast cancer cell lines generally express low levels of retinoic acid receptors (RARs), particularly RARα (*4*) (*5*) (*6*). Transfection of ATRA-resistant breast cancer cell lines with vectors encoding the RARα gene induced these cells to become sensitive to ATRA (*7*). Furthermore, it has been shown that activation of RARα alone is sufficient for full induction of retinoid responses in breast cancer cells (*8*).

Amplification of Her2/neu (also known as erbB2) is correlated with poor prognosis and survival outcome in patients with breast cancer (*9-11*). This is partly because Her2/neu can induce breast cancer cells resistance to chemotherapeutic and biological agents, including tumor necrosis factor-α (TNFα), tamoxifen, cisplatin, doxorubicin, and paclitaxel (*12-19*). While comparing the characteristics of ATRA-sensitive and ATRA-resistant breast cancer cell lines, we observed that many ATRA-resistant cell lines, with the exception of SKBr3 cells, have moderate to high expression levels of Her2/neu (*7,20-22*). Thus we hypothesized that Her2/neu induces ATRA resistance in breast cancer cells. Here we report that Her2/neu induces ATRA resistance in breast cancer cells by reducing RARα expression. We further demonstrated that Her2/neu uses the growth factor receptor bound protein-2 (Grb2) and Akt, two well-known downstream signaling proteins, to decrease RARα expression and induce ATRA resistance.

Materials and Methods

Cell lines

MCF-7 cells were obtained from American Type Cell Culture (Manassas, VA). MCF-7 cells transfected with the heregulin β-2 gene (MCF-7/HRG), the Her2/neu gene (MCF-7/HER2), and the epidermal growth factor receptor (EGFR) gene (MCF-7/EGFR) were kindly provided by Dr. Ruth Lupu (Berkeley, CA), Dr. Mien-Chie Hung (Houston, TX) and Dr. Francis G. Kern (Birmingham, AL), respectively. These cells were originally termed as MCF-7/T7 (*23*), MCF-7/HER2-18 (*13*), and MCE5 (*24*). Cells were cultured in Dulbecco's modified Eagles's medium (DMEM)/F12 medium supplemented with 5% heat-inactivated fetal bovine serum (FBS). MCF-7/EGFR cells were cultured in phenol red-free DMEM/F12 medium supplemented with 10% charcoal-stripped fetal bovine serum (CSS). Parental MDA-MB-453 cells were obtained from ATCC. MDA-MB-453 cells stably transfected with the HA-tagged cDNA encoding the dominant negative Akt mutant (K179M) were provided by Dr. Mien-Chie Hung and had been previously described (*25*).

Antibodies and ligands

Monoclonal antibodies specific for Her2/neu and Estrogen Receptor-α (ERα) were purchased from Oncogene Research Products (Boston, MA) and Novocastra Laboratories Ltd. (Burlingame, CA), respectively. Antibodies specific for EGFR and heregulin were obtained from NeoMarkers (Fremont, CA). Polyclonal RARα, RARβ, and RARγ antibodies were purchased

from Santa Cruz Biotechnology (Santa Cruz, CA). β-Actin and Grb2 antibodies were purchased from Sigma Chemical Co. (St. Louis, MO) and BD Transduction Laboratories (San Diego, CA), respectively. Anti-mouse and anti-rabbit secondary antibodies were obtained from Amersham Life Sciences (Cleveland, OH). ATRA was obtained from Sigma Chemical Co. Heregulin β1 was purchased from NeoMarkers. Trastuzumab (Herceptin®) was kindly provided by Genentech (San Francisco, CA).

Liposomal oligos

Nuclease resistant P-ethoxy oligos (18 bases) were purchased from Oligos Etc., Inc. (Wilsonville, OR). We have previously reported the sequences of the Grb2 antisense and the control oligos (*26,27*) as follows: Grb2 antisense, 5'-ATATTTGGCGATGGCTTC-3'; control oligo, 5'-GGGCTTTTGAACTCTGCT-3'. Grb2 antisense and control oligos were mixed with dioleoylphosphocholine (Avanti Polar Lipids, Alabaster, AL) in the presence of tertiary butanol and prepared as described (*26,27*).

Cell growth and viability assay

Breast cancer cells were seeded in 96-well plates in 0.1 ml of DMEM/F12 medium supplemented with 5% FBS. The next day, ATRA was added to the cells. When the sensitivity to ATRA was studied in MCF-7/EGFR cells, the culture medium was changed to phenol red-free DMEM/F12 supplemented with 10% CSS before adding ATRA. This medium is necessary to maintain high expression of EGFR in transfected cells (*24*). After 5 days of incubation, cell

growth and viability was measured by using the CellTiter 96 AQueous nonradioactive proliferation assay (Promega, Madison, WI).

Western blots

Cell lysates were obtained from untreated exponentially growing cells or from cells treated with ATRA. Proteins were electrophoresed and electrotransferred as previously described (*26,27*). Membranes were incubated with the appropriate primary and secondary antibodies. Protein bands were visualized by enhanced chemiluminescence (Kirkegaard and Perry Laboratories, Gaithersburg, MD). Images were scanned and quantified by using an Alpha Innotech densitometer using the Alpha Imager application program (Alpha Innotech, San Leandro, CA).

Statistical analysis

Statistical analysis was performed using StatView 5.0 (SAS Institute, Cary, NC). The differences between individual treatments of cells were analyzed using two-tailed *t* test.

Results

Her2/neu and heregulin induced ATRA resistance in breast cancer cells

To determine whether Her2/neu could induce ATRA resistance in breast cancer cells, the sensitivity of parental MCF-7 cells to the growth inhibitory effects of ATRA was compared with those of MCF-7 cells transfected with Her2/neu or heregulin, since Her2/neu is known to be transactivated by heregulin (*28-31*). We chose MCF-7 cells because these cells are sensitive to ATRA, have very low levels of Her2/neu (Fig. 1A, inset), and due to their ease of transfection, have been used as a model to study the function of various genes in breast cancer cells (*32*). As expected, MCF-7 cells stably transfected with either the Her2/neu gene (MCF-7/Her2) or the heregulin (MCF-7/HRG) gene have very high levels of the respective transfected genes (Fig. 1A, inset).

After 5 days of treatment with ATRA, the proliferation of parental MCF-7 cells (MCF-7/WT) was inhibited in a dose-dependent manner (Fig. 1A). At 1 μM concentration, ATRA inhibited MCF-7/WT cell growth by 63%. The sensitivity of vector-transfected cells (MCF-7/V) to ATRA was similar to that of MCF-7/WT cells (data not shown). However, ATRA did not inhibit the proliferation of neither MCF-7/HER2 nor MCF-7/HRG cells (Fig. 1A). This is despite the fact that the expression levels of estrogen receptor-α (ERα) are similar among MCF-7/WT, MCF-7/Her2 and MCF-7/HRG cells (Fig. 1A, inset).

Since Her2/neu and EGFR are related family members, we determined whether EGFR could also induce ATRA resistance. The levels of EGFR in MCF-7 cells transfected with vector control (MCF-7/V) are almost undetectable, whereas the levels of EGFR in MCF-7 cells stably

transfected with EGFR (MCF-7/EGFR cells) are very high (Fig. 1B, inset). However, the expression levels of ERα in both cell lines are quite similar (Fig. 1B, inset). ATRA inhibited the growth of MCF-7/V and MCF-7/EGFR cells to a very similar extent, approximately 40% (Fig. 1B).

Heregulin, when added exogenously, could also reduce the sensitivity of MCF-7 cells to ATRA (Fig. 2). When MCF-7 cells were incubated with 10 nM concentration of ATRA in phenol red-free DMEM/F12 medium + 10% CSS, the growth of MCF-7 cells was reduced by 56%, whereas in the presence of 100 ng/ml heregulin, the same dose of ATRA reduced MCF-7 cell growth by 20% ($p = 0.006$). This reduced sensitivity of MCF-7 cells to ATRA by heregulin was observed when cells were incubated with up to 250 nM ATRA (Fig. 2). However, heregulin did not affect the sensitivity of MCF-7 cells to ATRA when the cells were incubated with higher doses of ATRA. At 1 μM concentration, ATRA reduced the growth of MCF-7 cells by 71% in the absence of heregulin, and 55% in the presence of heregulin ($p > 0.05$). Thus, in the presence of heregulin, MCF-7 cells became less sensitive to low doses of ATRA. These data indicate that overexpression or activation of Her2/neu led to ATRA resistance in breast cancer cells.

Her2/neu and heregulin reduced RARα protein expression

Since the sensitivity of breast cancer cells to ATRA has been correlated with RARα expression (*5-8,20*), we examined the expression of RARs in MCF-7 parental cells and its variants. Compared with MCF-7/WT cells, MCF-7/HRG and MCF-7/HER2 cells had lower RARα protein expression (Fig. 3). Densitometric data indicated that RARα protein expression levels in the MCF-7/V, MCF-7/HRG and MCF-7/HER2 cells were approximately 90%, 41%,

and 63% of the level for MCF-7/WT cells. The expression levels of RARβ and RARγ proteins were not modulated in any of the transfected MCF-7 cells (Fig. 3), indicating that Her2/neu, when overexpressed or activated by heregulin, can decrease endogenous RARα expression.

It has been demonstrated that ATRA treatment led to rapid degradation of RARα protein (*33,34*). We next investigated whether Her2/neu could modulate this ATRA-induced degradation. MCF-7/WT and MCF-7/HER2 cells were incubated with 1 μM concentration of ATRA for 2, 24, and 48 h. After 2 h of treatment with ATRA, RARα protein expression was about 59% lower in MCF-7/WT and MCF-7/HER2 cells (Fig. 4). By 24 h of treatment, however, the levels of RARα proteins recovered to that of untreated MCF-7/WT cells (Fig. 4). On the other hand, the expression of RARα protein in MCF-7/HER2 cells remained suppressed even after 48 h of treatment (Fig. 4). These data indicate that, contrary to what was observed in parental cells, Her2/neu could prevent the recovery of RARα protein to pretreatment steady-state levels.

Trastuzumab increased ATRA sensitivity in Her2-overexpressing cells by increasing RARα protein expression

The antibody trastuzumab specifically blocks Her2/neu function and expression (*35-37*). Thus we determined whether trastuzumab, by blocking Her2/neu signaling, could increase RARα expression and thereby sensitize Her2-overexpressing breast cancer cells to ATRA. MDA-MB-453 cells, which express high levels of Her2/neu (*26*), were treated with 1 μM concentration of trastuzumab for 3 days. Compared with untreated cells, MDA-MB-453 cells treated with trastuzumab had lower levels of Her2/neu but higher levels of RARα protein (Fig. 5A). The sensitivity of MDA-MB-453 cells to ATRA was then determined in the presence and absence of

trastuzumab. When 1 μM trastuzumab was added to MDA-MB-453 cells, growth was inhibited by <6%. When ATRA and trastuzumab were added simultaneously to the cells, MDA-MB-453 cells became sensitive to 1 μM ATRA (Fig. 5B, group II versus group I; $p = 0.012$). Growth inhibition was approximately 39% when cells were incubated with ATRA and trastuzumab simultaneously. Preincubation of MDA-MB-453 cells with trastuzumab for 3 days could further sensitize MDA-MB-453 cells to ATRA (Fig. 5B, group III compared with group II). At 0.1 μM ATRA, growth inhibition of MDA-MB-453 cells was only 11% when trastuzumab was added simultaneously with ATRA. However, when cells were pretreated with trastuzumab, growth inhibition was increased to 32% ($p = 0.018$). Similarly, increase in growth inhibition by trastuzumab pretreatment was observed at 1.0 μM ATRA concentration (from 37 to 53%; $p = 0.019$). This increased growth inhibition was maintained even when cells were not continuously exposed to trastuzumab (Fig. 5B, group IV) since at 0.1 and 1.0 μM ATRA concentrations, growth inhibition was 31 and 58%, respectively. There is no statistical difference in the growth inhibitory values between groups III and IV.

Her2/neu used Grb2 and Akt proteins to induce ATRA resistance

We have previously demonstrated that Grb2 protein is vital to the proliferation of breast cancer cells that have high expression levels of Her2/neu or heregulin (*26,27*), so we examined whether Grb2 protein may also be vital to ATRA sensitivity.

Liposomal Grb2 antisense oligos (L-Grb2), but not liposomal control oligos (L-control), could downregulate Grb2 protein expression (Fig. 6A; *26,27*). L-Grb2 and L-control failed to modulate the sensitivity of MCF-7/WT cells to ATRA (Fig. 6B). However, both MCF-7/HER2

and MCF-7/HRG cells became sensitive to ATRA in the presence of 12 μM L-Grb2 (Fig. 6C and D). At 1 μM ATRA concentration, the growth of MCF-7/HER2 and MCF-7/HRG cells was inhibited by 53 and 72%, respectively. These growth inhibitory values were significantly higher than when MCF-7/HER2 and MCF-7/HRG cells were incubated with L-Grb2 alone ($p = 0.037$ and 0.006, respectively). The increased ATRA sensitivity was specific, because L-control did not modulate the sensitivity of MCF-7/HER2 or MCF-7/HRG cells to ATRA (Fig. 6C and D). L-Grb2 also increased the sensitivity of MDA-MB-453 cells to ATRA (Fig. 6E). When MDA-MB-453 cells were incubated with 6 μM L-Grb2 alone, growth inhibition was 32%. However, when MDA-MB-453 cells were coincubated with L-Grb2 and 1 μM ATRA, growth inhibition was increased to 52% ($p = 0.018$).

We have earlier shown that Grb2 protein regulates Akt activity in breast cancer cells that have high levels of Her2/neu or heregulin (*27*). Since downregulation of Grb2 protein sensitized Her2/neu-overexpressing breast cancer cells to ATRA, inhibition of Akt activity might also sensitize breast cancer cells to ATRA. We compared the RARα expression and the ATRA sensitivity of MDA-MB-453 parental cells to those stably transfected with the dominant negative Akt mutant (MDA-MB-453/DN Akt). MDA-MB-453/DN Akt cells had a higher endogenous RARα expression level (Fig. 7A) and higher ATRA sensitivity (Fig. 7B) than the parental MDA-MB-453 cells. Parental MDA-MB-453 cells were insensitive to 1 μM ATRA. But under the same conditions, ATRA induced 42% growth inhibition in MDA-MB-453/DN Akt cells (Fig. 7B; $p < 0.001$).

Discussion

Our data indicate that Her2/neu, when overexpressed or activated, could induce ATRA resistance in breast cancer cells. Her2/neu can induce tumor resistance to various chemotherapeutic and biological agents (*37*). However, little is known about the role of Her2/neu in regulating RARα expression level or in regulating breast cancer resistance to ATRA. There are multiple isoforms (α, β, γ) of both the RARs and the retinoid X receptors (RXRs) (*38*). ATRA is a pan-agonist for RARs (*38*); upon binding to ATRA, RARs and RXRs form heterodimers and bind to retinoic acid response elements found in the promoters of target genes to modulate their transcription (*38*). It has been shown that in breast cancer, expression and activation of RARα alone are sufficient for retinoid-mediated responses (*8*). Here, we showed that overexpression of Her2/neu or its activating ligand heregulin reduces RARα expression and induces ATRA resistance. We further demonstrated that trastuzumab could increase RARα expression and resensitize breast cancer cells to ATRA.

Both Grb2 and Akt proteins are known to be vital for Her2/neu signaling (*39*). Upon activation, Her2/neu becomes tyrosine phosphorylated and binds to Grb2 (*40*). Grb2 then links Her2/neu to the activation of multiple downstream signaling pathways. Although overexpression of Grb2 itself does not lead to cellular transformation (*41*), Grb2 is crucial for transformation and proliferation induced by various tyrosine kinases, including that of Her2/neu (*26,27,42*). However, Grb2 has not been implicated in the modulation of ATRA or chemotherapy sensitivity.

We have shown that Grb2 regulates Akt activity in heregulin-stimulated and Her2/neu-overexpressing breast cancer cells (*26,27*). Increased Akt activity has been found in many types of cancer. Activation of Akt could be due to AKT gene amplification (*43*), inactivating mutations

of its suppressor PTEN (*44*), or stimulation by growth factors and their receptors (*45-47*). Regardless of the activation mechanism, increased Akt activity can enhance proliferation and prolong cell survival. Akt has been found to modulate the activities of multiple proteins but not to regulate RARα expression. We are currently investigating whether the regulation of RARα expression is mediated directly by Akt or by proteins downstream of Akt and whether RARα regulation is at the transcriptional or translational level.

Her2/neu may induce ATRA resistance in breast cancer cells through other mechanisms besides modulating RARα expression. For example, transfection of c-jun into breast cancer cells increased AP-1 transcriptional activity and ATRA resistance (*48*). Higher basal AP-1 activity has been reported in cells that have constitutive activation of Her2/neu (*49*). Thus, Her2/neu may also induce ATRA resistance by increasing AP-1 transcriptional activity.

Even though ATRA resistance had been reported in both EGFR- and Her2/neu-overexpressing breast cancer cell lines, we did not find EGFR to be directly involved in inducing ATRA resistance in breast cancer cells. EGFR and Her2/neu are family members with a high structural homology (*50-54*). However, the signal transduction pathways they utilize are not always identical. For example, we found that serum growth factors and Grb2 predominantly regulate Akt activity in Her2/neu-overexpressing cells, while serum growth factors and Grb2 predominantly regulate Erk1,2 activities in EGFR-overexpressing cells (*26,55*). In that context, Her2/neu, but not EGFR, induces ATRA resistance in breast cancer cells.

Amplification of Her2/neu has been correlated with poor prognosis in patients with breast cancer (*9,10*). Thus therapeutic strategies that aim to inhibit Her2/neu, such as the trastuzumab antibody, and the tumor-suppressor genes E1A and Pea-3 (*56,57*), have been developed to treat such breast cancer patients. It has been suggested that the therapeutic potential of these agents

can be further improved by combining these agents with chemotherapeutic drugs (*37*). Here we have identified a novel alternative therapeutic strategy against Her2/neu-overexpressing breast tumors: combining the biological agent ATRA with inhibition of the Her2/neu-Grb2-Akt pathway.

Figure Legend

Figure 1. Overexpression of Her2/neu or heregulin inhibited the growth inhibitory effects of ATRA in MCF-7 cells. (A) Parental (MCF-7/WT), Her2-transfected (MCF-7/HER2), and heregulin-transfected (MCF-7/HRG) cells were plated at 1 X 10^3 cells/well in 96-well plates in DMEM/F12 medium + 5% FBS. (B) Vector-transfected (MCF-7/V) and EGFR-transfected (MCF-7/EGFR) cells were plated at 1.5 X 10^3 cells/well in 96-well plates in phenol red-free DMEM/F12 medium + 10% CSS. All cell lines were incubated with increasing doses of ATRA (0-1000 nM) for 5 days. Cell growth and viability were determined by the CellTiter 96 AQueous nonradioactive proliferation assay. Growth of treated cells was compared with that of untreated cells; results are expressed as percentage of untreated cells. Each data point represents an average of triplicate wells ± standard deviation. Insets, (A) Western blot was used to determine the expression levels of HER2/neu, heregulin, and ERα in MCF-7/WT, MCF-7/HER2, and MCF-7/HRG cells; (B) Western blot was used to determine the expression levels of EGFR and ERα in MCF-7/V and MCF-7/EGFR cells.

Figure 2. Heregulin reduced the sensitivity of MCF-7 cells to ATRA. MCF-7 cells were plated at 1.5 X 10^3 cells/well in 96-well plates in DMEM/F12 medium + 5% FBS. After overnight adherence, the medium was changed to phenol red-free DMEM/F12 medium + 10% CSS. MCF-7 cells were treated with increasing doses of ATRA (0-1000 nM) in the presence or absence of heregulin (100 ng/ml). After 5 days, cell growth and viability were determined. The growth of treated cells was compared with that of untreated cells cultured under the same conditions; results are expressed as percentage of untreated cells. Each data point represents an average of triplicate

wells ± standard deviation. *t*-test (at 95% confidence) was used to determine the statistical significance of the cells treated with the same doses of ATRA in the absence and the presence of heregulin (*, $p < 0.05$).

Figure 3. Her2/neu and heregulin reduced RARα protein expression. Protein lysates were obtained from untreated exponentially growing cells. Western blots were performed to determine the expression of RARα, RARβ, RARγ proteins. Densitometric scans were performed on western blots to measure the ratio of RARα to β-actin. The percentage of RARα expression was calculated as (ratio of RARα to β-actin in transfected cells/ratio of RARα to β-actin in parental cells) × 100.

Figure 4. Her2/neu suppressed the recovery of RARα protein upon ATRA incubation. Four hundred thousand MCF-7/WT cells and MCF-7/HER2 cells each were plated in T-25 flasks in DMEM/F12 medium + 5% FBS. Cells were treated with 1 μM concentration of ATRA for 0, 2, 24, and 48 h. MCF-7/WT protein lysates (25 μg) and MCF-7/HER2 protein lysates (40 μg) were used for western blots. Densitometric scans were performed on western blots to measure the ratio of RARα to β-actin. The expression levels of RARα protein were normalized to 100% in untreated parental and untreated transfected cells.

Figure 5. Trastuzumab increased RARα expression and ATRA sensitivity in MDA-MB-453 cells. (A) Two hundred thousand MDA-MB-453 cells were plated in T-25 flasks. After 3 days of incubation, protein lysates (25 μg) were obtained from untreated and trastuzumab (1 μM)-treated MDA-MB-453 cells. Western blots were performed to determine the expression levels of

Her2/neu and RARα proteins in the cell lysates. (B) MDA-MB-453 cells were plated at 2000 cells/well in 96-well plates and were incubated with ATRA (0, 0.01, 0.10, and 1.00 μM concentrations) in the absence (group I) and presence of trastuzumab (group II). MDA-MB-453 cells were pretreated with trastuzumab (groups III and IV) as described in Panel A. Cells were then replated at 2000 cells/well in 96-well plates before incubated with ATRA. Trastuzumab was continuously given to group III but not to group IV. Cell growth and viability were determined. Growth of treated cells was compared with that of untreated cells cultured under the same conditions; results were expressed as percentage of untreated cells. Each bar represents the average of quadruplicate wells ± standard deviation. *t*-test was used to determine the statistical significance (at 95% confidence) between the cells treated with trastuzumab only and the cells treated with the trastuzumab and ATRA combination (*, $p < 0.05$).

Figure 6. L-Grb2 increased ATRA sensitivity in breast cancer cells that have high levels of Her2/neu or heregulin. (A) MDA-MB-453 cells, plated at 1 X 10^5 cells/well in a 6-well plate, were treated with 10 μM L-Grb2 or L-control for 3 days. Cell lysates were obtained, and western blot was performed to determine Grb2 protein expression. (B-D) Parental and transfected MCF-7 cells were plated at 2000 cells/well in 96-well plates and incubated with increasing doses of ATRA (0 - 2.5 μM) in the presence and absence of 12 μM concentration of L-Grb2 or L-control. After 5 days of incubation, cell growth and viability were determined. (E) MDA-MB-453 cells were plated in T-25 flasks at 2 X 10^5 cells/flask and preincubated with 6 μM of L-Grb2 or L-control for 3 days. MDA-MB-453 cells were then replated at 2000 cells/well in 96-well plates before incubated with ATRA and L-Grb2 or L-control. After 5 days of incubation, cell growth

and viability were determined. Growth of treated cells was compared with that of untreated cells; results are expressed as percentage of untreated cells ± standard deviation. Each bar represents an average of triplicate wells ± standard deviation. *t*-test was used to determine the statistical significance (at 95% confidence) between the cells treated with L-Grb2 only and the cells treated with the L-Grb2 and ATRA combination (*, $p < 0.05$).

Figure 7. MDA-MB-453 cells transfected with the DN Akt gene have higher RARα protein expression and are more sensitive to ATRA than their parental counterparts. (A) Protein lysates were obtained from parental MDA-MB-453 cells and its variant transfected with the HA-tagged cDNA encoding the DN Akt gene (MDA-MB-453/DN Akt). Western blots were performed to determine RARα protein expression. (B) Parental MDA-MB-453 cells and MDA-MB-453/DN Akt cells were plated at 1000 cells/well in 96-well plates before incubated with 1 μM concentration of ATRA for 5 days. Cell growth and viability were determined. Growth of treated cells was compared with that of untreated cells; results are expressed as percentage of untreated cells. Each bar represents an average of triplicate wells ± standard deviation. *t*-test (at 95% confidence) was used to determine the statistical significance of the two treatment groups (*, $p < 0.05$).

References

(*1*) Lotan R: Different susceptibilities of human melanoma and breast carcinoma cell lines to retinoic acid-induced growth inhibition. Cancer Res 1979;39:1014-19.

(*2*) Fontana J, Hobbs P, Dawson M: Inhibition of mammary carcinoma growth by retinoidal benzoic acid derivatives. Exp Cell Biol 1988;56:254-63.

(*3*) Fraker L, Halter S, Forbes J: Growth inhibition by retinol of a human breast carcinoma cell line in vitro and in athymic mice. Cancer Res 1984;44:5757-62.

(*4*) Roman S, Clarke C, Hall R, Alexander I, Sutherland R: Expression and regulation of retinoic acid receptors in human breast cancer cells. Cancer Res 1992;52:2236-42.

(*5*) van der Burg B, van der Leede B, Kwakkenbos-Isbrucker L, Salverda S, de Laat S, van der Saag P: Retinoic acid resistance of estradiol-independent breast cancer cells coincides with diminished retinoic acid receptor function. Mol Cell Endocrinol 1993;91:149-57.

(*6*) Fitzgerald P, Teng M, Chandraratna R, Heyman R, Allegretto E: Retinoic acid receptor α expression correlates with retinoid-induced growth inhibition of human breast cancer cells regardless of estrogen receptor status. Cancer Res 1997;57:2642-50.

(*7*) Sheikh M, Shao Z, Li X, Dawson M, Jetten A, Wu S, et al: Retinoid-resistant estrogen receptor-negative human breast cancer cells transfected with retinoic acid receptor-α acquires sensitivity to growth inhibition by retinoids. J Biol Chem 1994;269:21440-47.

(*8*) Schneider S, Offterdinger M, Huber H, Grunt T: Activation of retinoic acid receptor α is sufficient for full induction of retinoid responses in SK-BR-3 and T47D human breast cancer cells. Cancer Res 2000;60:5479-87.

(*9*) Slamon D, Clark M, Wong S, Levin W, Ullrich A, McAuire W: Human breast cancer: correlation of relapse and survival with amplification of the Her-2 neu oncogene. Science 1987;235:177-81.

(*10*) Slamon D, Godolphin W, Jones L, Holt J, Wong S, Keith D, et al: Studies of the HER-2/neu protooncogene in human breast and ovarian cancer. Science 1989;244:707-12.

(*11*) Paterson M, Dietrich, KD, Nanyluk J, Paterson A, Lees A, Jamil H, et al: Correlation between c-erbB-2 amplification and risk of recurrent disease in node-negative breast cancer. Cancer Research 1991;51:556-67.

(*12*) Hudziak R, Lewis G, Winget M, Fendly B, Shepard M, Ullrich A: p185HER2 monoclonal antibody has antiproliferative effects in vitro and sensitizes human breast tumor cells to tumor necrosis factor. Mol Cell Biol 1989;9:1165-72.

(*13*) Benz C, Scott G, Sarup J, Johnson R, Tripathy D, Coronado E, et al: Estrogen-dependent, tamoxifen-resistant tumorigenic growth of MCF-7 cells transfected with HER2/neu. Breast Cancer Res Treatment 1992;24:85-95.

(*14*) Pietras R, Fendly B, Chazin V, Pegram M, Howell S, Slamon D: Antibody to HER-2/neu receptor blocks DNA repair after cisplatin in human breast and ovarian cancer cells. Oncogene 1994;9:1829-38.

(*15*) Pietras R, Arboleda J, Reese D, Wongvipat N, Pegram M, Ramos L, et al: HER-2 tyrosine kinase pathway targets estrogen receptor and promotes hormone-independent growth in human breast cancer cells. Oncogene 1995;10:2345-446.

(*16*) Liu Y, el-Ashry D, Chen D, Ding I, Kern F: MCF-7 breast cancer cells overexpressing transfected c-erbB-2 have an in vitro growth advantage in estrogen-depleted conditions

and reduced estrogen-dependence and tamoxifen-sensitivity in vivo. Breast Cancer Res Treat 1995;34:97-117.

(*17*) Yu D, Liu B, Tan M, Junzhi L, Wang S-S, Hung M-C: Overexpression of c-*erb*B2/*neu* in breast cancer cells confers increased resistance to Taxol via *mdr*-1-independent mechanisms. Oncogene 1996;13:1359-65.

(*18*) Baselga J, Norton L, Albanell J, Kim Y-M, Mendelsohn J: Recombinant humanized anti-Her2 antibody (Herceptin TM) enhances the antitumor activity of paclitaxel and doxorubicin against Her2/neu overexpressing human breast cancer xenografts. Cancer Res 1998;58:2825-31.

(*19*) Kurokawa H, Lenferink A, Simpson J, Pisacane P, Sliwkowski M, Forbes J, et al: Inhibition of HER2/neu (erbB-2) and mitogen-activated protein kinase enhances tamoxifen action against HER2-overexpressing, tamoxifen-resistant breast cancer cells. Cancer Res 2000;60:5887-94.

(*20*) Sheikh M, Shao Z, Chen J, Hussain A, Jetten A, Fontana J: Estrogen receptor-negative breast cancer cells transfected with the estrogen receptor exhibit increased RAR alpha gene expression and sensitivity to growth inhibition by retinoic acid. J Cell Biochem 1993;53:394-404.

(*21*) Rishi A, Gerald T, Shao Z, Li X, Baumann R, Dawson M, et al: Regulation of the human retinoic acid receptor alpha gene in the estrogen receptor negative human breast carcinoma cell lines SKBR-3 and MDA-MB-435. Cancer Res 1996;56:5246-52.

(*22*) De Luca L, Scita G, Takatsuka J: Retinoic acid downregulates growth, fibronectin and RAR alpha in 3T3 cells: Ha-ras blocks this response and RA metabolism. J Cell Physiol 1997;173:297-300.

(*23*) Tang C, Perez C, Grunt T, Waibel C, Cho C, Lupu R: Involvement of heregulin-b2 in the acquisition of the hormone-independent phenotype of breast cancer cells. Cancer Research 1996;1996:3350-58.

(*24*) Miller DL, el-Ashry D, Cheville AL, Liu Y, McLeskey SW, Kern FG: Emergence of MCF-7 cells overexpressing a transfected epidermal growth factor receptor (EGFR) under estrogen-depleted conditions: evidence for a role of EGFR in breast cancer growth and progression. Cell Growth Differ 1994;5:1263-74.

(*25*) Zhou BP, Hu MC, Miller SA, Yu Z, Xia W, Lin SY, et al: HER-2/neu blocks tumor necrosis factor-induced apoptosis via the Akt/NF- kappaB pathway. J Biol Chem 2000;275:8027-31.

(*26*) Tari A, Hung M-C, Li K, Lopez-Berestein G: Growth inhibition of breast cancer cells by Grb2 downregulation is correlated with inactivation of mitogen-activated protein kinase in EGFR, but not in ErbB2, cells. Oncogene 1999;18:1325-32.

(*27*) Lim S-J, Lopez-Berestein G, Hung M-C, Lupu R, Tari A: Grb2 downregulation leads to Akt inactivation in heregulin-stimulated and ErbB2-overexpressing breast cancer cells. Oncogene 2000;19:6271-76.

(*28*) Lupu R, Colomer R, Kannan B, Lippman M: Characterization of a growth factor binds exclusively to the erbB2 receptor and induces cellular responses. Proc Natl Acad Sci, USA 1992;89:2287-91.

(*29*) Peles E, Bacus S, Koski R: Isolation of the Neu/Her-2 stimulatory ligand: A 44 kDa glycoprotein that induces differentiation of mammary tumor cells. Cell 1992;69:205-16.

(*30*) Plowman G, Green J, Culouscou J-M, Rothwell V, Buckley S: Heregulin induces tyrosine phosphorylation of HER4/p180erbB4. Nature 1993;366:473-75.

(*31*) Sliwkowski M, Schaefer G, Akita R, Lofgren J, Fitzpatrick V, Nuijens A, et al: Coexpression of erbB2 and erbB3 proteins reconstitutes a high affinity receptor for heregulin. J Biol Chem 1994;269:14661-65.

(*32*) Kern F, McLeskey S, Zhang L, Kurebayashi J, Liu Y, Ding I, et al: Transfected MCF-7 cells as a model for breast-cancer progression. Breast Cancer Res Treat 1994;31:153-65.

(*33*) Scita G, Darwiche N, Greenwald E, Rosenberg M, Politi K, De Luca L: Retinoic acid down-regulation of fibronectin and retinoic acid receptor alpha proteins in NIH-3T3 cells. Blocks of this response by ras transformation. J Biol Chem 1996;271:6502-08.

(*34*) Zhu J, Gianni M, Kopf E, Honore N, Chelbi-Alix M, Koken M, et al: Retinoic acid induces proteasome-dependent degradation of retinoic acid receptor alpha (RARalpha) and oncogenic RARalpha fusion proteins. Proc Natl Acad Sci U S A 1999;96:14807-12.

(*35*) Fendly B, Winget M, Hudziak R, Lipari M, Napier M, Ullrich A: Characterization of murine monoclonal antibodies reactive to either the human epidermal growth factor receptor or HER2/neu gene product. Cancer Res 1990;50:1550-58.

(*36*) Carter P, Presta L, Gorman C, Ridgway J, Henner D, Wong W, et al: Humanization of an anti-p185HER2 antibody for human cancer therapy. Proc Natl Acad Sci USA 1992;89:4285-89.

(*37*) Sliwkowski M, Lofgren J, Lewis G, Hotaling T, Fendly B, Fox J: Nonclinical studies addressing the mechanism of action of trastuzumab (Herceptin). Semin Oncol 1999;26:60-70.

(*38*) Mangelsdorf D, Umesono K, Evans R: The retinoid receptors. In Sporn M, Roberts A, Goodman D, editors. The retinoids: biology, chemistry and medicine. New York: Raven Press, 1994, p. 319-50.

(*39*) Reese D, Slamon D: HER-2/neu signal transduction in human breast and ovarian cancer. Stem Cells 1997;15:1-8.

(*40*) Meyers S, LaBudda K, McGlade J, Hayman M: Analysis of the role of the Shc and Grb2 proteins in signal transduction by the v-ErbB protein. Mol Cell Biol 1994;14:3253-62.

(*41*) Lowenstein E, Daly R, Batzer A, Li W, Margolis B, Lammers R, et al: The SH2 and SH3 domain-containing protein GRB2 links receptor tyrosine kinases to ras signaling. Cell 1992;70:431-42.

(*42*) Xie Y, Pendergast A, Hung M-C: Dominant-negative mutants of Grb2 induced reversal of the transformed phenotypes caused by the point mutation-activated rat HER-2/Neu. Journal Biological Chemistry 1995;270:30717-24.

(*43*) Bellacosa A, de Feo D, Godwin A, Bell D, Cheng J, Altomare D, et al: Molecular alterations of the AKT2 oncogene in ovarian and breast carcinomas. Int J Cancer 1995;64:280-5.

(*44*) Steck P, Pershouse M, Jasser S, Yung W, Lin H, Ligon A, et al: Identification of a candidate tumour suppressor gene, MMAC1, at chromosome 10q23.3 that is mutated in multiple advanced cancers. Nat Genet 1997;15:356-62.

(*45*) Burgering B, Coffer P: Protein kinase B (c-Akt) in phosphatidylinositol 3-OH kinase signal transduction. Nature 1995;376:599-602.

(*46*) Franke T, Yang S, Chan T, Datta K, Kazlauskas A, Morrison D, et al: The protein kinase encoded by the Akt protooncogene is a target of the PDGF-activated phosphatidylinositol 3-kinase. Cell 1995;81:727-36.

(*47*) Alessi D, Andjelkovic M, Caudwell F, Cron P, Morrice N, Cohen P, et al: Mechanism of activation of protein kinase B by insulin and IGF-1. EMBO J 1996;15:6541-51.

(*48*) Yang L, Kim H, Munoz-Medellin D, Reddy P, Brown P: Induction of retinoid resistance in breast cancer cells by overexpression of c-Jun. Cancer Res 1997;57:4652-61.

(*49*) Galang CK, Garcia-Ramirez J, Solski PA, Westwick JK, Der CJ, Neznanov NN, et al: Oncogenic Neu/ErbB-2 increases ets, AP-1, and NF-kappaB-dependent gene expression, and inhibiting ets activation blocks Neu-mediated cellular transformation. J Biol Chem 1996;271:7992-8.

(*50*) Akiyama T, Sudo C, Ogawara H, Toyoshima K, Yamamoto T: The product of human c-erb-2 gene: a 185 kilodalton glycoprotein with tyrosine kinase activity. Science 1986;232:1644-46.

(*51*) Coussens L, Yang-Feng T, Liao Y, Chen E, Gray A, McGrath J, et al: Tyrosine kinase receptor with extensive homology to EGF receptor shares chromosomal location with neu oncogene. Science 1985;230:1132-39.

(*52*) Bargmann C, Hung M-C, Weinberg R: The *neu* oncogene encodes an epidermal growth factor receptor-related protein. Nature 1986;319:226-34.

(*53*) Schechter A, Hung M-C, Vaidyanthan L, Weinberg R, Yang-Feng T, Francke U, et al: The neu gene: An erbB-homologous gene distinct from and unlinked to the gene encoding the EGF receptor. Science 1985;229:976-87.

(*54*) Yamamoto T, Ikawa S, Akiyama T, Semba K, Nomura N, Miyajima N, et al: Similarity of protein encoded by the human c-erbB2 gene to epidermal growth factor receptor. Nature 1986;319:230-34.

(*55*) Tari A, Lopez-Berestein G: Serum predominantly leads to activation of MAPK and Akt kinases in EGFR and ErbB2 overexpressing cells, respectively. Int J Cancer 2000;86:295-97.

(*56*) Yu D, Hamada J, Zhang H, Nicolson G, MC H: Mechanisms of c-erbB2/neu oncogene-induced metastasis and repression of metastatic properties by adenovirus 5 E1A gene products. Oncogene 1992;7:2263-70.

(*57*) Xing X, Wang S, Xia W, Zou Y, Shao R, Kwong K, et al: The ets protein PEA3 suppresses HER-2/neu overexpression and inhibits tumorigenesis. Nat Med 2000;6:189-95.

Notes

A. M. Tari and S.-J. Lim contributed equally to this work.

Present address of S.-J. Lim: College of Pharmacy, Seoul National University, San 56-1, Shinlim-Dong, Kwanak-Gu, Seoul, KOREA 151-742

This work was supported in part by The Elsa Pardee Foundation (to A. M. T.), The University of Texas M. D. Anderson Cancer Center Breast Cancer Research Program/US Army Breast Cancer Research Training Grant Program, Grant No. DAMD 17-99-1-9264 (to S.-J. Lim) and NIH Grant K23-CA82119 (to F. J. E.).

We are grateful to Dr. Reuben Lotan for his advice and suggestions. We are also grateful to Dr. Ruth Lupu and Dr. Francis Kern for providing us the MCF-7/T7 (MCF7-HRG) and the MCE5 (MCF-7/EGFR) cells.

Figure 1

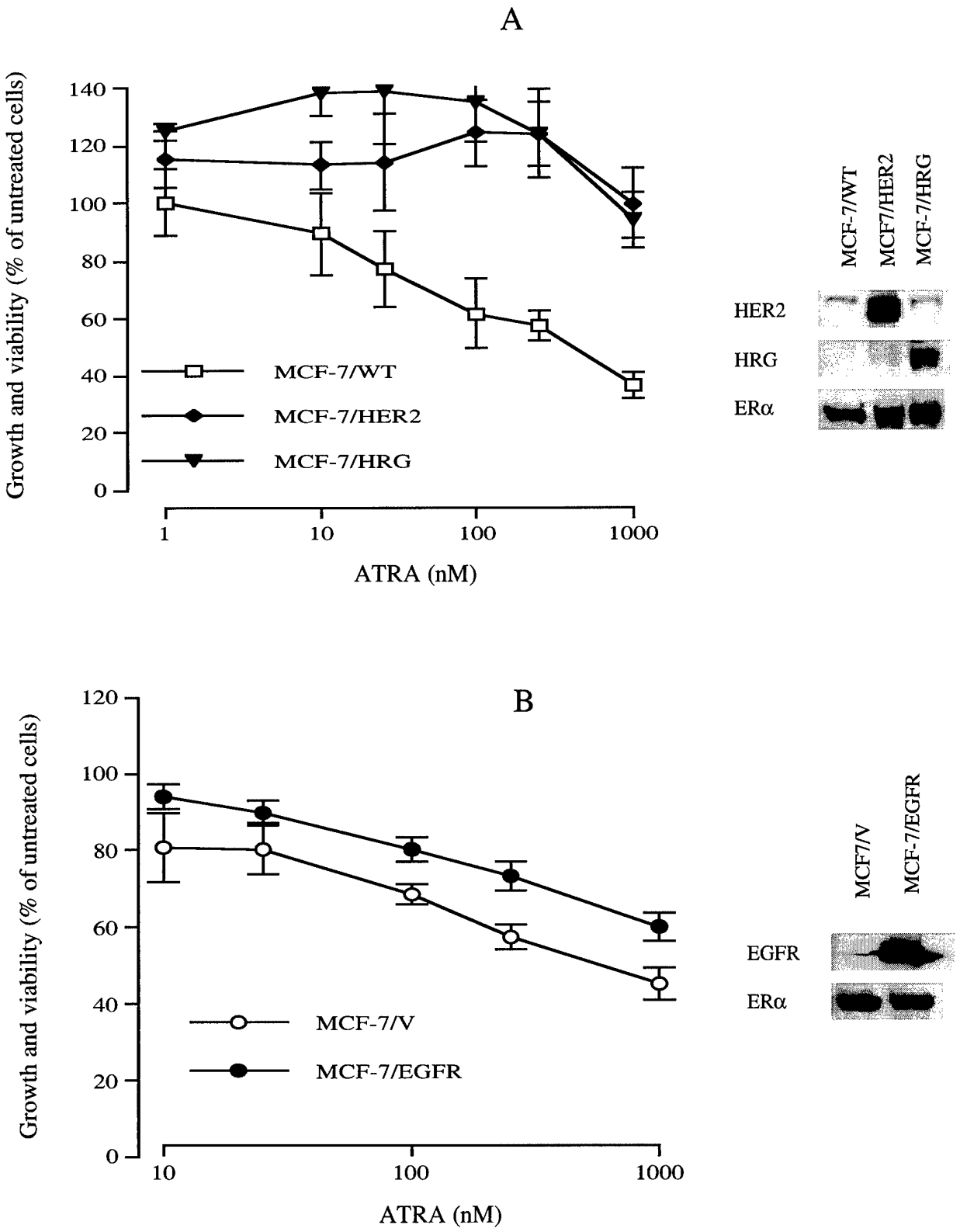
A
Growth and viability (% of untreated cells)
140
120
100
80
60
40
20
0
MCF-7/WT
MCF-7/HER2
MCF-7/HRG
1
10
100
1000
ATRA (nM)
MCF-7/WT
MCF7/HER2
MCF-7/HRG
HER2
HRG
ERα
B
Growth and viability (% of untreated cells)
120
100
80
60
40
20
0
MCF-7/V
MCF-7/EGFR
10
100
1000
ATRA (nM)
MCF7/V
MCF-7/EGFR
EGFR
ERα

Figure 2

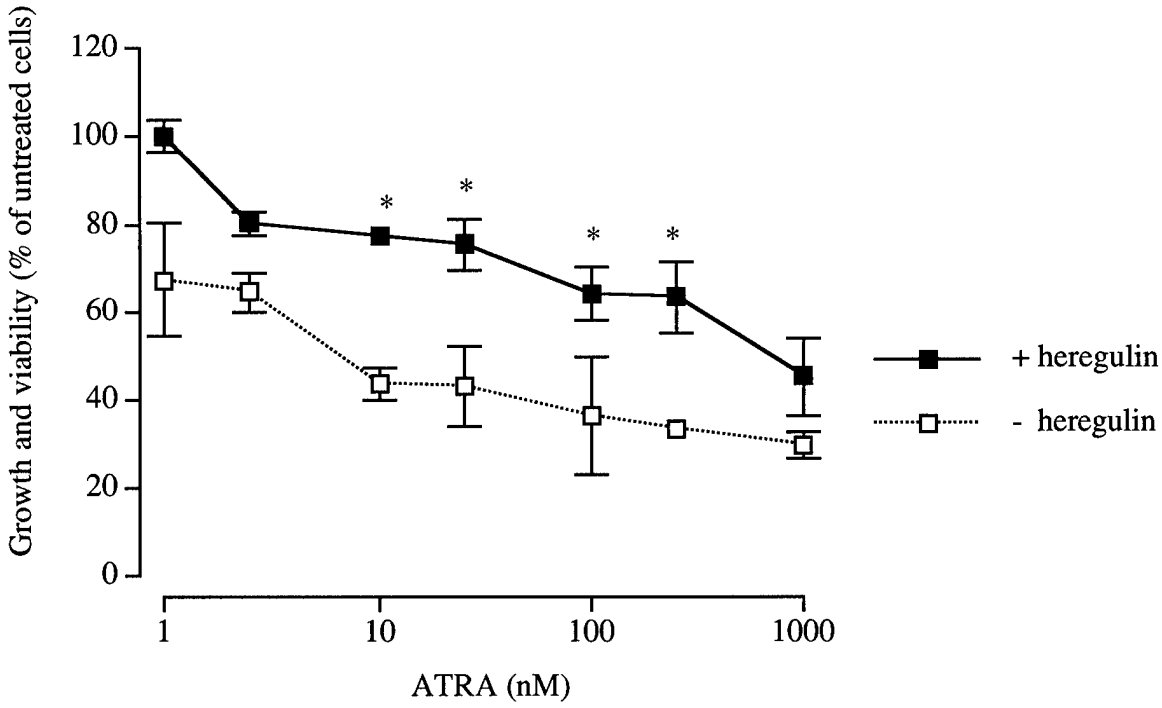
Growth and viability (% of untreated cells)
120
100
80
60
40
20
0
*
*
*
*
1
10
100
1000
ATRA (nM)
+ heregulin
- heregulin

Figure 3

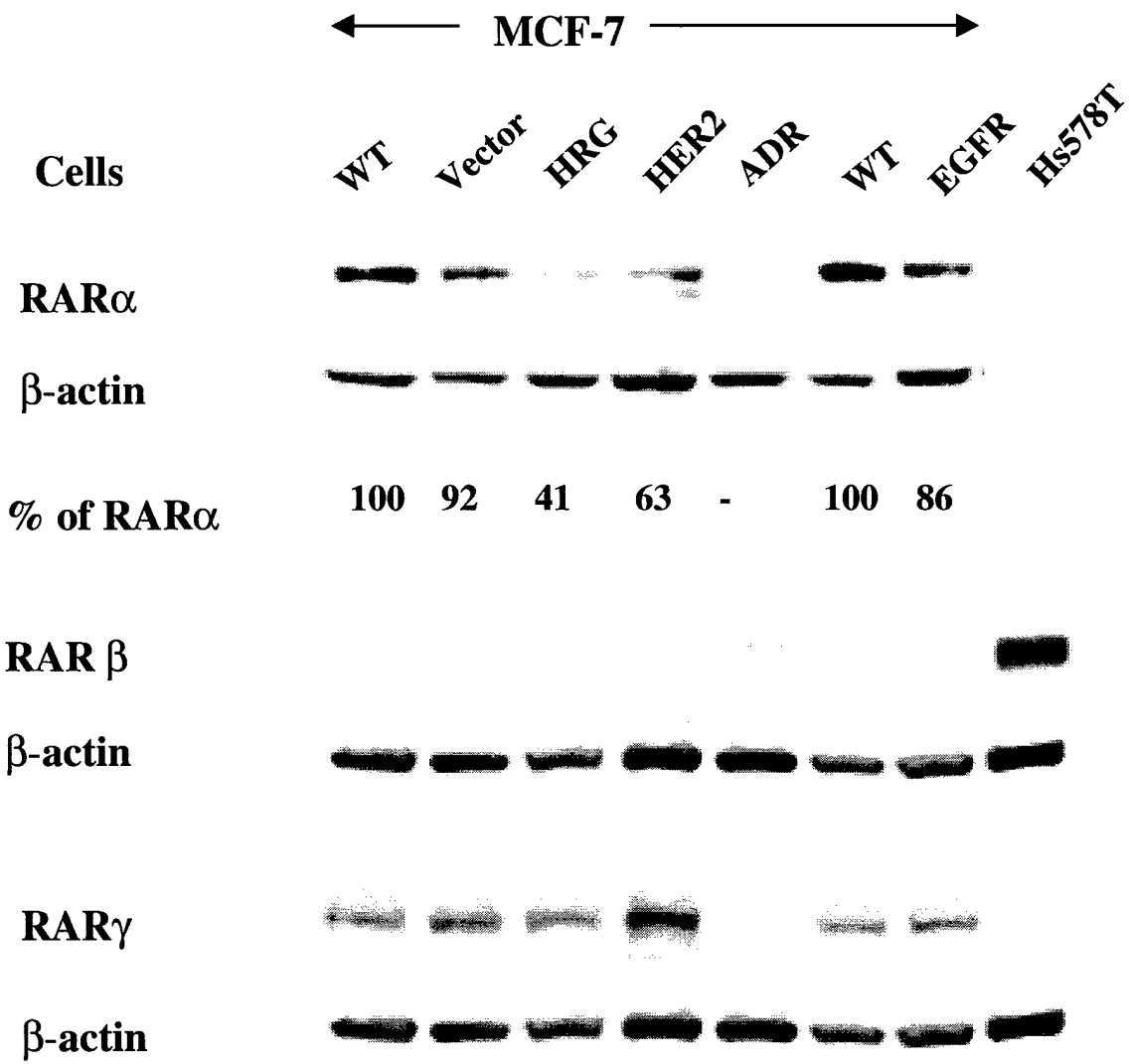
MCF-7
Cells
WT
Vector
HRG
HER2
ADR
WT
EGFR
Hs578T
RARα
β-actin
% of RARα
100
92
41
63
-
100
86
RAR β
β-actin
RARγ
β-actin

Figure 4

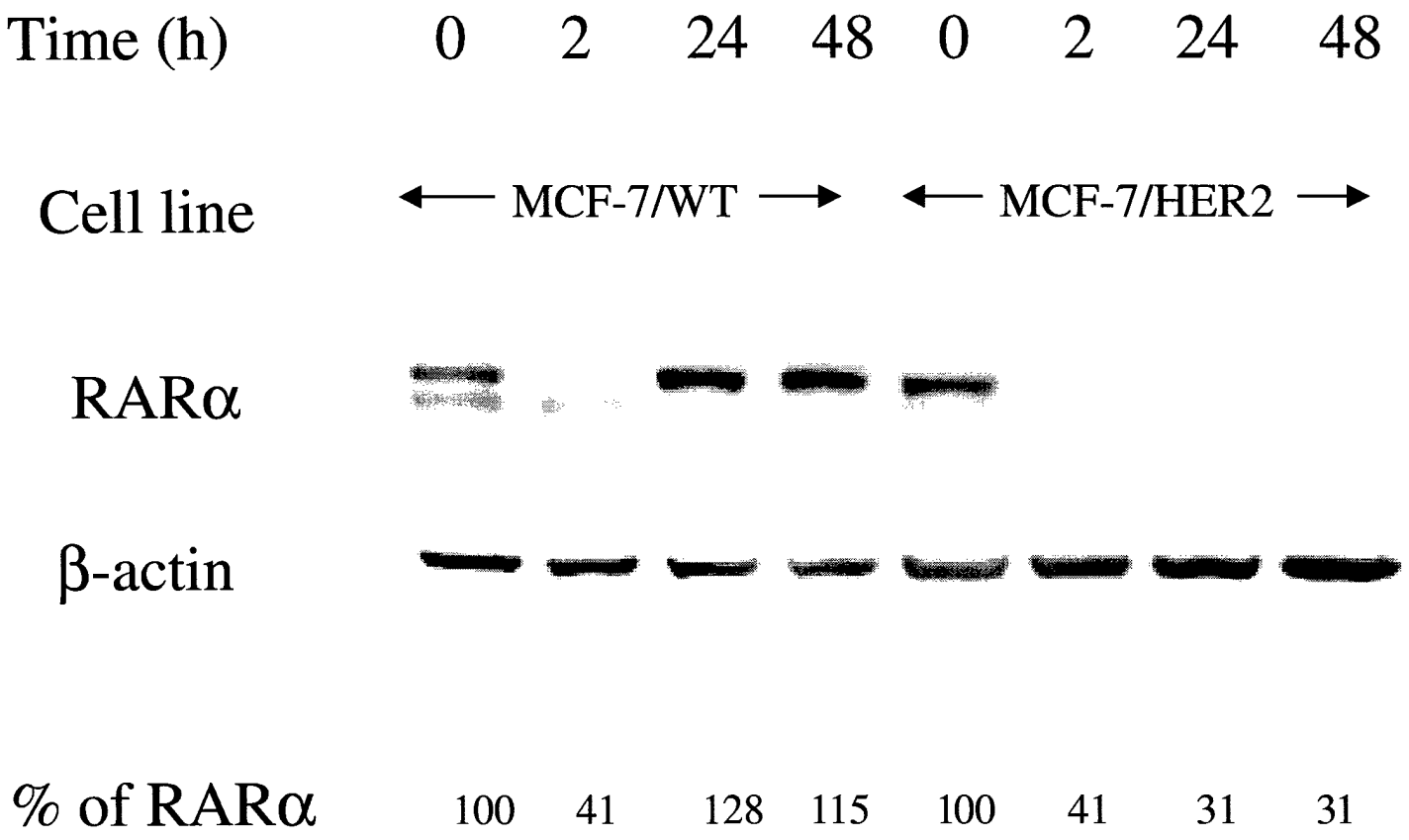
Time (h)
0 2 24 48 0 2 24 48
Cell line
← MCF-7/WT → ← MCF-7/HER2 →
RARα
β-actin
% of RARα
100 41 128 115 100 41 31 31

Figure 5

A

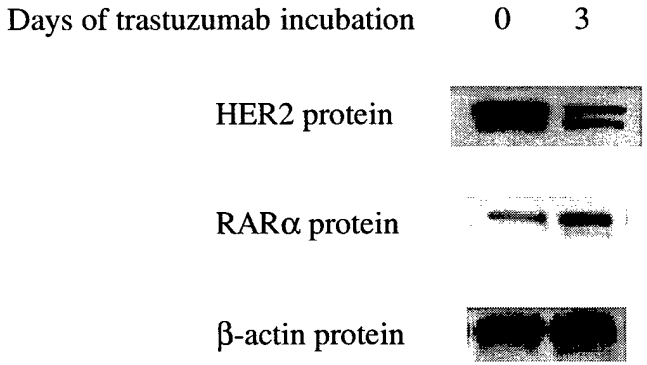
Days of trastuzumab incubation
0
3
HER2 protein
RARα protein
β-actin protein

B

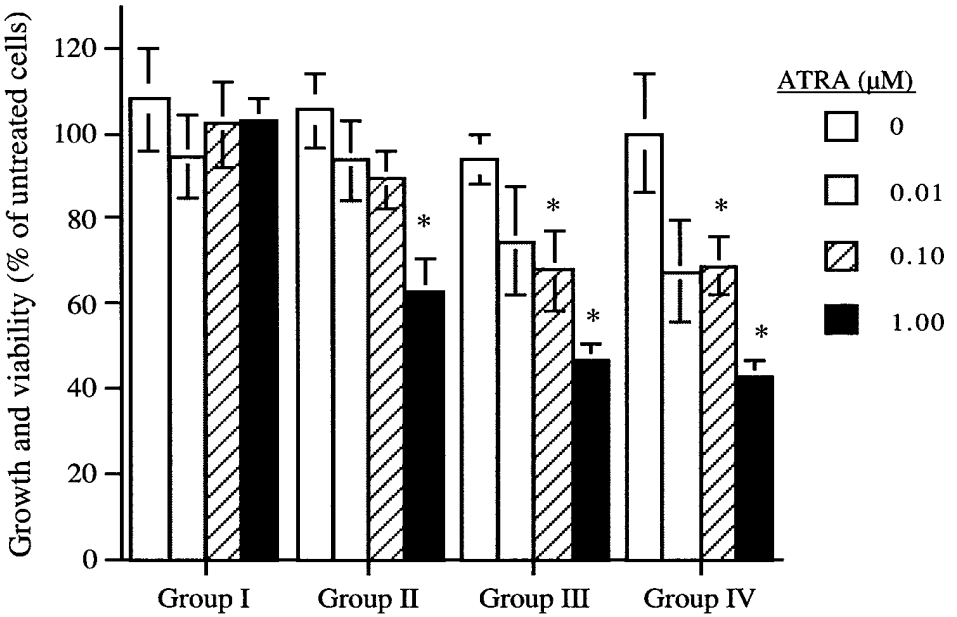
Growth and viability (% of untreated cells)
120
100
80
60
40
20
0
Group I
Group II
Group III
Group IV
ATRA (μM)
0
0.01
0.10
1.00
*

Figure 6

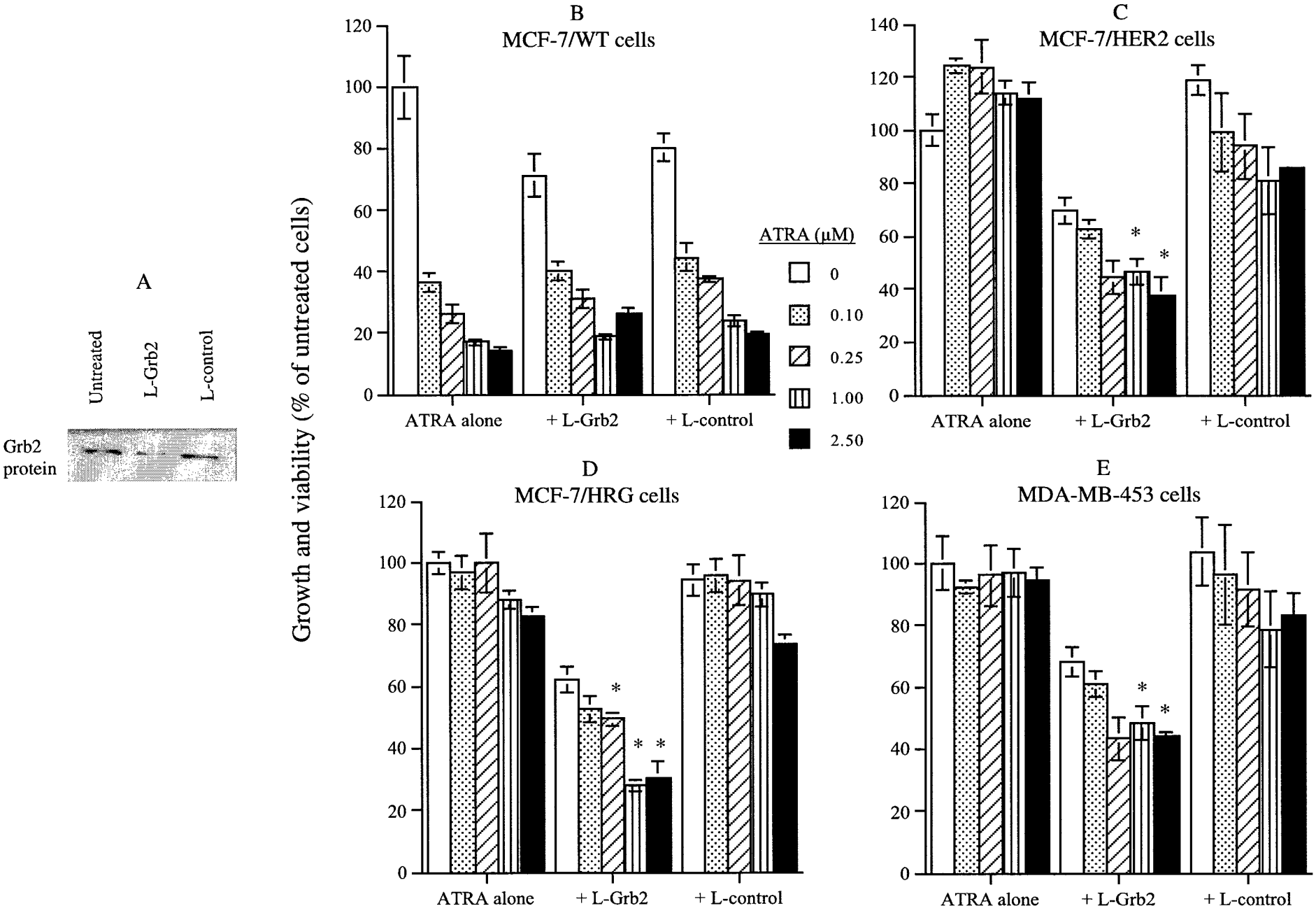
A
Untreated
L-Grb2
L-control
Grb2 protein
B
MCF-7/WT cells
C
MCF-7/HER2 cells
D
MCF-7/HRG cells
E
MDA-MB-453 cells
Growth and viability (% of untreated cells)
ATRA (μM)
0
0.10
0.25
1.00
2.50
ATRA alone
+ L-Grb2
+ L-control

Figure 7

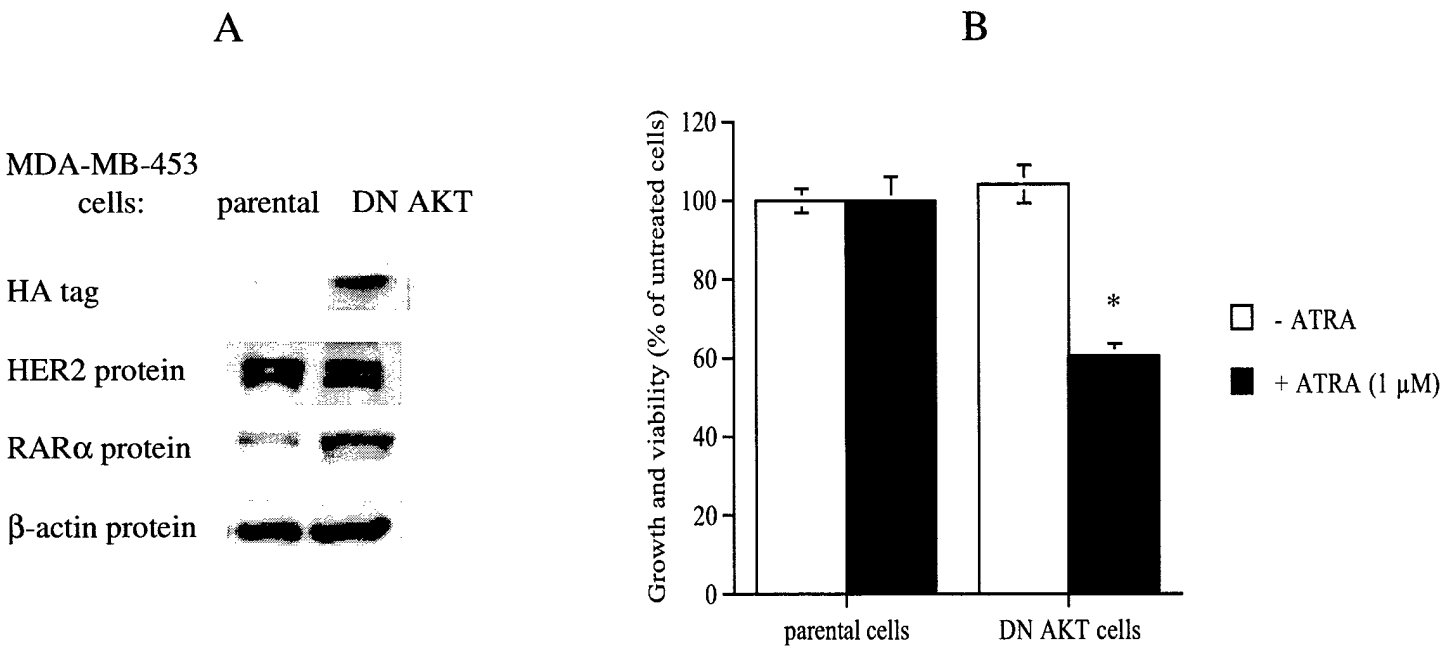
A
MDA-MB-453 cells:
parental
DN AKT
HA tag
HER2 protein
RARα protein
β-actin protein
B
Growth and viability (% of untreated cells)
120
100
80
60
40
20
0
*
parental cells
DN AKT cells
- ATRA
+ ATRA (1 μM)

MOLECULAR AND CELLULAR BIOLOGY, Dec. 2000, p. 9092–9101 Vol. 20, No. 23
0270-7306/00/$04.00+0
Copyright © 2000, American Society for Microbiology. All Rights Reserved.

Evidence of Rab3A Expression, Regulation of Vesicle Trafficking, and Cellular Secretion in Response to Heregulin in Mammary Epithelial Cells

RATNA K. VADLAMUDI, RUI-AN WANG, AMJAD H. TALUKDER, LIANA ADAM, RANDY JOHNSON, AND RAKESH KUMAR*

The University of Texas M. D. Anderson Cancer Center, Houston, Texas 77030

Received 11 July 2000/Returned for modification 18 August 2000/Accepted 30 August 2000

Heregulin β1 (HRG), a combinatorial ligand for human growth factor receptors 3 and 4, is a regulatory polypeptide that promotes the differentiation of mammary epithelial cells into secretory lobuloalveoli. Emerging evidence suggests that the processes of secretory pathways, such as biogenesis and trafficking of vesicles in neurons and adipose cells, are regulated by the Rab family of low-molecular-weight GTPases. In this study, we identified Rab3A as a gene product induced by HRG. Full-length Rab3A was cloned from a mammary gland cDNA library. We demonstrated that HRG stimulation of human breast cancer cells and normal breast epithelial cells induces the expression of Rab3A protein and mRNA in a cycloheximide-independent manner. HRG-mediated induction of Rab3A expression was blocked by an inhibitor of phosphatidylinositol 3-kinase but not by inhibitors of mitogen-activated protein kinases $p38^{MAPK}$ and $p42/44^{MAPK}$. Human breast epithelial cells also express other components of regulated vesicular traffic, such as rabphilin 3A, Doc2, and syntaxin. Rab3A was predominantly localized in the cytosol, and HRG stimulation of the epithelial cells also raised the level of membrane-bound Rab3A. HRG treatment induced a profound alteration in the cell morphology in which cells displayed neuron-like membrane extensions that contained Rab3A-coated, vesicle-like structures. In addition, HRG also promoted the secretion of cellular proteins from the mammary epithelial cells. The ability of HRG to modify exocytosis was verified by using a growth hormone transient-transfection system. Analysis of mouse mammary gland development revealed the expression of Rab3A in mammary epithelial cells. Furthermore, expression of the HRG transgene in Harderian tumors in mice also enhanced the expression of Rab3A. These observations provide new evidence of the existence of a Rab3A pathway in mammary epithelial cells and suggest that it may play a role in vesicle trafficking and secretion of proteins from epithelial cells in response to stimulation by the HRG expressed within the mammary mesenchyma.

In many eukaryotic cells, the secretion of biomolecules is mediated through both the constitutive and regulated transport of vesicles (34). Constitutive exocytosis is characterized by the continuous flow and fusion of vesicles to the plasma membrane immediately after synthesis of these vesicles; regulated exocytosis involves triggered fusion of preformed vesicles (9). The mammary epithelium secretes several proteins at the time of differentiation. Current evidence suggests that these proteins are secreted through both constitutive and regulated secretory pathways in the mammary epithelium (28, 41). Very little is known, however, about the mechanisms of regulated secretion in the mammary gland or the nature of the molecular players involved in such processes.

The Rab family of GTP-binding proteins has been implicated in vesicular trafficking in eukaryotic cells (16, 37). Many Rab family members are expressed in all mammalian cell types. The expression of Rab3A, however, is generally restricted to certain types of cells and organs, e.g., in neuronal, neuroendocrine, and adipose cells involved in regulated exocytosis. Regulated exocytosis, studied extensively in the neuronal system, is involved in cellular functions, such as neurotransmitter release, neuroendocrine hormone release, and zymogen secretion (18, 39). There are four members of the Rab3 subfamily: Rab3A, Rab3B, Rab3C, and Rab3D. Rab3A and -C are expressed predominantly in brain and neuroendocrine cells (15), Rab3D is widely expressed in adipocytes (4), and Rab3B is expressed in epithelial cells (29). Nonneuronal expression of Rab3A in adipocytes (5) and in the parathyroid gland (23) has been reported. Although the role of Rab3A in the neuronal system is well known, nothing is known about the potential role of Rab3A in mammary gland secretion.

Mammary gland development proceeds in distinct stages defined by the hormonal status of the animal (21). Heregulin β1 (HRG), a combinatorial ligand for human epidermal growth factor (HER) receptors 3 and 4, is a secretory polypeptide that affects growth stimulation and the differentiation, invasiveness, and migration of breast cancer cells (1, 8, 25, 30, 33, 45). HRG is known to be expressed in the mammary mesenchyma adjacent to lobuloalveolar structures and is maximally expressed during pregnancy (33). HRG plays a role in the morphogenesis and ductal migration of mammary epithelial cells (33, 45). HRG also promotes the in vitro responsiveness of mammary epithelial cells to lactogenic hormones (30). The ectopic delivery of HRG to the fat pad via implanted pellets induces the differentiation of the mammary epithelium into secretory lobuloalveoli (25). The mechanism by which HRG affects the secretory phenotype of mammary epithelial cells remains unexplored.

In this study, we investigated the possible role of HRG in regulated exocytosis in mammary epithelial cells. Our results demonstrated the expression of Rab3A in both cancerous and normal mammary epithelial cells and showed that HRG pro-

* Corresponding author. Mailing address: Department of Cellular and Molecular Oncology, The University of Texas M. D. Anderson Cancer Center-108, 1515 Holcombe Blvd., Houston, TX 77030. Phone: (713) 745-3558. Fax: (713) 745-3792. E-mail: rkumar@notes.mdacc.tmc.edu.

motes the accumulation of Rab3A-associated vesicles and makes cells competent for regulated exocytosis in mammary epithelial cells.

MATERIALS AND METHODS

Cell cultures and reagents. MCF-7 human breast cancer cells (1) were maintained in Dulbecco's modified Eagle's medium-F12 (1:1) supplemented with 10% fetal calf serum. HC11 mouse epithelial cells (generously provided by Daniel Madina, Baylor College of Medicine, Houston, Tex.) were maintained in RPMI 1640 medium supplemented with 8% fetal calf serum, 10 ng of EGF per ml and 5 μg of insulin per ml. Antibodies against Rab3A and vinculin were purchased from Santa Cruz (Santa Cruz, Calif.) and Sigma Chemical Company (St. Louis, Mo.), respectively. Antibodies against cytokeratin 5 and T7 were from Novagen (Milwaukee, Wis.). Antibody against HER2 was purchased from Neomarkers (Fremont, Calif.). Lactogenic hormone treatment and preparation of competent HC11 cells were performed according to Marte et al. (30).

Cell extracts, immunoblotting, and immunoprecipitation. For preparation of cell extracts, cells were washed three times with phosphate-buffered saline and lysed in radioimmunoprecipitation assay buffer supplemented with 100 mM NaF, 200 μM $NaVO_5$, 1 mM phenylmethylsulfonyl fluoride, 10-μg of leupeptin per ml, and 10 μg of aprotinin per ml for 15 min on ice. The lysates were centrifuged in an Eppendorf centrifuge at 4°C for 30 min. Cell lysates were resolved on a sodium dodecyl sulfate (SDS)–10% polyacrylamide gel, transferred to nitrocellulose, and probed with the appropriate antibodies, using an enhanced chemiluminescence method (6).

Cloning and construction of Rab3A cDNA. A mammary gland DNA library in the pcDNA3 vector was purchased from Invitrogen. Bacterial clones (10^6) were screened with a ^{32}P-labeled, 303-bp, Rab3A-specific probe generated from reverse transcription (RT)-PCR using MCF-7 cell total RNA. Filters were hybridized under high-stringency conditions (50% formamide buffer), washed, and developed by autoradiography. Positive clones were purified and sequenced. An open reading frame of Rab3A was isolated by PCR using 1.3-kb cDNA isolated from mammary gland and subcloned into pcDNA3.1/HIS (Invitrogen) to generate T7-tagged Rab3A (primers: forward, 5′-AAGATGGCATCGGCCACAGA-3′; reverse, 5′-CTCGCAGGCGCAGTCC-3′).

RT-PCR and Northern blot analysis. RT-PCR was performed using the Access RT-PCR system (Promega, Madison, Wis.) per the manufacturer's instructions. The following primers were used for Rab3A: forward (288 to 313), 5′-TACCGGACCATCACCACCGCATAC-3′; reverse (591 to 565), 5′-CAGATGACATCCACCAGGCGCTCAAA-3′. Total cytoplasmic RNA (20 μg) was analyzed by Northern blot analysis using either 303-bp Rab3A-specific PCR product or 1.3-kb Rab3A cDNA probe.

Membrane fractionation. Serum-starved MCF-7 cells (3×10^7) were treated with or without HRG (30 ng/ml) for 8 h. Cells were scraped and resuspended in 300 μl of ice-cold hypotonic buffer containing 20 mM HEPES, 5 mM KCl, 1.5 mM $MgCl_2$, 1 mM dithiothreitol, and protease inhibitor cocktail. Cells were processed in a glass homogenizer and centrifuged at 3,000 rpm (Eppendorf) for 5 min. The resulting postnuclear supernatant was centrifuged at 10,000 × *g* for 1 h, and the obtained pellet was designated the membrane portion. The membrane pellet was resuspended in SDS buffer (the volume equal to that of the cytosol fraction), and an aliquot (40 μl) was subjected to SDS-polyacrylamide gel electrophoresis (PAGE).

Triton X-114 fractionation was performed as described by Bordier (7). Triton X-114 (final concentration, 0.1% [vol/vol]) was added to the postnuclear supernatant from the MCF-7 cells (3×10^7) and incubated on ice for 30 min. Liquid phases were allowed to separate by keeping the samples at 37°C for 5 min, followed by centrifugation for 5 min. The proteins in aqueous and detergent phases were precipitated with trichloroacetic acid and were solubilized in 100 μl of 1× SDS buffer; 40 μl of the sample was analyzed by SDS-PAGE.

Assays for protein synthesis and secretions. Subconfluent cultures in six-well plates were serum starved for 4 days and stimulated with HRG for 6 h. Some cultures were incubated with inhibitors LY294002 (20 μM), PD98059 (20 μM), and SB203580 (20 μM) for 30 min before the addition of HRG. Cellular proteins were metabolically labeled with [^{35}S]methionine (10 μCi/ml of medium) during the last 4 h of HRG treatment. Treatment was carried out in 1 ml of medium. Proteins secreted into the culture supernatants were analyzed by loading 100 μl of the conditioned medium onto SDS-polyacrylamide gels, followed by fluorography.

GH secretion assays. The growth hormone (GH) release assay was performed according to the method described by Wick et al. (44). Cells were transfected with 1 μg of pXGH5 plasmid by using Fugene6 (Boehringer) and were treated 24 h later with HRG (30 ng/ml) for 3 days without serum. Cells were washed once with a low-salt solution (140 mM NaCl–4.7 mM KCl–2.5 mM $CaCl_2$–1.2 mM $MgSO_4$–1.2 mM KH_2PO_4–20 mM HEPES [pH 7.4]–11 mM glucose) and incubated for 20 min in a high-salt solution (same as the low-salt solution except for 60 mM KCl and 80 mM NaCl). The amount of GH released into the medium was measured using a radioimmunoassay kit (Nichols Institute, San Juan Capistrano, Calif.).

Immunohistochemistry and immunofluorescence confocal studies. Mouse mammary glands from different stages of development were cut out, fixed with 10% neutral buffered formaldehyde, and processed routinely into paraffin sections. The expression of Rab3A in paraffin sections was revealed by using the peroxidase-antiperoxidase method. Briefly, the sections were deparaffinized with xylene and rehydrated with graded ethanol. The sections were then incubated with rabbit anti-Rab3A (1:50) for 2 h, goat anti-rabbit immunoglobulin G (1:100) for 1 h, and rabbit peroxidase-antiperoxidase (1:200) for 1 h at room temperature. The staining was visualized with diaminobenzidine-H_2O_2 and counterstained with hematoxylin. For specificity control, the sections were stained with antigen-preabsorbed antibodies. For immunofluorescence studies, cells were transfected with T7-tagged Rab3A, and localization of Rab3A was visualized using indirect immunofluorescence as previously described (1).

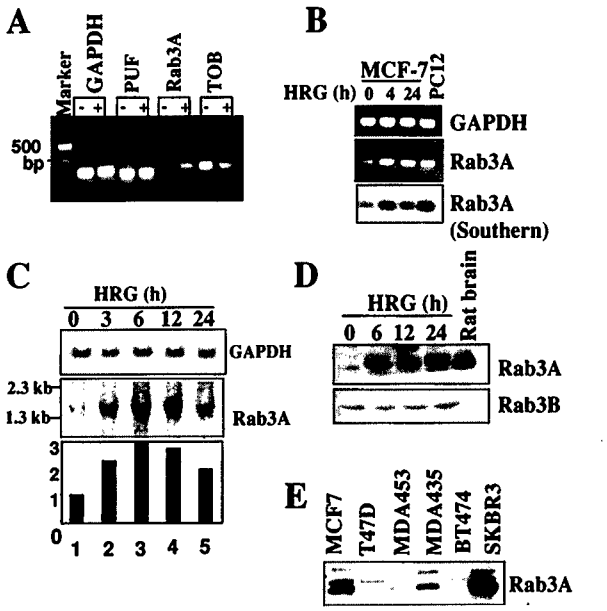

FIG. 1. Identification of Rab3A as an HRG-inducible gene. (A) RT-PCR analysis of three genes initially identified in the gene array filter. −, untreated; +, HRG treated for 6 h; TOB, transducer of ErbB-2; PUF, c-*myc* transcription factor. (B) Kinetics of Rab3A expression in HRG-stimulated MCF-7 cells. Expression was analyzed by RT-PCR and subjected to Southern hybridization with a rat Rab3A cDNA (18). GAPDH, glyceraldehyde-3-phosphate dehydrogenase. (C) Northern blot analysis of Rab3A in HRG-treated MCF-7 cells using a 303-bp Rab3A probe. (D) Serum-starved cells were treated with HRG, and Rab3A expression was analyzed by Western blotting. Rat brain extract, positive control. (E) Western blot analysis of Rab3A protein in breast cancer cell lines.

Transgenic studies. A breeding pair of HRG-transgenic mice were kindly provided by Philip Leder (27). The genotype of the animals was confirmed by Southern blotting of tail DNA. About 50% of transgenic offspring showed hyperplasia of the Harderian gland, as reported earlier (27). Hyperplastic Harderian glands from transgenic lines and normal Harderian glands from wild-type animals were dissected and processed for RNA extraction using the Trizol method. Paraffin sections of the glands were also obtained with 10% paraformaldehyde fixation. Sections were stained with Rab3A polyclonal antibody. Expression of HRG and Rab3A was analyzed by RT-PCR. The HRG primers were as follows: forward, 5′-ATGTCTGAGCGCAAAGAAGGCAGA-3′; and reverse, 5′-TTGCTGATCACTTTGCACATATAC-3′.

RESULTS

Identification of Rab3A as an HRG-inducible gene product. To identify HRG-regulated genes in mammary epithelial cells, we screened MCF-7 cells for inducible genes using Atlas cDNA expression arrays (Clontech). Total RNA was isolated from control cells and HRG-treated MCF-7 cells, and cDNAs were generated by using a reverse transcriptase in the presence of [α-^{32}P]deoxycytidine triphosphate and were hybridized to gene array filters. This screening identified Rab3A as an HRG-inducible gene in breast epithelial cells (Fig. 1A). RT-PCR analysis demonstrated a time-dependent stimulation of Rab3A mRNA. The identity of the amplified band was confirmed by sequencing and Southern analysis (Fig. 1B). When a 303-bp PCR probe was used for Rab3A, Northern blot analysis showed

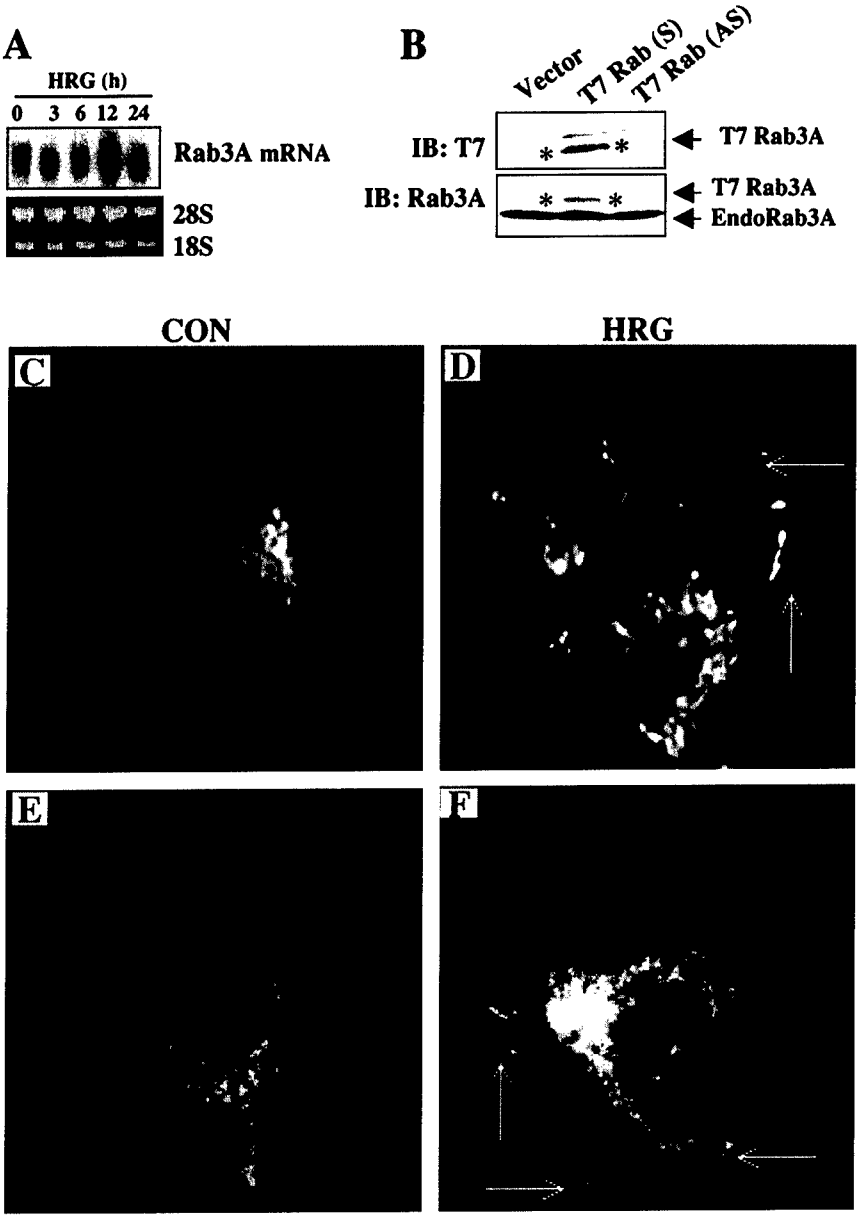

FIG. 2. HRG regulates the localization of Rab3A. (A) Northern blotting analysis of Rab3A in MCF-7 cells using a full-length Rab3A cDNA isolated from a mammary gland cDNA library. (B) Transient expression of T7-tagged Rab3A in MCF-7 cells. (Upper panel) Immunoblotting with a T7 monoclonal antibody. (Lower panel) The above blot was stripped and reprobed with a Rab3A antibody which recognizes both T7-tagged and endogenous Rab3A. IB, immunoblotting; S, sense construct; AS, antisense construct. Asterisks show the T7-tagged Rab3A protein band. (C to F) MCF-7 cells were transiently transfected with T7-Rab3A (C and E) and treated with HRG for 6 h (D and F). Localization of T7-Rab3A was visualized by immunostaining and confocal microscopy (×65 magnification). Arrows point to the neuron-like membrane extensions observed in HRG-treated cells. CON, control.

a significant increase in the steady-state levels of 1.3-kb mRNA for Rab3A, with maximal induction occurring 6 to 12 h after HRG treatment (Fig. 1C). Since there was no precedent of growth factor-inducible upregulation of Rab3A in breast cells, the experiment was independently repeated three times and similar results were obtained each time. The observed increase in Rab3A mRNA was accompanied by an enhancement in the level of 26-kDa Rab3A (Fig. 1D). The expression of Rab3A was easily detectable in human breast cancer cell lines (Fig. 1E). Taken together, these results suggest that Rab3A is expressed in MCF-7 cells and may be upregulated by HRG.

Expression of Rab3A in mammary epithelial cells. To confirm the expression of Rab3A in mammary cells, we screened a human mammary gland cDNA library with the PCR probe obtained from the RT-PCR. Screening resulted in the isolation of nine positive clones ranging from 1.2 to 1.3 kb. Comparison of the DNA sequence of isolated Rab3A cDNA clones with those in GenBank revealed that the sequences were 100% identical to human Rab3A (GenBank accession number M28210). The full-length 1.3-kb Rab3A cDNA was used to reconfirm the HRG-induced upregulation of Rab3A mRNA (Fig. 2A). Next, we studied HRG regulation of Rab3A using immunostaining and confocal microscopy. We used a T7-tagged Rab3A expression vector. The 1.3-kb cDNA that was isolated from mammary glands contained a full-length open reading frame of Rab3A, which was subcloned into pcDNA3.1 to obtain the T7 epitope-tagged Rab3A expression vector. Expression of T7-tagged Rab3A was verified by transient transfection into MCF-7 cells

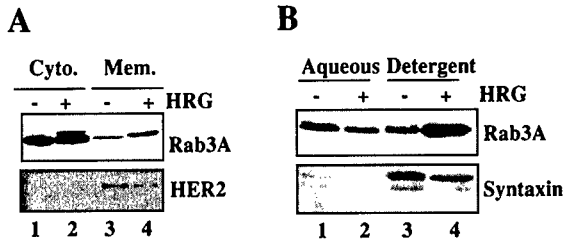

FIG. 3. Distribution of Rab3A in MCF-7 cells. (A) Cytosol (Cyto.) and membrane (Mem.) fractions from control (−) and HRG-treated (+) (30 ng/ml, 8 h) cells were analyzed by Western blotting. (B) Postnuclear supernatants from control (−) and HRG-treated (+) (8 h) cells were extracted with Triton X-114 as described (7). The levels of Rab3A present in aqueous (lanes 1 and 2) and detergent (lanes 3 and 4) phases were determined by Western blotting.

and by Western blot analysis using a T7 monoclonal antibody (Fig. 2B). MCF-7 cells were transiently transfected with T7-Rab3A and treated with HRG. Control MCF-7 cells exhibited Rab3A staining localized on punctate structures that were distributed randomly in the cytosolic compartment and resembled secretory vesicles. A similar pattern of punctate staining was earlier observed in insulin-secreting HIT-T15 cells when Rab3A was overexpressed (24). Interestingly, HRG treatment induced a dramatic change in the cell morphology: cells displayed neuron-like membrane extensions that contained Rab3A-coated, vesicle-like structures (Fig. 2C). A similar pattern of Rab3A-coated structures was observed in PC12 cells treated with nerve growth factor (10). There was no vesicle formation by transforming growth factor α, a close relative of the EGF family of ligands (data not shown). To further confirm the role of HRG in vesicle trafficking, we attempted to costain Rab3A along with another characterized protein associated with vesicles, such as rabphilin 3A or Doc2. However, since suitable, commercially available forms of these two antibodies had an isotypic nature similar to that of T7-Rab3A, this could not be accomplished. Therefore, as an alternate approach, we stained the cells with the Doc2 monoclonal antibody alone, a molecule that is implicated in regulated exocytosis and expressed in MCF-7 cells. In untreated control cells, Doc2 was primarily localized to perinuclear areas and HRG stimulation resulted in the appearance of an increased number of punctate structures directed toward the membrane (data not shown). These results suggested that HRG regulates both Rab3A expression and vesicle transport in breast epithelial cells.

HRG redistributes Rab3A to membranes. To analyze the localization of Rab3A in mammary epithelial cells, MCF-7 cells were treated with or without HRG, and cell lysates were fractionated into the cytosol and membrane. Rab3A was predominantly localized in the cytoplasmic fraction in unstimulated MCF-7 cells. However, HRG treatment enhanced the level of membrane-bound Rab3A (Fig. 3A). Since Rab3A is known to associate with membranes via geranylgeranyl groups (19), we performed partitioning studies by using the Triton X-114 partition method (7). The Triton X-114 partition assay has been widely used to identify membrane-associated geranylgeranylated Rab3A (19). In this assay, geranylgeranylated and/or farnesylated proteins are recovered in the detergent phase, while nonprenylated proteins are retained in the aqueous phase. HRG treatment of cells was accompanied by a significant increase in the amount of accumulated Rab3A in the detergent phase (Fig. 3B, compare lanes 2 and 4). Syntaxin 4, an integral membrane protein, was used as an internal control. It was present only in the detergent phase, and there was no effect of HRG on its level. These results indicate that in addition to its effect on the synthesis of Rab3A, the HRG-stimulated signaling pathway may have a role in the redistribution of Rab3A, probably via geranylgeranylation.

HRG signaling and Rab3A expression. HRG is known to stimulate a number of signaling pathways, including phosphatidylinositol (PI) 3-kinase and the mitogen-activated protein kinase $p42/44^{MAPK}$ and $p38^{MAPK}$ pathways (1, 38). In order to delineate the nature of the signaling pathway(s) leading to upregulation of Rab3A in HRG-treated cells, we employed three specific inhibitors, LY294002, PD98059, and SB203580, which specifically inhibit PI 3-kinase, $p42/44^{MAPK}$, and $p38^{MAPK}$, respectively. Pretreatment of cells with LY294002 but not with PD98059 or SB203580 completely blocked HRG-mediated upregulation of Rab3A (Fig. 4, compare lanes 2 and 4), suggesting a potential role for PI 3-kinase in the observed HRG-mediated induction of Rab3A expression.

Upregulation of Rab3A expression by HRG and lactogenic hormones in normal mammary epithelial cells. Using the HC11 mouse model system, we investigated whether HRG regulates the expression of Rab3A in normal mammary epithelial cells. The growth of HC11 mammary epithelial cells is stimulated by HRG, and pretreatment of these cells promotes responsiveness to lactogenic hormones and enhances secretion of β-casein (30). HRG treatment of HC11 cells in our study significantly increased levels of Rab3A mRNA (Fig. 5A) and Rab3A protein (Fig. 5B). Confocal analysis of HC11 cells showed that HRG significantly induced cytoplasmic vesicles and that transfected T7-Rab3A was distributed mainly on vesicles (Fig. 5C, upper panels). The control cells showed diffuse cytoplasmic staining. To verify that the increased vesicle formation was not an artifact of Rab3A overexpression by transient transfection, we next employed a monoclonal antibody against Rab3A to localize the endogenous Rab3A and analyzed cells treated with or without HRG by confocal microscopy. HRG treatment of HC11 cells significantly induced cell shape changes and increased formation of Rab3A-coated vesicles and their translocation towards membranes (Fig. 5C, lower panels).

We next investigated whether the lactogenic hormones dexamethasone, insulin, and prolactin (DIP), which together induce differentiation and secretion of milk proteins (30), could also influence the expression of Rab3A. Treatment of HC11 cells with DIP significantly upregulated Rab3A (Fig. 5D). Neither insulin alone nor prolactin alone affected the level of Rab3A, but dexamethasone alone induced Rab3A expression.

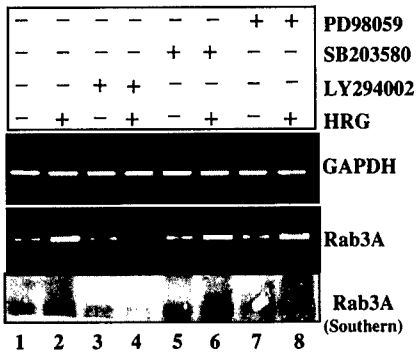

FIG. 4. HRG-mediated upregulation of Rab3A requires the PI 3-kinase pathway. MCF-7 cells were treated with HRG for 8 h. Some cultures were pretreated with PI 3-kinase inhibitor LY294002 (20 μM), $p38^{MAPK}$ inhibitor SB203580 (20 μM), and $p42/44^{MAPK}$ inhibitor PD98059 (20 μM) 30 min before HRG treatment. Expression of Rab3A was analyzed by RT-PCR followed by agarose gel electrophoresis and Southern blotting.

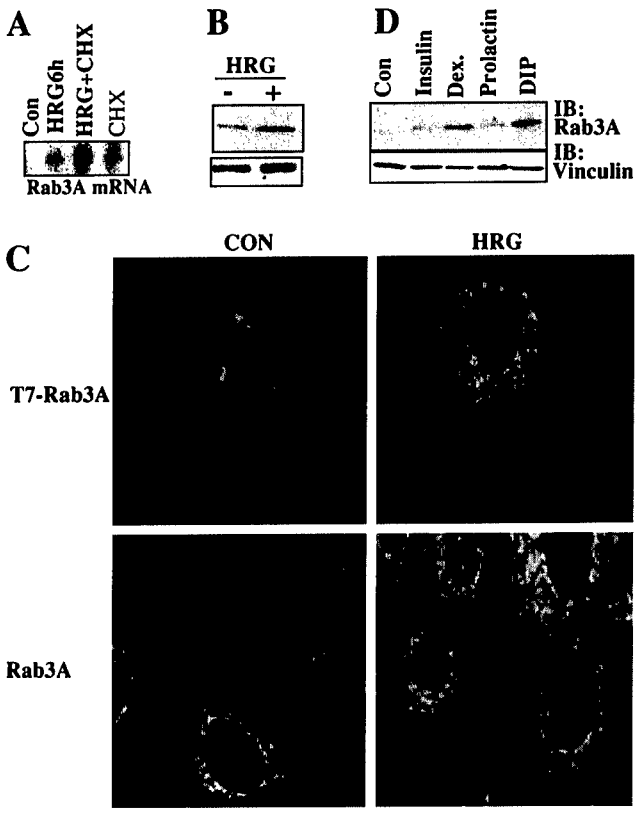

FIG. 5. Expression and localization of Rab3A in normal mammary epithelial cells. (A) Serum-starved HC11 cells were treated with HRG for 6 h, and the expression of Rab3A was examined by Northern blot analysis. Con, control. CHX, cycloheximide. (B) Expression of Rab3A protein in HC11 cells. −, untreated; +, HRG treated. (C) (Upper panels) HC11 cells were transiently transfected with T7-Rab3A treated with HRG for 6 h, and localization of T7-Rab3A was visualized by immunostaining and confocal microscopy. (Lower panels) HC11 cells were treated with or without HRG for 6 h, and localization of endogenous Rab3A was visualized by immunostaining with a monoclonal antibody and by confocal microscopy. CON, control. (D) HC11 cells were allowed to become competent for differentiation, as described in Materials and Methods, and were treated with DIP components separately or together. Rab3A expression was analyzed by immunoblotting (IB). Con, control.

HRG enhances secretion of cellular proteins from mammary epithelial cells. Next we investigated whether HRG could regulate the secretion of cellular proteins from mammary epithelial cells. To increase the sensitivity of the detection system, we analyzed the accumulation of secreted proteins in the conditioned medium from metabolically labeled cells. Three different mammary epithelial cell lines with different levels of Rab3A expression (MCF-7, high; HC11, medium; and BT-474, low) were used. HRG stimulation of MCF-7 cells resulted in a significant enhancement of several proteins in the culture supernatants (Fig. 6A, compare lanes within MCF-7 column). Similarly, HRG stimulation of HC11 also led to secretion of cellular proteins. However, in BT-474 cells, which have low levels of Rab3A, the levels of secreted proteins were significantly lower than those in MCF-7 and HC11 cells.

To examine the effects of signaling pathways on the secretion of proteins from HRG-treated cells, we pretreated cells with signaling inhibitors LY294002, PD98059, and SB203580. Blockage of the PI 3-kinase pathway with LY294002 was accompanied by a significant reduction in the ability of HRG to induce the secretion of cellular proteins. However, the secretion of two proteins in the molecular mass range of 40 to 50 kDa was induced by LY294002, suggesting the involvement of the PI 3-kinase pathway in the secretion of most but not all proteins in HRG-treated cells. Pretreatment of MCF-7 cells with PD98059 or SB203580 was also inhibited during the HRG-mediated secretion of cellular proteins, with SB203580 being more potent than PD98059.

To further visualize the effect of signaling inhibitors on HRG-associated secretory function, MCF-7 cells were transfected with T7-tagged Rab3A and treated with various inhibitors in the presence or absence of HRG, and T7-tagged Rab3A was localized by confocal microscopy (Fig. 7). HRG-treated cells exhibited an increase in the number of Rab3A-associated vesicles, and vesicles were predominantly localized to the membrane with a number of extensions. In contrast, T7-Rab3A-coated vesicles were distributed randomly in the cytoplasm in cells treated with PD98059 and LY294002. Interestingly, in SB203580-treated cells, T7-Rab3A-coated vesicles were clustered in one place. Together, these observations suggest that even though PI 3-kinase was involved in the HRG induction of Rab3A, other signaling pathways, including $p38^{MAPK}$ and $p42/44^{MAPK}$, are also involved in HRG-mediated secretion and vesicular trafficking.

Expression of components of regulated exocytosis in human and mouse mammary epithelial cells. Rab3A has been implicated in regulated exocytosis in neuronal and endocrine systems. Upregulation of Rab3A expression by HRG and lactogenic hormones, each of which promotes differentiation of mammary gland cells, raises the possibility that Rab3A is also involved in regulated exocytosis in mammary epithelial cells. Since regulated exocytosis involves interaction among several proteins on vesicles, membranes, and cytoplasmic regulators, we analyzed mammary epithelial cells for the expression profile of proteins known to be involved in regulated exocytosis in the neuronal system. Mammary epithelial cells express a number of proteins involved in regulated exocytosis, including rabphilin 3A, Sec8, synaptogyrin, syntaxin 4, SNAP-25, rabaptin, and Doc2 (Fig. 8). However, we observed no detectable levels of integral membrane proteins, such as synaptogyrin, synapsin, and complexin.

Effect of HRG stimulation on regulated secretion from mammary epithelial cells. To evaluate the effect of HRG upon regulated exocytosis, we used a GH transient-transfection sys-

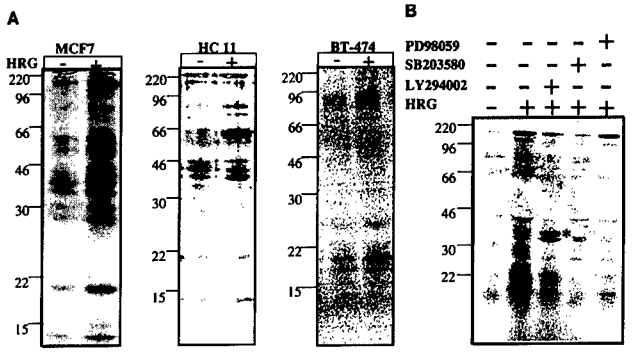

FIG. 6. HRG induces secretion of cellular proteins. (A) MCF-7, HC11, and BT-474 cells were serum starved, labeled with [^{35}S]methionine, and treated with HRG for 6 h. Conditioned media containing labeled proteins were analyzed by SDS-PAGE. −, untreated; +, HRG treated. (B) MCF-7 cells were pretreated with PI 3-kinase inhibitor LY294002 (20 μM), $p38^{MAPK}$ inhibitor SB203580 (20 μM), or $p42/44^{MAPK}$ inhibitor PD98059 (20 μM) 30 min before HRG treatment. Secreted proteins were analyzed. The asterisk indicates two protein bands which are secreted by HRG after blockage of the PI 3-kinase pathway with LY294002. Absence (−) or presence (+) of inhibitors and HRG is indicated. Molecular weights are given in thousands (A and B).

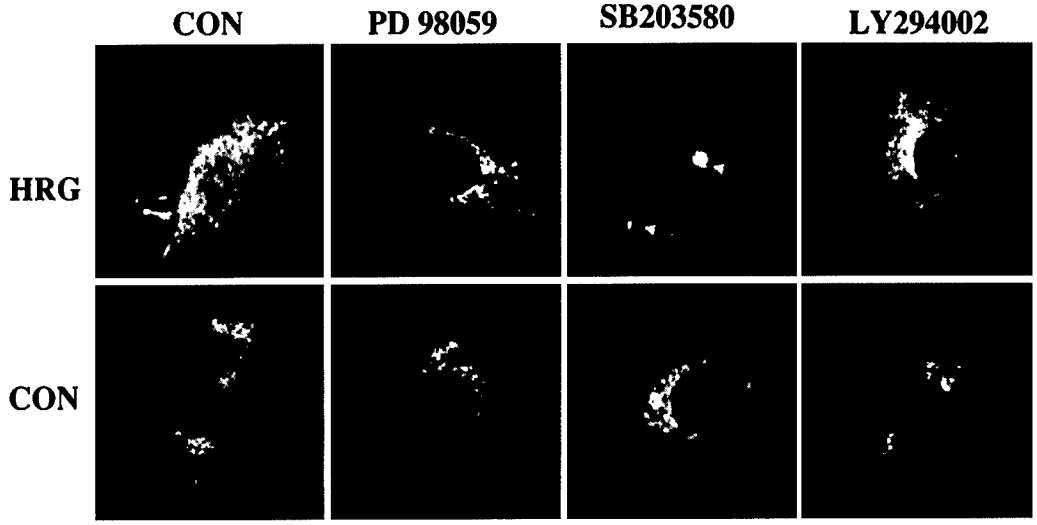

FIG. 7. Effect of signaling pathways on secretory functions in HRG-treated cells. MCF-7 cells were transiently transfected with T7-Rab3A and treated with HRG for 6 h. Where indicated, $p42/44^{MAPK}$ inhibitor PD98059, $p38^{MAPK}$ inhibitor SB20358, or PI 3-kinase inhibitor LY294002 was added to the medium (final concentration, 20 μM) 30 min before the addition of HRG. T7-tagged Rab3A was localized by confocal microscopy (magnification, ×65). CON, control. The long arrow indicates the neuron-like extensions seen in HRG-treated cells. The short arrows indicate the clustering of vesicles in one place in HRG-treated cells when $p38^{MAPK}$ was blocked by SB203580.

tem. Expressed GH is stored in dense-core vesicles in the regulated secretory pathway in chromaffin granules and is released upon stimulation of the vesicles with various agonists in a Ca^{2+}-dependent manner (11, 44). MCF-7 and HC11 cells were transfected with pXGH5 (the GH plasmid), which was treated with HRG, and the amount of GH protein released into the medium was analyzed. HRG-treated cells were stimulated with elevated potassium in the presence of Ca^{2+}. HRG treatment significantly potentiated the potassium-stimulated release of GH into the medium (Fig. 9A). In addition, HRG treatment of MCF-7 cells significantly increased the amount of secretion of GH by the Ca^{2+} ionophore ionomycin (Fig. 9B). Pretreatment of HC11 cells with HRG significantly increased the amount of GH released into the medium by the lactogenic hormones DIP (Fig. 9C). To determine whether HRG alters Rab3A expression's effect on the secretory function, MCF-7 cells were cotransfected with Rab3A and GH plasmids in the presence or absence of HRG, and secretion of GH into the culture supernatant was measured. Expression of Rab3A was accompanied by a slight enhancement in the secretion of GH. However, expression of Rab3A in the presence of HRG resulted in increased levels of secreted GH (Fig. 9D, compare lane 4 with lanes 2 and 3). These results suggested that HRG-responsive signaling pathways participate in promoting secretion by HRG, in addition to upregulation of Rab3A in HRG-treated cells.

Expression of Rab3A in mammary epithelial cells in vivo. To demonstrate the expression of Rab3A in mammary gland cells, we isolated RNA from various stages of mammary gland development and analyzed the expression of Rab3A mRNA by RT-PCR. Rab3A expression was detected during all stages of mammary gland development; the level of Rab3A expression increased slightly during pregnancy. Interestingly, the mammary gland showed elevated expression of HRG during late pregnancy and early lactation (Fig. 10A). Western blot analysis of whole-tissue lysates indicated the presence of Rab3A in all stages of mammary gland development (Fig. 10B). The temporal and spatial expression of Rab3A in the mammary gland was assessed by using immunohistochemistry. Rab3A was found to be present in both ductal and alveolar epithelial cells but not in myoepithelial cells through all stages of mammary gland development. Rab3A was also seen in the adipose cells of the mammary gland (Fig. 10C to J). The specificity of the staining was confirmed by blocking the staining with the epitope-specific peptide. These results confirm that mammary epithelial cells express Rab3A in vivo.

HRG regulation of Rab3A expression in vivo. To evaluate the HRG modulation of Rab3A in vivo, we used mouse mammary tumor virus-driven HRG-transgenic mice, which develop mammary adenocarcinomas and Harderian tumors (27). Since Harderian tumors are usually detected by 3 weeks of age, as

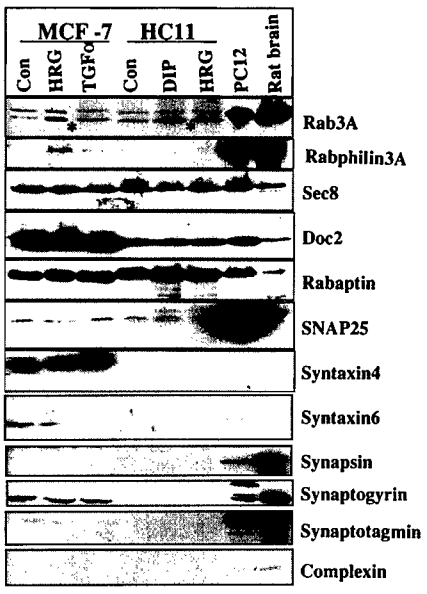

FIG. 8. Mammary epithelial cells express components of regulated exocytosis. MCF-7 and HC11 cells were treated with or without HRG (30 ng/ml) or transforming growth factor α (TGFα) (30 ng/ml) or DIP, and cell lysates were analyzed for expression of indicated proteins by Western blotting using specific antibodies. PC12 and rat brain lysates were used as positive controls. CON, control. Asterisks indicate the endogenous Rab3A band.

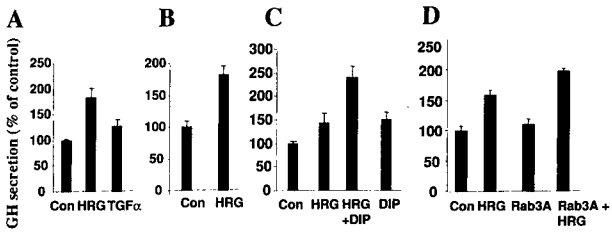

FIG. 9. Effect of HRG on regulated exocytosis in mammary epithelial cells. (A) MCF-7 cells were transiently transfected with pXGH5 (a reporter plasmid for exocytosis). Cells were treated with either HRG (30 ng/ml) or transforming growth factor α (TGFα) (30 ng/ml) in serum-free conditions for 3 days and stimulated with elevated K^+ for 20 min in the presence of Ca^{2+} as described (7). GH released into the medium was measured by radioimmunoassay, and results are presented as a percentage of the control. (B) MCF-7 cells treated with or without HRG were stimulated with ionomycin (10 μM) as described for panel A. (C) HC11 cells transfected with pXGH5 plasmid were treated with HRG alone, HRG followed by DIP, and DIP alone. (D) MCF-7 cells were transfected with pXGH5 and Rab3A either alone or together, treated with or without HRG for 72 h in serum-free conditions, and stimulated with elevated K^+ for 20 min in the presence of Ca^+. GH accumulation in the culture supernatant was measured by radioimmunoassay. The experiment was repeated three times with similar results. Error bars represent standard errors of the means (n = 3). Con, control.

opposed to 12 to 16 months for mammary gland tumors, we used Harderian tumors to establish the proof of principle of our hypothesis in vivo. Interestingly, overexpression of HRG in Harderian tumors was accompanied by increased Rab3A expression. Harderian glands from wild-type and HRG-transgenic mice were analyzed by RT-PCR for the expression of HRG and also for Rab3A. HRG-transgenic mice have significantly elevated levels of HRG transcript compared to those in wild-type mice (Fig. 11). Interestingly, HRG-transgenic mice also exhibited two- to threefold higher levels of Rab3A, as determined by Southern analysis. Expression of Rab3A was also verified by immunostaining (Fig. 11C). HRG-transgenic mouse tissue sections showed increased Rab3A immunostaining compared to the tissue of wild-type mice. Together, these results imply a close relationship between the expression of HRG and Rab3A in vivo.

DISCUSSION

Rab GTPases represent a large family of small G proteins that play an important role in exocytosis, endocytosis, and vesicular trafficking (16). Rab proteins, like the Ras family of proteins, exist in active (GTP-bound) and inactive (GDP-bound) form; the GTP-bound form associates with vesicles. The conversion of GTP to GDP is regulated by GEP regulatory proteins (also called GDP/GTP exchange proteins) and the GDP dissociation inhibitor, while the conversion of GTP to GDP is regulated by GTPase-activating proteins (32). Further, Rab proteins are geranylgeranylated at their C terminus, and this process is required for their membrane association (37). The Rab3 subfamily of proteins is particularly implicated in the secretion of neuroendocrine hormones and neurotransmitters. Very little information is available on Rab3A expression and potential secretory function in mammary epithelial cells.

The results of our study show that Rab3A is a target of HRG in mammary epithelial cells. Our conclusion that these cells express Rab3A and that Rab3A expression is induced by HRG and differentiation of the mammary epithelial cells is based on the following evidence. (i) HRG stimulated the expression of Rab3A mRNA, as measured by using RT-PCR and Northern blot analysis. (ii) HRG increased the levels of Rab3A protein. (iii) HRG and lactogenic hormones enhanced expression of Rab3A in normal mouse mammary epithelial cells. (iv) Full-length Rab3A cDNA was isolated from a human mammary gland cDNA library. (v) Treatment of MCF-7 and HC11 cells with HRG increased the accumulation of Rab3A-containing

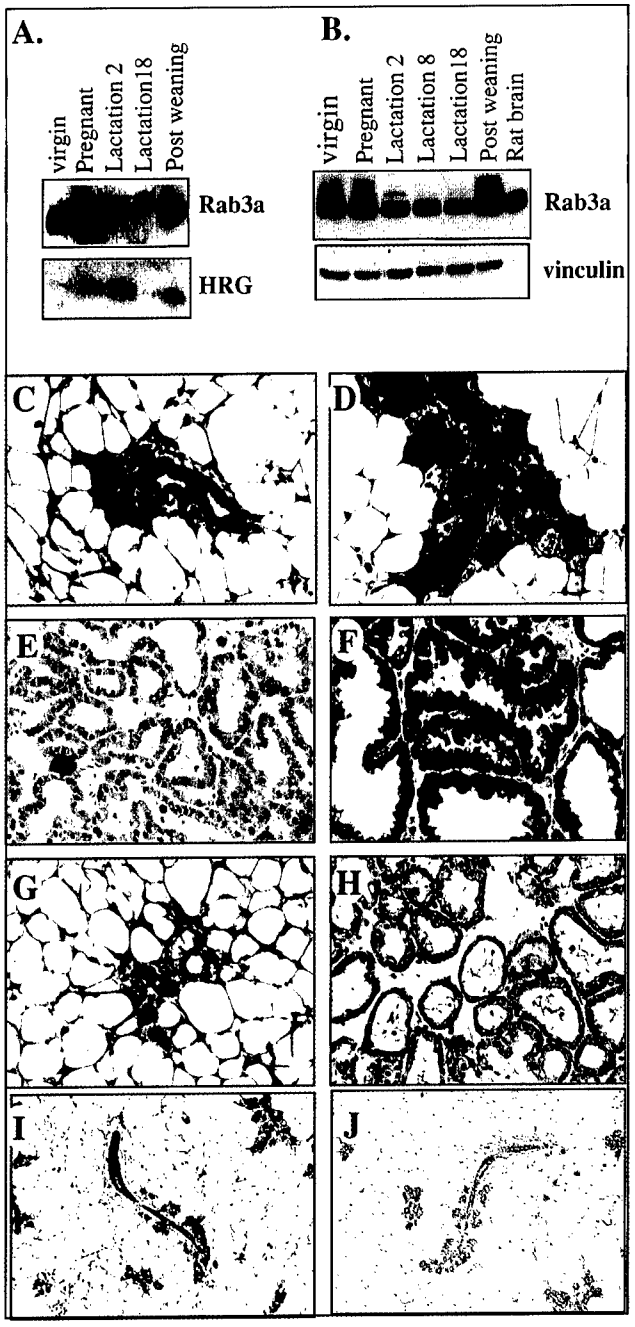

FIG. 10. Expression of Rab3A in the mammary gland in vivo. Mammary gland tissue was isolated from various stages of mammary gland development. (A) Expression of Rab3A and HRG analyzed by RT-PCR. (B) Western analysis of Rab3A in whole-gland tissue lysates. Lactation 2, second day of lactation. (C to J) Immunohistochemical demonstration of Rab3A expression in various stages of mammary gland development. Rab3A was present in the epithelial cells of the ducts (C) (virginity), end buds (D and I) (pregnancy), alveoli (E and F) (lactation, days 2 and 18), and involuted and/or regressed mammary tissues (G) but not in the myoepithelial cells, as revealed by staining with the marker protein MK-5 (H). A positive control for Rab3A antibody is shown (I). To create a negative control, the staining was blocked by preabsorbing the primary antibody with synthetic peptide (J) (pregnancy). Magnification, ×200 (C to H); ×100, (I and J).

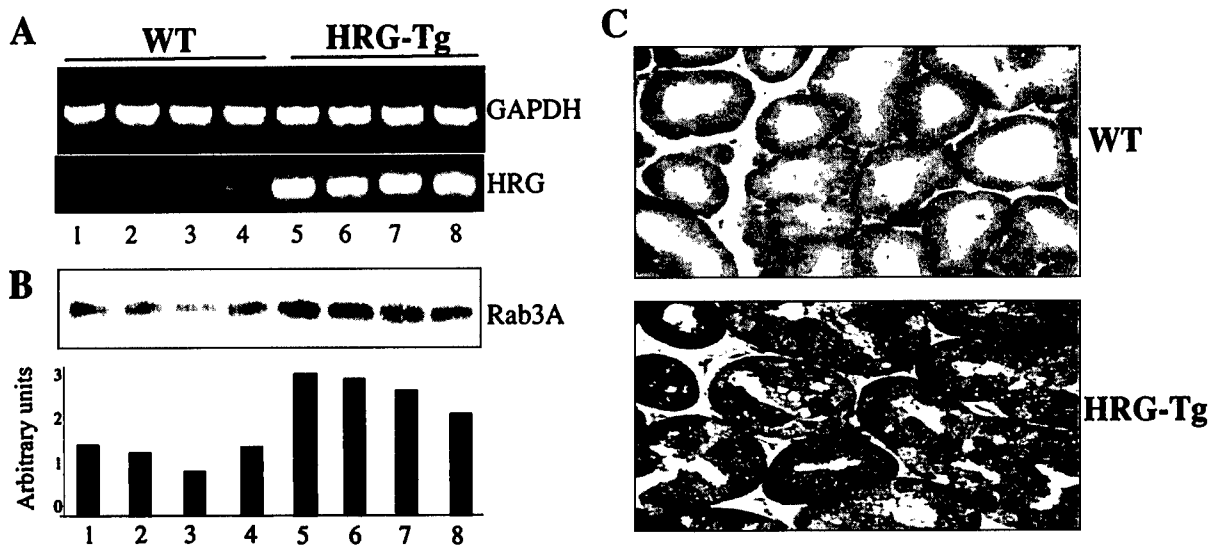

FIG. 11. HRG regulation of Rab3A expression in vivo. (A and B) Harderian glands from four wild-type (WT) (lanes 1 to 4) and HRG-transgenic (HRG-Tg) (lanes 5 to 8) mice were analyzed for HRG and Rab3A expression. (A) Expression of HRG was analyzed by RT-PCR. Glyceraldehyde-3-phosphate dehydrogenase (GAPDH) levels were used as a loading control. (B) Expression of Rab3A was analyzed by RT-PCR, followed by Southern blotting. (C) Rab3A immunostaining analysis in the representative Harderian gland sections from WT and HRG-Tg mice.

vesicles. (vi) There was immunohistochemical localization of Rab3A in epithelial cells within the mammary gland sections.

Early studies showed that HRG induces differentiation in mammary epithelial cells (30). Differentiation and secretion of proteins are essential functions of mammary gland cells. Our data showing that HRG induces expression of Rab3A and makes cells competent to release stored secretory proteins suggest that HRG may use Rab3A to make mammary epithelial cells competent for differentiation. Our data also imply that extracellular molecules secreted from the mammary epithelial cells may be controlled by regulated exocytosis. Using the calcium ionophore ionomycin, Turner et al. (41) showed that lactating mammary cells possess both Ca^{2+} pathways and Ca^{2+}-independent pathways for protein secretion. The results from the present study suggest that HRG participates in the reported Ca^{2+}-dependent secretion of mammary epithelial cells.

Many of the Rab family proteins are regulated by posttranslational mechanisms, including geranylgeranylation, phosphorylation, and GDP/GTP exchange (14, 37). Such posttranslational modifications are essential for regulated exocytosis. There are, however, a few examples of upregulation of the expression of Rab proteins. (i) Brain-derived neurotrophic factor, which promotes differentiation and maturation, can upregulate stimulation-evoked neurotransmitter release by increasing levels of exocytosis-related and synaptic vesicle proteins, including Rab3A (40). (ii) Gamma interferon in mononuclear cells selectively increases the synthesis and processing of Rab5 by geranylgeranylation (2). (iii) Rab3D is upregulated during adipocyte differentiation (4) and myeloid differentiation (31). Our data showing HRG-stimulated upregulation of Rab3A suggest that regulated secretion may play a role in differentiated mammary epithelial cells.

Rab proteins are shown to have a role in vesicle docking. Rab proteins cycle between an activated (GTP) membrane-bound pool and a cytosolic GDP-bound pool complexed to the members of the guanine nucleotide dissociation inhibitor gene family (32). At steady state, Rabs are predominantly membrane associated, and about 10 to 50% of the total Rab3A can be found in the cytosol (37). The Rab3 subfamily consists of four members, Rab3A, -3B, -3C, and -3D. Rab3 subfamily members have a distinct expression pattern: Rab3A and Rab3C are predominantly expressed in neurons (15), Ran3D in adipocytes (4), and Rab3B in epithelial cells (29). Nonneuronal expression of Rab3A was also reported in adipocytes (5) and in the parathyroid gland (23). Immunolocalization studies revealed that Rab3A was associated with large dense-core vesicles in PC12 cells (13). Rab3A was shown to be associated with the insulin-containing granules in pancreatic beta cells (35). Interestingly, in parathyroid gland chief cells, the majority of Rab3A was found in the cytosol (23). In this context, results from the present study also show that in MCF-7 breast cancer cells, the Rab3A was predominantly localized in the cytoplasm, and HRG increased the pool of membrane-bound Rab3A, probably due to increased geranylgeranylation. Recently, another growth factor, insulin, was shown to upregulate geranylgeranylation of Rab3A by activating geranylgeranyltransferase II (19). Thus, HRG-mediated posttranslational modifications of Rab3A may also have a role in secretory function.

The targeting of vesicles to organelles requires a set of proteins and several levels of interaction between proteins (34). Cellular pathways activated by HRG have a role in the reorganization of cytoskeletal cells and the migration of mammary epithelial cells (1, 38, 42). Recent evidence also suggests a close link between Rab-mediated vesicle docking and actin- and microtubule-based cytoskeleton reorganization (43). Other examples of interactions between exocytosis and cytoskeletal proteins include (i) regulation of secretory granule exocytosis by RhoA and/or RhoC proteins in anterior pituitary cells (12), (ii) stabilization of the neuronal cytoskeleton by Rab3 (3), and (iii) interaction of Rab3A-binding protein rabphilin with alpha-actinin, an actin-binding protein (26). Since vesicle transport involves passing through cytoskeleton barriers, our results raise the possibility that HRG treatment-associated reorganization of cytoskeletal structures plays a role in making mammary epithelial cells competent for regulated exocytosis.

Existing evidence suggests that Rab3A acts by regulating the late steps in synaptic vesicle fusion. Overexpression of Rab3A inhibited exocytosis in PC12 and chromaffin cells (22, 35). However, overexpression of Rab3A had no significant effect on the release of human C peptide, while expression of the GT-

Pase-deficient Rab3A mutant prevented exocytosis in insulin-secreting cells (24). Rab3A knockout mice exhibited enhanced exocytosis after the arrival of nerve impulse (17), confirming its role as a regulator at the last stage of exocytosis. Even though Rab3A is a key regulator in exocytosis, its activity is regulated in turn by a number of other factors, including GTP/GDP exchange proteins, rabphilin 3A, and geranylgeranylation. Complex regulation of Rab3A indicates that the overall effects of Rab3A on exocytosis may reflect the cumulation of its regulation at multiple steps rather than of its expression alone. Interestingly, HRG induces synthesis and HRG secretion of a number of proteins in breast epithelial cells. Although the induction of Rab3A expression requires a functional PI 3-kinase pathway, HRG-induced secretion of cellular proteins requires additional signaling pathways, such as the $p38^{MAPK}$ and $p42/44^{MAPK}$ pathways. Since these proteins were newly synthesized after HRG treatment, some of the signaling pathways may be involved in the synthesis of these proteins. Also, blockage of the $p38^{MAPK}$ pathway resulted in the accumulation of vesicles as clusters in the cytoplasm, suggesting that signaling from the $p38^{MAPK}$ pathway may be involved in the trafficking of vesicles during HRG-regulated secretion. At this moment, we do not know the identity of the secreted proteins in HRG-treated cultures, but planned studies will investigate the nature of the proteins.

Some of the actions of Rab3A are shown to be mediated via its effector molecule, rabphilin 3A. Rabphilin 3A binds Rab3A and colocalizes on secretory organelles. Overexpression of rabphilin 3A enhances both basal and induced secretion (11). In the mammary epithelial cells, overexpression of Rab3A alone had little effect on K^+-evoked secretion. However, exposure of cells to HRG significantly enhanced the secretory function of Rab3A-overexpressing cells. Our findings suggest that in addition to induction of Rab3A protein, HRG signaling may be involved in other aspects of the exocytosis pathway, including posttranslational modification of Rab3A, regulation of rabphilin 3A, and storage and trafficking of vesicles.

Accumulating evidence suggests that the basic mechanisms of membrane fusion follow the SNARE hypothesis (20, 36). According to the SNARE model, exocytosis involves interactions between v-SNARE proteins (present on vesicles) and t-SNARE proteins (present on target membranes) and is regulated by a number of proteins. SNAP-25 and the syntaxins belong to the t-SNARE complex, while synaptotagmin and synapsin belong to the v-SNARE complex. Rabphilin, Doc2, and Sec8 are complex regulatory proteins. Our data suggest that several components of regulatory exocytosis are expressed in mammary epithelial cells. The presence of proteins belonging to t-SNARE and regulatory subunits and the lack of expression of membrane components of v-SNARE in synaptic vesicles suggest that the vesicle components in mammary epithelial cells are different from those in neurons but probably utilize regulators similar to those used by neurons. This was the case with adipocytes, in which the nonneuronal expression of Rab3A was detected without any detectable levels of synaptophysin, an abundant integral protein of synaptic vesicles (5).

In summary, the results of our study demonstrate the expression of Rab3A in mammary epithelial cells in vivo and in vitro and show that Rab3A expression and function may be positively regulated by HRG and lactogenic hormones. These observations suggest that Rab3A plays a role in exocytosis within mammary epithelial cells.

ACKNOWLEDGMENTS

This study was supported in part by NIH grants CA80066 and CA65746 and the breast and ovarian research programs of The University of Texas M. D. Anderson Cancer Center to R.K.

We are grateful to Philip Leder for providing HRG-transgenic mice, Pietro De Camilli for rat Rab3A cDNA, Ronald W. Holz for pXGH5 construct, and Daniel Medina for HC11 cells.

REFERENCES

1. **Adam, L., R. K. Vadlamudi, S. Kondapaka, J. Chernoff, J. Mendelsohn, and R. Kumar.** 1998. Heregulin regulates cytoskeletal reorganization and cell migration through the p21-activated kinase-1 via phosphatidylinositol-3 kinase. J. Biol. Chem. **273:**28238–28246.
2. **Alvarez-Dominguez, C., and P. D. Stahl.** 1998. Interferon-gamma selectively induces Rab5a synthesis and processing in mononuclear cells. J. Biol. Chem. **273:**33901–33904.
3. **Ayala, J., B. Olofsson, N. Touchot, A. Zahraoui, A. Tavitian, and A. Prochiantz.** 1989. Developmental and regional regulation of rab3: a new brain specific "ras-like" gene. J. Neuro. Sci. Res. **22:**241–246.
4. **Baldini, G., T. Hohl, H. Y. Lin, and H. F. Lodish.** 1992. Cloning of a Rab3 isotype predominantly expressed in adipocytes. Proc. Natl. Acad. Sci. USA **89:**5049–5052.
5. **Baldini, G., P. E. Scherer, and H. F. Lodish.** 1995. Nonneuronal expression of Rab3A: induction during adipogenesis and association with different intracellular membranes than Rab3D. Proc. Natl. Acad. Sci. USA **92:**4284–4288.
6. **Bandyopadhyay, D., M. Mandal, L. Adam, J. Mendelsohn, and R. Kumar.** 1998. Physical interaction between epidermal growth factor receptor and DNA-dependent protein kinase in mammalian cells. J. Biol. Chem. **273:** 1568–1573.
7. **Bordier, C.** 1981. Phase separation of integral membrane proteins in Triton X-114 solution. J. Biol. Chem. **256:**1604–1607.
8. **Burden, S., and Y. Yarden.** 1997. Neuregulins and their receptors: a versatile signaling module in organogenesis and oncogenesis. Neuron **18:**847–855.
9. **Burgoyne, R. D., and A. Morgan.** 1993. Regulated exocytosis. Bioessays **293:** 305–310.
10. **Chung, S., G. Joberty, E. A. Gelino, I. G. Macara, and R. W. Holz.** 1999. Comparison of the effects on secretion in chromaffin and PC12 cells of Rab3 family members and mutants. J. Biol. Chem. **274:**18113–18120.
11. **Chung, S., Y. Takai, and R. W. Holz.** 1995. Evidence that the Rab3A-binding protein, rabphilin3a, enhances regulated secretion. J. Biol. Chem. **270:** 16714–16718.
12. **Cussac, D., P. Leblanc, A. L'Heritier, J. Bertoglio, P. Lang, C. Kordon, A. Enjalbert, and D. Saltarelli.** 1996. Rho proteins are localized with different membrane compartments involved in vesicular trafficking in anterior pituitary cells. Mol. Cell. Endocrinol. **119:**195–206.
13. **Darchen, F., J. Senyshyn, W. H. Brondyk, R. W. Holz, I. G. Macara, C. Tougard, and J. P. Henry.** 1995. Association of the GTP binding protein Rab3A with chromaffin granules. J. Cell Sci. **108:**1639–1649.
14. **Davidson, H. W., C. H. McGowan, and W. E. Balch.** 1992. Evidence for the regulation of exocytic transport by protein phosphorylation. J. Cell Biol. **116:** 1343–1355.
15. **Fischer von Mollard, G., G. A. Mignery, M. Baumert, M. S. Perin, T. J. Hanson, P. M. Burger, R. Jahn, and T. C. Sudhof.** 1990. rab3 is a small GTP-binding protein exclusively localized to synaptic vesicles. Proc. Natl. Acad. Sci. USA **87:**1988–1992.
16. **Geppert, M., and T. C. Sudhof.** 1998. RAB3 and synaptotagmin: the yin and yang of synaptic membrane fusion. Annu. Rev. Neurosci. **21:**75–95.
17. **Geppert, M., Y. Goda, C. F. Stevens, and T. C. Südhof.** 1997. The small GTP-binding protein Rab3A regulates a late step in synaptic vesicle fusion. Nature **387:**810–814.
18. **Geppert, M., V. Y. Bolshakov, S. A. Siegelbaum, K. Takei, P. De Camilli, R. E. Hammer, and T. C. Sudhof.** 1994. The role of Rab3A in neurotransmitter release. Nature **369:**493–497.
19. **Goalstone, M. L., J. W. Leitner, I. Golovchenko, M. R. Stjernholm, M. Cormont, Y. L. Marchand-Brustel, and B. Draznin.** 1999. Insulin promotes phosphorylation and activation of geranylgeranyltransferase II. Studies with geranylgeranylation of rab-3 and rab-4. J. Biol. Chem. **274:**2880–2884.
20. **Hay, J. C., and R. H. Scheller.** 1997. SNAREs and NSF in targeted membrane fusion. Curr. Opin. Cell. Biol. **9:**505–512.
21. **Hennighausen, L., and G. W. Robinson.** 1998. Think globally, act locally: the making of a mouse mammary gland. Genes Dev. **12:**449–455.
22. **Holz, R. W., W. H. Brondyk, R. A. Senter, L. Kuizon, and I. G. Macara.** 1994. Evidence for the involvement of Rab3A in Ca(2+)-dependent exocytosis from adrenal chromaffin cells. J. Biol. Chem. **269:**10229–10234.
23. **Huang, Z., C. Ritter, A. Brown, J. Finch, Y. Abu-Amer, P. Ross, and E. Slatopolsky.** 1999. Cloning and localization of Rab3 isoforms in bovine, rat, and human parathyroid glands. Biochem. Biophys. Res. Commun. **255:**645–651.
24. **Iezzi, M., G. Escher, P. Meda, A. Charollais, G. Baldini, F. Darchen, C. B. Wollheim, and R. Regazzi.** 1999. Subcellular distribution and function of Rab3A, B, C, and D isoforms in insulin-secreting cells. Mol. Endocrinol. **13:** 202–212.
25. **Jones, F. E., D. J. Jerry, B. C. Guarino, G. C. Andrews, and D. F. Stern.** 1996. Heregulin induces in vivo proliferation and differentiation of mammary epithelium into secretory lobuloalveoli. Cell Growth Differ. **7:**1031–1038.

26. **Kato, M., T. Sasaki, T. Ohya, H. Nakanishi, H. Nishioka, M. Imamura, and Y. Takai.** 1996. Physical and functional interaction of rabphilin-3A with alpha-actinin. J. Biol. Chem. **271:**31775–31778.
27. **Krane, I. M., and P. Leder.** 1996. NDF/heregulin induces persistence of terminal end buds and adenocarcinomas in the mammary glands of transgenic mice. Oncogene **12:**1781–1788.
28. **Linzell, J. L., and M. Peaker.** 1971. Mechanism of milk secretion. Physiol. Rev. **51:**564–597.
29. **Lledo, P. M., P. Vernier, J. D. Vincent, W. T. Mason, and R. Zorec.** 1993. Inhibition of Rab3B expression attenuates Ca(2+)-dependent exocytosis in rat anterior pituitary cells. Nature **364:**540–544.
30. **Marte, B. M., M. Jeschke, D. Graus-Porta, P. Hofer, B. Groner, Y. Yarden, and N. E. Hynes.** 1995. Neu differentiation factor/heregulin modulates growth and differentiation of HC11 mammary epithelial cells. Mol. Endocrinol. **9:**14–23.
31. **Nishio, H., T. Suda, K. Sawada, T. Miyamoto, T. Koike, and Y. Yamaguchi.** 1999. Molecular cloning of cDNA encoding human Rab3D whose expression is upregulated with myeloid differentiation. Biochim. Biophys. Acta **1444:** 283–290.
32. **Novick, P., and M. Zerial.** 1997. The diversity of Rab proteins in vesicle transport. Curr. Opin. Cell Biol. **9:**496–504.
33. **Peles, E., S. S. Bacus, R. A. Koski, H. S. Lu, D. Wen, S. G. Ogden, R. B. Levy, and Y. Yarden.** 1992. Isolation of the neu/HER-2 stimulatory ligand: a 44 kd glycoprotein that induces differentiation of mammary tumor cells. Cell **69:** 205–216.
34. **Pfeffer, S. R.** 1999. Transport vesicle targeting: tethers before SNAREs. Nat. Cell Biol. **1:**E17–E22.
35. **Regazzi, R., M. Ravazzola, M. Iezzi, J. Lang, A. Zahraoui, E. Andereggen, P. Morel, and Y. Takai.** 1996. Expression, localization and functional role of small GTPases of the Rab3 family in insulin-secreting cells. J. Cell Sci. **109:** 2265–2273.
36. **Rothman, J. E.** 1994. Mechanisms of intracellular protein transport. Nature **372:**55–63.
37. **Schimmoller, F., I. Simon, and S. R. Pfeffer.** 1998. Rab GTPases: directors of docking. J. Biol. Chem. **273:**22161–22164.
38. **Spencer, K. S. R., D. Grausoporta, J. Leng, N. E. Hynes, and R. L. Klemke.** 2000. ErbB2 is necessary for induction of carcinoma cell invasion by ErbB family receptor tyrosine kinases. J. Cell Biol. **148:**385–397.
39. **Takai, Y., T. Sasaki, H. Shirataki, and H. Nakanishi.** 1996. Rab3A small GTP-binding protein in Ca(2+)-dependent exocytosis. Genes Cells **1:**615–632.
40. **Takei, N., K. Sasaoka, K. Inoue, M. Takahashi, Y. Endo, and H. Hatanaka.** 1997. Brain-derived neurotrophic factor increases the stimulation-evoked release of glutamate and the levels of exocytosis-associated proteins in cultured cortical neurons from embryonic rats. J. Neurochem. **68:**370–375.
41. **Turner, M. D., M. E. Rennison, S. E. Handel, C. J. Wilde, and R. D. Burgoyne.** 1992. Proteins are secreted by both constitutive and regulated secretory pathways in lactating mouse mammary epithelial cells. J. Cell Biol. **117:**269–278.
42. **Vadlamudi, R. K., L. Adam, A. H. Talukder, J. Mendelsohn, and R. Kumar.** 1999. Serine phosphorylation of paxillin by heregulin-beta 1: role of p38 mitogen activated protein kinase. Oncogene **18:**7253–7264.
43. **Walch-Solimema, C., R. N. Collins, and P. J. Novick.** 1997. Sec2p mediates nucleotide exchange on Sec4p and is involved in polarized delivery of post-Golgi vesicles. J. Cell Biol. **137:**1495–1509.
44. **Wick, P. F., R. A. Senter, L. A. Parsels, M. D. Uhler, and R. W. Holz.** 1993. Transient transfection studies of secretion in bovine chromaffin cells and PC12 cells. Generation of kainate-sensitive chromaffin cells. J. Biol. Chem. **268:**10983–10989.
45. **Yang, Y., E. Spitzer, D. Meyer, M. Sachs, C. Neimann, G. Hartmann, K. M. Weidner, C. Birchmeier, and W. Birchmeier.** 1995. Sequential requirement of hepatocyte growth factor and neuregulin in the morphogenesis and differentiation of the mammary gland. J. Cell Biol. **131:**215–226.

THE JOURNAL OF BIOLOGICAL CHEMISTRY Vol. 276, No. ??, Issue of ???? ??, pp. 1–xxx, 2001
Printed in U.S.A.
© 2001 by The American Society for Biochemistry and Molecular Biology, Inc.

Molecular Cloning and Characterization of PELP1, a Novel Human Coregulator of Estrogen Receptor α*

Received for publication, April 27, 2001, and in revised form, July 5, 2001
Published, JBC Papers in Press, July 31, 2001, DOI 10.1074/jbc.M103783200

Ratna K. Vadlamudi‡, Rui-An Wang, Abhijit Mazumdar, Yoon-sok Kim§, Jaekyoon Shin§, Aysegul Sahin, and Rakesh Kumar

From the University of Texas M. D. Anderson Cancer Center, Houston, Texas 77030 and the §Samsung Biomedical Research Institute and Sungkyunkwan University School of Medicine, Suwon, 440-746 Korea.

Nuclear hormone receptors (NRs) are transcription factors whose activity is regulated by ligands and by coactivators or corepressors. We report the characterization of a new NR coregulator: proline-, glutamic acid-, leucine-rich protein 1 (PELP1), a novel human protein that comprises 1,282 amino acids and is localized on chromosome 17. The primary structure of PELP1 consists of several motifs present in most transcriptional regulators including nine NR-interacting boxes (LXXLL motifs), a zinc finger, and glutamic acid- and proline-rich regions. We demonstrate that PELP1 is a coactivator of estrogen receptor α (ERα). PELP1 enhances 17β-estradiol-dependent transcriptional activation from the estrogen response element in a dose-dependent manner. PELP1 interacts with ERα and also with general transcriptional coactivators p300 and cAMP response element-binding protein-binding protein. PELP1 was differentially expressed in various human and murine tissues with the highest expression levels in the testes, mammary glands, and brain. We also provide evidence supporting the developmental regulation of PELP1 expression in murine mammary glands, the detectable expression of PELP1 in human mammary cancer cell lines, and the enhanced expression of PELP1 in human breast tumors. These findings suggest that PELP1 is a novel coregulator of ERα and may have a role in breast cancer tumorigenesis.

The nuclear hormone receptors (NRs)[1] constitute a large family of transcription factors that regulate gene expression in a ligand-dependent manner. NRs play an important role in vertebrate development and have been implicated in a broad range of cellular responses, such as differentiation, proliferation, and homeostasis (1, 2). Currently, the NR superfamily is divided into three subfamilies: the type I subfamily encodes steroid hormone receptors, such as receptors of estrogen (ER), progestin, androgen, and glucocorticoids; the type II subfamily encodes receptors for non-steroidal hormones, such as receptors for retinoic acid, thyroid hormone, and vitamin D receptor; and the type III subfamily encodes orphan receptors with no well characterized ligands (3).

NRs share several structural features including an N-terminal ligand-independent transcriptional activation function domain 1 (AF1); a C-terminal ligand binding domain (LBD) that interacts with ligands; a central, highly conserved DNA binding domain (DBD) that targets NRs to specific DNA motifs; and a C-terminal ligand-dependent transcriptional activation function domain (AF2) (3, 4). The binding of hormones to a NR triggers a conformational change that allows the NR to bind the responsive elements in the target gene promoters. The LBDs of NRs are diverse in sequence, accounting for ligand specificity, but they share a consistent overall structure (3). AF2 is highly conserved among various NRs, but AF1 is not conserved (2).

The transcriptional activity of NRs is not only regulated by hormones but also affected by several regulatory proteins called coactivators and corepressors (3, 5). Coactivators do not usually bind to DNA but are recruited to the target gene promoters through protein-protein interactions with the NRs (6). The p160 family is a well studied family of NR coactivators, and its members are steroid receptor coactivator SRC1, glucocoticoid receptor-interacting protein GRIP1/TIF2, and P/CIP (also known as AIB1, TRAM1, RAC3) (7). A second coactivator family includes the cAMP response element-binding protein-binding protein CBP and p300 (8). Among the corepressors, nuclear receptor corepressor (NcoR) and silencing mediator for retinoic and thyroid receptor (SMRT) have been widely characterized and implicated in the transcriptional silencing of thyroid hormone receptor-, retinoic acid receptor-, retinoid X receptor-, and vitamin D receptor-responsive genes in the absence of ligand (3). Corepressors have been shown to associate preferentially with antagonist-occupied NRs (9). A few bifunctional coregulators that can act as both coactivators and corepressors of NRs have also been reported recently, and examples include mouse zinc finger protein, a regulator of apoptosis and cell cycle arrest (ZAC1) (10); a NR-binding set domain-containing protein (NSD1) (11); and RIP140 (12).

Evidence suggests that multiprotein complexes containing coactivators, NRs, and transcriptional regulators assemble in response to hormone binding and activate transcription (3). Researchers are actively investigating the molecular mechanisms whereby hormones elicit tissue type- and cell type-specific responses and the composition of coactivator proteins in-

* This study was supported in part by the National Institutes of Health Grants CA80066 and CA84456 and Cancer Center Core Grant CA16672, Breast Cancer Research Program of the University of Texas M. D. Anderson Cancer Center. The costs of publication of this article were defrayed in part by the payment of page charges. This article must therefore be hereby marked "*advertisement*" in accordance with 18 U.S.C. Section 1734 solely to indicate this fact.

‡ To Whom correspondence should be addressed: Dept. of Cellular and Molecular Oncology, the University of Texas M. D. Anderson Cancer Center 108, 1515 Holcombe Blvd., Houston, TX 77030. Tel.: 713-745-5239; Fax: 713-745-3792; E-mail: rvadlamu@mdanderson.org.

[1] The abbreviations used are: NR(s), nuclear receptor(s); ER, estrogen receptor; AF, activation function; LBD, ligand binding domain; DBD, DNA binding domain; SRC1, steroid receptor coactivator 1; GRIP, glucocorticoid receptor interacting protein; CBP, cAMP response element-binding protein-binding protein; E_2, 17β-estradiol; ERE, estrogen response element; PELP1, proline glutamic acid- and leucine-rich protein 1; PBS, phosphate-buffered saline; luc, luciferase; gal, galactosidase; CAT, chloramphenicol acetyltransferase; GST, glutathione *S*-transferase.

volved. Structural analysis of coactivators has identified a motif consisting of five amino acids LXXLL (where X is any amino acid), which is sufficient to mediate coregulator binding to the liganded NRs (13). The coactivators SRC1, CBP, and p300 have intrinsic histone acetyltransferase activity (14). In contrast, NcoR and SMRT associate with histone deacetylases and mSin3A (15). The association of the histone acetyltransferase and histone deacetylase activity with the coactivators and corepressors suggests that the modulation of chromatin structures constitutes a potential mechanism whereby coregulators function (2). Another mechanism of regulation of gene transcription, in addition to chromatin remodeling, is the phosphorylation of coactivators and corepressors (16).

Steroid hormone 17β-estradiol (E_2) plays an important role in controlling the expression of genes involved in a wide variety of biological processes, including development, homeostasis, regulation of the cardiovascular system, the determination of bone density, and breast tumor progression (17). The biological effects of estrogen are mediated by its binding to the structurally and functionally distinct estrogen receptors (ERα and ERβ); ERα is the major ER in the mammary epithelium (18). Like other steroid receptors, ERα comprises an N-terminal AF1 domain, a DBD, and a C-terminal LBD that contains an AF2 domain (19). Upon the binding of E_2 to ERα, the ligand-activated ERα translocates to the nucleus, binds to the 13-base pair palindromic estrogen response enhancer element (ERE) in the target genes, and stimulates gene transcription, thus promoting the growth of breast cancer cells (20). It is generally accepted that some of the diverse functions of estrogens depend on differential recruitment of coregulators to the E_2·ER complex. The transcription functions of ER may be influenced by several coregulators, including SRC1, GRIP1, AIB1, CBP/p300, TIF1, PGC1, and DAX1 (3, 21, 22). Although much is known about the structure of coregulators, very little is known about the physiological role of coregulator proteins in the development, hormone regulation, and progression of cancer.

In the present study, we describe the cloning and characterization of PELP1, a new member of the family of coregulators of NRs. We also provide evidence that PELP1 is a novel coactivator of the ER pathway and that it may be up-regulated in human breast cancer.

MATERIALS AND METHODS

Cell Cultures and Reagents—MCF-7, T47D, and ZR75R human breast cancer cells (23) were maintained in Dulbecco's modified Eagle's medium and F-12 (1:1) supplemented with 10% fetal calf serum. Antibodies against actin, vinculin, and E_2 were purchased from Sigma Chemical Co. Antibodies against ERα were purchased from Upstate Biotechnology. Anti-T7 epitope antibody was purchased from Novagen. Antibodies against CBP and p300 were purchased from Santa Cruz Biotechnology. Charcoal-stripped serum (DCC serum) was purchased from Sigma.

Isolation of PELP1 cDNA—PELP1 identification, purification, endoproteinase digestion, high performance liquid chromatography purification, and peptide sequencing have been described (24). Peptide sequences used for screening the library were GSPDGSLQTGKPSAPK(S), LDVGEAMAP(Q), VQPEPEPEPGLLLEVEEPGTEEERGADD, and VQPPPETPAEEEMETETEAEALQEKEQ. A HeLa cDNA library (Stratagene) was screened with ^{32}P-labeled oligonucleotide probes that were synthesized according to PELP1 sequences. Hybridization was performed at 42 °C in formamide buffer, and membranes were washed three times in 2× SSC in 0.1% SDS at 42 °C. Positive clones were plaque purified, and the N-terminal region (400 base pairs) of the longest clone (1,300 base pairs) was used to rescreen the HeLa library as described above. Positives from the secondary screening were plaque purified, and the full-length PELP1 clone was constructed using overlapping internal restriction sites. A full-length open reading frame of PELP1 was subcloned into pcDNA3.1 His vector (Invitrogen) using *Eco*RI and *Xho*I sites to make T7-tagged PELP1 expression vector. PELP1(1–540) and PELP1(541–1282) constructs were created in pcDND3.1 His vector utilizing an internal unique *Bam*HI site.

Generation of PELP1 Antiserum—A 19-mer peptide encoding amino acids 558–576 (RDSLSPGQERPYSTVRTKV) of the *PELP1* gene was synthesized and conjugated to keyhole limpet hemocyanin. Using a standard inoculation protocol (Research Genetics, Huntsville, AL) the conjugated peptide was then used to produce a rabbit polyclonal antiserum.

Cell Extracts, Immunoblotting, and Immunoprecipitation—To prepare cell extracts, cells were washed three times with phosphate-buffered saline (PBS) and then lysed in RIPA buffer (50 mM Tris-HCl, pH 7.5, 150 mM NaCl, 0.5% Nonidet P-40, 0.1% SDS, 0.1% sodium deoxycholate, 1× protease inhibitor mixture (Roche Biochemical), and 1 mM sodium vanadate) for 15 min on ice. The lysates were centrifuged in an Eppendorf centrifuge at 4 °C for 15 min. Cell lysates containing equal amounts of protein (~200 μg) were resolved on SDS-polyacrylamide gels (8% acrylamide), transferred to nitrocellulose membranes, probed with the appropriate antibodies, and developed using either the enhanced chemiluminescence method (ECL) or the alkaline phosphatase-based color reaction method. Immunoprecipitation was performed for 2 h at 4 °C using 1 μg of antibody/mg of protein (25).

Reporter Gene Assays—For reporter gene transient transfections, HeLa and MCF-7 cells were cultured in minimal essential medium without phenol red containing 10% DCC serum for 24 h and then transfected reporter plasmids without or with PELP1 expression plasmid using Fugene-6 reagent according to the manufacturer's instructions (Roche Diagnostics). 24 h later, cells were treated with the indicated ligands for 16–24 h. Cells were lysed with passive lysis buffer, and the luciferase (luc) assay was performed using a luciferase reporter assay kit (Promega). The total amount of DNA used was kept constant by adding parental vector. The activity of β-galactosidase (β-gal) reporter was used to correct the transfection efficiencies. SRC1, GRIP1 plasmids were used as positive controls. Chloramphenicol acetyltransferase assays were performed using an assay kit from Promega. Transfections were carried out in six-well plates, and each transfection was performed in triplicate wells. Luciferase assays using gal4-ER/gal4-luc were performed as described (26).

Immunohistochemistry—The mouse organs were dissected and fixed with 10% formaldehyde or with Bouin's solution overnight and processed using standard techniques in paraffin sections. Immunohistochemistry was done as described previously (27). Briefly, the sections were deparaffinized with xylene, rehydrated using graded ethanol, and incubated in 0.3% hydrogen peroxide and methanol for 30 min to inactivate the endogenous peroxidase. The sections were then boiled for 10 min in 0.01 M citrate buffer and cooled for 30 min at room temperature to unmask the antigen epitopes. The sections were incubated sequentially with 2% normal goat serum in 1% bovine serum albumin and PBS for 30 min and with rabbit anti-PELP1 antibody (1:500 diluted in 2% normal goat serum, 1% bovine serum albumin, and PBS) overnight at room temperature. The sections were washed three times with 0.05% Tween in PBS for 10 min and incubated with horseradish peroxidase-donkey anti-rabbit IgG (1:100, Sigma) for 1 h. After being washed with PBS, the antigen sites were visualized with DAB-H_2O_2 and counterstained with Mayer's hematoxylin. For staining specificity control, preimmune serum from the same animal and peptide absorbed antiserum were used to replace the first antibody for staining.

Tumor Samples—Human biopsies were obtained from the breast cancer core laboratories at the M. D. Anderson Cancer Center. Samples were frozen in liquid nitrogen and stored at −80 °C. Eight matching pairs of tumor and adjacent normal tissues were analyzed. Biopsy tissues were homogenized in Triton X-100 lysis buffer (20 mM HEPES, 150 mM NaCl, 1% Triton X-100, 0.1% deoxycholate, 2 mM EDTA, 2 mM EDTA, 2 mM sodium orthovanadate, and protease inhibitor mixture; Roche Molecular Biochemicals), and equal amounts of protein were analyzed by Western blotting.

RESULTS

cDNA Cloning and DNA Sequence Analysis—Earlier in an attempt to identify the Src homology 2 domain-binding proteins, we identified a protein with a molecular mass of about 160 kDa. The identification, purification, and peptide sequencing of p160 kDa protein have been reported earlier (24). Using the peptide sequence of p160 protein, we screened an HeLa cDNA library and isolated a cDNA clone (accession no. U88153) that contained an open reading frame of 3,846 base pairs and also the entire peptide sequences reported for the p160 protein (14). This protein is unusually rich in the amino acids proline (13.2%), glutamic acid (12.4%), and leucine (12.9%) and is

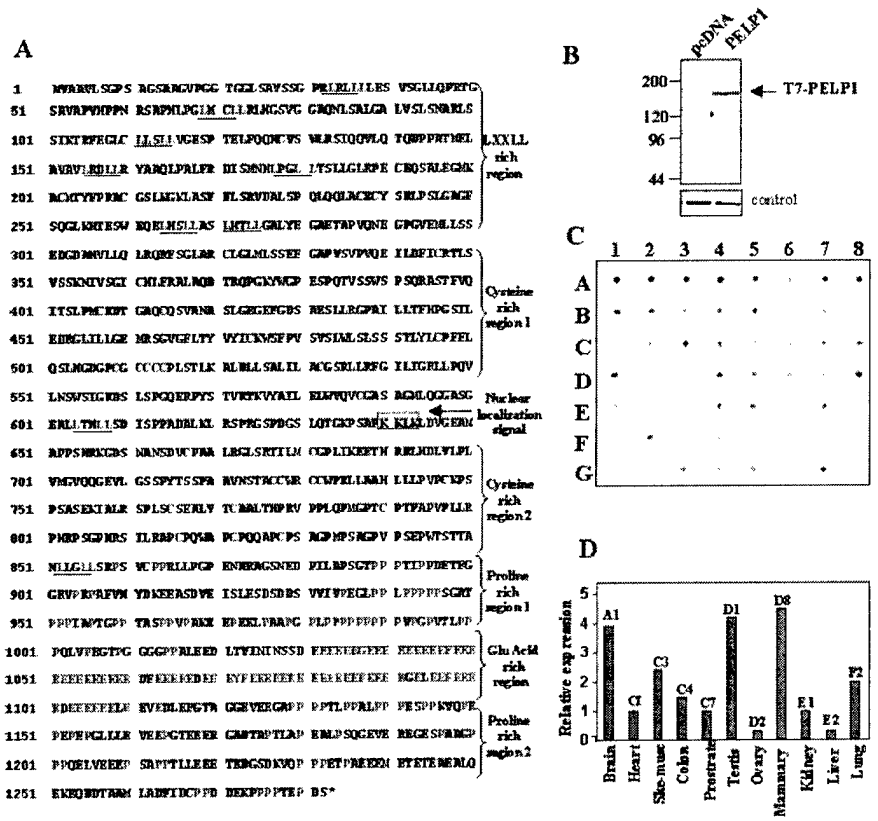

FIG. 1. **PELP1 amino acid sequence and expression in human tissues.** *Panel A*, deduced amino acid sequence of PELP1. The *numbers* on the *left* correspond to the amino acid numbers. NR recognition motifs are *underlined*, and the nuclear localization sequence is *boxed*. Domains rich in LXXLL motifs, cysteine, proline, and acidic amino acids are shown on the *right*. *Panel B*, pcDNA or PELP1-pcDNA was transiently expressed in MCF-7 cells, and the expressed protein was detected using a monoclonal antibody against T7. *Panel C*, Northern analysis of the expression of PELP1 using a multiple human poly(A)$^+$ RNA master blot from CLONTECH, probed with a PELP1 open reading frame. *A1*, brain; *A2*, amygdala; *A3*, caudate nucleus; *A5*, cerebral cortex; *A6*, frontal lobe; *A7*, hippocampus; *A8*, medulla ablongata; *B1*, occipital lobe; *B2*, putamen; *B3*, substantia nigra; *B4*, temporal lobe; *B5*, thalamus; *B6*, nucleus accumbsus; *B7*, spinal cod; *C1*, heart; *C2*, aorta; *C3*, skeletal muscle; *C4*, colon; *C5*, bladder; *C6*, uterus; *C7*, prostate; *C8*, stomach; *D1*, testis; *D2*, ovary; *D3*, pancreas; *D4*, pituitary gland; *D5*, adrenal gland; *D6*, thyroid gland; *D7*, salivary gland; *D8*, mammary gland; *E1*, kidney; *E2*, liver; *E3*, small intestine; *E4*, spleen; *E5*, thymus; *E6*, peripheral leukocyte; *E7*, lymph node; *E8*, bone marrow; *F1*, appendix; *F2*, lung; *F3*, trachea; *F4*, placenta; *G1*, fetal brain; *G2*, fetal heart; *G3*, fetal kidney; *G4*, fetal liver; *G5*, fetal spleen; *G6*, fetal thymus; *G7*, fetal lung. *Panel D*, the expression of PELP in RNA dot blots was quantitated, and data from representative tissues are shown. The GenBank accession number for PELP1 cDNA is U88153.

therefore named proline-, glutamic acid-, and leucine-rich protein 1 (PELP1). A search of the newly released Human Genomic Sequence data base revealed that PELP1 is localized at chromosome 17. The present study was undertaken to characterize this novel protein and to explore its functions.

The deduced amino acid sequence of PELP1 is shown in Fig. 1*A*. The PELP1 protein has no overall homology with any protein in the GenBank data base. However, the amino acid sequence of PELP1 has several interesting features (Fig. 1*A*). PELP1 has a centrally located consensus nuclear localization motif starting with amino acids 640–641 (28). PELP1 contains nine LXXLL motifs. LXXLL motifs are present in several NR coactivators, including SRC1, GRIP1, and P300 and mediate ligand-dependent binding of coactivators with NR (13). The PELP1 C terminus has two regions rich in proline (31% proline, amino acids 851–1020; 23% proline, amino acids 1129–1282). Proline-rich sequences in transcription factors have been reported, and a region containing 25% proline has been shown to function as a transcriptional activation domain in CTF1/NF1 (29). The C-terminal region of PELP1 contains regions unusually rich in acidic amino acids. PELP1 also contains two regions rich in cysteine residues, which may potentially form three zinc fingers, but these regions show no homology with the well established zinc finger domains in the protein domain data base. In addition, PELP1 has several consensus phosphorylation sites. To verify that the PELP1 clone encodes a physiological gene product, the expression of PELP1 cDNA was examined in a transient expression assay using the human breast cancer cell line MCF-7 (Fig. 1*B*). To detect the expression of PELP1 cDNA, we incorporated T7 epitope tag at the N terminus of the open reading frame. The expression of T7-tagged cDNA of PELP1 produced a protein with a molecular mass of about 160 kDa. The expression of PELP1 mRNA was analyzed using a multiple human tissue poly(A)$^+$ RNA dot-blot (CLONTECH). As shown in Fig. 1, *C* and *D*, PELP1 was expressed differentially in various human tissues, with the highest expression levels in testis, mammary gland, brain, skeletal muscle, and lung tissues.

PELP1 Acts as a Coactivator of ERα—The presence of nine LXXLL motifs and the abundant expression of PELP1 in mammary glands provide a basis to hypothesize that PELP1 has a role in the ER pathway. To explore this hypothesis, we used a well established gal4-ER/gal4-luc assay system (30). This system involves the transient transfection of two plasmids gal4-AF2 (LBD of ERα) and gal4-luc reporter, wherein activation of the luc depends on stimulation of the AF2 domain by E_2. PELP1 was cotransfected with gal4-AF2, gal4-luc plasmids into HeLa cells, which are known to contain no or undetectable ER. The levels of luc reporter transcriptional activity were higher in cells treated with E_2 than in untreated control cells

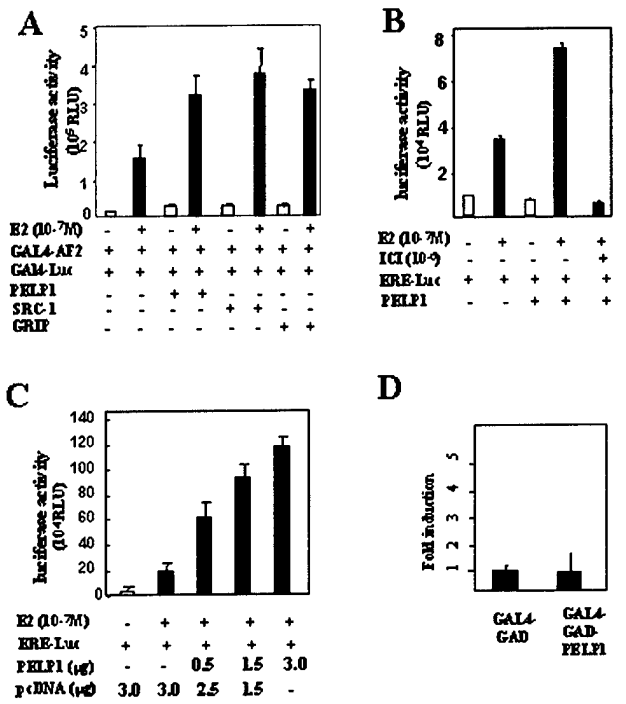

FIG. 2. **PELP1 enhances ERα-dependent transcription and interacts with endogenous ERα.** *Panel A*, HeLa cells were cotransfected with 100 ng of gal4-AF2, gal4-luc, and with 1 μg of PELP1 or SRC1 or GRIP1 or control plasmid. Cells were treated with or without 10^{-7} M E_2, and luc activity was measured 24 h later. *Panel B*, MCF-7 cells were cotransfected with 100 ng of ERE-luc and 1 μg of PELP1. After 24 h, cells were treated with 10^{-7} M E_2 or E_2 and 10^{-6} M ICI182780, and luc activity was measured after 24 h. *Panel C*, MCF-7 cells were transfected with 100 ng of ERE-luc and increasing concentrations of PELP1 and treated with E_2. The mean results of triplicate samples are shown. The luc experiments were repeated three times, and similar results were obtained. *Panel D*, MCF-7 cells were cotransfected with 100 ng of GAL4-luc reporter and gal4-GBD vector or gal4-GBD-PELP1, and luc activity was measured after 48 h.

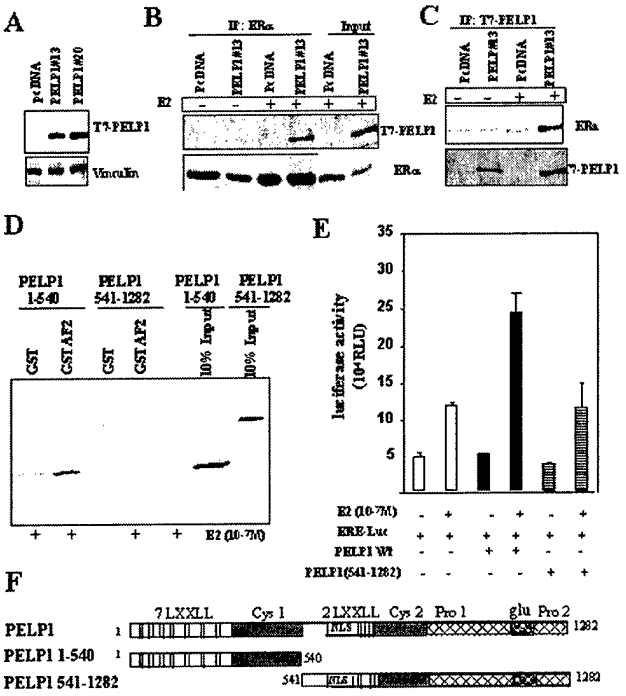

FIG. 3. **PRLP1 interacts with ERα.** *Panel A*, expression of T7-tagged PELP1 in MCF-7 stable cell lines as detected by Western blotting using anti-T7 mAb. *Panels B* and *C*, MCF-7 cells stably expressing pcDNA or PELP1 were treated with E_2 for 30 min, and nuclear extracts were prepared. Equal amounts of proteins were immunoprecipitated with anti-ER or anti-T7 mAb and analyzed by Western blotting with T7 and ER antibodies. Input represents 10% of the total amount used for immunoprecipitations. *Panel D*, interaction of PELP1 and ERα AF2 domain *in vitro*. PELP1(1–540) and PELP1(541–1282) were labeled with [^{35}S]methionine using the TNT reaction (Promega) and incubated with GST-AF2 in the presence of 100 nM E_2. Bound proteins were visualized by SDS-polyacrylamide gel electrophoresis and developed by phosphorimaging. *Panel E*, MCF-7 cells were transfected with 100 ng of ERE-luc and with 1 μg of PELP1 or 1 μg of PELP1(541–1273). 24 h later cells were treated with E_2, and luciferase activity was measured after 24 h. *Panel F*, schematic representation of the PELP1 deletion constructs used.

(Fig. 2*A*). The expression of PELP1 had no apparent effect on the reporter activity in the absence of ligand. However, in the presence of 100 nM E_2 cotransfection of cells with PELP1 but not the control vector significantly increased gal-luc reporter activity in a manner similar to that observed in the well characterized coactivators SRC1 and GRIP1 (Fig. 2*A*).

To confirm these results, we performed another assay, using ERE-luc reporter in ERα-positive MCF-7 human breast cancer cells. The ERE-luc activity after transient coexpression of PELP1 with ERE-luc reporter was 7 times that of control cells, a significantly greater increase than that induced by E_2 treatment alone, which resulted in an ERE-luc activity level 3.6 times that of controls (Fig. 2*B*). PELP1 had no significant effect on the activity of ERE-luc in the absence of ligand. In addition, PELP1-mediated enhancement of the transcriptional activity was completely blocked by the addition of pure anti-estrogen ICI 182780. The PELP1-mediated increase in the ERE-luc activity was dose-dependent, with the highest activity at 3 μg of DNA (Fig. 2*C*). To examine the possibility that PELP1 has intrinsic transcriptional activity, full-length PELP1 cDNA was fused to gal4-DBD, and its effect on the transcriptional activity of gal4-responsive luc reporter was analyzed. We did not observe any significant activity of PELP1 compared with gal4-DBD vector. These results suggest that PELP1 acts as a coactivator of ER/ERE pathway and is functionally distinct from SRC family of coactivators which possess intrinsic transcriptional activity.

PELP1 Interacts with ERα—We next sought to determine whether PELP1 interacts with ERα. Because we did not have an antibody effective in recognizing PELP1 in immunoprecipitations, we initially developed stable MCF-7 cell lines expressing T7-tagged PELP1 cDNA (Fig. 3*A*). Two clones expressing detectable levels of PELP1 were identified. The expression of PELP1 did not affect the growth rate of the cells in either the presence or the absence of E_2 (data not shown). To examine the interaction of PELP1 with endogenous ERα, MCF-7 cells expressing PELP1 were treated with or without E_2, and nuclear extracts were immunoprecipitated with ERα or T7 antibodies. ERα antibody effectively immunoprecipitated PELP1 only when cells were treated with E_2; in the absence of ligand, no interaction was observed (Fig. 3*B*). Similarly, in reciprocal immunoprecipitations PELP1 effectively immunoprecipitated ER only when cells were treated with E_2 (Fig. 3*C*). These results suggest that PELP1 interacts with ERα in a ligand-dependent manner.

To address the role of LXXLL motifs in the binding and coactivation of ERα, we created two deletion constructs: the first construct PELP1(1–540) contains seven LXXLL motifs, and the second construct PELP1(541–1282) lacks seven LXXLL motifs (Fig. 3*F*). Initially the ability of both constructs to bind AF2 domain of ERα was analyzed by GST-pull down assays. GST AF2 but not GST alone pulled down the PELP1(1–540) (Fig. 3*D*), and there was no detectable binding of AF2 to

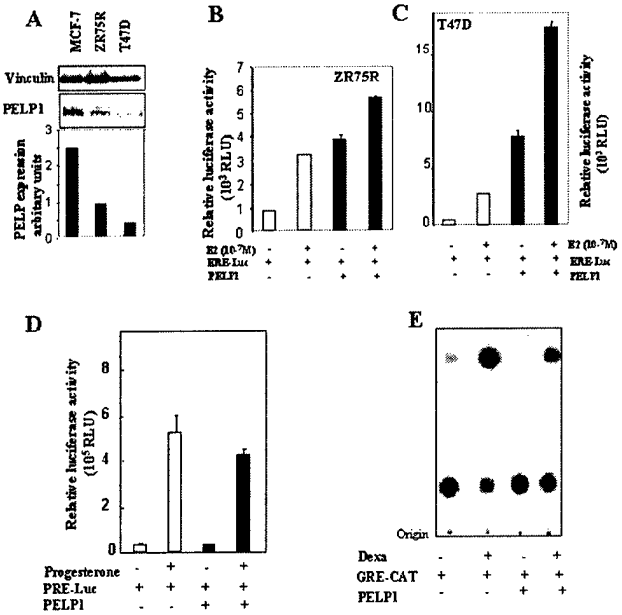

FIG. 4. **PELP1 differentially regulates transcriptional activation in a cell- and promoter-dependent manner.** *Panel A*, Western blot showing the endogenous levels of PELP1 in three breast cancer cell lines. *Panel B*, ZR75R cells were cotransfected with 100 ng of ERE-luc and 1 μg of PELP1. After 24 h, cells were treated with 10^{-7} M E_2, and luc activity was measured after 24 h. *Panel C*, T47D cells were cotransfected with 100 ng of ERE-luc and 1 μg of PELP1. After 24 h, cells were treated with 10^{-7} M E_2, and luc activity was measured after 24 h. *Panel D*, MCF-7 cells were cotransfected with 100 ng of PRE-luc and 1 μg of PELP1 or control vector. After 24 h, cells were treated without or with 500 nM progesterone for an additional 24 h. *Panel E*, MCF-7 cells were cotransfected with 1 μg of GRE-CAT reporter and with 1 μg of PELP1 or control vector. 48 h later cells were treated without or with 500 nM dexamethasone for 24 h, and cell extracts were assayed for CAT activity. Results shown are representative of three separate experiments.

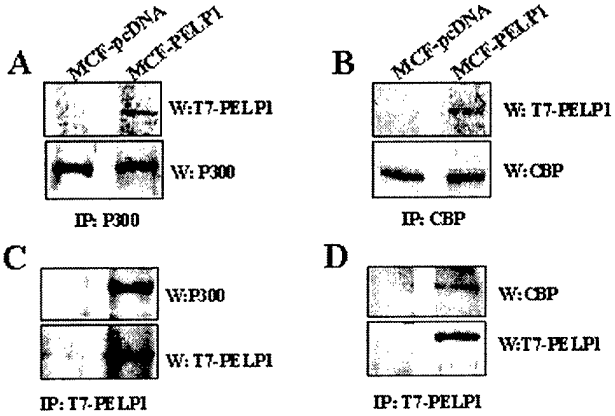

FIG. 5. **Interaction of PELP1 with CBP and with P300.** *Panels A* and *B*, equal amounts of cell lysates from MCF-7 cells stably expressing pcDNA or T7-PELP1 (clone 20) were subjected to immunoprecipitation with CBP and p300 antibodies followed by Western blotting with T7 monoclonal antibody. *Panels C* and *D*, reverse experiment in which 3 mg of cell lysates from MCF-7 cells stably expressing pcDNA or T7-PELP1 (clone 20) were subjected to immunoprecipitation with T7 monoclonal antibody and Western blotted with p300 or CBP.

PELP1(541–1282). These results suggest that the 540-amino acid region containing seven LXXLL motifs is important for the binding of ERα. Furthermore, transfection of PELP1(541–1282), which has a deletion of seven LXXLL motifs, failed to activate the transcription by E_2 in ERE reporter assays (3E). Together these results suggest that LXXLL motifs are required for the binding, and such binding is essential for the activation function of PELP1.

PELP1 Differentially Regulates Steroid Receptors in a Cell- and Promoter Context-dependent Manner—To explore the possibility that differential expression of PELP1 and cellular context impacts ERα transactivation distinctly, we next determined the ERE-driven transactivation of a reporter system in breast cancer cells lines MCF-7, ZR75R, and T47D, which have high, moderate to low, and low levels of endogenous PELP1, respectively (see Fig. 6*D* for the PELP1 levels). All three of the model cells have been shown to contain functional ERα and respond to E_2. Cotransfection of PELP1 in low expressing T47D cells significantly increased the E_2 responses of the ERE reporter to 30-fold over control (Fig. 4*C*) compared with high expressing MCF-7 cells which responded to 7-fold increase over control (Fig. 2*B*). Moderate PELP1-expressing ZR75R cells showed a 10-fold increase in luciferase activity by E_2 (Fig. 4*B*). Interestingly, overexpression of PELP1 alone in ZR75R and T47D cells was sufficient to activate the ERE reporter activity in the absence of E_2. The lower response of PELP1 on MCF7 cells could possibly be attributed to the saturation of these cells with high levels of endogenous PELP1, and MCF7 cells have higher basal ERE reporter activity compared with T47D cells. These results suggest that PELP1 signaling is dependent on the cell/tissue context.

We next tested the possibility of whether PELP1 is specific coregulator of ERα or if it can act as a coactivator for other members of steroid receptors. To address this possibility, we used reporter genes for two other steroid receptors progesterone and glucocorticoid, which are known to be expressed in mammary epithelial cells. Cotransfection of PELP1 with PRE-luc or GRE-CAT reporter did not result in a significant activation of the reporter activity in presence or absence of the ligand. In contrast, there was a moderate decrease in the ligand-induced activation. These results suggest that PELP1 may be a specific activator of ERα, and its coactivation function is promoter-dependent.

PELP1 Interacts with General Transcriptional Activators CBP and p300—Earlier studies have shown that NR coactivators interact with CBP and p300, general transcriptional activators (8). Because PELP1 augmented E_2-mediated transcription, we sought to determine whether PELP1 also interacts with CBP and p300. Cell lysates from the stable cell lines expressing T7-tagged PELP1 were subjected to immunoprecipitation with CBP or p300 and Western blotted with T7 antibody. Both p300 and CBP specifically coimmunoprecipitated T7-PELP1 (Fig. 5, *A* and *B*). This result was validated by a reverse experiment involving immunoprecipitation of T7-tagged PELP1 followed by Western blotting with antibodies directed against CBP or p300 (Fig. 5, *C* and *D*). These results suggest that PELP1 interacts with the general transcriptional coactivators CBP and p300.

PELP1 Expression in Mouse Tissues and in Human Breast Cancer Cell Lines—To characterize PELP1 protein further, we generated polyclonal antiserum directed at a peptide sequence containing amino acids 557–576 of PELP1. Western blot analysis of the total lysates from MCF-7 cells and from one of the stable clones showed a band with a molecular mass of about 160 kDa. No such band was observed when preimmune serum from the same rabbit was used in Western blotting (Fig. 6*A*, *right panel*). Also, the observed PELP1 protein band was completely abolished when the serum was preincubated with immunized peptide (Fig. 6*A*, *middle panel*). These results suggested that the antibody specifically recognized PELP1 protein. MCF-7 cell lysates were fractionated into cytosolic and nuclear fraction, and localization of PELP1 was analyzed by Western

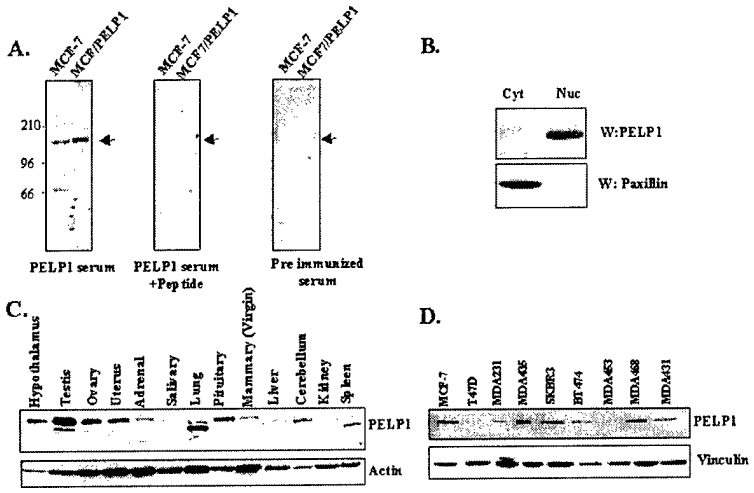

FIG. 6. **Characterization of PELP1 antibody.** *Panel A*, 200 μg of total cell lysate from MCF-7 cells or MCF-7 stable cells expressing PELP1 was Western blotted with 1:500 PELP1 antiserum (*left*), blotted with PELP1 antiserum preadsorbed with peptide (*middle*), and blotted with preimmune serum from the same rabbit (*right*). *Panel B*, localization of PELP1 as analyzed by cellular fractionation. MCF-7 cells were fractionated into nuclear and cytoplasmic fractions, and localization of PELP1 was analyzed by PELP1 antiserum. Paxillin was used as a marker of cytoplasmic fraction. *Panel C*, expression of PELP1 was analyzed in mouse tissue by Western blotting using PELP1 antiserum. *Panel D*, expression of PELP1 in breast cancer cell lines. Blots were stripped and reprobed with vinculin, which was used as a loading control.

blotting. PELP1 is present predominantly in the nuclear fraction, and some staining was also observed in the cytosolic fraction (Fig. 6*B*). We next examined the expression of PELP1 in various mouse tissues using PELP1 antibody. As shown in Fig. 6*C*, the expression of PELP1 could be seen in most of the tissues with the highest expression levels in testis, ovaries, uterus, and pituitary. In some tissues, the antibody also reacted with a second protein band that may represent a degradation product of PELP1 or, alternatively, an isoform of PELP1. PELP1 expression was also observed in several commonly used human breast cancer cell lines (Fig. 6*D*).

PELP1 Localization in Various Murine Tissues—We next examined the localization of PELP1 in various tissues by immunohistochemical staining (Fig. 7). PELP1 staining was seen in all of the tissues examined but was localized differently in each organ. The protein was present in both the nuclei and the cytoplasm in differing degrees depending on the tissue. For example, in pregnant ovaries and fallopian tubes, PELP1 was localized predominantly in the nuclei of cells from the corpus luteum and the epithelium of fallopian tubes, but a considerable level of cytoplasmic staining also occurred in these cells (Fig. 7). In the lung, parts of the epithelial cell nuclei were stained. In the testis, PELP1 was localized in the nuclei.

Developmental Regulation of PELP1 in Mammary Glands—To determine whether PELP1 expression is developmentally regulated in mammary glands, we extracted protein at various stages of mammary gland development and analyzed the expression of PELP1 by Western blot analysis (Fig. 8*A*). PELP1 expression was detected during all stages of mammary gland development but was significantly higher during pregnancy and also significantly lower during lactation than during any other stages of development. The temporal and spatial expression of PELP1 in mammary glands was assessed using immunohistochemistry (Fig. 8, *B–E*), which showed that PELP1 expression was localized predominantly in the nuclei with lesser amounts in the cytoplasm of the ductal and alveolar epithelial cells and in the nuclei of the stromal fat cells. In the pregnant mammary gland, the epithelial cell nuclei showed a much stronger staining compared with other developmental stages (Fig. 8*C*). The specificity of the staining was confirmed by blocking the staining with the epitope-specific peptide. These results confirm that mammary epithelial cells express

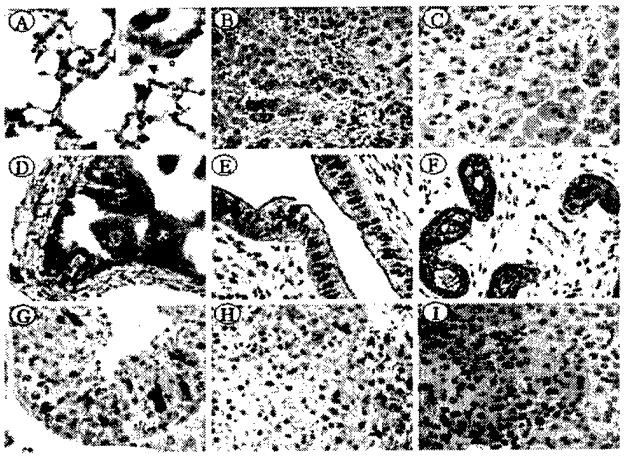

FIG. 7. **Localization of PELP1 in various mouse organs *in vivo*.** Immunohistochemistry shows sections of various murine organs stained with PELP1 antiserum: *panel A*, lung; *panel B*, anterior pituitary; *panel C*, adrenal gland; *panel D*, fallopian tubules; *panel E*, uterus; *panel F*, uterus gland; *panel G*, testis; *panel H*, corpus leuteum; and *panel I*, corpus leutium stained with PELP1 antiserum serum preabsorbed with synthetic peptide as a specificity control.

PELP1 *in vivo* and that its expression is regulated developmentally.

PELP1 Expression and Breast Tumors—Because PELP1 acts as a coactivator of the ER pathway and because the ER pathway has been implicated in breast cancer progression, we hypothesized that PELP1 expression is deregulated in breast cancer. To explore this possibility, we analyzed the level of PELP1 expression in 16 samples of paired normal and breast cancer tumor biopsies. As shown in Fig. 9, normal breast tissue expressed very low levels of PELP1, whereas five of eight breast tumors tested had PELP1 levels 3–5 times those of normal tissue. Although these results suggested that the expression of PELP1 is up-regulated in breast tumors, a larger study is needed to verify these results.

DISCUSSION

We report the cloning and characterization of PELP1, a novel member of the steroid receptor coactivator family. Transient

transfection assays with the ERE-containing reporter genes clearly demonstrated that PELP1 acts as a coactivator of ERα (Fig. 2). Our conclusion that PELP1 is a coactivator of ERα is based on the following observations: 1) Coexpression of PELP1 in the gal4-AF2/gal4-luc reporter assay augmented transcriptional activity of E_2 in HeLa cells; 2) PELP1 augmented the transcriptional activation of ERE-luc reporter by E_2 in a dose-dependent manner in breast cancer MCF-7 cells; 3) PELP1 interacted with endogenous ERα in a ligand-dependent manner in immunoprecipitation assays; 4) PELP1 interacted with the ERα *in vivo*, as determined by confocal microscopy. The expression of PELP1 in mammary glands, its effect on E_2-dependent transcription, and its interaction with ERα suggest that PELP1 is an important component of the ER pathway in mammary epithelial cells.

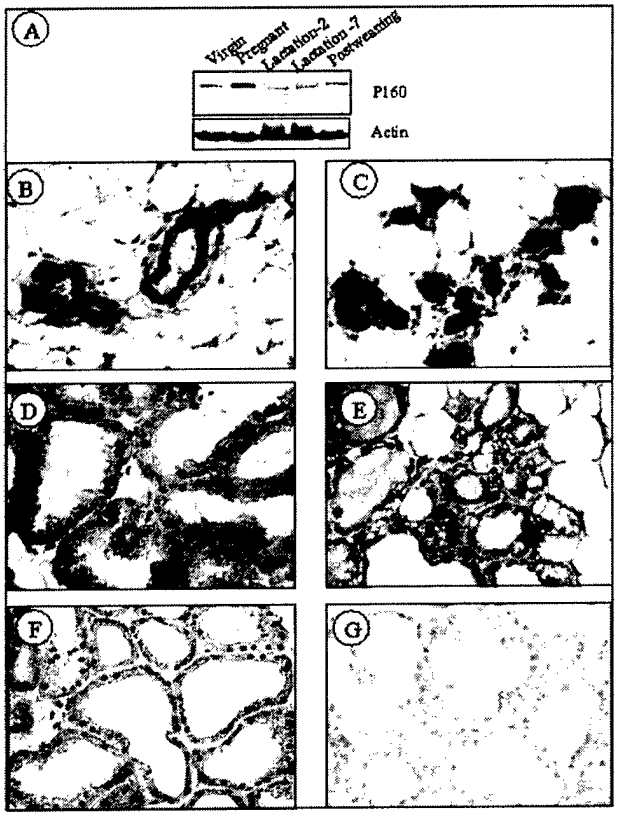

FIG. 8. **PELP1 expression in mammary glands *in vivo*.** Mammary glands were isolated from various developmental stages of murine mammary glands. *Panel A*, Western blot analysis of PELP1 in whole gland tissue lysates. *Panels B–E*, immunohistochemical detection of PELP1 expression in various stages of mammary gland development. Sections were stained with PELP1 antiserum and counterstained with hematoxylin. *Panel B*, virgin; *panel C*, pregnant; *panel D*, lactation; and *panel E*, postweaning. PELP1 expression was localized predominantly in the nuclei with lesser amounts in the cytoplasm of the ductal and alveolar epithelial cells and in the nuclei of the stromal fat cells. In the pregnant mammary gland (*panel C*), the epithelial cell nuclei showed much stronger staining. *Panel F*, staining of a section of lactating mammary gland with PELP1 antibody without hematoxylin counterstaining. *Panel G*, section of lactating mammary gland stained with PELP1 antiserum that was preadsorbed with synthetic peptide and used as a control.

A well studied group of coactivators of ER is the p160 family of coactivators. These coactivators share a common structure frame that includes an N-terminal basic helix-loop-helix domain, a PAS domain, a C-terminal transcriptional activation domain, and a central region containing three LXXLL motifs (29). Among the three known members of the p160 family, 40% similarity at the amino acid level was observed. p160 coactivators also interact with general coactivators such as CBP and p300. Recent evidence suggests that multiprotein complexes, including liganded NR, coregulator, and general transcription machinery, regulate the transcriptional activation by NRs (3, 8, 16). Although PELP1 migrated as a 160-kDa protein and stimulated E_2-mediated transcription, the only similarity between the amino acid sequence of PELP1 and that of p160 coactivators is that both contain LXXLL motifs. PELP1 also lacks the conserved basic helix-loop-helix and PAS domains present in p160 coactivators and therefore represents a novel member of the steroid coregulators. Further, PELP1 showed no intrinsic transcriptional activity when tethered to the gal4 binding domain. Lack of intrinsic transcriptional activity was also observed in some coactivators such as PCAF (31) and TIP60 (32). These results suggest that PELP1 may enhance the transcription by recruiting necessary factors to the liganded ER complex. We are currently investigating the potential PELP1-interacting proteins by the yeast two-hybrid system.

ER transactivation functions are believed to be mediated by the binding of coactivators and by the recruitment of resulting complexes to the promoter (5, 33). The surface of the E_2-dependent AF2 domain consists of a cluster of residues from helices 3, 5, and 12 which form a hydrophobic patch on the surface of liganded LBD (34, 35). The hydrophobic patch on AF2 binds to coactivators such as the p160 family of proteins via their LXXLL motifs. Structural and functional analysis of several coactivators revealed that coactivators interact with ligand-bound AF2 domains via LXXLL motifs, which have been shown to be sufficient in mediating the binding of coactivators to liganded NRs (16). LXXLL motifs are present not only in p160 coactivators, but also in general coactivators including CBP, p300, and P/CAF. Furthermore, corepressor proteins such as RIP140, TIF1, and orphan receptor DAX1 also use

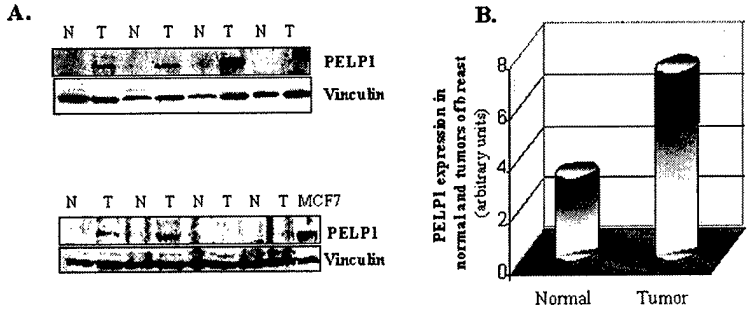

FIG. 9. **PELP1 expression in normal and tumors of breast.** *Panel A*, cell lysates from paired samples of normal breast and breast tumors were analyzed by Western blotting using PELP1 antiserum (*top section*) and subsequently reprobed with vinculin antibody, which served as a loading control (*middle section*). *Panel B*, the average expression of PELP1 in normal breast tissue and breast tumors was quantitated by the Sigma Scan program and is shown in the *bar graph*.

these motifs to interact with NRs (21, 36). The number of LXXLL motifs in the coactivators varies: SRC1, GRIP1, and AIB1 have three such motifs (3), and PELP1 has nine motifs. Similar to SRC1, PELP1 contains two LXXLL motifs that are located in its central region, and the other seven LXXLL motifs are concentrated in the N-terminal region. The N-terminal region containing seven LXXLL motifs alone is sufficient to bind to ERα. We do not know which of the PELP1 seven LXXLL motifs mediate interaction with ERα receptor; deletion studies are in progress to identify the function of each motif. It has been reported that another nuclear receptor coregulator, human RIP140, also contains nine LXXLL motifs. RIP140 is shown to interact with ER and stimulate ER-dependent transcription (12). Recent evidence suggests that RIP140 also function as a corepressor for nuclear orphan receptor TR2 pathways (36, 37). We do not know whether PELP1 has any role in the transcriptional regulation of class II NRs (non-steroidal NR, retinoic acid receptor, retinoid X receptor, and thyroid hormone receptor) or class III NRs (orphan receptors) and are currently planning studies to address these possibilities.

It has been speculated that differential expression of coactivators among tissues contributes at least partly to the different responses elicited by hormones. Coactivators of ERα such as SRC1, GRIP1, and CBP/P300 exhibit ubiquitous expression patterns and are therefore less likely to be involved in tissue-specific actions of ERα. AIB1, a member of the p160 family of coactivators, has been shown to be overexpressed in ER-positive cell lines and breast tumors (38). Recently, coactivators other than those in the p160 family of coactivators were reported to regulate the transactivation potential of ERα. One such coregulator, peroxisome proliferator-activated receptor γ coactivator (PGC-1) is expressed selectively in the brain, heart, kidneys, adipose tissue, and skeletal muscles (22). PELP1 is expressed in high levels in the testes, mammary glands, placenta, and brain and potentially has a role in the NR function in these tissues. Further, developmental regulation of PELP1 in mammary glands may be a reflection of differential response of steroid hormones during development.

The ER signaling pathway has been implicated in the progression of breast cancer tumorigenesis. Coregulators that regulate the activity of ER play a role in tumor progression. AIB1 was shown to be amplified and overexpressed in breast and ovarian cancer (38). In the present study, we observed that PELP1 expression was 3–5 times higher in breast tumors than in normal tissues. PELP1 expression was also observed in several breast cancer cell lines. PELP1 localized to the nuclei regulates ER activation and interacts with general coactivators such as CBP/p300. All of these findings suggest that overexpression of PELP1 may impact the nuclear signaling pathways and modulate the responses of estrogen and anti-estrogens in hormone-dependent cancers.

In summary, we have demonstrated that PELP1 is a ligand-dependent coregulator of estrogen receptor. The primary structure of PELP1 contains several motifs commonly present in the transcriptional regulators including LXXLL motifs, zinc finger, and glutamic- and proline-rich regions. Moreover, PELP1 acts as a coactivator in the ER pathway and is overexpressed in breast cancer.

Acknowledgments—We are grateful to Donald McDonald for ERE-luc, Bert O'Malley and Ming Tsai for SRC1, Michael Stallcup for GRIP, Malcom Parker for gal4-ER-AF2 and GST-AF2 constructs, and Liana Adam and Rozita Bagheri-Yarmand for exploratory studies.

REFERENCES

1. Kliewer, S. A., Lehmann, J. M., and Willson, T. M. (1999) *Science* **284,** 757–760
2. Xu, L., Glass, C. K., and Rosenfeld, M. G. (1999) *Curr. Opin. Genet. Dev.* **9,** 140–147
3. McKenna, N. J., Lanz, R. B., and O'Malley, B. W. (1999) *Endocr. Rev.* **20,** 321–344
4. Tsai, M. J., and O'Malley, B. W. (1994) *Annu. Rev. Biochem.* **63,** 451–486
5. Glass, C. K., Rose, D. W., and Rosenfeld, M. G. (1997) *Curr. Opin. Cell Biol.* **9,** 222–232
6. Ma, H., Hong, H., Huang, S. M., Irvine, R. A., Webb, P., Kushner, P. J., Coetzee, G. A., and Stallcup, M. R. (1999) *Mol. Cell. Biol.* **19,** 6164–6173
7. Torchia, J., Glass, C., and Rosenfeld, M. G. (1998) *Curr. Opin. Cell Biol.* **10,** 373–383
8. Chakravarti, D., LaMorte, V. J., Nelson, M. C., Nakajima, T., Schulman, I. G., Juguilon, H., Montminy, M., and Evans, R. M. (1996) *Nature* **383,** 99–103
9. Wagner, B. L., Norris, J. D., Knotts, T. A., Weigel, N. L., and McDonnell, D. P. (1998) *Mol. Cell. Biol.* **18,** 1369–1378
10. Huang, S. M., and Stallcup, M. R. (2000) *Mol. Cell. Biol.* **20,** 1855–1867
11. Huang, N., Vom, B., Garnier, J. M., Lerouge, T., Vonesch, J. L., Lutz, Y., Chambon, P., and Losson, R. (1998) *EMBO J.* **17,** 3398–3412
12. Cavailles, V., Dauvois, S., L'Horset, F., Lopez, G., Hoare, S., Kushner, P. J., and Parker, M. G. (1995) *EMBO J.* **14,** 3741–3751
13. Heery, D. M., Kalkhoven, E., Hoare, S., and Parker, M. G. (1997) *Nature* **387,** 733–736
14. Spencer, T. E., Jenster, G., Burcin, M. M., Allis, C. D., Zhou, J., Mizzen, C. A., McKenna, N. J., Onate, S. A., Tsai, S. Y., Tsai, M. J., and O'Malley, B. W. (1997) *Nature* **389,** 194–198
15. Nagy, L., Kao, H. Y., Chakravarti, D., Lin, R. J., Hassig, C. A., Ayer, D. E., Schreiber, S. L., and Evans, R. M. (1997) *Cell* **89,** 373–380
16. Glass, C. K., and Rosenfeld, M. G. (2000) *Genes Dev.* **14,** 121–141
17. Couse, J. F., and Korach, K. S. (1999) *Endocr. Rev.* **20,** 358–417
18. Warner, M., Nilsson, S., and Gustafsson, J. A. (1999) *Curr. Opin. Obstet. Gynecol.* **11,** 249–254
19. Kumar, V., Green, S., Stack, G., Berry, M., Jin, J. R., and Chambon, P. (1987) *Cell* **51,** 941–951
20. Dubik, D., and Shiu, R. P. (1988) *J. Biol. Chem.* **263,** 12705–12708
21. Zhang, J., Thomsen, J., Johansson, J., Gustafsson, J., and Treuter, E. (2000) *J. Biol. Chem.* **275,** 39855–39859
22. Tcherepanova, I., Puigserver, P., Norris, J. D., Spiegelman, B. M., and McDonnell, D. P. (2000) *J. Biol. Chem.* **275,** 16302–16308
23. Adam, L., Vadlamudi, R., Kondapaka, S. B., Chernoff, J., Mendelsohn, J., and Kumar, R. (1998) *J. Biol. Chem.* **273,** 28238–28246
24. Joung, I., Strominger, J. L., and Shin, J. (1996) *Proc. Natl. Acad. Sci. U. S. A.* **93,** 5991–5995
25. Adam, L., Vadlamudi, R., Mandal, M., Chernoff, J., and Kumar, R. (2000) *J. Biol. Chem.* **275,** 12041–12050
26. Mazumdar, A., Wang, R. A., Mishra, S. K., Adam, L., Bagheri-Yarmand, R., Mandal, M., Vadlamudi, R. K., and Kumar, R. (2001) *Nat. Cell Biol.* **3,** 30–37
27. Wang, R. A., Nakane, P. K., and Koji, T. (1998) *Biol. Reprod.* **58,** 1250–1256
28. Chelsky, D., Ralph, R., and Jonak, G. (1989) *Mol. Cell. Biol.* **9,** 2487–2492
29. Mermod, N., O'Neill, E. A., Kelly, T. J., and Tjian, R. (1989) *Cell* **58,** 741–753
30. Fan, S., Wang, J., Yuan, R., Ma, Y., Meng, Q., Erdos, M. R., Pestell, R. G., Yuan, F., Auborn, K. J., Goldberg, I. D., and Rosen, E. M. (1999) *Science* **284,** 1354–1356
31. Krumm, A., Madisen L., Yang, X., Goodman, R., Nakatani, Y., and Groudine, M. (1998) *Proc. Natl. Acad. Sci. U. S. A.* **95,** 14501–14506
32. Brady, M. E., Ozanne, D. M., Gaughan, L., Waite, I., Cook, S., Neal, D. E., and Robson, C. N. (1999) *J. Biol. Chem.* **274,** 17599–17604
33. Horwitz, K. B., Jackson, T. A., Bain, D. L., Richer, J. K., Takimoto, G. S., and Tung, L. (1996) *Mol. Endocrinol.* **10,** 1167–1177
34. Feng, W., Ribeiro, R. C., Wagner, R. L., Nguyen, H., Apriletti, J. W., Fletterick, R. J., Baxter, J. D., Kushner, P. J., and West, B. L. (1998) *Science* **280,** 1747–1749
35. Henttu, P. M., Kalkhoven, E., and Parker, M. G. (1997) *Mol. Cell. Biol.* **17,** 1832–1839
36. Lee, C. H., and Wei, L. N. (1999) *J. Biol. Chem.* **274,** 31320–31326
37. Lee, C. H., Chinpaisal, C., and Wei, L. N. (1998) *Mol. Cell. Biol.* **18,** 6745–6755
38. Anzick, S. L., Kononen, J., Walker, R. L., Azorsa, D. O., Tanner, M. M., Guan, X. Y., Sauter, G., Kallioniemi, O. P., Trent, J. M., and Meltzer, P. S. (1997) *Science* **277,** 965–968

Protein Kinases in Mammary Gland Development and Cancer

RAKESH KUMAR* AND RUI-AN WANG

Department of Molecular and Cellular Oncology

The University of Texas M. D. Anderson Cancer Center, Houston, Texas 77030.

KEY WORDS Receptor tyrosine kinases, HER2, heregulin, development, cancer

Running Title: MAMMARY GLAND AND CANCER

*Correspondence to: Rakesh Kumar, Ph.D., The University of Texas M. D. Anderson Cancer Center, Box 108, 1515 Holcombe Blvd, Houston, TX 77030.

Support: National Institutes of Health grants CA65746 and CA90970.

ABSTRACT Protein kinases, the enzymes responsible for phosphorylation of a wide variety of proteins, are the largest class of genes known to regulate growth, development, and neoplastic transformation of mammary gland. Mammary gland growth and maturation consist of a series of highly ordered events involving interactions among several distinct cell types that are regulated by complex interactions among many steroid hormones and growth factors. The mammary gland is one of the few organ systems in mammals that complete their morphologic development postnatally during two discrete physiologic states, puberty and pregnancy. Thus the mammary gland is an excellent model for studying normal development and the early steps of tumor formation. The susceptibility of the mammary gland to tumorigenesis is influenced by its normal development, particularly during stages of puberty and pregnancy. Numerous experimental and epidemiological studies have suggested that specific details in the development of the mammary gland play a critical role in breast cancer risk. Mammary gland development is characterized by dynamic changes in the expression and functions of protein kinases. Perturbations in the regulated expression or function of protein kinases or their associated signaling pathways can lead to malignant transformation of the breast. For example, overexpression of several receptor-tyrosine kinases, including human epidermal growth factor receptor and HER2/c-*neu*, has been shown to contribute to the development of breast cancer. Since receptor-tyrosine kinases regulates several essential processes such as mitogenesis, motility, invasion, cell survival and angiogenesis, targeting receptor-tyrosine kinases may have important implications in designing the strategies against breast cancer.

INTRODUCTION

Breast cancer is the leading type of cancer in women and is the second leading cause of cancer death among women. In the United States in 1998, an estimated 178,700 new cases of breast cancer were expected to be diagnosed, and 43,500 women were expected to die of this disease. Approximately 2,000,000 women have been diagnosed with breast cancer. Breast cancer also occurs in men, although far more rarely than in women; treatment for breast cancer in men is guided by our understanding of the disease in women.

Our limited understanding of the biology and developmental genetics of the normal mammary gland has been a barrier to progress in treating breast cancer. Much of the biological research in the recent past has focused on understanding the initiation and development of the disease. Data from emerging models suggest that we need to better understand crucial signaling components in the normal mammary gland before any beneficial impact on the prevention and treatment of breast cancer can be expected.

In this review, we summarize some of the recent findings about the role, the expression, and biological effects of both tyrosine and serine/threonine protein kinases during development and tumorigenesis of the mammary gland. Because of the nature and depth of the information available on this subject, we could only include representative studies, and we apologize to those whose work could not be covered.

MAMMARY GLAND DEVELOPMENT

Mammary gland growth and maturation consist of a series of highly ordered events involving interactions among several distinct cell types that are regulated by complex interactions among many steroid hormones and growth factors. In 4-week-old mice, the mammary glands become increasingly sensitized to elevations in ovarian hormones, which signal the terminal end buds (club-shaped epithelial structures) to grow away from the nipple region to fill the fat pad. During this rapid but

tightly regulated growth phase, an extensive network of epithelial ductal tree-like branching develops. When the expanding mammary ductal mass reaches the limits of its fat pad, the terminal end bud structures are permanently replaced by mitotically quiescent terminal end ducts and alveolar buds. At the onset of pregnancy, rapid epithelial cell proliferation begins again, resulting in additional ductal branching and lobuloalveolar growth from the ductal skeleton. These alveoli are the functional units of milk production at lactation, the time at which the gland is fully differentiated (Fig.1). After lactation ceases, the gland undergoes massive restructuring and apoptosis, leading to involution and return of the primary ductal structures (Nandi, 1959; Daniels et al., 1987; Medina, 1996).

A balance between cell proliferation, cell differentiation, and cell death in the stem cell population and throughout the mammary gland is critical for normal development. In contrast, perturbations in this balance can contribute to cancer development. Conditions that upregulate cell proliferation or downregulate apoptosis can allow accumulation of mutations that contribute to the subsequent development of breast cancer. It is not clear, however, how normal mechanisms and signaling pathways controlling growth and apoptosis in the human breast act in tumor development, in protection from tumor development or in tumor dissemination.

MAMMARY GLAND CARCINOGENESIS

Epidemiologic studies have suggested that specific details in the development of the mammary gland play a critical role in breast cancer risk (Kelsy and Gammon, 1997; Anderson et al., 1997). Some of the risk factors for breast cancer include nulliparity or first full-term pregnancy after age 30, early menarche, late menopause and a family history of breast cancer (Rondinelli et al., 1995; Russo and Russo, 1980). In contrast, early parity, late menarche, early menopause, and long periods of lactation provide a protective effect against breast cancer (Russo and Russo, 1982; Henderson et al., 1993). Therefore, systemic endocrine patterns and reproductive changes occurring in the human breast have important implications for breast cancer. The observation that the same endocrine events control

mammary development and influence breast-cancer risk strengthens the hypothesis that mammary gland development and carcinogenesis are fundamentally linked. For example, exposure of early-stage rat mammary glands to carcinogens resulted in significant mutations associated with malignant transformation and increased the susceptibility to tumor formation. Although these hormonal risk factors provide clues for target cell predisposition to breast cancer, the underlying mechanisms, including the role of signaling pathways, remain poorly understood.

The susceptibility of the mammary gland to tumorigenesis is influenced by its normal development, particularly during puberty and pregnancy stages that are characterized by marked alterations in cell proliferation and differentiation. The nature of these changes suggests that tumorigenesis is closely related to normal developmental pathways in the breast (Russo and Russo, 1982; Henderson et al., 1993). Thus, understanding the mechanisms by which reproductive events regulate breast cancer development will require a better understanding of the genes that control mammary proliferation and motility. Protein kinases that function by phosphorylation of a wide variety of proteins, are the largest class of genes known to regulate the normal development and neoplastic transformation of mammary gland. Protein kinases are grouped into two categories- tyrosine kinase and serine/threonine kinases. Depending on the subcellular localization, protein kinases are also divided into receptor and non-receptor kinases. About forty protein kinases have been found to be expressed in mammary glands (Table 1).

THE HUMAN EGF RECEPTOR FAMILY IN BREAST CANCER

Growth factors are secreted polypeptides that regulate the growth of both normal and neoplastic cells. Proto-oncogenes are a group of normal genes that play important roles in the regulation of cell proliferation. Evidence that the gene products of several activated proto-oncogenes are either growth factor receptors or growth factors initially suggested a possible link between proto-oncogenes and growth factors (Ullrich and Schlessinger, 1990). Recent studies have established an essential role of

growth factors and their receptors in the regulation of proliferation of mammary epithelial and cancer cells.

Currently, the EGF family of growth factors consists of seven members- EGF, transforming growth factor-α (TGF-α), heparin-binding EGF-like growth factor (HB-EGF), amphiregulin (AR), betacellulin (BTC), epiregulin (ER) and heregulins (HRG) (Peles and Yarden, 1993; Riese and Stern, 1998). The EGF family of ligands binds to transmembrane receptor tyrosine kinases, commonly known as HER receptors (**H**uman **E**pidermal growth factor **R**eceptor) (Klapper et al., 2000; Olayioye et al., 2000; Mendelsohn and Baselga, 2000). The HER family consists of four distinct members, including the EGF receptor (also known as HER1), HER2 (also known as c-*erbB*-2 or c-*neu*), HER3, and HER4. These receptors are composed of an extracellular binding domain, a transmembrane lipophilic segment, and an intracellular protein tyrosine kinase domain with a regulatory carboxy terminal segment, with the only exception of HER3, which has a deficient tyrosine kinase domain. All of these receptors share sequence homology with the tyrosine kinase domain of EGF receptor (Hynes and Stern, 1994). Binding of ligand to the HER receptor triggers the formation of homo- or hetero-dimeriztion of HER members leading to receptor autophophorylation, recruitment of adaptor molecules, and activation of signal transduction pathways leading to gene expression and different phenotypic changes (Graus-Porta et al., 1997). Aberrant expression and activation of EGFR is observed in various human tumors. HER2 has been shown to be overexpressed, amplified, or both, in a number of human malignancies, including breast and ovarian cancers (Pinkas-Kramarski et al., 1997; Alroy and Yarden, 1997). Over expression of the HER receptors has been shown to be closely associated with an increased progression and metastasis, an aggressive clinical course, and decreased disease-free survival cancer patients. Over expression of some growth factor receptors has been shown to induce transformed properties in the recipient cells (Riedel et al., 1998; Zhang et al., 1996), possibly because of excessive activation of signal transduction pathways.

The regulation of HER family members by the EGF family of ligands is complex, as binding of ligands to these receptors can lead to the formation of multiple distinct homo or heterodimers among the HER receptors and thus presumably, engagement of distinct signaling pathways. In addition to dimerization, ensuing receptor trans-autophosphorylation results in the dissociation of the original (primary) receptor dimer and phosphorylated receptor monomer then interacts with a new (nonphosphorylated) receptor to form a secondary dimer. Treatment of cells with EGF yields HER2-HER3 secondary dimers, and HRG treatment induces the formation of HER3-EGFR (secondary) dimers (Gamet et al., 1997). It has been proposed that such signaling through various combinations of HER receptors may be responsible for distinct biological functions (Alroy and Yarden, 1997). HER3 is unique among the HER family members, as it has an impaired tyrosine kinase domain due to substitution of three amino acids in the kinase domain (Guy et al., 1994). Despite the lack of kinase activity of HER3, ligand binding to HER3 leads to increased HER3 tyrosine phosphorylation, probably due to formation of a high-affinity co-receptor complex through heterodimeric interaction with HER2 (Horan et al., 1995). It is believed that among HER family, the HER2/HER3 dimer complex elicits the most potent mitogenic signal (Alimandi et al., 1995; Pinkas-Kramarski et al., 1996). This may be related to the fact that the carboxy-terminal phosphorylation domain of HER3 contains several consensus sites for the binding of signal-transducing proteins implicated in mitogenic signaling, including phosphatidylinositol 3-kinase (PI 3-kinase) (Prigent and Gullick, 1994; Alimandi et al., 1995; Pinkas-Kramarski et al., 1996). A ligand that interacts with HER2 in the absence of other HER family members has yet to be identified. The ligands for HER family receptors are summarized in table 2, and the variety of dimerization among HER family members elicited by specific ligands is depicted in Fig2.

The dimerization and activation of HER receptors result in the phosphorylation of tyrosine residues, and provides docking sites for intracellular molecules that possess Src homology 2 (SH2) or phosphotyrosine (PTB) binding domains (Heldin, 1995; Weiss AND Schlessinger, 1998; Shoelson

1997; Sudol, 1998). These proteins includes kinases such as Src, Chk, PI-3K as well as adaptor proteins such as Shc, Crk, Grb2, Grb7 and Gab1. There is a large scale of overlap among the pathways activated by the four HERs, leading to activation of MAP kinase pathway via the coupling of Shc or Grb2. However, there is also a preferential modulation of specific pathways (Olayioye et al., 2000). For example, among the HER family members, HER3 is the most efficient activator of PI-3 kinase pathway due to presence of multiple binding sites for p85 on HER3 (Prigent and Gullick, 1994). In general, the multiple choices of ligand combinations and different dimerization offer a wide range of signaling options to regulate phenotypic changes in cancer cells.

HER FAMILY LIGANDS IN MAMMARY GLAND TUMORIGENESIS

Perturbations in the regulated expression or function of protein kinases or their associated signaling pathways can lead to malignant transformation of the breast. For example, overexpression of several tyrosine kinases have been shown to contribute to the development of breast cancer in both humans and animal model systems. These kinases are human epidermal growth factor receptor, and HER2/c-*neu*. Similarly, the ligands for protein kinases, including EGF, TGF-alpha, amphiregulin, cripto, and HRG, play important roles in normal ductal and alveolar development as well as in transformation of the mammary gland (Colemen et al., 1990; Vonderhaar, 1987; Kenney et al., 1995).

Growth and morphogenesis of the mammary gland are driven not only by an intrinsic genetic program but also by signals or growth factors provided by neighboring cells and tissues. Like many other organs, the normal development of mammary gland also depends on the epithelium and mesenchyme/stromal interaction and also the interaction within the epithelium. Heregulin (HRG) is a combinatorial ligand for HER-3 and -4 and transactivates HER2 and EGF receptors. HRG is expressed within the mammary mesenchyme adjacent to lobuloalveolar structures. HRG expression is regulated during mammary gland development and is maximally expressed during pregnancy and early lactation (Schroeder and Lee, 1998; Jones et al., 1996). In breast tumor cells, HRG seems to have a mitogenic

effect and induces differentiation and the synthesis of milk proteins. HRG induces in vivo proliferation and differentiation of normal mammary epithelium into secretory lobuloalveoli (Jones et al., 1996). Furthermore, targeted expression of a HRG transgene resulted in persistence of terminal end buds and late development of mammary adenocarcinomas, suggesting that HRG may inhibit signals that normally lead to terminal differentiation (Krane and Leder, 1996; Neimann et al., 1998). HRG also mediates the proliferative effects of progestins in mouse mammary adenocarcinomas (Balana et al., 1999). Finally, accumulating evidence suggests that the HRG promote cell motility, invasiveness and the development of more aggressive phenotype in mammary cancer cells (Adam et al., 1998; Adam et al., 2000; Vadlamudi et al., 1999a,b; Vadlamudi et al., 2000).

PROTEIN KINASES IN MAMMARY GLAND DEVELOPMENT AND CANCER

I. RECEPTOR TYROSINE KINASES

One of the most powerful tools to ascertain about the role of a given protein is the development of a knockout mouse. In this context, deletion of HER family of receptors has been shown to be lethal due to early embryonic defects in heart and brain development in knockout mice (Lee et al., 1995; Gassmann et al., 1995; Riethmacher et al., 1995; Erickson et al., 1997). Therefore, our current understanding of the roles of HER family members in the mammary gland comes from cell culture and transgenic models.

EGFR is found to be essential for the ductal morphogenesis of the mammary gland. Expression of EGFR was found to be throughout all the developmental stages and preferentially, in the ductal epithelium (Shroeder and Lee, 1998). In the *wa-2* mice that harbor a point mutation in the kinase domain of EGFR, the mammary gland was very sparsely developed (Fowler et al., 1995). Furthermore, overexpression of a kinase-inactive form of EGFR under the control of the MMTV promoter in the murine mammary gland also resulted in a retarded ductal development during puberty, but lobuloalveolar development was not affected (Xie et al., 1997). An EGFR ligand knockout mice study

also revealed a role for EGFR in mammary gland development during ductal development. Of the three EGFR specific ligands, EGF, AR and TGFα, AR is preferentially expressed in the epithelium of developing ducts. Targeted disruption of AR but not EGF and TGFα, resulted in an impaired ductal growth without any affect on lobular alveolar development. Complete disruption of all these three ligands, however, abrogated the lactogenesis (Luetteke et al., 1999). In brief, AR plays an essential role in the action of EGFR during ductal development of mammary glands, while TGFα and EGF are functionally redundant but required for the fully normal development of mammary gland.

HER2 plays an essential role in normal mammary gland development, particularly, during alveolar morphogenesis. In addition, overexpression of the activated hybrid receptor containing the intracellular domain of HER2 can also induce alveolar morphogenesis in the absence of growth factors (Niemann et al., 1998). In accordance, transgenic mice expressing dominant negative HER2 failed to develop functional alveoli, while ductual branching was not affected (Jones and Stern, 1999).

The roles of HER3 and HER4 in mammary gland development appear to be mainly related to lobuloalveolar morphogenesis. This may be related to the fact that HRG, the primary ligand for these receptors, is expressed during pregnancy and early lactation phase when lobuloalveolar morphogenesis takes place (Yang et al., 1995). This observation also derives support from in vitro studies showing the effectiveness of HRG antisense oligonucleotides in blocking lobuloalveolar but not ductal morphogenesis in an organ culture model (Yang et al., 1995). Also, planting slow HRG-releasing beads in the mammary fat pads induces lobuloalveolar development of the mammary glands (Jones et al., 1996). The heterodimerization between HER3 and HER2 seems to be important in inducing lobuloalveolar development. The homodimerization of HER2 achieved by blocking HER3 with specific antibody only induces cell proliferation, but not morphogenesis, in the cultured HB2 human mammary epithelial cells (Baeckstrom et al., 2000). HER4 mainly acts as a differentiation factor. The expression of HER4 is elevated in the mature female mice (Shroeder and Lee, 1998; Darcy et al.,

2000). During pregnancy, HER4 is expressed but not activated till late when differentiation and secretory activity predominate over proliferation. HER4 activity peaked at lactation, when mammary glands undergo terminal differentiation (Schroeder and Lee, 1998). In transgenic mice with alveoli expressing the dominant negative HER4, the mammary glands were condensed and lacked normal lumenal lactation products. The whey acidic protein, and α–lactalbumin protein but not the β-casein production were much reduced in these alveoli (Jones et al., 1999). The phosphorylation of Stat5a, which is critical for the functional differentiation of mammary gland (Liu et al., 1996, 1997; Hennighausen et al., 1997) was markedly reduced in these alveoli.

Met is the receptor for hepatocyte growth factor/scatter factor (HGF/SF). The function of Met has been linked with the cell mitogenic response, cell motility and the promotion of ordered spatial arrangement of tissue. In a cultured human breast cancer cell line, Met was seen to be expressed in cells bordering lumen-like structures that resemble ducts. Met expression has also been reported in the normal human mammary ductal cells (Niemann et al., 1992). The mRNA expression of both Met and its ligand HGF are progressively reduced during pregnancy, are virtually undetectable during lactation, and increase during the phase of involution to prepregnancy levels (Soriano et al., 1998). The reduction in HGF and Met expression corresponds to periods in which functions other than tubulogenesis predominate in the mammary gland, namely alveologenesis (mid to late pregnancy) and milk protein synthesis (lactation). Moreover, adding of prolactin significantly reduce the level of Met mRNA in the cultured murine mammary epithelial cells. In vitro cell culture analysis also established the role of Met in inducing the morphogenic process of mammary glands (Yang et al., 1995). EpH4 mouse mammary epithelial cells cultured in matrigel form branched tubules in the presence of hepatocyte growth factor/scatter factor (HGF/SF), the ligand of Met. The branch induced by HGF was abrogated by the PI3 kinase inhibitor wortmannin and LY294002 (Nieman et al., 1998). This effect can also be evoked by transfection of a Met specific substrate, Gab1, which can activate the PI3 kinase pathway. These

studies suggested that Met is required for the development of ductal networks in the mammary glands. In breast cancer, both hepatocyte growth factor and Met have been reported to have an elevated level of expression and their expression level had a close relation with the rapid progression, more frequent recurrence and poor prognosis (Yamashita et al., 1994; Beviglia et al., 1997; Ghoussoub et al., 1998; Edakuni et al., 2001)

Ron, a member of the Met family, is the receptor for the macrophage stimulating factor/Scatter factor II. In normal mammary tissue, Ron is at a barely detectable level (Maggiora et al., 1998), and there is no study yet reported about its role in the normal development of mammary gland. Activation of Ron in vitro promoted the proliferation, migration and tubulogenesis of cultured MDCK canine kidney cells and can not transform the NIH3T3 fibroblast cells (Santoro et al., 1996). Ron was reported to be overexpressed in more than 50% of the breast cancers. And activation of Ron in cultured breast cancer cells ZR75 caused increased proliferation, migration and invasive (Maggiora et al., 1998).

DDR1 (Discoidin domain receptor 1) is the receptor for several types of collagen, and it is also a member of RTK family. A recent DDR1-gene knockout study revealed the essential role of this receptor kinase and also its ligand, the collagens in mammary gland development. The DDR1 binding sites were found in the ducts, but the most striking phenomena was the retarded lobuloalveolar development and impaired lactogenesis. (Vogel et al., 2001).

II. NON-RECEPTOR TYROSINE KINASES

Janus kinases (Jak) are non-receptor tyrosine kinases, and play an important figure in the pathway for the functional differentiation of mammary gland. Upon binding with the ligand, prolactin receptor phosphorylate and activate Jak2 which in turn phophosrylate transcription factors such as Stat5a, which then translocate to nucleus and activate genes for lactation such as β-casein and whey acidic protein (WAP) (Hennighausen et al., 1997). Recently studies have shown that Jaks also

phosphorylate the kinase domain of non-activated HER2, the physiological significance of which remains to be established.

Etk/Bmx, a member of the Tec family of nonreceptor protein-tyrosine kinases, is characterized by an N-terminal pleckstrin homology domain and has been shown to be a downstream effector of phosphatiylinositol-3 kinase. The expression of wild-type Etk in a non-invasive human breast cancer MCF-7 cells significantly increased proliferation and anchorage-independent growth of epithelial cancer cells. Conversely, expression of kinase-inactive mutant Etk-KQ suppressed the proliferation, anchorage-independent growth, and tumorigenicity of human breast cancer MDA-MB435 cells (Bagheri-Yarmand et al., 2001). So far, there is no study reported on the in vivo study of Etk and breast cancer.

III. SERINE/THREONINE KINASES

TGF-beta receptors are serine/threonine kinases, including type I and type II receptor. Upon binding with their ligands, type I and type II receptors form heterodimers which then autophosphorylate serine and threonine residues. The downstream signaling molecules are mainly members of Smad family. After activation, TGF-beta1 receptors phosphorylate Smad 1-3, depending on the organ and tissue, which then recruits Smad4, and then the complex translocates to the nucleus where it regulates transcriptional activity of a specific set of genes. There are also inhibitory Smads, namely Smad6 and 7, which inhibits the translocation of Smads from cytoplasm to nucleus, conferring to this system a fine tuning knob. Besides this main Smad pathway, TGF-beta can also activate the mitogen-activated protein kinase (MAPK) pathway, and the different biological responses to TGF-beta, which depend to varying degrees on activation of either or both of these two pathways (Wakefield et al., 2001).

Several known members of the TGF-beta receptor superfamily like TβRI and TβII, ActRI and ActRII, as well as a variety of ligands were found to be expressed in regulated pattern in the mammary

glands. These include TGFβ 1, 2, and 3; activin, inhibin, and BMP4. In general, the role of this system is to exert an inhibitory effect on both growth and differentiation, provide a balance to other growth and/or differentiation stimulating systems as described above. Experiments have shown that overexpression of TGFβ transgenes during puberty reduces the rate of growth of the ductal tree and simplifies the pattern of arborization, while expression during pregnancy also interferes with lactation. It is recently shown that TGFβ-3 is critical for inducing apoptosis in the onset of involution (Nguyen and Pollard, 2000). Expression studies in the normal mouse gland indicate that TGFβ is synthesized in the mammary epithelium, with the three isoforms showing somewhat different spatial and temporal distributions. Exogenous TGFβ applied directly to the gland in situ inhibits epithelial cell division within hours, and strongly stimulates extracellular matrix synthesis over a longer time course. The down stream signaling pathway of the TGFβ system functions in mammary gland, but is not yet well documented. So far, there is no report on Smad expression in the mammary glands, and the significance of the cross-talk between TGFβ receptor—Smad and Ras—MAPK pathway in also largely unknown.

Akt, also known as PKB (protein kinase B), is a key figure in cell survival. In addition to Akt, two other members of the Akt family, Akt2 and Akt3.have also been identified. The three members of this family are all serine/threonine protein kinases that share similar structural features including a pleckstrin homology (PH) domain and two threonine and serine phosphorylation sites (Marte and Downward, 1997). The activation of Akt is PI-3 kinase dependent. Activated Akt inhibits cell apoptosis by phosphorylation and inactivation of fork-head transcription factor (FKHR) (Brunet et al., 1999; Tang et al., 1999). The function of Akt in mammary gland development seems to be that of supportive for the cell survival. Akt expression is elevated in late pregnancy and lactation (Chodosh et al., 2000), a period when there is almost no mammary epithelial cell apoptosis. In early involution, when massive mammary epithelial cell apoptosis occurs, the expression of Akt decreases (Chodosh et

al., 2000; Schwertfeger et al., 2001). In transgenic mammary overexpressing Akt driven by an MMTV promoter, the involution process slowed down and apoptosis was markedly reduced at the initial stage (Schwertfeger et al., 2001).

A recent report of transgenic mice study revealed the involvement of Akt in the mammary gland tumorigenesis. Mammary epithelium-specific expression of polyoma virus middle T antigen resulted in a rapid development of multifocal metastatic mammary tumors, whereas transgenic mice expressing a mutant middle T antigen decoupled from the PI-3 kinase develop extensive hyperplasias that are highly apoptotic. Expression of constitutive active Akt interferes with normal mammary gland involution, but tumors were not developed However, coexpression of constitutive active Akt with mutant middle T antigen resulted in a dramatic acceleration of mammary tumorigenesis correlated with reduced apoptotic cell death. Moreover, coexpression of active Akt with mutant middle T resulted in phosphorylation of FKHR and translational upregulation of cyclin D1 levels. These observations indicate that activation of Akt can contribute to tumor progression by providing an important cell survival signal (Hutchinson et al., 2001).

Cyclin dependent kinases (CDK) are a family of serine/threonine kinases that play important roles in controlling cell cycle progression. There are at least nine CDKs (CDK1-9) identified, they associate with around twenty cylin cofactors (Cyclin A to T) in different combinations to regulate the progression of cell cycle (Senderowicz, 2000). Though a large amount of data has accumulated on CDK's relation with tumorigenesis, little is known about their role in normal mammary gland development. Indeed, some cyclins, such as cyclin A and cyclin D1 expression in mammary glands were found to be developmentally regulated, i.e., they have an highly elevated level of expression in early pregnancy, corresponding to the high mitotic rate at the time. Overexpression of cyclin A in the mammary glands of transgenic mice results in the induction of nuclear abnormalities and increased apoptosis (Bortner and Rosenberg, 1995). Deletion of cyclin D1 caused impairment of lobular alveolar development during pregnancy (Sicinski et al., 1995; Fantl et al., 1995), and this phenotype can be

rescued by getting rid of the cell cycle inhibitor $p27^{kip1}$ simultaneously (Geng et al., 2001). Over expression of either cyclin D1 or E in mice mammary gland both induced hyperplasia and carcinomas (Wang et al, 1994; Bortner and Rosenberg, 1997). In breast cancer patients, it is reported that most of the cases have an overexpression of cyclin D1 (Barnes and Gillet, 1998). Consequently, knocking out of cyclin D1 was found to confer the mice resistance to stimulation of HER2 and Ras, but not c-myc and Wnt-1 (Yu et al., 2001).

P21-activated kinase 1 (Pak1) is an intracellular serine/threonine kinase that works downstream of PI-3 kinase and Akt. The function of Pak1 is primarily linked with cell skeleton organization. Recent studies showed that breast cancer has elevated Pak1 expression and activity level that has a positive correlation with the advances of the cancer (Fig. 2) (Vadlamudi et al., 2000). It was demonstrated that in cultured breast cancer cells, up-regulation of Pak1 activity by growth factor potentates cell skeleton reorganization and increased cell migration. Overexpression of constitutively active Pak1 promotes the anchorage independent growth of the MCF-7 breast cancer cells. In addition, Pak1 mediated the effect of VEGF in promoting angiogenesis, which is also critical for the survival and growth of cancer cells (Vadlamudi et al., 2000).

Hunk (Hormone upregulated and neu-associated kinase) is a recently identified serine/threonine kinase in the mammary gland. During postnatal mammary development, Hunk mRNA expression is restricted to a subset of mammary epithelial cells and is temporally regulated with highest levels of expression occurring during early pregnancy. In addition, treatment of mice with 17 beta-estradiol and progesterone results in the rapid and synergistic upregulation of Hunk expression in a subset of mammary epithelial cells, suggesting that expression of this kinase is regulated by ovarian hormones. . Consistent with the tightly regulated pattern of Hunk expression during pregnancy, mammary glands from transgenic mice which overexpress Hunk in the mammary epithelium manifest temporally distinct defects in epithelial proliferation and differentiation during pregnancy, and fail to undergo normal lobuloalveolar development. It seems that Hunk may contribute to changes in the mammary

gland that occur during pregnancy in response to ovarian hormones (Gardner et al., 2000a). The role of Hunk in mammary carcinogenesis has not been reported yet.

Pnck (Pregnancy upregulated non-ubiquitous CaM kinase) is a another newly identified serine/threonine kinase from the muirne mammary gland. Pnck is temporally regulated during murine mammary development with highest levels of expression observed late in pregnancy, concomitant with decreased cellular proliferation and terminal differentiation of the mammary epithelium. Consistently, Pnck is up-regulated in confluent mammary epithelial cells and is down-regulated as serum-starved cells are stimulated to reenter the cell cycle. The expression of Pnck in mammary gland is epithelial cell specific and heterogeneous. Expression of Pnck is restricted to a subset of human breast cancer cell lines as well as the epithelial tumor cell lines which are raised from transgenic mice. Moreover, Pnck was found to be highly overexpressed in a subset of human primary breast cancers compared with benign mammary tissue. Gardner et al suggest that Pnck may play a role in mammary development, and that expression of this kinase may be restricted to a mammary epithelial cell type that is transformed in a subset of human breast cancers (Gardner HP et al., 2000b).

CONCLUSIONS

Normal mammary gland development is regulated by a very fine balance between cell proliferation, cell differentiation, and cell death in the stem cell population, and deregulation of this balance leads to cancer development. When deregulated, cellular pathways that promote cell growth and survival leads to the subsequent development of breast cancer. It remains to be fully understood why normal mechanisms and signaling pathways become deregulated in the mammary gland and how many of these pathways are required for development of breast cancer. Accumulating data support an important role of HER family members in epithelial cell signaling and functions, including mitogenesis, motility and invasion, angiogenesis in normal mammary gland development. Similarly, a wealth of information is now available about the involvement of cytoplasmic kinases that also

transduce signals from receptor-tyrosine kinases to the nucleus, in the development and maintenance of malignant phenotypes in breast cancer. It is increasingly accepted that deregulation of receptor-generated signals involving phosphorylation-triggered cascades may promote non-attenuation of target genes in the nucleus, and thus, contribute to the mammary gland tumorigenesis. However, very little is known about the nature of physiological substrates of these kinases, and how exactly these activated substrates participates in the regulation of cellular processes in mammary gland. An important area that needs extensive study is the potential mechanistic roles of protein kinases and their substrates during the process of carcinogenesis in mammary gland. In addition, we do not know why at certain stages of development, mammary gland acquire an enhanced susceptibility to carcinogenesis. It is expected that with the recent technologic advances in transgenic and knockout methodology and ready availability of phospho-specific antibodies against signaling components, we should be able to gain further insights about the roles of protein kinases in mammary gland development and cancer.

ACKNOWLEDGEMENTS

Research in authors laboratories is supported by the National Institutes of Health grants CA65746 and CA 80066.

REFERENCES

Adam L, Vadlamudi R, Kondapaka SB, Chernoff J, Mendelsohn J, Kumar R. 1998. Heregulin Regulates Cytoskeletal Reorganization and Cell Migration through the p21-activated Kinase-1 via Phosphatidylinositol-3 Kinase. J Biol Chem 273: 28238-28246.

Adam L, Vadlamudi R, Mandal M, Chernoff J, Kumar R. 2000. Regulation of Microfilament Reorganization and Invasiveness of Breast Cancer Cells by p21-activated Kinase-1 K299R. J Biol Chem 275:12041-12050.

Alroy I, Yarden Y. 1997. The ErbB signaling network in embryogenesis and oncogenesis: signal diversification through combinatorial ligand-receptor interactions. FEBS Lett 410: 83-86.

Alimandi M, Romano A, Curia MC, Muraro R, Fedi P, Aaronson SA, Di Fiore PP, Kraus MH. 1995. Cooperative signaling of ErbB3 and ErbB2 in neoplastic transformation and human mammary carcinomas. Oncogene 10:1813-1821.

Anderson E, Clarke RB, Howell A. 1997. Changes in the normal human breast throughout the menstrual cycle: relevance to breast carcinogenesis. Endocrine-Related Cancer 4: 23-33.

Bagheri-Yarmand R, Mandal M, Taludker AH, Wang RA, Vadlamudi RK, Kung HJ, Kumar R. 2001. Etk/bmx tyrosine kinase activates pak1 and regulates tumorigenicity of breast cancer cells. J Biol Chem 276: 29403-29409.

Balana ME, Lupu R, Labriola L, Charreau EH, Elizalde PV. 1999. Interactions between progestins and heregulin (HRG) signaling pathways: HRG acts as mediator of progestins proliferative effects in mouse mammary adenocarcinomas. Oncogene 18: 6370-6379.

Barnes DM, Gillet CE. 1998. Cyclin D1 in breast cancer. Breast Cancer Res Treat 52:1-15.

Beviglia L, Matsumoto K, Lin CS, Ziober BL, Kramer RH.1997. Expression of the c-Met/HGF receptor in human breast carcinoma: correlation with tumor progression. Int J Cancer 74:301-309.

Bortner DM, Rosenberg MP. 1995. Overexpression of cyclin A in the mammary glands of transgenic mice results in the induction of nuclear abnormalities and increased apoptosis. Cell Growth Differ 6:1579-1589.

Bortner DM, Rosenberg MP. 1997. Induction of mammary gland hyperplasia and carcinomas in transgenic mice expressing human cyclin E. Mol Cell Biol 17: 453-459.

Brunet A, Bonni A, Zigmond MJ, Lin MZ, Juo P, Hu LS, Anderson MJ, Arden KC, Blenis J, Greenberg ME. 1999. Akt promotes cell survival by phosphorylating and inhibiting a Forkhead transcription factor. Cell 96: 857-68.

Colemen S, Silberstein GB, Daniel CW. 1990. Ductal morphogenesis in the mouse mammary gland: evidence supporting a role for EGF. Dev Biol 127:304-315.

Chodosh LA, Gardner HP, Rajan JV, Stairs DB, Marquis ST, Leder PA. 2000. Protein kinase expression during murine mammary development. Dev Biol 219: 259-276.

Daniels CW, Siberstein GB. 1987. Postnatal development of the rodent mammary gland. In M.C. Neville and CW. Daniels (eds.), The mammary gland: development, regulation, and function. New York, Plenum Publishing Corp. pp3-36.

Darcy KM, Zangani D, Wohlhueter AL, Huang RY, Vaughan MM, Russell JA, Ip MM. 2000. Changes in ErbB2 (her-2/neu), ErbB3, and ErbB4 during growth,

differentiation, and apoptosis of normal rat mammary epithelial cells. J Histochem Cytochem 48:63-80.

Edakuni G, Sasatomi E, Satoh T, Tokunaga O, Miyazaki K. 2001.Expression of the hepatocyte growth factor/c-Met pathway is increased at the cancer front in breast carcinoma. Pathol Int 51:172-178.

Erickson SL, O'Shea KS, Ghaboosi N, Loverro L, Frantz G, Bauer M, Lu LH, Moore MW. 1997. ErbB3 is required for normal cerebellar and cardiac development: a comparison with ErbB2-and heregulin-deficient mice. Development 124: 4999-5011.

Fantl V, Stamp G, Andrews A, Rosewell I, Dickson C.1995. Mice lacking cyclin D1 are small and show defects in eye and mammary gland development. Genes Dev 9:2364-2372.

Gamett DC, Pearson G, Cerione RA Friedberg I. 1997. Secondary Dimerization between Members of the Epidermal Growth Factor Receptor Family. J Biol Chem 272:12052-12056.

Gardner HP, Belka GK, Wertheim GB, Hartman JL, Ha SI, Gimotty PA, Marquis ST, Chodosh LA. 2000a. Developmental role of the SNF1-related kinase Hunk in pregnancy-induced changes in the mammary gland. Development 127: 4493-4509.

Gardner HP, Ha SI, Reynolds C, Chodosh LA. 2000b. The caM kinase, Pnck, is spatially and temporally regulated during murine mammary gland development and may identify an epithelial cell subtype involved in breast cancer. Cancer Res. 60: 5571-5577.

Gassmann M, Casagranda F, Orioli D, Simon H, Lai C, Klein R, Lemke G. 1995. Aberrant neural and cardiac development in mice lacking the ErbB4 neuregulin receptor. Nature 378: 390-394.

Geng Y, Yu Q, Sicinska E, Das M, Bronson RT, Sicinski P. 2001. Deletion of the p27Kip1 gene restores normal development in cyclin D1-deficient mice. PNAS 98:194-199.

Ghoussoub RA, Dillon DA, D'Aquila T, Rimm EB, Fearon ER, Rimm DL. 1998.Expression of c-met is a strong independent prognostic factor in breast carcinoma. Cancer 82:1513-1520.

Graus-Porta D, Beerli RR, Daly JM, Hynes NE. 1997. ErbB-2, the preferred heterodimerization partner of all ErbB receptors, is a mediator of lateral signaling. EMBO J 16:1647-1655.

Guy PM, Platko JV, Cantley LC, Cerione RA, Carraway KL 3rd.1994. Insect cell-expressed p180erbB3 possesses an impaired tyrosine kinase activity. Proc Natl Aca Sci USA 91:8132-8136.

Heldin CH. 1995. Dimerization of cell surface receptors in signal transduction. Cell 80:213-223.

Henderson BE, Ross RK, Pike MC. 1993. Hormonal chemoprevention of cancer in women. Science 259: 633-638.

Hennighausen L, Robinson GW, Wagner KU, Liu X. 1997.Developing a mammary gland is a stat affair. J Mammary Gland Biol Neoplasia 2:365-372

Horan T, Wen J, Arakawa T, Liu N, Brankow D, Hu S, Ratzkin B, Philo JS. 1995. Binding of Neu Differentiation Factor with the extracellular Domain of Her2 and Her3. J Biol Chem 270: 24604-24608.

Hutchinson J, Jin J, Cardiff RD, Woodgett JR, Muller WJ. 2001. Activation of Akt (protein kinase B) in mammary epithelium provides a critical cell survival signal required for tumor progression. Mol Cell Biol 21: 2203-2212.

Hynes NC, Stern DF. 1994. The biology of the erbB-2/neu/HER2 and its role in cancer. Biochim Biophys Acta 1198:165-184

Jones FE, Jerry DJ, Guarino BC, Andrews GC, Stern D. 1996. Heregulin induces in vivo proliferation and differentiation of mammary epithelium into secretary lobuloalveoli. Cell Growth & Diff 7:1031-1038.

Jones FE, Stern DF. 1999. Expression of dominant-negative ErbB2 in the mammary gland of transgenic mice reveals a role in lobuloalveolar development and lactation. Oncogene 18:3481-3490.

Jones FE, Welte T, Fu XY, Stern DF. ErbB4 signaling in the mammary gland is required for lobuloalveolar development and Stat5 activation during lactation. J Cell Biol. 1999 Oct 4;147(1):77-88.

Kenney NJ, Huang RP, Johnson G, Okamura D, Matheny W, Plowman G, Smith GH, Salomon DS, Adamson ED. 1995. Detection and location of amphiregulin and cripto-1 in the developing mouse mammary gland. Mol Reprod Dev 41: 277-286.

Kelsy JL, Gammon MD. 1997. The epidemiology of breast cancer. CA-A Cancer J Clinic 41:146-165.

Klapper LN, Kirschbaum MH, Sela M, Yarden Y. 2000. Biochemical and clinical implications of the ErbB/HER signaling network of growth factor receptors. Adv Cancer Res 77:25-79.

Krane I M, Leder P. 1996. NDF/heregulin induces persistence of terminal end buds and adenocarcinomas in the mammary glands of transgenic mice. Oncogene 12:1781-1788.

Lee KF, Simon H, Chen H, Bates B, Hung MC, Hauser C. 1995. Requirement for neuregulin receptor erbB2 in neural and cardiac development. Nature 378: 394-398.

Liu X, Robinson GW, Hennighausen L. 1996. Activation of Stat5a and Stat5b by tyrosine phosphorylation is tightly linked to mammary gland differentiation. Mol Endocrinol 10:1496-1506.

Liu X, Robinson GW, Wagner KU, Garrett L, Wynshaw-Boris A, Hennighausen L. 1997. Stat5a is mandatory for adult mammary gland development and lactogenesis. Genes Dev 11:179-186.

Luetteke NC, Qiu TH, Fenton SE, Troyer KL, Riedel RF, Chang A, Lee DC. 1999. Targeted inactivation of the EGF and amphiregulin genes reveals distinct roles for EGF receptor ligands in mouse mammary gland development. Development. 1999 Jun;126(12):2739-50.

Maggiora P, Marchio S, Stella MC, Giai M, Belfiore A, De Bortoli M, Di Renzo MF, Costantino A, Sismondi P, Comoglio PM. 1998. Overexpression of the RON gene in human breast carcinoma. Oncogene 16:2927-2933.

Marte BM, Downward J. 1997. PKB/Akt: connecting phosphoinositide 3-kinase to cell survival and beyond. Trends Biochem Sci 22:355-358.

Medina D. 1996. The mammary gland: a unique organ for the study of development and tumorigenesis. J Mammary Gland Biol Neoplasia 1:5-19.

Mendelsohn J, Baselga J. 2000. The EGF receptor family as targets for cancer therapy. Oncogene 19:6550-6565.

Muraoka RS, Lenferink AE, Simpson J, Brantley DM, Roebuck LR, Yakes FM, Arteaga CL. 2001. Cyclin-dependent kinase inhibitor p27(Kip1) is required for mouse mammary gland morphogenesis and function. J Cell Biol 153:917-932.

Nandi S. 1959. Hormonal control of mammogenesis and lactogenesis in the C3H/He Crgl mouse. University California Publi Zool 65:1-128.

Neimann C, Brinkmann V, Spitzer E, Hartmann G, Sachs M, Naundorf H, Birchmeier W. 1998. Reconstitution of mammary gland development in vitro: requirement of c-met and c-erbB2 for branching and alveolar morphogenesis. J Cell Biol 19: 533-545.

Olayioye MA, Neve RM, Lane HA, Hynes NE. 2000. The ErbB signaling network: receptor heterodimerization in development and cancer. EMBO J 19: 3159-3167.

Peles E, Yarden Y. 1993. Neu and its ligands: from an oncogene to neural factors. BioEssays 15:815-824.

Pinkas-Kramarski R, Soussan L, Waterman H, Levkowitz G, Alroy I, Klapper L, Lavi S, Seger R, Ratzkin BJ, Sela M, Yarden Y. 1996. Diversification of Neu differentiation factor and epidermal growth factor signaling by combinatorial receptor interactions. EMBO J 15:2452-2467.

Pinkas-Kramarski R, Soussan L, Waterman H, Levkowitz G, Alroy I, Klapper L, Lavi S, Seger R, Ratzkin BJ, Sela M, Yarden Y. 1997. Diversification of NDF and EGF signaling by combinational receptor interactions. EMBO J 15:2452-2467.

Prigent SA, Gullick WJ. 1994. Identification of c-erbB-3 binding sites for phosphatidylinositol 3'-kinase and SHC using an EGF receptor/c-erbB-3 chimera. EMBO J 13:2831-2841.

Riedel H, Massoglia S, Schlessinger J, Ullrich A. 1988. Ligand activation of overexpressed epidermal growth factor receptors transform NIH3T3 mouse fibroblasts. Proc Natl Acad Sci USA 85: 1477-1481.

Riese DJII, Stern DF. 1998. Specificity within the EGF family/ErbB receptor family signaling network. BioEssays 20:41-48.

Riethmacher D, Sonnenberg-Riethmacher E, Brinkmann V, Yamaai T, Lewin GR, Birchmeier C. 1997. Severe neuropathies in mice with targeted mutations in the ErbB3 receptor. Nature 389: 725-730.

Rondinelli RH, Haslam SZ, Fluck MM. 1995. The tole of ovarian hormones, age and mammary gland development in polymavirus mammary tumorigenesis. Oncogene 11:1817-1827.

Russo J, Russo IH. 1980. Susceptibility of the mammary gland to carcinogenesis. II. Pregnancy interruption as a risk factor in tumor incidence. Am J Pathol 100: 497-512.

Russo J, Russo IH. 1982. Differentiation of the mammary gland and susceptibility to carcinogenesis. Breast Cancer Res Treat 2:5-73.

Santoro MM, Collesi C, Grisendi S, Gaudino G, Comoglio PM. 1996. Constitutive activation of the RON gene promotes invasive growth but not transformation. Mol Cell Biol 16: 7072-7083.

Schroeder JA, Lee DC. 1998. Dynamic expression and activation of erbB receptors in the developing mouse mammary gland. Cell Growth Differ 9: 451-464.

Schwertfeger KL, Richert MM, Anderson SM. 2001. Mammary gland involution is delayed by activated akt in transgenic mice. Mol Endocrinol 15:867-881.

Senderowicz AM. 2000. Small molecule modulators of cyclin-dependent kinases for cancer therapy. 19:6600-6606.

Shoelson SE. 1997. SH2 and PTB domain interactions in tyrosine kinase signal transduction. Curr Opin Chem Biol 1:227-234.

Sicinski P, Donaher JL, Parker SB, Li T, Fazeli A, Gardner H, Haslam SZ, Bronson RT, Elledge SJ, Weinberg RA. 1995. Cyclin D1 provides a link between development and oncogenesis in the retina and breast. Cell 82:621-630.

Soriano JV, Pepper MS, Orci L, Montesano R. 1998. Roles of hepatocyte growth factor/scatter factor and transforming growth factor-beta1 in mammary gland ductal morphogenesis. J Mammary Gland Biol Neoplasia 3: 133-150.

Sudol M. 1998. From Src homology domains to other signaling modules: proposal of the 'protein recognition code'. Oncogene, 17:1469-1474.

Tang ED, Nunez G, Barr FG, Guan KL. 1999. Negative regulation of the forkhead transcription factor FKHR by Akt. J Biol Chem 274: 16741-16746.

Ullrich A, Schlessinger J. 1990. Signal transduction by receptors with tyrosine kinase activity. Cell 61: 203-212.

Vadlamudi R, Adam L, Tseng B, Costa L, Kumar R. 1999a.Transcriptional up-regulation of paxillin expression by heregulin in human breast cancer cells. Cancer Res 59: 2843-2846.

Vadlamudi R, Adam L, Talukder A, Mendelsohn J, Kumar R. 1999b. Serine phosphorylation of paxillin by heregulin-beta1: role of p38 mitogen activated protein kinase. Oncogene 18: 7253-7264.

Vadlamudi R, Adam L, Wang RA, Mandal M, Sahin A, Chernoff J, Hung M-H, Kumar R. 2000. Regulatable expression of p21-activated kinase-1 promotes anchorage-independent growth and abnormal organization of mitotic spindles in human epithelial breast cancer cells. J Biol Chem 275:36238-36244.

Vogel WF, Aszodi A, Alves F, Pawson T. 2001. Discoidin domain receptor 1 tyrosine kinase has an essential role in mammary gland development. Mol Cell Biol 21: 2906-17.

Vonderhaar BK.1987. Local effects of EGF, TGF-alpha, and EGF-loke growth factors on lobuloalveolar development of the mouse mammary gland in vivo. J Cell Physiol 132: 581-584.

Wang TC, Cardiff RD, Zukerberg L, Lees E, Arnold A, Schmidt EV. 1994. Mammary hyperplasia and carcinoma in MMTV-cyclin D1 transgenic mice. Nature 369:669-671.

Wakefield LM, Piek E, Bottinger EP. 2001. TGFβ signaling in mammary gland development and tumorigenesis. J Mamm Gland Biol Neopl 6: 67-82.

Weiss A, Schlessinger J. 1998; Switching signals on and off by receptor dimerization. Cell 94:277-280.

Yamashita J, Ogawa M, Yamashita S, Nomura K, Kuramoto M, Saishoji T, Shin S.1994. Immunoreactive hepatocyte growth factor is a strong and independent predictor of recurrence and survival in human breast cancer. Cancer Res 54:1630-1633.

Yang Y, Spitzer E, Meyer D, Sachs M, Niemann C, Hartmann G, Weidner KM, Birchmeier C, Birchmeier W. 1995. Sequential requirement of hepatocyte growth factor and neuregulin in the morphogenesis and differentiation of the mammary gland. J Cell Biol 131: 215-226.

Yu Q, Geng Y, Sicinski P. 2001. Specific protection against breast cancers by cyclin D1 ablation.Nature 411:1017-1021.

Zhang K, Sun J, Liu N, Wen D, Chang D, Thomason A, Yoshinaga SK. 1996. Transformation of NIH3T3 cells by HER3 or HER4 reptors requires the presence of HER1 or HER2. J Biol Chem 271:3884-3890.

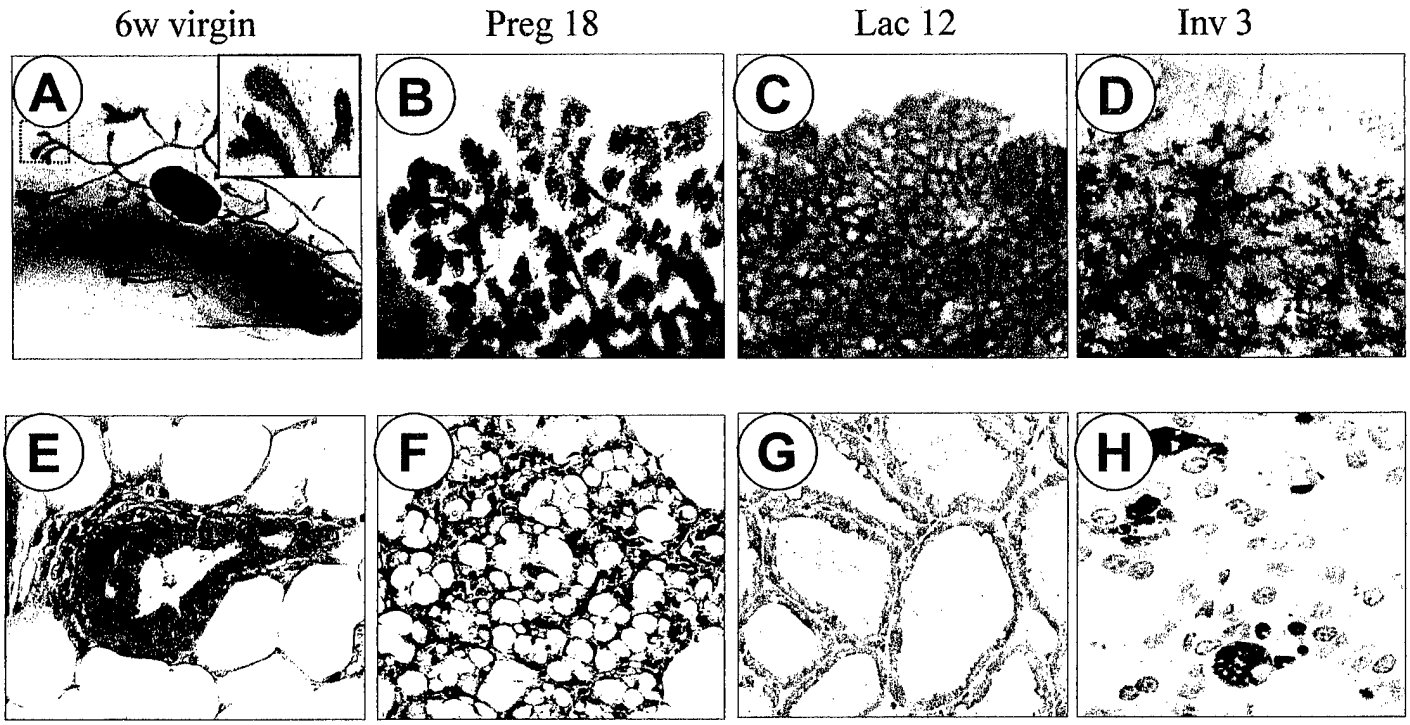

Fig 1. Development of murine mammary gland. A-D, Whole-mount staining. E-G, H.E. Staining. H, TUNEL staining counterstained with hematoxylin.

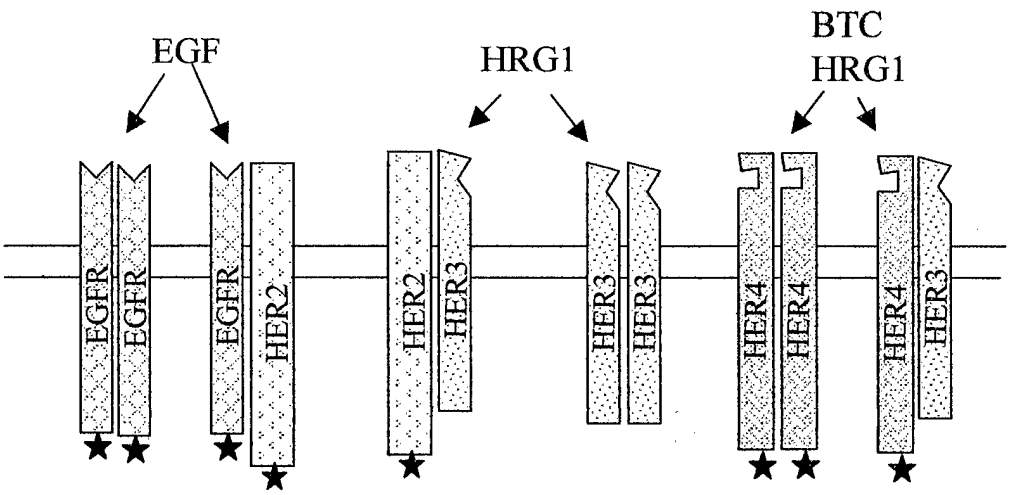

Fig 2. Heterodimerization among HER family members induced by specific ligands. Star stands for kinase. Note there is no ligands known for HER2 yet, and HER3 is impaired in terms of kinase activity.

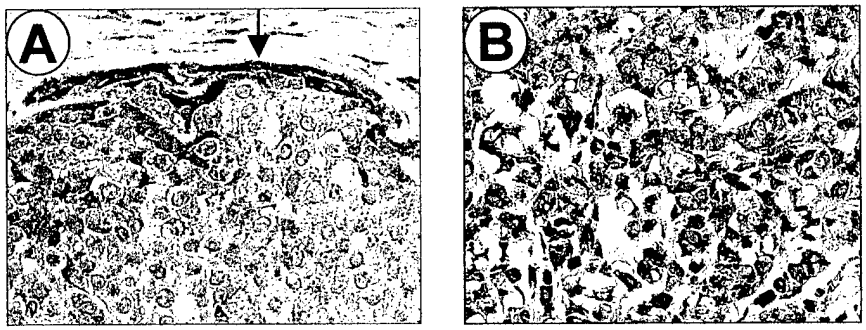

Fig 2. Pak1 expression in breast cancer. A. Grade II breast cancer has a relative low lower level of Pak1 expression, but the cells in the leading edge have a much higher expression. B. GradeIII breast cancer have a high level of Pak1 expression.

Table 1 List of Protein Kinases Expressed in Mammary Gland

Receptor Tyrosine Kinases	Tie1	Prkmk3
AX1/Ufo	Tie2	c-Src
EphA2	Tyro10	Srm
EphA7	Tyro3	Tec
EphB3		Tyk2
FGFR	***None Receptor Tyrosine Kinases***	***Serine/Threonine kinases***
FLT3	c-Abl	TGFβR
HER1,2,4	Csk	Akt
IGF1R	Ctk	Mlk1
InsR	c-Fes	Pak1
c-kit	Fyn	Plk
Met	Hck	Hunk
MuSK	Jak1	Pnck
Ron	Jak2	
RyK	Lyn	

Table 2. Ligands of HER family receptor tyrosine kinases

	Ligands
EGFR	EGF, TGFα, AR, BTC, HB-EGF, EPR
HER2	?
HER3	HRG1, HRG2
HER4	BTC, HB-EGF, EPR, HRG1-4

Transcriptional repression of oestrogen receptor by metastasis-associated protein 1 corepressor

Abhijit Mazumdar*†, Rui-An Wang*†, Sandip K. Mishra*, Liana Adam*, Rozita Bagheri-Yarmand*, Mahitosh Mandal*, Ratna K. Vadlamudi* and Rakesh Kumar*‡

*Department of Molecular and Cellular Oncology, University of Texas M. D. Anderson Cancer Center, 1515 Holcombe Boulevard, Houston, Texas 77030, USA
†These authors contributed equally to this work
‡e-mail: rkumar@notes.mdacc.tmc.edu

Activation of the heregulin/HER2 pathway in oestrogen receptor (ER)-positive breast-cancer cells leads to suppression of oestrogen-receptor element (ERE)-driven transcription and disruption of oestradiol responsiveness, and thus contributes to progression of tumours to more invasive phenotypes. Here we report the identification of metastatic-associated protein 1 (MTA1), a component of histone deacetylase (HDAC) and nucleosome-remodelling complexes, as a gene product induced by heregulin-β1 (HRG). Stimulation of cells with HRG is accompanied by suppression of histone acetylation and enhancement of deacetylase activity. MTA1 is also a potent corepressor of ERE transcription, as it blocks the ability of oestradiol to stimulate ER-mediated transcription. The histone-deacetylase inhibitor trichostatin A blocks MTA1-mediated repression of ERE transcription. Furthermore, MTA1 directly interacts with histone deacetylase-1 and -2 and with the activation domain of ER-α. Overexpression of MTA1 in breast-cancer cells is accompanied by enhancement of the ability of cells to invade and to grow in an anchorage-independent manner. HRG also promotes interaction of MTA1 with endogenous ER and association of MTA1 or HDAC with ERE-responsive target-gene promoters *in vivo*. These results identify ER-mediated transcription as a nuclear target of MTA1 and indicate that HDAC complexes associated with the MTA1 corepressor may mediate ER transcriptional repression by HRG.

Growth of human breast cells is closely regulated by receptors of both steroid and peptide hormones[1]. Members of both receptor classes are important prognostic factors in human breast cancer as well as determinants of endocrine therapy in breast cancer patients. After the initial stages of breast-cancer progression, tumours frequently acquire resistance to -steroid hormones with concurrent amplification of growth-factor receptors; this alteration is associated with a poor prognosis. For example, overexpression of c-*erb*B-2 (also known as human epidermal growth-factor receptor, HER2) in ER-positive breast-cancer cells leads to reduced sensitivity of these cells to oestrogen both *in vitro* and *in vivo*[2–5]. In addition, accumulating evidence indicates that the progression of breast-cancer cells to a more invasive phenotype may be regulated not only by HER2 overexpression but also by a mesenchymal growth factor, HRG, which is a ligand for HER3 and HER4 and which transactivates HER2 (ref. 6). Recently, we and others have shown that HRG activation promotes the development of aggressive phenotypes in breast-cancer cells[7–10].

There is also considerable evidence to indicate that the development of hormone independence in breast cancer cells may be influenced by crosstalk between steroid-hormone and HER2/HRG pathways. For example, expression of the HER2 pathway in MCF-7 cells results in downregulation of ER expression and inactivation of ERE-driven reporter transcription[8,9]. The finding that signalling by HRG promotes ligand-independent suppression of ER transcription also supports a link between the HER2 and ER receptor pathways[6–9]. In spite of these findings, the molecular basis of hormone independence and the putative function of these histone modifications remain unexplored.

The eukaryotic genome is compacted with histone and other proteins to form chromatin, which consists of repeating units of nucleosomes[11]. For transcription factors to access DNA, the repressive chromatin structure needs to be remodelled. Dynamic alterations in chromatin structure can facilitate or suppress access of transcription factors to nucleosomal DNA, leading to transcriptional regulation. One way to achieve this is through alterations in the acetylation state of nucleosomal histones[11–13]. Acetylation of core histones occurs at lysine residues on their amino-terminal

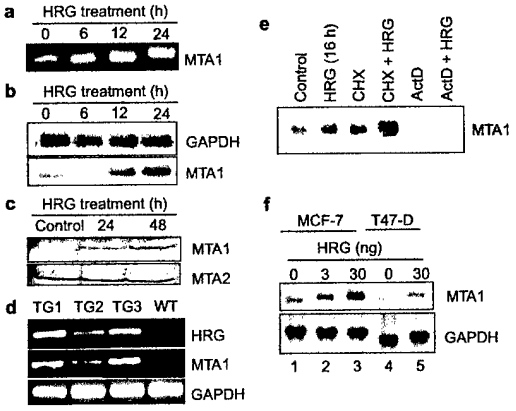

Figure 1 **HRG regulation of MTA1 expression.** **a**, RT-PCR analysis of MTA1 expression. **b**, Northern-blot analysis of HRG regulation of MTA1 expression in MCF-7 cells. **c**, Western-blot analysis of HRG regulation of MTA1 or MTA2 expression in MCF-7 cells. **d**, RT-PCR analysis of HRG and MTA1 expression in Harderian-gland tumours from HRG transgenic mice. TG1, TG2 and TG3, Harderian-gland tumours from HRG transgenic mice. WT, wild-type mice. **e**, Regulation of MTA1 mRNA by HRG in MCF-7 cells. CHX, cyclohexamide; ActD, actinomycin D. **f**, Dose-dependent upregulation of MTA1 mRNA in MCF-7 cells (lanes 1–3) and T47-D cells (lanes 4 and 5); $n = 3$.

© 2000 Macmillan Magazines Ltd

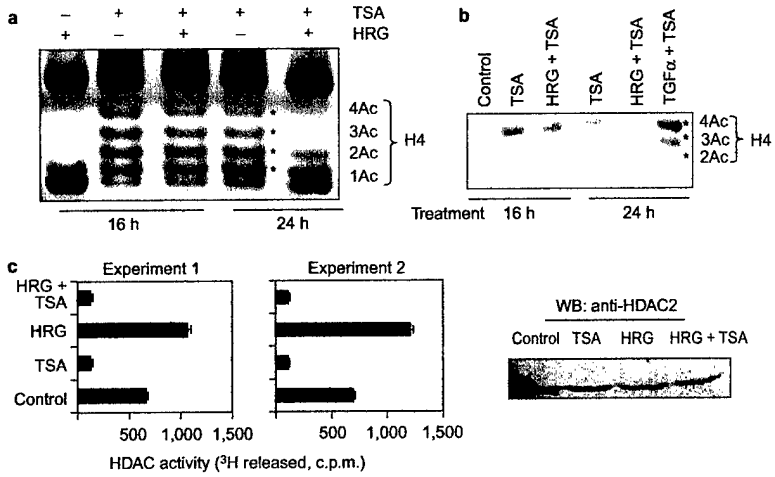

Figure 2 **HRG regulation of HDAC activity.** **a**, Urea–polyacrylamide-gel analysis of histone H4 acetylation in TSA-treated MCF-7 cells in the presence or absence of HRG. **b**, Western-blot analysis of histone H4 acetylation using an antibody against acetylated H4. **c**, Regulation of TSA-sensitive deacetylase activity by HRG in MCF-7 cells. TSA, 300 nM; HRG, 1 nM; $n = 4$. WB, western blot.

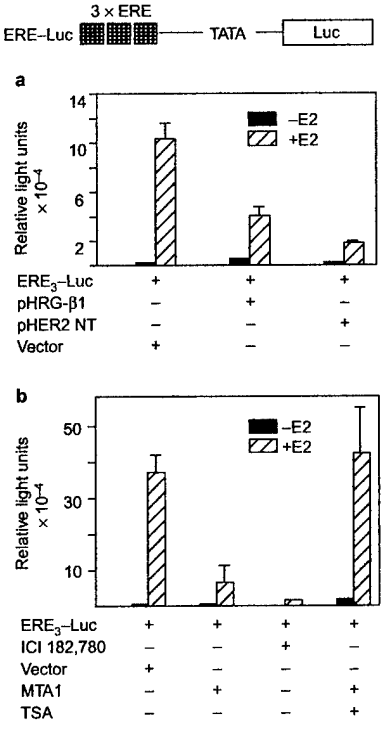

Figure 3 **MTA1 represses ERE-mediated transcription.** **a**, Repression of 17β-oestradiol (10^{-9} M)-mediated stimulation of ERE–luciferase activity in MCF-7 cells by heregulin gene (pHRGβ1) and point-mutated HER2 (pHER2NT). Shown above is a schematic representation of the ERE–Luc construct. **b**, MCF-7 cells were transfected with ERE–Luc in the presence or absence of MTA1. Where indicated, cultures were treated with TSA (300 nM); $n = 3$.

tails, thus neutralizing the positive charge of the histone tails and reducing their affinity for DNA. Hyperacetylated chromatin is generally associated with transcriptional activation, whereas hypoacetylated chromatin is associated with transcriptional repression[14]. The acetylation state of histones is regulated by a dynamic interaction of two groups of recently identified enzymes — histone acetyltransferases (HATs) and HDACs. HATs and HDACs thus constitute important links between chromatin structure and transcription outcome.

Several recent studies have raised the possibility of a close connection between HDACs and cancer. As HDAC-mediated deacetylation of nucleosomal histones is known to be associated with transcriptional repression of some genes, it has been proposed that deregulation of HDAC recruitment to specific promoters is a potential mechanism by which these HDACs contribute to tumorigenesis. Several recent findings[15–18], which have revealed the identity of a polypeptide (NuRD-70) of nucleosome remodelling and HDAC complex with that of MTA1 have indicated a possible function of HDACs in tumour progression. MTA1 also physically interacts with HDAC1 (ref. 19). The MTA1 gene was originally identified by differential expression in rat mammary adenocarcinoma metastatic cells, and has since been shown to correlate well with the metastatic potential of several human cell lines and tissues[20–22].

Although MTA1 has been shown to be a part of the HDAC complex, the nature of its target or targets remains unidentified. As one of the mechanisms by which hormone independence by HRG is developed includes repression of the ER pathway, and as MTA1 is a component of the HDAC complex, we explored the hypothesis that HRG regulates expression of MTA1, which, as a part of the HDAC complex, may antagonize the activation of the ER pathway by oestradiol. Here we provide new evidence that MTA1 is a target of HRG and represses ER-mediated transcription by recruiting HDACs.

Results

HRG stimulation of MTA1 expression in breast-cancer cells. Because deregulation of the HRG pathway into ER-positive breast-cancer cells leads to suppression of ER-driven transcription[9], and because MTA1 is a component of the HDAC complex[15–18], we initially investigated whether HRG could upregulate the expression of

© 2000 Macmillan Magazines Ltd

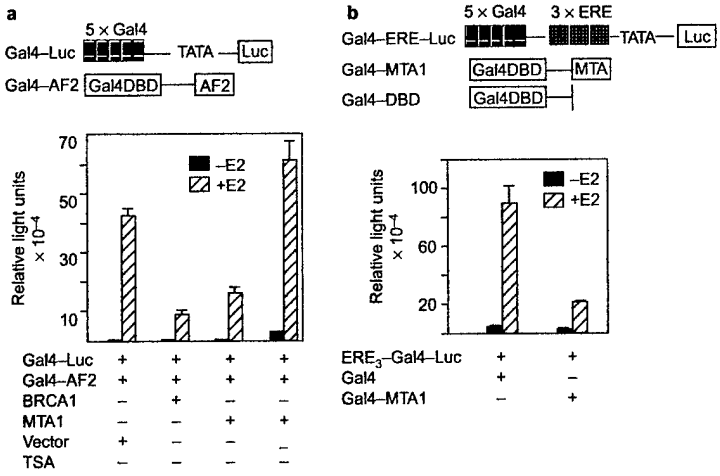

Figure 4 **MTA1 regulation of the function of the ER AF2 domain. a**, MCF-7 cells were co-transfected with Gal4–AF2 and Gal4–Luc (each containing five copies of the Gal4-binding domain) with or without MTA1. BRCA1 was used as a positive control to show its suppression. **b**, E2-dependent direct interactions between Gal4–MTA1 and ERE_3–Gal4–Luc (n = 4). Schematic representations of the constructs used are shown at the top.

MTA1. Using a pair of specific MTA1 primers[20], analysis of RNAs from breast cancer MCF-7 cells by polymerase chain reaction with reverse transcription (RT-PCR) revealed time-dependent stimulation of MTA1 messenger RNA by HRG (Fig.1a). We confirmed the identity of the amplified MTA1 band by sequencing and Southern blotting (data not shown). Using a 291-base-pair PCR probe for MTA1, northern blotting showed a significant increase in steady-state levels of 2.9-kilobase (kb) mRNA for MTA1 in a time-dependent manner (Fig. 1b). Western blotting with an anti-MTA1 antibody[23] also showed that the level of MTA1 of relative molecular mass 80,000 (M_r 80K) was significantly increased in HRG-treated MCF-7 cells (Fig. 1c). HRG had no effect on expression of MTA2 protein. As treatment with HRG for 12 h had no effect on the levels of thymidine incorporation into DNA, or on the cell-cycle distribution of this incorporation (data not shown), the observed effect of HRG on MTA1 expression may not be reflective of the proliferative status of the cell. To evaluate HRG modulation of MTA1 *in vivo*, we used a mouse mammary tumour virus (MMTV)-promoter-driven HRG-transgenic mouse line, which develops mammary adenocarcinomas and Harderian-gland tumours[24]. As Harderian-gland tumours are usually detected by 3 weeks of age, as opposed to 12–16 months for mammary-gland tumours, we used the presence of Harderain-gland tumours to establish the proof-of-principle of our hypothesis *in vivo*. Expression of HRG transgene in Harderian-gland tumours in a MMTV/HRG transgenic mouse model[24] was accompanied by increased expression of MTA1 (Fig. 1d). Treatment of cultures with actinomycin D, an inhibitor of transcription, completely inhibited HRG-mediated induction of MTA1 mRNA (Fig. 1e). Treatment of cells with cycloheximide stabilized the levels of MTA1 mRNA expression; treatment with HRG, however, superinduced the expression of MTA1 mRNA. Induction of MTA1 expression by HRG was also dose-dependent (Fig. 1f). To confirm that MTA1 is expressed in mammary epithelium cancer cells, we also cloned the full-length MTA1 complementary DNA from the human mammary gland cDNA library (data not shown).

Suppression of histone acetylation in HRG-treated cells. As MTA1, a component of the NuRD complex, was induced by HRG, we next examined the influence of HRG on the status of histone acetylation. We treated MCF-7 cells for 16 or 24 h with or without HRG in the presence or absence of trichostatin-A (TSA), a specific HDAC inhibitor, and evaluated the status of histone acetylation using acetic acid–urea–acrylamide gels. Addition of TSA to control cells

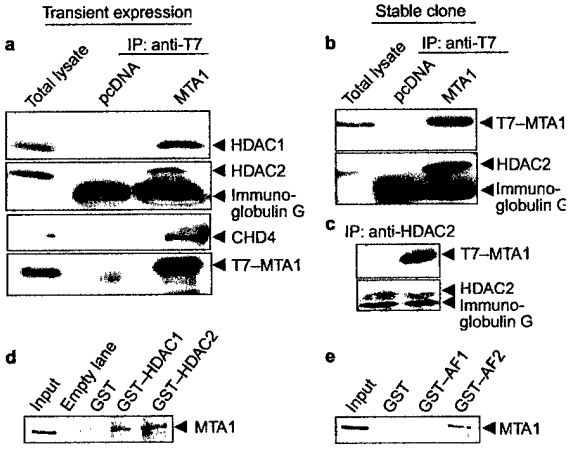

Figure 5 **Direct association of MTA1 with HDACs and ER. a**, MTA1 interacts with HDAC complexes *in vivo*. MCF-7 cells were transiently transfected with T7–MTA1 or control vector. Immunoprecipitation (IP) was carried out using anti-T7 monoclonal antibody; western blotting was carried out with the indicated antibodies. **b**, **c**, T7–MTA1 associates with HDAC2 in the stable cell lines. Cell extracts were immunoprecipitated with anti-T7 antibody, and the same blot was immunoblotted with anti-HDAC2 and anti-T7 antibodies (**b**). In a reverse experiment, extracts were immunoprecipitated with anti-HDAC2 antibody and immunoblotted with anti-T7 and anti-HDAC2 antibodies (**c**). **d**, MTA1 directly interacts with HDAC. GST pull-down assay, showing the association of HDAC with *in vitro*-translated MTA1. **e**, GST pull-down assay, demonstrating a direct interaction between MTA1 and the ligand-binding domian (AF2) of ER (n = 4).

was accompanied by an expected increase in the acetylation of histone 4 (H4, Fig. 2a). However, HRG treatment for longer than 16 h suppressed the levels of H4 acetylation, particularly on bands 4 and 3 (Fig. 2a). Similar results were obtained for cell lysates from the above experiment when immunoblotted with an anti-H4 antibody (Fig. 2b). However, this antibody predominantly recognized acetylated

© 2000 Macmillan Magazines Ltd

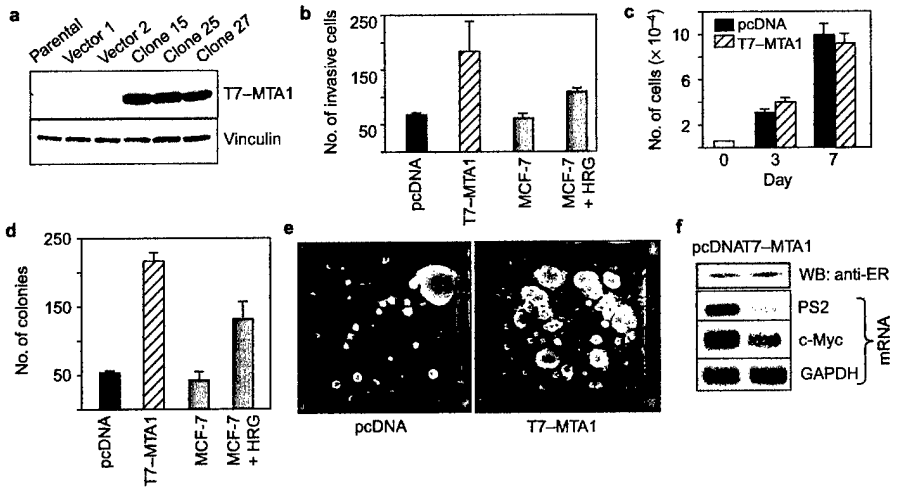

Figure 6 **Characterization of MCF-7 cells overexpressing MTA1. a**, Western-blot analysis of control and T7–MTA1-expressing clones, using anti-T7 monoclonal antibody. The blot was reprobed with anti-vinculin antibody as a loading control. **b**, Invasiveness of MCF-7 cells expressing T7–MTA1 (clone 15) or control vector pcDNA. As a positive reference control for comparison, MCF-7 cells were treated with HRG and another group was left untreated. **c**, Effect of T7–MTA1 expression on the growth rate of cells, as shown by MTT assay. **d**, Effect of T7–MTA1 expression on anchorage-independent growth of MCF-7 cells. As a positive control, MCF-7 cells were treated with HRG and another group was left untreated. **e**, Representative photographs of soft-agar colonies of the indicated strains. **f**, Expression of ER protein and pS2, c-Myc and GAPDH mRNAs in MCF-7 cells expressing vector or T7–MTA1 (n = 3). WB, western blot.

H4 bands 4, 3 and 2 (in decreasing order). This was a specific effect of HRG, as another growth factor, TGF-α, produced no such inhibitory effect (Fig. 2b). HRG treatment of MCF-7 cells was also accompanied by an enhancement of TSA-sensitive HDAC activity without any effect on expression of HDAC2 protein (Fig. 2c). These findings indicate that HRG may interfere with the acetylation of H4, presumably through stimulation of MTA1 expression.

Repression of ERE-mediated transcription by MTA1. Because MTA1 has been shown to be a component of the NuRD complex and to have HDAC activity[15–18], and because HRG induces MTA1 expression as well as histone deacetylation, we hypothesized that MTA1, in conjunction with HDAC complexes, may repress ERE transcription and may thus provide a molecular explanation for the reported suppression of the ER pathway by HRG[7,8]. As shown in Fig. 3a, co-transfection of ERE–luciferase with either HRG or activated (point-mutated) HER2, but not with control vector, was accompanied by significant suppression of ERE–reporter transcription, indicating the possible existence of crosstalk between the HER2/HRG and ER pathways.

To investigate whether HRG-inducible MTA1 serves as specific corepressor of ERE transcription, we repeated the above experiment with MTA1 expression vector. Transient expression of MTA1 effectively blocked the ability of oestradiol to stimulate ERE transcription (Fig. 3b). The inhibitory effect of MTA1 on ERE transcription was antagonized by TSA, a specific inhibitor of HDAC enzyme, indicating that MTA1 potentially recruits HDAC to repress ERE-mediated transcription.

We next examined the recruitment of MTA1 complex(es) to ER elements, using a Gal4–ER/Gal4–Luc assay system[25,26]. This system involves transient transfection of two plasmids, Gal4–AF2 (the ligand-binding domain of ER-α) and Gal4–luciferase reporter; luciferase activation depends on E2 stimulation of the AF2 domain. As shown in Fig. 4a, E2-mediated activation of the AF2 domain could also be repressed by MTA1 expression, and this repression was relieved by TSA. These observations indicate that the observed MTA1 regulation of AF2 function may be independent of the DNA-binding activity of ER and that this may involve HDACs. Many repressors have been shown to repress transcription of specific promoters when recruited by heterologous DNA-binding domain[15,16]. To confirm further the function of MTA1 in ERE transcription, we constructed a reporter gene containing five Gal4 sites placed in front of three ERE sites, and used the GAL4 DNA-binding domain fused MTA1 to recruit MTA1 to the ERE promoter. Expression of Gal4–MTA1 repressed the E2-mediated activity of ERE by up to 80% (Fig. 4b). The repressing effect of MTA1 on the ERE-mediated transcription was not restricted to the ER, as MTA1 also effectively blocked the activation of GRE-mediated transcription by progestin and dexamethasone in a TSA-sensitive manner (see Supplementary Information). Overall, these results establish a new function of MTA1 in repression of the ERE- and GRE-mediated transcription.

Association of MTA1 with HDAC and ER. To determine whether the observed repression of ERE transcription by MTA1 was associated with recruitment of HDAC complexes *in vivo*, we next examined the association between T7-tagged MTA1 and the components of HDACs by co-immunoprecipitation and western blotting (Fig. 5a). Transient expression of T7-tagged MTA1, but not of control T7 vector, in MCF-7 cells was accompanied by interactions with HDAC1, HDAC2 and chromodomain protein 4 (CHD4). Similar results were also obtained when extracts from the stable cell lines were analysed. As shown in Fig. 5b, immunoprecipitation of the extracts from stable cell lines with anti-T7 antibody (Fig. 5b) or anti-HDAC2 antibody (Fig. 5c) further confirmed the existence of a physical association between HDAC2 and T7-MTA1.

To investigate whether the observed association between MTA1 and HDAC1 or HDAC2 was direct or was mediated through other proteins, we examined the binding ability of *in vitro*-translated MTA1 protein with glutathione-S-transferase (GST)-tagged HDAC1 and HDAC2. MTA1 interacted with GST–HDAC1 and GST–HDAC2, but not with GST alone, in GST pull-down assays (Fig. 5d). A physical interaction has also been reported between MTA1 and HDAC1 (ref. 19).

As MTA1 repressed ERE-mediated transcription by recruiting HDAC, we hypothesized that MTA1 physically interacts with ER to

© 2000 Macmillan Magazines Ltd

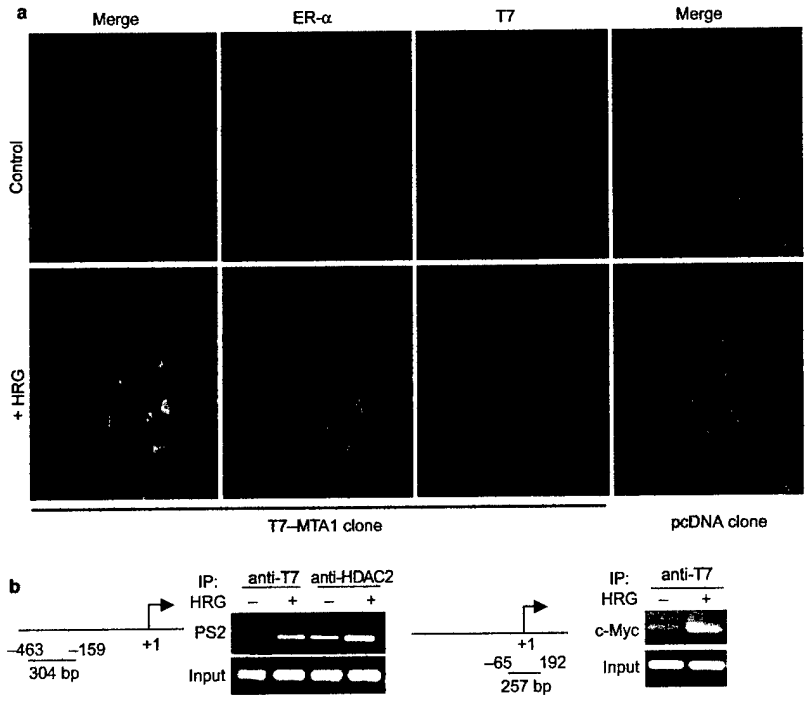

Figure 7 **HRG promotes interaction of MTA1 with the endogenous ER pathway. a**, T7–MTA1 and ER-α partially co-localize in the nuclei of MCF-7 cells expressing T7–MTA1. Confocal images of single optical sections are shown. Double labelling was carried out with a rabbit antibody against human ER-α (green) and a mouse monoclonal antibody against T7 to visualize MTA-1 (red). HRG treatment induced co-localization of ER with T7–MTA1 in large nuclear domains, as shown by the presence of yellow colour in the merged images. **b**, Analysis of MTA1–HDAC2 association on ERE-responsive promoters by chromatin-immunoprecipitation assay. MCF-7 cells were treated with or without HRG (30 ng ml^{-1} for 16 h), and chromatin lysates were immunoprecipitated (IP) with anti-T7 or anti-HDAC2 antibodies; samples were processed as described in Methods. Upper panels of the blots show PCR analysis of pS2 (304 bp) and c-Myc (257 bp) promoter fragments associated with T7–MTA1 or HDAC2 (schematic representations are shown to the left of blots); lower panels show PCR analysis of the DNA input.

influence its function. To explore this possibility, we examined the binding ability of *in vitro*-translated MTA1 with GST-tagged AF1 and AF2 domains of ER in GST pull-down assays. MTA1 protein effectively interacted with GST–AF2 (the ligand-binding domain of ER), but not with GST alone or with GST–AF1 (Fig. 5e). These results support the hypothesis that MTA1 acts as a transcription repressor by recruiting the HDAC complex.

Effect of MTA1 on the biology of breast-cancer cells. To delineate further the potential contribution of MTA1 in breast-cancer cells, we established stable MCF-7 clones expressing T7-tagged MTA1 or control vector (Fig. 6a). For subsequent studies, we used MCF-7 clone 15 expressing T7-MTA1, and control-vector-transfected MCF-7 cells (clone V2). We analysed the influence of MTA1 expression on the invasion of MCF-7 cells using a Boyden chamber. Vector-transfected cells showed low invasiveness (Fig. 6b), whereas expression of MTA1 resulted in a significant increase in cell invasiveness (Fig. 6b). As a positive reference control, we treated MCF-7 cells with HRG, a known inducer of invasiveness in these cells[10], and left another group untreated. To examine the potential influence of MTA1 expression on the growth characteristics of breast epithelial cancer cells, we measured the growth rate and ability of cells to grow in an anchorage-independent manner. Expression of MTA1 had little or no significant effect on the growth rate of MCF-7 cells on plastic (Fig. 6c). However, MTA1 expression significantly enhanced the ability of MCF-7 cells to form colonies on soft agar (Fig. 6d). As a positive control, we treated MCF-7 cells with HRG and left another group untreated. Overexpression of MTA1 was accompanied by a significant, reproducible enhancement of the ability of cells to form larger colonies in soft agar, as compared to those formed by vector-transfected control cells (Fig. 6e). Although MTA1 expression had no effect on the level of ER, MTA1-overexpressing breast-cancer cells exhibited a reduction in the levels of ER target genes, including those encoding pS2 and c-Myc (Fig. 6f). Together, these observations indicate that cells expressing MTA1 may affect the status of ER-responsive genes and that these cells may acquire more invasive phenotypes.

HRG promotes interaction of MTA1 with endogenous ER. Having shown that MTA1 has a role in the invasiveness of breast-cancer cells, we next investigated the effect of HRG on the potential interaction between MTA1 and endogenous ER in MCF-7 cells expressing T7-tagged MTA1 or control vector. We fixed cells treated with or without HRG, co-stained them with antibodies against ER or T7-tag, and quantified the resulting immunofluorescence by laser-scanning confocal microscopy. MTA1 was abundantly present in the nuclei of T7–MTA1-expressing cells, exhibiting a fine granular pattern in untreated control cells (Fig. 7a, upper-left panel; see also Fig. 7a, T7). In contrast, T7–MTA1 was expressed in larger nuclear domains in HRG-treated clones (Fig. 7a, lower-left panel). No positive staining was detected in cell transfected with empty vector (Fig. 7a, right panels). Interestingly, within the larger nuclear domains, MTA1 partially colocalized with ER-α only upon HRG treatment (represented by yellow staining). Very fine serial confocal sectioning revealed that ER staining was dispersed as several smaller nuclear dots decorating the surface of the larger anti-MTA1-

© 2000 Macmillan Magazines Ltd

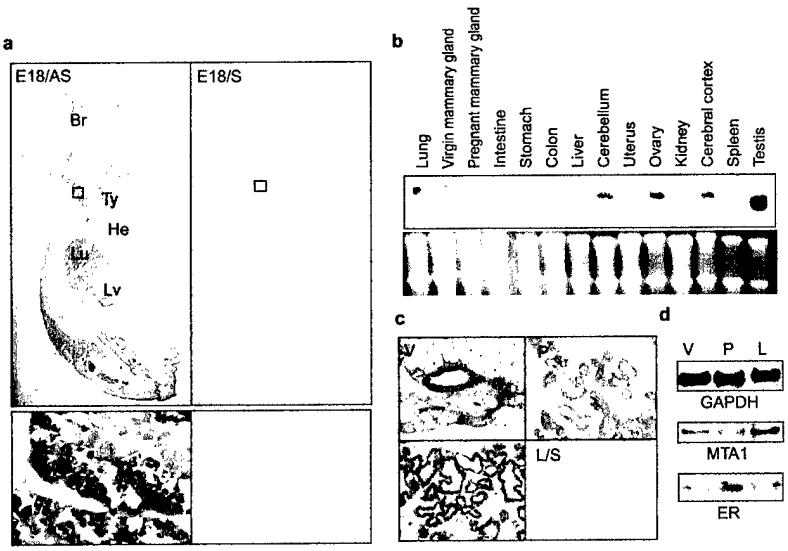

Figure 8 **MTA1 expression during embryogenesis and mammary-gland development. a**, MTA1 expression in an E18 embryo. MTA1 expression was detected by a specific anti-sense MTA1 riboprobe (E18/AS). Sense-probe hybridization was used to show the background staining (E18/S). Br, brain; Lu, lung; Ty, thymus; Lv, liver. Lower panels are enlargements of the boxed areas in the upper panels. **b**, Northern-blot analysis of MTA1 expression in the indicated mouse tissues. **c**, *In situ* hybridization analysis of MTA1 expression. V, virgin mammary gland at day 21; P, pregnant mammary gland at day 15; L, lactating mammary gland at day 12; L/S, control *in situ* hybridization, using the sense MTA1 probe, in lactating mammary gland. **d**, Northern-blot analysis of expression of MTA1 and ER in the samples described in **c** ($n = 2$).

reactive nuclear domains. As shown in Fig. 7a, overexpression of T7–MTA1 was not sufficient to induce a significant increase in the interaction between T7–MTA1 and ER, whereas HRG treatment could rapidly trigger this process. These observations raise the possibility that the observed MTA1–ER interaction may be an indirect effect of HRG, and may potentially involve an unidentified component or components of HRG pathways that lead to MTA1.

HRG treatment induces MTA1–HDAC association on ERE-responsive promoters *in vivo*. To assess directly the potential significance of the physical interaction between MTA1 and ER in HRG-activated cells, we investigated whether MTA1 and HDAC associate on the chromatin of endogenous RE-containing promoters, using a chromatin-immunoprecipitation (ChIP) assay. We treated MCF-7 cells expressing T7-tagged MTA1 with HRG and left another group untreated, and processed them with formaldehyde and sonicated chromatin for immunoprecipitation with specific antibodies against T7 or HDAC2. We analysed genomic DNA fragments bound to T7–MTA1 or to HDAC2 by quantitative PCR using primers spanning ERE elements present in the promoters of the genes encoding pS2 (ref. 27) and c-Myc (ref. 28), to assay for potential HRG-triggered association of T7–MTA1 or HDAC2 with the promoters of two ERE target genes. HRG treatment triggered significant increases in the amount of chromatin from the promoters of both the pS2 and c-Myc genes (5.8- and 4.1-fold, respectively, relative to untreated cells) that was associated with T7–MTA1 (Fig. 7b). Alterations in the amount of HRG-responsive increase of pS2-promoter DNA with HDAC2 were also significant, but less profound (1.8-fold increase relative to untreated cells, Fig. 7b). We repeated these experiments three times with similar results, and have thus demonstrated the potential complexity of regulation of promoter chromatin by multi-protein complexes. As the association of MTA1 with the ERE-responsive promoters of ER target genes was dependent on HRG treatment, the observed effects may involve HRG-triggered cellular events, and hence may be indirect. Together, these findings strongly support the idea that MTA1 interacts with endogenous ER and that both MTA1 and HDAC2 associate with ERE-containing promoters in HRG-treated cells.

Expression of MTA1 during embryogenesis and mammary-gland development. During embryonic development, HDAC may work constantly to control the on/off function of the genes that regulate cell proliferation and differentiation. However, little is known of the expression profile of HDAC components. We investigated MTA1 expression in mouse embryonic development by *in situ* hybridization. As shown in Fig 8a, MTA1 mRNA was expressed in most tissues, with highest levels present in rapidly proliferating tissues such as liver, lung and thymus. MTA1 mRNA signals in the vertebral column, heart and intestinal tract were significantly weaker. At high magnification, MTA1 signals were detected in the cytoplasm of neuronal cells in the cervical neuronal arch (Fig. 8a, lower panels). In accordance with the results of *in situ* hybridization, high levels of MTA1 mRNA expression were detected in the brain, lung and testis; high levels of MTA1 mRNA expression were also detected in the mammary gland by northern blotting of RNAs from several organs from female mice (Fig. 8b).

In situ-hybridization analysis of mouse mammary gland showed that MTA1 mRNA was present in the cytoplasm of virgin ducts, in the growing-end buds of the pregnant mammary gland, and in lactating alveoli (Fig. 8c). The signal was much stronger in the lactating alveoli and the virgin mammary gland than in the pregnant and the involuting mammary gland. Signals from the pregnant mammary gland were relatively weaker. Low levels of MTA1 expression were detected in the virgin fat-pad tissues.

As MTA1 regulates the function of ER in breast-cancer cells, we next examined the expression pattern of MTA1 during mammary-gland development, and the relationship between MTA1 expression and ER expression. The northern-blot analysis showed that MTA1 was expressed during all stages of mammary-gland development (Fig. 8d). The highest levels of MTA1 expression were observed during lactation, when ER levels were lower. These results indicate that MTA1 may regulate the expression of one or more ER target genes, and could influence ER function.

© 2000 Macmillan Magazines Ltd

Discussion

We have shown that MTA1 is a target of HRG in breast-cancer cells and that MTA1 represses ER-mediated transcription by recruiting HDACs. Recruitment of HDAC to promoters has emerged as a general mechanism of transciption repression of target genes. For example, recruitment of HDAC complex to target genes of the retinoic-acid receptor represses transcription and prevents differentiation, and treatment with retionic acid induces differentiation by displacing HDAC complex from PML–RAR-α (refs 29, 30). Similarly, transcription-repressor complexes containing HDAC have been discovered in the RB/E2F[31] and Myc/Mad (reviewed in ref. 32) pathways. Recruitment of HDACs to specific promoters may be mediated either through direct interactions with regulatory proteins such as transcription factor YY1 (ref. 33), or through interaction with corepressors containing an HDAC-interacting domain, such as Sin3A. Nuclear hormone receptors have been shown to bind to the corepressor N-CoR, which directly interacts with the Sin3A–HDAC corepressor complex[16].

Our observation that MTA1 can directly interact with HDAC1/2 and the AF2 domain of ER is important because it indicates that the reported association between MTA1 and HDACs in the NuRD complex[15–18] may reflect direct MTA1 interaction. In addition, we have identified specific nuclear targets and a corepressor function for MTA1, as it effectively suppressed ligand-induced activation of ER.

Expression of MTA1 correlates well with the metastasis potential of several human cancer cell lines and tissues[20–22]. However, direct evidence to link enhanced MTA1 expression with metastasis is currently lacking. MTA1 has been found to contain a domain (known as the WFY domain) that is similar to two regions of N-CoR[17]. The WFY domain of MTA1 is less likely to be involved in recruiting HDACs in our system, because we detected no appreciable interaction between MTA1 and N-CoR (data not shown). However, specific domains of MTA1 may directly associate with both HDAC2 and AF-2 (Fig. 5c). In summary, we have identified ER-mediated transcription as a nuclear target of corepressor MTA1, and have provided new evidence to support the idea that HDAC complexes are involved in MTA1-mediated transcriptional repression of oestrogen. □

Methods

Cell culture, transfection, cell extracts and reagents.

Breast-cancer MCF-7 cells[10] were maintained in DMEM–F12 (1:1 ratio) supplemented with 10% FCS. Cell lysates were prepared as described[10] and were resolved on a 10% SDS–polyacrylamide gel, transferred to nitrocellulose, and probed with the appropriate antibodies. Antibodies against HDAC1 and HDAC2 were from Santa Cruz; anti-T7 antibody was from Novagen. Transfection was carried out using the Fugene-6 kit (Roche) according to the manufacturer's instructions.

Northern blotting and promoter–reporter assays.

Total cytoplasmic RNA (20 μg) was analyzed by northern blotting[10]. For promoter assays, cells were transiently co-transfected with a reporter construct and β-galactosidase. Cells were collected with passive lysis buffer or were processed for CAT assay (Promega).

Construction of reporter systems.

3 × ERE–TATA–luciferase plasmid was from D. McDonnell (Duke Univ., Durham, North Carolina). 5 × GAL4 plasmid was from F. Claret, M. D. Anderson Cancer Center. Full-length MTA1 cDNA was isolated from a human mammary gland cDNA library (Invitrogen). MTA1 cDNA containing the entire reading frame of MTA1 was subcloned into pcDNA3.1–T7 vector using restriction sites *Eco*RI and *Xba*I to generate T7-tagged MTA1. To construct 5 × Gal4–ERE–luciferase construct, 5 × Gal4 sites were isolated by PCR using Gal4 5 × luciferase as a backbone (*Sma*I and *Kpn*I sites were added to primers) and subcloned into *Sma*I and *Kpn*I sites of 3 × ERE–TATA–luciferase plasmid. The identities of constructs were verified by sequencing.

In vitro transcription and translation.

In vitro transcription and translation of MTA1 proteins was carried out using the TNT transcription–translation system (Promega). MTA1 cDNA (1 μg) in pcDNA 3.1 vector was *in vitro* translated in the presence of [^{35}S]methionine in a reaction volume of 50 μl using the T7–TNT kit (Promega). The reaction was diluted to 1 ml with NP40 lysis buffer; an aliquot (250 μl) was used for each GST pull-down assay. Translation was verified by subjecting 2 μl of the reaction mixture to SDS–PAGE and autoradigraphy.

Histone–urea gels and deacetylase assays.

Histones were purified and resolved onto a 15% urea gel as described[34]. HDAC activity was measured by scintillation counting of [^{3}H]acetic acid released from ^{3}H-acetylated histones as described[17].

GST pull-down assay.

GST pull-down assays were carried out by incubating equal amounts of GST, GST–AF1, GST–AF2, GST–HDAC1 or GST–HDAC2 immobilized on glutathione–sepharose beads (Amersham) with *in vitro*-translated ^{35}S-labelled MTA protein. The mixture was incubated for 2 h at 4 °C and washed with NP40 lysis buffer; bound proteins were eluted with 2 × SDS buffer, separated by SDS–PAGE and developed by fluorography[35].

Production of stable cell lines expressing MTA1.

MCF-7 cells were transfected with pcDNA3.1 or pcDNA.T7–MTA1 using the calcium-phosphate method. Forty-eight hours after transfection, cells were selected in media containing 1 mg ml^{-1} G418. Several individual clones were isolated and expanded, and expression of exogenous MTA1 was verified by immunoblotting using anti-T7 monoclonal antibody.

Cell-proliferation, invasion and soft-agar assays.

Cell-invasion assays were carried out using Boyden chambers as described[36]. Cells were plated on the upper well of a Boyden chamber at a concentration of 20,000 cells per well. The lower side of the separating filter was coated with chemoattractant (thick layer of a 1:2 dilution of Matrigel (Life Technologies)) in serum-free medium. The number of cells that successfully migrated through the filter and invaded the 2-mm Matrigel layer, as well as those that remained on the upper side of the filter, were counted after staining with propidium iodide (Sigma). The percentage of the total number of cells that migrated was recorded; data are means ± s.e.m. from triplicate wells in three separate experiments.

Cell-proliferation assays were carried out using the 3-(4,5-dimethyl-thiazol-2-yl)diphenyltetraszolium bromide (MTT) dye method as described[9,10]. Soft-agar colony-growth assays were carried out as described[37]. Briefly, 1 ml of 0.6% DIFCO agar in DMEM supplemented with 10% FBS and insulin was layered onto 60 × 15-mm tissue-culture plates. MCF-7 cells (10,000 cells) were mixed with 1 ml of 0.36% Bactoagar solution in DMEM prepared in a similar manner and layered on top of the 0.6% Bactoagar layer. Plates were incubated at 37 °C in 5% CO_2 for 21 days.

Immunofluorescence confocal studies.

Cellular localization of T7–MTA1 and ER was determined using indirect immunofluorescence as described[10]. Briefly, cells grown on glass coverslips were fixed (without permeabilization) in ethanol/methanol (1:1) at −20 °C for 3 min. Cells were treated with or without anti-T7 monoclonal antibody or anti-ER antibody and were then treated with Alexa-546-labelled goat anti-mouse antibody or Alexa-488 (Molecular Probes). For controls, cells were treated only with the secondary antibodies. Images are z-sections taken at the same cellular level and magnification. Confocal analysis was carried out using a Zeiss laser-scanning confocal microscope and the established methods, involving processing of the same section for each detector (two excitations corresponding to 546 and 488 nm) and comparing images pixel by pixel. Co-localization of the two proteins is indicated by the presence of yellow color as a result of overlapping red and green pixels.

Chromatin immunoprecipitation (ChIP) assays.

Quantitative ChIP assays were carried out as described[38,39]. Cells were treated with 37% formaldehyde solution (final concentration 1%) to crosslink T7–MTA1 or HDAC2 to DNA. Cells were washed twice with PBS (pH 7.4) containing protease-inhibitor cocktail (Roche) and were then lysed with lysis buffer containing 1% SDS and sonicated as described[38]. Supernatants from sonicated lysates were diluted ten-fold with chromatin-dilution buffer containing 0.01% SDS, 1.1% Triton X-100 and protease-inhibitor cocktail. For input DNA, 1% of the chromatin solution was kept aside before immunoprecipitation. Chromatin solutions were immunoprecipitated with anti-T7 (Novagen) or anti-HDAC2 antibody (Santa Cruz) at 4 °C overnight. Beads were washed as described[1] on a rotating platform before finally eluting antibody-bound chromatin by incubation with 400 μl of 1% SDS containing 0.1 M $NaHCO_3$. The eluate, as well as the input chromatin, was heated to 65 °C for 6 h to reverse the formaldehyde crosslinks, and was then subjected to phenol-chloroform extraction. The supernatant was ethanol-precipitated and resuspended in 50 μl of 10 mM Tris–1 mM EDTA, pH 7.4. Quantitative PCR analysis was carried out with 10 μl of DNA sample restricted to 25 cycles. Our pS2 gene primers[27] amplify the region including the ER-responsive element from position −463 to −159; c-Myc gene primers[28] amplify the region from −65 to +192. PCR products were resolved on 1.5% agarose gel and visualized with ethidium bromide. Images were quantified using Sigma gel-analysis software, version 1.

In situ hybridization.

For *in situ* hybridization, mouse mammary-gland tissues or 18-day-old embryos (E18) were cut out and fixed with 10% neutral-buffered formaldehyde and processed routinely to make paraffin sections as described[40]. *In situ* hybridization was carried out in frozen sections using the digoxigenin-labelled riboprobe (Roche). A 290-bp fragment of mouse MTA1 cDNA corresponding to bases 1,781–2,070 of the human MTA1 mRNA region was amplified by RT-PCR, subcloned into the TOPO II vector (Promega) and used for riboprobe synthesis. RNA probes were labelled with digoxigenin and hybridized for 16–20 h in buffer containing 1 μg ml^{-1} riboprobes, 50% formamide, 300 mM NaCl, 10 mM Tris pH 7.4, 10 mM NaH_2PO_4 pH 6.8, 5 mM EDTA pH 8.0, 0.2% Ficoll 400, 0.2% polyvinyl pyrolidone, 10% dextran sulphate, 200 μg ml^{-1} yeast total RNA and 50 mM dithiothreitol. Alkaline-phosphatase-labelled sheep anti-digoxigenin antibody was applied and signals were visualized by NBT-BCIP. Sense-probe hybridization was used for background control.

RECEIVED 15 MAY 2000; REVISED 14 AUGUST 2000; ACCEPTED 18 SEPTEMBER 2000; PUBLISHED 6 DECEMBER 2000.

1. Nass, S. J. & Davidson, N. E. The biology of breast cancer. *Hematol. Oncol. Clin. N. Am.* 13, 311–332 (1999).
2. Muss, H. B. *et al.* c-erbB-2 expression and response to adjuvant therapy in women with node-posi-

© 2000 Macmillan Magazines Ltd

tive early breast cancer. *N. Engl. J. Med.* **330**, 1260–1266 (1994).
3. Borg, A. *et al.* ERBB2 amplification is associated with tamoxifen resistance in steroid-receptor positive breast cancer. *Cancer Lett.* **81**, 137–144 (1994).
4. Wright, C. *et al.* Relationship between c-erbB-2 protein product expression and response to endocrine therapy in advanced breast cancer. *Br. J. Cancer* **65**, 118–121 (1992).
5. Benz, C. C. *et al.* Estrogen-dependent, tamoxifen-resistant tumorigenic growth of MCF-7 cells transfected with HER2/neu. *Breast Cancer Res. Treat.* **24**, 85–95 (1995).
6. Hynes, N. C. & Stern, D. F. The biology of erbB-2/neu/HER-2 and its role in cancer. *Biochim. Biophys. Acta* **1198**, 165–184 (1994).
7. Pietras, R. J. *et al.* HER-2 tyrosine kinase pathway targets estrogen receptor and promotes hormone-independent growth in human breast cancer cells. *Oncogene* **10**, 2435–2446 (1995).
8. Kumar, R., Mandal, M., Ratzkin, B. J., Liu, N. & Lipton, A. NDF induces expression of a novel 46 kD protein in estrogen receptor positive breast cancer cells *J. Cell. Biochem.* **62**, 102–112 (1995).
9. Tang, C. K. *et al.* Involvement of heregulin-beta2 in the acquisition of the hormone-independent phenotype of breast cancer cells. *Cancer Res.* **56**, 3350–3358 (1996).
10. Adam, L. *et al.* Heregulin regulates cytoskeletal reorganization and cell migration through the p21-activated kinase-1 via phosphatidylinositol-3 kinase. *J. Biol. Chem.* **273**, 28238–28246 (1998).
11. Owen-Hughes, T. & Workman, J. L. Experimental analysis of chromatin function in transcription control. *Crit. Rev. Eukaryot. Gene. Expr.* **4**, 403–441 (1994).
12. Owen-Hughes, T., Utley, R. T., Cote, J., Peterson, C. L. & Workman, J. L. Persistent site-specific remodeling of a nucleosome array by transient action of the SWI/SNF complex. *Science* **273**, 513–516 (1996).
13. Paranjape, S. M., Kamakaka, R. T. & Kadonaga, J. T. Role of chromatin structure in the regulation of transcription by RNA polymerase II. *Annu. Rev. Biochem.* **63**, 265–297 (1994).
14. Brownell, J. E. *et al.* Tetrahymena histone acetyltransferase A: a homolog to yeast Gcn5p linking histone acetylation to gene activation. *Cell* **84**, 843–851 (1996).
15. Hassig, C. A., Fleischer, T. C., Billin, A. N., Schreiber, S. L. & Ayer, D. E. Histone deacetylase activity is required for full transcriptional repression by mSin3A. *Cell* **89**, 341–347 (1997).
16. Laherty, C. D. *et al.* Histone deacetylases associated with the mSin3 corepressor mediate mad transcriptional repression. *Cell* **89**, 349–356 (1997).
17. Xue, Y. *et al.* NURD, a novel complex with both ATP-dependent chromatin-remodeling and histone deacetylase activities. *Mol. Cell* **2**, 851–861 (1998).
18. Zhang, Y. *et al.* Analysis of the NuRD subunits reveals a histone deacetylase core complex and a connection with DNA methylation. *Genes Dev.* **13**, 1924–1935 (1999).
19. Toh, Y. *et al.* Molecular analysis of a candidate metastasis-associated gene, MTA1, possible interaction with histone deacetylase 1. *J. Exp. Clin. Cancer Res.* **19**, 105–111 (2000).
20. Toh, Y., Pencil, S. D. & Nicolson, G. L. A novel candidate metastasis-associated gene, *mta1*, differentially expressed in highly metastatic mammary adenocarcinoma cell lines. cDNA cloning, expression, and protein analyses. *J. Biol. Chem.* **269**, 229–263 (1994).
21. Toh, Y. *et al.* Overexpression of the MTA1 gene in gastrointestinal carcinomas: correlation with invasion and metastasis. *Int. J. Cancer* **74**, 459–463 (1997).
22. Toh, Y., Kuwano, H., Mori, M., Nicolson, G. L. & Sugimachi, K. Overexpression of metastasis-associated MTA1 mRNA in invasive oesophageal carcinomas. *Br. J. Cancer* **79**, 1723–1726 (1999).
23. Kleene, R., Zdzieblo, J., Wege, K. & Kern, H-F. A novel zymogen granule protein (ZG29p) and the nuclear protein MTA1p are differentially expressed by alternative transcription initiation in pancreatic acinar cells of the rat. *J. Cell Sci.* **112**, 2539–2548 (1999).
24. Krane, I. M. & Leder, P. NDF/heregulin induces persistence of terminal end buds and adenocarcinomas in the mammary glands of transgenic mice. *Oncogene* **12**, 1781–1788 (1996).
25. Henttu, P. M., Kalkhoven, E. & Parker, M. G. AF-2 activity and recruitment of steroid receptor coactivator 1 to the estrogen receptor depend on a lysine residue conserved in nuclear receptors. *Mol. Cell. Biol.* **17**, 1832–1839 (1997).
26. Fan, S. *et al.* BRCA1 inhibition of estrogen receptor signaling in transfected cells. *Science* **284**, 1354–1356 (1999).
27. Berry, M., Nunez, A. M. & Chambon, P. Estrogen-responsive element of the human pS2 gene is an imperfectly palindromic sequence. *Proc. Natl Acad. Sci USA* **86**, 1218–1222 (1989).
28. Dubik, D. & Shiu, R. P. C. Mechanism of estrogen activation of c-myc oncogene expression. *Oncogene* **7**, 1587–1594 (1992).
29. Lin, R. J. *et al.* Role of the histone deacetylase complex in acute promyelocytic leukaemia. *Nature* **391**, 811–814 (1998).
30. Grignani, F. *et al.* Fusion proteins of the retinoic acid receptor-alpha recruit histone deacetylase in leukaemia. *Nature* **391**, 815–818 (1998).
31. Brehm, A. *et al.* Retinoblastoma protein recruits histone deacetylase to repress transcription. *Nature* **391**, 597–601 (1998).
32. Kouzarides, T. Histone acetylases and deacetylases in cell proliferation. *Curr. Opin. Genet. Dev.* **9**, 40–48 (1999).
33. Yang, W. M., Inouye, C., Zeng, Y., Bearss, D. & Seto, E. Transcriptional repression by YY1 is mediated by interaction with a mammalian homolog of the yeast global regulator RPD3. *Proc. Natl Acad. Sci. USA* **93**, 12845–12850 (1996).
34. Boffa, L. C., Vidali, G., Mann, R. S. & Allfrey, V. G. Suppression of histone deacetylation *in vivo* and *in vitro* by sodium butyrate. *J. Biol. Chem.* **253**, 3364–3366 (1978).
35. Yang, W. M., Yao, Y. L., Sun, J. M., Davie, J. R. & Seto, E. Isolation and characterization of cDNAs corresponding to an additional member of the human histone deacetylase gene family. *J. Biol. Chem.* **272**, 28001–28007 (1997).
36. Adam, L., Vadlamudi, R., Mandal, M., Chernoff, J. & Kumar, R. Regulation of microfilament reorganization and invasiveness of breast cancer cells by p21-activated kinase-1 K299R. *J. Biol. Chem.* **275**, 12041–12050 (2000).
37. Vadlamudi, R. *et al.* Regulatable expression of p21-activated kinase-1 promotes anchorage-independent growth and abnormal organization of mitotic spindles in human epithelial breast cancer cells. *J. Biol. Chem.* **275**, 36238–36244 (2000).
38. Braunstein, M., Rose, A. B., Holmes, S. G., Allis, C. D. & Broach, J. R. Transcritional silencing in yeast is associated with reduced nucleosome acetylation. *Genes Dev.* **7**, 592–604 (1993).
39. Hecht, A., Strahl-Bolsinger, S. & Grunstein, M. Spreading of transcriptional repressor SIR3 from telomeric heterochromatin. *Nature* **383**, 92–96 (1996).
40. Wang, R. A. & Zhao, G. Q. Transforming growth factor beta signal transducer Smad2 is expressed in mouse meiotic germ cells, Sertoli cells, and Leydig cells during spermatogenesis. *Biol. Reprod.* **61**, 999–1004 (1999).

ACKNOWLEDGEMENTS

We thank D. Allies for anti-acetylated H4 antibody, D. McDonnell for 3X-ERE TATA, P. Leder for heregulin transgenic mice, F. Claret for 5XGAL4, W. Wang for Gal4–MTA1 and anti-CHD4 antibody, D. Shapiro for ERE-reporter systems, M. R. Parker for AF1 and AF2 fusion-protein expression vectors, E. Seto for HDACs expression vectors, S. Roth for HDAC assay substrate and useful tips, D. Stern for HER2 constructs, M-C. Hung for the Gal4 system, W. Schmid for GRE–CAT promoter constructs, R. Kleene for anti-MTA1 antibody, and D. Reinberg for anti-MTA2 antibody. This study was supported by NIH grants CA80066, CA65746 and CA84456, by the Breast Cancer Research Program of The University of Texas M. D. Anderson Cancer Center (to R.K.), and by Cancer Center Core grant CA16672.

Correspondence and requests for materials should be addressed to R.K. Supplementary Information is available on *Nature Cell Biology*'s website (http://cellbio.nature.com) or as paper copy from the London editorial office of *Nature Cell Biology*.

© 2000 Macmillan Magazines Ltd

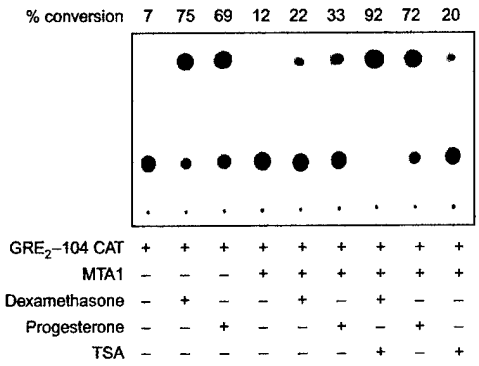

Figure S1 **MTA1 act as a global steroidal repressor.** MCF-7 cells were co-transfected with a GRE–CAT promoter–reporter construct and MTA1 or with a vector control. Some cultures were treated with dexamethasone (500 nM) or progesterone (500 nM) for 16 h, and cell extracts were assayed for CAT activity ($n = 4$).

© 2000 Macmillan Magazines Ltd

Oncogene (2001) 20, 2537–2543
© 2001 Nature Publishing Group All rights reserved 0950–9232/01 $15.00
www.nature.com/onc

Transcriptional upregulation and activation of p55Cdc via p34^{cdc2} in Taxol-induced apoptosis

Keishi Makino[1], Dihua Yu[2] and Mien-Chie Hung*[,1,2]

[1]*Department of Molecular and Cellular Oncology, The University of Texas MD Anderson Cancer Center, Houston, Texas, TX 77030, USA;* [2]*Department of Surgical Oncology, The University of Texas MD Anderson Cancer Center, Houston, Texas, TX 77030, USA*

Paclitaxel (Taxol) is a potent and highly effective antineoplastic agent for the treatment of advanced, drug-refractory, metastatic breast cancers. Taxol not only induces tubulin polymerization, stabilizes microtubules, blocks cell cycle progression, and induces apoptosis, but it also alters gene expression. Here, we have identified that Taxol can upregulate expression of the gene encoding the cell cycle protein p55Cdc by using cDNA array technique. Taxol induced p55Cdc mRNA expression through activation of the p55Cdc promoter, which led to increase p55Cdc protein expression. Taxol also activated p55Cdc-associated kinase. In addition, overexpression of the p55Cdc gene resulted in cell death in both HeLa cells and NIH3T3 cells in a dose-dependent manner. A dominant-negative mutant of p34^{cdc2} blocked Taxol-induced p55Cdc activation and inhibited p55Cdc-induced and Taxol-induced cell death. Our data suggest that transcriptional upregulation of p55Cdc and activation of p55Cdc by Taxol-mediated p34^{cdc2} activation play a critical role in Taxol-induced cell death. *Oncogene* (2001) **20,** 2537–2543.

Keywords: cDNA array; Taxol; p55Cdc; p34^{cdc2}; apoptosis

Introduction

Paclitaxel (Taxol), a diterpene compound, was originally isolated from the stem bark of *Taxus brevifolia* and shown to have antiproliferative activity in various cultured cancer cells and antineoplastic activity in cancer patients (Wani *et al.*, 1971). These effects appear to be related to Taxol's ability to bind tubulin, to promote microtubule assembly, and to stabilize microtubules by bundle formation (Kumar, 1981; Schiff *et al.*, 1979; Schiff and Horwitz, 1980). Taxol has also been shown to alter gene expression (Ding *et al.*, 1990; Bogdan and Ding., 1992). Thus, identification and characterization of changes in gene expression profiles in response to Taxol treatment may lead to a better understanding of mechanisms for Taxol-mediated activity and facilitate design of novel cancer therapies. The recently described cDNA array or DNA chip technology allows monitoring of expression of thousands of genes simultaneously and provides a format for identifying genes and changes in their activities (Shena *et al.*, 1995; Shalon *et al.*, 1996; Heller *et al.*, 1997; DeRisi *et al.*, 1996). The p55Cdc gene product is a cell cycle protein expressed in proliferating cells but not in differentiated, growth-arrested cells (Weinstein *et al.*, 1994). This protein has homology to *Saccharomyces cerevisiae* proteins Cdc4 and Cdc20, which are believed to regulate DNA synthesis and mitosis, respectively (Weinstein *et al.*, 1994; Choi *et al.*, 1990). Furthermore, overexpression of p55Cdc in a myeloid leukemic cell line resulted in increased serum- and factor-starved apoptosis, and inducible expression increased cell death in the same cell line (Kao *et al.*, 1996; Lin *et al.*, 1998). Using the cDNA array technique in this study, we found that Taxol could induce p55Cdc gene expression in HeLa cells. Taxol also induced both p55Cdc mRNA and protein expression in a dose-dependent manner. Furthermore, p55Cdc expression resulted in increased cell death, but dominant-negative p34^{cdc2} could inhibit p55Cdc-induced and Taxol-induced cell death. These results suggest that p55Cdc may play a role in Taxol-mediated apoptosis.

Results and discussion

To elucidate Taxol-mediated gene expression profiles in cultured cells, we performed differential hybridization analysis of cDNAs from HeLa, MDA-MB-435, 435-eB.1 (Her2/neu stable transfectant of MDA-MB-435) and MCF-10A cell lines grown with or without Taxol treatment and then hybridized to an Atlas cDNA expression array (Clontech). The expression of eight genes in HeLa, 18 genes in MDA-MB-435, 31 genes in 435-eB,1 and 17 genes in MCF-10A cells were upregulated with Taxol treatment (data not shown). Expression of nuclear factor 90 (NF90), fos-related antigen-2 (FRA-2), p55Cdc and transcriptional factor PAX3 were commonly high and transcriptional initiation factor TFIID subunit TAFII31, transferrin receptor, RNA polymerase II elongation factor SIII

*Correspondence: M-C Hung, The Department of Molecular and Cellular Oncology, Box 108, The University of Texas MD Anderson Cancer Center, 1515 Holcombe Boulvard, Houston, TX 77030, USA
Received 9 October 2000; revised 31 January 2001; accepted 12 February 2001

and CD44 were lower in these cell lines (data not shown). Among these, p55Cdc expression with Taxol treatment was 20-fold higher than that of nontreatment in HeLa cell (Figure 1a), and six- or twofold higher in 435-eB.1 or MCF-10A cells (data not shown). Thus, in all three cell lines tested, the p55Cdc RNA expression was found to be increased by Taxol treatment, though the increased level is not exactly the same. To confirm upregulation of p55Cdc expression by Taxol, we performed RT–PCR in various cell lines. The upregulation was detected in HeLa and MCF-7 cells (Figure 1b). To determine whether an increase in p55Cdc RNA resulted in an increase in p55Cdc protein, protein lysates were prepared from HeLa and MCF-7 cells after Taxol treatment. As shown in Figure 1c, 0.1 μM Taxol clearly caused an increase in p55Cdc protein levels in these cell lines. The p55Cdc protein is known to play a role in mitosis (Shteinberg *et al.*, 1999; Kotani *et al.*, 1999), Taxol induce mitotic block at the metaphase/anaphase transition in HeLa cells by stabilizing spindle microtubles (Jordan *et al.*, 1993). Activity of the p55Cdc-associated myelin basic protein kinase peaks in the G2/M phase in HeLa cells, paralleling Taxol-induced mitotic block (Farruggio *et al.*, 1999). To examine whether Taxol could activate the p55Cdc-associated kinase, p55Cdc proteins were immunoprecipitated with anti-p55Cdc antibody from Taxol-treated or -untreated HeLa cell lysates and tested for the kinase activity of phosphorylation of myelin basic proteins. As shown in Figure 1d, Taxol not only induced expression of p55Cdc, but also enhanced activity of the p55Cdc-associated kinase.

To determine whether Taxol can induce transcriptional activity of the p55Cdc promoter, we subcloned 1000 bp of the rat p55Cdc promoter (Weinstein *et al.*, 1998) into the pGL2 vector, which contains the luciferase reporter gene. The construct was transiently transfected into HeLa cells with or without Taxol treatment, and then the transcriptional activity of the p55Cdc promoter was measured at various time. After 48 h, the relative activity of the p55Cdc-driven luciferase reporter gene was 5.6 times greater in the treated cells (Figure 2). Thus, Taxol can activate the p55Cdc promoter and enhance p55Cdc transcription, which contributes to increased p55Cdc RNA and protein expression and p55Cdc-associated kinase activity.

When the orderly progression of the cell cycle disrupted, an abnormal mitosis (mitotic catastrophe) occurs. This aberrant process takes place when cell cycle components are overexpressed or sustain mutations (Russel and Nurse, 1987; Heald *et al.*, 1993). Deregulation of these cell cycle components leads to hyperactiva-

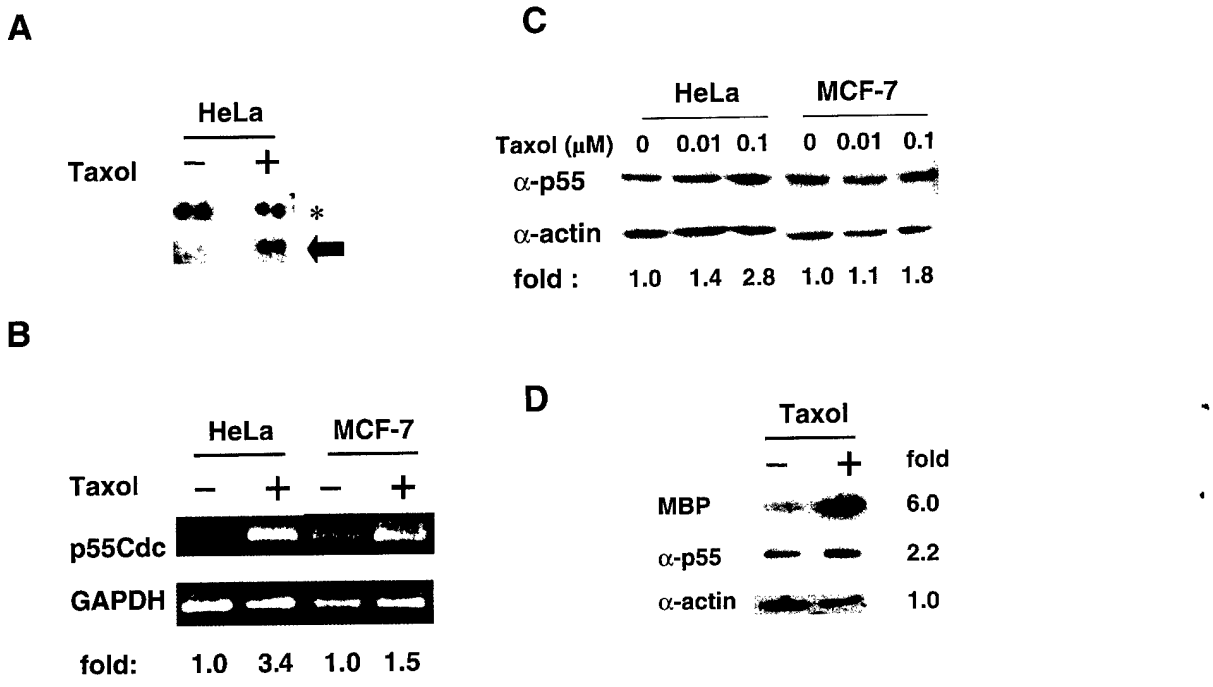

Figure 1 mRNA and protein expression of p55Cdc by Taxol treatment. (**a**) HeLa cells were treated with 0.1 μM Taxol (+) or without Taxol (−), and gene expression was analysed using cDNA array. Arrow indicates p55Cdc gene expression, and asterisk indicates SAS (transmembrane 4 superfamily protein) which was located near by p55Cdc on the membranes. (**b**) HeLa and MCF-7 cells were treated with (+) or without (−) 0.1 μM Taxol for 24 h, and p55Cdc gene expression was analysed by RT–PCR. GAPDH was used as a control. The numbers at the bottom show fold induction. (**c**) p55Cdc protein expression was analysed in HeLa and MCF-7 cells by Western blot analysis after exposure to Taxol for 24 h. Actin was used as a protein loading control. The numbers at the bottom show fold induction. (**d**) Activation of the p55Cdc- associated kinase by Taxol treatment. Extracts were prepared from HeLa cells treated with 0.1 μM Taxol (+) or without Taxol (−) for 24 h and incubated with anti-p55Cdc antibody. Immunoprecipitates were assayed for associated kinase activity toward myelin basic protein (MBP). Samples were analysed by SDS–PAGE followed by phosphoimaging

tion of cdc2 at an inappropriate time during the cell cycle. Cdk activation induced by inappropriately bypassing mitotic checkpoints may result in death to the cell in a manner similar to that seen in mitotic catastrophe (Shi *et al*., 1994; Meikrantz *et al*., 1994). To address whether p55Cdc plays a functional role in Taxol-mediated responses, we examined the effect of increased p55Cdc expression on programmed cell death. We amplified the full-length ORF of the p55Cdc cDNA, which was subcloned into pCGN-p55Cdc and transiently transfected into HeLa cells and 293T cells (Figure 3a). Overexpression of HA-tagged p55Cdc resulted in decreased expression of cyclin B1 (Figure 3a). These finding indicate that overexpression of p55Cdc results in activation of cyclosome/anaphase promoting complex (APC). Next, we asked whether overexpression of p55Cdc results in decrease in cell viability. The pCGN-p55Cdc expression vector were cotransfected with a pCMV-luciferase reporter gene construct which expressed in living cells but not in dead cells. Luciferase activity was quantitated and normalized by β-gal activity. Expression of p55Cdc resulted in decreased survival in a dose-dependent manner (Figure 3b). Thus, upregulation of p55Cdc expression can activate cyclosome/APC and lead to decrease cell viability.

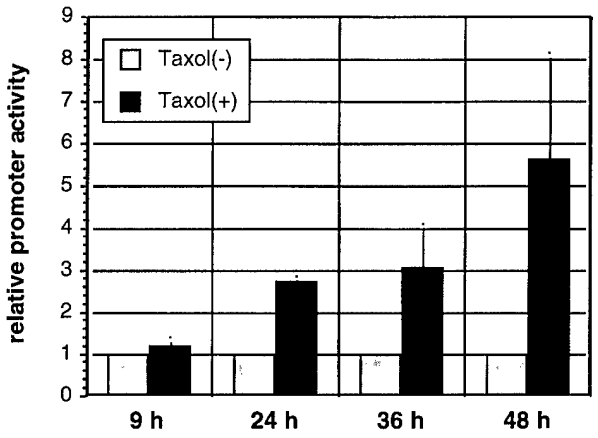

Figure 2 Activation of the p55Cdc promoter with Taxol treatment. Five micrograms of the luciferase reporter gene driven by the p55Cdc promoter were transfected into HeLa cells on 100 mm dishes. Twenty-fours after transfection, cells were split onto six-well plates with (+) or without Taxol (−). Luciferase activity was measured at indicated time points and normalized by measurement of protein concentration and β-gal activity. Data represent the average of three independent experiments

Since Taxol can induce both cell death and p55Cdc expression, we ask whether Taxol-induced p55Cdc expression may contribute to Taxol-induced apoptosis. We had previously shown that activation of $p34^{cdc2}$ at G2/M phase of cell cycle is required for Taxol-induced apoptosis in breast cancer cells because Taxol-mediated activation of $p34^{cdc2}$ kinase occurred prior to Taxol-induced apoptosis and inhibition of Taxol-mediated activation of $p34^{cdc2}$ kinase by the dominant-negative mutant of $p34^{cdc2}$ diminished Taxol-induced apoptosis (Yu *et al*., 1998). Because p55Cdc is phosphorylated by cdc2-cyclinB, and this phosphorylation is required for p55Cdc-dependent cyclosome/APC activation (Kotani *et al*., 1999), we therefore investigate whether Taxol-induced $p34^{cdc2}$ activation is involved in Taxol-mediated p55Cdc activation and if a potential relationship between $p34^{cdc2}$ and p55Cdc induces cell death. We

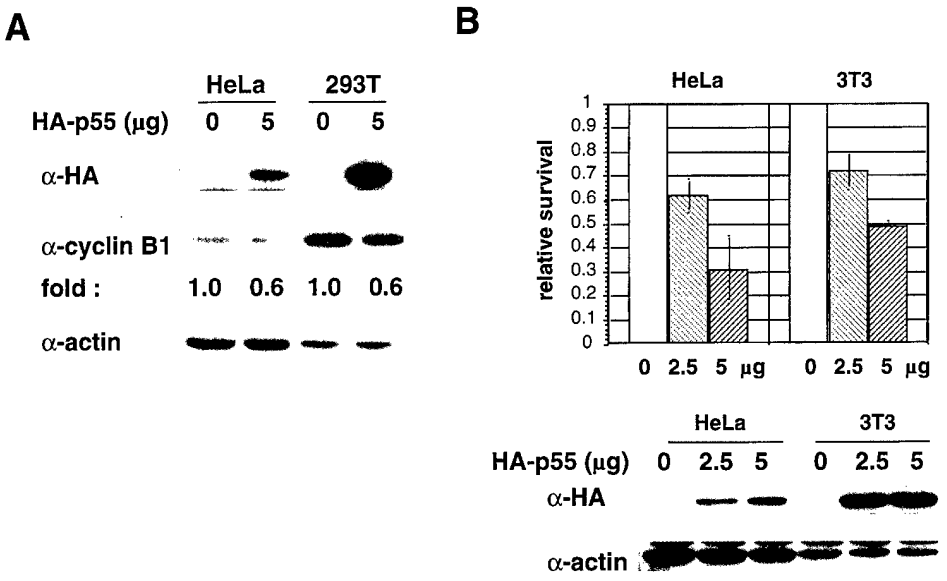

Figure 3 Effect of overexpression of p55Cdc on cell survival. (**a**) Lysate prepared from HeLa cells and 293T cells transfected with HA-tagged p55Cdc expression vectors (0 or 5 μg) were detected by anti-HA and anti-Cyclin B1 antibodies. (**b**) Two different dose (2.5 or 5 μg) of HA-tagged p55Cdc expression vectors were cotransfected with luciferase reporter plasmids and β-gal plasmids for normalizing transfection efficiencies in HeLa and NIH3T3 cells. Twenty-four hours after transfection, medium were changed to serum free conditions and cells were incubated for another 48 h. Cells were harvested, luciferase activity was measured, and survival ratios (HA-p55Cdc/vector only) were determined. Data represent the average of three independent experiments. HA-tagged p55Cdc protein expression was confirmed by Western blot analysis using anti-HA antibody

cotransfected pCGN-p55Cdc and pCMV-cdc2-dn expression vectors into HeLa cells. The dominant-negative mutant of cdc2 inhibited p55Cdc-induced (Figure 4a-1) and Taxol-induced cell death (Figure 4a-2), but not serum-starved cell death (Figure 4a-3). Thus, the pathways of p55Cdc- and Taxol- induced cell death seems to be different from serum-starved induced cell death. The overexpression of p55Cdc resulted in decrease in expression of cyclin B1. However, coexpression of dominant-negative cdc2 inhibited p55Cdc overexpression mediated cyclin B1 regulation (Figure 4b). Furthermore, forced expression of p55Cdc and Taxol treatment resulted in activation of the p55Cdc-associated kinase. Expression of dominant-negative cdc2 inhibited p55Cdc overexpression- and Taxol-induced p55Cdc-associated kinase activity (Figure 4c).

The expression level of p55Cdc is known to fluctuate during the cell cycle. Protein levels of p55Cdc peak in M phase and phosphorylation of p55Cdc is detected during mitosis (Weinstein, 1997; Kramer *et al*., 1998). To study whether the Taxol-induced expression of p55Cdc occurred as a result of mitotic-arrest by Taxol, cells were synchronized at the G1/S boundary by double thymidine block and then treated with Taxol for 8 h. Both mRNA and protein levels of p55Cdc were low at G1/S boundary (Figure 5a,b). However, increased expression of both mRNA and protein of p55Cdc were observed after 8 h Taxol treatments (Figure 5a,b). Furthermore, when cells were treated at 8 h after the release from thymidine block, there is no increase in p55Cdc expression. As a matter of fact, double block was observed and protein level was

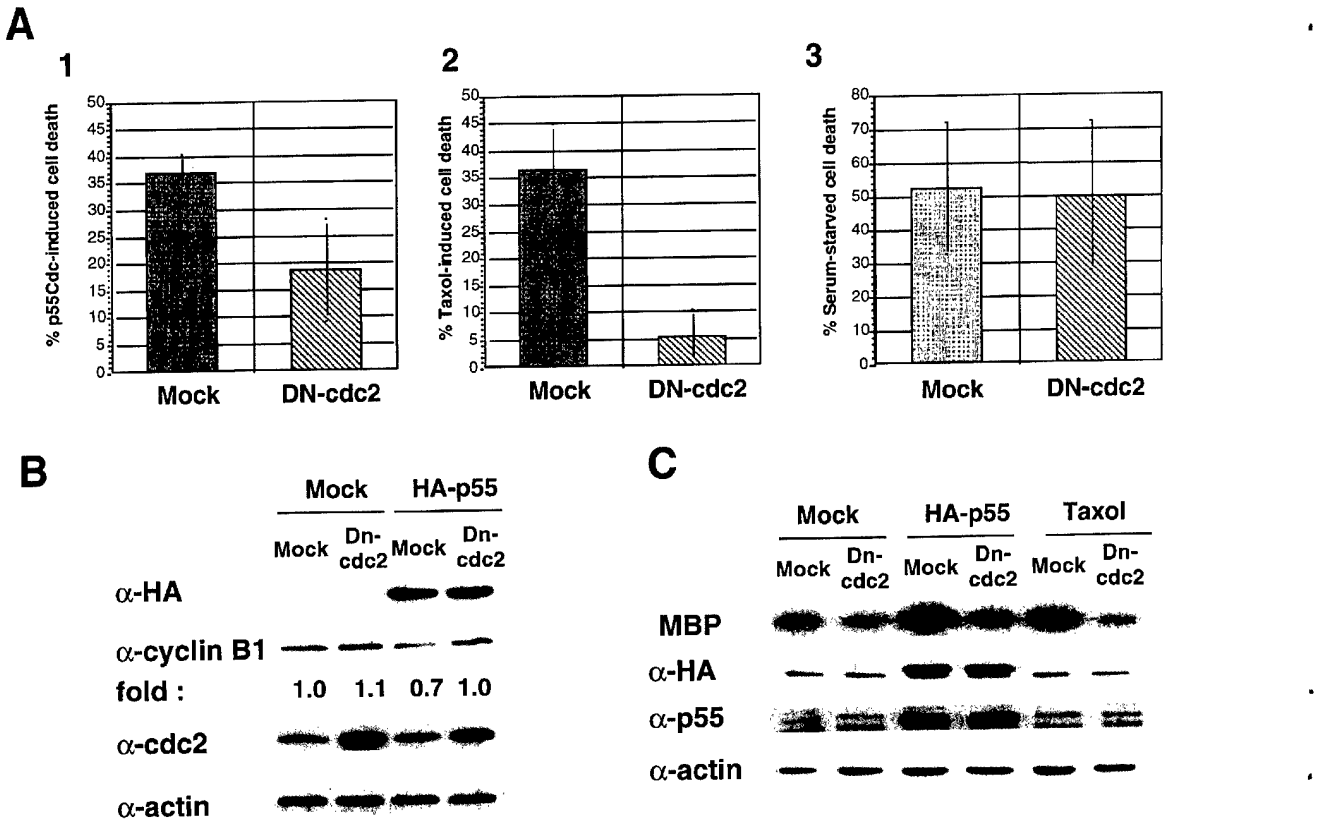

Figure 4 Effect of dominant-negative mutant of $p34^{cdc2}$ on p55Cdc-induced and Taxol-induced cell death. (**a**) Inhibition of p55Cdc-induced and Taxol-induced cell death by the dominant-negative mutant of $p34^{cdc2}$ (DN-cdc2). (1) 2.5 μg of HA-tagged p55Cdc expression vectors or control empty vectors were cotransfected into HeLa cells with DN-cdc2 or empty vectors (Mock) and with luciferase and β-gal plasmids normalizing transfection efficiencies. Luciferase activity was measured, and survival ratios (HA-p55Cdc/vector only) were determined. Per cent cell death were calculated by subtraction the numbers of survival ratios of HA-p55Cdc from these of empty vector and compared between DN-cdc2 and Mock transfections. (2,3) HeLa cells were cotransfected with DN-cdc2 or empty vectors (Mock) and luciferase and β-gal plasmids. Luciferase activity was measured, survival ratios (Taxol/nontreatment or serum-starved/nontreatment) were determined. Per cent cell death were calculated by subtraction the numbers of survival ratios of Taxol treatment or serum-starvation treatment from these of nontreatment and compared between DN-cdc2 and Mock transfections. Data represent the average of three independent experiments. (**b**) Inhibition of p55Cdc-mediated APC/cyclosome activation by DN-cdc2. HA-tagged p55Cdc expression vectors or control empty vectors were cotransfected into 293T cells with DN-cdc2 or empty vectors (Mock). The transfection efficiency of 293 T is approximately 30–40% under our standard protocols. The cell lysates were immunoblotted with anti-p55Cdc, anti-Cyclin B1 and anti-cdc2 antibodies. Actin was used as a protein loading control. (**c**) Inhibition of p55Cdc-induced and Taxol-induced p55Cdc associated kinase activity by DN-cdc2. Cells were treated as in **a** and were collected and assayed for p55Cdc-associated kinase activity as in Figure 1D. The protein levels of HA and p55Cdc were determined by Western blot analysis. Actin was used as a protein loading control

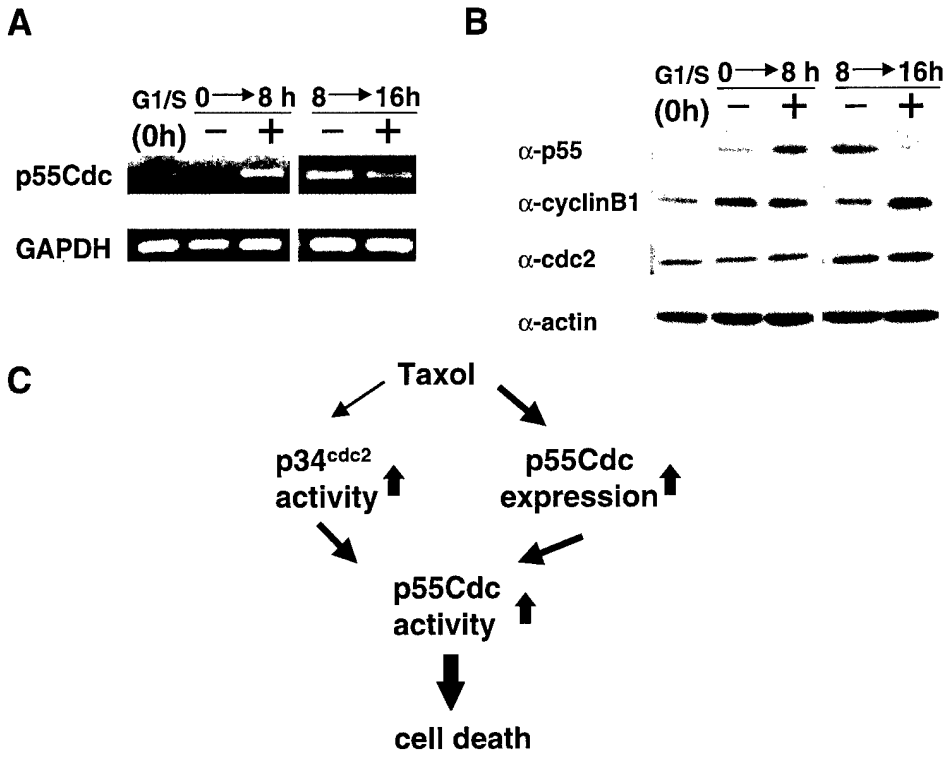

Figure 5 Effect of mitotic arrest on both mRNA and protein expression of p55Cdc. HeLa cells were synchronized at the G1/S boundary by double thymidine block and released into the cell cycle. The cells were then exposed to Taxol (0.1 μM, (+)) for 8 h at the beginning of the release from thymidine block (most of cells were in G1/S phase) or at 8 h after the release from thymidine block (M phase) in the absence of serum. After 8 h incubation, cells were harvested and both RNA and cell lysates were prepared. (**a**) p55Cdc gene expression was analysed by RT–PCR. GAPDH was used as a control. (**b**) The cell lysates were immunoblotted with anti-p55Cdc, anti-Cyclin B1 and cdc2 antibodies. Actin was used as a protein loading control. (**c**) A model to demonstrate Taxol-mediated cell death through $p34^{cdc2}$ and p55Cdc

reduced (Figure 5b). Thus, these findings suggest that increased p55Cdc expression is probably induced as a result of mitotic-arrest by Taxol.

As mentioned previously, p55Cdc-associated kinase activity is correlated with Taxol-induced mitotic block. This mitotic block is followed by an abnormal exit from mitosis into an interphase-like state with no accompanying cytokinesis. The block appears to be sufficient to inhibit further cell proliferation and to induce cell death by apoptosis (Jordan *et al*., 1996). In the present work, we showed that Taxol can induce p55Cdc, which is a known regulator of mitosis. The data suggest that Taxol induces cell death not only by regulating stabilization of microtubles but also by directly regulating mitotic regulators. In this regard, both transcriptional upregulation of p55Cdc and activation of p55Cdc by Taxol-mediated $p34^{cdc2}$ kinase activity may contribute to the Taxol-induced cell death (Figure 5c).

Materials and methods

Cell culture

HeLa cells (human epithelioid cervical cancer cell line), NIH3T3 cells (mouse fibroblast cell lines) and human breast cancer cell lines MCF-7 and MDA-MB-435 were maintained in DMEM/F12 medium containing 10% fetal bovine serum (37°C, 5% CO_2). The 435-eB transfectants were established and cultured as previously reported (Yu *et al*., 1996). MCF-10A cells (normal human breast epithelial cell line) were maintained in DMEM/F12 medium containing 5% horse serum with insulin (10 μg/ml), epidermal growth factor (20 ng/ml), cholera endotoxin (100 ng/ml), hydrocortisone (0.5 μg/ml), and calcium (1.05 mM). Cells were seeded at densities of 1×10^5 cells/ml so that they grew in log phase for the duration of each experiment. Two days after seeding, cells were grown in fresh medium with Taxol (0.1 μM) or without Taxol (Bristol-Meyers Squibb Co.) for 24 h.

Differential hybridization of cDNA expression arrays

Total RNA was isolated from cells using Trizol reagent (Life Technologies) according to the protocol recommended by the manufacturer. Poly $(A)^+$ RNA was purified from 250–300 μg of total RNA using the Oligotex purification (QIAGEN) according to the protocol recommended by the manufacturer. RNA was precipitated at −70°C for 1 h with 3 M sodium acetate (pH 5.2) and 100% ethanol. After drying, the RNA pellet was resuspended in 7.5 μl of DEPC-treated water and 2 μl of CDS primer (0.02 μM) (Clontech) and incubated at 70°C for 10 min. After placing the reaction mixture on ice, 2 μl of 10 × reaction buffer, 2 μl of 25 mM $MgCl_2$, 1 μl of dNTPs (5 mM dATP, dGTP, and dTTP and 50 nM dCTP), 2 μl of 100 mM DTT and 3.5 μl of

[α-^{32}P]dCTP (10 μCi) were added, and the mixture was incubated at 42°C for 5 min. One microliter of SuperScriptII reverse transcriptase (Life Technologies) was added, and incubated at 42°C for 1 h. After purification using a spin column, cDNAs were hybridized to two Atlas human cDNA expression arrays (Clontech) in separate bags for 18 h at 50°C. After washing with 0.1 × SSC and 0.1% SDS at room temperature for 10 min and with 0.3 × SSC and 0.1% SDS at 68°C for 30 min, the expression arrays were exposed to a phosphoimaging plate for 18 h. The data were analysed using ImageQuant software (Molecular Dynamics). The GAPDH gene was used as an internal control for hybridization efficiency and cDNA concentration.

RT–PCR

Reverse transcription was performed on 5 μg of total RNA using the SuperScript preamplification system (Life Technologies). The full-length ORF of the p55Cdc cDNA was amplified by PCR from 5% of the RT products using forward primer (5′-GGGCTCTAGAATGGCACAGTTC-3′) and reverse primer (5′-GGGTTCTAGATCAGCGGATGCCT-3′), both containing a *Xba*I site (underlined). Thirty cycles of RT–PCR were performed with denaturation 94°C for 1 min, annealing at 60°C for 1 min, and extension at 72°C for 1 min. Products were analysed by electrophoresis through a 1% agarose gel.

Western blotting

Equal amounts of protein from cell lysates were separated on 8% polyacrylamide gels and transferred to nitrocellulose filters. Each filter was blocked at room temperature for 1 h with PBS containing 0.05% Tween 20 and 5% dry milk. They were then incubated at 4°C overnight in the same solution with anti-HA antibody (1 : 1000) (Boehringer-Mannheim Corp.), anti-p55Cdc antibody (1 : 600) (Santa Cruz), anti-CyclinB1 antibody (1 : 1000) (Neo Marker), anti-cdc2 antibody (1 : 1000) (Neo Marker), or anti-actin antibody (1 : 3000) (Sigma). The filters were washed three times for 10 min each in PBS containing 0.05% Tween 20, and then incubated with horseradish peroxidase-conjugated anti-mouse IgG antibody against HA, anti-goat IgG antibody against p55Cdc, or anti-rabbit IgG antibody against CyclinB1, cdc2 and actin (Boehringer-Mannheim Corp.) for 40 min. Specific proteins were detected using an enhanced chemiluminescence system (Amersham Corp.).

Immunoprecipitation and kinase assays

293T cells were cotransfected with pCGN-p55Cdc or a pGEM control vector and either pCMVcdc2-dn (a dominant negative p34^{cdc2} expression vector) or a pCDNA3 control vector encapsulated in DC-Chol liposome. Forty-eight hours later, cells were lysed with immunoprecipitation (IP) buffer [0.5% NP-40, 150 mM NaCl, 50 mM Tris (pH 8.0)] containing 2% aprotinin, 5 mM PMSF, 100 mM NaF, 2 mM Na_3VO_4 and 1 mM EDTA. Five hundred micrograms of protein from each sample was incubated at 4°C with 1 μg of antibody overnight and for another 2 h after addition of protein G-agarose. The immunoprecipitates were washed three times with IP buffer and twice with kinase buffer [20 mM HEPES (pH 7.4), 150 mM KCl, 5 mM $MnCl_2$, 5 mM NaF, 1 mM DTT] and then resuspended in 40 μl of kinase buffer containing 5 μg of myelin basic protein and 10 μCi of [γ–^{32}P]ATP. Following 30 min incubations at 30°C, the reactions were terminated with 40 μl of 2 × Laemmli SDS sample buffer. Samples were incubated for 5 min at 96°C and resolved by 15% SDS–PAGE.

Cloning of the p55Cdc promoter and generation of a p55Cdc promoter-luciferase reporter construct

Rat genomic DNA was isolated from the normal rat fibroblast cell line Rat1 using Insta gane Matrix (Bio-Rad) according to the protocol recommended by the manufacturer. A 1000 bp region of the rat p55Cdc promoter (Weinstein *et al*., 1998) was amplified by PCR using forward primer (5′-CCCAAGCTTGGGGCTTCCCTTCTTC-3′) and reverse primer (5′-TAAAGCTTCGCCGAACAGTTATT-3′), both containing a *Hind*III site (underlined). Thirty-five cycles were performed with denaturation at 95°C for 1 min, annealing at 55°C for 1 min, and extension at 72°C for 1 min. The PCR fragments were digested with *Hind*III, and ligated into a pGL2 vector (Promega) containing a luciferase reporter gene. DNA sequencing of double-strand plasmid DNAs was performed at DNA Core Facility in MD Anderson Cancer Center.

Luciferase assays

HeLa cells were cotransfected with the pGL2-p55Cdc promoter vector and a β-actin-lacZ vector using the cationic liposome method. Cells were lysed with 1 × lysis buffer (Promega) after 9, 24, 36 and 48 h. After centrifugation, half of the supernatant was used for a β-galactosidase (β-gal) assay to determine transfection efficiency, and one-sixth was added to reconstituted luciferase assay reagent in a luciferase assay kit (Promega). Light emission was detected by a luminometer.

Construction of the p55Cdc expression vector.

The full-length ORF of the *p55Cdc* cDNA was amplified by PCR from RT-products from HeLa mRNA by the forward primer (5′-GGGCTCTAGAATGGCACAGTTC-3′) and reverse primer (5′-GGGTTCTAGATCAGCGGATGCCT-3′), both containing a *Xba*I site (underlined). The PCR fragments were digested with *Xba*I and ligated into a pCGN expression vector containing an HA epitope tag at the NH2 terminal. DNA sequencing of double-strand plasmid DNAs was performed at DNA Core Facility in MD Anderson Cancer Center. To express HA epitope-tagged p55Cdc, the pCGN-p55Cdc vector was transfected into HeLa cells by the liposome-mediated gene transfer method.

Double thymidine cell cycle synchronization at G1/S phase

HeLa cells were treated with 1 mM thymidine for 24 h, followed by a 8 h release in fresh DMEM/F12 medium with 10% fetal bovine serum and successive retreatment with thymidine for 14 h and released to enter cell cycle (Lu and Hunter, 1995)

Acknowledgments
This work was supported by NIH grants CA58880 and Ovarian SPORE grant P50 CA83639 (to M-C Hung) and by a postdoctoral fellowship from the US Army Breast Cancer Research Training Grant Program, Grant No. DAMD17-99-1-9264 (to K Makino).

References

Bogdan C and Ding A. (1992). *J. Leukoc. Biol.*, **52,** 119–121.
Choi WJ, Clark MW, Chen JX and Jong AY. (1990). *Biochem. Biophys. Res. Commun.*, **172,** 1324–1330.
DeRisi J, Penland L, Brown PO, Bittner ML, Meltzer PS, Ray M, Chen Y, Su YA and Trent JM. (1996). *Nat. Genet.*, **14,** 457–460.
Ding AH, Porteu F, Sanchez E and Nathan CF. (1990). *Science*, **248,** 370–372.
Farruggio DC, Townsley FM and Ruderman JV. (1999). *Proc. Natl. Acad. Sci. USA*, **96,** 7306–7311.
Heald R, McLoughlin M and McKeon F. (1993). *Cell*, **74,** 463–474.
Heller RA, Schena M, Chai A, Shalon D, Bedilion T, Gilmore J, Woolley DE and Davis RW. (1997). *Proc. Natl. Acad. Sci. USA*, **94,** 2150–2155.
Jordan MA, Toso RJ, Thrower D and Wilson L. (1993). *Proc. Natl. Acad. Sci. USA*, **90,** 9552–9556.
Jordan MA, Wendell K, Gardiner S, Derry WB, Copp H and Wilson L. (1996). *Cancer Res.*, **56,** 816–825.
Kao CT, Lin M, O'Shea-Greenfield A, Weinstein J and Sakamoto KM. (1996). *Oncogene*, **13,** 1221–1229.
Kotani S, Tanaka H, Yasuda H and Todokoro K. (1999). *J. Cell. Biol.*, **146,** 791–800.
Kramer ER, Gieffers C, Holz G, Hengstshlager M and Peters JM. (1998). *Curr. Biol.*, **8,** 1207–1210.
Kumar N. (1981). *J. Biol. Chem.*, **256,** 10435–10441.
Lin M, Mendoza M, Kane L, Weinstein J and Sakamoto KM. (1998). *Exp. Hematol.*, **26,** 1000–1006.
Lu KP and Hunter T. (1995). *Prog. Cell Cycle Res.*, **1,** 187–205.
Meikrantz W, Gisselbrecht S, Tam SW and Schlegal R. (1994). *Proc. Natl. Acad. Sci. USA*, **91,** 3754–3758.
Russel P and Nurse P. (1987). *Cell*, **49,** 559–567.
Schena M, Shalon D, Davis RW and Brown PO. (1995). *Science*, **270,** 467–470.
Schiff PB, Fant J and Horwitz SB. (1979). *Nature*, **277,** 665–667.
Schiff PB and Horwitz SB. (1980). *Proc. Natl. Acad. Sci. USA*, **77,** 1561–1565.
Shalon D, Smith SJ and Brown PO. (1996). *Genome Res.*, **6,** 639–645.
Shi L, Nishioka WK, Th'ng J, Bradbury EM, Litchfield D and Greenberg AH. (1994). *Science*, **263,** 1143–1145.
Shteinberg M, Protopopov Y, Listovsky T, Brandeì M and Hershko A. (1999). *Biochem. Biophys. Res. Commun.*, **260,** 193–198.
Wani MC, Taylor HL, Wall ME, Coggon P and McPhail AT. (1971). *J. Am. Chem. Sci.*, **93,** 2325–2327.
Weinstein J, Jacobsen FW, Hsu-Chen J, Wu T and Baum LG. (1994). *Mol. Cell. Biol.*, **14,** 3350–3363.
Weinstein J. (1997). *J. Biol. Chem.*, **272,** 28501–28511.
Weinstein J, Karim J, Geschwind DH, Nelson SF, Krumm J and Sakamoto KM. (1998). *Mol. Genet. Metab.*, **64,** 52–57.
Yu D, Liu B, Tan M, Li J, Wang SS and Hung M-C. (1996). *Oncogene*, **13,** 1359–1365.
Yu D, Jing T, Liu B, Yao J, Tan M, McDonnell T and Hung M-C. (1998). *Mol. Cell*, **2,** 581–591.

[CANCER RESEARCH 61, 2838–2842, April 1, 2001]

Advances in Brief

Ultraviolet Irradiation Induces BRCA2 Protein Depletion through a p53-independent and Protein Synthesis-dependent Pathway[1]

Shao-Chun Wang, Keishi Makino, Li-Kuo Su, Annie Y. Pao, Jeong Soo Kim, and Mien-Chie Hung[2]

Department of Molecular and Cellular Oncology, The University of Texas M. D. Anderson Cancer Center, Houston, Texas 77030

Abstract

It has been suggested that BRCA2, the protein product of the breast cancer susceptibility gene *BRCA2*, is involved in DNA damage repair. It is therefore likely that BRCA2 plays a role in a signaling pathway induced by DNA-damaging agents. To test this possibility, we examined the alteration of the BRCA2 protein level in human cell lines after UV irradiation. We found that UV irradiation down-regulated BRCA2 in a dose-dependent manner in all cell lines tested. The down-regulation of BRCA2 occurred soon (within 4 h) after UV treatment. Surprisingly, down-regulation of BRCA2 by UV does not require functional p53, which has been suggested to be required for the down-regulation of BRCA1 and BRCA2 mRNAs by DNA-damaging agents. Moreover, the proteosome- and calpain-mediated protein degradation pathways do not have an important role in the UV-induced BRCA2 depletion. However, blocking protein synthesis temporally inhibited the depletion of BRCA2 and BRCA1 in some cell lines. Ectopic expression of BRCA2 in cells increased resistance of cells to high-dose UV irradiation. These results demonstrate that BRCA2 is involved in a DNA-damaging signaling pathway induced by UV radiation and that expression of BRCA2 can protect cells from UV-mediated cell death.

Introduction

Patients carrying heterozygous germ-line mutations in the breast cancer susceptibility gene *BRCA2* are predisposed to breast, ovarian, and other types of cancer (1–3). The wild-type allele of the *BRCA2* gene is usually lost in tumors of patients carrying germ-line *BRCA2* mutations, indicating a prominent role of *BRCA2* in the development of cancer. Recently, we and others have demonstrated that the expressions of *BRCA2* RNA and protein are regulated in a cell cycle-dependent manner, with a peak expression during S and M phases of the cell cycle (4–7). Studies using *Brca2* knockout mice suggested a role of BRCA2 in DNA damage signaling and repair (reviewed in Refs. 1–3). Mouse embryos carrying homozygous mutations of *Brca2* are developmentally retarded and usually die early in embryogenesis. Homozygous *Brca2* mutant mice that survive to birth showed a wide range of defects, including the development of lethal thymic lymphomas. In addition, mouse embryonic stem cells and embryo fibroblast cells lacking functional *Brca2* are deficient in DNA repair. These observations together suggest a guardian function for BRCA2 in maintaining genome integrity by participating in the repair of DNA damage. This suggestion is further supported by the physical association between BRCA2 and RAD51, a human homologue of the *Escherichia coli* DNA double-strand-break repair protein RecA.

UV radiation is a potent DNA-damaging agent that activates a wide spectrum of signaling pathways in cells. One of such responses is the increased level of wild-type p53, probably because of its increased protein stability by site-specific phosphorylation induced by UV (8). Mouse embryos lacking functional *Brca2* have been shown to be hypersensitive to UV irradiation (9). This observation suggests that Brca2 is essential for the mouse embryo cells to survive DNA damage caused by UV. However, it remains to be determined whether BRCA2 also involves in stress responses to UV irradiation in human adult cells.

BRCA2 has been shown to physically associate with the tumor suppressor p53 and therefore is linked to the p53-dependent transactivation function (reviewed in Ref. 9 and references therein). Consistently, homozygous *Brca2* mutant mouse embryos develop better when they also lack a functional *p53* gene, suggesting a functional association between these two genes. It has been shown that loss of the p53 checkpoint function combined with BRCA2 deficiency may trigger tumor formation and cancer progression (10). The functional and physical link between BRCA2 and p53 raises an intriguing question as to whether the response of BRCA2, if any, to DNA damage caused by genotoxic agents requires functional p53.

In this report, we show that UV irradiation results in depletion of BRCA2 protein, and that this process does not require functional p53 but requires protein synthesis. We also show that forced expression of BRCA2 increased cell resistance to UV irradiation.

Materials and Methods

Materials. 293 cells were maintained in high-glucose DMEM-10% fetal bovine serum containing 25 mM HEPES. Other cell lines were maintained in DMEM/F-12 medium with 10% fetal bovine serum. The monoclonal antibody N61 against BRCA2 has been described (7). Antibodies against p53 (Oncogene Science, Cambridge, MA), BRCA1 (Neomarker, Union City, CA), pRB (Santa Cruz Biotechnology, Santa Cruz, CA), and PARP[3] (PharMingen, San Diego, CA) were purchased. Genistein, MG115, MG132, and ALLN were purchased from Calbiochem (La Jolla, CA). z-VAD-fmk was purchased from Enzyme Systems Products (Livermore, CA). Cycloheximide and TNF-α were from Sigma Chemical Co. (St. Louis, MO).

BRCA2 Expression Plasmids. Fragments of the wild-type human BRCA2 cDNA were isolated by RT-PCR and completely sequenced. The full-length BRCA2 cDNA was then assembled from these fragments and was inserted into a modified pcDNA3 plasmid. The m1 BRCA2 mutant, which mimics a pathogenic germ-line mutation and has a two-nucleotide deletion at codon 17, was generated using mutagenesis PCR.

Immunoblot Analysis. Cells were harvested and lysed in ice-cold NETN buffer [150 mM NaCl, 1 mM EDTA, 20 mM Tris (pH 8.0), and 0.5% NP40]. Lysates containing an equal amount of protein (60–120 μg) were separated by SDS-PAGE and blotted to polyvinylidene difluoride membrane (Bio-Rad,

Received 4/10/00; accepted 2/13/01.

The costs of publication of this article were defrayed in part by the payment of page charges. This article must therefore be hereby marked *advertisement* in accordance with 18 U.S.C. Section 1734 solely to indicate this fact.

[1] This study is supported in part by the M. D. Anderson Breast Cancer Research Program (to M-C. H. and L-K. S.) and NIH Grants RO1 CA58880, CA60856, and CA77858. K. M. is a postdoctoral fellow supported by Department of Defense Breast Cancer Training Grant DAMD17-99-1-9264.

[2] To whom requests for reprints should be addressed, at The University of Texas M. D. Anderson Cancer Center, Department of Molecular and Cellular Oncology, Box 108, 1515 Holcombe Boulevard, Houston, TX 77030. Phone: (713) 792-3668; Fax: (713) 794-0209; E-mail: mchung@mail.mdanderson.org.

[3] The abbreviations used are: PARP, poly(ADP-ribose) polymerase; z-VAD-fmk, z-Val-Ala-Asp-fluoromethyl ketone; TNF, tumor necrosis factor; EGFR, epidermal growth factor receptor; NF-κB, nuclear factor-κB.

Hercules, CA). Proteins were then identified using antibodies per the manufacturer's instructions.

UV Survival Assays. 293 cells were plated in six-well plates or 60-mm dishes and transfected with the appropriate plasmid DNA as described in the figure legends using the cationic liposome LPD1 (a gift kindly provided by Drs. Leaf Huang and Song Li, University of Pittsburgh, Pittsburgh, PA). Sixteen h later, the transfected cells were split. For the luciferase assay, the cultures in six-well plates were split into two wells and treated with UV radiation (80 J/m^2) 36 h after plating. The cultures were maintained, and the medium was changed every 3 days. Ten days later, the cells were lysed, and the luciferase activity was determined using a luciferase assay system (Promega Corp., Madison, WI) following the manufacturer's instructions. Results from four independent experiments were averaged. For the clonogenic assay, 1×10^5 cells were transfected in 60-mm plates and then plated in 100-mm tissue culture dishes 48 h after transfection. After incubation for 36 h, the cells were treated with UV irradiation (80–120 J/m^2), and the cultures were maintained until the surviving cells formed colonies.

Results

UV Irradiation Altered BRCA2 Protein Expression. To investigate the effect of UV irradiation on BRCA2 protein expression, we examined a panel of human cell lines including an immortalized normal breast epithelial cell line (MCF-10A), an osteogenic sarcoma cell line (U-2 OS), a pancreatic cancer cell line (CAPAN-1), two breast cancer cell lines (MDA-MB-435 and MDA-MB-231), and an ovarian cancer cell line (SKOV3-ip1; Table 1). UV irradiation down-regulated BRCA2 protein levels in a dose-dependent manner in each cell line tested (Fig. 1*A*). Although low-dose UV irradiation down-regulated BRCA2 to various extents among these cell lines, UV doses >12 J/m^2 consistently reduced the BRCA2 protein in all cell lines tested. The CAPAN-1 cell line expresses a truncated BRCA2 because of a single nucleotide deletion (6174dT) in exon 11 of the *BRCA2* gene (7). The truncated BRCA2 protein, which is not able to associate with p53 (11), was still down-regulated by UV irradiation. More importantly, UV-induced down-regulation of BRCA2 protein did not require functional p53. BRCA2 protein depletion by UV can be observed in cell lines expressing wild-type p53 (MCF-10A and U-2 OS), mutant p53 (MDA-MB-231, MDA-MB-435, and CAPAN-1), or no p53 (SKOV3-ip1). As expected, the p53 protein level was induced by UV irradiation in a dose- and time-dependent manner in the two cell lines expressing wild-type p53 (MCF-10A and U-2 OS) and was not altered in cell lines expressing mutant p53 (Fig. 1*A*). It is known that BRCA2 expression is reduced in cells growth arrested at the G_0-G_1 phases of the cell cycle (5, 7). To rule out the possibility that BRCA2 down-regulation by UV may be a secondary effect caused by cell cycle arrest at G_0-G_1 phases after UV irradiation, we examined the effects of UV treatment on cell cycle progression. As shown in Fig. 1*B* using MCF-10A and U2-OS cells as examples, the BRCA2 protein down-regulation by UV irradiation did not correlate with cell cycle alteration based on fluorescence-activated flow cytometry (FACS). Thus, the down-regulation of BRCA2 by UV treatment cannot be attributed to the effects of UV irradiation on cell cycle progression.

Table 1 *The p53 status of cell lines used in this work*

Cell line	Origin	*p53* status
MCF-10A	Breast epithelium	Wild-type
U-2 OS	Osteosarcoma	Wild-type
MDA-MB-435	Breast cancer	Mutant
MDA-MB-231	Breast cancer	Mutant
SKOV3-ip1	Ovarian cancer	Null
CAPAN-1	Pancreatic cancer	Mutant
A431	Epidermoid cancer	Mutant

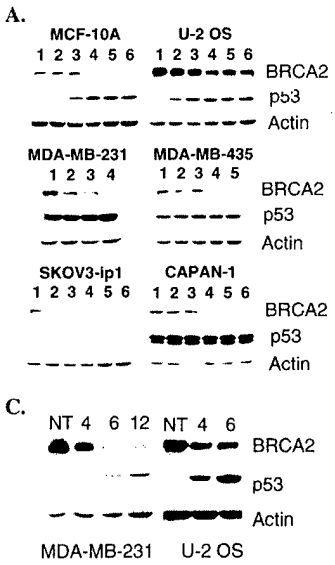

B.

MCF-10A	G0/G1	S	G2/M
0 J/m^2	48.6	36.5	14.9
6 J/m^2	28.9	40.6	30.6
12 J/m^2	27.4	61.6	11.0
24 J/m^2	34.7	45.5	19.8

U2-OS	G0/G1	S	G2/M
0 J/m^2	54.9	26.4	18.7
6 J/m^2	37.0	50.0	13.1
12 J/m^2	36.1	53.8	10.1
24 J/m^2	33.9	54.4	11.7

Fig. 1. UV-mediated down-regulation of BRCA2 protein. *A*, human cell lines were irradiated with different doses of UV (*Lane 1*, no treatment; *Lane 2*, 6 J/m^2; *Lane 3*, 12 J/m^2; *Lane 4*, 24 J/m^2; *Lane 5*, 32 J/m^2; *Lane 6*, 42 J/m^2). Cell lysates were prepared 12 h after the UV treatment, and proteins were detected by immunoblotting. α-Actin was used as a control for equal loading of protein. The BRCA2 protein in CAPAN-1 cells is a COOH-terminal truncated mutant (7). *B*, UV effects of the cell cycle. Cell cycle progression of MCF-10A and U2-OS in *A* was determined by FACS analysis 12 h after UV treatment. The percentage of cells in each cell cycle phase is shown. *C*, rapid BRCA2 down-regulation induced by UV. MDA-MB-231 and U-2 OS cells were treated with 24 J/m^2 of UV and incubated for different times (h) as indicated before the cells were lysed. *NT*, no treatment.

Requirement of Protein Synthesis of UV-mediated Depletion of BRCA2 and BRCA1. To further address the mechanism of the UV-induced BRCA2 down-regulation, we determine the kinetics of BRCA2 depletion in response to UV irradiation (Fig. 1*C*). UV-mediated down-regulation of BRCA2 protein occurred within 4 h after UV irradiation in U-2 OS and MDA-MB-231 cells.

The rapid depletion prompted us to test whether protein degradation contributed to the UV-mediated BRCA2 down-regulation by blocking protein synthesis with the protein translation inhibitor cycloheximide. To our surprise, cycloheximide treatment of U-2 OS cells actually prevented BRCA2 depletion within 9.5 h of incubation after UV irradiation, suggesting the involvement of protein synthesis in the down-regulation process (Fig. 2*A*). However, in U-2 OS cells, the inhibitory effect of cycloheximide was relieved after prolonged incubation (15 h; Fig. 2*C*). On the other hand, BRCA2 depletion by UV irradiation in MDA-MB-231 cells remained blocked by cycloheximide, even after prolonged incubation (17 h; Fig. 2, *B* and *D*). In this experiment, the inhibition of protein neosynthesis was confirmed by the lack of p53 induction by UV in cycloheximide-treated U-2 OS cells (8). In both cell lines tested, UV treatment also caused down-regulation of BRCA1 protein accompanied with a slower migration of the BRCA1 protein, which likely resulted from protein phosphorylation induced by UV, as reported previously (12, 13). Interestingly, although cycloheximide treatment could not block UV-mediated BRCA1 down-regulation in U-2 OS cells, cycloheximide completely blocked BRCA1 protein depletion by UV irradiation in MDA-MB-231 cells (Fig. 2).

To circumvent the unexpected effect of cycloheximide, a pulse-chase experiment was performed. MDA-MB-231 cells were metabolically pulse labeled with [^{35}S]methionine for newly synthesized protein before being irradiated with UV. The BRCA2 protein level was monitored at different chasing time points after UV irradiation by immunoprecipitation with an anti-BRCA2 antibody (Fig. 2*E*). There was a clear reduction in the BRCA2 protein level by 2 h after UV

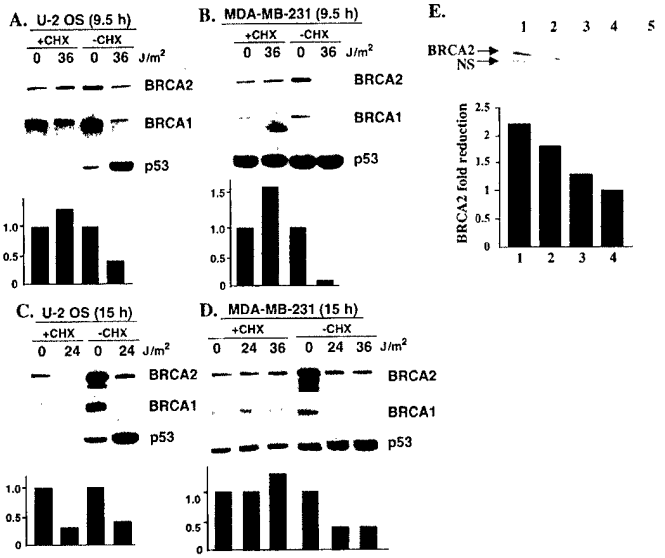

Fig. 2. BRCA2 protein depletion caused by UV irradiation requires protein synthesis. U-2 OS (*A* and *C*) and MDA-MB-231 (*B* and *D*) cells, treated or not treated with 50 μM of cycloheximide (*CHX*), were irradiated with UV (24 J/m^2) and incubated for different periods of time as indicated (*A* and *B*, 9.5 h; *C* and *D*, 15 h). Proteins were detected by immunoblotting. The levels of BRCA2 were quantified using the NIH Image program and shown as *columns*. The BRCA2 level in cells without treating with UV was set as 1. *E*, UV irradiation causes BRCA2 protein degradation. MDA-MB-231 cells were pulse labeled with [^{35}S]methionine (1 mCi/ml) for 2 h, irradiated with 42 J/m^2 of UV, then incubated in the absence of [^{35}S]methionine for different periods of time before being lysed. BRCA2 protein was immunoprecipitated and detected by autoradiography. The intensities of the BRCA2 protein signals were measured using Phosphorimage as shown by the *columns*. The BRCA2 level of the sample irradiated with UV and incubated for 4 h before lysis was set as 1. *Lane 1*, the pulse-labeled cells were lysed immediately after labeling; *Lane 2*, labeled cells were incubated for 4 h after labeling without UV irradiation; *Lane 3*, labeled cells were incubated for 2 h, irradiated, and further incubated for another 2 h; *Lane 4*, labeled cells were irradiated with UV right after labeling and incubated for 4 h before lysis; *Lane 5*, same as *Lane 2* but used mouse plus rabbit IgG for immunoprecipitation. NS, non-specific.

irradiation. The result strongly suggests that UV irradiation causes BRCA2 protein degradation.

BRCA2 Protein Depletion by UV through a Novel Pathway. Although the regulation of BRCA2 RNA level by UV has been reported, the regulation of BRCA2 protein by UV irradiation has not been addressed (12, 14). The ubiquitin-proteosome pathway is an important mechanism to modulate protein stability. To determine whether the proteosome pathway is involved in UV-mediated BRCA2 depletion, three proteosome inhibitors, MG132, MG115, and ALLN (15), were used to treat U-2 OS cells upon UV irradiation. Although treatment with these inhibitors resulted in a significantly greater level of p53, which is controlled by ubiquitin-mediated protein depletion (16), these three inhibitors did not inhibit BRCA2 depletion induced by UV (Fig. 3*A*).

We also investigated the potential involvement of other proteases in the UV-induced BRCA2 depletion. p53 is also known to be a target of calpain-mediated proteolysis (17). Treatment with the calpain inhibitor ALLN (18) stabilized p53 but did not inhibit BRCA2 depletion induced by UV. The involvement of CPP32/caspase-3-like protease in UV-induced BRCA2 down-regulation has also been excluded because treatment with z-VAD-fmk, a broad-spectrum caspase inhibitor (19), failed to affect the stability of BRCA2 after UV irradiation (Fig. 3*B*).

It has been shown that UV signaling can be mediated through the activity of tyrosine kinase receptors on the cell membrane (20, 21). The possibility of the involvement of EGFR in UV-mediated BRCA2 down-regulation was investigated using the human epidermoid carcinoma cell line A431. A431 cells overexpress EGFR (22) and harbor mutated endogenous p53 (23). Treatment of cells with the tyrosine kinase receptor inhibitor genistein inhibited EGFR activity, as indicated by the decrease of tyrosine phosphorylation of EGFR, but had no effect on the UV-mediated BRCA2 depletion (Fig. 3*C*). In addition, treatment with TNF-α, a cytokine that acts in a synergistic manner with UV in stress signaling (24), did not result in BRCA2 depletion (Fig. 3*D*). These results suggest that UV-mediated BRCA2 protein depletion occur through a novel mechanism.

BRCA2 and UV Protection. Because UV irradiation caused BRCA2 down-regulation, we tested whether forced expression of BRCA2 could protect cells from UV-mediated cell killing using a clonogenic assay and a luciferase reporter assay. 293 cells, whose endogenous BRCA2 decreased upon UV irradiation similar to other cell lines examined (Fig. 4*B*), were transfected with a plasmid expressing either wild-type or m1 mutant *BRCA2* cDNA and then irradiated with UV. UV-treated cells were cultured for a few weeks, and surviving colonies were counted. There were about twice as many surviving colonies from cells transfected with the wild-type *BRCA2*-expressing plasmid than from cells transfected with the m1 BRCA2 mutant expressing plasmid (Fig. 4*C*).

A luciferase expression assay was also used to test the UV protection function of BRCA2. 293 cells were transfected with a luciferase reporter plasmid together with a plasmid expressing either the wild-type or the m1 mutant BRCA2 cDNA. Transfected cells were treated with UV and cultured for ~10 days. Luciferase activity expressed in these cells was measured and used as an indicator for cell survival. Consistent with the result of the clonogenic experiment, there were more surviving cells in cells transfected with wild-type BRCA2-expressing plasmid than in those transfected with m1 mutant BRCA2-expressing plasmid (Fig. 4*D*). These results showed that increased expression of wild-type BRCA2 protected cells from UV-induced cell killing.

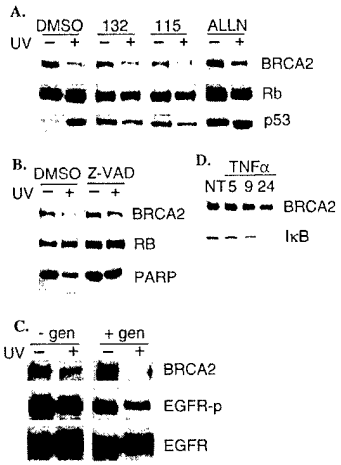

Fig. 3. UV-induced BRCA2 protein depletion via a proteosome-independent, calpain-independent, and TNF-α-independent pathway. *A*, U-2 OS cells were first treated with proteosome inhibitor MG132 (5 μM), MG115 (25 μM), or calpain inhibitor ALLN (10 μM), or with DMSO as the solvent control for 30 min. Cells were then mock irradiated or irradiated with 24 J/m^2 of UV. Cell lysates were prepared after incubation for 4 h in the presence of the inhibitors, and the indicated proteins were detected by immunoblotting. The retinoblastoma protein (*RB*) was used as an equal loading control. The accumulation of p53, which is subject to proteosome- and calpain-mediated depletion, in mock UV-irradiated cells demonstrated the effectiveness of inhibitor treatments. *B*, U-2 OS cells were treated with the calpain and caspase 3 inhibitor z-VAD (40 μM), and the level of BRCA2 protein was determined by immunoblotting as in *A*. The level of PARP was lower after UV irradiation because of cleavage by caspase-3. PARP cleavage by caspase-3 was inhibited in the presence of z-VAD-fmk. *C*, A431 cells, which overexpress EGFR, were treated (+ *gen*) or not treated (− *gen*) with genistein (20 ng/ml) for 14 h in medium containing 5% serum. The cells were then irradiated with UV (24 J/m^2) and incubated for 6 h before lysis. Cell lysates were then prepared, and proteins were detected by immunoblotting. EGFR-p was activated, therefore tyrosine phosphorylated, EGFR. *D*, the breast cancer cell line MDA-MB-231 was treated with TNF-α (10 ng/ml) for 5, 9, or 24 h, and the level of BRCA2 protein was determined by immunoblotting. Concomitant depletion of IκB by TNF-α as reported previously (27) was shown. *NT*, no treatment.

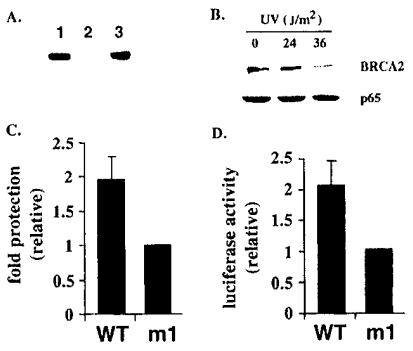

Fig. 4. Inhibition of cell death from UV irradiation by BRCA2 expression. *A*, expression of the BRCA2 protein from the expression plasmids was confirmed after transient transfection. Mouse NIH3T3 cells were used for the transfection because the BRCA2 antibody used did not detect mouse Brca2 in immunoblotting (7). *Lane 1*, NIH3T3 cells transfected with wild-type BRCA2 expression plasmid; *Lane 2*, NIH3T3 cells transfected with an empty expression plasmid; *Lane 3*, lysate of U-2 OS cells used as a positive control. *B*, BRCA2 protein in 293 cells is also down-regulated by UV irradiation. The p65 subunit of NF-κB was shown as equal loading control. *C*, 293 cells were transfected by a plasmid encoding either wild-type (*WT*) or mutant (*m1*) BRCA2. Transfected cells were allowed to recover for 24 h. Cells (1×10^5) were then plated on each dish and subjected to UV irradiation. The colonies that survived after incubation were then stained and counted, and the relative colony numbers were determined. The average of four independent experiments is shown. *D*, 293 cells were cotransfected with a plasmid encoding either wild-type (*WT*) or mutant (*m1*) *BRCA2* and a plasmid carrying the luciferase gene under the control of the CMV promoter. A plasmid carrying the β-galactosidase gene under the control of the α-actin promoter was also included for normalizing transfection efficiencies. The transfected 293 cells were subjected to UV irradiation and maintained in cell cultures for at least 1 week until the surviving colonies formed, and the luciferase activity was then measured. The percentage of protection (treated/untreated) was determined and compared between the two BRCA2 constructs. The average of four independent experiments is shown; *bars*, SD.

Discussion

We showed in this report that BRCA2 protein level was reduced within 4 h after cells were irradiated with UV. The rapid depletion of BRCA2 suggests that the down-regulation of BRCA2 was not the result of UV-induced cell cycle arrest. This suggestion was also supported by our observation that the down-regulation of BRCA2 protein did not correlate with the cell cycle alteration after UV irradiation. UV irradiation has been shown to down-regulate the BRCA2 mRNA level (12, 14). The rapid reduction of BRCA2 protein level after UV irradiation indicates that the reduction of BRCA2 protein is not simply the consequence of the reduction of BRCA2 mRNA level.

It has been reported that the BRCA1 and BRCA2 mRNAs were reduced in cells treated with Adriamycin and UV in a p53-dependent manner (14). It also has been reported that BRCA1 expression was reduced in response to Adriamycin and mitomycin C in the presence of wild-type p53 (25). However, our results clearly show that both BRCA2 and BRCA1 protein levels were decreased by UV irradiation, regardless of the p53 status of cells investigated. Consistently, the COOH-terminal region of BRCA2, which binds to p53 and modulates its transcriptional function (11), was not required for the UV-mediated depletion of BRCA2. The COOH terminus-truncated BRCA2 protein in CAPAN-1 cells was degraded by UV similar to wild-type BRCA2 in other cell lines.

The depletion of BRCA2 protein by UV irradiation appeared to require protein synthesis, because the protein synthesis inhibitor cycloheximide blocked this process. It is possible that UV irradiation induces the expression of a short-lived factor(s) that is critical for the degradation of BRCA2. Identification of such factor(s) would be a significant step in understanding BRCA2 regulation mechanism under genotoxic stresses. Extended incubation overcame the cycloheximide inhibition and resulted in further BRCA2 protein depletion in the absence of protein synthesis (Fig. 2*C*). This result indicates that protein degradation contributes to the UV-mediated BRCA2 depletion, which is also supported by the result of the pulse-chase experiment (Fig. 2*E*). It is worth mentioning that cycloheximide blocked BRCA1 protein depletion by UV irradiation in MDA-MB-231 but not in U-2 OS cells, indicating that UV may modulate BRCA2 and BRCA1 protein levels through different mechanisms in different cell types.

Our results strongly suggest that down-regulation of BRCA2 in UV-irradiated cells is mediated by a new mechanism. It does not rely on the function of the proteosome and calpain systems, which are the most common biological mechanisms for protein depletion. Inhibitors for proteosome (MG132, MG115, and ALLN) and caspase (z-VAD-fmk) did not prevent UV-induced BRCA2 down-regulation. Calpain inhibitors ALLN (15) and z-VAD-fmk (19) also did not inhibit this process. Because calpain is necessary for the degradation of IκB for the induction of NF-κB in UV-irradiated cells (26), our result suggests that NF-κB does not participate in the UV-induced BRCA2 down-regulation. Activation of the signaling pathway of TNF-α receptor, which has been shown to contribute to UV-induced apoptosis (24), did not result in significant BRCA2 down-regulation, suggesting that the TNF-α pathway is not involved in this process. Similarly, the UV-mediated down-regulation of BRCA2 does not depend on signaling through EGFR, which has been shown as a target of UV signaling (21). Additional studies are necessary to further understand in detail the mechanism(s) for UV-mediated BRCA2 and BRCA1 down-regulation.

A role of BRCA2 in the repair of UV-induced DNA damage has been hypothesized. Our results that ectopic expression of wild-type BRCA2 protected cells from UV-induced cell killing support this hypothesis. It is therefore surprising that the BRCA2 level decreased in cells irradiated with UV. However, the BRCA2 level was reduced not completely diminished. The amount of remaining BRCA2 may still provide protection to cells. This is consistent with the fact that homozygous *Brca2* mutant cells, which do not have any functional *Brca2*, are more sensitive to UV than the wild-type or heterozygous *Brca2* mutant cells (9). One possible consequence of the reduced BRCA2 level in UV-irradiated cells could be to render cells that sustain extensive DNA damage to cell death rather than to be transformed because of their carrying mutated DNA. Further investigations will be necessary to better understand the role of BRCA2 in UV-induced stress responses.

References

1. Bertwistle, D., and Ashworth, A. Functions of the *BRCA1* and *BRCA2* genes. Curr. Opin. Genet. Dev., *8:* 14–20, 1998.
2. Zhang, H., Tombline, G., and Weber, B. L. BRCA1, BRCA2, and DNA damage response: collision or collusion? Cell, *92:* 433–436, 1998.
3. Zheng, L., Li, S., Boyer, T. G., and Lee, W-H. Lessons learned from BRCA1 and BRCA2. Oncogene, *19:* 6159–6175, 2000.
4. Vaughn, J. P., Cirisano, F. D., Huper, G., Berchuck, A., Futreal, P. A., Marks, J. R., and Iglehart, J. D. Cell cycle control of BRCA2. Cancer Res., *56:* 4590–4594, 1996.
5. Wang, S-C., Su, L-K., Lin, S-H., and Hung, M-C. Changes in *BRCA2* expression during progression of the cell cycle. Biochem. Biophys. Res. Commun., *234:* 247–251, 1997.
6. Bertwistle, D., Swift, S., Marston, N. J., Jackson, L. E., Crossland, S., Crompton, M. R., Marshall, C. J., and Ashworth, A. Nuclear location and cell cycle regulation of the BRCA2 protein. Cancer Res., *57:* 5485–5488, 1997.
7. Su, L-K., Wang, S-C., Qi, Y., Luo, W., Hung, M-C., and Lin, S-H. Characterization of BRCA2: temperature sensitivity of detection and cell-cycle regulated expression. Oncogene, *17:* 2377–2381, 1998.
8. Pitkanen, K., Haapajarvi, T., and Laiho, M. UVC-induction of p53 activation and accumulation is dependent on cell cycle and pathways involving protein synthesis and phosphorylation. Oncogene, *16:* 459–469, 1998.
9. Patel, K. J., Vu, V. P., Lee, H., Corcoran, A., Thistlethwaite, F. C., Evans, M. J., Colledge, W. H., Friedman, L. S., Ponder, B. A., and Venkitaraman, A. R. Involvement of Brca2 in DNA repair. Mol. Cell, *1:* 347–357, 1998.
10. Lee, H., Trainer, A. H., Friedman, L. S., Thistlethwaite, F. C., Evans, M. J., Ponder, B. A., and Venkitaraman, A. R. Mitotic checkpoint inactivation fosters transformation in cells lacking the breast cancer susceptibility gene, *Brca2*. Mol. Cell, *4:* 1–10, 1999.

11. Marmorstein, L. Y., Ouchi, T., and Aaronson, S. A. The *BRCA2* gene product functionally interacts with p53 and RAD51. Proc. Natl. Acad. Sci. USA, *95:* 13869–13874, 1998.
12. Fan, S., Twu, N-F., Wang, J-A., Yuan, R-Q., Andres, J., Goldberg, I. D., and Rosen, E. M. Down-regulation of *BRCA1* and *BRCA2* in human ovarian cancer cells exposed to Adriamycin and ultraviolet radiation. Int. J. Cancer, *77:* 600–609, 1998.
13. Scully, R., Chen, J., Ochs, R. L., Keegan, K., Hoekstra, M., Feunteun, J., and Livingston, D. M. Dynamic changes of BRCA1 subnuclear location and phosphorylation state are initiated by DNA damage. Cell, *90:* 425–435, 1997.
14. Andres, J. L., Fan, S., Turkel, G. J., Wang, J-A., Twu, N-F., Yuan, R-Q., Lamszus, K., Goldberg, I. D., and Rosen, E. M. Regulation of BRCA1 and BRCA2 expression in human breast cancer cells by DNA-damaging agents. Oncogene, *16:* 2229–2241, 1998.
15. Rock, K. L., Gramm, C., Rothstein, L., Clark, K., Stein, R., Dick, L., Hwang, D., and Goldberg, A. L. Inhibitors of the proteasome block the degradation of most cell proteins and the generation of peptides presented on MHC class I molecules. Cell, *78:* 761–771, 1994.
16. Scheffner, M., Werness, B. A., Huibregtse, J. M., Levine, A. J., and Howley, P. M. The E6 oncoprotein encoded by human papillomavirus types 16 and 18 promotes the degradation of p53. Cell, *63:* 1129–1136, 1990.
17. Kubbutat, M. H. G., and Vousden, K. H. Proteolytic cleavage of human p53 by calpain: a potential regulator of protein stability. Mol. Cell Biol., *17:* 460–468, 1997.
18. Wang, K. K. W., and Yuen, P. Calpain inhibition: and overview of its therapeutic potential. Trends Pharmacol. Sci., *15:* 412–419, 1994.
19. Nicholson, D. W., and Thornberry, N. A. Caspases: killer proteases. Trends Biochem. Sci., *22:* 299–306, 1997.
20. Sachsenmaier, C., Radler-Pohl, A., Zinck, R., Nordheim, A., Herrlich, P., and Rahmsdorf, H. J. Involvement of growth factor receptors in the mammalian UVC response. Cell, *78:* 963–972, 1994.
21. Rosette, C., and Karin, M. Ultraviolet light and osmotic stress: activation of the JNK cascade through multiple growth factor and cytokine receptors. Science (Washington DC), *274:* 1194–1197, 1996.
22. Haigler, H., Ash, J. F., Singer, S. J., and Cohen, S. Visualization by fluorescence of the binding and internalization of epidermal growth factor in human carcinoma cells A-431. Proc. Natl. Acad. Sci. USA, *75:* 3317–3321, 1978.
23. Reiss, M., Brash, D. E., Munoz-Antonia, T., Simon, J. A., Ziegler, A., Vellucci, V. F., and Zhou, Z. L. Status of the *p53* tumor suppressor gene in human squamous carcinoma cell lines. Oncol. Res., *4:* 349–357, 1992.
24. Sheikh, M. S., Antinore, M. J., Huang, Y., and Fornace, A. J. J. Ultraviolet-irradiation-induced apoptosis is mediated via ligand independent activation of tumor necrosis factor receptor I. Oncogene, *17:* 2555–2563, 1998.
25. MacLachlan, T. K., Dash, B. C., Dicker, D. T., and El-Deiry, W. S. Repression of BRCA1 through a feedback loop involving p53. J. Biol. Chem., *275:* 31869–31875, 2000.
26. Bender, K., Gottlicher, M., Whiteside, S., Rahmsdorf, H. J., and Herrlich, P. Sequential DNA damage-independent and -dependent activation of NF-κB by UV. EMBO J., *17:* 5170–5181, 1998.
27. Brown, K., Gerstberger, S., Carlson, L., Franzoso, G., and Siebenlist, U. Control of IκBα proteolysis by site-specific, signal-induced phosphorylation. Science (Washington DC), *267:* 1485–1488, 1995.

Nuclear localization of EGF receptor and its potential new role as a transcription factor

Shiaw-Yih Lin*†, Keishi Makino*†, Weiya Xia*, Angabin Matin*, Yong Wen*, Ka Yin Kwong*, Lilly Bourguignon‡ and Mien-Chie Hung*§

*Department of Molecular and Cellular Oncology, Breast Cancer Basic Research Program, The University of Texas M.D. Anderson Cancer Center, Houston, TX 77030, USA

†These authors contributed equally to this work.

‡Endocrine Unit (111N), San Francisco VA Medical Center, UCSF, San Francisco, CA 94121, USA

§e-mail: mhung@notes.mdacc.tmc.edu

Epidermal growth factor receptor (EGFR) has been detected in the nucleus in many tissues and cell lines. However, the potential functions of nuclear EGFR have largely been overlooked. Here we demonstrate that nuclear EGFR is strongly correlated with highly proliferating activities of tissues. When EGFR was fused to the GAL4 DNA-binding domain, we found that the carboxy terminus of EGFR contained a strong transactivation domain. Moreover, the receptor complex bound and activated AT-rich consensus-sequence-dependent transcription, including the consensus site in cyclin D1 promoter. By using chromatin immunoprecipitation assays, we further demonstrated that nuclear EGFR associated with promoter region of cyclin D1 *in vivo*. EGFR might therefore function as a transcription factor to activate genes required for highly proliferating activities.

Epidermal growth factor receptor (EGFR) is a transmembrane glycoprotein that possesses intrinsic tyrosine kinase activity[1]. Studies on EGFR have been focused mainly on the conventional signal transduction pathways such as mitogen-activated protein kinase[2], phospholipase C-γ (ref. 3) and phosphatidylinositol-3-OH kinase[4]. However, it has long been known that many functions of EGFR, such as EGF-induced DNA synthesis and its mitogenic effect, require other mechanisms besides those early transient responses[5–7]. In addition, Wakshull and Wharton[8] have reported that stabilized complexes of EGF–EGFR on the cell surface were not able to induce DNA synthesis although the transient responses were activated. It is evident that a critical activity of EGFR signalling is still missing from the current model.

For years, EGFR and its ligands have repeatedly been observed in the nucleus, for example in cell lines, in human placenta, in regenerating liver[9] and in many different cancer types[10–13]. Yet the function of nuclear EGFR is far from clear. Here we demonstrate that the nuclear localization of EGFR is correlated with the highly proliferative status of tissues. In addition, we provide evidence to support the potential roles of nuclear EGFR as a transcription factor or coactivator, which might activate the genes required for its mitogenic effects, such as the gene that encodes cyclin D1. Our studies might contribute to uncovering the crucial activity of EGFR that the whole scheme has lacked for decades.

Results

Nuclear EGFR in highly proliferative tissues. The localization of EGFR in the nucleus has been demonstrated by many different groups in a variety of systems[9–13]. After careful analysis of those studies, we found a common feature in their results that demonstrated a strong correlation between nuclear EGFR and the highly proliferating status of tissues. To address this issue further, we examined EGFR expression in five different tissues with these features, including uterus from pregnant mice, mouse embryos, normal human mouth mucosa and human cancer tissues. Fig. 1A (top left) shows the immunostaining of EGFR on the uterus taken from a C3H-hen mouse on day 6 of pregnancy. The expression of EGFR was high and many of the cells showed the strong nuclear staining of the receptor. In contrast, EGFR was weakly expressed in the uterus from non-pregnant mice, in which almost none of the cells showed the significant nuclear staining (Fig. 1A, top right). The results of three control experiments shown in Fig. 1A (bottom) confirmed the specificity of the EGFR signal. We also observed heavy staining of nuclear EGFR in a 10-day-old mouse embryo, which is another example of highly proliferating tissues (data not shown). Next, we stained the samples from human normal oral mucosa, which contains both highly proliferating basal cells and fully differentiated non-growing squamous cells. We detected EGFR staining only in the nuclei of the basal cells, as shown in Fig. 1B (top). We stained the same tissue with Ki 67 antibody to confirm the correlation between nuclear receptor expression and the proliferating status of tissue (13.8% Ki 67-positive for basal cells, against 0.4% Ki 67-positive for fully differentiated cells) (data not shown). Finally, we examined samples of human cancer tissue, which is an important pathological example with highly proliferating activities. Although the membrane staining of EGFR was readily detectable (Fig. 1C, bottom right), we observed EGFR clearly localized in the nuclei in both the oral cancer sample (Fig. 1C, top) and the breast cancer sample (data not shown). The similar nuclear staining of EGFR was also clearly detected by using another anti-EGFR antibody (EGF-R Ab1; Oncogene Science) against a different epitope, which confirmed the specificity of the detected signals (data not shown). Thus, in five different tissues with highly proliferating cells *in vivo*, we observed clear nuclear EGFR staining with different anti-EGFR antibodies. Our data therefore strongly supported the correlation between nuclear EGFR and tissues with high proliferation.

Nuclear EGFR in cell lines cultured *in vitro*. In addition to the tissue samples, we examined EGFR-overexpressing cell lines for the presence of nuclear EGFR. Because most EGFR is expressed on the cell surface in cell culture, which in turn might mask a weak EGFR signal in the nucleus, we performed confocal microscopy to ensure the accuracy of the localization images. As shown in Fig. 1D, two EGFR overexpressors, A431 (top panels)

© 2001 Macmillan Magazines Ltd

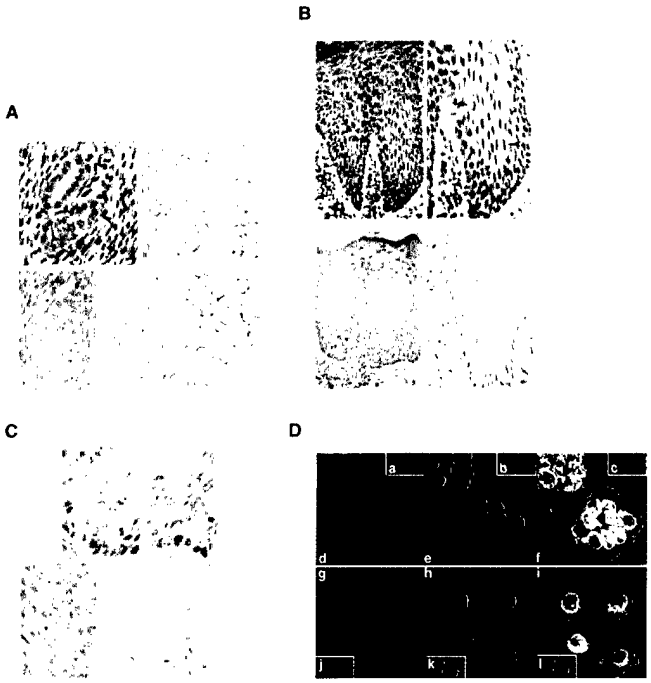

Figure 1 **Immunohistochemical staining of different tissues for EGFR. A,** Uterus from a pregnant mouse (top left) and a non-pregnant mouse (top right). The bottom panels show control experiments: 10 × EGFR competitive peptide was added (bottom left); PBS was used instead of primary antibody (bottom middle), and 468-cell-derived tumours were used as a positive staining control (bottom right). **B,** Normal human mouth mucosa, magnified ×100 (top left) and ×200 (top right). The bottom panels show the respective negative controls using antibody with 10 × competitive peptide (bottom left) or PBS instead of primary antibody (bottom right). **C,** Human oral cancer sample, magnified ×400 (top). The bottom panels show negative and positive controls as described for **A**. **D,** Cell lines immunostained with anti-EGFR antibody and analysed by confocal microscopy. The yellow signals indicate the localization of EGFR in the nucleus. **a, j,** Fluorescein isothiocyanate (FITC)-conjugated pre-immune serum as a negative control; **b, k,** propidium staining; **c,** superimposition of **a** and **b**; **l,** superimposition of **j** and **k**; **d, g,** FITC-conjugated anti-EGFR antibody; **e, h,** propidium iodide staining; **f,** superimposition of **d** and **e**; **i,** superimposition of **g** and **h**.

and MDA-MB-468 (bottom panels) were immunostained with anti-EGFR antibody (EGFR (1005)-G; Santa Cruz). Cells were double-labelled by fluorescein isothiocyanate (FITC)-conjugated anti-EGFR antibody (Fig. 1Dg) to localize EGFR (green signal) and by propidium iodide to localize nuclei (Fig. 1De, Dh; red signal). When two images were merged, we found a significant portion of EGFR localized in the nucleus (Fig. 1Df, Di; yellow signal). The same procedure was also performed by using FITC-conjugated preimmune serum as a negative control (Fig. 1Da, Dj). Nuclear staining was readily detectable by propidium iodide (Fig. 1Db, Dk), but no yellow signal was detectable when two images were merged (Fig. 1Dc, Dl), ensuring the specificity of the nuclear EGFR detected in Fig. 1Df, Di. We consider the EGFR signal observed to be specific because nuclear EGFR was also detected when two other antibodies recognizing different epitopes were used (EGF-R Ab-1 (Oncogene Science) and EGFR Ab-3 (NeoMarkers); data not shown).

To confirm the presence of EGFR in the nuclear fraction and to determine the phosphorylation status of the nuclear receptor, we next subjected nuclear extracts from A431 and MDA-MB-468 cells to immunoprecipitation with anti-EGFR antibody followed by immunoblotting with either anti-phosphotyrosine antibody (Fig. 2A, top) or anti-EGFR antibody (Fig. 2A, bottom). We found that nuclear EGFR levels increased on treatment with EGF and that EGFR that accumulated in the nucleus was highly tyrosine-phosphorylated. Similar results were also obtained when cells were treated with another ligand for EGFR, transforming growth factor-α (data not shown).

To rule out the possibility that the signal seen in the nuclear extracts was due to contamination, the nuclei from unstimulated and EGF-stimulated MDA-MB-468 cells (N^- and N^+, respectively) were mixed with the non-nuclear fraction from unstimulated cells (S^-) or cells stimulated with EGF for 30 min (S^+). The nuclei were then again separated from the non-nuclear fraction and washed extensively, and the nuclear extract was then analysed by immunoblotting with anti-phosphotyrosine antibody. In this way we demonstrated that even if the non-nuclear fraction of the EGF-activated cell lysate was mixed and incubated for 30 min with nuclei from the untreated cells, the EGFR in that fraction did not diffuse into or contaminate the nuclear fraction (Fig. 2B, lane 5). We therefore concluded that the nuclear EGFR that we detected was not due to passive contamination of the nuclear fraction by EGFR from the plasma membrane or cytoplasm. This experiment also demonstrated that the cell-surface and cytoplasmic EGFR did not passively pass into the nuclei but indicated the existence of a specific pathway for transporting the receptor into the nuclei. This pathway was evidently not intact when the cells were disrupted because of the failure of the isolated nuclei to take up EGFR from the non-nuclear fraction.

Nuclear EGFR can be from the cell surface. Having established a putative pathway for the nuclear import of EGFR, we sought to determine how fast this translocation occurred and where the

© 2001 Macmillan Magazines Ltd

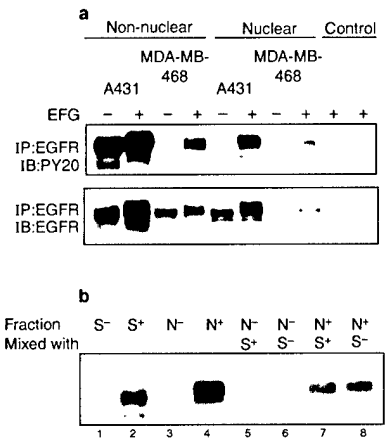

Figure 2 **Detection of EGFR in the nuclear fractions of A431 and MDA-MB-468 cells. a**, The nuclear (80 μg) and non-nuclear (20 μg) fractions from cells treated with (+) or without (–) EGF were subjected to immunoprecipitation with monoclonal antibody against human EGFR or c-Myc (control) and then blotted with anti-phosphotyrosine (PY20) antibody (top) or with sheep anti-human EGFR antibody (bottom). **b**, Nuclei were prepared from unstimulated and EGF-stimulated MDA-MB-468 cells (N^- and N^+, respectively) and then mixed with the non-nuclear fraction from the cells stimulated with EGF for 30 min (S^+). The nuclei were then separated from the S^+ fraction, and the nuclear extract was isolated and analysed by immunoblotting with anti-phosphotyrosine (PY20) antibody.

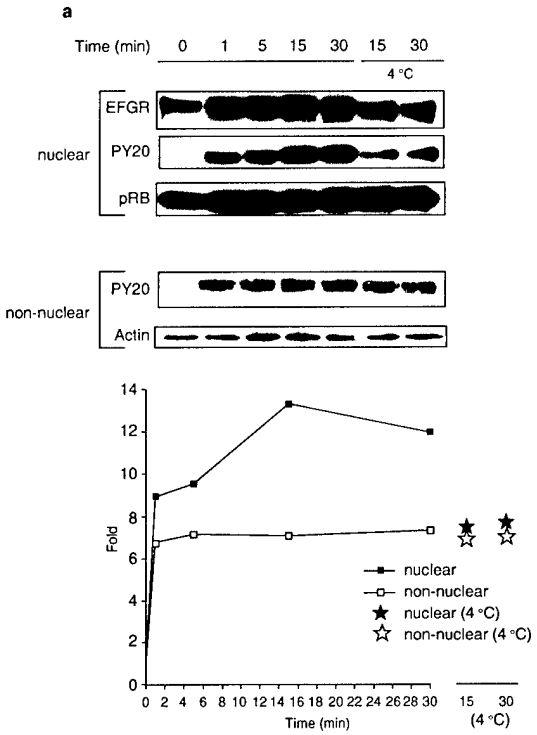

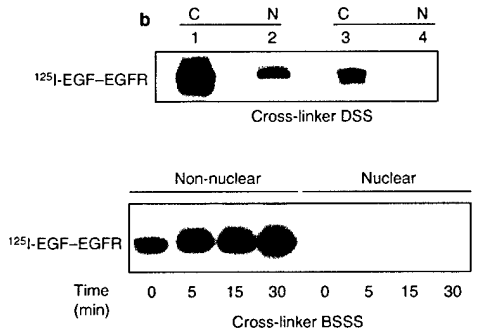

Figure 3 **Time-course study of EGFR nuclear localization. a**, A431 cells were stimulated with EGF and incubated at 37 °C for 1–30 min or at 37 °C for 1 min and then at 4 °C for a further 14 min (lane 6) or 29 min (lane 7). The nuclear extract (top) and non-nuclear fraction (middle) were then subjected to western blotting with anti-EGFR and anti-phosphotyrosine (PY20) antibodies or with pRB antibody as the loading control. The results were then plotted diagrammatically as shown in the bottom panel. The density of the bands at zero time were defined as 1 after subtraction of the background by using NIH Image software to quantify the signals. **b**, Specific cell-surface labelling of EGFR by cross-linking with ^{125}I-EGF. Top, ^{125}I-EGF–EGFR cross-linked proteins in the non-nuclear (lane 1) and nuclear (lane 2) fractions revealed by autoradiography. In the presence of unlabelled EGF, the level of cross-linking was decreased (lanes 3 and 4). Bottom, cross-linking as described above, except that a non-membrane-permeable cross-linker was used.

nuclear EGFR came from. To determine the kinetics of the translocation, we incubated A431 cells with EGF for 1–30 min. Fig. 3a (top) shows that phosphorylated nuclear EGFR was detected as early as 1 min after treatment with EGF, with the peak detected at about 15–30 min. This rapid translocation was also seen in MDA-MB-468 cells (data not shown). However, when cells were treated with EGF for 1 min and the warm medium was replaced with cold medium to stop membrane trafficking, the translocation of the receptor was abolished even though cells were continuously incubated in the medium with the same concentration of ligand (Fig. 3a, top; lanes 6 and 7).

In contrast, the level of phosphorylated EGFR in the non-nuclear fraction remained the same in this time period (Fig. 3a, middle). In addition, stopping the membrane trafficking did not affect the EGFR phosphorylation in the non-nuclear fraction (Fig. 3a, middle; lanes 6 and 7). These results not only confirmed that the increase of the phosphorylated EGFR in the nuclear extract was not due to contamination by the non-nuclear fraction, but also indicated that the nuclear receptor might have come from the cell membrane (Fig. 3a, bottom).

To further confirm this possibility, we cross-linked ^{125}I-labelled EGF to EGFR on the cell surface of MDA-MB-468 cells by means of the non-cleavable, amine-reactive homobifunctional cross-linker disuccinimidyl suberate (DSS)[14] (Fig. 3b, top) or a non-cleavable, membrane-impermeable cross-linking reagent, bis(sulphosuccinimidyl) suberate (BSSS) (Fig. 3b, bottom). As shown in Fig. 3b (top), we detected a clear cross-linked ^{125}I-EGF–EGFR band in the nuclear extract (lane 2). This band could be competed away in the presence of an excess of unlabelled EGF (lane 4), thus confirming the specificity of the binding. The movement of the ^{125}I-EGF–EGFR complex was detected in the nuclear extract as early as 5 min after cross-linking (Fig. 3b, bottom). Because BSSS could not pass through the cell membrane alone, detection of the ^{125}I-EGF–EGFR complex supported the idea that EGFR was moving into the nuclei from the cell surface after stimulation with EGF.

A strong transactivation domain in EGFR. Having confirmed the time- and ligand-dependent nuclear translocation of EGFR, we

© 2001 Macmillan Magazines Ltd

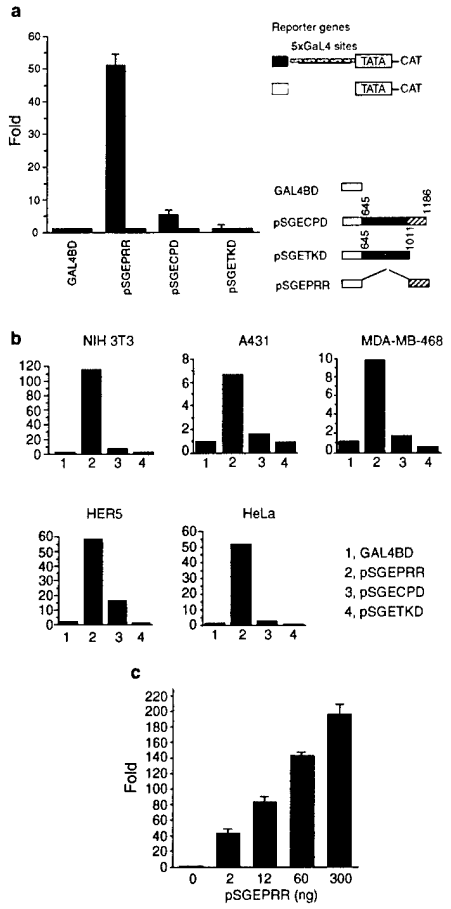

Figure 4 **Activation of gene expression by the C-terminus of EGFR (PRR domain).** **a**, The relative CAT activity of the reporter gene was measured when different GAL4-EGFR expression constructs were co-transfected into NIH 3T3 cells. **b**, Results of experiments similar to those in **a** except that other cell lines and a luciferase reporter were used. **c**, Dose-dependent transactivation in NIH 3T3 cells

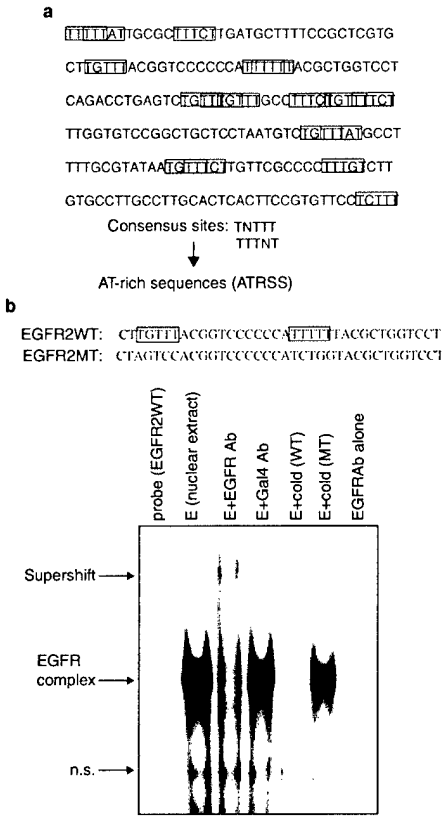

Figure 5 **AT-rich consensus sequences (ATRSs) identified by CASTing.** Top, sequences of six identified clones with the ATRS marked in each; bottom, an EGFR-associated protein complex specifically bound to a DNA probe containing putative EGFR-binding sites.

next sought to determine the receptor's biological function(s) in the nucleus. Previous studies had already shown that EGF and EGFR both formed complexes with chromatin, especially in transcriptionally active regions[15], thus indicating that EGFR and its ligand might have roles in modulating gene expression. We therefore first tried to determine whether any domain of EGFR exhibited transactivation activity. By motif analysis we found that the C-terminus of EGFR contained a proline-rich sequence, which was a typical feature of a transactivation domain for transcription factors. When we fused the C-terminus of EGFR (pSEGPRR) to the GAL4 DNA-binding domain, we found that this chimaeric construct strongly activated (up to 60-fold) the transcription of a reporter gene containing five GAL4-binding sites linked to chloramphenicol transferase (CAT) complementary DNA in NIH 3T3 cells (Fig. 4a). In contrast, the tyrosine kinase domain and the whole cytoplasmic domain of EGFR either did not activate (tyrosine kinase domain) or only slightly activated (whole cytoplasmic domain) the transcription of the reporter.

The observed transactivating activity was evidently dependent on DNA binding because the carboxy terminus of EGFR failed to activate the reporter gene when the GAL4-binding sites were deleted. This activity was also evidently general rather than cell-type-specific because it occurred in all five cell lines that we tested (Fig. 4b). Finally, this transactivation activity was dose-dependent. By increasing the amount of expression vector, we observed a very clear dose-dependent activation (Fig. 4c).

The weaker transactivation activity of the whole cytoplasmic domain suggested the presence of a negative control activity in the tyrosine kinase domain. It is interesting to note that the tyrosine kinase domain contains the negative regulatory sites identified by other groups in the early studies[16]. It remains to be determined whether those negative sites are involved in regulating the transactivation activity of EGFR exerted by its C terminus.

DNA-binding site(s) for EGFR complexes. We next sought to determine whether EGFR, as a putative transcription factor, could bind to DNA, and, if it does, to identify its DNA-binding site(s) by the cyclic amplification and selection of targets (CASTing) method[17]. In brief, cell lysate prepared from EGF-treated A431 cells as the source of EGFR was incubated with an excess of oligonucleotides containing a 36-nucleotide core of random sequences flanked by two polymerase chain reaction (PCR) primers (see Methods). To identify the EGFR containing DNA-binding complexes, anti-EGFR antibody (Ab12; NeoMarkers) was added to the reaction mixture to supershift the complexes of interest. We observed a very faint band appearing after the antibody was added.

© 2001 Macmillan Magazines Ltd

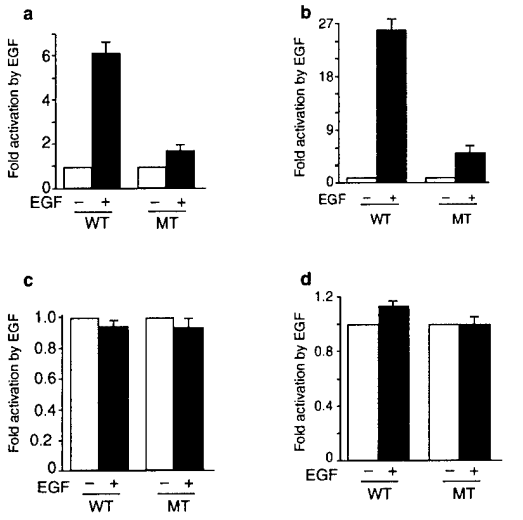

Figure 6 **Activation of ATRS-specific reporter gene expression by EGF in EGFR-overexpressing cell lines. a**, A431 cells; **b**, MDA-MB-468 cells; **c**, HBL 100 cells; **d**, CHO cells. All four lines were transfected with a luciferase vector containing four repeats of wild-type (WT) or mutated (MT) ATRS sequences, with (+) or without (–) EGF (100 ng ml^{-1}).

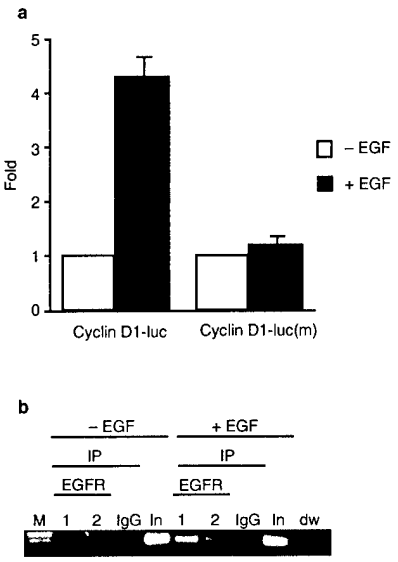

Figure 7 **ATRS-dependent activation of cyclin D1 promoter by EGF, and association of EGFR with cyclin D1 promoter *in vivo*. a**, MDA-MB-468 cells were transfected with a luciferase vector containing the cyclin D1 promoter with two intact ATRS or the same promoter with the ATRS mutated. After 24 h of incubation, cells were treated with (+) or without (–) EGF (100 ng ml^{-1}). **b**, A431 cells were treated with (+) or without (–) EGF (100 ng ml^{-1}) for 30 min and cross-linked with 1% formaldehyde; nuclear lysate was then prepared. After precipitation with the anti-EGFR antibodies (1, Santa Cruz; 2, NeoMarkers) or normal rabbit IgG, the cyclin D1 promoter region was amplified by PCR. Input nuclear DNA (In) or water (dw) were used as PCR controls.

We believed that the faint band observed should have contained EGFR because a supershift was detected only with anti-EGFR antibody but not with the control anti-GAL4 antibody or mouse preimmune serum (data not shown, and see Fig. 5b). In addition, the anti-EGFR antibody alone did not bind to the probe when the cell lysate was left out of the reaction mixture. After excision of the band, we eluted and amplified the DNA by PCR. The same procedure was repeated for a further three rounds. The final DNA products were then subcloned and sequenced. When we compared the sequences from all six clones, we identified an AT-rich minimal consensus sequence (ATRS) that appeared in all six clones, 18 times in total. We therefore considered this consensus sequence a putative EGFR-associating sequence (Fig. 5a).

Next, using one of the cloned sequences as the probe, we performed gel-retardation assays to confirm the specific association between EGFR and our identified sequences. As expected, we observed the specific binding of an EGFR-containing complex to the probe, which could be competed away by an excess of unlabelled wild-type oligonucleotides but not by the oligonucleotides in which the consensus sites were mutated (Fig. 5b). We therefore concluded that the ATRS that we identified was a true DNA-binding site for the EGFR complex.

EGFR-binding-site-dependent gene activation. Next, we constructed four repeats of either the ATRS sites or the mutated sites in a luciferase reporter construct containing the mouse thymidine kinase gene (*tk*) minimal promoter. When the reporter genes were transfected into EGFR-overexpressing cell lines (A431 and MDA-MB-468), EGF activated the wild-type reporter construct strongly but the mutant construct only weakly (Fig. 6a, b). In contrast, neither the wild-type nor the mutant reporter was activated by EGF in the cells with low levels of EGFR (HBL100) or no EGFR (Chinese hamster ovary) (Fig. 6c, d). However, EGFR-dependent activation could be restored in these two cell lines upon the co-transfection of the EGFR expression vector (data not shown). Thus, the ATRS, which can bind to the nuclear EGFR complex, responds to EGFR-dependent activation, whereas the mutant ATRS, which fails to bind to nuclear EGFR, loses it ability to respond to the EGFR-dependent activation. This result strongly supports the idea that ATRS might be one of the target sequences activated by nuclear EGFR.

Cyclin D1 as one of the potential targets for nuclear EGFR. Finally, we sought to identify the potential targets for nuclear EGFR so that we could determine its biological significance. Because nuclear EGFR was correlated with highly proliferative activity of cells, we suspected that its target genes were likely to be involved in cell proliferation. One of the candidates is cyclin D1. Cyclin D1 is a cell-cycle regulator essential for G1 progression. Overexpression of cyclin D1 has been shown to shorten G1 and to accelerate cell proliferation. We found two ATRSs located in the proximal region of the cyclin D1 promoter between nucleotides –74 and –70 (TTTAT) and –31 and –27 (TTTGT), respectively. To test whether these two ATRSs in the cyclin D1 promoter were responsive to EGFR activity, the reporter gene containing 163 base pairs of the cyclin D1 promoter (cyclin D1-luc) was tested. Many known transcription-factor-binding sites had been eliminated from this construct but it still contained two ATRSs as described above. EGF activated the wild-type reporter up to fourfold but the activation was abolished when these two ATRS were mutated (cyclin D1-luc(m)) by changing the two ATRSs to CCTAT and GGTGT, respectively (Fig. 7a).

Furthermore, to examine whether EGFR can bind directly to the promoter region of cyclin D1 *in vivo*, we performed chromatin immunoprecipitation assays with anti-EGFR antibodies to precipitate EGFR with or without stimulation by EGF (100 ng ml^{-1}). As shown in Fig. 7b, the EGFR was found to be physically associated with the promoter region of cyclin D1 only in EGF-treated cell extracts precipitated by EGFR-specific antibodies, not in those

© 2001 Macmillan Magazines Ltd

precipitated by normal IgG. Therefore, EGFR can bind to the cyclin D1 promoter *in vivo*.

Discussion

In the study described here, we have demonstrated that EGFR shares several features with transcription factors: it can be located in the nucleus, it contains a transactivation domain, it associates with genes and it activates sequence-specific gene expression. Our results therefore support a model in which nuclear EGFR might function as a transcription factor. Although other groups have observed the binding of EGFR to chromatin, ours is the first study to demonstrate that EGFR can bind to specific DNA sequences to activate gene expression. The demonstration of cyclin D1, a well-known cell-growth-promoting factor, as its potential target might explain why the nuclear localization of EGFR was strongly correlated with the tissues with high proliferation activity.

At present we do not know whether EGFR binds to ATRS directly. However, it has previously been shown that rat Schwannoma-derived growth factor (SDGF), a ligand for EGFR, can bind to AT-rich DNA sequences that perfectly match the ATRS and must be transported into nucleus to induce a mitogenic response[18]. Our study therefore raises the interesting idea that EGFR and its ligands might function together as transactivation complexes in which the ligand serves as the DNA-binding domain and the receptor as the transactivation domain.

It is not clear how EGFR is translocated to the nucleus. We found that EGFR contained a putative nuclear localization signal (NLS) in amino-acid residues 645–657 of the cytoplasmic domain (RRRHIVRKRTLRR). When fused to this polypeptide, β-galactosidase could be directed into the nucleus (data not shown). EGFR might therefore be translocated into the nucleus through the conventional nuclear importing system associated with the nuclear pore complex (that is, the Ran/Importin pathway).

Many other transmembrane receptors have also been detected in the nucleus[19], including the receptors for insulin[20], nerve growth factor[15,21] fibroblast growth factor[22,23], platelet-derived growth factor[15], growth hormone[24], interleukin-1[25], c-erbB-4 (ref. 26) and HER-2/*neu*[27,28]. Nuclear localization might therefore be a general feature of many transmembrane receptors. However, despite many previous reports on nuclear receptors, the functions of transmembrane receptors in the nucleus have never been explained. Because we believe that the gap causing slow progress in this field is due mainly to the lack of functional studies, we have begun to fill this gap by clearly identifying the potential functions of nuclear EGFR. In fact, the transactivating activity that we identified in EGFR has also previously been observed by our group in HER-2/*neu*[27]. It is possible that many other receptors also have this activity and so can regulate their specific target genes. Consequently, further studies of the functions of those nuclear receptors should open up a new direction in the field of receptor signalling that has long been overlooked.

Methods

Cell culture and nuclear fractionation.

All cell lines were normally grown in DMEM/F-12 with 10% fetal calf serum. Before stimulation with EGF, cells were serum-starved for 24 h. Then, cells were stimulated with EGF (100 ng ml^{-1}) for various periods. Cells were then lysed in a lysis buffer (20 mM HEPES, pH 7.0, 10 mM KCl, 2 mM $MgCl_2$, 0.5% Nonidet P40, 1 mM Na_3VO_4, 1 mM PMSF, 0.15 U ml^{-1} aprotinin) and homogenized by 30 strokes in a tightly fitting Dounce homogenizer. The homogenate was centrifuged at 1,500 *g* for 5 min to sediment the nuclei. The supernatant was then resedimented at 15,000 *g* for 5 min, and the resulting supernatant formed the non-nuclear fraction. The nuclear pellet was washed three times and resuspended in the same buffer containing 0.5 M NaCl to extract nuclear proteins. The extracted material was sedimented at 15,000 *g* for 10 min and the resulting supernatant was termed the nuclear fraction.

Immunohistochemical staining.

Immunostaining was done with a modification of the avidin–biotin complex technique described previously[29]. The confocal microscope used in this analysis was a Multiprobe 2001 Inverted CLSM system (Molecular Dynamics, Sunnyvale, California).

Western blotting and immunoprecipitation.

Cellular extract immunoprecipitated by anti-human EGFR monoclonal antibodies (Amersham and NeoMarkers) was separated by SDS–PAGE and transferred to a nitrocellulose membrane. Immunoblotting was performed with anti-EGFR antibody (UBI and NeoMarkers) or anti-phosphotyrosine monoclonal antibody (mAb2; Oncogene Science) as primary antibody followed by horseradish-peroxidase-conjugated rabbit anti-sheep or anti-mouse antibodies as secondary antibodies and detected by chemoluminescence (ECL; Amersham).

Kinetic study of nuclear localization of EGFR.

A431 cells were first stimulated with EGF (100 ng ml^{-1}). They were then incubated at 37 °C for 1–30 min or incubated at 37 °C for 1 min and then switched to cold medium containing the same concentration of EGF for a further 14 or 29 min. The nuclear and the non-nuclear fractions were then isolated and subjected to western blotting with anti-EGFR or anti-phosphotyrosine (PY20) antibody on nitrocellulose membranes. The same membranes were also probed with pRB (for the nuclear fraction) or actin (for the non-nuclear fraction) as a loading control.

Chemical cross-linking.

MDA-MB-468 cells were grown in low-serum medium for 24 h. The plates were cooled to 4 °C before adding medium containing ^{125}I-EGF (1 μCi ml^{-1}) and further incubating for 20 min. Phosphate buffer containing BSSS (3 mM) was then added to the plates and incubated with gentle rocking for 30 min on ice. The cross-linking was quenched by washing cells with cold buffer containing 25 mM Tris-HCl, pH 7.4, 140 mM NaCl. This was followed by washing with 50 mM glycine hydrochloride, pH 3.0, 150 mM NaCl to remove excess non-cross-linked ^{125}I-EGF. After further washing with cold PBS, warm medium was placed on the cells, which were incubated at 37 °C for a further 15 min to allow cross-linked proteins to enter cells. The cells were then lysed as before, and nuclear and non-nuclear fractions were subjected to 8% SDS–PAGE.

Plasmids and transfection.

The cytoplasmic domain (amino acids 645–1186), tyrosine kinase domain (645–1011) and C-terminal proline-rich region (1011–1086) of human EGFR were amplified by PCR and subcloned in-frame into pSG424 to generate for each domain a fusion protein containing GAL4 DNA-binding proteins. The fusion protein constructs were then transfected into a variety of cell lines along with GAL4CAT or GAL4Luc reporter plasmids via liposomal DC-Chol provided by Dr Leaf Huang at the University of Pittsburgh.

CASTing and EMSA.

Cyclic amplification and selection of targets (CASTing) was performed as described previously[17]. In brief, a 76-bp oligonucleotide containing a random stretch of 36 nucleotides (5′-GACGTCTCGAGAATTCATCG(N)$_{36}$CGATGGATCCATCCATGTCAGACT-3′), a 5′-end PCR primer (5′-GACGTCTCGAGAATTCATCG-3′) and a 3′-end PCR primer 5′-CGATGGATCCATCCATGTCAGACT-3′) were synthesized. Double-stranded DNA was generated and ^{32}P-labelled as the probe by PCR. A431 cell lysate was incubated on ice for 30 min with anti-EGFR antibody (Ab12; NeoMarkers) in a buffer containing 25 mM HEPES, 100 mM KCl, 0.5 mM $MgCl_2$, 1 mg ml^{-1} bovine serum albumin, 10% glycerol, 5 mM dithiothreitol and 0.1 mg poly(dI-dC). The probe was then added to the reaction mixture and incubated at room temperature for a further 30 min before electrophoresis on a 4% non-denaturing polyacrylamide gel. The shifted band was excised and bound DNAs were eluted. The eluted DNAs were then amplified and labelled by PCR with the two primers described above. After four rounds of selection, the amplified products were subcloned into pBluescript and sequenced. For electrophoretic mobility-shift assay (EMSA), A431 nuclear extract was dialysed with the binding buffer first and then incubated on ice for 30 min with EGFR or control antibody in the same buffer. EMSAs were then performed exactly as described above.

Chromatin immunoprecipitation assay (CHIP).

The methods of Braunstein *et al.*[30] and Oriand[31] were adopted as follows. A431 cells in five 10-cm dishes were serum-starved for 24 h and stimulated with EGF (100 ng ml^{-1}) for 30 min. The cells were then treated with formaldehyde (1% final concentration) for 10 min to cross-link proteins to DNA before harvesting. Cells were scraped off the plate, washed with ice-cold phosphate-buffered saline and resuspended in 500 μl of hypotonic buffer (10 mM Tris-HCl, pH 7.4, 10 mM KCl, 1 mM dithiothreitol), and passed 20 times through a 25-gauge needle. Nuclei were spun down, resuspended in 200 μl SDS lysis buffer (1% SDS, 10 mM EDTA, 50 mM Tris-HCl, pH 8.0, and protease inhibitors), and sonicated for two 30-s bursts separated by cooling on ice. After centrifugation, the supernatant was diluted 1:10 with immunoprecipitation buffer (50 mM Tris-HCl, pH 8.0, 150 mM NaCl, 5 mM EDTA, 0.5% NP40). The cell lysate was precleared by incubation at 4 °C for 1 h with normal rabbit IgG and for a further 1 h with Protein A–agarose beads. The cleared lysates were incubated with two different anti-EGFR antibodies (Santa Cruz or NeoMarkers), or normal rabbit IgG at 4 °C overnight. Immunoprecipitated complexes were collected by adding Protein A–agarose beads for 2 h at 4 °C. Immunoprecipitates were washed once with RIPA buffer (150 mM NaCl, 50 mM Tris-HCl, pH 8.0, 0.1% SDS, 0.5% sodium deoxycholate, 1.0% NP40), once in high-salt wash (500 mM NaCl, 1.0% NP40, 0.1% SDS, 50 mM Tris-HCl, pH 8.0), once in LiCl wash (250 mM LiCl, 1.0% NP40, 0.5% sodium deoxylcholate, 1 mM EDTA, 50 mM Tris-HCl, pH 8.0) and twice in TE buffer (10 mM Tris-HCl, pH 8.0, 1 mM EDTA). The beads were then treated with RNase (50 μg ml^{-1}) for 30 min at 37 °C. The samples were adjusted to 0.25% SDS, 250 μg ml^{-1} proteinase K and incubated at 37 °C overnight. The cross-links were reversed by heating at 65 °C for 6 h and the DNA was then extracted with phenol/chloroform (1:1) and was precipitated with ethanol. Specific sequences of cyclin D1 promoter in the immunoprecipitates were detected by PCR with primers S (5′-GAGGGGACTAATATTTCCAGCAA-3′) and AS (5′-TAAAGGGATTTCAGCTTAGCA-3′).

RECEIVED 18 JANUARY 2001; REVISED 6 APRIL 2001; ACCEPTED 5 JUNE 2001;
PUBLISHED 9 AUGUST 2001.

1. Cohen, S., Ushiro, H., Stoscheck, C. & Chinkers, M. A native 170,000 epidermal growth factor receptor-kinase complex from shed plasma membrane vesicles. *J. Biol. Chem.* **257**, 1523–1531

© 2001 Macmillan Magazines Ltd

(1982).
2. Boonstra, J. *et al.* The epidermal growth factor. *Cell. Biol. Int.* **19**, 413–30 (1995).
3. Anderson, D. *et al.* Binding of SH2 domains of phospholipase C γ1, GAP, and Src to activated growth factor receptors. *Science* **250**, 979–982 (1990).
4. Hu, P. *et al.* Interaction of phosphatidylinositol 3-kinase-associated p85 with epidermal growth factor and platelet-derived growth factor receptors. *Mol. Cell. Biol.* **12**, 981–990 (1992).
5. Carpenter, G. & Cohen, S. Epidermal growth factor. *Annu. Rev. Biochem.* **48**, 193–216 (1979).
6. Knauer, D. J., Wiley, H. S. & Cunningham, D. D. Relationship between epidermal growth factor receptor occupancy and mitogenic response. Quantitative analysis using a steady state model system. *J. Biol. Chem.* **259**, 5623–5631 (1984).
7. Defize, L. H., Moolenaar, W. H., van der Saag, P. T. & de Laat, S. W. Dissociation of cellular responses to epidermal growth factor using anti-receptor monoclonal antibodies. *EMBO J.* **5**, 1187–1192 (1986).
8. Wakshull, E. M. & Wharton, W. Stabilized complexes of epidermal growth factor and its receptor on the cell surface stimulate RNA synthesis but not mitogenesis. *Proc. Natl Acad. Sci. USA* **82**, 8513–8517 (1985).
9. Zimmermann, H. *et al.* The overexpression of proliferating cell nuclear antigen in biliary cirrhosis in the rat and its relationship with epidermal growth factor receptor. *J. Hepatol.* **23**, 459–464 (1995).
10. Tervahauta, A., Syrjanen, S. & Syrjanen, K. Epidermal growth factor receptor, c-erbB-2 proto-oncogene and estrogen receptor expression in human papillomavirus lesions of the uterine cervix. *Int. J. Gynecol. Pathol.* **13**, 234–240 (1994).
11. Kamio, T., Shigematsu, K., Sou, H., Kawai, K. & Tsuchiyama, H. Immunohistochemical expression of epidermal growth factor receptors in human adrenocortical carcinoma. *Hum. Pathol.* **21**, 277–282 (1990).
12. Gusterson, B. *et al.* Evidence for increased epidermal growth factor receptors in human sarcomas. *Int. J. Cancer* **36**, 689–693 (1985).
13. Lipponen, P. & Eskelinen, M. Expression of epidermal growth factor receptor in bladder cancer as related to established prognostic factors, oncoprotein (c-erbB-2, p53) expression and long-term prognosis. *Br. J. Cancer* **69**, 1120–1125 (1994).
14. Pilch, P. F. & Czech, M. P. Interaction of cross-linking agents with the insulin effector system of isolated fat cells. Covalent linkage of ^{125}I-insulin to a plasma membrane receptor protein of 140,000 daltons. *J. Biol. Chem.* **254**, 3375–3381 (1979).
15. Rakowicz-Szulczynska, E. M., Rodeck, U., Herlyn, M. & Koprowski, H. Chromatin binding of epidermal growth factor, nerve growth factor, and platelet-derived growth factor in cells bearing the appropriate surface receptors. *Proc. Natl Acad. Sci. USA* **83**, 3728–3732 (1986).
16. Khazaie, K., Schirrmacher, V. & Lichtner, R. B. EGF receptor in neoplasia and metastasis. *Cancer Metastasis Rev.* **12**, 255–274 (1993).
17. Wright, W. E., Binder, M. & Funk, W. Cyclic amplification and selection of targets (CASTing) for the myogenin consensus binding site. *Mol. Cell. Biol.* **11**, 4104–4110 (1991).
18. Kimura, H. Schwannoma-derived growth factor must be transported into the nucleus to exert its mitogenic activity. *Proc. Natl Acad. Sci. USA* **90**, 2165–2169 (1993).
19. Jans, D. A. & Hassan, G. Nuclear targeting by growth factors, cytokines, and their receptors: a role in signaling? *BioEssays* **20**, 400–411 (1998).
20. Vigneri, R., Goldfine, I. D., Wong, K. Y., Smith, G. J. & Pezzino, V. The nuclear envelope. The major site of insulin binding in rat liver nuclei. *J. Biol. Chem.* **253**, 2098–2103 (1978).
21. Rakowicz-Szulczynska, E. M., Herlyn, M. & Koprowski, H. Nerve growth factor receptors in chromatin of melanoma cells, proliferating melanocytes, and colorectal carcinoma cells in vitro. *Cancer Res.* **48**, 7200–7206 (1988).
22. Maher, P. A. Nuclear translocation of fibroblast growth factor (FGF) receptors in response to FGF-2. *J. Cell Biol.* **134**, 529–536 (1996).
23. Stachowiak, M. K., Maher, P. A., Joy, A., Mordechai, E. & Stachowiak, E. K. Nuclear accumulation of fibroblast growth factor receptors is regulated by multiple signals in adrenal medullary cells. *Mol. Biol. Cell* **7**, 1299–1317 (1996).
24. Lobie, P. E., Wood, T. J., Chen, C. M., Waters, M. J. & Norstedt, G. Nuclear translocation and anchorage of the growth hormone receptor. *J. Biol. Chem.* **269**, 31735–31746 (1994).
25. Curtis, B. M., Widmer, M. B., deRoos, P. & Qwarnstrom, E. E. IL-1 and its receptor are translocated to the nucleus. *J. Immunol.* **144**, 1295–1303 (1990).
26. Srinivasan, R., Gillett, C. E., Barnes, D. M. & Gullick, W. J. Nuclear expression of the c-erbB-4/HER-4 growth factor receptor in invasive breast cancers. *Cancer Res.* **60**, 1483–1487 (2000).
27. Xie, Y. & Hung, M. C. Nuclear localization of p185neu tyrosine kinase and its association with transcriptional transactivation. *Biochem. Biophys. Res. Commun.* **203**, 1589–1598 (1994).
28. Cohen, J. A., Yachnis, A. T., Arai, M., Davis, J. G. & Scherer, S. S. Expression of the neu proto-oncogene by Schwann cells during peripheral nerve development and Wallerian degeneration. *J. Neurosci. Res.* **31**, 622–634 (1992).
29. Hsu, S. M., Raine, L. & Fanger, H. Use of avidin–biotin–peroxidase complex (ABC) in immunoperoxidase techniques: a comparison between ABC and unlabeled antibody (PAP) procedures. *J. Histochem. Cytochem.* **29**, 577–580 (1981).
30. Braunstein, M., Rose, A. B., Holmes, S. G., Allis, C. D. & Broach, J. R. Transcriptional silencing in yeast is associated with reduced nucleosome acetylation. *Genes Dev.* **7**, 592–604 (1993).
31. Orlando, V. & Paro, R. Mapping Polycomb-repressed domains in the bithorax complex using *in vivo* formaldehyde cross-linked chromatin. *Cell* **75**, 1187–1198 (1993).

ACKNOWLEDGEMENTS

We thank You-Wei Chen for his assistance with the confocal microscopic analysis. The work was supported partly by NCI grants (to L.B. and M.-C.H.), an M.D. Anderson Faculty Achievement Award (to M.-C.H.) and a predoctoral fellowship from the DOD Breast Cancer Research Program (to S.-Y. L.). K.M. and Y.W. are supported by a DOD Breast Cancer Research Training Grant.

Correspondence and requests for materials should be addressed to M.-C.H.

© 2001 Macmillan Magazines Ltd

poles. These findings support the conclusion that separase has a general role in anaphase spindle dynamics, but its mechanism remains unclear.

Important questions for the future will be to determine whether the spindle defect is due to the failure to cleave other substrates or to the absence of a non-protease function of separase. Characterization of the phenotype of a catalytically inactive separase mutants expressed during anaphase should help to resolve these issues. In addition, cells lacking separase activity do not efficiently degrade mitotic cyclins[7,19]. Therefore, separase might also affect spindle dynamics indirectly by its effects on the levels of mitotic cyclins.

Slk19 also plays an important role in the first meiotic anaphase, when it is required to prevent separase action on centromere-associated Rec8 (ref. 20). The maintenance of centromeric cohesion until anaphase II is crucial for proper meiotic chromosome segregation. This role of Slk19 does not, however, seem to require separase cleavage[1] and the mechanism remains to be determined. Perhaps unphosphorylated Slk19 acts as a competitive inhibitor of separase action on kinetochores during anaphase I. This model predicts that recognition (but not clipping) of the separase cleavage site on Slk19 would be required for its meiosis I function.

The identification of at least one new separase substrate suggests that separase might have a broad role in regulating mitosis. Because animal cells also have a separase system for dissolving sister cohesion[4,8], these cells might also harbour a complex set of separase substrates. In addition, some of the potential separase substrates do not have mitotic functions. This raises the possibility that separase could also regulate other processes. It is worth noting that the separase mutations that are commonly studied were selected specifically for their mitotic defects and so probably do not represent complete null mutations[15,21]. A re-examination of the phenotypes associated with bona fide null mutations might reveal additional separase functions. Addressing this seductive possibility will require extensive analysis.

David Pellman is at the Dana-Farber Cancer Institute, 44 Binney Street, Boston, Massachusetts 02115, USA
email: david_pellman@dfci.harvard.edu
Michael F. Christman is in the Department of Microbiology, University of Virginia, 1300 Jefferson Park Avenue, Charlottesville, Virginia 22908, USA
email: mfc3f@virginia.edu

1. Sullivan, M., Lehane, C. & Uhlmann, F. *Nature Cell Biol.* **3**, 771–772 (2001).
2. Nasmyth, K., Peters, J. M. & Uhlmann, F. *Science* **288**, 1379–1385 (2000).
3. Uhlmann, F., Wernic, D., Poupart, M. A., Koonin, E. V. & Nasmyth, K. *Cell* **103**, 375–386 (2000).
4. Waizenegger, I. C., Hauf, S., Meinke, A. & Peters, J. M. *Cell* **103**, 399–410 (2000).
5. Funabiki, H. *et al. Nature* **381**, 438–441 (1996).
6. Ciosk, R. *et al. Cell* **93**, 1067–1076 (1998).
7. Cohen-Fix, O. & Koshland, D. *Genes Dev.* **13**, 1950–1959 (1999).
8. Zou, H., McGarry, T. J., Bernal, T. & Kirschner, M. W. *Science* **285**, 418–422 (1999).
9. Zeng, X. *et al. J. Cell Biol.* **146**, 415–425 (1999).
10. Zachariae, W. & Nasmyth, K. *Genes Dev.* **13**, 2039–2058 (1999).
11. Juang, Y. L. *et al. Science* **275**, 1311–1314 (1997).
12. Rao, H., Uhlmann, F., Nasmyth, K. & Varshavsky, A. *Nature* **410**, 955–959 (2001).
13. Alexandru, G., Uhlmann, F., Mechtler, K., Poupart, M. & Nasmyth, K. *Cell* **105**, 459–472 (2001).
14. Bachmair, A., Finley, D. & Varshavsky, A. *Science* **234**, 179–186 (1986).
15. Uzawa, S., Samejima, I., Hirano, T., Tanaka, K. & Yanagida, M. *Cell* **62**, 913–925 (1990).
16. McGrew, J. T., Goetsch, L., Byers, B. & Baum, P. *Mol. Biol. Cell* **3**, 1443–1454 (1992).
17. Kumada, K. *et al. Curr. Biol.* **8**, 633–641 (1998).
18. Jensen, S., Segal, M., Clarke, D. J. & Reed, S. I. *J. Cell Biol.* **152**, 27–40 (2001).
19. Tinker-Kulberg, R. L. & Morgan, D. O. *Genes Dev.* **13**, 1936–1949 (1999).
20. Kamieniecki, R. J., Shanks, R. M. & Dawson, D. S. *Curr. Biol.* **10**, 1182–1190 (2000).
21. Baum, P., Yip, C., Goetsch, L. & Byers, B. *Mol. Cell Biol.* **8**, 5386–5397 (1988).

EGF receptors as transcription factors: ridiculous or sublime?

Mark G. Waugh and J. Justin Hsuan

The notion that a transmembrane receptor at the cell surface can somehow reappear as a transcription factor in the nucleus is bound to be controversial. However, there are two reported examples of this. If this hypothesis can withstand the inevitable and necessary battery of additional empirical tests, then our understanding of signal transduction needs to move in a new direction.

On pages 802–808 of this issue, Hung and co-workers report that following epidermal growth factor (EGF) stimulation at the cell surface, full-length EGF receptors (EGFR) migrate to the nucleus, where they bind an AT-rich consensus sequence (ATRS) via an undefined domain and enhance transcription via a proline-rich region near their carboxy-terminal domain (Fig. 1) (ref. 1). Moreover, they show that EGFRs associate with the promoter region of cyclin D1, a protein that can play a key role in mitogenesis. These results challenge the textbook dogma that receptor tyrosine kinases stimulate mitogenic pathways only through sustained activation of second messenger cascades at the plasma membrane or in endosomes[2,3].

Before this, the prevailing mechanism by which EGF was believed to promote mitogenesis could be summarized as follows. EGFR monomers on the cell surface bind a single molecule of EGF. EGFR molecules then dimerize and undergo autophosphorylation of multiple tyrosine residues in their cytoplasmic tails. These residues become docking sites for cytosolic and membrane-associated effectors containing phosphotyrosine-binding SH2 or PTB domains, such as phosphoinositide 3-kinase (PI3K), phospholipase C (PLC) and the adapter molecule Grb2. The ensuing assembly of specific target proteins on the inner leaflet of the plasma membrane culminates in the formation of second messengers such as polyphosphoinositides and inositol polyphosphates, and the activation of key mitogenic pathways, such as the Ras/MAPK cascade. The targets of these pathways include transcription factors (Fig. 2), which translocate from the cytosol to the nucleus when stimulated by their respective upstream kinases or phosphatases. Although previous studies have suggested that various receptor tyrosine kinases can migrate to the nucleus, what is most striking about Hung and co-workers' paper is its suggestion that activated EGFR molecules can themselves enhance gene expression by binding to DNA in the nucleus[1]. The ability to bypass the protein phosphorylation cascades, widely thought to be essential in transducing mitogenic stimuli, has important implications for treating conditions requiring increased cell proliferation or its

© 2001 Macmillan Magazines Ltd

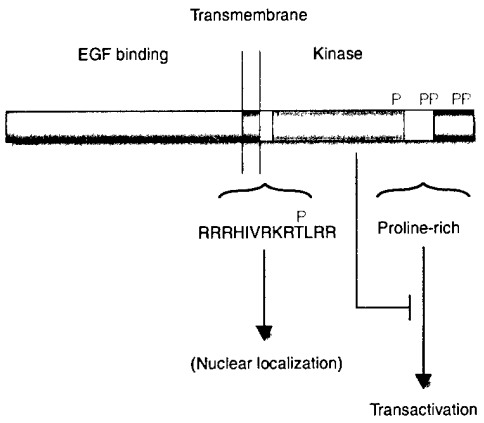

Figure 1 **Epidermal growth factor receptor (EGFR) domain topology. Regions that are relevant to the proposed nuclear localization of EGFR are indicated schematically, including the putative nuclear localization sequence (NLS) in the juxtamembrane region (yellow) and the proline-rich transactivation domain near the carboxy terminus (orange). The major autophosphorylation sites and protein kinase C phosphorylation site are also indicated (red P).**

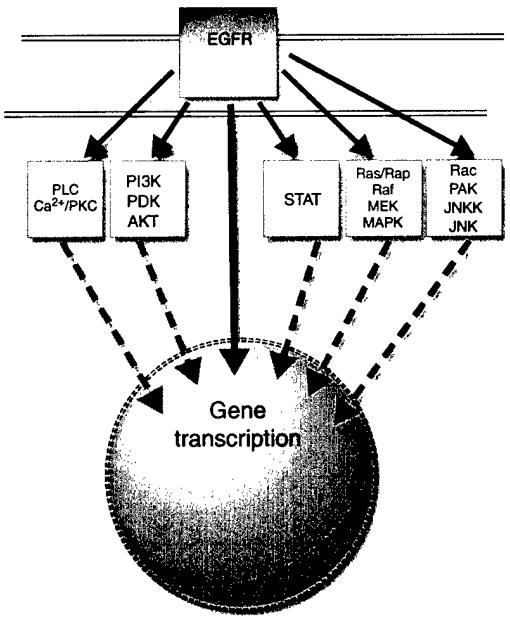

Figure 2 **Signal transduction from epidermal growth factor receptors (EGFRs) to nuclear transcription. Multiple signalling cascades transduce signals from activated EGFR at the cell surface to the nucleus. All depend on protein phosphorylation, culminating in the nuclear import of activated serine/threonine kinases (red) and the phosphorylation of target transcription factors. EGFRs are also found in the nucleus and have been postulated to have intrinsic transcription factor activity.**

inhibition, such as wound repair and cancer, respectively.

Through their proposal that activated EGFRs behave as transcription factors, Hung and co-workers provide an explanation for several puzzling reports suggesting nuclear translocation by several transmembrane receptors in addition to EGFR (c-erbB), including the receptor tyrosine kinases for c-erbB2 (ref. 4), c-erbB-4 (ref. 5), platelet-derived growth factor, fibroblast growth factor (FGF), nerve growth factor and insulin[6]. In their earlier report of transactivation by the cytoplasmic domain of c-erbB2 (but not by the full-length protein)[4], Hung and co-workers also speculated that members of the large family of receptor tyrosine kinases might be functional transcription factors. This suggested a reason why growth-factor-dependent DNA synthesis might require receptor translocation in addition to the signal transduction cascades initiated at the cell surface.

> ... Hung and co-workers provide an explanation for several puzzling reports suggesting nuclear translocation by several transmembrane receptors...

It will be interesting to see whether other families of ligand-activated plasma membrane receptor, such as G-protein-coupled and cytokine receptors, also have transcription factor activity. Several of these can affect gene expression and have been found in the nucleus, such as the receptors for angiotensin, growth hormone, interleukins 1α and 1β, and interferons β and γ (ref. 6). One conceivable advantage of direct receptor action in the nucleus is to maintain specificity, which is otherwise compromised by the degeneracy of signalling pathways that are shared by many different cell surface receptors.

Several reports have also described the migration of growth factors, hormones and cytokines to the nucleus, many of which have been shown to have a functional nuclear localization sequence[6] (NLS). The NLS binds importin α and the complex is then targeted to the nuclear pore complex by association with importin β. It remains to be shown whether or not the putative EGFR NLS

© 2001 Macmillan Magazines Ltd

reported by Hung and co-workers (Fig. 1) is responsible for nuclear localization *in vivo*[1]. Nuclear import of proteins that do not have a functional NLS might be mediated by glycosylation[6] or associated proteins. For example, the FGF receptor has recently been found to bind directly to importin β (ref. 8), although more work is needed to establish whether or not this represents a general mechanism used by other receptors.

Two properties are required to define eukaryotic transcription factors: DNA binding at specific sequences and transactivation (the ability to enhance transcription by RNA polymerase II). Although EGFRs have been shown to bind DNA preferentially at ATRS sites and to stimulate transcription from reporter constructs, transactivation was only detected using the isolated EGFR proline-rich domain (Fig. 1) fused to a Gal4 DNA-binding domain. Furthermore, specific DNA binding was tested using EGFR-containing cell lysates and might be indirect. Consequently, an outstanding question is whether nuclear translocation and gene induction by endogenous EGFRs have any physiological importance, either alone or combined with other EGF-dependent signalling pathways. The critical tests of biological necessity and sufficiency in intact cells have yet to be applied.

Perhaps the most intriguing problem yet to be faced concerns the steric quandary raised by the proposed transition from transmembrane receptor to transcription factor: how can a 170 kDa integral membrane protein enter the nucleus a few minutes after activation at the cell surface? Proteolysis does not seem to be relevant because nuclear EGFRs seem to be intact. Also, there is no mechanism by which EGFRs could leave their membrane bilayer, and endosome trafficking through 10–20 nm nuclear pores seems to be impossible. The only established pathway for EGFRs to enter cells is via clathrin-coated pits but receptors sequestered in this way are usually destined for degradation by lysosomes[9]. It has been suggested that caveolae transport growth hormone and interferon γ to nuclei, but there is no empirical evidence for this pathway. The role of EGFRs as transcription factors will not enter the textbooks until a plausible trafficking route is identified.

If correct, however, the idea that EGFRs act directly as transcription factors might have significant clinical ramifications. Hung and co-workers show that the proportion of EGFRs that can be identified within nuclei correlates with the proliferative status of tissues[1]. They also note that overexpression and increased nuclear levels of the c-erbB family in proliferative disorders are not in themselves new findings. However, if EGFR directly activates transcription, their study raises the possibility that inappropriate transcription from EGFR target genes contributes to a number of pathologies, including cancer. EGFR overexpression is known to cause mislocalization and aberrant signalling. For example, EGFRs are normally confined to the basolateral surface of polarized epithelial cells but, when they are overexpressed, receptors also appear at the apical surface[10]. EGFRs that are misdirected through overexpression to the apical surface undergo prolonged activation, giving rise to augmented phosphorylation of focal adhesion kinase and β-catenin. If a similar scenario is extrapolated to nuclear EGFR signalling then EGFR-dependent transcriptional activation might only become apparent in some tissues as a consequence of deregulated EGFR production. If so, it might be possible to exploit the nuclear localization and putative transcriptional role of EGFR for therapeutic purposes. Indeed, there is already at least one successful effort to use nuclear EGFR as a means of introducing Auger-electron-emitting ^{111}In-radiolabelled EGF to the nucleus[11]. In addition, anti-EGFR antibodies have been conjugated to a reporter gene to use EGFR transport to the nucleus as a means of introducing and transcribing exogenous DNA in the nucleus[12]. Given the newly proposed role of EGFR as a transcription factor, such radiopharmaceutical and genetic approaches might be a particularly effective means of controlling pathologies associated with EGFR overexpression, and might complement approaches designed to inhibit signalling cascades.

> ... If correct, however, the idea that epidermal growth factor receptors act directly as transcription factors might have significant clinical ramifications...

Clearly, whether further studies challenge or support the proposed nuclear role of EGFR, the study by Hung and co-workers in this issue provides the springboard for incisive experiments in this previously unexplored area of receptor biology. □

Mark G. Waugh and J. Justin Hsuan are at the Centre for Molecular Cell Biology, Department of Medicine, Royal Free and University College Medical School, Royal Free Campus, Hampstead, London, NW3 2PF, UK
e-mail: m.waugh@rfc.ucl.ac.uk; j.hsuan@rfc.ucl.ac.uk

1. Lin, S.-Y. *et al. Nature Cell Biol.* **3**, 802–808 (2001).
2. Yarden, Y. & Sliwkowski, M. X. *Nature Rev. Mol. Cell Biol.* **2**, 127–137 (2001).
3. Leof, E. B. *Trends Cell Biol.* **10**, 343–348 (2000).
4. Xie, Y. & Hung, M. C. *Biochem. Biophys. Res. Commun.* **203**, 1589–1598 (1994).
5. Srinivasan, R., Gillett, C. E., Barnes, D. M. & Gullick, W. J. *Cancer Res.* **60**, 1483–1487 (2000).
6. Jans, D. A. & Hassan, G. *BioEssays* **20**, 400–411 (1998).
7. Duverger, E., Pellerin-Mendes, C., Mayer, R., Roche, A. C. & Monsigny, M. *J. Cell Sci.* **108**, 1325–1332 (1995).
8. Reilly, J. F. & Maher, P. A. *J. Cell Biol.* **152**, 1307–1312 (2001).
9. Carpenter, G. *BioEssays* **22**, 697–707 (2000).
10. Kuwada, S. K. *et al. Am. J. Physiol.* **275**, C1419–1428 (1998).
11. Reilly, R. M. *et al. J. Nucl. Med.* **41**, 429–438 (2000).
12. Chen, J. *et al. Cancer Gene Ther.* **5**, 357–364 (1998).

News and Views contributions

The News and Views section provides a forum in which new advances in the field of cell biology, as reported in published papers, can be communicated to a wide audience.

Most News and Views pieces are linked to Articles that appear in *Nature Cell Biology*, but some may focus on papers of exceptional significance that are published elsewhere. Unsolicited contributions will not normally be considered, although prospective authors are welcome to make proposals to the Editor before the paper is published.

As a general guideline, News and Views pieces should be about 1,300 words, with one or two display items (figures, boxes and tables). They should make clear the advance (the 'news') and communicate a sense of excitement, yet provide a critical evaluation of the work in context of the rest of the field. We encourage personal 'views', criticisms and predictions, but authors should not refer to their own work, except in passing. Detailed guidelines are available on request from cellbio@nature.com and on *Nature Cell Biology*'s Web site (http://cellbio.nature.com).

© 2001 Macmillan Magazines Ltd

DOC-2 inhibits ILK activity and induces anoikis in breast cancer cells

Shao-Chun Wang*[1], Keishi Makino*[1], Weiya Xia[1], Jeong Soo Kim[1], Seock-Ah Im[2], Hua Peng[1], Samuel C. Mok [3], Sonja E. Singletary[4], and Mien-Chie Hung[1‡]

The University of Texas M. D. Anderson Cancer Center, Department of Molecular and Cellular Oncology[1], Department of Neuro-Oncology[2], Department of Surgical Oncology[4], Houston, Texas; Laboratory of Gynecologic Oncology, Division of Gynecologic Oncology, and Department of Obstetrics, Gynecology and Reproductive Biology, Brigham and Women's Hospital, Dana Farber Harvard Cancer Center[3].

* These two authors contributed equally.

‡ To whom correspondence should be addressed: The University of Texas, M. D. Anderson Cancer center, Department of Molecular and Cellular Oncology, Box 108, 1515 Holcombe Blvd., Houston, TX 77030. Phone: (713) 792-3668. Fax: (713) 794-0209. E-mail: mchung@mail.mdanderson.org

Key words: ILK, DOC-2, anoikis, breast cancer, HER-2/*neu*

Abstract

DOC-2 was identified due to the loss of its expression in primary ovarian cancer cells. It is believed that loss of DOC-2 expression is one of the early events of ovarian malignancy. These results suggest a function of DOC-2 as a tumor suppressor. However, it is not clear how DOC-2 negatively regulates cancer cell growth. In this report, we demonstrate that DOC-2 expression in breast cancer cells resulted in sensitivity to suspension-induced cell death (anoikis). This event was associated with the down-regulation of the integrin-linked kinase (ILK) activity. Since ILK is a key factor in regulating the cellular signaling in responding to the extracellular signals through adhesion molecules like integrins, our results indicate that DOC-2 may prevent tumor growth and invasion by modulating the anti-apoptotic ILK pathway.

The human DOC-2 gene (differentially-expressed in ovarian carcinoma 2) was originally isolated based on a differential RNA fingerprint screening of normal versus cancer epithelial ovarian cells (Mok et al., 1994; Mok et al., 1998). Expression of the DOC-2 gene is mitigated or lost in multiple ovarian cancer cell lines as well as in tissues derived from serous ovarian tumors when compared with the expression levels in normal ovarian cells (Mok et al., 1994; Mok et al., 1998). The DOC-2 protein contains a phosphotyrosine interacting domain (PID) at the N terminal region and multiple proline-rich SH3 binding motifs at the C terminus (Mok et al., 1998). These motifs are conserved in the mouse homologue of DOC-2, p96/mDab2, suggesting critical biological functions associated with these motifs (Xu et al., 1998). The SH3 binding motifs of the mouse p96/mDab2 protein have been shown to interact with the SH3 domains of Grb2 and reduce the binding between Grb2 and Sos (Xu et al., 1998). These observations suggest that DOC-2 may be involved in the signaling pathway mediated by tyrosine phosphorylations.

In normal tissues, DOC-2 expression is distributed in the surface epithelial cells of ovary or the ductal epithelial cells of breast (Fazili et al., 1999; Mok et al., 1994; Mok et al., 1998; Sheng et al., 2000). Loss of DOC-2 expression in ovarian cancer appears to be an early tumorigenesis event in serous but not mucinous ovarian cancer (Fazili et al., 1999; Mok et al., 1998). It has been reported that DOC-2 expression is correlated with the presence of basement membrane in ovarian and breast tumors, suggesting that DOC-2 exerts its anti-tumor function by controlling the positioning of the epithelial cells to basement membrane (Sheng et al., 2000). Consistently, reconstitution of DOC-2

expression in human ovarian cancer cells resulted in reduction of growth rate in culture and tumorigenicity in nude mice (Mok et al., 1998). However, the mechanism of the tumor suppression function of DOC-2 remains unclear.

To further explore the function of DOC-2, we constructed a recombinant adenovirus of DOC-2. Infection of two breast cancer cell lines, SK-BR-3 and MDA-MB-453, showed a dose-dependent manner of adenovirus-mediated DOC-2 expression (Figure 1). Both cell lines express low or undetectable levels of endogenous DOC-2 protein. Even though flow cytometry analysis indicated that DOC-2 expression did not significantly affect the proliferation of these cell lines in attached cell culture (data not shown), ectopic DOC-2 expression in SK-BR-3 cells significantly sensitized the cells to apoptosis induced by cell detachment (anoikis) (Figure 2, A and C). This phenomenon is not limited to SK-BR-3 cells. Viral infection of DOC-2 in the MDA-MB-453 breast cancer cells exhibited an even more dramatic effect by DOC-2 expression in sensitization of anoikis (Figure 2, B and C).

Under our experimental condition, DOC-2 expression did not alter the activation of the ERK signaling pathway, nor the JNK stress responsive pathway (Figure 3). Since both SK-BR-3 and MDA-MB-453 cells express high level of the tyrosine kinase receptor HER-2/*neu*, and that HER-2/*neu* overexpression has been reported to enhance cell survival in anchorage-independent growth (Yu & Hung, 1991), we next checked the protein levels and the tyrosine phosphorylation status of HER-2/*neu* in these cell lines.

DOC-2 expression apparently did not have effect on either protein expression or the autophosphorylation status of HER-2/*neu* (Figure 3).

The induced apoptosis in detached cells by DOC-2 suggests that DOC-2 may block the anti-apoptotic arm downstream the integrin signaling pathway. The major survival determinant in the integrin pathway is the integrin-linked kinase (ILK) (Dedhar, 2000). ILK is a serine/threonine kinase and plays a critical role for cell proliferation, survival, and tumor development (Dedhar, 2000; Persad et al., 2000). ILK interacts with the cytoplasmic domain of integrin β1 and β3 and can be stimulated by extracellular matrix attachment. ILK can also be activated by growth factor stimulation in a PI-3 kinase-dependent manner (Delcommenne et al., 1998). Overexpression of ILK in breast cancer cells confers resistance to anoikis, while down-regulation of ILK in breast cancer cells sensitized the cells to anoikis (Attwell et al., 2000). Since SK-BR-3 and MDA-MB-453 cells express high levels of ILK [Makino, unpublished results], we tested the possible involvement of ILK in the DOC-2 signaling pathway by examining the kinase activity of ILK in cells overexpressing DOC-2 (Figure 4). DOC-2 expression resulted in significant down-regulation of the ILK activity in SK-BR-3 and MDA-MB-453 cells and the level of down-regulation was corresponding to the induction levels of anoikis as evaluated by TUNNEL assay mentioned above (Figure 2).

We have demonstrated that the putative tumor suppressor gene DOC-2 sensitizes breast cancer cells to apoptosis induced by loss of attachment to extracellular matrix. This event was accompanied by enzymatic down-regulation of the ILK kinase, a key anti-

apoptotic mediator in processing signals stimulated by changes in the extracellular environment. Our study indicates that DOC-2 suppresses the development of breast cancer by targeting the oncogenic activity of ILK. These results also suggest a link between the DOC-2 function and the integrin-mediated signaling for cell survival. The question whether this tumor suppression function of DOC-2 is associated with its previously reported ability to interrupt the Grb2-Sos signaling cascade remains to be explored (Xu et al., 1998). With this regard, it is noteworthy that the Shc2-Grb2-Sos signaling pathway has been shown to be involved in the activation of PI-3K activity (Gu et al., 2000), and that activation of PI-3K results in the activation of a number of downstream regulators including ILK (Dedhar, 2000; Delcommenne et al., 1998). Alternatively, DOC-2 may modulate the activity of ILK by directly inhibiting the cross talk between integrins and ILK. The answer of this question will be critical to understanding of the pathogenesis and the development of a potential therapy for ovarian and breast cancer.

References

Attwell, S., Roskelley, C. & Dedhar, S. (2000). *Oncogene*, **19,** 3811-3815.

Dedhar, S. (2000). *Curr. Opin. Cell Biol.*, **12,** 250-256.

Delcommenne, M., Tan, C., Gary, V., Rue, L., Woodgett, J. & Dedhar, S. (1998). *Proc. Natl. Acad. Sci. USA*, **95,** 11211-11216.

Fazili, Z., Sun, W., Mittelstaedt, S., Cohen, C. & Xu, X.-X. (1999). *Oncogene*, **18,** 3104-3113.

Gu, H., Maeda, H., Moon, J.J., Lord, J.D., Yoakim, M., Nelson, B.H. & Neel, B.G. (2000). *Mol. Cell. Biol.*, **20,** 7109-7120.

Mok, S. C.,, Wong, K.K., Chan, R.K.W., Ching, C.C., Tsao, S.W., Knapp, R.C. & Berkowitz, R.S. (1994). *Gyn. Oncology*, **52,** 247-252.

Mok, S.C., Chan, W.Y., Wong, K.K., Cheung, K.K., Lau, C.C., Ng, S.W., Baldini, A., Colitti, C.V., Rock, C.O. & Berkowitz, R.S. (1998). *Oncogene*, **16,** 2381-2387.

Persad, S., Attwell, S., Gray, V., Delcommenne, M., Troussard, A., Sanghera, J. & Dedhar, S. (2000). *Proc. Natl. Acad. Sci. USA*, **97,** 3207-3212.

Sheng, Z., Sun, W., Smith, E., Cohen, C., Sheng, Z. & Xu, X.-X. (2000). *Oncogene*, **19,** 4847-4854.

Xu, X.-X., Yi, T., Tang, B. & Lambeth, J.D. (1998). *Oncogene*, **16,** 1561-1569.

Yu, D. & Hung, M.-C. (1991). *Oncogene*, **6,** 1991-1996.

Figure Legends

Figure 1. Dose-dependent expression of DOC-2 by adenovirus infection. 1×10^6 of cells were plated in 100 mm tissue culture plates for 48 h. Cells were then infected by DOC-2 viruses (Ad.DOC-2) of different titers (MOI) for overnight in the absence of serum. The infection mix was then removed and the cells were cultured in medium containing 10% of fetal bovine serum for 36 h before being harvested for cell lysates. A, For SK-BR-3 cells infection with the control virus of luciferase (Ad.Luc) was used as the negative control. B, For the experiment of MDA-MB-453 cells, Ad.DOC-2 and Ad.Luc of 400 MOI in total with different combinations as indicated were used to co-infect the cells. The CPP32 protein (panels A and B) as well as HER-2 (panel B) were shown as equal loading controls.

Figure 2. DOC-2 expression inhibited anoikis. A, SK-BR-3 cells were infected by 200 MOI of DOC-2 virus (Ad.DOC-2) or control luciferase (Ad.Luc) as described in Figure 1. The infected cells were then trypsinized and plated in 100 mm plates coated with poly-(2-hydroxyethyl methacrylate) (poly-HEMA) and incubated for 36 h in serum-free medium. Cells were then harvested, washed, and collected on a slide by a cytospin centrifuge. The cell pellet was then fixed in 4% paraformaldehyde at 4° for overnight. The fixed cells were then permeablized by 0.5% Triton X-100 and deproteinated with proteinase K. The apoptotic DNA fragments were then labeled by terminal deoxynucleotidyl transferase (TdT) (Gibco BRL, MD) and biotinylated dUTP (Boehringer Mannheim, IN). Labeled cells were stained with the HRP-conjugated

avidin-biotinylated complex (Vector, CA) and developed in the aminoethylcarbazole chromogen substrate solution. The ratio between infections by Ad.DOC-2 and by Ad.Luc is shown. B, TUNNEL assay for MDA-MB-453 cells infected by 400 MOI of Ad.DOC-2 or Ad.Luc as described in A. C, Representative slides showing the different levels of anoikis of SK-BR-3 and MDA-MB-453 cells as detected by TUNNEL assay. Examples of positive cells are marked by arrows.

Figure 3. DOC-2 expression did not affect the ERK, JNK, or HER-2/*neu* activity. The lysates isolated from the cells infected by Ad.DOC-2 or Ad.Luc as indicated in Figure 2 were separated by SDS-PAGE and the resulted blots were probed with antibodies of DOC-2 (Upstate), phosphorylated ERK and total ERK (Santa Cruz), phosphorylated tyrosine (4G10; Upstate), total HER-2/*neu* (Oncogene Science), and ILK (Upstate). A. SK-BR-3 cells. B. MDA-MB-453 cells.

Figure 4. DOC-2 expression inhibited ILK kinase activity. After infection by either Ad.DOC-2 or Ad.Luc for 36 h in the absence of serum, cell lysates were prepared in the immunoprecipitation buffer [0.5% NP-40, 150 mM NaCl, 50 mM Tris (pH 8.0), 2% aprotinin, 5 mM PMSF, 100 mM NaF, 2 mM Na_3VO_4, 1 mM EDTA]. Five hundred micrograms of protein from each sample was incubated at 4° with 1 μg of anti-ILK antibody or normal rabbit IgG overnight and for another 2 h after addition of protein A-agarose. The immunoprecipitates were washed three times with IP buffer and twice with kinase buffer [20 mM HEPES (pH7.4), 150 mM KCl, 5 mM $MnCl_2$, 5 mM NaF, 1 mM DTT] and then resuspended in 40 μl of kinase buffer containing 5 μg of myelin basic

protein and 10 μCi of [γ-^{32}P]ATP. Following 30 min incubations at 30°, the reactions were terminated with 40 μl of 2 X Laemmli SDS sample buffer. Samples were incubated for 5 min at 96° and resolved by 15% SDS-PAGE and visualized by autoradiography. The data were quantified by ImageQuant software of a Phosphoimager (Molecular Dynamics, Sunnyvale, CA). The fold reduction of ILK kinase activity by DOC-2 expression is shown. A. SK-BR-3 cells. B. MDA-MB-453 cells.

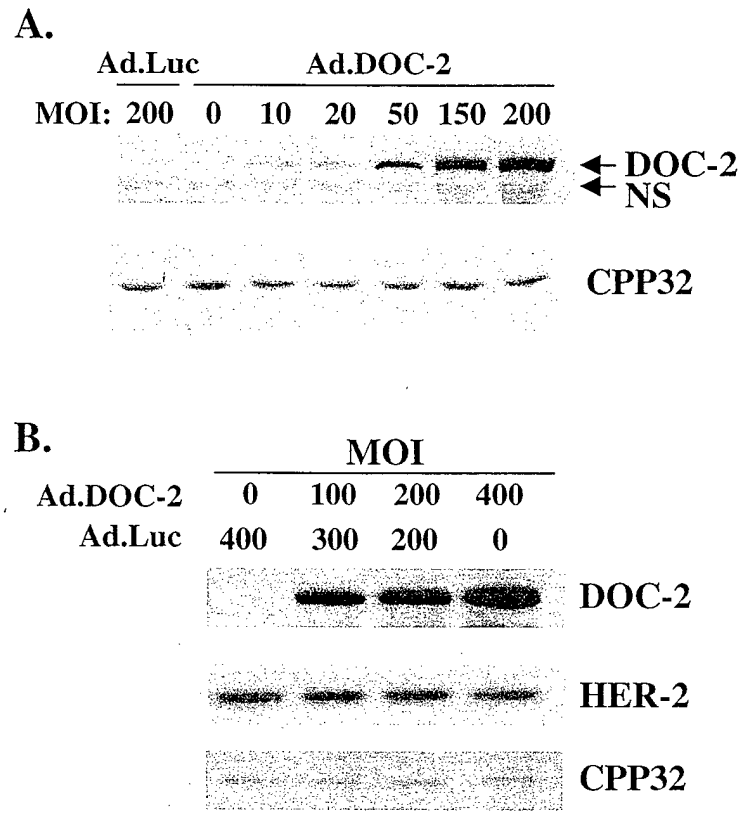
A.
Ad.Luc
Ad.DOC-2
MOI: 200 0 10 20 50 150 200
DOC-2
NS
CPP32
B.
MOI
Ad.DOC-2 0 100 200 400
Ad.Luc 400 300 200 0
DOC-2
HER-2
CPP32

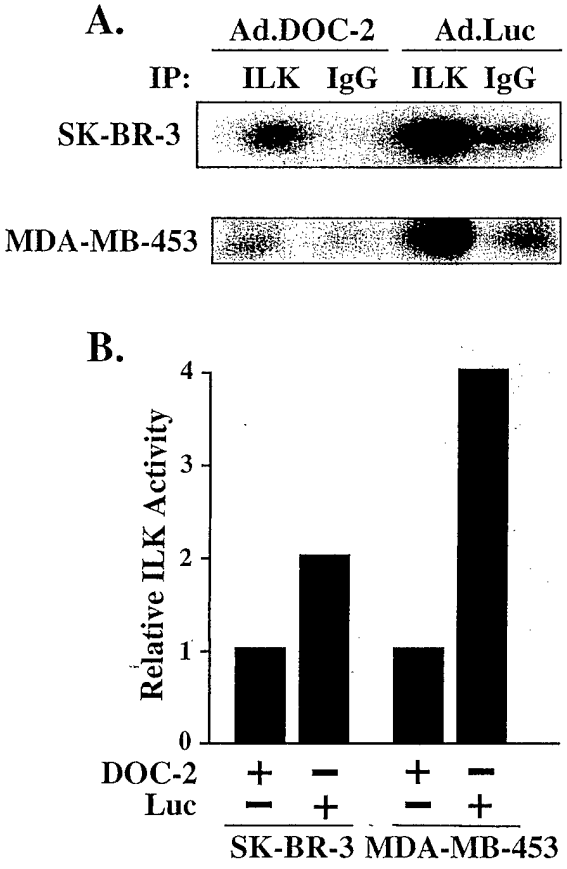
A.
Ad.DOC-2
Ad.Luc
IP:
ILK
IgG
ILK
IgG
SK-BR-3
MDA-MB-453
B.
Relative ILK Activity
0
1
2
3
4
DOC-2
Luc
+
−
−
+
+
−
−
+
SK-BR-3
MDA-MB-453

A.

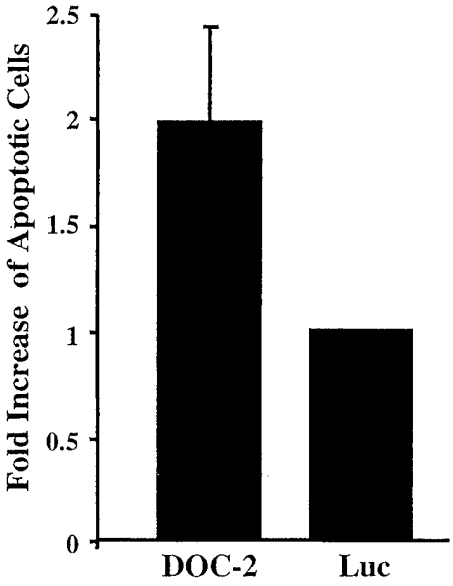
Fold Increase of Apoptotic Cells
2.5
2
1.5
1
0.5
0
DOC-2
Luc

B.

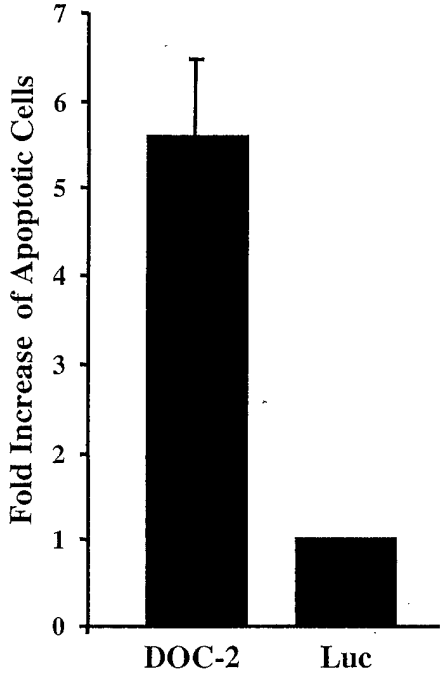
Fold Increase of Apoptotic Cells
7
6
5
4
3
2
1
0
DOC-2
Luc

C.

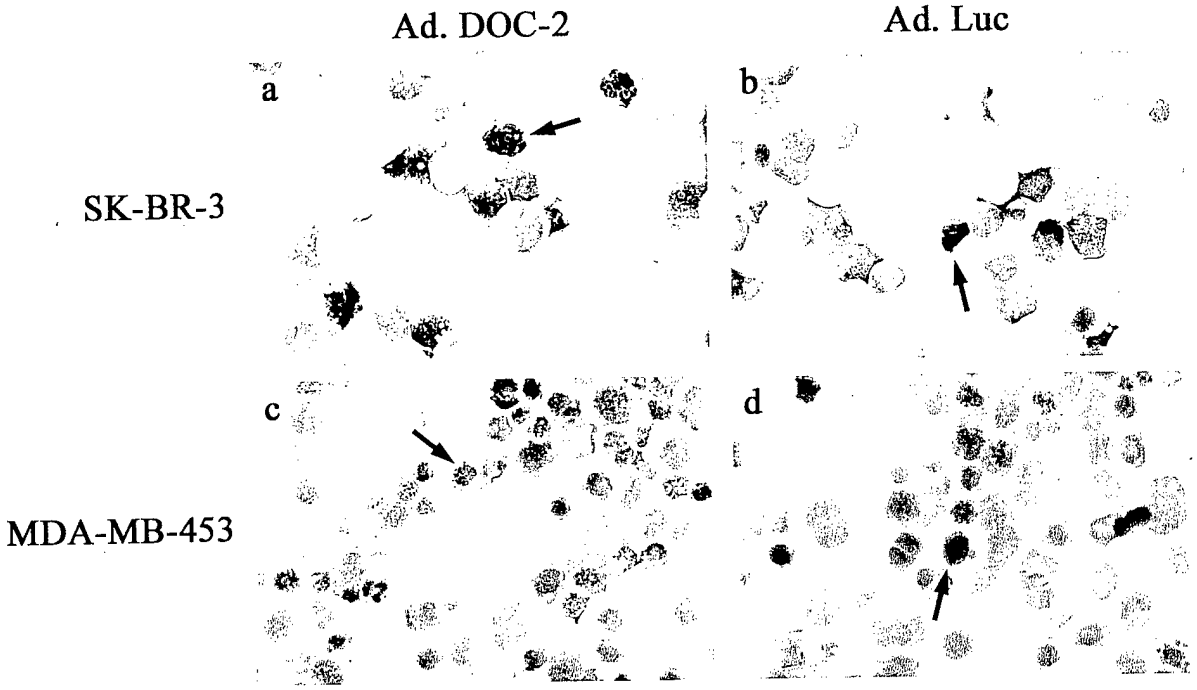
Ad. DOC-2
Ad. Luc
a
b
SK-BR-3
c
d
MDA-MB-453

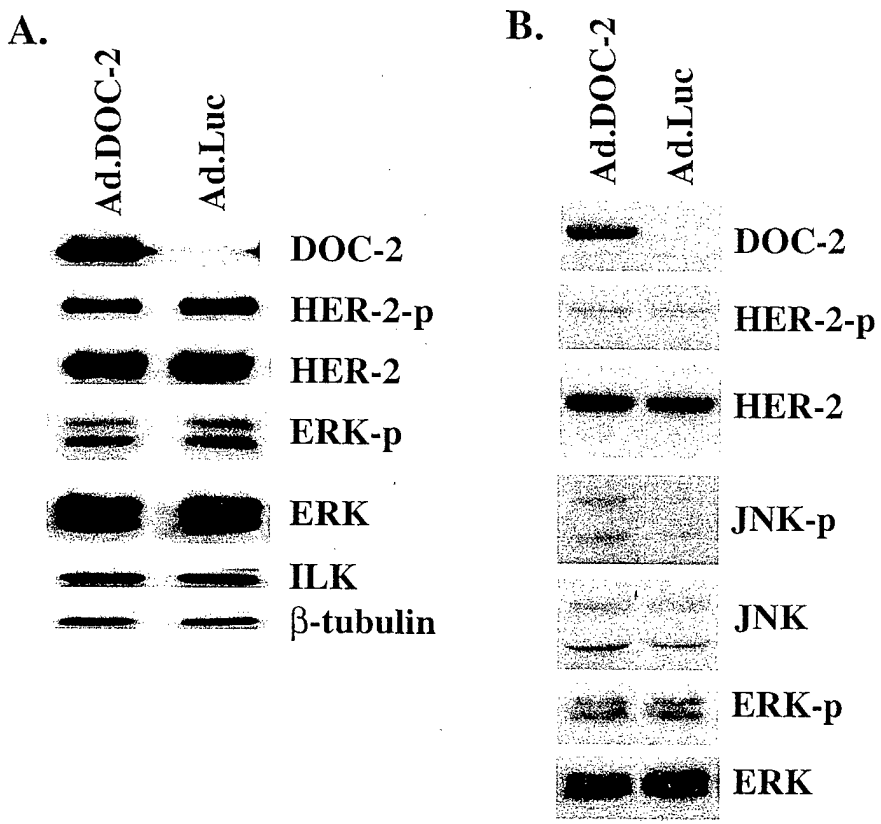
A.
Ad.DOC-2
Ad.Luc
DOC-2
HER-2-p
HER-2
ERK-p
ERK
ILK
β-tubulin
B.
Ad.DOC-2
Ad.Luc
DOC-2
HER-2-p
HER-2
JNK-p
JNK
ERK-p
ERK

Multiple signaling pathways involved in activation of matrix metallo-proteinase-9 (MMP-9) by heregulin-β1 in human breast cancer cells

Jun Yao†, Shunbin Xiong†, Kristine Klos, Nina Nguyen, Rebecca Grijalva, Ping Li, and Dihua Yu*

Department of Surgical Oncology, The University of Texas M. D. Anderson Cancer Center, Houston, Texas 77030, USA

Running Title: Activation of MMP-9 by heregulin-β1

† These authors contributed equally

* Correspondence: D. Yu, Department of Surgical Oncology, Box 107, The University of Texas M. D. Anderson Cancer Center, 1515 Holcombe Boulevard, Houston, TX 77030, USA Phone: (713) 792-3636 Fax: (713) 794-4830 Email: dyu@mdacc.org

Matrix metalloproteinase-9 (MMP-9[1]) plays important roles in tumor invasion and angiogenesis. Secretion of MMP-9 has been reported in various cancer types including lung cancer, colon cancer, and breast cancer. In our investigation of MMP-9 regulation by growth factors, MMP-9 was activated by heregulin-β1 as shown by zymography in both SKBr3 and MCF-7 breast cancer cell lines. Increase in MMP-9 activity was due to increased MMP-9 protein and mRNA levels, which mainly results from transcriptional upregulation of MMP-9 by heregulin-β1. Heregulin-β1 activates multiple signaling pathways in breast cancer cells, including Erk, p38 kinase, PKC, and PI3-K pathways. We examined the pathways involved in heregulin-β1-mediated MMP-9 activation using chemical inhibitors that specifically inhibit each of these heregulin-β1-activated pathways. The PKC inhibitor RO318220 and p38 kinase inhibitor SB203580 completely blocked heregulin-β1-mediated activation of MMP-9. MEK-1 inhibitor PD098059 partially blocked MMP-9 activation, whereas PI3-K inhibitor wortmannin had no effect on heregulin-β1-mediated MMP-9 activation. Therefore, at least three signaling pathways are involved in the activation of MMP-9 by heregulin-β1. Since MMP-9 is tightly associated with invasion/metastasis and angiogenesis, our studies suggest that blocking heregulin-β1-mediated activation of MMP-9 by inhibiting the related signaling pathways may provide new strategies for inhibition of cancer metastasis and angiogenesis.

Keywords: MMP-9; heregulin-β1; signaling; breast cancer; invasion

---

[1] the abbreviations used are: MMP-9, matrix metalloproteinase-9; Erk, extracellular response kinase; PKC, protein kinase C; PI3-K, phosphatidylinositol 3-kinase; PMA, phorbol 12-myristate 13-acetate; JNK, Jun amino-terminus kinase; TGF, transforming growth factor.

Introduction

Matrix metalloproteinase-9 (MMP-9) belongs to a family of zinc- and calcium-dependent metalloproteinases which are involved in the breakdown of extracellular matrix during tissue remodeling. Along with other metalloproteinases, MMP-9 plays a key role in physiological processes such as development, wound healing, angiogenesis, and also in pathological processes such as inflammation, tumor invasion and metastasis (reviewed by Parks & Mecham, 1998).

Elevated expression of MMP-9 is associated with increased metastatic potential in many cancer types including breast cancer, prostate cancer, brain cancer, and melanoma (Hujanen *et al.*, 1994; Jones *et al.*, 1999; Rao *et al.*, 1993; Sehgal *et al.*, 1996). For example, MMP-9 was detected in 68% of primary breast carcinomas, either in the stromal compartment or adjacent to tumor cells (Jones *et al.*, 1999). A significant correlation between the expression of MMP-9 and tumor grade has also been reported in bladder cancer (Davies *et al.*, 1993b). Also, MMP-9 activity was dramatically higher in human malignant brain tumors compared to less malignant or normal brain tissue extracts (Rao *et al.*, 1993). Furthermore, elevated serum level of MMP-9 was shown to correlate with spontaneous metastasis in rat mammary tumor models (Nakajima *et al.*, 1993). Inhibition of MMP-9 expression and/or activity resulted in reduction of tumor invasion and metastasis in animal studies (Davies *et al.*, 1993a; Garbisa *et al.*, 1987; Lozonschi *et al.*, 1999). Mice deficient in MMP-9 were viable but exhibited an abnormal pattern of skeletal growth plate vascularization (Vu *et al.*, 1998). Cultured growth plate cells from MMP-9-null mice showed a delayed release of some angiogenic activators, suggesting that MMP-9 may play a positive role in regulating angiogenesis. This finding is supported by a recent report that cell surface-localized MMP-9 proteolytically activated pro-TGFβ and promoted tumor invasion and angiogenesis (Yu & Stamenkovic, 2000). However, MMP-9 can also cleave plasminogen to generate angiostatin, an angiogenesis inhibitor (Patterson & Sang, 1997).

Secretion of MMP-9 can be stimulated by a variety of factors including cytokines, growth factors, phorbol esters, and bacteria endotoxins. For example, epidermal growth factor and amphiregulin stimulate MMP-9 secretion in the SKBr3 human breast cancer cell line (Kondapaka *et al.*, 1997; Shima *et al.*, 1993). TGF-β also activates MMP-9 in

breast cancer and prostate cancer cells (Samuel *et al.*, 1992; Sehgal *et al.*, 1996; Welch *et al.*, 1990). In addition, expressions of oncogenic Ras and Src in cancer cells also lead to expression of MMP-9, suggesting that various stimuli may activate cellular signaling pathways controlled by these oncoproteins to upregulate MMP-9 (Ballin *et al.*, 1988; Sato *et al.*, 1993). Induction of MMP-9 is also regulated through cell-cell contacts and cell-extracellular matrix interaction. For example, fibroblasts cultured with colon carcinoma cells were induced to secrete MMP-9 (Segain *et al.*, 1996).

Regulation of MMP-9 activation by various stimuli in different cellular settings may involve different signal transduction pathways. MMP-9 activity was markedly stimulated in tumor cell lines by PMA, a known PKC activator, suggesting a possible role for PKC in activation of MMP-9 (Huhtala *et al.*, 1991; Moll *et al.*, 1990). In addition, PMA-induced MMP-9 activities in UM-SCC-1 cell line were abolished by inhibition of p38 kinase (Simon *et al.*, 1998). Inhibition of Erk activation by MEK inhibitor PD098059 blocked MMP-9 production and attenuated the *in vivo* invasiveness of head and neck squamous carcinoma cells (Simon *et al.*, 1999). Involvement of JNK signaling pathway in regulation of MMP-9 is also reported (Gum *et al.*, 1997). Finally, secretion of newly synthesized MMP-9 from HT1080 human fibrosarcoma cells was regulated by phospholipase D activity (Williger *et al.*, 1999), which may regulate MMP-9 production at a late stage.

Heregulins are a family of growth factors that regulate growth, differentiation, and survival of breast cancer cells and various other cancer cells (Holmes *et al.*, 1992; Lupu *et al.*, 1990; Peles *et al.*, 1992). Heregulin binds directly to membrane receptors HER3 and HER4 which form heterodimers with HER2 (Carraway *et al.*, 1994; Plowman *et al.*, 1993; Sliwkowski *et al.*, 1994). Heregulin is produced by both stroma cells such as fibroblasts and tumor cells including breast carcinomas and melanomas (Holmes *et al.*, 1992; Wen *et al.*, 1992). Messenger RNA transcripts of heregulin were detected in about 25% of human mammary carcinomas (Normanno *et al.*, 1995), a percentage similar to HER2 overexpression. However, there is no significant association between expression of these two molecules. The role of heregulins in tumor invasion and metastasis is not yet clear. In this study, we demonstrated that heregulin-β1 induced MMP-9 secretion

from MCF-7 and SKBr3 breast cancer cell lines via activation of multiple signaling pathways that led to transcriptional upregulation of MMP-9.

Results

HRG-β1 induced MMP-9 secretion in SKBr3 and MCF-7 breast cancer cells

A panel of breast cancer cell lines was examined for their response to heregulin-β1 treatment to secrete MMP-9. The cell lines included MDA-MB-435, MDA-MB-231, MDA-MB-453, BT-474, SKBr3, MCF-7, and 435.eB1, a stable transfectant expressing high levels of erbB2 derived from MDA-MB-435 cells. Heregulin-β1 treatment significantly increased MMP-9 gelatinolytic activity in MCF-7 and SKBr3 cell lines, but not in other breast cancer cell lines (Figure 1a and data not shown). In contrast, activities of MMP-2, another closely related MMP, was not induced by heregulin-β1 treatment in all cell lines examined at the same time. Induction of MMP-9 gelatinolytic activity was time- and concentration-dependent and could be readily detected when SKBr3 cells were treated with as low as 2 ng/ml heregulin-β1 for 24 hours (Figure 1b). MCF-7 cells had a higher basal level of MMP-9 activity than SKBr3 cells. Nevertheless, induction of MMP-9 activity could be detected in MCF-7 cells 24 hours after heregulin-β1 (>5 ng/ml) treatment.

Western blot analysis of MMP-9 demonstrated that heregulin-β1 induced MMP-9 protein secretion from SKBr3 (Figure 2a) and MCF-7 cells (data not shown). The MMP-9 protein levels correlated well with MMP-9 gelatinolytic activity shown in the zymographic assays (Figure 1). Therefore, increased MMP-9 gelatinolytic activity induced by heregulin-β1 was due to increased MMP-9 protein production and secretion. To further examine whether heregulin-β1-mediated increase of MMP-9 protein level was mostly due to increased MMP-9 messenger RNA expression, northern hybridization analysis and RT-PCR were performed to detect MMP-9 mRNA in heregulin-β1 treated and untreated SKBr3 cells. Untreated SKBr3 cells had a basal MMP-9 mRNA level that was barely detectable by northern hybridization (Figure 2b). However, an increase in MMP-9 mRNA level could be detected 6 hours after heregulin-β1 treatment. The MMP-9 mRNA levels continued to increase until 24 hours after heregulin-β1 treatment (Figure

2b). RT-PCR was more sensitive than northern hybridization and detected a basal signal in untreated SKBr3 cells (Figure 2c). Additionally, RT-PCR results confirmed that MMP-9 mRNA level increased 6 hours after heregulin-β1 treatment of SKBr3 cells (Figure 2c) and MCF-7 cells (data not shown). Therefore, increased MMP-9 messenger RNA levels contributed to increased MMP-9 protein levels in heregulin-β1-treated SKBr3 and MCF-7 cells. Notably, the increase of MMP-9 mRNA levels was not due to increased MMP-9 mRNA stability, because heregulin-β1 did not significantly change MMP-9 mRNA decay rate (data not shown).

Heregulin-β1 increased MMP-9 promoter activities in SKBr3 and MCF-7 cells

To examine whether the increase in MMP-9 mRNA level was due to increased transcription from the MMP-9 promoter, a luciferase reporter gene driven by a 2.2kb MMP-9 promoter (pMMP9-2.2k-luc) or by a shorter 670bp MMP-9 promoter (pMMP9-670-luc) was transfected into SKBr3 cells and luciferase activities were measured (Figure 3a). Heregulin-β1 treatment led to an approximately 2.4-fold increase of luciferase activity using both pMMP9-2.2k-luc and pMMP9-670-luc. This indicated that heregulin-β1 indeed upregulated MMP-9 at the transcriptional level and that the proximal 670bp promoter region may contain the heregulin-β1-response element(s) inside the 2.2kb MMP-9 promoter. To confirm this observation, pMMP9-670-Luc reporter plasmid was transfected into MCF.HRG cells that constitutively secret the functional EGF-like domain of human heregulin-β1, as well as into the MCF.Zeo control cell line. Figure 3b shows that luciferase activity increased more than 2.5-fold in MCF.HRG cells compared to that of MCF.Zeo cells. In addition, we cloned the 670bp MMP-9 promoter region devoid of the minimal promoter region (-46bp to transcriptional start) into a TK promoter-luciferase reporter and transfected it into both MCF-7 and SKBr3 cells treated with or without heregulin-β1. Luciferase activities from MMP9-670-TK-luc reporter gene also showed an approximately 2.4-fold increase in heregulin-β1-treated MCF-7 or SKBr3 cells compared with untreated cells (Figure 3c). All these data confirmed that heregulin-β1 indeed induced transcription from the MMP-9 promoter. It should be noted that the transcription induction by heregulin-β1 was modest when compared to the

dramatic increases of gelatinolytic activities in heregulin-β1-stimulated SKBr3 cells. This suggested that other mechanisms in addition to transcriptional upregulation could be involved in heregulin-β1-induced MMP-9 activation.

To further define the heregulin-β1-responsive elements in the 670 bp MMP-9 proximal promoter, a series of promoter 5'-deletion constructs linked to the luciferase reporter gene was transfected into heregulin-β1 treated and untreated SKBr3 cells. Luciferase assays showed that promoter deletion from the 5' end up to -241bp did not significantly change the basal MMP-9 promoter activity, but slightly decreased the response of the promoter to heregulin-β1 treatment (Figure 3d). The shortest reporter construct with only an 84 bp promoter region (pMMP9-84-luc) had dramatically decreased basal promoter activity and also completely lost response to heregulin-β1 treatment. The data suggested that a major heregulin-β1-response element(s) resides in promoter region –84bp to –241bp and that the promoter regions from –241bp to –670bp also contribute to heregulin-β1-induced transactivation.

Multiple signaling pathways regulated heregulin-β1-induced MMP-9 secretion

We have previously shown that heregulin-β1 can activate several signaling pathways in MCF-7 and SKBr3 cells including Erk, p38 kinase, PI3-K, and PKC pathways (Tan *et al.*, 1999; Xiong *et al.*, 2001). To examine which of these signaling pathways may be involved in induction of MMP-9 by heregulin-β1, we used chemical inhibitors of these signaling pathways to examine the requirement of activation of each pathway in heregulin-β1-mediated MMP-9 upregulation. PD098059 is known to selectively block the activity of MAP kinase kinase (MEK), an activator of Erk kinases. SB203580 is a specific inhibitor for p38 kinase. RO318220 inhibits PKC activity and wortmannin inhibits PI3-K activity. Different concentrations of these chemical inhibitors were added to heregulin-β1-treated SKBr3 cells. Heregulin-β1-induced MMP-9 activation was partially blocked by PD098059 at concentrations above 10μM, which partially inhibited heregulin-β1-induced Erk activation (Figure 4a). However, PD098059 had no effect on MMP-2 activity (Figure 4a). Wortmannin had no apparent effect on heregulin-β1-mediated activation of MMP-9 even at a high concentration of 40 nM that effectively

inhibited heregulin-β1-mediated activation of Akt, a downstream target of PI3-K (Figure 4b). Therefore, the Erk pathway contributes to heregulin-β1-induced activation of MMP-9 while the PI-3K pathway, despite its activation by heregulin-β1, does not contribute to MMP-9 activation.

Interestingly, inhibition of p38 kinase by SB203580 and inhibition of PKC by RO318220 all effectively blocked heregulin-β1-mediated activation of MMP-9 (Figure 4c and 4d). SB203580 inhibited heregulin-β1 mediated MMP-9 upregulation in a concentration dependent manner and it completely blocked MMP-9 induction by heregulin-β1 at a concentration of 10μM (Figure 4c). PKC inhibitor RO318220 was the most potent inhibitor of heregulin-β1-induced MMP-9 activation. It completely inhibited MMP-9 activation at a concentration of 5μM (Figure 4d). This finding was further confirmed by applying two other PKC inhibitors RO320432 and GO6976 (Figure 4d). PKC consists of a family of isoforms including PKC α, β, ε, and ζ, which are differentially activated and perform different functions. It is known that the IC50 of these PKC inhibitors for PKCα and β are similar, but RO318220 inhibits PKCε at a lower concentration than RO320432 and GO6979 does not inhibit PKCε (Gschwendt *et al.*, 1996). Thus, more potent inhibition of MMP-9 activation by RO318220 suggested that PKCε may be an important PKC isoform in mediating the upregulation of MMP-9 by heregulin-β1.

We next investigated whether these chemical inhibitors may block heregulin-β1-induced upregulation of MMP-9 mRNA and transcription. Northern analysis demonstrated that the MEK inhibitor PD098059 partially blocked heregulin-β1-induced upregulation of MMP-9 mRNA (Figure 5a), which is consistent with its partial inhibition of MMP-9 activity (Figure 4a). Both RO318220 and SB203580 completely blocked the hregulin-β1-induced increase of MMP-9 mRNA level (Figure 5a). Furthermore, the luciferase assay on pMMP9-670-luc transfected SKBr3 cells treated with or without heregulin-β1 revealed that PD098059 weakly inhibited MMP-9 transcriptional upregulation by heregulin-β1 (Figure 5b). In contrast, SB203580 effectively blocked heregulin-β1-mediated MMP-9 transcriptional upregulation and had no effect on MMP-9 promoter basal activity. Notably, the PKC inhibitor RO318220 inhibited both heregulin-

β1-mediated MMP-9 transcriptional upregulation and MMP-9 basal transcription (Figure 5b). These data suggested that (1) PKC contributes to both basal and heregulin-β1-induced expression of MMP-9, (2) PKC and p38 kinase regulate heregulin-β1-induced transcription of MMP-9 from the MMP-9 promoter, and (3) Erk kinase may partially contribute to heregulin-β1-induced upregulation of MMP-9 expression and activity at post-translational levels.

It has been reported previously that MMP-9 plays an important role in tumor cell invasion (Hujanen *et al.*, 1994; Jones *et al.*, 1999; Rao *et al.*, 1993; Sehgal *et al.*, 1996). To explore the biological impact of heregulin-β1-induced MMP-9 upregulation, we examined the effects of these chemical kinase inhibitors on heregulin-β1-induced invasion of SKBr3 breast cancer cells by *in vitro* invasion assay. As shown in Figure 6a, heregulin-β1-induced SKBr3 cell invasion could be significantly inhibited by PD98059 and SB203580 (approximately 70% inhibition) and almost completely blocked by RO318220 (more than 90% inhibition). The results demonstrated that heregulin-β1-induced breast cancer cell invasion can be blocked by multiple kinase inhibitors that inhibit heregulin-β1 down-stream signaling pathways for MMP-9 upregulation. This indicated that MMP-9 upregulation contributed to heregulin-β1-induced breast cancer cell invasion.

Discussion

In this study, we demonstrated that heregulin-β1 was able to upregulate MMP-9 secretion in SKBr3 and MCF-7 breast cancer cell lines. This induction was specific for MMP-9 since heregulin-β1 did not induce secretion of MMP-2, another closely related gelatinase, under the same experimental conditions (Figure 1). Despite high homology in their amino acid sequences, the promoters of MMP-9 and MMP-2 consist of different *cis*-elements (Parks & Mecham, 1998), hence respond to different stimuli.

Among a panel of seven breast cancer cell lines, significant increases of MMP-9 activity after heregulin-β1 treatment were observed in SKBr3 and MCF-7 cell lines. Both MCF-7 and SKBr3 cells have relatively high expression of HER3 receptors for

heregulins (Aguilar *et al.*, 1999), which may contribute to the induction of MMP-9 by heregulin-β1. However, other cell lines with high HER3 expression (such as MDA-MB-453 or BT474) did not respond to heregulin-β1 to upregulate MMP-9. This can generally be ascribed to cell type specificity, as different cell lines may have different levels of signaling molecules and downstream transcription factors. We have demonstrated that blockage of either Erk kinase activation, p38 activation, or PKC activation could inhibit MMP-9 production (Figures 4 and 5). Therefore, the inability of breast cancer cells to activate all these pathways to certain threshold levels might account for their inability to produce MMP-9. An extensive examination of the activation levels of signaling pathways in heregulin-β1 responsive and non-responsive cell lines may clarify this issue.

Heregulin-β1-induced increases of MMP-9 gelatinolytic activity were accompanied by increased MMP-9 protein level, which is likely the result of upregulated MMP-9 mRNA level (Figure 2). In contrast to the dramatic increase in MMP-9 protein level after heregulin-β1 treatment, induction of transcription from the MMP-9 promoter as indicated by the luciferase assay was moderate (about 2.4 fold, Figure 3). Furthermore, no significant change in MMP-9 mRNA stability was observed in SKBr3 cells untreated or treated with heregulin-β1 (data not shown). Thus, the apparent difference in the degrees of MMP-9 upregulation at protein and RNA levels could be due to the regulation of MMP-9 via other mechanisms such as translational and/or post-translational regulations. Alternatively, some heregulin-β1-responsive elements may reside outside the 2.2kb MMP-9 promoter region used in our study. Lastly, transcriptional upregulation of MMP-9 by heregulin-β1 could be moderate in nature, since heregulin-β1-induced transactivation from other promoters was reported to be moderate as well (Gramolini *et al.*, 1999; Khurana *et al.*, 1999, Xiong *et al.*, 2001).

It has been reported that inhibition of the Erk kinase pathway blocked MMP-9 production in other cell lines (Simon *et al.*, 1999). However, only partial inhibition of heregulin-β1-induced MMP-9 upregulation by PD098059 was observed in SKBr3 cells (Figure 4a) when cells were treated with 20μM PD098059. This partial inhibition might be due to incomplete block of the Erk activation in SKBr3 cells at the 20μM concentration of PD098059 (Figure 4a, right). Further increase of PD098059

concentration in culture medium to 40μM resulted in precipitation and crystallization of PD098059. Thus, we were unable to determine whether higher concentrations of PD098059 could completely inhibit Erk activity and block heregulin-β1–induced MMP-9 upregulation in SKBr3 cells.

A striking finding in this study was that induction of MMP-9 by heregulin-β1 was not dependent on the activation of a single signaling pathway but rather dependent on at least three signaling pathways; namely the Erk pathway, PKC pathway, and p38 kinase pathway. Although each single pathway was previously shown to be involved in MMP-9 production in different cellular settings (Huhtala *et al.*, 1991; Moll *et al.*, 1990; Simon *et al.*, 1998; Simon *et al.*, 1999), our study is the first to report that heregulin-β1 can upregulate MMP-9 via simultaneous activation of multiple pathways in breast cancer cells (Figure 6b). The chemical inhibitors we used to block the function of various kinases are reported to be highly specific (Simon *et al.*, 1998; Simon *et al.*, 1999) and caused no apparent phenotypical changes in cells during the assay. Among these, inhibitors that block PKC and p38 pathways had the most potent inhibitory effects, suggesting that PKC and p38 kinases may be more critical than the Erk kinase in heregulin-β1-mediated MMP-9 induction in breast cancer cells. Interestingly, inhibition of the PI3-K pathway had no effect on MMP-9 induction by heregulin-β1. We have previously reported that heregulin-β1 regulates MCF-7 cell aggregation through the PI3-K pathway (Tan *et al.*, 1999). Therefore, heregulin-β1 can regulate distinct cellular processes through different signaling pathways.

Considering the possible involvement of several signaling pathways in MMP-9 activation, we propose two models to interpret our results. In the first model, we hypothesize that there is "cross-talk" between signaling pathways so that blocking one of the signaling pathways may affect the activation of another pathway. Indeed, some recent publications point out that PKC may function upstream of the p38 kinase pathway (Kozawa *et al.*, 2000; Simon *et al.*, 1998). However, it is unlikely that all three pathways (Erk, p38, PKC) are activated in a sequential order. Therefore, an alternative model is that signals from all three pathways could merge on a common target complex and activation of this common target requires input from each single pathway. When the overall input reaches a threshold, transcription of MMP-9 is turned on. This model

explains why blockage of a single pathway may abolish MMP-9 expression, and also why increased signals from one pathway (e.g. Erk pathway or PKC pathway) could lead to MMP-9 production (Gum *et al.*, 1997; Huhtala *et al.*, 1991; Moll *et al.*, 1990). We are currently investigating these possibilities.

Our finding that multiple signaling pathways control the upregulation of MMP-9 by heregulin-β1 (and possibly stimulation by other growth factors) has broadened our knowledge on the regulation of this important molecule involved in tumor invasion and metastasis. Our study implies that activation of MMP-9 by heregulin-β1 may highly depend on the nature of different breast tumors, such as their receptor levels and intracellular signaling networks. In addition, we can target more than one signaling pathway to repress MMP-9 expression. Indeed, applications of PD098059, SB203580, and RO318220 all dramatically inhibited breast cancer cell invasion *in vitro* (Figure 6a). These data provide insights and more options for future clinical interventions of heregulin-β1-induced MMP-9 upregulation and invasion of breast cancers.

Materials and Methods

Reagents

Recombinant human heregulin-β1 was purchased from NeoMarkers (Fremont, CA). Wortmannin, PD098059, GO6976, RO318220, RO320432, SB203580, and PMA were from Calbiochem (La Jolla, CA). MMP-9 antibody (Ab-1) was purchased from Calbiochem (La Jolla, CA). Antibodies against Akt, p38, and Erk (including phosphorylated forms) were purchased from New England BioLabs (Beverly, MA). MMP-9 CAT reporter plasmids were kindly provided by Dr. Douglas Boyd from the University of Texas M. D. Anderson Cancer Center. These include a panel of serial deletion constructs (pMMP9-670CAT, pMMP9-323CAT, pMMP9-241CAT, and pMMP9-84CAT). The promoter regions were subcloned using PCR method into pGL3-Basic luciferase reporter (Promega) to make pMMP9 luciferase reporters. The 2.2kb MMP-9 promoter was obtained by PCR using HT1080 genomic DNA as a template and primers of, forward 5'-GGTACCAGAGCCAGGCAGTTCTGG GCTTGAACACTA-3', reverse 5'-GAATTCCACTGGGGCAACCCCCTGTCTTCC-3'. The PCR fragment is subcloned into pMMP9-670Luc and fused with the proximal promoter to generate pMMP9-2.2k-Luc.

Zymographic Assay

Cells were seeded onto 6-well tissue culture plates in DMEM/F12 medium with 10% FBS and were cultured to 80% confluence. Cells were then washed and starved in serum-free media for 16 hours. Recombinant heregulin-β1 was added to a final concentration of 10ng/ml. After 24hr, conditioned media were collected and concentrated 10-fold using Centricon spin columns (Amicon, Beverly, MA) from 2 ml to 0.2 ml. Concentrated samples were subjected to 7.5% SDS-PAGE with gel containing 1% gelatin (Sigma). After electrophoresis, the gel was washed four times in 50 mM Tris-HCl buffer (pH 7.5) containing 2% Triton X-100. The gel was then washed once in 50 mM Tris-HCl buffer (pH 7.5) containing 0.2% Triton X-100, 150 mM sodium chloride, 10 mM calcium chloride, and 1 μM zinc chloride, and incubated in the same buffer overnight at 37°C. The gel was then stained using 0.2% Coomassie Brilliant Blue R250 in 45% methanol

and 10% acetic acid for one hour and was destained in 20% ethanol and 5% acetic acid until the bands were seen.

Northern Hybridization

Total RNA was prepared using RNAzolB reagent (TEL-TEST Inc., Friendswood, TX) following manufacturer's instructions. Plasmid carrying partial MMP-9 cDNA (pCR92ColIV) was kindly provided by Dr. Douglas Boyd from the University of Texas M. D. Anderson Cancer Center. PCR92ColIV was digested with HindIII and EcoRI to release a ~500bp fragment which is unique in sequence and does not have a homologous region in other MMPs. 20 μg total RNA were separated by a 1% agarose gel containing 0.4 M formaldehyde and 1x MOPS buffer. RNA was transferred to a nylon membrane (Hybond-N+, Amersham) and crosslinked using UV Stratalinker (Stratagene). The membrane is prehybridized in hybridization buffer containing 50% formamide, 5× SSPE, 2× Denhardt's reagent, and 0.1% SDS at 42°C for 1 hour. ^{32}P-labeled MMP-9 probe was added to prehybridized membrane and hybridized overnight at 42°C. The membrane was washed with 0.5x SSC and 0.05% SDS for 20 min at 60°C followed by washing in the same buffer for 5 min at room temperature. The membrane was then dried and subjected to autoradiography.

RT-PCR

Reverse transcription reaction was performed using SuperScript™ Pre-amplification System from Life Technologies Inc. (Rockville, MD) following the protocol provided by the supplier. Primer sequences for MMP-9 cDNA PCR are 5'-CTCCTCCCTTTCCTCC AGAACAGAA-3' (forward) and 5'-GGAGCCGCTCTCCAA GAAGCTT-3' (reverse). Primer sequences for β-actin cDNA PCR are 5'-GGCATGGG TCAGAAGGATTCG-3' and 5'-AGCACAGCCTGGATAGCAACG- 3'. Primers were used at a final concentration of 0.5μM. Reaction mixture was first denatured at 94°C for 1min. The PCR condition was 94°C 30 sec, 58°C 30 sec, 72°C 45 sec, for 30 cycles, followed by 94°C 30 sec and 72°C 5min.

Luciferase Assay

MCF-7 and SKBr3 cells were transfected with LipofectAMINE following the protocol provided by the supplier (Life Technologies, Inc.) After 5 hr, the media was changed to serum-free media. After overnight culture, heregulin-β1 was added to fresh serum-free media at a final concentration of 10 ng/ml and cells were incubated for 24 hr and scraped off into 1 ml PBS. Cells were spun down and lysed in 200μl Passive Lysis Buffer (Promega). After one cycle of freeze-and-thaw, cells were spun down and 10μl supernatant were used in luciferase assay using Microtiter® Plate Luminometer (Dynex Technologies, Chantilly, VA).

In vitro Chemoinvasion Assay

SKBr3 cells in serum-free DMEM/F12 were pretreated with inhibitors (20μM PD098059, 2μM RO318220, and 5μM SB203580) for one hour before addition of 20ng/ml heregulin-β-1 for 24 hours. Polycarbonate-membrane invasion chambers from 24-well Transwell plates (Corning Incorporated, Corning NY) were coated with a 1:80 dilution of Matrigel matrix (BD Biosciences, Bedford, MA) and allowed to dry overnight. Chambers were rehydrated for 3 hours in PBS before SKBr3 cells (3.5×10^4 cells in 0.1ml of DMEM/F12 + 0.1%BSA) were loaded into the chambers with or without heregulin and inhibitors. 0.6ml of 40μg/ml Fibronectin (BD Biosciences, Bedford, MA) in the bottom of the wells served as chemoattractants and 0.6ml DMEM/F12 + 0.1%BSA as a negative control. The invasion was allowed to proceed for 72 hours, followed by fixation, staining, and counting of cells as previously described (Tan *et al.*, 1997).

Acknowledgments: We thank Dr. Douglas Boyd for valuable reagents. This research was supported by grants P30-CA16672 and 2RO1-CA60448 (to D. Y.) from the National Institutes of Health; DAMD17-98-2-8338 (to D. Y.) and DAMD17-99-1-9271 (to D. Y.) from the United States Army Research and Material Command; and The University of Texas M. D. Anderson Breast Cancer Basic Research Program Fund (to D. Y.). J. Y. is an awardee of the Rosalie B. Hite predoctoral fellowship.

References

Aguilar, Z., Akita, R.W., Finn, R.S., Ramos, B.L., Pegram, M.D., Kabbinavar, F.F., Pietras, R.J., Pisacane, P., Sliwkowski, M.X. & Slamon, D.J. (1999). *Oncogene*, **18,** 6050-62.

Ballin, M., Gomez, D.E., Sinha, C.C. & Thorgeirsson, U.P. (1988). *Biochemical & Biophysical Research Communications*, **154,** 832-8.

Carraway, K.L., 3rd, Sliwkowski, M.X., Akita, R., Platko, J.V., Guy, P.M., Nuijens, A., Diamonti, A.J., Vandlen, R.L., Cantley, L.C. & Cerione, R.A. (1994). *Journal of Biological Chemistry*, **269,** 14303-6.

Davies, B., Brown, P.D., East, N., Crimmin, M.J. & Balkwill, F.R. (1993a). *Cancer Research*, **53,** 2087-91.

Davies, B., Waxman, J., Wasan, H., Abel, P., Williams, G., Krausz, T., Neal, D., Thomas, D., Hanby, A. & Balkwill, F. (1993b). *Cancer Research*, **53,** 5365-9.

Garbisa, S., Pozzatti, R., Muschel, R.J., Saffiotti, U., Ballin, M., Goldfarb, R.H., Khoury, G. & Liotta, L.A. (1987). *Cancer Research*, **47,** 1523-8.

Gramolini, A.O., Angus, L.M., Schaeffer, L., Burton, E.A., Tinsley, J.M., Davies, K.E., Changeux, J.P. & Jasmin, B.J. (1999). *Proceedings of the National Academy of Sciences of the United States of America*, **96,** 3223-7.

Gschwendt, M., Dieterich, S., Rennecke, J., Kittstein, W., Mueller, H.J., & Johannes, F.J. (1996). *FEBS Letters*, **392**, 77-80.

Gum, R., Wang, H., Lengyel, E., Juarez, J. & Boyd, D. (1997). *Oncogene*, **14,** 1481-93.

Holmes, W.E., Sliwkowski, M.X., Akita, R.W., Henzel, W.J., Lee, J., Park, J.W., Yansura, D., Abadi, N., Raab, H. & Lewis, G.D. (1992). *Science*, **256,** 1205-10.

Huhtala, P., Tuuttila, A., Chow, L.T., Lohi, J., Keski-Oja, J. & Tryggvason, K. (1991). *Journal of Biological Chemistry*, **266,** 16485-90.

Hujanen, E.S., Vaisanen, A., Zheng, A., Tryggvason, K. & Turpeenniemi-Hujanen, T. (1994). *International Journal of Cancer*, **58,** 582-6.

Jones, J.L., Glynn, P. & Walker, R.A. (1999). *Journal of Pathology*, **189,** 161-8.

Khurana, T.S., Rosmarin, A.G., Shang, J., Krag, T.O., Das, S. & Gammeltoft, S. (1999). *Molecular Biology of the Cell*, **10,** 2075-86.

Kondapaka, S.B., Fridman, R. & Reddy, K.B. (1997). *International Journal of Cancer*, **70,** 722-6.

Kozawa, O., Kawamura, H., Hatakeyama, D., Matsuno, H. & Uematsu, T. (2000). *Cellular Signalling*, **12,** 375-380.

Lozonschi, L., Sunamura, M., Kobari, M., Egawa, S., Ding, L. & Matsuno, S. (1999). *Cancer Research*, **59,** 1252-8.

Lupu, R., Colomer, R., Zugmaier, G., Sarup, J., Shepard, M., Slamon, D. & Lippman, M.E. (1990). *Science*, **249,** 1552-5.

Moll, U.M., Youngleib, G.L., Rosinski, K.B. & Quigley, J.P. (1990). *Cancer Research*, **50,** 6162-70.

Nakajima, M., Welch, D.R., Wynn, D.M., Tsuruo, T. & Nicolson, G.L. (1993). *Cancer Research*, **53,** 5802-7.

Normanno, N., Kim, N., Wen, D., Smith, K., Harris, A.L., Plowman, G., Colletta, G., Ciardiello, F. & Salomon, D.S. (1995). *Breast Cancer Research & Treatment*, **35,** 293-7.

Parks, W.C. & Mecham, R.P. *Matrix Metalloproteinases*. Academic Press.

Patterson, B.C. & Sang, Q.A. (1997). *Journal of Biological Chemistry*, **272,** 28823-5.

Peles, E., Bacus, S.S., Koski, R.A., Lu, H.S., Wen, D., Ogden, S.G., Levy, R.B. & Yarden, Y. (1992). *Cell*, **69,** 205-16.

Plowman, G.D., Culouscou, J.M., Whitney, G.S., Green, J.M., Carlton, G.W., Foy, L., Neubauer, M.G. & Shoyab, M. (1993). *Proceedings of the National Academy of Sciences of the United States of America*, **90,** 1746-50.

Rao, J.S., Steck, P.A., Mohanam, S., Stetler-Stevenson, W.G., Liotta, L.A. & Sawaya, R. (1993). *Cancer Research*, **53,** 2208-11.

Samuel, S.K., Hurta, R.A., Kondaiah, P., Khalil, N., Turley, E.A., Wright, J.A. & Greenberg, A.H. (1992). *EMBO Journal*, **11,** 1599-605.

Sato, H., Kita, M. & Seiki, M. (1993). *Journal of Biological Chemistry*, **268,** 23460-8.

Segain, J.P., Harb, J., Gregoire, M., Meflah, K. & Menanteau, J. (1996). *Cancer Research*, **56,** 5506-12.

Sehgal, I., Baley, P.A. & Thompson, T.C. (1996). *Cancer Research*, **56,** 3359-65.

Shima, I., Sasaguri, Y., Kusukawa, J., Nakano, R., Yamana, H., Fujita, H., Kakegawa, T. & Morimatsu, M. (1993). *British Journal of Cancer*, **67,** 721-7.

Simon, C., Goepfert, H. & Boyd, D. (1998). *Cancer Research*, **58,** 1135-9.

Simon, C., Hicks, M., Nemechek, A., Mehta, R., O'Malley, B.J., Geopfert, H., Flaitz, C. & Boyd, D. (1999). *British Journal of Cancer*, **80,** 1412-19.

Sliwkowski, M.X., Schaefer, G., Akita, R.W., Lofgren, J.A., Fitzpatrick, V.D., Nuijens, A., Fendly, B.M., Cerione, R.A., Vandlen, R.L. & Carraway, K.L., 3rd. (1994). *Journal of Biological Chemistry*, **269,** 14661-5.

Tan, M., Grijalva, R. & Yu, D. (1999). *Cancer Research*, **59,** 1620-25.

Tan, M., Yao, J., and Yu, D. (1997). *Cancer Research*, **57**, 1199-205.

Vu, T.H., Shipley, J.M., Bergers, G., Berger, J.E., Helms, J.A., Hanahan, D., Shapiro, S.D., Senior, R.M. & Werb, Z. (1998). *Cell*, **93,** 411-22.

Welch, D.R., Fabra, A. & Nakajima, M. (1990). *Proceedings of the National Academy of Sciences of the United States of America*, **87,** 7678-82.

Wen, D., Peles, E., Cupples, R., Suggs, S.V., Bacus, S.S., Luo, Y., Trail, G., Hu, S., Silbiger, S.M. & Levy, R.B. (1992). *Cell*, **69,** 559-72.

Williger, B.T., Ho, W.T. & Exton, J.H. (1999). *Journal of Biological Chemistry*, **274,** 735-8.

Xiong, S.B., Grijalva, R., Zhang, L., Nguyen, N.T., Pisters, P.W., Pollock, R.E. & Yu, D. (2001). *Cancer Research*, **61**, 1727-32.

Yu, Q. & Stamenkovic, I. (2000). *Genes & Development*, **14,** 163-76.

Legends to Figures

Figure 1 Heregulin-β1 increased MMP-9 activity in breast cancer cells. (**a**) Induction of MMP-9 gelatinolytic activity by heregulin-β1 in SKBr3 and MCF-7 breast cancer cell lines. Cells were starved in serum-free medium for 12 hr and then treated with recombinant heregulin-β1 at a final concentration of 20 ng/ml. Cells were harvested 24 hr later and conditioned medium concentrated and subjected to zymography. Relative fold of induction of MMP-9 in SKBr3 and MCF-7 cells was quantitated by densitometry. Supernatant from mouse cell line B104-1-1 was used as a positive control of MMP-2. (**b**) Dose- and time-dependent activation of MMP-9 by heregulin-β1 in SKBr3 and MCF-7 breast cancer cell lines. Zymographic assay was performed as in (**a**) with the indicated concentrations of heregulin-β1 for 24hr (left) or the indicated time with 10 ng/ml heregulin-β1.

Figure 2 Upregulation of MMP-9 protein and mRNA expression by heregulin-β1 in breast cancer cells. (**a**) Western blot analysis of MMP-9 protein expression in conditioned medium after heregulin-β1 stimulation. SKBr3 cells were starved for 12 hr and stimulated with the indicated concentrations of heregulin-β1. Conditioned media were collected after 20hr and concentrated. Western blot analysis was performed using an antibody against MMP-9. (**b**) and (**c**) Heregulin-β1 increased messenger RNA level of MMP-9 in SKBr3 cells. SKBr3 cells were starved and treated with 10ng/ml heregulin-β1 for the indicated times. Total RNAs were prepared and equal amounts of RNA were subjected to Northern analysis (**b**) or used to perform RT-PCR experiments (**c**). MMP-9

signal was shown as a PCR band of 520 bp and β-actin mRNA of 287bp was also amplified by RT-PCR in the same reaction as a loading control.

Figure 3 Heregulin-β1 induced transcription upregulation from MMP-9 promoter in SKBr3 and MCF-7 cells. (**a**) SKBr3 cells were transfected with luciferase reporter plasmids carrying a full-length MMP-9 promoter (pMMP9-2.2k-luc), or a proximal promoter (pMMP9-670-luc). Cells were starved overnight after transfection and then stimulated with 10ng/ml heregulin-β1 for 24 hr. Cell lysates were prepared and subjected to luciferase assay. (**b**) MCF-7.Zeo and MCF.HRG cell lines were transfected with pMMP9-670-luc and luciferase assay performed 40 hrs after transfection. (**c**) MCF-7 and SKBr3 cells were transfected with pMMP9-670-TK-Luc. Cells were treated with heregulin-β1 and the luciferase assays were performed as in (**a**). (**d**) Defining heregulin-β1-responsive region in MMP-9 proximal promoter. SKBR3 cells were transfected with the indicated luciferase reporter constructs carrying different length of MMP-9 promoter regions. Heregulin treatment and luciferase assay were performed as in (**a**).

Figure 4 Effects on heregulin-β1-induced activation of MMP-9 using chemical inhibitor PD098059 (**a**), wortmannin (**b**), SB203580 (**c**), and PKC inhibitors (**d**). SKBr3 cells were starved for 12 hours and then stimulated with 10 ng/ml heregulin-β1 in the presence of the indicated concentrations of the chemical inhibitors. After 24 hours of incubation, conditioned media were collected, concentrated, and subjected to zymographic assay (**a-d**, left panels). To test the efficacy of inhibitors, SKBr3 cells were starved for 12 hours, pretreated with the inhibitors at the indicated concentrations for 1 hour, and stimulated by

10ng/ml heregulin-β1 for 7 min. Cell lysates were prepared and subjected to Western blot analysis using antibodies against Erk, Akt, and p38 (**a-c**, right panels).

Figure 5 Effect of PD098059, SB203580, and RO318220 on heregulin-β1-induced upregulation of MMP-9 mRNA level and MMP-9 transcription. (**a**) SKBr3 cells were starved and treated with 10ng/ml heregulin-β1 in the presence or absence of the indicated inhibitors (20μM PD098059, 10μM SB203580, or 5μM RO318220) for 20 hours. Total RNA were prepared and subjected to Northern analysis with the MMP-9 cDNA probe (upper panel) or with GAPDH probe as an internal loading control. (**b**) SKBr3 cells were transfected with pMMP9-670Luc. Cells were starved after transfection and treated with 10ng/ml heregulin-β1 for 24 hours along with the same concentrations of chemical inhibitors used in (**a**) or with DMSO as a control. Cell lysates were then prepared and subjected to luciferase assay.

Figure 6 (a) Inhibition of invasion of heregulin-β1-treated SKBr3 cell by PD098059, RO318220, and SB203580. SKBr3 cells in serum-free DMEM/F12 were pretreated with or without inhibitors (20μM PD098059, 2μM RO318220, and 5μM SB203580) for one hour, then 20ng/ml heregulin-β-1 was added. Cells were collected 24 hours later, retreated, and plated in the upper chambers ($3.5X10^4$ cells in 0.1ml DMEM/F12 + 0.1%BSA) and allowed to invade for 72 hours. Negative controls are untreated cells with no chemoattractant (fibronectin) in the bottom chamber of the Transwell. Invading cells were counted in 6 High Power Fields per well. Duplicate wells were assayed for each sample. The bars represent the percent of invading cells compared to the heregulin-

treated sample without inhibitors. The experiments have been repeated three times. **(b)** A model of pathways involved in heregulin-β1-induced MMP-9 expression. Heregulin-β1 binds to ErbB3 or/and ErbB4 receptors which induce heterodimization of these receptors with the ErbB2 receptor. This leads to activation of down-stream signaling pathways, among which are MEK → Erk, PLCγ → PKC, PAK1 → p38, and PI3-K → Akt pathways. This study shows that Erk, PKC, and p38 pathways are involved in heregulin β1-induced upregulation of MMP-9.

a

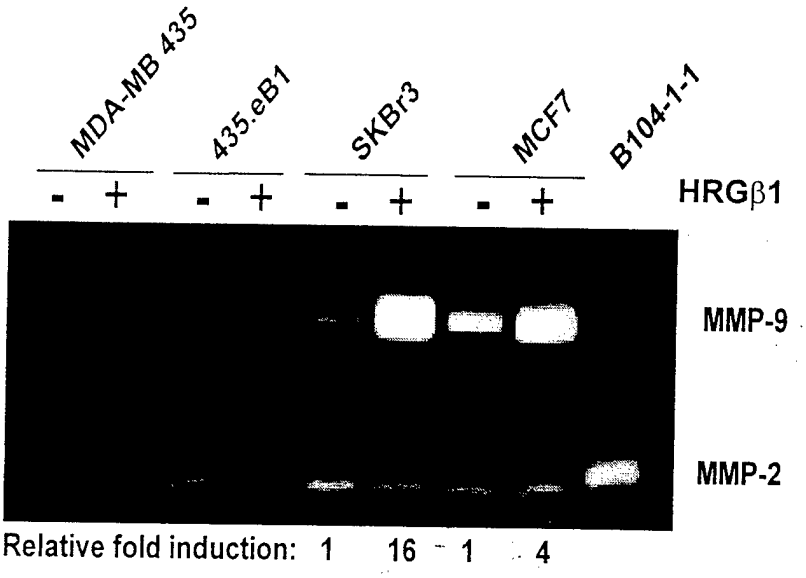
MDA-MB 435
435.eB1
SKBr3
MCF7
B104-1-1
- + - + - + - +
HRGβ1
MMP-9
MMP-2
Relative fold induction: 1 16 1 4

b

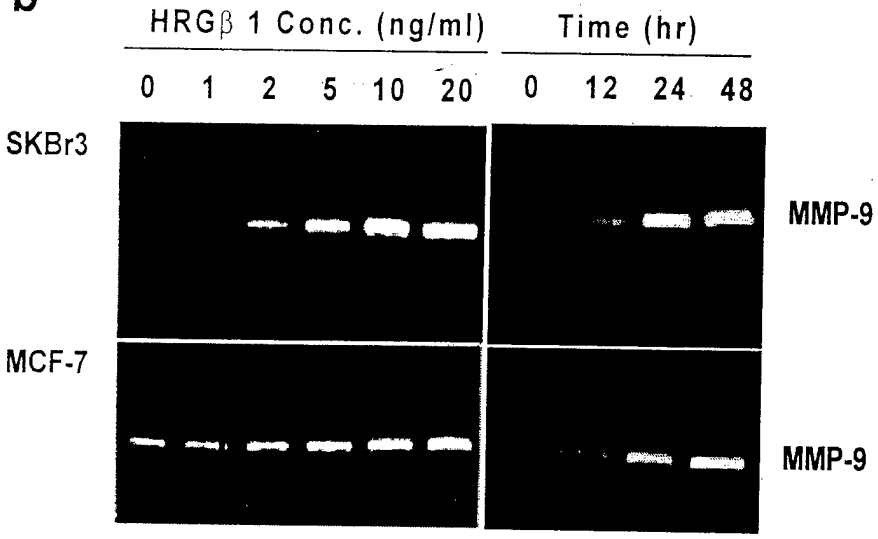
HRGβ 1 Conc. (ng/ml)
Time (hr)
0 1 2 5 10 20 0 12 24 48
SKBr3
MCF-7
MMP-9
MMP-9

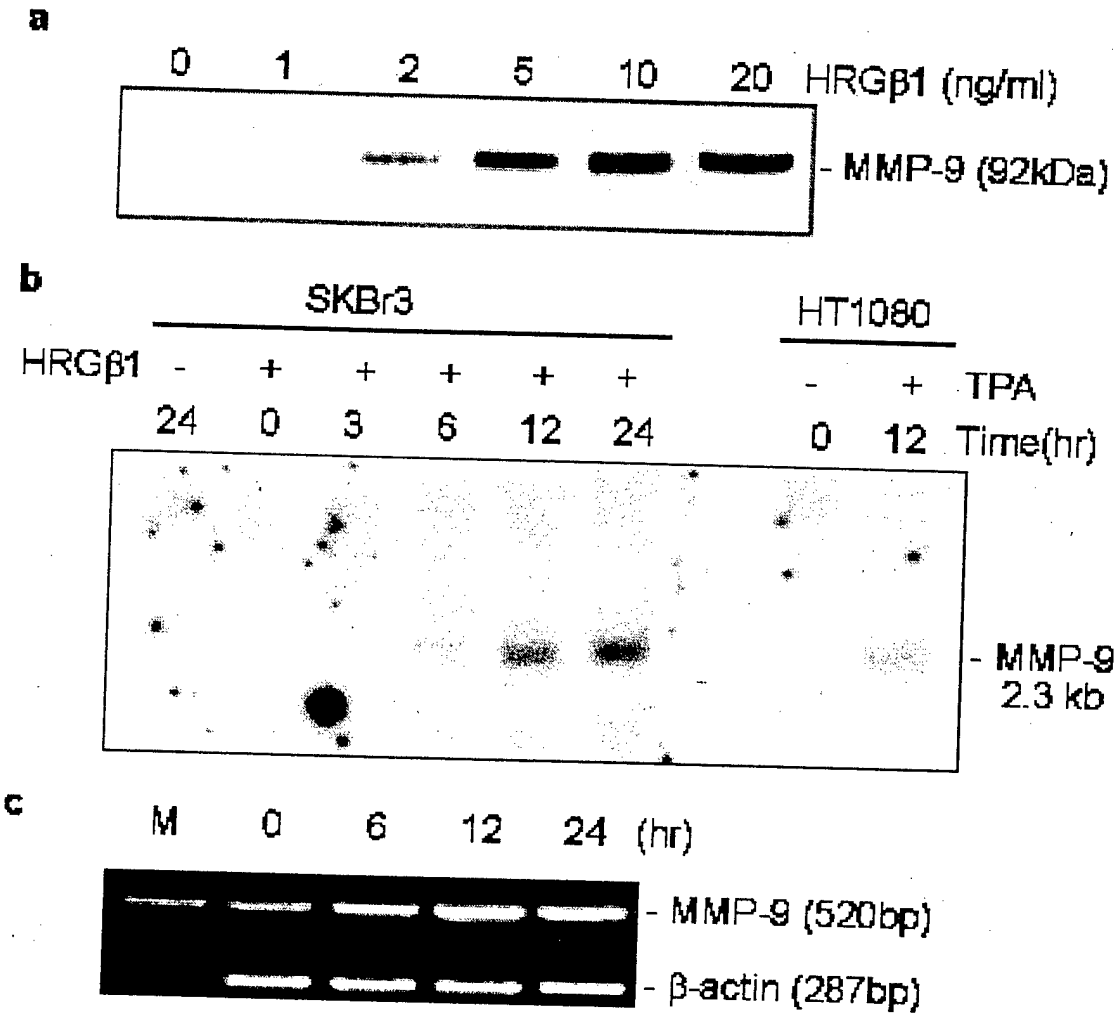
a
0 1 2 5 10 20 HRGβ1 (ng/ml)
- MMP-9 (92kDa)
b
SKBr3
HT1080
HRGβ1 - + + + + + - + TPA
24 0 3 6 12 24 0 12 Time(hr)
- MMP-9
2.3 kb
c
M 0 6 12 24 (hr)
- MMP-9 (520bp)
- β-actin (287bp)

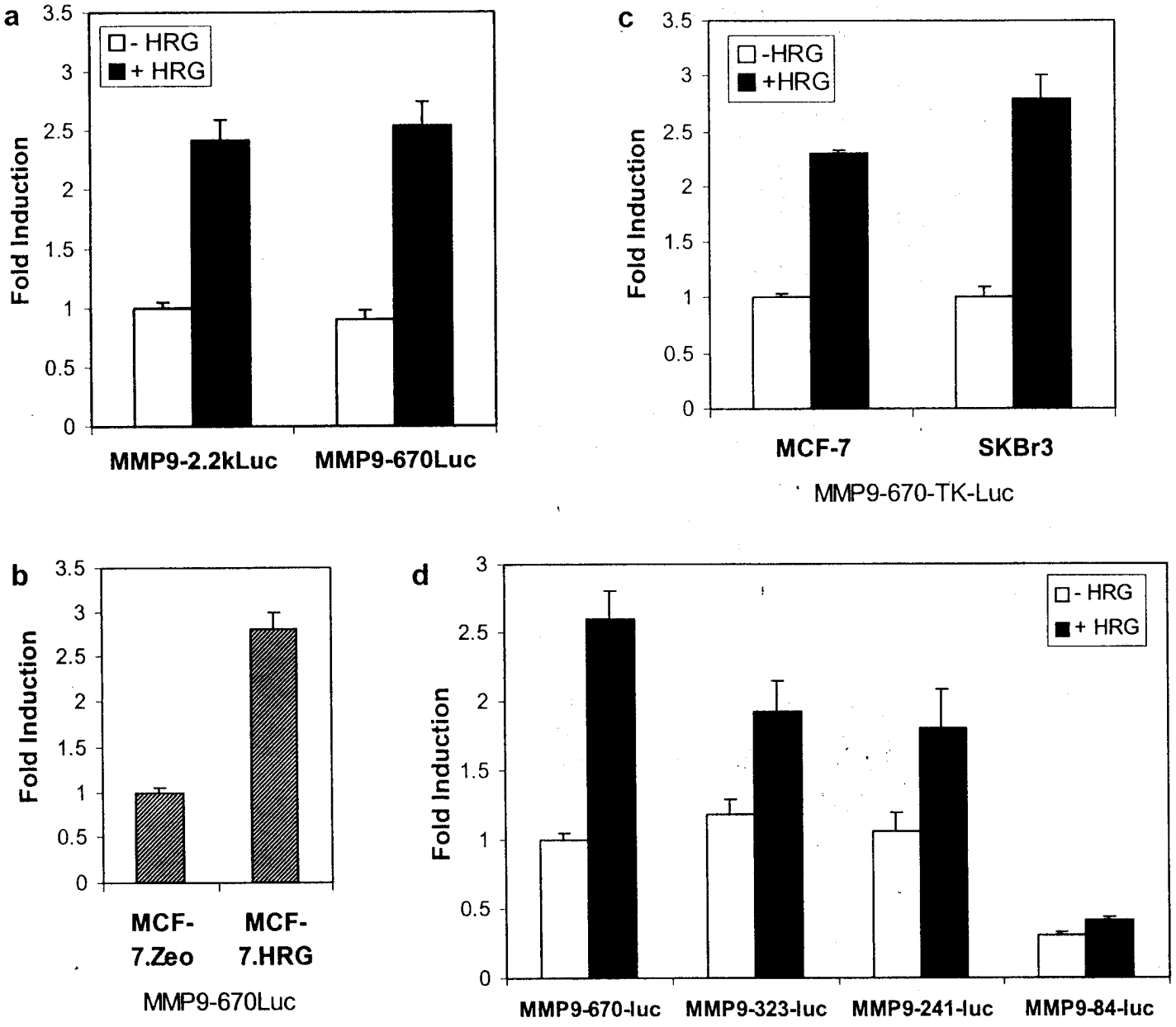
a
- HRG
+ HRG
Fold Induction
3.5
3
2.5
2
1.5
1
0.5
0
MMP9-2.2kLuc
MMP9-670Luc
c
-HRG
+HRG
Fold Induction
MCF-7
SKBr3
MMP9-670-TK-Luc
b
Fold Induction
MCF-7.Zeo
MCF-7.HRG
MMP9-670Luc
d
- HRG
+ HRG
Fold Induction
MMP9-670-luc
MMP9-323-luc
MMP9-241-luc
MMP9-84-luc

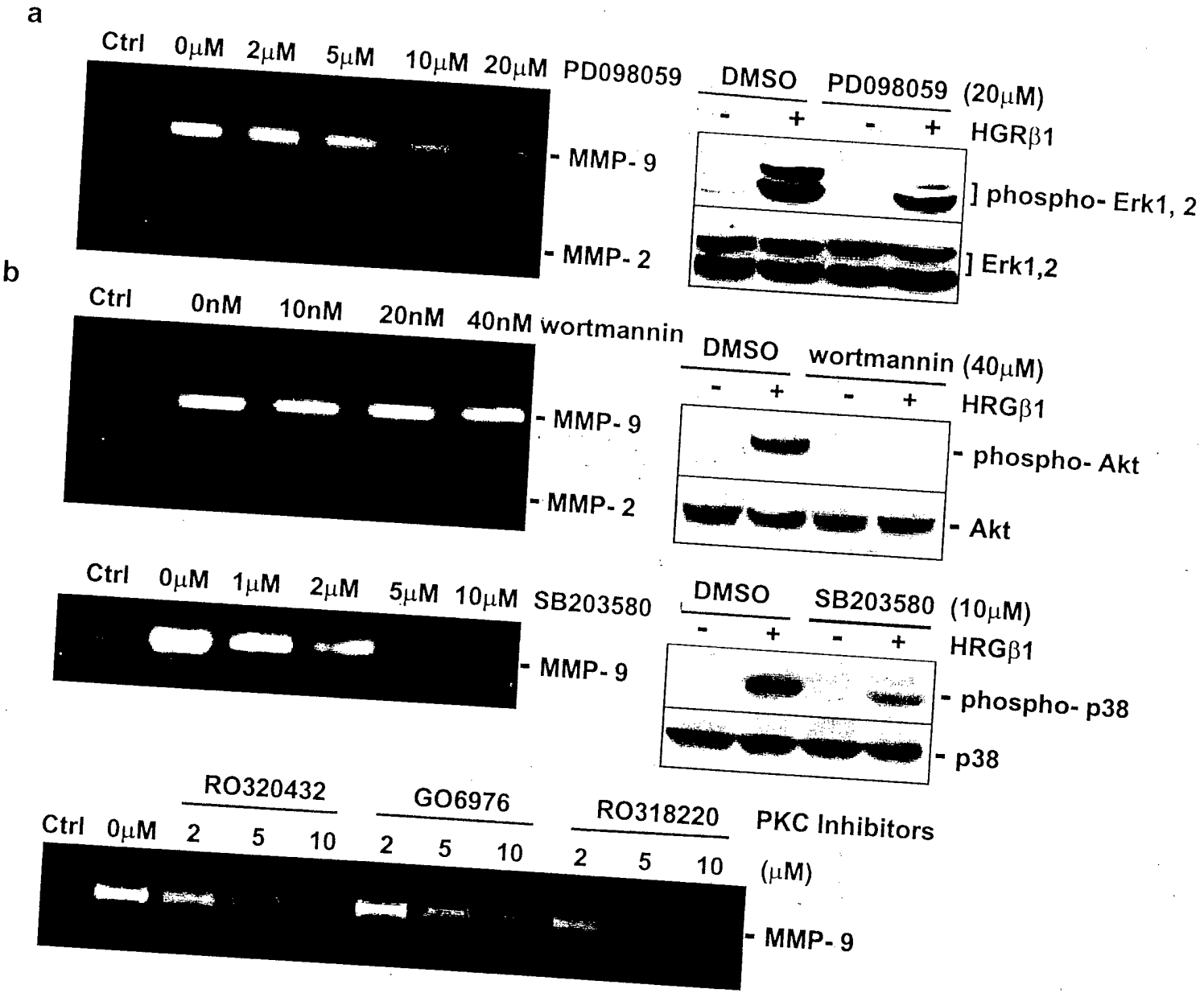
a
Ctrl 0μM 2μM 5μM 10μM 20μM PD098059
- MMP- 9
- MMP- 2
DMSO PD098059 (20μM)
- + - +
HGRβ1
] phospho- Erk1, 2
] Erk1,2
b
Ctrl 0nM 10nM 20nM 40nM wortmannin
- MMP- 9
- MMP- 2
DMSO wortmannin (40μM)
- + - +
HRGβ1
- phospho- Akt
- Akt
c
Ctrl 0μM 1μM 2μM 5μM 10μM SB203580
- MMP- 9
DMSO SB203580 (10μM)
- + - +
HRGβ1
- phospho- p38
- p38
d
RO320432 GO6976 RO318220 PKC Inhibitors
Ctrl 0μM 2 5 10 2 5 10 2 5 10 (μM)
- MMP- 9

a

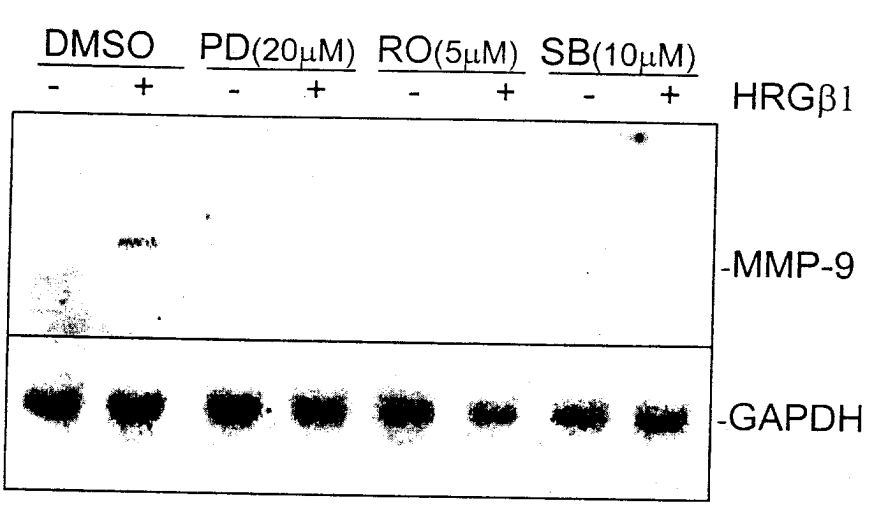
DMSO
PD(20μM)
RO(5μM)
SB(10μM)
- + - + - + - +
HRGβ1
-MMP-9
-GAPDH

b

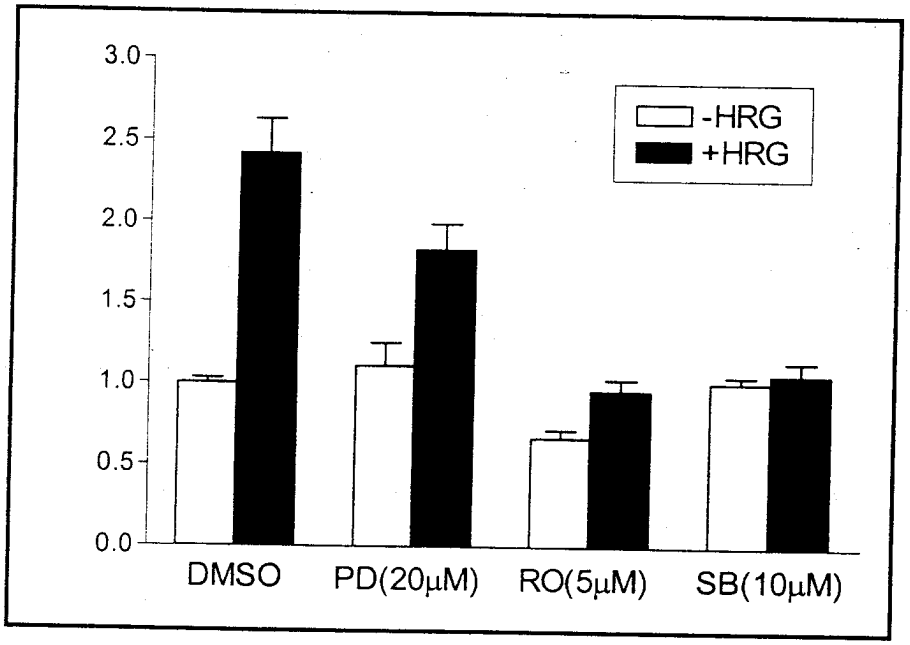
3.0
2.5
2.0
1.5
1.0
0.5
0.0
-HRG
+HRG
DMSO
PD(20μM)
RO(5μM)
SB(10μM)

a

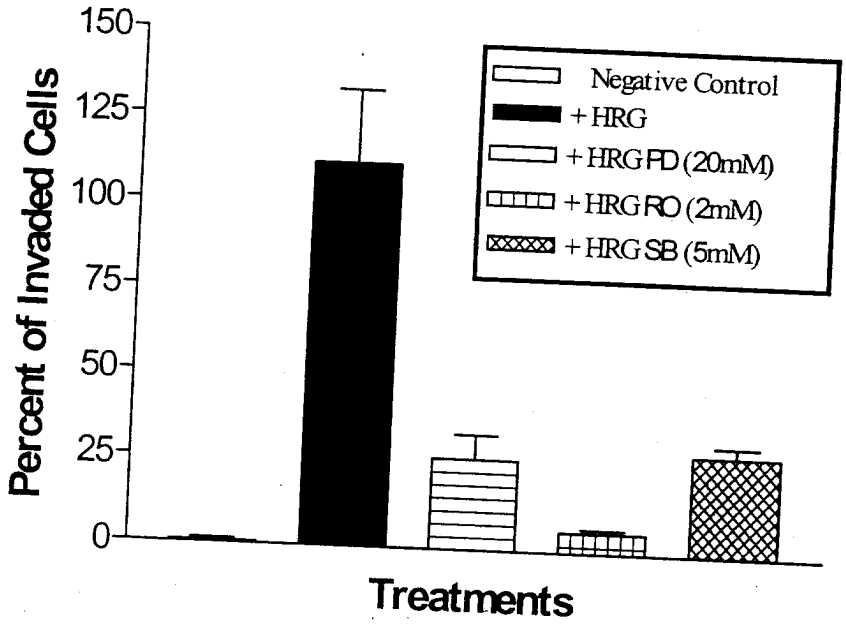
150
125
100
75
50
25
0
Percent of Invaded Cells
Negative Control
+HRG
+HRG PD (20mM)
+HRG RO (2mM)
+HRG SB (5mM)
Treatments

b

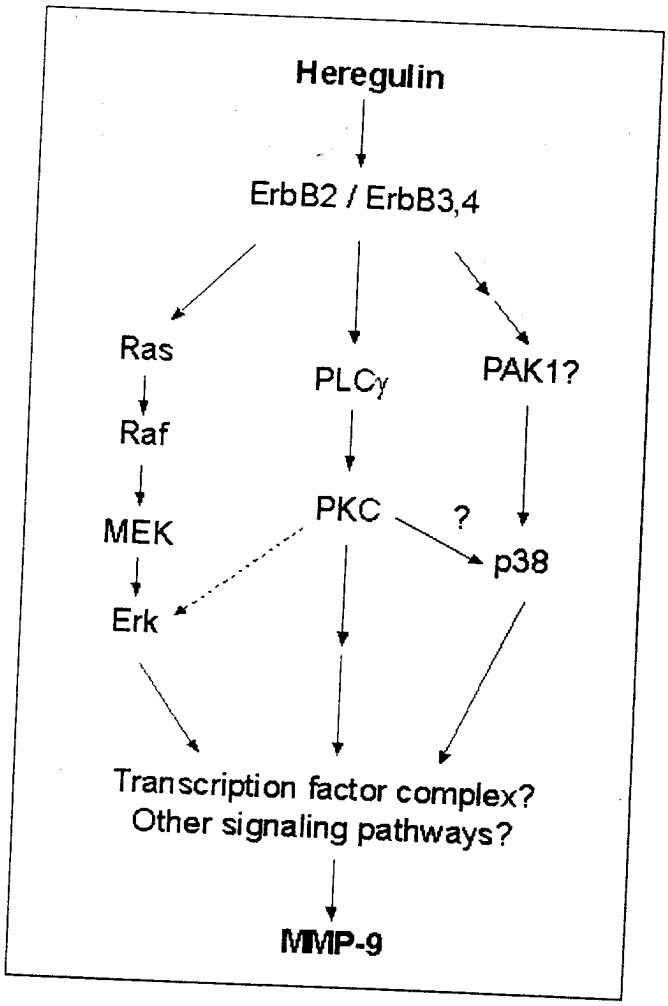
Heregulin
ErbB2 / ErbB3,4
Ras
Raf
MEK
Erk
PLCγ
PKC
PAK1?
?
p38
Transcription factor complex?
Other signaling pathways?
MMP-9

Enhanced Sensitization to Taxol-induced Apoptosis by Herceptin Pretreatment in ErbB2-Overexpressing Breast Cancer Cells

Sangkyou Lee, Wentao Yang, Shankar Sellappan, Kristine Klos, Mark X. Sliwkowski, Gabriel Hortobagyi, Mien-Chie Hung, and Dihua Yu[2]

Departments of Surgical Oncology [S.L., W.Y., S.S., K.K., D.Y.], Breast Medical Oncology [G.H.], and Molecular and Cellular Oncology [M.C.H., D.Y.], The University of Texas M.D. Anderson Cancer Center, Houston, Texas 77030; Genentech, Inc. [M.X.S.], One DNA way, South San Francisco, California; 94080

Running title: Super-Chemosensitization by Herceptin Pretreatment

Key words: Herceptin, taxol, ErbB2, pretreatment, apoptosis

Notes:

1. This research was supported by Genentech Inc. Research Grant LS99-260 (to D.Y.), Grants P30-CA16672 (Cancer Center Core Grant) and 2RO1-CA60488 (to D.Y.) from the NIH, and The University of Texas M.D. Anderson Breast Cancer Basic Research Program Fund (to D.Y.).

2. Requests for reprints should be addressed to Dihua Yu, M.D., Ph.D. at Department of Surgical Oncology, M.D. Anderson Cancer Center, 1515 Holcombe Blvd., Houston, Texas, U.S.A. 77030. Phone: 713-792-3636; Fax: 713-794-4830; Email:dyu@notes.mdacc.tmc.edu.

Abbreviations: DAB, 3-3'-diaminobenzidine; DTT, dithiothreitol; FBS, fetal bovine serum; FITC, fluorecein isothiocyanate; HPFs, high power fields; IP, immunoprecipitation; m.f.p., mammary fat pad; PBS, phosphate-buffered saline; PI, propidium iodide; SDS-PAGE, sodium dodecyl sulfate polyacrylamide gel electrophoresis; TdT, terminal deoxynucleotidyl transferase; TUNEL, terminal deoxynucleotidyl transferase-mediated dUTP-biotin nick end labeling; Tyr, tyrosine.

ABSTRACT

The recombinant humanized anti-ErbB2/HER2 monoclonal antibody Herceptin™ (Trastuzumab) has been shown to significantly enhance the tumoricidal effects of anti-tumor drugs such as paclitaxel (taxol) in patients with ErbB2-overexpressing breast cancers. Here, we investigated the molecular mechanisms by which Herceptin enhances the anti-tumor effects of taxol. Since activation of $p34^{Cdc2}$ is required for taxol-induced apoptosis and since overexpression of ErbB2 blocks taxol-induced apoptosis by inhibiting $p34^{Cdc2}$ activation, we studied the effect of Herceptin treatment on $p34^{Cdc2}$ kinase activation and apoptosis in taxol-treated human breast carcinoma cell lines MDA-MB-435, SKBr3, MDA-MB-453, and 435.eB, which is an ErbB2 transfectant of MDA-MB-435. Herceptin treatment downregulated ErbB2, reduced the inhibitory phosphorylation of Cdc2 on Tyr15, and downregulated the expression of $p21^{Cip1}$, a Cdc2 inhibitor. Herceptin plus taxol treatment led to higher levels of $p34^{Cdc2}$ kinase activity and apoptosis in ErbB2-overexpressing breast cancer cells, which is likely due to inhibition of Cdc2-Tyr15 phosphorylation and $p21^{Cip1}$ expression. Since significant dephosphorylation of Cdc2-Tyr15 and down-regulation of $p21^{Cip1}$ occur at least 24 h after Herceptin treatment, we investigated whether 24 h Herceptin pretreatment will render ErbB2-overexpressing breast cancer cells more sensitive to taxol-induced apoptosis compared to the simultaneous treatment of Herceptin plus taxol. Indeed, Herceptin pretreatment increased taxol-induced apoptosis and cytotoxicity *in vitro*, and more effectively inhibited the growth of tumor xenografts with enhanced *in vivo* apoptosis. Thus, Herceptin treatment of ErbB2-overexpressing cells can inhibit ErbB2-mediated Cdc2-Tyr15 phosphorylation and $p21^{Cip1}$ upregulation, which allows effective $p34^{Cdc2}$ activation and induction of apoptosis upon taxol treatment. Herceptin pretreatment renders ErbB2-overexpressing breast cancers more susceptible to taxol-induced cell death, which may have important clinical therapeutic implications.

INTRODUCTION

The erbB2 gene (also known as HER2, *neu*) encodes a 185-kDa transmembrane glycoprotein ($p185^{ErbB2}$), that belongs to the epidermal growth factor receptor (EGFR) family of receptor tyrosine kinases (RTKs) (1, 2). The ErbB2 RTK can be involved in the regulation of a variety of vital functions controlled by any of the ErbB-receptor family members, including cell growth, differentiation, and apoptosis (3). The ErbB2 RTK plays an important role in human malignancies. It is overexpressed in approximately 30% of human breast carcinomas (4, 5) and in many other types of human malignancies (6). Studies of individuals with ErbB2 - overexpressing tumors have shown that they have a significantly lower overall survival rate and a shorter time to relapse than those patients whose tumors did not overexpress ErbB2. ErbB2 overexpression has been correlated positively with lymph node metastasis in node-positive patients (5, 7-9). We have also observed that ErbB2 overexpression can enhance the intrinsic metastatic potential of breast cancer cells (10).

In addition to conferring aggressive malignant behavior, ErbB2 overexpression has been observed to affect the sensitivity of breast cancer cells to several anticancer agents (3). Our previous studies demonstrated that ErbB2 overexpression in breast cancer cells confers increased resistance to the chemotherapeutic agent paclitaxel (taxol) (11, 12). This is supported by another study in which Herceptin, a humanized anti- ErbB2 antibody, enhanced the antitumor activity of taxol and doxorubicin against ErbB2-overexpressing human breast cancer xenografts (13). Furthermore, results of the Herceptin phase III trial demonstrated that the taxol response rate of patients with ErbB2-overexpressing breast cancers was significantly higher among patients receiving taxol plus Herceptin than those receiving taxol alone (14, 15).

Herceptin (or Trastuzumab) was developed from anti-$p185^{ErbB2}$ murine monoclonal antibody (muMAb 4D5) that binds to the extracellular domain of ErbB2 and downregulates the expression of cell-surface ErbB2 proteins (16). Herceptin has demonstrated tumor inhibitory and chemosensitizing effects to taxol and several chemotherapeutic agents in preclinical studies and in phase II and phase III clinical trials (13, 14, 17, 18). Currently, Herceptin is the only U.S. FDA approved antibody therapeutic for treatment of cancers that overexpress ErbB2. Impressively, Herceptin treatment significantly improved the taxol response rates of patients with ErbB2 overexpressing breast cancers (14, 15).

Taxol is a potent and highly effective anti-neoplastic agent in the treatment of advanced, drug-refractory, metastatic breast cancers (19, 20). Taxol induces tubulin polymerization and microtubule formation (21), blocks the cell cycle in mitosis, and induces programmed cell death (apoptosis) (22). Taxol may induce apoptosis through different mechanisms depending on cell lines and culture conditions, which can involve JNK activation, NF-κB activation, p66 Shc phosphorylation, or MAP kinase pathways (ERK and p38) and can be p53 independent (23-28)). Recently, we demonstrated that activation of $p34^{Cdc2}$ is required for taxol-induced apoptosis of breast cancer cells (12). Furthermore, we found that at least two mechanisms are involved in the ErbB2 inhibition of $p34^{Cdc2}$ activation and taxol-induced apoptosis. First, ErbB2 overexpression can inhibit $p34^{Cdc2}$ activation and apoptosis in taxol-treated breast cancer cells by upregulating $p21^{Cip1}$, an inhibitor of cell cycle dependent kinases (12). Second, ErbB2 overexpression can inhibit $p34^{Cdc2}$ activation and taxol-induced apoptosis by increasing phosphorylation of Cdc2 on Tyr15, a critical inhibitory phosphorylation site on $p34^{Cdc2}$ (29).

Based on these understandings of the mechanisms of ErbB2-mediated taxol resistance, we hypothesized that Herceptin may sensitize ErbB2 overexpressing breast cancer cells to taxol-induced apoptosis by allowing efficient activation of $p34^{Cdc2}$ kinase after taxol treatment. In this

study, we investigated whether Herceptin treatment of ErbB2 overexpressing breast cancer cells, by down-regulation of ErbB2, could lead to inhibition of $p21^{Cip1}$ expression and reduced Cdc2-Tyr15 phosphorylation, which allows for efficient $p34^{Cdc2}$ activation and apoptosis when cells are treated with taxol. We also investigated whether Herceptin pretreatment, which renders ErbB2 overexpressing breast cancer cells more susceptible to $p34^{Cdc2}$ activation and apoptosis upon taxol treatment, more effectively sensitized these cells to taxol-induced apoptosis.

MATERIALS AND METHODS

Cell Lines and Culture. Human breast cancer cell lines MDA-MB-435, the 435.eB transfectants, SKBr3, and MDA-MB-453 were obtained, established, and cultured as previously described (11, Yu, 1998b #1837).

Antibodies and Reagents. Herceptin was provided by Genentech, Inc. (South San Francisco, CA). Rhu IgG1 was purchased from Calbiochem (San Diego, CA), and paclitaxel (taxol) from the Bristol Myers-Squibb Company (Princeton, NJ). Human $p185^{ErbB2}$ monoclonal antibody (Ab-3) was purchased from Oncogene Science, Inc. (Cambridge, MA), and human $p21^{Cip1}$ polyclonal and $p34^{Cdc2}$ monoclonal antibodies from Santa Cruz Biotechnology, Inc. (Santa Cruz, CA). Phospho Tyr15-$p34^{Cdc2}$ polyclonal antibody was purchased from Cell Signaling Technology, Inc. (Beverly, MA).

Herceptin Treatment and Western Blot Analysis. Cells were cultured to approximately 80% confluence before Herceptin treatment. Cells were then incubated with either 10 or 20 nM Herceptin for 24, 36, or 48 h, depending on the cell line. Cells were washed with cold PBS and lysed with immunoprecipitation buffer (1% Triton X-100; 150 mM NaCl; 10 mM Tris at pH 7.4, 1 mM ethylene glycol-bis–tetraacetic acid; 0.2 mM sodium vanadate; 1 mM EDTA; 0.2 mM

phenylmethylsulfonyl fluoride; and 0.5% NP-40). One hundred micrograms of protein from each sample was separated by 8% or 12% SDS-PAGE, transferred to a nitrocellulose membrane (Bio-Rad, Hercules, CA), and probed by specific antibodies against $p185^{ErbB2}$, phospho Tyr15-$p34^{Cdc2}$, $p21^{Cip1}$, and $p34^{Cdc2}$. Protein signals were detected using the enhanced chemiluminescence detection system (Amersham Corp., Arlington Heights, IL).

Immunocomplex-kinase Assays. Fourteen hours after cells were plated, the culture medium was replaced with medium containing 0.5% FBS with or without Herceptin (10 or 20 nM) for 24 h. Then cells were treated with or without taxol (0.02 or 0.05 μM) for different time periods (3 or 6 h). Immunocomplex-kinase assays of $p34^{Cdc2}$ kinase activity were performed as previously described (12).

Flow Cytometry Analyses of Apoptotic Cells. Cells were cultured in 0.5% FBS in the absence or presence (Herceptin pretreatment) of Herceptin (5, 10, and 20 nM) for 24 h. Cells were then treated with or without taxol (0.02 and 0.05 μM) or Herceptin (0, 5, 10, and 20 nM) plus taxol for 1 h, washed once, and incubated for another 24 h in the absence or presence of Herceptin. Cells were harvested by trypsinization, fixed in 1% formaldehyde on ice for 20 min, and washed once with 70% ethanol. For multiparameter flow cytometry analysis, the cells were incubated in terminal deoxynucleotidyl transferase solution (0.1 M sodium cacodylate; 1 mM $CoCl_2$; 0.1 mM dithiothreitol; 0.005 mg/ml bovine serum albumin; 10 U TdT; and 0.5 nM biotin-16-dUTP) at 37°C for 30 min, transferred to 100 μl of staining solution (4×SSC; 5% dry milk; 0.15% Triton X-100; and 2.5 ng/μl Avidin-FITC), and incubated in the dark at room temperature for 30 min. Finally, the cells were stained in 500 μl of propidium iodide solution (0.5 μg/ml of PI and 0.1% Rnase A). Flow cytometry analyses were performed on a FACScan flow cytometer (Becton Dickenson, San Jose, CA). Cell cycle profiles were analyzed with Multicycle software (Phoenix

Flow Systems, San Diego, CA), and FITC signals were analyzed with Epics Elite software (Coulter Corp., Miami, FL).

Clonogenic Assay. Cells (1,500-4,000 per well) were seeded on 24-well plates. The culture medium was replaced 14 h later with medium containing 0.5% FBS with or without Herceptin. After incubation for 24 h, taxol or Herceptin plus taxol was added at taxol concentrations ranging from 0 to 2.5 μM and incubated for 1 h. Cells were then washed with serum-free medium and incubated in the presence or absence of Herceptin. The culture medium was changed every 2 days until colonies were stained with crystal violet on day 8. Colonies containing more than 10 cells were counted under the microscope.

Tumorigenecity Assay. The 435.eB cells in log-phase growth were trypsinized, washed twice with PBS, and centrifuged at 250×g. The viable cells were then counted. 1×10^6 viable cells in 0.15 ml of Matrigel (BD Biosciences, Bedford, MA) were injected into the mammary fat pad (m.f.p.) of ten-week old female ICR-SCID mice (Harlan, Indianapolis, IN) under aseptic conditions. Nine or ten mice were injected for each treatment group. Tumors were measured by calipers in two orthogonal diameters, and the volumes were calculated using the formula for a prolate ellipsoid: volume (mm^3) = $L\times W^2/2$, where L and W are the major and minor diameters (in millimeters), respectively. Tumor volumes are presented as mean values.

Immunohistochemical Staining of ErbB2. Immunohistochemical staining was performed on 5 μm slides. After deparaffinization and rehydration, sections were subjected to heat-induced epitope retrieval by immersion in a 0.01 mol/L citrate buffer (pH 6.0). Endogenous peroxidase activity was blocked for 30 min in 3% hydrogen peroxide. The slides were then incubated for 30 min at RT in a humidified chamber with anti-ErbB2 antibody (A0485, DAKO). The immunoperoxidase staining was done using the LSAB2 peroxidase kit (DAKO). The antigen-antibody immunoreaction was visualized using DAB as the chromogen. The slides were washed,

counterstained with hematoxylin, dehydrated with alcohol, cleared in xylene, and mounted. Patient samples that were previously shown to express high levels of ErbB2 were used as positive controls. The negative control was performed by replacing the primary antibody with normal horse serum. Moderate to strong membrane staining in more than 10% of the tumor cells were scored as HER2 overexpression.

In Situ TUNEL Assay *In Vivo*. The breaking ends of fragmented DNA in apoptotic cells were detected in situ by nick end-labeling with the TUNEL method using ApopTag Plus Peroxidase in situ apoptosis detection kit (Intergen, NY). Briefly, slides were digested with 20 μg/ml proteinase K (Boehringer Mannheim) for 15 min at room temperature. Endogenous peroxidase activity was blocked with 3% hydrogen peroxide for 5 min. Equilibration buffer was then applied directly to the slide for 30 min. Slides were incubated with digoxigenin-dUTP and TdT in a humidified chamber at 37°C for 1 h. The reaction was terminated with a 10 min incubation in stop/wash buffer. After washing in PBS, the sections were covered with anti-digoxigenin-peroxidase for 30 min at room temperature, followed by color development with DAB. The slides were counter stained with hematoxylin. The positive control slides included in the kit were stained as described above as positive controls. The negative controls were done by substituting TdT with PBS.

Assessment of Apoptotic Cells. Apoptotic cells and bodies were counted from 10 HPFs with ×400 magnification. Cells were considered apoptotic if the whole nuclear area of the cell labeled positively. Apoptotic bodies were defined as small positively labeled globular bodies in the cytoplasm of the tumor cells, which could be found either singly or as groups.

RESULTS

Down-regulation of $p21^{Cip1}$ and Decreased Cdc2-Tyr15 Phosphorylation in

Herceptin-treated ErbB2 Overexpressing Breast Cancer Cells. Our previous studies demonstrated that activation of $p34^{Cdc2}$ kinase is required for taxol-induced apoptosis and that overexpression of ErbB2 inhibits activation of $p34^{Cdc2}$ and apoptosis of taxol-treated cells by up-regulation of $p21^{Cip1}$ and phosphorylation of Cdc2-Tyr15 (12, Chadebech, 2000 #2243, 29). To investigate whether Herceptin, which is known to down-regulate ErbB2 expression, will decrease ErbB2-mediated $p21^{Cip1}$ upregulation and Cdc2-Tyr15 phosphorylation in ErbB2-overexpressing breast cancer cells, MDA-MB-435, 435.eB, SKBr3, and MDA-MB-453 cells were treated with 10 nM Herceptin or control human IgG for various time intervals. Western blot analyses demonstrated that 24 h and 36 h Herceptin treatments down-regulated ErbB2 protein expression in 435.eB, SKBr3, and MDA-MB-453 cells, which overexpress ErbB2 naturally as well as ectopically (Fig.1). Notably, parallel to or following ErbB2 down-regulation, reduced phosphorylation on Tyr15 of $p34^{Cdc2}$ and decreased $p21^{Cip1}$ protein levels were also detected in these cells after 24 h or 36 h Herceptin treatment (Fig.1). The control IgG had no significant effect on ErbB2 expression, Cdc2-Tyr15 phosphorylation, or $p21^{Cip1}$ expression. This data indicates that Herceptin effectively down-regulated ErbB2 expression, leading to inhibition of ErbB2-mediated $p21^{Cip1}$ upregulation and Cdc2-Tyr15 phosphorylation in ErbB2-overexpressing breast cancer cells.

Herceptin Renders ErbB2-Overexpresing Cells More Susceptible to $p34^{Cdc2}$ Activation upon Taxol Treatment. It is known that dephosphorylation on Tyr15 of $p34^{Cdc2}$ can lead to activation of this cyclin-dependent kinase (30). Additionally, we have previously shown that $p21^{Cip1}$ inhibits Cdc2 Kinase activity and reducing $p21^{Cip1}$ expression by antisense $p21^{Cip1}$ oligonucleotide allowed effective Cdc2 activation when cells were treated with taxol (12). We therefore examined whether decreased Cdc2-Tyr15 phosphorylation and reduced $p21^{Cip1}$

expression by Herceptin treatment could result in activation of $p34^{Cdc2}$ kinase in ErbB2 overexpressing breast cancer cells and whether better activation of $p34^{Cdc2}$ will be observed in ErbB2-overexpressing breast cancer cells treated with Herceptin plus taxol. The 435.eB transfectants were either untreated, cultured with human IgG control antibody, treated with 0.02 μM taxol, 20 nM Herceptin, or Herceptin plus taxol simultaneously (Fig. 2A, lanes 1-5). In addition, since decreased Cdc2-Tyr15 phosphorylation and reduced $p21^{Cip1}$ expression were detected at least 24 h after Herceptin treatment, cells were pretreated with Herceptin for 24 h and subsequently added with taxol (Fig. 2A, lane 6). The kinase activity of $p34^{Cdc2}$ immunoprecipitated with anti-$p34^{Cdc2}$ antibody was measured using Histone H1 as substrate. As expected, activation of Cdc2 kinase was readily detected in 435.eB cells treated with taxol. Activation of $p34^{Cdc2}$ kinase was indeed detected after 24 h of Herceptin treatment. Moreover, simultaneous treatment with Herceptin plus taxol showed an additive effect on the activation of $p34^{Cdc2}$ (Fig. 2A). The additive effect on $p34^{Cdc2}$ activation is more apparent in cells pretreated with Herceptin for 24 h followed by taxol treatment (sequential treatment, Fig. 2A). Similar effects on Cdc2 activation were also observed in SKBr3 cells upon taxol treatment, Herceptin treatment, and 24 h of Herceptin pretreatment followed by taxol (Fig. 2B). These results demonstrate more effective $p34^{Cdc2}$ activation in ErbB2-overexpressing breast cancer cells with Herceptin plus taxol treatment.

Herceptin Pretreatment Further Increases Taxol–induced Apoptosis. We previously reported that $p34^{Cdc2}$ activation is required for taxol-induced apoptosis in ErbB2-overexpressing breast cancer cells (12). The data above demonstrates that $p34^{Cdc2}$ kinase activity was increased by Herceptin treatment in ErbB2-overexpressing breast cancer cells. Thus, we next examined whether Herceptin treatment could enhance taxol-induced apoptosis and whether Herceptin

pretreatment is more effective in sensitizing ErbB2-overexpressing breast cancer cells to taxol-induced apoptosis than simultaneous Herceptin plus taxol treatment. The 435.eB transfectant and SKBr3 cells were treated as in figure 2A, i.e., cultured in regular medium with human IgG control antibody, with Herceptin, with taxol, with Herceptin plus taxol added simultaneously, or with pretreatment of Herceptin for 24 h before addition of taxol (Fig. 3). After cells were collected, cell cycle stages and apoptosis were simultaneously determined by measuring DNA content with propidium iodide and by labeling DNA strand breaks with biotinylated dUTP shown as FITC-positive cells (31). Very low levels of apoptosis were detected in cells cultured in regular medium, with human IgG control antibody, or with Herceptin, whereas taxol induced apoptotic cell death in both the 435.eB transfectant and SKBr3 cells (Fig. 3). In 435.eB transfectants simultaneously treated with Herceptin plus taxol, Herceptin treatment slightly increased taxol-induced apoptosis (Fig. 3A and B). Notably, in 435.eB transfectants pretreated with Herceptin for 24 h followed by taxol treatment, taxol-induced apoptosis was significantly increased by Herceptin pretreatment (Fig.3A and B). In SkBr3 cells, simultaneous treatment with Herceptin and taxol had an additive effect leading to a substantial increase of apoptosis. Moreover, Herceptin pretreatment demonstrated a synergistic effect on taxol-induced apoptosis in SKBr3 cells (Fig.3C). Thus, data from both the 435.eB transfectant and SKBr3 cells demonstrate improved sensitization to taxol-induced apoptosis by Herceptin pretreatment than from the Herceptin-taxol simultaneous treatment.

Enhanced Sensitization to Taxol Killing in ErbB2-overexpessing Breast Cancer Cells by Herceptin Pretreatment. To examine whether Herceptin pretreatment further enhances the cytotoxic effect of taxol over the Herceptin-taxol simultaneous treatment, clonogenic assays were performed using 435.eB transfectants and SkBr3 cells. Cells were treated with various

concentrations of taxol plus IgG, simultaneously with taxol plus Herceptin, or pretreated with Herceptin for 24 h followed by taxol. The number of surviving colonies after each treatment were counted eight days post-treatment. As expected, taxol reduced colony formation in a taxol concentration-dependent manner (Fig. 4). Simultaneous treatment of Herceptin plus taxol moderately increased the cytotoxic effect of taxol on these two cell lines. Notably, Herceptin pretreatment significantly enhanced the cytotoxicity of taxol. Specifically, less than 1 % of the colonies survived after Herceptin pretreatment followed with a near IC50 concentration of taxol (0.02 μM for 435.eB cells), whereas ~25 % of the colonies survived after the simultaneous Herceptin-taxol treatment with the same concentration of taxol (Fig. 4A). Better sensitization to taxol killing by Herceptin pretreatment was also observed in SKBr3 cells (Fig. 4B). These data indicate that Herceptin pretreatment sensitizes the ErbB2-overexpressing breast cancer cells to taxol killing better than the simultaneous treatment.

Greater Inhibition of Tumor Growth by Herceptin Pretreatment. To further determine whether Herceptin pretreatment may provide an advantage for tumor growth inhibition *in vivo*, female ICR-SCID mice were inoculated with 435.eB transfectants into the m.f.p. to allow for the growth of tumor xenografts. Seven days after injection, mice were divided into five groups with at least nine animals in each group. The first group began treatment starting on day seven with the rhu IgG monoclonal antibody (0.3 mg/kg) twice a week for five weeks as controls and the second group was treated with Herceptin at the same dose and schedule. The third group was injected with taxol (10 mg/kg) i.p. on days 12 and 15 along with the rhu IgG monoclonal antibody (0.3 mg/kg). Treatment continued with the rhu IgG monoclonal antibody twice a week for another four weeks. The fourth group was given taxol (10 mg/kg) i.p. on days 12 and 15 along with Herceptin (0.3 mg/kg). Treatment continued with Herceptin twice a week for four

weeks. The fifth group was first treated with Herceptin (0.3 mg/kg) on days 7, 9, and 11. Then, mice were given taxol (10 mg/kg) i.p. on days 12 and 15 along with Herceptin (0.3 mg/kg). Herceptin treatment continued twice a week for four weeks. A low dose of Herceptin (0.3 mg/kg) was selected in order to detect possible differences between the simultaneous treatment group (group 4) and the pretreatment group (group 5). Compared with the control group (group 1), treatment with either Herceptin (group 2) or taxol (group 3) delayed tumor growth, whereas simultaneous treatment with Herceptin plus taxol (group 4) showed slightly better tumor inhibition (Fig. 6A). Notably, Herceptin pretreatment followed by taxol (group 5) inhibited tumor growth to greater extents than the simultaneous treatment. This data indicates that Herceptin pretreatment can improve its sensitization effect on tumor growth inhibition by taxol in ErbB2-overexpressing breast cancers.

To investigate if down-regulation of ErbB2 and better induction of apoptosis are the underlying mechanisms for the enhanced tumor growth inhibition by Herceptin pretreatment, tumor samples were collected from each group and examined for ErbB2 expression and *in vivo* apoptosis. Overexpression of ErbB2 was found by immunohistochemical staining of tumor slides with anti-ErbB2 antibody from IgG control treated (group 1) and taxol treated (group 3) mice. However, ErbB2 expression levels were significantly reduced in Herceptin-containing treatment groups (groups 2, 4, and 5). In situ TUNEL assays detected fragmented DNAs within the nuclei of the tumor cells in each group and intense TUNEL signals were occasionally observed in nuclear fragments or apoptotic bodies (Fig. 6B). Compared to IgG control tumors (11 apoptotic cells per 10 HPFs), Herceptin treated or taxol treated tumors showed a slight increase in apoptosis (18 apoptotic cells and 22 apoptotic cells, respectively, per 10 HPFs), while Herceptin plus taxol treated tumors demonstrated dramatic increase of *in vivo* apoptosis (group 4, 36/10HPFs, Fig. 6C). Notably, an even higher incidence of apoptosis was detected in Herceptin

pretreated tumors (group 5, 62/10HPFs) than in Herceptin and taxol simultaneously treated tumors. These data indicate that Herceptin pretreatment primed the ErbB2-overexpressing breast tumors for efficient apoptosis induction in response to taxol treatment, which paralleled the enhanced sensitization to tumor inhibition by taxol.

DISCUSSION

Here, we demonstrated that Herceptin treatment of ErbB2 overexpressing human breast cancer cells down-regulated ErbB2 expression, decreased the inhibitory phosphorylation of Cdc2 on Tyr15 and the expression of $p21^{Cip1}$, thus, allowing efficient $p34^{Cdc2}$ activation and apoptosis induction upon taxol treatment. We also provided evidence that Herceptin pretreatments led to improved sensitization of ErbB2-overexpressing breast cancer cells to taxol-induced apoptosis, cytotoxicity, and tumor growth inhibition than the currently used Herceptin and taxol simultaneous treatment strategy.

Herceptin down-regulated the ErbB2 protein in 435.eB transfectant, MDA-MB-453 cells, and SKBr3 cells. Herceptin-mediated ErbB2 down-regulation is known to result from multiple steps such as receptor internalization, protein degradation, and receptor recycling (32, 33). However, the efficiencies of these processes may vary among different cell lines. Additionally, different cell lines may have divergent downstream elements in their signal transduction pathways that are responsible for their responses to ErbB2 down-regulation by Herceptin (34). Thus, it is not surprising that variation in response to Herceptin-mediated ErbB2 down-regulation was seen among ErbB2-overexpressing breast cancer cells (Fig. 1). This is also consistent with clinical trial data that breast cancers with ErbB2-overexpression have a Herceptin response rate of only about 15% [Gilewski, 2000 #2252; (35).

We have previously found that activation of $p34^{Cdc2}$ is required for taxol-induced apoptosis, but overexpression of ErbB2 inhibits Cdc2 activation upon taxol treatment leading to inhibition of apoptosis (12). In this study, we showed that Herceptin treatment permits efficient $p34^{Cdc2}$ activation upon taxol treatment of ErbB2 overexpressing human breast cancer cells (Fig. 2). The Herceptin-mediated efficient $p34^{Cdc2}$ activation upon taxol treatment is likely the result of reversals of two known ErbB2-mediated Cdc2 inhibitory mechanisms, i.e., Herceptin decreased the ErbB2-mediated inhibitory phosphorylation of Cdc2 on Tyr15 and blocked the ErbB2-mediated upregulation of $p21^{Cip1}$ (Fig. 1). We propose that the reversals of these two known ErbB2-mediated Cdc2 inhibitory mechanisms are important molecular mechanisms contributing to Herceptin-mediated sensitization of ErbB2-overexpressing cells to taxol-induced apoptosis (Fig. 3), which requires Cdc2 activation.

On the other hand, multiple mechanisms or signaling pathways may be involved in Herceptin-mediated taxol sensitization in addition to the ones demonstrated here. For example, although Herceptin pretreatment only led to slightly better activation of $p34^{Cdc2}$ than simultaneous treatment (Fig. 2), Herceptin pretreatment resulted in significant sensitization to taxol-induced apoptosis, cell killing, and tumor inhibition (Figs. 3-5). This suggests that $p34^{Cdc2}$ activation is only one of those multiple mechanisms or signaling pathways induced by Herceptin leading to taxol sensitization. Consistent with this notion, it has been recently reported that anti-ErbB2 monoclonal antibody 4D5, from which Herceptin was developed, resulted in rapid dephosphorylation of ErbB2, accumulation of the cyclin-dependent kinase inhibitor $p27^{kip1}$, and inactivation of cyclin-Cdk2 complexes (36). Notably, Cdk2 kinase activities were dramatically inhibited when MDA-MB-435 cells were treated with taxol (12). Another group recently showed that taxol treatments significantly reduced the level of Cdk2 protein in MCF7 cells (28). Thus, it is possible that Cdk2 inhibition may also contribute to Herceptin-mediated sensitization

of ErbB2-overexpressing breast cancer cells to taxol. In addition, taxol-mediated down-regulation of IκB-α through the up-regulation of IκB kinase β subunit (26) and taxol-mediated serine phosphorylation of the 66-kDa Shc isoform may also be signaling events contributing to cell death (27). We are currently investigating the involvement of these mechanisms in Herceptin-mediated taxol sensitization.

It has been reported that Herceptin enhances the anti-tumor activity of taxol and doxorubicin against ErbB2-overexpressing human breast cancer xenografts (13). The report is consistent with data from the Herceptin phase III clinical trial, in which Herceptin and taxol were administered simultaneously (37, 38). Here, we report an insightful finding that Herceptin pretreatment sensitizes ErbB2-overexpressing cells to taxol-induced apoptosis, cell killing, and tumor inhibition to greater extents than simultaneous treatment with Herceptin plus taxol (Figs. 3-5). This improved taxol sensitization may be attributed to, at least partly, reduced Cdc2 inhibitory phosphorylation on Tyr15 and down-regulation of $p21^{cip1}$, which are achieved at least 24 h after Herceptin treatment in cultured cells (Fig. 1), allowing more efficient activation of Cdc2 and better induction of apoptosis (Figs. 2, 3). In our *in vivo* tumorigenecity assays, we pretreated mice with Herceptin five days before giving taxol. This pretreatment consisted of three Herceptin injections once every other day to allow enough time for inhibition of both Cdc2-Tyr15 phosphorylation and $p21^{cip1}$ expression. Although we were unable to determine Cdc2 kinase activities in tumor samples, in situ TUNEL assays demonstrated that Herceptin pretreated tumors are more susceptible to taxol-induced apoptosis than the simultaneous treatment group (Fig. 5B,C). More importantly, the enhanced apoptosis in tumor samples correlated with improved inhibition of tumor xenografts in mice. Despite the need to investigate other possible mechanisms underlying the improved tumor inhibition by Herceptin pretreatment, our findings that Herceptin pretreatment better sensitizes ErbB2-overexpressing breast cancer

cells to taxol than the simultaneous treatment with taxol could have important therapeutic implications. It will be very important to determine whether Herceptin pretreatment may provide further improved clinical responses to taxol in breast cancer patients compared to the current practice of the simultaneous administration of Herceptin and taxol.

ACKNOWLEDGMENTS

We thank Drs. Ming Tan, Lianglin Zhang, and Jon Trent for helpful discussions and technical suggestions.

REFERENCES:

1. Yamamoto, T., Ikawa, S., Akiyama, T., Semba, K., Nomura, N., Miyajima, N., Saito, T., and Toyoshima, K. Similarity of protein encoded by the human c-*erb*B-2 gene to epidermal growth factor, Nature. *319:* 230-234, 1986.

2. Bargmann, C. I., Hung, M.-C., and Weinberg, R. A. The *neu* oncogene encodes an epidermal growth factor receptor-related protein, Nature. *319:* 226-230, 1986.

3. Yu, D. and Hung, M.-C. Role of erbB2 in breast cancer chemosensitivity, BioEssays. *22:* 673-680, 2000.

4. Slamon, D. J., Clark, G. M., Wong, S. G., Levin, W. J., Ullrich, A., and McGuire, W. L. Human breast cancer: correlation of relapse and survival with amplification of the HER-2/*neu* oncogene, Science. *235:* 177-182, 1987.

5. Slamon, D. J., Godolphin, W., Jones, L. A., Holt, J. A., Wong, S. G., Keith, D. E., Levin, W. J., Stuart, S. G., Udove, J., Ullrich, A., and McGuire, W. L. Studies of the HER-2/*neu* proto-oncogene in human breast and ovarian cancer, Science (Washington, D.C.). *244:* 707-712, 1989.

6. Yu, D. and Hung, M.-C. HER-2/neu gene in human cancers. *In:* E. Freireich and S. A. Stass (eds.), Molecular Basis of Oncology, Vol. 5, pp. 131-162. Cambridge: Blackwell Scientific Publications Inc., 1995.

7. Tauchi, K., Hori, S., Itoh, H., Osamura, R. Y., Tokuda, Y., and Tajima, T. Immunohistochemical studies on oncogene products (c-erbB-2, EGFR, c-myc) and estrogen receptor in benign and malignant breast lesions: with special reference to their prognostic significance in carcinoma, Virchows Arch. A Pathol. Anat. Histopathol. *416:* 65-73, 1989.

8. Lacroix, H., Iglehart, J. D., Skinner, M. A., and Kraus, M. H. Overexpression of erbB-2 or EGF-receptor proteins present in early stage mammary carcinoma is detected simultaneously in matched primary tumors and regional metastasis, Oncogene. *4:* 145-151, 1989.

9. van de Vijver, M. J., Peterse, J. L., Mooi, W. J., Wisman, P., Lomans, J., Dalesio, O., and Nusse, R. *Neu*-protein overexpression in breast cancer: association with comedo-type ductal carcinoma in situ and limited prognostic value in stage II breast cancer, N. Engl. J. Med. *319:* 1239-1245, 1988.

10. Tan, M., Yao, J., and Yu, D. Overexpression of the c-erbB-2 gene enhanced intrinsic metastatic potential in human breast cancer cells without increasing their transformation abilities, Cancer Res. *57:* 1199-1205, 1997.

11. Yu, D., Liu, B., Tan, M., Li, J., Wang, S.-S., and Hung, M.-C. Overexpression of c-erbB-2/neu in breast cancer cells confers increased resistance to Taxol via mdr-1-independent mechanisms, Oncogene. *13:* 1359-1365, 1996.

12. Yu, D., Jing, T., Liu, B., Yao, J., Tan, M., McDonnell, T. J., and Hung, M.-C. Overexpression of ErbB2 blocks Taxol-induced apoptosis by upregulation of $p21^{Cip1}$, which inhibits $p34^{Cdc2}$ kinase, Molecular Cell. *2:* 581-591, 1998a.

13. Baselga, J., Norton, L., Albanell, J., Kim, Y.-M., and Mendelsohn, J. Recombinant humanized anti-HER2 antibody (Herceptin®) enhances the antitumor activity of paclitaxel and doxorubicin against HER2/neu overexpressing human breast cancer xenografts, Cancer Res. *58:* 2825-2831, 1998.

14. Pegram, M. D., Lipton, A., Hayes, D. F., Weber, B. L., Baselga, J. M., Tripathy, D., Baly, D., Baughman, S. A., Twaddell, T., Glaspy, J. A., and Slamon, D. J. Phase II study of receptor-enhanced chemosensitivity using recombinant humanized anti-

p185HER2/neu monoclonal antibody plus cisplatin in patients with HER2/neu-overexpressing metastatic breast cancer refractory to chemotherapy treatment, J. Clin. Oncol. *16:* 2659-2671, 1998.

15. Dickman, S. Antibodies stage a comeback in cancer treatment, Science. *280:* 1196-1197, 1998.

16. Shepard, H. M., Lewis, G. D., Sarup, J. C., Fendly, B. M., Maneval, D., Mordenti, J., Figari, I., Kotts, C. E., Palladino Jr., M. A., Ullrich, A., and Slamon, D. Monoclonal antibody therapy of human cancer: Taking the HER2 protooncogene to the clinic, J. Clin. Immuno. *11:* 117-127, 1991.

17. Baselga, J., Tripathy, D., Mendelsohn, J., Baughman, S., Benz, C. C., Dantis, L., Sklarin, N. T., Seidman, A. D., Hudis, C. A., Moore, J., Rosen, P. P., Twaddell, T., Henderson, I. C., and Norton, L. Phase II study of weekly intravenous recombinant humanized anti-p185her2 monoclonal antibody in patients with HER2/neu-overexpressing metastatic breast cancer, J. Clin. Oncol. *14:* 737-744, 1996.

18. Pietras, R. J., Pegram, M. D., Finn, R. S., Maneval, D. A., and Slamon, D. J. Remission of human breast cancer xenografts on therapy with humanized monoclonal antibody to HER-2 receptor and DNA-reactive drugs, Oncogene. *17:* 2235-2249, 1998.

19. Holmes, F. A., Walters, R. S., Theriault, R. L., Forman, A. D., Newton, L. K., Raber, M. N., Buzdar, A. U., Frye, D. K., and Hortobagyi, G. N. Phase II trial of Taxol, an active drug in the treatment of metastatic breast cancer, J. Natl. Cancer Inst. *83:* 1797-1805, 1991.

20. Chevalier, B., Fumoleau, P., Kerbrat, P., Dieras, V., Roche, H., Krakowski, I., Azli, N., Bayssas, M., Lentz, M. A., and Van Glabbeke, M. Docetaxel is a major cytotoxic drug for the treatment of advanced breast cancer: a phase 2 trial of the clinical screening

cooperative group of the European Organization for Research and Treatment of Cancer, J. Clin. Oncol. *13:* 314-322, 1995.

21. Horwitz, S. B. Mechanism of action of Taxol, Trends. Pharma. Sci. *13:* 134-136, 1992.

22. Wahl, A. F., Donaldson, K. L., Fairchild, C., Lee, F. Y. F., Foster, S. A., Demers, G. W., and Galloway, D. A. Loss of normal p53 function confers sensitization to Taxol by increasing G2/M arrest and apoptosis, Nat. Med. *2:* 72-79, 1996.

23. Lee, L. F., Li, G., Templeton, D. J., and Ting, J. P. Paclitaxel (Taxol)-induced gene expression and cell death are both mediated by the activation of c-Jun NH2-terminal kinase (JNK/SAPK), J. Biol. Chem. *273:* 28253-28260, 1998.

24. Wang, T. H., Popp, D. M., Wang, H. S., Saitoh, M., Mural, J. G., Henley, D. C., Ichijo, H., and Wimalasena, J. Microtubule dysfunction induced by paclitaxel initiates apoptosis through both c-Jun N-terminal kinase (JNK)-dependent and -independent pathways in ovarian cancer cells, J. Biol Chem. *274:* 8208-8216, 1999.

25. Yamamoto, K., Ichijo, H., and Korsmeyer, S. J. BCL-2 phosphorylated and inactivated by an ASK1/Jun N-terminal protein kinase pathway normally activated at G(2)/M, Mol. Cell. Biol. *19:* 8469-8478, 1999.

26. Huang, Y., Johnson, K. R., Norris, J. S., and Fan, W. Nuclear factor-kappaB/IkappaB signaling pathway may contribute to the mediation of paclitaxel-induced apoptosis in solid tumor cells, Cancer Res. *60:* 4426-4432, 2000.

27. Yang, C. P. and Horwitz, S. B. Taxol mediates serine phosphorylation of the 66-kDa Shc isoform, Cancer Res. *60:* 5171-5178, 2000.

28. Bacus, S. S., Gudkov, A. V., Lowe, M., Lyass, L., Yung, Y., Komarov, A. P., Keyomarsi, K., Yarden, Y., and Seger, R. Taxol-induced apoptosis depends on MAP kinase pathways (ERK and p38) and is independent of p53, Oncogene. *20:* 147-155, 2001.

29. Jing, T., Tan, M., Lee, S., Nagata, Y., Liu, J., Arlinghaus, R., Hung, M. C., and Yu, D. S. Phosphorylation on Tyrosine-15 of p34Cdc2 by erbB2 Receptor Tyrosine Kinase Inhibits p34Cdc2 Activation, Nat. Cell Biol. *Under review:*, 2001.

30. Coleman, T. R. and Dunphy, W. G. Cdc2 regulatory factors, Curr. Opin. Cell Biol. *6:* 877-882, 1994.

31. Darzynkiewicz, Z., Bruno, S., Del Bino, G., Gorczyca, W., Hotz, M. A., Lassota, P., and Traganos, F. Features of apoptotic cells measured by flow cytometry, Cytometry. *13:* 795-808, 1992.

32. Klapper, L. N., Waterman, H., Sela, M., and Yarden, Y. Tumor-inhibitory antibodies to HER-2/ErbB-2 may act by recruiting c-Cbl and enhancing ubiquitination of HER-2, Cancer Res. *60:* 3384-3388, 2000.

33. Hurwitz, E., Stancovski, L., Sela, M., and Yarden, Y. Suppression and promotion of tumor growth by monoclonal antibodies to ErbB-2 differentially correlate with cellular uptake, Proc. Natl. Acad. Sci. *92:* 3353-3357, 1995.

34. Madhani, H. D. Accounting for specificity in receptor tyrosine kinase signaling, Cell. *106:* 9-11, 2001.

35. Stebbing, J., Copson, E., and O'Reilly, S. Herceptin (trastuzamab) in advanced breast cancer, Cancer Treatment Reviews. *26:* 287-290, 2000.

36. Lane, H. A., Beuvink, I., Motoyama, A. B., Daly, J. M., Neve, R. M., and Hynes, N. E. ErbB2 Potentiates Breast Tumor Proliferation through Modulation of $p27^{Kip1}$-Cdk2 Complex Formation: Receptor Overexpression Does Not Determine Growth Dependency, Mol. Cell. Biol. *20:* 3210-3223, 2000.

37. Slamon, D., Leyland-Jones, B., Shak, S., Paton, V., Bajamonde, A., Fleming, T., Eiermann, W., Wolter, J., Baselga, J., and Norton, L. Addition of Herceptin (Humanized

anti-HER2 antibody) to first line chemotherapy for HER2 overexpressing metastatic breast cancer (HER2+/MBC) markedly increases anticancer activity: a randomized, multinational controlled phase III trial, Proc. Am. Soc. Clin. Oncol. *17:* 98A, 1998.

38. Cobleigh, M. A., Vogel, C. L., Tripathy, D., Robert, N. J., Scholl, S., Fehrenbacher, L., Paton, V., Shak, S., Lieberman, G., and Slamon, D. Efficacy and safety of Herceptin (Humanized anti-HER2 antibody) as a single agent in 222 women with HER2 overexpression who relapsed following chemotherapy for metastatic breast cancer, Proc. Am. Soc. Clin. Oncol. *17:* 97A, 1998.

FIGURE LEDGEND

Fig. 1. Herceptin downregulated ErbB2, reduced phosphorylation on Tyr15 of $p34^{Cdc2}$, and inhibited $p21^{Cip1}$ expression in ErbB2-overexpressing breast cancer cells. MDA-MB-435 cells and 435.eB transfectants (A), SkBr3 and MDA-MB-453 cells (B) were treated with incremental concentrations of Herceptin (10 and 20 nM) or IgG for various times (0, 24, or 36 h). Western blot analysis was performed as described in "Materials and Methods". All experiments described in this study have been repeated at least three times.

Fig. 2. Herceptin treatment sensitized ErbB2-overexpressing breast cancer cells to $p34^{Cdc2}$ activation upon taxol treatment. A, Activation of $p34^{Cdc2}$ kinase in differentially treated 435.eB transfectants. Cells were untreated (lane 1), treated with 20 nM human IgG (lane 2), 0.02 μM taxol (lane 3), 20 nM Herceptin (lane 4), 20 nM Herceptin plus 0.02 μM taxol simultaneously for 3 hours (lane 5), or 20 nM Herceptin for 24 hours as a pretreatment then 0.02 μM taxol for three hours (lane 6). Immunocomplex–kinase assays were performed as described in " Materials and Methods". B, Activation of $p34^{Cdc2}$ Kinase in SKBr3 cells. Cells were cultured in medium containing 20 nM human IgG (lane 1, control), 0.05 μM taxol (lane 2), 5 nM Herceptin (lane 3), or pretreated with 10 nM Herceptin for 24 h before addition of 0.05 μM taxol (lane 4). Cell were continuously treated for 6 h and immunocomplex–kinase assays were performed as described in " Materials and Methods".

Fig. 3. Herceptin pretreatment further enhanced taxol–induced apoptosis than the simultaneous Herceptin and taxol treatment in 435.eB transfectants (A, B) and in SKBr3 cells (C). Cells were treated as in Figure 2A. Cells were collected and analyzed for taxol-induced apoptosis by double-label flow cytometry analysis as described in "Materials and Methods". Apoptotic cells

with DNA strand breaks are shown to have higher levels of Biotin-16-dUTP labeling above the sloped lines. Percentage of cell population in G_2/M and with strong dUTP labeling are indicated at the top of frame (A). A graphic presentation of FITC positive cells in A as percentages of apoptosis (B). SKBr3 cells were treated with 5 nM or 10 nM Herceptin and /or 0.05 uM taxol as indicated (C). Cells were collected, and analyzed for taxol-induced apoptosis by double-label flow cytometry as described in "Materials and Methods". The percentages of FITC positive apoptotic cells after each treatment are shown in bar diagrams (C).

Fig. 4. Enhanced sensitization to taxol killing by Herceptin pretreatment compared to the simultaneous treatment in ErbB2-overexpessing 435.eB transfectants (A) and SKBr3 cells (B). Cells were treated with 20 nM Herceptin for 24 h prior to addition of 0.02 μM taxol (435.eB transfectants) or 10 nM Herceptin for 24 h prior to addition of 0.05 μM taxol (SKBr3 cells). Clonogenic assays were performed to analyze cytotoxicity as described in " Materials and Methods".

Fig. 5. Herceptin pretreatment inhibited tumor growth more effectively than the simultaneous treatment. A. Female ICR-SCID mice (total 47 mice) were injected with 435.eB transfectants (1X 10^6 cells/mice) to induce tumor xenografts. Seven days later, mice were divided into five groups, with at least nine mice in each group. The first group was treated with the rhu IgG monoclonal antibody (0.3 mg/kg) twice a week for five weeks and the second group was treated with Herceptin at the same dose and schedule. The third group was injected with taxol (10 mg/kg) i.p. on days 12 and 15 along with the rhu IgG monoclonal antibody (0.3 mg/kg). Treatment continued with the rhu IgG monoclonal antibody twice a week for another four weeks. The fourth group was given taxol (10 mg/kg) i.p. on days 12 and 15 along with Herceptin (0.3

mg/kg). Treatment continued with Herceptin twice a week for four weeks. The fifth group was pretreated with Herceptin (0.3 mg/kg) on days 7, 9, and 11, then given taxol (10 mg/kg) i.p. on days 12 and 15 along with Herceptin (0.3 mg/kg). Treatment continued with Herceptin twice a week for four weeks. Tumor volume was measured and calculated as described in " Materials and Methods". B. Immunohistochemical staining with anti-ErbB2 antibody and in situ TUNEL assay of apoptosis *in vivo*. a-e: ErbB2 immunohistochemical staining of tumor slides from different treatment groups 1 -5 (×200). f-j: In situ TUNEL assay of tumor slides from different treatment groups 1 -5 (×400). The percentages of TUNEL positive apoptotic cells in each treatment group were quantified and shown as bar diagrams (C).

Fig. 1

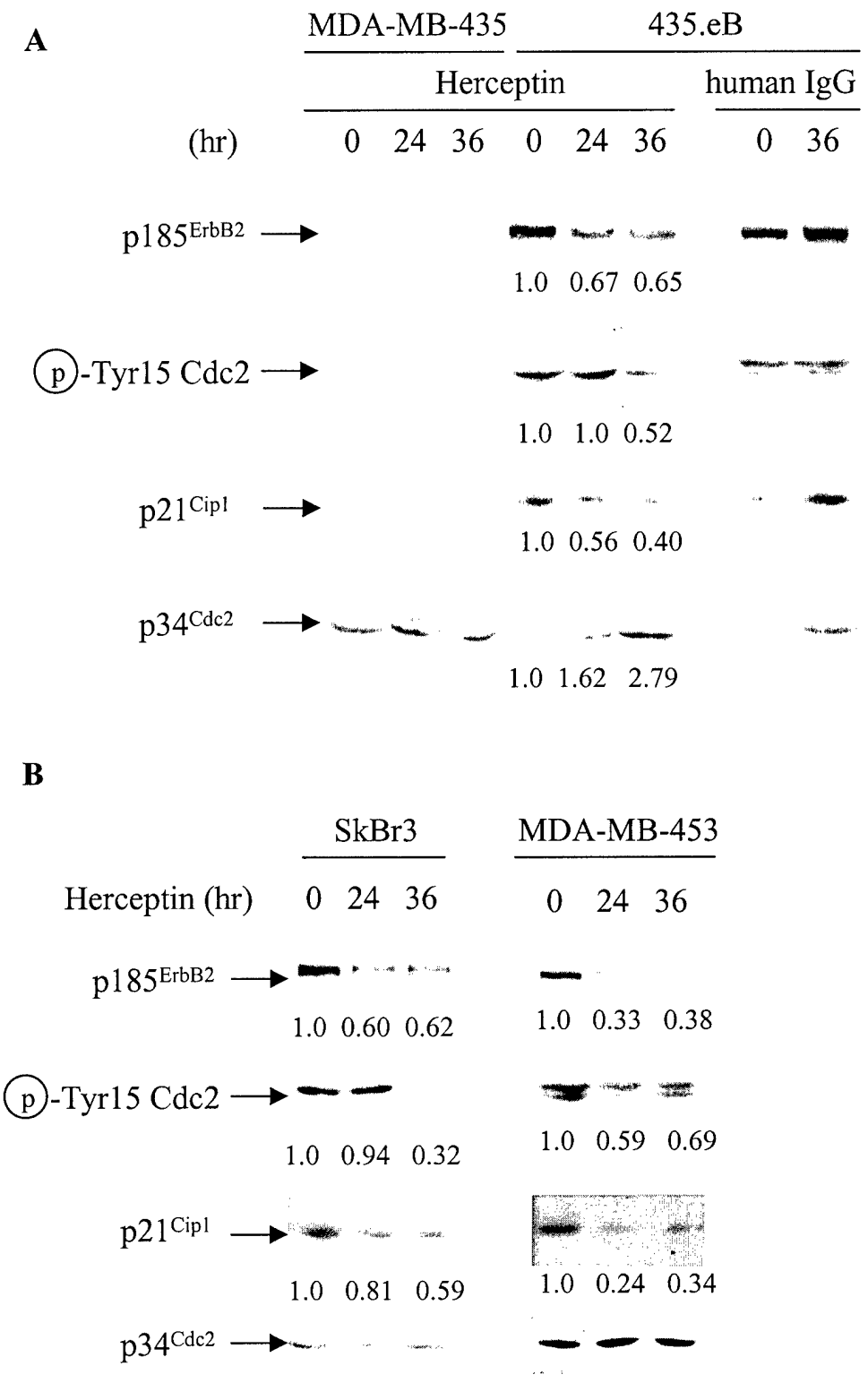
A
MDA-MB-435
435.eB
Herceptin
human IgG
(hr)
0 24 36 0 24 36 0 36
p185ErbB2
1.0 0.67 0.65
p-Tyr15 Cdc2
1.0 1.0 0.52
p21Cip1
1.0 0.56 0.40
p34Cdc2
1.0 1.62 2.79
B
SkBr3
MDA-MB-453
Herceptin (hr)
0 24 36 0 24 36
p185ErbB2
1.0 0.60 0.62
1.0 0.33 0.38
p-Tyr15 Cdc2
1.0 0.94 0.32
1.0 0.59 0.69
p21Cip1
1.0 0.81 0.59
1.0 0.24 0.34
p34Cdc2

Fig. 2

A. 435.eB

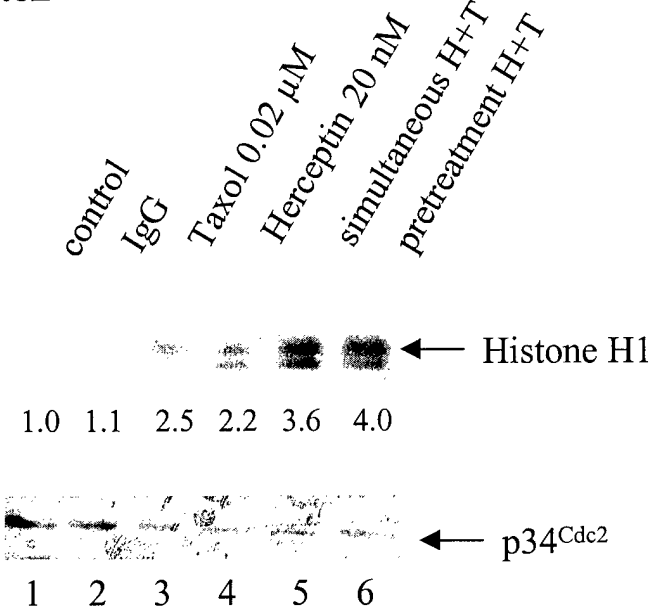

B. SKBr3

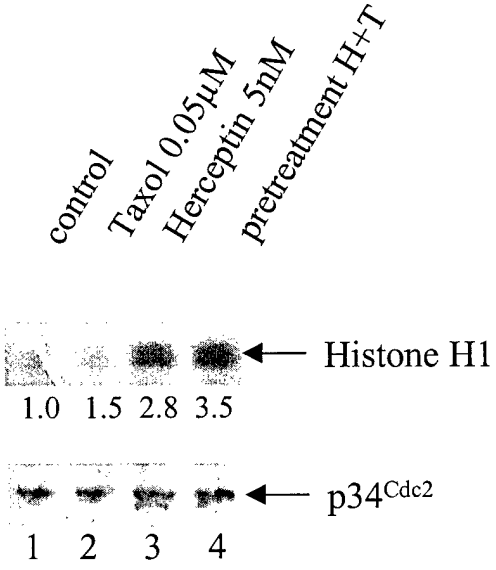

Fig. 3

A. 435.eB

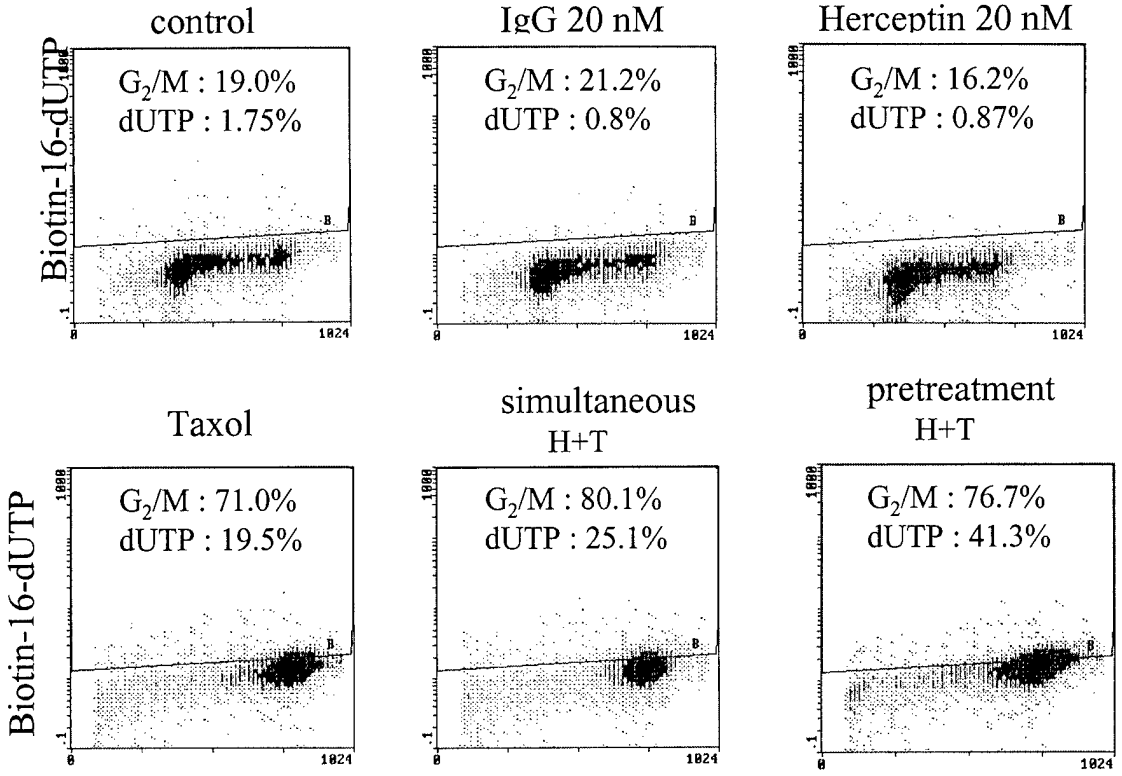

B. 435.eB

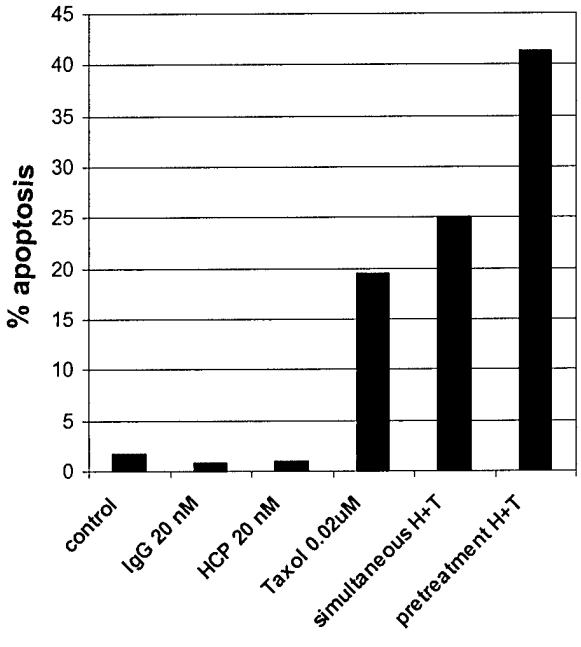

C. SKBr3

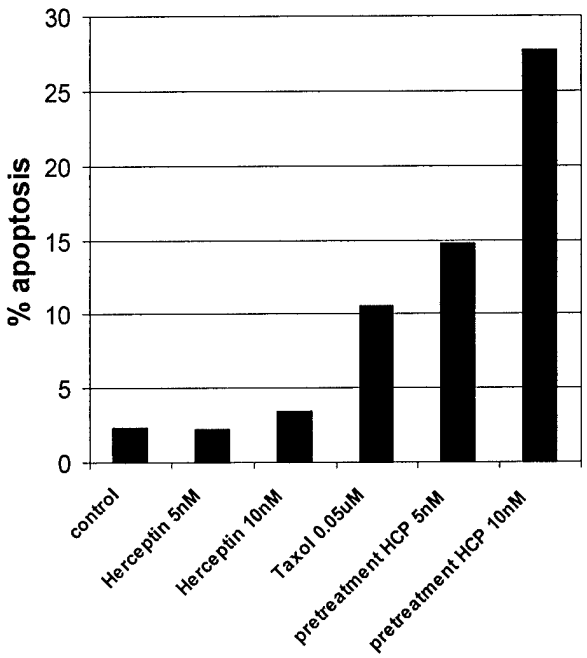

Fig. 4

A 435.eB

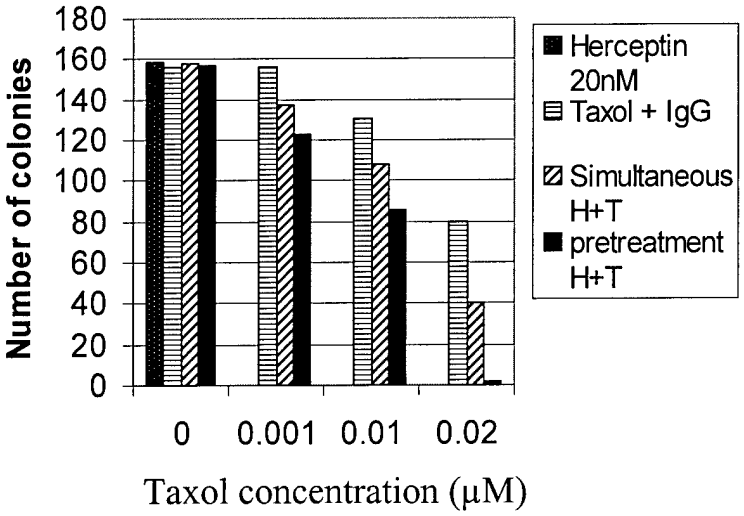

B SKBr3

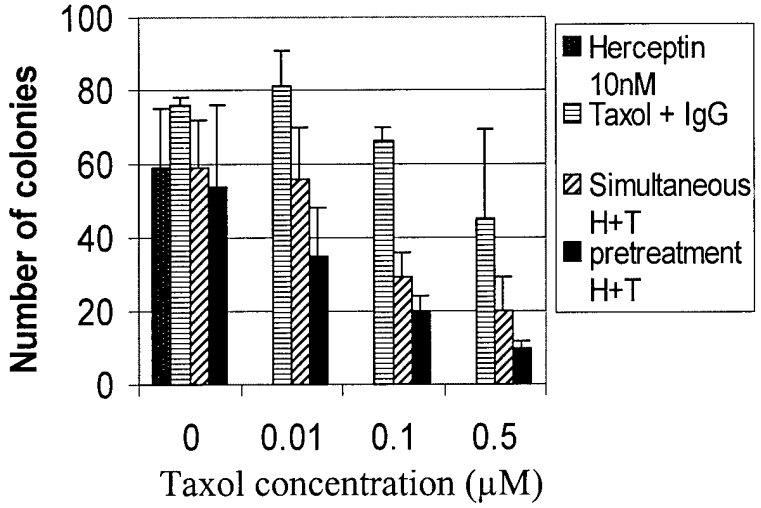

Fig. 5

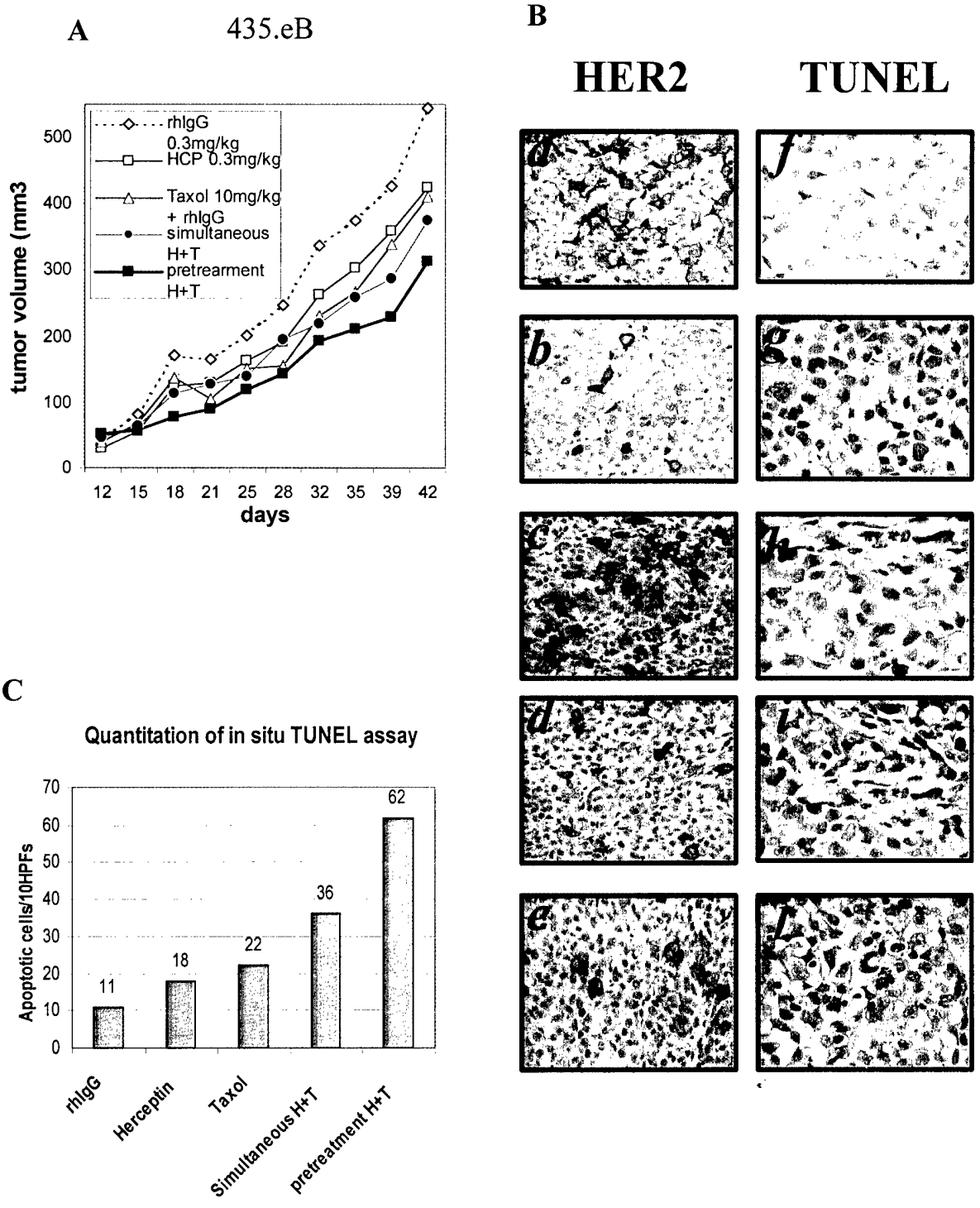
A
435.eB
rhIgG 0.3mg/kg
HCP 0.3mg/kg
Taxol 10mg/kg
+ rhIgG simultaneous H+T
pretrearment H+T
tumor volume (mm3
0
100
200
300
400
500
12 15 18 21 25 28 32 35 39 42
days
B
HER2
TUNEL
a
b
c
d
e
f
g
h
i
j
C
Quantitation of in situ TUNEL assay
Apoptotic cells/10HPFs
0
10
20
30
40
50
60
70
11
18
22
36
62
rhIgG
Herceptin
Taxol
Simultaneous H+T
pretreatment H+T

.CER RESEARCH 60, 6841–6845, December 15, 2000]

.dvances in Brief

HER-2/neu Promotes Androgen-independent Survival and Growth of Prostate Cancer Cells through the Akt Pathway[1]

Yong Wen,[2] Mickey C-T. Hu,[2] Keishi Makino, Bill Spohn, Geoffrey Bartholomeusz, Duen-Hwa Yan, and Mien-Chie Hung[3]

Department of Molecular and Cellular Oncology, The University of Texas M. D. Anderson Cancer Center, Houston, Texas 77030

Abstract

***HER-2/neu* has been implicated in the activation of androgen receptor (AR) and in inducing hormone-independent prostate cancer growth. Here we report that *HER-2/neu* activates Akt (protein kinase B) to promote prostate cancer cell survival and growth in the absence of androgen. Blocking of the Akt pathway by a dominant-negative Akt or an inhibitor LY294002 abrogates the *HER-2/neu*-induced AR signaling and cell survival/growth effects in the absence or presence of androgen. Akt specifically binds to AR and phosphorylates serines 213 and 791 of AR. Thus, Akt is a novel activator of AR required for *HER-2/neu* signaling to androgen-independent survival and growth of prostate cancer cells.**

Introduction

Androgen plays a critical role in controlling the growth and survival of prostate cancer cells, and androgen ablation therapy usually achieves significant clinical responses in the beginning. Under the selective pressure of androgen withdrawal, however, prostate cancers progress to an androgen-independent stage (1). The mechanism for this progression to androgen independence is not completely understood. Although androgen-independent progression has been correlated with mutation of the *AR*[4] gene (2, 3), most androgen-independent prostate cancer cells express AR and the androgen-dependent gene *PSA*, implying that these cells maintain a functional AR signaling pathway. Furthermore, it has been shown that MAP kinases are involved in activation of AR signal transduction (4, 5), suggesting that reactivation of the AR pathway by a hormone-independent mechanism may lead to androgen-independent prostate cancers. Recently, overexpression of *HER-2/neu* has been implicated in the activation of AR and in inducing hormone-independent prostate cancer growth (5, 6). *HER-2/neu*, a M_r 185,000 transmembrane receptor tyrosine kinase with homology to members of the EGF receptor family, is overexpressed in ~30% of human breast and ovarian cancers (7). Unlike the other members of EGF receptors, *HER-2/neu* has an intrinsic tyrosine kinase activity that activates the receptor-mediated signal transduction in the absence of ligand. Although EGF binds to an EGF receptor to induce receptor dimerization and activate PI3K (8), *HER-2/neu* homodimer constitutively activates the PI3K-Akt pathway without extracellular stimulation (9). Activation of PI3K generates phosphatidylinositol-3,4,5-triphosphate, which in turn binds to the pleckstrin homology domain of serine/threonine kinase Akt, resulting in recruitment of Akt to the cell membrane. A conformational change of Akt follows, which enables residues Thr-308 and Ser-473 to be phosphorylated by upstream kinases, PDK-1 and PDK-2 or ILK, respectively (10). Activated Akt phosphorylates specific targets such as Bad (11), pro-caspase-9 (12), and transcription factor FKHRL1 (13) at the Akt phosphorylation consensus sequence R-X-R-X-X-S/T, thus promoting cell survival and blocking apoptosis. In this way, the PI3K-Akt pathway plays a critical role in antiapoptosis that may contribute to the pathogenesis of cancer (10). In the present study, we examined whether Akt and *HER-2/neu* are involved in the AR signaling pathway and whether they play a role in androgen-independent survival or growth of prostate cancer cells. We show that *HER-2/neu* activated Akt to promote prostate cancer cell survival and growth in the absence of androgen. The *HER-2/neu*-induced AR signaling and cell survival/growth effects were blocked by the DN-Akt or an inhibitor LY294002. Moreover, Akt specifically binds to AR and phosphorylates Ser-213 and Ser-791 of AR. Thus, our findings provide a molecular mechanism for the *HER-2/neu*-induced androgen-independent survival and growth of prostate cancer cells.

Materials and Methods

Reporter and Cell Survival Assays. LNCaP cells were plated the day before transfection at a density of 2×10^5 cells/well in six-well plates. The cells were cotransfected with a luc reporter plasmid (0.3 μg of PSA-luc or PRE-luc) and a β-gal expression plasmid (0.2 μg of CMV-β-gal) and expression plasmids or an empty vector (0.9 μg each) as indicated using liposomes. After transfection, the cells were cultured in phenol red-free medium supplemented with 5% of the c-FBS in the absence or presence of the synthetic androgen R1881 (NEN; 0.1 or 1.0 nM). Cell lysates were collected 48 h after transfection, and the luc activity of each sample was measured with the luc assay kit (Promega). β-gal activity was determined to normalize variations in transfection efficiency. The PSA-luc reporter construct (PSA-luc) was generated by subcloning a genomic DNA (~1.5 kb) containing the PSA promoter (640-bp) and enhancer (~820-bp) into the luc expression vector. The PRE-luc reporter (PRE-luc) contains two copies of the progesterone/androgen response element (14). For survival assays, LNCaP cells were prepared as described above and cotransfected with 0.2 μg of CMV-luc plasmid and 2 μg of each expression plasmid as indicated. The transfected cells were cultured in the absence or presence of androgen as described above. The relative survival rate (percentage of cell survival) between the cultures in the absence and presence of androgen was determined by the luc activities and shown as a ratio, using the activity in the medium containing androgen as 100%. The data represent the mean value of at least three independent experiments, and statistical significance was calculated with the χ^2 test using SPSS software. $P < 0.05$ was set as the criterion for statistical significance.

Cell Proliferation Assays. LNCaP cells were plated the day before transfection at 50% confluence in 100-mm dishes. The cells were cotransfected with

Received 7/19/00; accepted 10/31/00.

The costs of publication of this article were defrayed in part by the payment of page charges. This article must therefore be hereby marked *advertisement* in accordance with 18 U.S.C. Section 1734 solely to indicate this fact.

[1] This work was supported by Grants R01-CA58880 and R01-CA77858 and Cancer Core Grant 16672 from the National Cancer Institute, by the Nellie Connally Breast Cancer Research Fund, and by the Faculty Achievement Award at M. D. Anderson Cancer Center (to M-C. H.). Y. W. and K. M. are predoctoral and postdoctoral fellows, respectively, supported by United States Army Breast Cancer Research Training Grant DMAD 17-99-1-9264).

[2] These authors contributed equally to this work.

[3] To whom requests for reprints should be addressed, at Department of Molecular and Cellular Oncology, Box 108, The University of Texas M. D. Anderson Cancer Center, 1515 Holcombe Boulevard, Houston, TX 77030. Phone: (713) 792-3668; Fax: (713) 794-4784; E-mail: mhung@notes.mdacc.tmc.edu.

[4] The abbreviations used are: AR, androgen receptor; PSA, prostate-specific antigen; MAP, mitogen-activated protein; EGF, epidermal growth factor; PI3K, phosphatidylinositol 3-kinase; HA, hemagglutinin; CMV, cytomegalovirus; mAb, monoclonal antibody; β-gal, β-galactosidase; c-FBS, charcoal-treated FBS; BrdUrd, bromodeoxyuridine; wt, wild type; mut, mutant; GST, glutathione *S*-transferase; RFP, red fluorescent protein; luc, luciferase; DN-Akt, dominant-negative Akt; CA-Aft, constitutively active Akt.

1.0 μg of pDsRed1-C1 plasmid (Clontech) and 15 μg of a constitutively active *HER2/neu* (*HER2/neu**), the Thr-1172 of which has been changed to Glu, or 15 μg of the control vector. After transfection, the cells were cultured in phenol red-free medium supplemented with 5% of c-FBS in the absence or presence of R1881 (0.1 nM). As controls, 36 h after transfection, the transfected cells were treated with 40 μM of LY294002 (Biomol), which is an inhibitor for the PI3K/Akt pathway. For BrdUrd labeling, 48 h after transfection, the cells were incubated with BrdUrd (10 μM) for 1 h. The transfected cells expressing the red fluorescent protein were selected by fluorescence-activated cell sorter and plated onto poly-L-lysine-coated slides using Cytospin II. The BrdUrd-labeled cells were detected using a BrdUrd labeling and detection kit (Roche) and evaluated under a fluorescent microscope. The percentages of BrdUrd-labeled cells were calculated based on ~400–800 RFP^+ cells from each sample.

Immunoprecipitation, Western Blot, and Immunocomplex Kinase Assays. LNCaP cells were washed with PBS, lysed in ice-cold RIPA buffer containing protease inhibitors, and centrifuged at 14,000 × *g* for 10 min at 4°C. For immunoprecipitation, 1 mg of each supernatant (cell lysate) was incubated with an anti-AR mAb (Pharmingen) or mouse IgG (negative control) overnight at 4°C. Then, protein G-agarose (Roche) was added and incubated for 2 h at 4°C with rotation. The immunocomplex was recovered by centrifugation, washed four times with lysis buffer, dissolved in loading buffer, and subjected to SDS-PAGE. For Western blot, the protein samples were subjected to SDS-PAGE and transferred onto nitrocellulose membranes. The membranes were blocked with 5% nonfat dry milk in PBS containing 0.05% Tween 20 and incubated with an anti-p-Akt (S-473) antibody (New England Biolabs) and then with horseradish peroxidase-conjugated secondary antibodies according to the manufacturer's instructions. The immunoblots were visualized by an enhanced chemiluminescence kit (ECL; Amersham). Immunocomplex kinase assays were performed as described previously (15). Specifically, 293T cells were transfected with the HA-tagged CA-Akt expression plasmid, the cells were harvested, and whole-cell lysates were prepared 48 h after transfection. After immunoprecipitation with an anti-HA mAb, phosphorylation of AR was determined by an immunocomplex kinase assay, using wt or mut GST-AR-N or GST-AR-C or histone 2B (Roche) as substrates. The GST-AR-N and GST-AR-C plasmids were constructed by subcloning of the cDNA fragments containing the N- or COOH-terminal domain of AR (AR-N or AR-C) by the PCR technique. The mutant GST-AR-N and GST-AR-C were generated by site-directed mutagenesis using specific oligonucleotides and a QuickChange site-directed mutagenesis kit (Stratagene) to change the Ser-213 and Ser-791 residues to Ala-213 and Ala-791, respectively. The GST-fusion proteins were purified by affinity chromatography on glutathione-Sepharose 4B (Amersham).

Pull-Down Assays. 293T cells were transfected with the HA-tagged CA-Akt expression plasmid, the cells were harvested, and whole-cell lysates were prepared 48 h after transfection. Fifty μl of glutathione-Sepharose were incubated with 90 μg of GST-AR-N or GST-AR-C or GST protein for 3 h and washed with washing buffer [50 mM Tris-HCl (pH 8.0), 150 mM NaCl, and 0.5% NP40] three times. The 293T cell lysates were mixed with the GST-AR-N or GST-AR-C or GST conjugated glutathione-Sepharose, incubated overnight at 4°C, and washed three times with washing buffer. The proteins bound to the GST-AR-N or GST-AR-C or GST-conjugated glutathione-Sepharose were analyzed by Western blotting using an anti-HA mAb (12CA5).

Results and Discussion

Because activation of the AR signaling pathway by an androgen-independent survival mechanism may promote survival of prostate cancer cells during androgen deprivation, we investigated whether Akt is involved in the AR pathway and plays a role in androgen-independent survival or growth of prostate cancer cells. The PSA promoter/enhancer contains high-affinity AR binding sites and is up-regulated by androgen (16, 17). To examine the effects of Akt on PSA transcriptional regulation, we cotransfected LNCaP cells with the PSA-luc reporter plus any one of the following: a CA-Akt, a DN-Akt, an empty vector, or a PTEN (18), which is a tumor suppressor phosphatase that inhibits the PI3K/Akt pathway. We then assayed for the luc activities. CA-Akt activated the PSA-luc reporter 5–7-fold in a dose-dependent manner, whereas DN-Akt suppressed the reporte ~2-fold (Fig. 1*a*), suggesting that Akt activates PSA transcription. To compare the transactivation activity of Akt in the absence and presence of the hormone, we carried out the same DNA transfection experiments as described above, except that the cells were cultured in phenol red-free medium supplemented with the charcoal-treated serum to allow precise control of the concentration of androgen. In the absence of androgen, CA-Akt stimulated the PSA-luc reporter ~5-fold (Fig. 1*b*, *Lane 4 versus Lane 1*), and DN-Akt inhibited the reporter ~2-fold (Fig. 1*b*, *Lane 7 versus Lane 1*), suggesting that Akt can activate the PSA promoter/enhancer in the absence of androgen. Consistent with this concept, PTEN, which is a well-known PI3K/Akt inhibitor, also blocked activation of the PSA promoter/enhancer (Fig. 1*b*, *Lanes 10–12*) in the absence or presence of androgen, further suggesting that the Akt pathway may be required for transactivation of the PSA promoter/enhancer. Moreover, the PSA transcriptional activity induced by CA-Akt in the absence of R1881 (Fig. 1*b*, *Lane 4 versus Lane 1*) is slightly stronger than that stimulated by R1881 alone (Fig. 1*b*, *Lane 3 versus Lane 1*); activation of PSA transcription appears to be less effective by R1881 in the presence of CA-Akt (~1.6-fold; Fig. 1*b*, *Lane 6 versus Lane 4*) than in the absence of

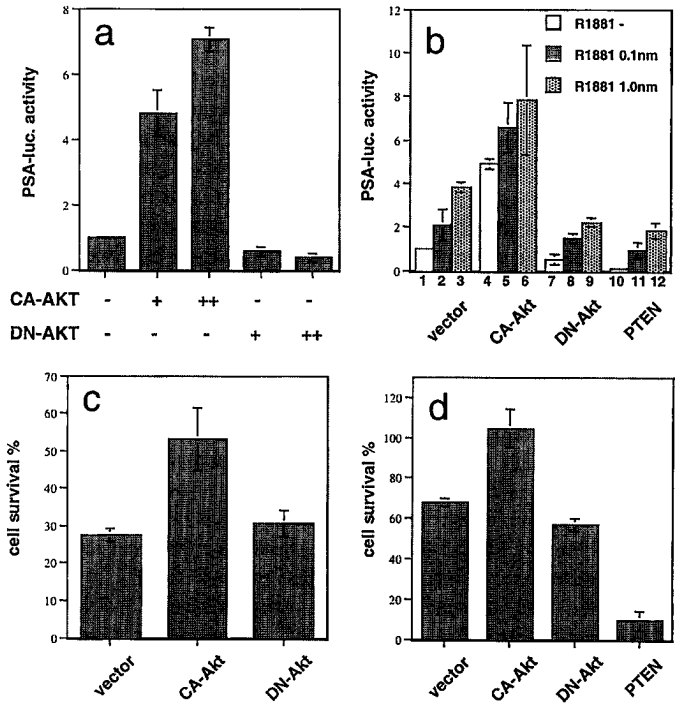

Fig. 1. Akt activates the PSA promoter/enhancer and promotes survival of androgen-dependent prostate cancer cells upon androgen deprivation. *a*, androgen-dependent LNCaP cells were cotransfected with the PSA-luc reporter and a CMV-β-gal vector plus a constitutively active Akt (*CA-Akt*) or a dominant-negative Akt (*DN-Akt*) or an empty vector as indicated and cultured in RPMI 1640 supplemented with 5% FBS. ++, double dose of +, which is 0.6 μg of DNA. The luc activity was measured after 48 h and expressed as an arbitrary unit; the β-gal activity was measured to normalize variations in transfection efficiency. *b*, LNCaP were cotransfected with the PSA-luc reporter and a CMV-β-gal vector plus CA-Akt or DN-Akt or PTEN or an empty vector and cultured in phenol red-free medium supplemented with 5% of the c-FBS in the absence or presence of the synthetic androgen R1881 (0.1 or 1.0 nM) as indicated. The normalized luc activity was indicated as described above. *c*, LNCaP cells were cotransfected with the CMV-luc reporter and a CMV-β-gal vector plus CA-Akt or DN-Akt or an empty vector and cultured in RPMI 1640 supplemented with 5% of either c-FBS or FBS. The percentage of cell survival represents the ratio of the normalized luc activities between the cells cultured in c-FBS and those cultured in FBS. *d*, LNCaP cells were cotransfected with the vectors as described above and cultured in phenol red-free medium supplemented with 5% c-FBS in the absence or presence of R1881 (0.1 nM). The percentage of cell survival indicates the ratio of the normalized luc activities between the cells cultured without R1881 and with R1881. The data represent the mean value of at least three independent experiments; *bars*, SD.

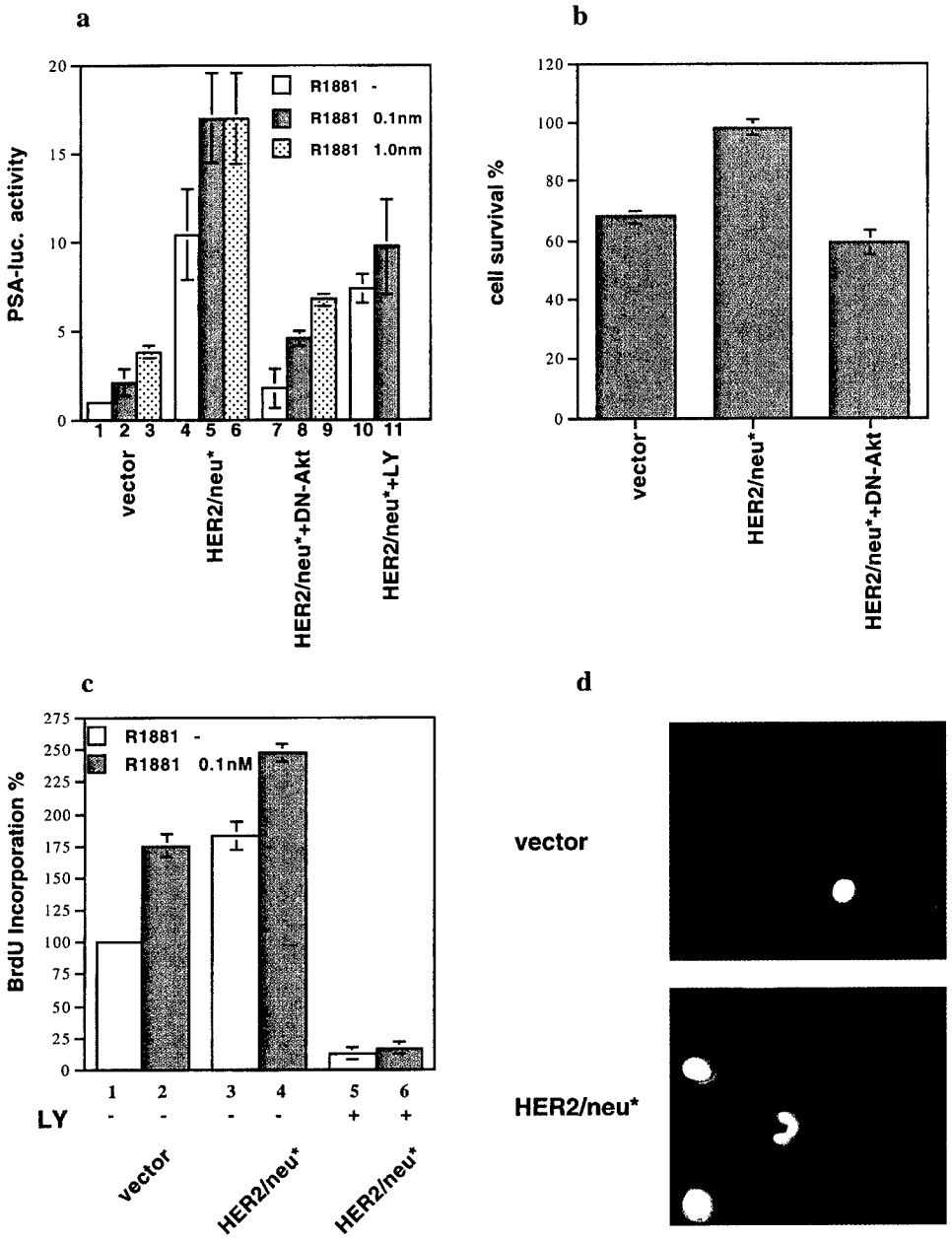

Fig. 2. *HER-2/neu* activates AR signaling and enhances survival and growth of androgen-dependent prostate cancer cells upon androgen withdrawal via the Akt pathway. *a,* LNCaP were cotransfected with the PSA-luc reporter and a CMV-β-gal vector and *HER-2/neu** or *HER-2/neu** plus DN-Akt or an empty vector and cultured in phenol red-free medium supplemented with 5% c-FBS in the absence or presence of R1881 (0.1 or 1.0 nM), with or without LY294002 (*LY*) as indicated. The normalized luc activity was indicated as described in the legend to Fig. 1. *Bars,* SD. *b,* LNCaP were cotransfected with the CMV-luc reporter and a CMV-β-gal vector and *HER-2/neu** or *HER-2/neu** plus DN-Akt or an empty vector and cultured in the same medium in the absence or presence of R1881 (0.1 nM). The percentage of cell survival represents the ratio of the normalized luc activities between the cells cultured without R1881 and with R1881. *Bars,* SD. *c,* LNCaP were cotransfected with pDsRed1-C1 encoding a RFP and *HER-2/neu** or an empty vector and cultured in the same medium in the absence or presence of R1881 (0.1 nM), with or without LY as indicated. The transfected cells were incubated with BrdUrd, the RFP^+ cells were sorted by fluorescence-activated cell sorter, and the sorted cells were plated onto the poly-L-lysine-coated slides using Cytospin II. The BrdUrd-labeled cells were detected and evaluated under a fluorescence microscope. The percentage of BrdUrd-labeled cells were determined based on ~400–800 RFP^+ cells from each sample; *bars,* SD. *d,* representative fluorescent pictures of the RFP^+ cells are depicted.

CA-Akt (~4-fold; Fig. 1*b*, *Lane 3 versus Lane 1*). Taken together, these results imply that Akt is involved in androgen-independent transactivation function.

To further examine whether the androgen-independent transactivation of Akt can be extended to cell survival of prostate cancer cells upon androgen withdrawal, we cotransfected LNCaP cells with the CMV-luc reporter plus CA-Akt or DN-Akt or an empty vector and then cultured the cells either in regular medium or in phenol red-free medium supplemented with the charcoal-treated serum. We used luc assays for the measurement of cell survival because luc is rapidly degraded after cell death, and it has been well established as a measure of cell viability (19, 20). CA-Akt enhanced LNCaP cell survival ~2-fold in the absence of the hormone, whereas DN-Akt failed to increase LNCaP cell survival (Fig. 1*c*). The relative survival rate (percentage of cell survival) was shown as a ratio between the survival of LNCaP cells in the absence and presence of androgen. To confirm that this Akt effect is independent of androgen, we performed similar DNA transfection experiments and cultured the cells in phenol red-free medium supplemented with the charcoal-treated serum with or without R1881. CA-Akt significantly increased LNCaP cell survival in the absence of R1881, whereas DN-Akt and PTEN decreased LNCaP cell survival in the absence of R1881 (Fig. 1*d*). Our data further support the notion that Akt mediates androgen-independent transactivation function and suggest that Akt may enhance prostate cancer cell survival during androgen deprivation.

Because *HER-2/neu* has been shown recently to activate AR signaling (9, 10) and we have demonstrated previously that *HER-2/neu* activates the Akt pathway, we determined whether Akt may be involved in the *HER-2/neu*-activated AR signaling. We cotransfected LNCaP cells with the PSA-luc reporter and an activated form of *HER-2/neu* (*HER-2/neu**) or *HER-2/neu** plus DN-Akt and cultured the cells in the hormone-free medium as described above. *HER-2/neu** activated the PSA promoter/enhancer ~8-fold (Fig. 2*a*, *Lane 5 versus Lane 2,* at 0.1 nM R1881) or ~5-fold (Fig. 2*a*, *Lane 6 versus Lane 3,* at 1.0 nM R1881) in the presence of R1881, and ~10-fold (Fig. 2*a*, *Lane 4 versus Lane 1*) in the absence of R1881. However, this stimulatory effect of *HER-2/neu** was dramatically reduced by DN-Akt or an Akt inhibitor LY294002 (Fig. 2*a*), suggesting that

activation of the AR pathway by *HER-2/neu* requires functional Akt. The PSA-luc reporter construct encodes 1400 bp of sequence consisting of a high-affinity androgen responsive element in the promoter and an androgen responsive region in an upstream enhancer (16, 17). To exclude the possibility that some other promoter or enhancer elements may attribute to PSA activation by androgen, we further analyzed the PRE-luc reporter, which contains two copies of high-affinity androgen response element (14). Similarly, *HER-2/neu** activated the PRE-luc reporter significantly in the presence or absence of R1881. However, this stimulatory effect was blocked by DN-Akt (data not shown), confirming that *HER-2/neu* activates AR signaling via the Akt pathway.

To address the critical question of whether *HER-2/neu* can enhance prostate cancer cell survival upon androgen deprivation, we cotransfected LNCaP cells with the CMV-luc reporter and *HER-2/neu** or *HER-2/neu** plus DN-Akt or PTEN and cultured the cells in the hormone-free medium with or without R1881 as described above. Importantly, *HER-2/neu** significantly increased survival (~30%) of LNCaP cells in the absence of R1881, whereas this enhancing effect by *HER-2/neu** was abolished by DN-Akt (Fig. 2*b*). These results suggest that *HER-2/neu* promotes prostate cancer cell survival upon androgen withdrawal through the Akt pathway. Furthermore, to examine whether *HER-2/neu* can stimulate prostate cancer cell proliferation during androgen withdrawal, we measured the DNA synthesis rate by the BrdUrd incorporation rate. We cotransfected LNCaP cells with a red fluorescent protein expression vector pDsRed1-C1 and *HER-2/neu** or an empty vector and cultured the cells in the hormone-free medium with or without R1881. In addition, one set of the *HER-2/neu**-transfected cells were treated with LY294002. Subsequently, the red fluorescence-positive cells were sorted, plated on slides by cytospin, and assayed for proliferation by BrdUrd incorporation. Significantly, *HER-2/neu** augmented the BrdUrd incorporation rate (*i.e.*, growth rate) of LNCaP cells ~2-fold (*Lane 3 versus Lane 1*) in the absence of R1881 and ~1.5-fold (*Lane 4 versus Lane 2*) in the presence of R1881 (Fig. 2*c*). Representative fluorescent pictures are shown (Fig. 2*d*). However, this growth-stimulatory effect of *HER-2/neu** was strongly blocked by LY294002 (Fig. 2*c*), confirming that activation of the androgen-independent growth by *HER-2/neu* requires a functional PI3-K/Akt pathway. Taken together, *HER-2/neu* promotes prostate cancer cell survival and growth upon androgen deprivation via the Akt pathway.

Because Akt can activate the AR pathway, we investigated whether the interactions between Akt and AR can occur *in vivo*. Whole-cell lysates of LNCaP cells were immunoprecipitated using an anti-AR mAb or mouse IgG, and the immunoprecipitated proteins were subjected to Western blotting using an antibody against phosphorylated Akt (p-Akt). Our results showed that p-Akt (activated Akt) was coimmunoprecipitated with an mAb against AR but not with the control IgG (Fig. 3*a*), suggesting that the endogenous AR is specifically associated with activated Akt *in vivo*. Comparison of the amino acid sequences of AR among human, rat, and mouse reveals two conserved putative consensus Akt phosphorylation sites, Ser-213 and Ser-791, based on the human sequence (Fig. 3*b*). Therefore, we examined which sites of the AR protein can interact with CA-Akt *in vitro*. We generated and purified GST-fusion proteins containing the NH_2-terminal half of AR (designated GST-AR-N) and the COOH-terminal portion of AR (designated GST-AR-C), where Ser-213 and Ser-791 residues reside in AR-N and AR-C, respectively. Whole-cell lysates of HA-CA-Akt transfected 293T cells were incubated with glutathione-Sepharose preloaded with either GST-AR-N or GST-AR-C or GST protein. The bound proteins were eluted and immunoblotted with an anti-HA mAb. Specific M_r 62,000 HA-Akt proteins were detected in the GST-AR-N- and GST-AR-C-bound fractions as

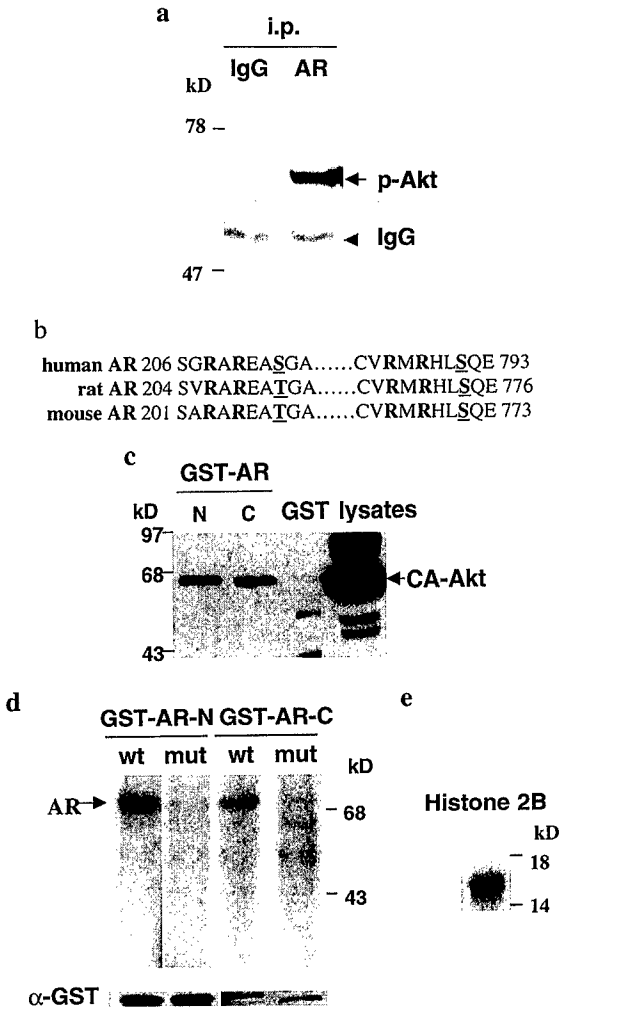

Fig. 3. Activated Akt is associated with AR *in vivo* and *in vitro* and specifically phosphorylates Ser-213 and Ser-791 of AR *in vitro*. *a*, the endogenous AR in LNCaP cell lysate was immunoprecipitated with an anti-AR mAb or a control mouse IgG and then analyzed by Western blot using an anti-p-Akt antibody. *b*, two consensus Akt phosphorylation sites (RXRXXS/T) are conserved among human, rat, and mouse AR amino acid sequences. The Ser-213 and Ser-791 residues are located within the NH_2-terminal half and the COOH-terminal domain of human AR, respectively. *c*, pull-down (*in vitro*) assays of HA-CA-Akt with GST-AR-N or GST-AR-C. 293T cells were transfected with the HA-tagged CA-Akt expression plasmid, the cells were harvested, and whole-cell lysates were prepared 48 h after transfection. Whole-cell lysates were incubated with each GST-fusion protein or GST and glutathione-Sepharose, washed, and total bound fractions were analyzed by SDS-PAGE, followed by Western blotting with an anti-HA monoclonal antibody. As a positive control, the HA-CA-Akt-transfected cell lysate was included in the Western blot analysis. *d*, 293T cells were transfected with the HA-CA-Akt expression plasmid, the cells were harvested, and whole-cell lysates were prepared 48 h after transfection. After immunoprecipitation with an anti-HA mAb, phosphorylation of AR was determined by an immunocomplex kinase assay, using wt or mut GST-AR-N and GST-AR-C as substrates. As a control for substrates, an equal amount of each GST-fusion protein (50 μg) was subjected to SDS-PAGE (10%), transferred to a nitrocellulose membrane, and analyzed by Western blot using an anti-GST antibody (*bottom panel*). *e*, as a kinase control for Akt, the same immunocomplex kinase assay was performed as described above using histone 2B as a substrate.

well as in the total lysates (positive control) but not in the GST (negative control) bound fractions (Fig. 3*c*). These results suggest that both domains (Akt phosphorylation sites) of the AR protein are specifically associated with CA-Akt protein *in vitro*. Furthermore, we determined whether these two Akt target sites can be phosphorylated by CA-Akt, using immunocomplex kinase assays. To test the specificities of Akt phosphorylation, these two Ser-213 and Ser-791 residues within GST-AR-N and GST-AR-C were mutated to Ala residues, designated GST-AR-N/mut and GST-AR-C/mut, respectively. To produce CA-Akt, 293T cells were transiently transfected with HA-

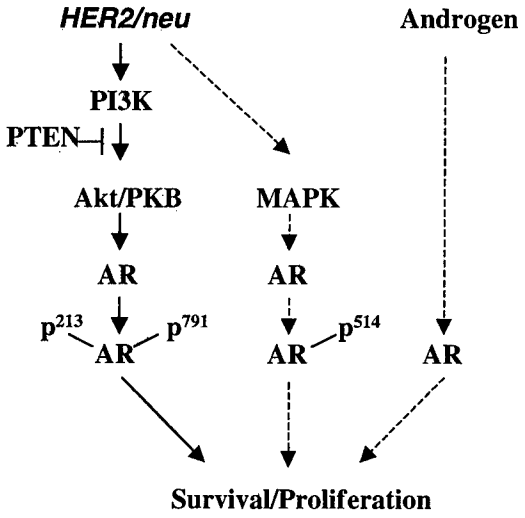

Fig. 4. A model of *HER-2/neu* activation of the Akt-AR pathway that promotes survival and proliferation of androgen-dependent prostate cancer cells upon androgen deprivation.

CA-Akt. Whole-cell lysates of the transfected cells were immunoprecipitated using an anti-HA mAb, and the immunoprecipitated proteins were subjected to immunocomplex kinase assays using GST-AR-N (wt or mut) and GST-AR-C (wt or mut) as substrates. Phosphorylation of GST-AR-N/wt and GST-AR-C/wt was readily detected, whereas phosphorylation of GST-AR-N/mut and GST-AR-C/mut was not detectable (Fig. 3*d*), suggesting that Ser-213 and Ser-791 were specifically phosphorylated by CA-Akt. As a positive control, the same immunoprecipitated proteins were subjected to an immunocomplex kinase assay using histone 2B as a substrate (Fig. 3*e*). As shown in Fig. 4, a model is depicted to illustrate the proposed parallel cell survival and proliferation pathways induced by *HER-2/neu* via the Akt pathway from the current study or the MAP kinase pathway as well reported previously (4, 5). To our knowledge, this is the first evidence that *HER-2/neu* activates AR via the Akt pathway and may provide an interpretation of how *HER-2/neu* can restore AR signaling to prostate cancer cells during androgen ablation. The effect of Ser-213 and Ser-791 mutants on AR function and response to *HER-2/neu*-Akt activation deserves further investigation and may open an alternative avenue for understanding the molecular mechanism of the androgen-independent survival and growth of prostate cancer cells. It may lead to a new direction for developing novel anticancer therapies for the androgen-refractory prostate cancers.

References

1. Schulze, H., Isaacs, J., and Senge, T. Inability of complete androgen blockade to increase survival of patients with advanced prostatic cancer as compared to standard hormonal therapy. J. Urol., *137:* 909–911, 1987.
2. Taplin, M. E., Bubley, G. J., Shuster, T. D., Frantz, M. E., Spooner, A. E., Ogata, G. K., Keer, H. N., and Balk, S. P. Mutation of the androgen-receptor gene in metastatic androgen-independent prostate cancer. N. Engl. J. Med., *332:* 1393–1398, 1995.
3. Tilley, W. D., Buchanan, G., Hickey, T. E., and Bentel, J. M. Mutations in the androgen receptor gene are associated with progression of human prostate cancer to androgen independence. Clin. Cancer Res., *2:* 277–285, 1996.
4. Abreu-Martin, M. T., Chari, A., Palladino, A. A., Craft, N. A., and Sawyers, C. L. Mitogen-activated protein kinase kinase kinase 1 activates androgen receptor-dependent transcription and apoptosis in prostate cancer. Mol. Cell. Biol., *19:* 5143–5154, 1999.
5. Yeh, S., Lin, H. K., Kang, H. Y., Thin, T. H., Lin, M. F., and Chang, C. From HER2/Neu signal cascade to androgen receptor and its coactivators: a novel pathway by induction of androgen target genes through MAP kinase in prostate cancer cells. Proc. Natl. Acad. Sci. USA, *96:* 5458–5463, 1999.
6. Craft, N., Shostak, Y., Carey, M., and Sawyers, C. L. A mechanism for hormone-independent prostate cancer through modulation of androgen receptor signaling by the HER-2/neu tyrosine kinase. Nat. Med., *5:* 280–285, 1999.
7. Slamon, D. J., Clark, G. M., Wong, S. G., Levin, W. J., Ullrich, A., and McGuire, W. L. Human breast cancer: correlation of relapse and survival with amplification of the *HER-2/neu* oncogene. Science (Washington DC), *235:* 177–182, 1987.
8. Hu, P., Margolis, B., Skolnik, E. Y., Lammers, R., Ullrich, A., and Schlessinger, J. Interaction of phosphatidylinositol 3-kinase-associated p85 with epidermal growth factor and platelet-derived growth factor receptors. Mol. Cell. Biol., *12:* 981–990, 1992.
9. Zhou, B. P., Hu, M. C., Miller, S. A., Yu, Z., Xia, W., Lin, S. Y., and Hung, M. C. HER-2/neu blocks tumor necrosis factor-induced apoptosis via the Akt/NF-κB pathway. J. Biol. Chem., *275:* 8027–8031, 2000.
10. Kandel, E. S., and Hay, N. The regulation and activities of the multifunctional serine/threonine kinase Akt/PKB. Exp. Cell Res., *253:* 210–229, 1999.
11. del Peso, L., Gonzalez-Garcia, M., Page, C., Herrera, R., and Nunez, G. Interleukin-3-induced phosphorylation of BAD through the protein kinase Akt. Science (Washington DC), *278:* 687–689, 1997.
12. Cardone, M. H., Roy, N., Stennicke, H. R., Salvesen, G. S., Franke, T. F., Stanbridge, E., Frisch, S., and Reed, J. C. Regulation of cell death protease caspase-9 by phosphorylation. Science (Washington DC), *282:* 1318–1321, 1998.
13. Brunet, A., Bonni, A., Zigmond, M. J., Lin, M. Z., Juo, P., Hu, L. S., Anderson, M. J., Arden, K. C., Blenis, J., and Greenberg, M. E. Akt promotes cell survival by phosphorylating and inhibiting a Forkhead transcription factor. Cell, *96:* 857–868, 1999.
14. Jenster, G., Spencer, T. E., Burcin, M. M., Tsai, S. Y., Tsai, M. J., and O'Malley, B. W. Steroid receptor induction of gene transcription: a two-step model. Proc. Natl. Acad. Sci. USA, *94:* 7879–7884, 1997.
15. Shao, R., Hu, M. C-T., Zhou, B. P., Lin, S-Y., Chaio, P. J., von Lindern, R. H., Spohn, B., and Hung, M-C. E1A sensitizes cells to tumor necrosis factor-induced apoptosis through inhibition of IκB kinases and nuclear factor κB activities. J. Biol. Chem., *274:* 21495–21498, 1999.
16. Schuur, E. R., Henderson, G. A., Kmetec, L. A., Miller, J. D., Lamparski, H. G., and Henderson, D. R. Prostate-specific antigen expression is regulated by an upstream enhancer. J. Biol. Chem., *271:* 7043–7051, 1996.
17. Cleutjens, K. B., van Eekelen, C. C., van der Korput, H. A., Brinkmann, A. O., and Trapman, J. Two androgen response regions cooperate in steroid hormone regulated activity of the prostate-specific antigen promoter. J. Biol. Chem., *271:* 6379–6388, 1996.
18. Di Cristofano, A., and Pandolfi, P. P. The multiple roles of PTEN in tumor suppression. Cell, *100:* 387–390, 2000.
19. Coombe, D. R., Nakhoul, A. M., Stevenson, S. M., Peroni, S. E., and Sanderson, C. J. Expressed luciferase viability assay (ELVA) for the measurement of cell growth and viability. J. Immunol. Methods, *215:* 145–150, 1998.
20. Cree, I. A. Luminescence-based cell viability testing. Methods Mol. Biol., *102:* 169–177, 1998.

p202, an Interferon-Inducible Protein, Mediates Multiple Anti-Tumor Activities in Human Pancreatic Cancer Xenograft Models[1]

Yong Wen[2], Duen-Hwa Yan[2], Bailiang Wang, Bill Sphon, Yi Ding, Ruping Shao, Yiyu Zou, Keping Xie, and Mien-Chie Hung[3]

Departments of Molecular and Cellular Oncology [Y.W., D.-H.Y., B.S., Y.D., R.S., Y.Z., M.-C.H.], Surgical Oncology [D.-H.Y., M.-C.H.], Gastrointestinal Medical Oncology [B.W., K.X.], The University of Texas, M. D. Anderson Cancer Center, 1515 Holcombe Blvd. Houston, Texas 77030

[1]Funded by grants from the NIH (CA77858) and Department of Defense (DAMD17-00-1-0312) (to M.-C.H.), from the University Cancer Foundation at the University of Texas M. D. Anderson Cancer Center and Texas Advanced Technology Program under Grant No. 003657-0082-1999 (to D.-H.Y.), from the American Cancer Society (RPG-00-054-01-CMS) (to K.X.), and from Cancer Center Core grant 16672.

[2]These authors contributed equally to this work.

[3] To whom requests for reprints should be addressed, at Department of Molecular and Cellular Oncology, The University of Texas, M. D. Anderson Cancer Center, 1515 Holcombe Blvd. Houston, Texas 77030. Phone: (713) 792-3668; Fax: 713-794-0209; E-mail: mchung@mdanderson.org

Running Title: The anti-tumor activities of p202 in pancreatic cancer

Key words: p202, tumorigenecity, metastasis, angiogenesis, gene therapy

Abstract

p202, an interferon-inducible protein, interacts with certain transcriptional activators leading to transcriptional repression. p202 expression has been associated with inhibition of cancer cell growth *in vitro* and *in vivo*. To examine a potential p202-mediated anti-tumor activity in pancreatic cancer, we used both ectopic and orthotopic xenograft models and demonstrated that p202 expression is associated with multiple anti-tumor activities that include inhibition of tumor growth, reduced tumorigenecity, prolonged survival, and remarkably, suppression of metastasis and angiogenesis. *In vitro* invasion assay also showed that p202-expressing pancreatic cancer cells are less invasive than those without p202 expression. That observation was supported by the findings that p202-expressing tumors showed reduced expression of angiogenic markers such as IL-8, and VEGF, and p202-expressing pancreatic cancer cells have reduced level of MMP-2 activity, a secreted protease activity important for metastasis. Importantly, we demonstrated a treatment efficacy by using p202/SN2 liposome complex in a nude mice xenograft model, suggesting a feasibility of using p202/SN2 liposome in future pre-clinical gene therapy experiments. Together, our results strongly suggest that p202 expression mediates multiple anti-tumor activities against pancreatic cancer, and that may provide a scientific basis for developing a p202-based gene therapy in pancreatic cancer treatment.

Introduction

Pancreatic cancer is highly aggressive and is a leading cause of cancer death in the western countries. The deadliness of this disease is illustrated by the prediction in 1999 that 28,600 new cases would be diagnosed and most of them would be fatal (1). The main reason for the extremely poor prognosis is the fact that patients often present with advanced stage at the time of diagnosis. The median survival varies between 4-6 months and the five-year survival rate is less than 2% (2). Currently, there is no effective treatment for this deadly disease since conventional chemotherapy and radiation treatments have had very limited success to improve patient survival (3). Therefore, novel treatment strategies against this disease are urgently needed.

p202 is an interferon-inducible protein and its expression is associated with growth inhibition (4, 5). The findings that p202 interacts with cell-cycle transcriptional regulators such as E2F-1/DP-1, E2F-4/DP-1, AP-1 (c-Fos/c-Jun), and c-Myc, and represses their transcriptional activities have provided insight into the molecular mechanism by which p202 mediates growth inhibition (6-10). We have previously documented that p202 inhibits human cancer cell growth *in vitro* and suppresses tumor growth *in vivo* (11, 12). Furthermore, we showed that p202 expression sensitizes breast cancer cells to TNF-α-induced apoptosis. The mechanism responsible for the p202-mediated sensitization is likely due to the inactivation of TNF-α-induced NF-κB by p202 (12). In light of the anti-apoptotic role of NF-κB in TNF-α-mediated apoptosis (13), we have hypothesized that NF-κB inactivation by p202 leads to the abolishment of the anti-apoptotic process and results in sensitizing cancer cells to TNF-α-induced apoptosis. On

the other hand, the aberrant NF-κB activity has been implicated, at least in part, in tumorigenesis and chemo-resistant phenotype of certain human cancers including pancreatic cancer (14, 15). Thus, it is likely that p202-based gene therapy may be particularly useful in targeting tumors that contain such aberrant NF-κB activity. In this study, we tested that possibility in pancreatic cancer cells that possess the constitutively active NF-κB (16). We showed that, in addition to the growth inhibition *in vitro* and tumor suppression *in vivo*, p202 expression was found associated with suppression of metastasis and angiogenesis in orthotopic pancreatic cancer xenogrft model. Importantly, we demonstrated a treatment efficacy of using p202/liposome gene therapy in a pancreatic cancer xenograft model. Together, our results raise a possibility of using p202-based gene therapy strategy in pancreatic cancer treatment.

Materials and Methods

Cell Culture. Human pancreatic cancer cell lines Capan-1, PANC-1, BxPC-3, AsPC-1, and CFPAC-1 were obtained from the American Type Culture Collection (ATCC) and maintained as recommended. Transfected cell lines were maintained in complete medium containing 500 μg/ml G418 (Life Technologies, Inc.).

Colony-forming Assay. Cells were transfected with a p202 expression vector (CMV-p202) (in which p202 cDNA is driven by CMV promoter), or an control vector (pcDNA3). Both plasmids contain neomycin resistant gene. Three weeks after

transfection and G418 selection, cell colonies were stained by 0.5% crystal violet containing 20% ethanol.

Western Blot Analysis. Protein lysate was prepared with RIPA-B cell lysis buffer containing 20 mM Na_2PO_4 (pH 7.4), 150 mM NaCl, 1% Triton X-100, 100 mM NaF, 2 mM Na_3VO_4, 5 mM PMSF, 1% aprotinin, and 10 μg/ml leupeptin. Rabbit anti-p202 polyclonal antibody was kindly provided by Dr. Divaker Choubey (Loyola University, Chicago). Donkey anti-rabbit IgG peroxidase (Jackson) was used as secondary antibody. Western blots were developed by enhanced chemiluminescence (ECL) (Amersham).

Northern Blot Analysis. Total RNA was isolated from PANC-1, pcDNA3, p202-1, and p202-2 cells using a TRIZOL RNA isolation kit (GIBCO BRL). Twenty micrograms of total RNA were separated by electrophoresis under denaturing conditions and then transferred to a Hybond N^+ membrane. Full-length p202 cDNA isolated from CMV-p202 plasmid by BamH1 digest was gel-purified and ^{32}P-labeled by using a random-labeling kit. Hybridization was performed at 65°C overnight in solution containing 1% BSA (W/V), 0.2 M sodium phosphate, 1 mM EDTA, 7% SDS (W/V), 15% formamide and 40 μg/ml salmon testes DNA (Sigma). The blot was subsequently washed three times in 40 mM sodium phosphate, 1 mM EDTA, 1% SDS (W/V) at 65°C for 5 min per wash, and twice at 70°C for 10 min per wash. The p202 RNA (1.8 kb) was visualized by using a PhosphoImager.

Transfection and Luciferase Assays. PANC-1, pcDNA3, and p202-1, and p202-2 cells were transfected with the 0.5 μg of κB-luc construct and 0.1 μg of the internal transfection control (pRL-TK, Promega). Forty-eight hours after transfection, cells were harvested and luciferase activity was measured using the dual luciferase assay system (Promega) according to the protocol supplied by the manufacture. The κB-luc activity was normalized by the internal control luciferase activity of pRL-TK. To determine the p202 dose effect, PANC-1 cells were co-transfected with 50 ng of CMV-luc and increasing amount (0, 0.5, or 2 μg) of CMV-p202. The total amount of DNA transfected at each p202 dose was kept constant (2.05 μg) by adding an appropriate amount of pcDNA3 vector. Luciferase activity was measured 48 h after transfection. The relative activities were calculated by setting the luciferase activities obtained from transfections without CMV-p202 (0 μg) at 100%. The data represent mean ± S.D. of two independent experiments.

Soft Agar Assay. Aliquots of cells (1×10^4) were mixed at 37°C with 0.5% agarose (sea plaque, low gelling temperature, FMC Bioproducts, Rockland, ME) in complete medium and gelled at 4°C for 15 min over a previously gelled layer of 1% agarose in complete medium in six-well dishes. After incubation for 3 weeks, 200 μl of 1 mg/ml p-iodonitrotetrazolium violet was added and incubated for additional 24 h. Colonies were photographed using a Zeiss microscope and counted using computer software associated with the microscope.

Ectopic Tumorigenicity Assays in Nude Mice. Aliquots of cells (1 x 10^6) in 200 μl of PBS were injected subcutaneously on both sides of the abdomen of 4-5-week old female nude mice. Tumor sizes were measured with a caliper every week. The tumor volume was calculated using the formula: Vol. = S×S×L/2, where S = the short length of the tumor in cm, and L = the long length of the tumor in cm.

Orthotopic Tumorigenicity and Survival Assays in Nude Mice. Aliquots of cells (1 x 10^6) were suspended in 50 μl of PBS as single-cell suspensions. Nude mice were anesthetized with methoxyflurane and placed in the supine position. An upper midline abdomen incision was made, and the pancreas was exteriorized. Tumor cells were injected into the tail of the pancreas and the abdomen was closed using wound clip. Animals were sacrificed 3 months after tumor inoculation. Tumors in the pancreas were harvested and weighed. Livers were fixed in Bouin's solution for 24 h to differentiate the neoplastic lesions from the organ parenchyma, and the metastases on the surface of liver were counted with the aid of a dissecting microscope. For survival assays, daily survival of mice was monitored and recorded as dead or euthanized when the animals reached the moribund stage.

***In Vitro* Invasion Assay.** The procedure was followed as described previously (17), except for the following modification: the 24-well chamber with an 8-μm pore size polycarbonate filter (Costar Co., Cambridge, MA) was coated with Matrigel (Bacton Dickenson Labware, Bedford, MA) according to the manufacture protocol.

Zymography. Cells were grown to 70% confluency in DMEM/F12 media containing 10% FBS and switched to serum free media (17). After two days of incubation, the conditioned media was collected, passed through a 0.22 μm filter, and then concentrated to a small volume on Centricon YM 30 filter units. Four micrograms of each sample was loaded on the gel. For the positive control, 0.25 μl of fetal calf serum was used. Zymography was performed using gelatin-embedded SDS gels as previously described (17).

Immunohistochemistry. Tumor tissue sections (5 μm thick) of the formalin-fixed, paraffin-embedded specimens were deparaffinized in xylene and rehydrated in graded alcohol. The endogenous peroxidase was blocked by the use of 3% hydrogen peroxide in PBS for 12 min. The samples were incubated for 20 min at room temperature with a protein blocking solution containing 5% normal horse serum and 1% normal goat serum and in PBS. Samples were then incubated at 4 °C in a 1:50 dilution of rabbit polyclonal anti-IL-8 antibody (Biosource International, Camarillo, CA), or 1:50 dilution of rabbit anti-VEGF antibody, followed by the incubation with peroxidase-conjugated anti-rabbit IgG at room temperature for 1 h, and with diaminobenzidene (Research Genetics) for 5 min. The sections were counter-stained with Mayer's hematoxylin (Biogenex Laboratories, San Ramon, CA) and mounted with a Universal mount (Research Genetics). Examined under a microscope, a positive reaction was indicated by a reddish-brown precipitate in the cytoplasm or the nucleus. Tissue sections vessels in solid tumors growing in the pancreas of nude mice were determined under light microscope after immune staining of sections with anti-CD31 antibodies. Cryostat sections of tumors

were fixed with 2% paraformaldehyde in PBS (pH 7.5) for 10 min at room temperature and processed for immunostaining as described above for paraffin embedded tissues.

p202 Gene Therapy Treatment in Human Pancreatic Cancer Xenograft Model. Aliquots of PANC-1 cells (1 x 10^6) in 200 μl of PBS were injected (per site) subcutaneously on both sides of the abdomen of 4-5-week old female nude mice. After tumors reached 5 mm in diameter, mice received treatment with p202/SN2 complex through intratumor injection. For each injection, 15 μg of CMV-p202 or the control vector, i.e., a luciferase cDNA driven by a CMV promoter (CMV-luc), was complexed with 30 μg of SN2. CMV-p202/SN2 complex was administrated twice a week. Mice in the control group were injected with either CMV-luc/SN2 complex or SN2 alone. Tumor size and treatment related side effect were monitored twice a week. SN2 is a liposome-based non-viral delivery system developed recently by our group (Zou and Hung, unpublished results).

Results

p202 expression inhibits human pancreatic cancer cell growth *in vitro*. To determine the growth inhibitory activity of p202 in human pancreatic cancer cells, we performed a colony-forming assay on five human pancreatic cancer cell lines, i.e., Capan-1, PANC-1, BxPC-3, AsPC-1, and CFPAC-1. (All of them are known to possess the constitutively active NF-κB (16).) As shown in Table 1, with all cell lines tested, the number of G418-resistant colonies in the p202-transfected cells was consistently fewer than that of the

pcDNA3-transfected cells with a reduction ranged from 75% (BxPC-3) to 100% (CFPAC-1). This result suggests that p202 possesses a strong growth inhibitory activity in human pancreatic cancer cells. Consistent to that observation, our effort to isolate p202 stable pancreatic cancer cell lines has yielded only two p202-expressing PANC-1 clones (i.e., p202-1 and p202-2) out of twenty G418-resistant clones screened by western analysis. p202-1 expresses a higher level of p202 protein than p202-2 (Fig. 1*a*), and that correlates well with the levels of p202 mRNA expression of these clones as determined by a northern blot analysis (Fig. 1*b*). To test if p202 expression inhibits NF-κB activity in the p202-expressing cells (12), we perform a gel-shift assay and found that the p202 expression level in p202-1 and p202-2 cells is efficient to abolish the DNA binding activity of NF-κB (data not shown). The reduced NF-κB DNA binding activity in p202-expressing cells was further confirmed by the reduced NF-κB-mediated promoter activity in p202-1 and p202-2 cells as compared with that in the control cells (pcDNA3) (Fig. 1*c*). As shown in Fig. 2*a*, the growth rate of p202-1 cells is the slowest as compared with that of PANC-1, vector control (pcDNA3), and the low p202 expressor, p202-2, cells. The different levels of p202 expression may account for the different growth rates seen between p202-1 and p202-2 cells. This result is consistent to our previous observation that the extent of growth inhibition is p202 dose dependent (11). To further confirm that observation, we performed a transient transfection assay in which a fixed amount (50 ng) of CMV-luc was co-transfected with increasing amount (0, 0.5, and 2 μg) of CMV-p202 in PANC-1 cells. Since the apparent luciferase activity is indicative of living cells, we showed that p202 expression caused overall growth inhibition in a dose-dependent manner (Fig. 2*b*). Under the same condition, no apparent apoptosis was observed as

determined by flow cytometry analysis to detect sub-G1 apoptotic cells (data not shown). Thus, our results support the idea that the level of p202 expression is proportional to its growth inhibitory activity. Consistent to the ability of p202 to suppress transformation phenotype (11, 12), both p202-1 and p202-2 cells showed a significant reduction in the number of soft-agar colonies as compared with that of the control cell lines, i.e., PANC-1 and pcDNA3 (Fig. 2*c*). Our results thus indicate that p202 is a potent growth inhibitor in suppressing pancreatic cancer cell growth.

p202 expression suppresses tumorigenicity in ectopic and orthotopic pancreatic cancer xenograft models. To determine if p202 expression could mediate an anti-tumor effect on pancreatic cancer cells *in vivo*, we first examined if p202 suppresses the tumorigenicity of PANC-1 cells. p202-1 and p202-2 cells were subcutaneously (s.c.) injected into nude mice and tumor growth was monitored thereafter. As shown in Fig. 3*a*, p202-1 tumors grew significantly slower than the vector-transfected PANC-1 tumors. p202-2 tumors (which express less p202 than p202-1 tumors) on the other hand started to show a modest growth reduction 12 weeks after injection as compared with that of the control tumors. Like in p202-mediated growth inhibition, the extent of anti-tumor activity observed here appears to be dependent on the level of p202 expression. To further examine the p202-mediated anti-tumor activity in an organ (pancreas)-specific environment, we injected p202-1 and p202-2 cells directly into mouse pancreas. Three months after injection, mice were sacrificed and tumor growth was measured. We found that, while PANC-1 tumors and vector control tumors grew readily in mouse pancreas at 100% frequency (5/5), p202-1 and p202-2 cells are tumorigenic at a much lower

frequency, i.e., 20% (1/5) and 40% (2/5), respectively (Table 2). Furthermore, the average tumor size (measured by weight) of the control tumors was about five times that of p202-1 or p202-2 tumors. When the survival rate was measured, we observed that mice bearing p202 tumors had a longer survival than those bearing control tumors without p202 expression (Fig. 3*b*). In particular, mice bearing p202-1 or p202-2 tumors had 50% survival at 90 days after implantation as opposed to the mice bearing either PANC-1 or vector control tumors that showed 0% survival at the same time. Our results clearly demonstrated a potent anti-tumor activity of p202 in orthotopic pancreatic cancer xenograft models, but to a less extent in the ectopic environment.

p202 expression suppresses metastasis in pancreatic tumors. Upon examining the orthotopic pancreatic tumor xenograft model, we observed liver metastasis in 40% (2/5) and 20% (1/5) of mice bearing either PANC-1 tumors or vector control tumors, respectively. In contrast, we found no detectable liver metastasis in mice bearing p202 tumors (Table 2). This result suggests a possible anti-metastasis function of p202 in pancreatic cancer cells. To test that possibility *in vitro*, we employed a double-chamber assay (17) in which the test cells were grown in the top chamber, and the bottom chamber was filled with conditioned media containing chemo-attractant, e.g., laminin. A Matrigel coated membrane was used to separate the two chambers. To migrate from the top chamber to the bottom chamber, cells must digest away the reconstituted basement membrane matrix by producing secretory proteases such as matrix metalloproteinases (MMPs) and then penetrate through pores on the membrane. Thus, this assay somewhat mimics a typical metastatic process, and the number of cells found on the bottom side of

the membrane (which can be visualized by Giemsa staining, i.e., blue cells (Fig. 4*a*)) is indicative of the metastatic potential of the test cells. Based on this criteria, we found that p202-1 possesses the least metastatic potential among the cell lines tested (Fig. 4*b*). p202-2 and p202-pool cells (i.e., the pooled p202-transfected clones) have slightly lower metastatic potential than that of PANC-1 or vector control cells (Fig. 4*a* and 4*b*). Since MMP-2 (72 kD) is one of the important MMPs secreted by cancer cells during the metastatic process (18), we examined if MMP-2 expression is altered in p202-1 and p202-2 cells by employing a zymography to analyze the MMP-2 activity in each cultured medium. As shown in Fig. 4*c*, the level of MMP-2 secreted by p202-1 cells is greatly reduced, but PANC-1, vector control (pcDNA3-1 and -2), and p202-2 cells maintain a high level of secreted MMP-2. Although the MMP-2 level is not significantly reduced in p202-2 cells, it is likely that the low p202 expression level accounts for the difference in both the MMP-2 activity and the *in vitro* invasiveness between p202-1 and p202-2 cells. The MMP-2 activity in serum serves as a positive control. Together, our *in vivo* and *in vitro* results support the idea that p202 expression suppresses metastatic potential of pancreatic cancer cells.

p202 expression suppresses angiogenesis in pancreatic tumors. It has been well documented that tumor growth and metastasis require persistent growth of new blood vessel (neovasculature) (19). To examine if the reduced tumorigenecity of p202-expressing pancreatic cancer cells is associated with a reduced angiogenesis, we analyzed the formation of neovasculature in p202-1 tumors and Panc-1 tumors obtained from the orthotopic pancreatic cancer xenografts. Fig. 5 shows that the number of blood vessels

(stained by antibody against a blood vessel marker, i.e., CD31 (20)) was significantly reduced in p202-1 tumor as compared with PANC-1 tumor. Since the expression of angiogenic factors such as IL-8 and VEGF are critical for the onset of angiogenesis (19), we examined a possible correlation between the expression of these proteins and the reduced angiogenesis in p202-1 tumors. Using immunohistochemical analysis with antibody specific to IL-8 or VEGF, we showed that p202-1 tumor has much reduced IL-8 and VEGF protein staining (dark gray color) as compared with that of PANC-1 tumor (Fig. 5). These results strongly suggest that p202 expression in pancreatic tumors is associated with suppression of angiogenesis.

p202/liposome treatment suppresses tumor growth in a pancreatic cancer xenograft model. Based on the strong anti-tumor activity of p202 in human pancreatic cancer cells described above (Fig. 2 and Table 2), we tested a potential therapeutic effect of p202 gene therapy treatment in a s.c. pancreatic cancer model. Briefly, the mice bearing s.c. PANC-1 tumors were treated by intratumor injection of CMV-p202/SN2 complex twice a week for eight weeks. (SN2 is a lipid formula developed in our laboratory, and when complex with DNA, it enhances *in vivo* and *in vitro* transfection efficiency (Zhou and Hung, unpublished results)). The control groups consisted of tumor-bearing mice treated with SN2 alone (SN2) or CMV-luc/SN2 complex. As shown in Fig. 6, while there was no significant difference in tumor growth between SN2 and CMV-luc/SN2 complex treatment groups, the CMV-p202/SN2 treated tumors exhibited a slower growth rate than that of the control treatments. This proof-of-concept experiment clearly shows a

feasibility of using CMV-p202/SN2 complex to achieve a therapeutic effect on an ectopic pancreatic cancer xenograft model.

Discussion

In this report, we showed that p202 expression resulted in a growth inhibition of pancreatic cancer cells *in vitro* and *in vivo*. The enforced expression of p202 correlates well with the inactivation of the otherwise constitutively active NF-κB. This observation is significant because persistent NF-κB activity was associated with anti-apoptosis and chemo-resistance in human cancers (14, 15), and that sets the stage for us to test if p202 expression can sensitize these pancreatic cancer cells to chemotherapy treatment. To date, very few chemo-drugs are found beneficial in treating pancreatic cancer (3), and the constitutive activation of NF-κB is likely to contribute to such chemo-resistant phenotype. It is therefore possible that a p202-based gene therapy may restore chemo-sensitivity and leads to a potential p202/chemo-drug combined treatment for pancreatic cancer. Experiments are underway to test that hypothesis.

We observed a more pronounced p202-mediated anti-tumor activity (i.e., reduced tumor growth and prolonged survival) in orthotopic pancreatic cancer xenograft model than that in a s.c. ectopic xenograft model. Although the reason for the differential therapeutic effect remains unknown, it does indicate that orthotopic xenograft model is not only a more relevant but also a better model to evaluate future treatment efficacy of p202-based gene therapy than the s.c. ectopic model. We also observed a decreased vascularity

(CD31 staining) and a decreased level of angiogenic factors, e.g., IL-8 and VEGF, in p202-expressing tumors. Thus, our results suggest that p202 inhibits the expression of angiogenic factors and that in turn leads to suppression of angiogenesis. Remarkably, we observed that mice bearing p202-expressing tumors apparently lacked liver metastasis, and that correlates with a reduced invasiveness and a reduction in MMP-2 expression *in vitro*. Together, our data present the first evidence to suggest that p202 expression is associated with suppression of both angiogenesis and metastasis.

Finally, we showed a significant therapeutic effect using CMV-p202/SN2 treatment in, albeit, a s.c. pancreatic cancer xenograft model. It nevertheless implicates a feasibility of using a p202-based gene therapy treatment for pancreatic cancer. Given that the orthotopic model is a better system to study the efficacy of p202 anti-tumor activity as indicated in this report, it is possible that CMV-p202/SN2 treatment may yield even better anti-tumor activity in orthotopic xenograft model. A success of a p202-based gene therapy in orthotopic model will pave the way for future experiments to determine the efficacy p202/chemo-drug combined treatment in pre-clinical gene therapy settings.

References

1. Landis SH, M. T., Bolden S, Wingo PA. Cancer statistics, 1999., CA Cancer J Clin. *49:* 8-31, 1999.
2. Rosewicz S, W. B. Pancreatic carcinoma., Lancet. *349:* 485-489, 1997.

3. Staley, C. A., Lee, J. E., Cleary, K. R., Abbruzzese, J. L., Fenoglio, C. J., Rich, T. A., and Evans, D. B. Preoperative chemoradiation, pancreaticoduodenectomy, and intraoperative radiation therapy for adenocarcinoma of the pancreatic head, Am J Surg. *171:* 118-24; discussion 124-5., 1996.

4. Choubey D, L. P. Interferon action: cytoplasmic and nuclear localization of the interferon-inducible 52-kD protein that is encoded by the Ifi 200 gene from the gene 200 cluster., J Interferon Res. *13:* 43-52, 1993.

5. Choubey D, L. P. Binding of an interferon-inducible protein (p202) to the retinoblastoma protein., J Biol Chem. *270:* 6134-6140, 1995.

6. Choubey D, L. S., Datta B, Gutterman JU, Lengyel P. Inhibition of E2F-mediated transcription by p202., EMBO J. *15:* 5668-5678, 1996.

7. Choubey D, G. J. Inhibition of E2F-4/DP-1-stimulated transcription by p202., Oncogene. *15:* 291-301, 1997.

8. Datta B, M. W., Burma S, Lengyel P. Increase in p202 expression during skeletal muscle differentiation: inhibition of MyoD protein expression and activity by p202., Mol Cell Biol. *18:* 1074-1083, 1998.

9. Min, W., Ghosh, S., and Lengyel, P. The interferon-inducible p202 protein as a modulator of transcription: inhibition of NFκB, c-Fos, and c-Jun activities., Mol. Cell. Biol. *16:* 359-368, 1996.

10. Wang, H., Liu, C., Lu, Y., Chatterjee, G., Ma, X. Y., Eisenman, R. N., and Lengyel, P. The Interferon- and Differentiation-inducible p202a Protein Inhibits the Transcriptional Activity of c-Myc by Blocking Its Association with Max, J Biol Chem. *275:* 27377-27385, 2000.

11. Yan DH, W. Y., Spohn B, Choubey D, Gutterman JU, Hung MC. Reduced growth rate and transformation phenotype of the prostate cancer cells by an interferon-inducible protein, p202., Oncogene. *18:* 807-811, 1999.

12. Wen Y, Y. D., Spohn B, Deng J, Lin SY, Hung MC. Tumor suppression and sensitization to tumor necrosis factor alpha-induced apoptosis by an interferon-inducible protein, p202, in breast cancer cells., Cancer Res. *60:* 42-46, 2000.

13. Barkett, M. and Gilmore, T. D. Control of apoptosis by Rel/NF-kappaB transcription factors, Oncogene. *18:* 6910-24., 1999.

14. Rayet, B. and Gelinas, C. Aberrant rel/nfkb genes and activity in human cancer, Oncogene. *18:* 6938-47, 1999.

15. Mayo, M. W. and Baldwin, A. S. The transcription factor NF-kappaB: control of oncogenesis and cancer therapy resistance, Biochim Biophys Acta. *1470:* M55-62., 2000.

16. Wang, W., Abbruzzese, J. L., Evans, D. B., Larry, L., Cleary, K. R., and Chiao, P. J. The nuclear factor-kappa B RelA transcription factor is constitutively activated in human pancreatic adenocarcinoma cells, Clin Cancer Res. *5:* 119-27, 1999.

17. Yu, D., Wang, S. S., Dulski, K. M., Tsai, C. M., Nicolson, G. L., and Hung, M. C. c-erbB-2/neu overexpression enhances metastatic potential of human lung cancer cells by induction of metastasis-associated properties, Cancer Res. *54:* 3260-6, 1994.

18. Ellerbroek, S. M. and Stack, M. S. Membrane associated matrix metalloproteinases in metastasis, Bioessays. *21:* 940-9, 1999.

19. Hanahan, D. and Folkman, J. Patterns and emerging mechanisms of the angiogenic switch during tumorigenesis, Cell. *86:* 353-64, 1996.

20. DeLisser, H. M., Newman, P. J., and Albelda, S. M. Platelet endothelial cell adhesion molecule (CD31), Curr Top Microbiol Immunol. *184:* 37-45, 1993.

Figure Legends

Fig. 1. Generation of the p202-expression PANC-1 cells. *a*, Two p202-expressing PANC-1 cell lines (p202-1 and p202-2) were generated and the p202 protein (52 kD) expression was analyzed by western blot using p202-specific antibody. The 68 kD non-specific band serves as an internal loading control. The positive control is AKR-2B cells stimulated by IFN-α (Control) and the vector (pcDNA3)-transfected cells serve as negative control. *b*, p202 mRNA expression in p202-1 and p202-2 cells. Twenty micrograms of total RNA isolated from PANC-1, pcDNA3, p202-1, and p202-2 cells were analyzed by northern blot using a full-length p202 cDNA as a probe. The p202-specific RNA (1.8 kb) is indicated. As internal loading controls, 18S and 28S rRNAs on the membrane after gel transfer were stained by ethidium bromide. *c*, p202 expression inhibits the NF-κB-mediated transcription. A luciferase gene driven by IκB promoter (κB-luc) was transfected into p202-1, p202-2, and vector control (pcDNA3) cells followed by luciferase assay. The relative luciferase activity is shown with that in pcDNA3 cells set at 100%.

Fig. 2. The p202-expressing PANC-1 cells exhibit a reduced growth *in vitro*. *a*, The growth rate of PANC-1 (parental), pcDNA3, p202-1, and p202-2 cells was measured by MTT assay. Each measurement was done in quadruplicates. *b*, The p202 dose effect on growth inhibition. PANC-1 cells were co-transfected with 50 ng of CMV-luc and increasing amount (0, 0.5, or 2 μg) of CMV-p202. The relative activities were calculated by setting the luciferase activities obtained from transfections without CMV-p202 (0 μg) at 100%. The data represent mean ± S.D. of two independent experiments. *c*, PANC-1,

pcDNA3, p202-1, and p202-2 cells were grown in soft agar. The colony number was scored three weeks after seeding by p-iodonitrotetrazolium violet staining. The relative number is presented using that of the parental cells as 100%.

Fig. 3. p202 expression mediates anti-tumor activity *in vivo*. *a*, Tumorigenicity assay. PANC-1 (control), p202-1, and p202-2 cells were subcutaneously implanted in the abdomen of 4-5-week old female nude mice (five mice per group). Tumor sizes were measured with a caliper every week. The tumor volume was calculated using the formula: Vol. = S×S×L/2, where S = the short length of the tumor in cm, and L = the long length of the tumor in cm. *b*, Mice bearing p202-expressing PANC-1 tumors in pancreas exhibited a longer survival rate. PANC-1, pcDNA-3, p202-1, and p202-2 cells were injected orthotopically into mouse pancreases. Time of death was recorded and the survival rate is calculated as the percentage of the survived animals (the starting animal number is set at 100%).

Fig. 4. p202 expression inhibits cell invasion *in vitro*. Cells were tested for their invasiveness by using a double-chamber assay in which a Matrigel coated membrane was used to separate two chambers. PANC-1, pcDNA3, a pool of p202-transfected clones (p202-pool), p202-1, and p202-2 cells were seeded in the top chamber with lower chamber filled with laminin (30 μg/ml)-containing conditioned medium. Seventy-two hours after seeding, the migrated cells on the bottom side of the membrane were scored by Giemsa's stain as indicated by the blue cells (*a*), and the quantification of the migrated cells is shown in (*b*). *c*, p202 expression is associated with a reduced level of secretory

MMP-2 in the medium. Cells (PANC-1, two vector-transfected cell lines (pcDNA3-1 and -2), p202-1, and p202-2) were grown in the serum-free medium. The secreted MMP-2 activity was assayed by a zymography. After 24 h incubation, the conditioned media were harvested and concentrated before subject to SDS-PAGE in which the gel was imbedded with 1.5% gelatin. The MMP-2 activity in serum serves as a positive control.

Fig. 5. p202 expression is associated with reduced angiogenesis and down-regulation of IL-8 and VEGF. PANC-1 and p202-1 tumors excised from the pancreas of the orthotopic xenografts were analyzed by immunohistochemical staining for vascularity (CD31 staining) and IL-8 and VEGF protein expression.

Fig. 6. Anti-tumor effect of p202/SN2 complex by intratumoral injection in a s.c. xenograft model. Tumors were produced by subcutaneously implanting PANC-1 cells into both flanks of each nude mouse. Tumor-bearing mice were divided into three treatment groups (five mice per group and two tumors per mouse): SN2 liposome alone (SN2), CMV-luc/SN2, and CMV-p202/SN2. SN2 (30 μg) with or without DNA (15 μg) in 100 μl PBS was injected twice a week into each tumor. Tumors were measured twice a week after treatment began, and the average tumor volume per treatment group at the indicated time is presented.

Table 1. Number of Colonies From Transfection of Pancreatic Cell Lines with p202 and Control Vector DNA.

Cell Line	pcDNA3	p202	% of control
Capan-1	130	3	2.3
PANC-1	508	108	21.0
BxPC-3	4	1	25.0
AsPC-1	232	31	13.4
CFPAC-1	6	0	0

a

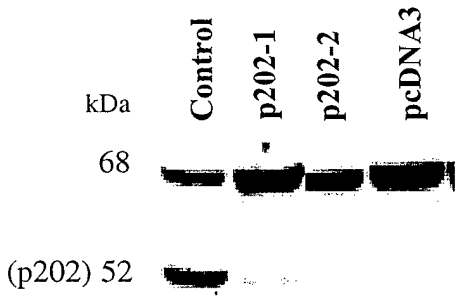
kDa
Control
p202-1
p202-2
pcDNA3
68
(p202) 52

b

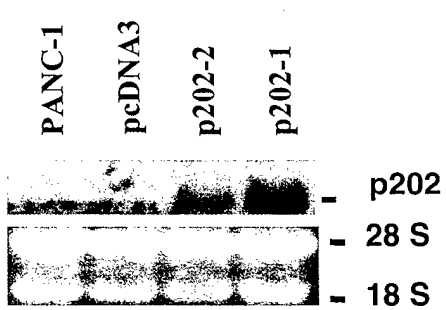
PANC-1
pcDNA3
p202-2
p202-1
p202
28 S
18 S

c

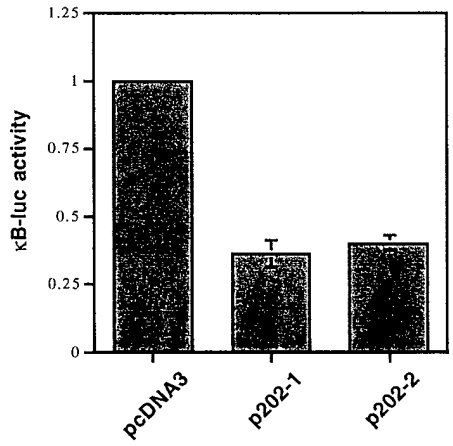
1.25
1
0.75
0.5
0.25
0
κB-luc activity
pcDNA3
p202-1
p202-2

a

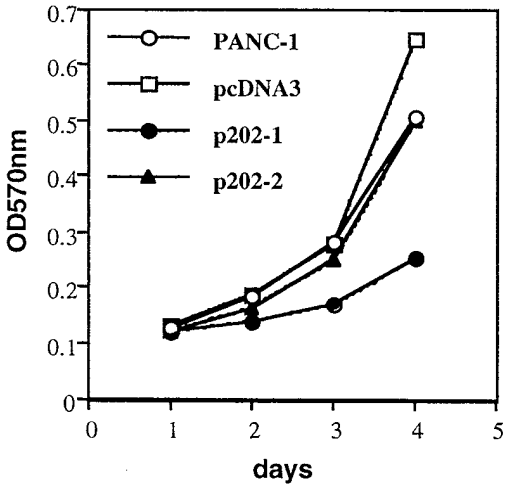
PANC-1
pcDNA3
p202-1
p202-2
OD570nm
days
0
0.1
0.2
0.3
0.4
0.5
0.6
0.7
0
1
2
3
4
5

b

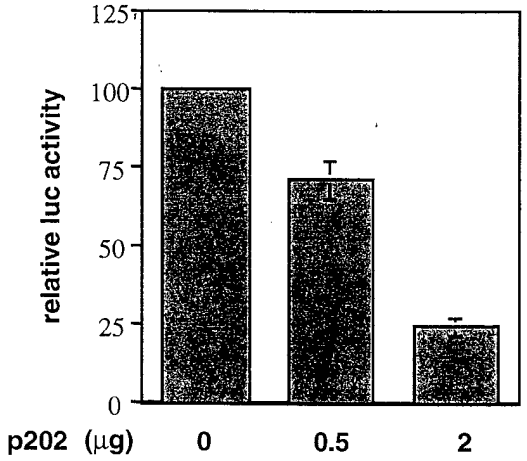
relative luc activity
125
100
75
50
25
0
p202 (μg)
0
0.5
2

c

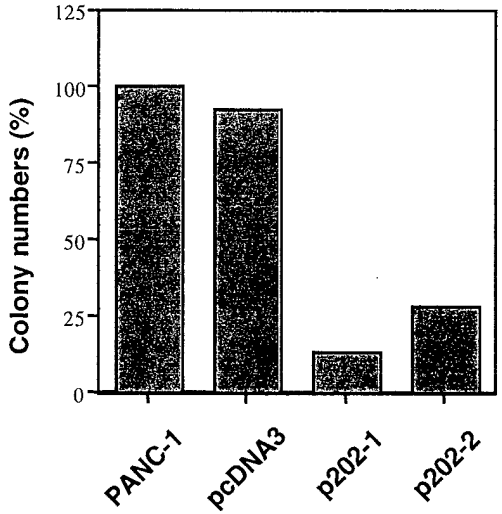
Colony numbers (%)
125
100
75
50
25
0
PANC-1
pcDNA3
p202-1
p202-2

a

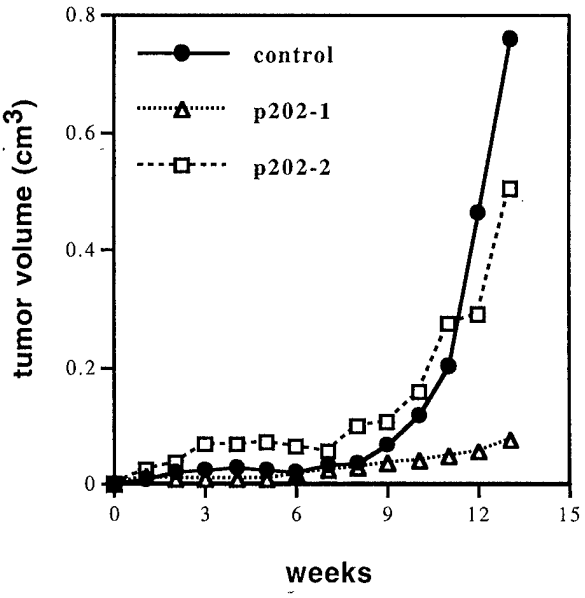
0.8
0.6
0.4
0.2
0
tumor volume (cm3)
control
p202-1
p202-2
0
3
6
9
12
15
weeks

b

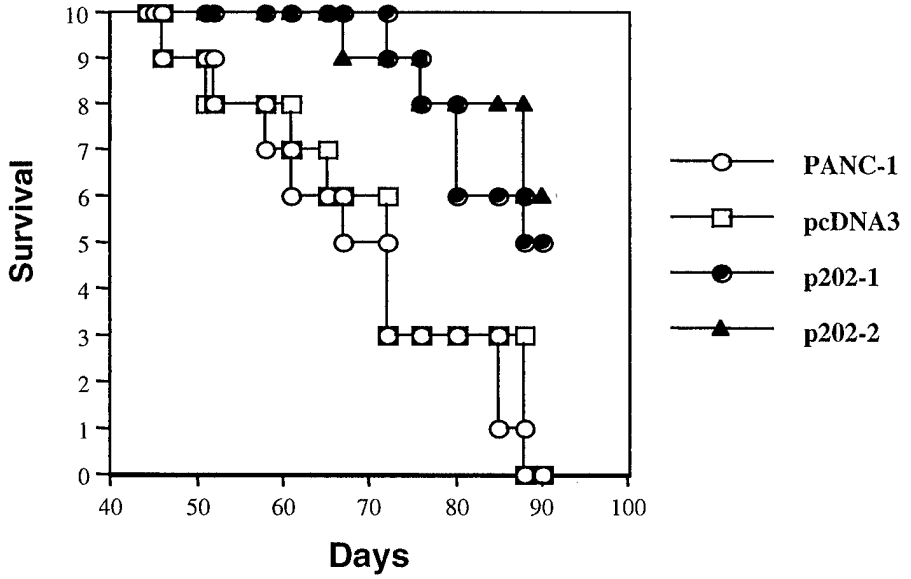
10
9
8
7
6
5
4
3
2
1
0
Survival
40
50
60
70
80
90
100
Days
PANC-1
pcDNA3
p202-1
p202-2

Table 2. Growth and Metastasis of PANC-1 Human Adenocarcinoma Cells in Nude Mice*

Lines	Orthotopic Growth (pancreas)		Gross Hepatic Metastasis	
	Incidence	**Median (tumor weight) (g)**	**Incidence**	**Median (Number)**
PANC-1	**5/5**	**0.30 (0.12, 0.20, 0.30, 0.51, 0.63)**	**2/5[a]**	**0 (0, 0, 0, 3, 4)**
pcDNA3	**5/5**	**0.22 (0.08, 0.13, 0.22, 0.32, 0.46)**	**1/5[b]**	**0 (0, 0, 0, 0, 5)**
P202-1	**1/5**	**0 (0, 0, 0, 0, 0.06)[#]**	**0/5**	**0 (all 0)[#]**
P202-2	**2/5**	**0 (0, 0, 0, 0.045, 0.05)[#]**	**0/5[c]**	**0 (all 0)[#]**

*Othortopic tumor transplantation (1 x 10^6 cells/mouse) was performed by intrapancreatic injection. Mice were killed after 3 months.

[a] 2 mice were found with peritoneal dissemination;

[b] 1 mouse was found with peritoneal dissemination;

[c] 1 mouse was found dead before experiment termination with no tumor and no metastasis.

[#] $p < 0.01$ as compared with control groups.

a

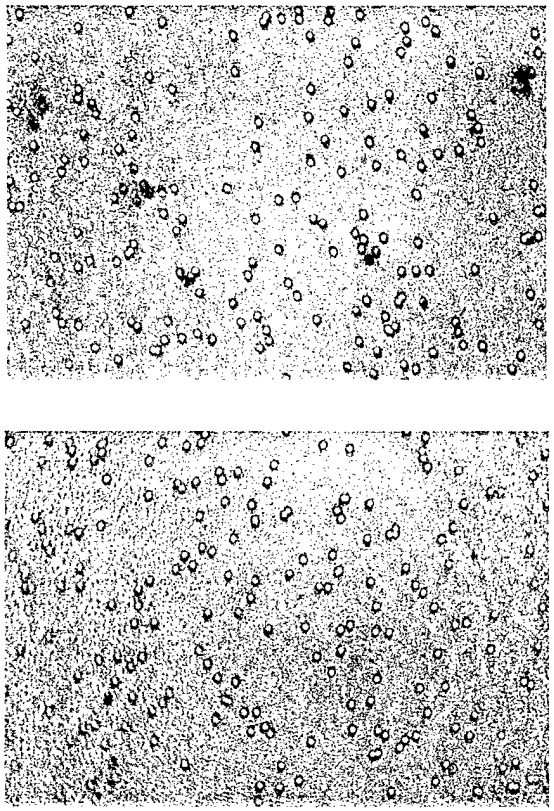
PANC-1
p202-1

b

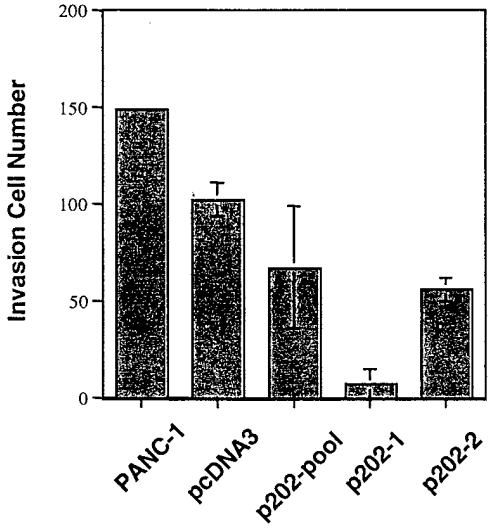
Invasion Cell Number
200
150
100
50
0
PANC-1
pcDNA3
p202-pool
p202-1
p202-2

c

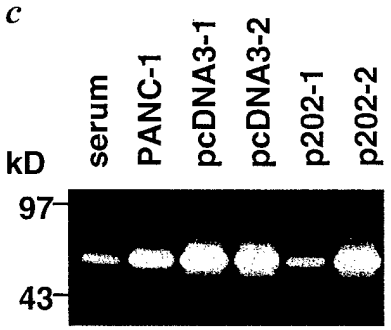
kD
serum
PANC-1
pcDNA3-1
pcDNA3-2
p202-1
p202-2
97
43

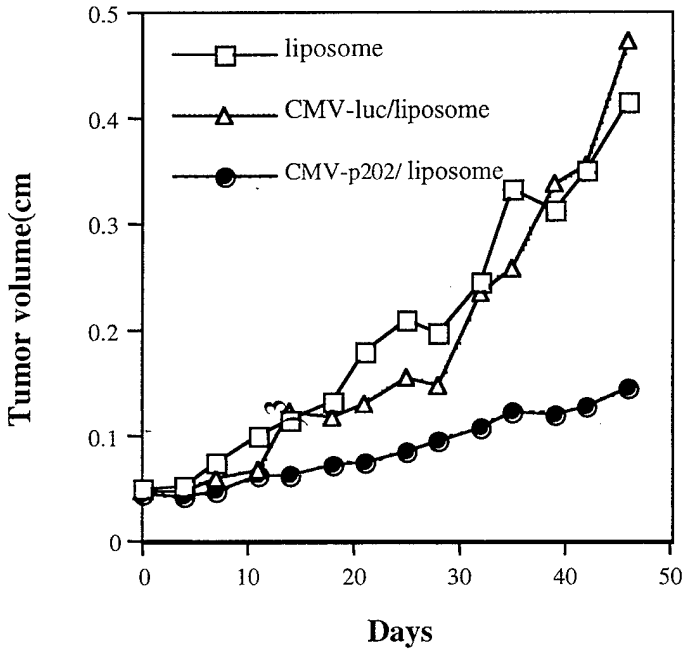
0.5
0.4
0.3
0.2
0.1
0
liposome
CMV-luc/liposome
CMV-p202/ liposome
Tumor volume(cm
0
10
20
30
40
50
Days

Pro-apoptotic Effect of Adenovirus-Mediated p202 Gene Transfer on Breast Cancer Cells[1]

Yi Ding, Li Wang, Bill Spohn, Ka Yin Kwong, Ruping Shao, Yong Wen, Zheng Li, Gabriel N. Hortobagyi, Mien-Chie Hung, and Duen-Hwa Yan[2]

Departments of Molecular and Cellular Oncology [Y.D., L.W., B.S. K.Y.K., R.S., Y.W., Z.L., M.-C.H., D.-H.Y.], Breast Medical oncology [G.N.H.], and Surgical Oncology [M.-C.H., D.-H.Y.]. The University of Texas M. D. Anderson Cancer Center, 1515 Holcombe Blvd. Houston, Texas 77030

[1]Funded by grants from the University Cancer Foundation at the University of Texas M. D. Anderson Cancer Center, Department of Defense (DAMD17-99-1-9270), and Texas Advanced Technology Program under Grant No. 003657-0082-1999 (to D.-H.Y.), from the NIH (CA77858) and Department of Defense (DAMD17-00-1-0312) (to M.-C.H.), from Breast Cancer Research Foundation/Estee Lauder Foundation (to G.N.H.), and from Cancer Center Core Grant 16672. Y.W. is a recipient of predoctoral fellowship from Department of Defense, Breast Cancer Research Training Grant (DMAD17-99-1-9264).

[2]To whom requests for reprints should be addressed at Department of Molecular and Cellular Oncology, The University of Texas, M. D. Anderson Cancer Center, 1515 Holcombe Blvd. Houston, Texas 77030. Phone: (713) 792-3677; Fax: 713-794-0209; E-mail: dyan@mdanderson.org

Running Title: Pro-apoptotic effect by adenovirus-mediated p202 gene delivery on breast cancer cells

Key words: p202, adenovirus, apoptosis, TNF-α, caspases

Abstract

p202, an interferon (IFN)-inducible protein, is a member of murine 200-amino acid repeat family. Ectopic expression of p202 in human breast cancer cells resulted in growth inhibition and sensitization to TNF-α-induced apoptosis. In this report, we used adenovirus-mediated gene delivery system to express p202 gene (Ad-p202) in the MDA-MB-468 breast cancer cell line and found that Ad-p202 infection induces growth inhibition as well as sensitizes the otherwise resistant cells to TNF-α-induced apoptosis. Importantly, we demonstrated for the first time that Ad-p202 infection alone induces apoptosis, and that requires the activation of caspases (caspase-3, in particular) for full apoptotic effect. Taken together, our results suggest that Ad-p202 is a potent growth-suppressing, pro-apoptotic agent that not only provides a useful tool to investigate the function of p202, but also can be used to further study the treatment efficacy in breast cancer xenograft model.

Introduction

p202, an IFN-inducible, chromatin-associated protein, belongs to a murine 200-amino acid repeat family (1, 2). The unique feature of p202 is illustrated by its ability to interact with several important transcriptional regulators that include E2Fs, Rb and the pocket proteins, p130 and p107, Fos/Jun, c-Myc, NF-κB, and p53BP-1 (reviewed in (3)), resulting in transcriptional repression of genes that are up-regulated by these transcriptional regulators. The exact role of p202 in IFN-mediated signal pathway is not well defined. However, consistent to the multiple anti-tumor activities of IFN (4),

enforced expression of p202 in stable murine fibroblasts and human cancer cell lines leads to retardation of cell growth and suppression of transformation phenotype (5-8). Furthermore, we showed that p202 stable breast cancer cells are sensitized to TNF-α-induced apoptosis (8), and that is associated with inactivation of the TNF-α-induced NF-κB via p202/NF-κB interaction. We therefore postulated that p202 inactivates NF-κB resulting in transcriptional repression of anti-apoptotic genes activated by NF-κB (9-11), and that leads to sensitization to TNF-α-induced apoptosis (8).

To generate a p202-based therapeutic agent for efficacy study in animal model and a tool to study the biological function of p202, we constructed Ad-p202. In this study, we showed that Ad-p202 infection into breast cancer cells resulted in growth inhibition and sensitization to TNF-α-induced apoptosis. Interestingly, we found that Ad-p202 infection alone induces apoptosis in breast cancer cells. In particular, the activation of caspase-3 appears to be critical for this process. Taken together, our results suggest that Ad-p202 is a potent growth-suppressing, pro-apoptotic agent that could be used to further study treatment efficacy in breast cancer xenograft model.

Materials and Methods

Generation of Ad-p202. Ad-p202 was constructed according to the protocol described previously (12). p202 cDNA (6) was subcloned into an adenovirus vector (pAdTrack-CMV) that carries a CMV promoter-driven green fluorescence protein (GFP), a separate CMV promoter directs p202 cDNA. A control virus, an adenoviral vector expressing

luciferase gene (Ad-Luc) and GFP was likewise generated. The expression of the GFP gene enabled us to monitor the infection efficiency by direct observation using a fluorescence microscope.

***In Vitro* Growth Assays.** MDA-MB-468 human breast cancer cells were maintained in DMEM/F-12 medium (HyClone Laboratories, Inc.) supplemented with 10% (v/v) fetal bovine serum. For MTT assay, 2 x10^3 cells were plated in 96-well culture plates in 0.1 ml of culture medium. Ad-p202 or Ad-Luc was added at multiplicity of infection (MOI) of 200 on the next day. At different times indicated, 20 μl of MTT (5 mg/ml stock solution) was added to each well. Cells were cultured for an additional 2 hours, then 100 μl of lysis buffer (20% SDS in 50% *N, N*-dimethylformamide, pH 4.7) was added to each well followed by five hours of incubation, and then absorbance was measured at 570 nm. [^{3}H] Thymidine incorporation assay was done as described previously (13).

Apoptosis Assays. Flow cytometry analysis: cells were collected at 72-h post-infection, washed once with phosphate-buffered saline (PBS) and suspended in 0.5 ml of PBS containing 0.1% (v/v) Triton X-100 for nuclei preparation. The suspension was filtered through a nylon mesh, then adjusted to a final concentration of 0.1% (w/v) RNase and 50 μg/ml propidium iodide. Apoptotic cells were quantitated by FACScan cytometer. DNA Fragmentation Assay was carried out as described previously (13).

Western Blot Analysis. MDA-MB-468 cells treated with or without TNF-α (R & D Systems, Inc., Minneapolis, MN) were infected with Ad-p202 or Ad-Luc at MOI of 200.

At 72-h post-infection, cells were lysed with RIPA lysis buffer. The protein extracts were subject to SDS-PAGE followed by western blotting according to the procedure described previously (8). Goat anti-p202 polyclonal antibody and anti-PARP antibody were obtained from Santa Cruz Biotechnology (Santa Cruz, CA) and BD Transduction Labs (Lexington, KY), respectively. Caspase inhibitors, Z-VAD and Z-DEVD-fmk were purchased from Enzyme Systems Products (Livermore, CA).

Gel-Shift Assay. The NF-κB gel-shift assay was performed as described previously (13).

Results and Discussion

Ad-p202 mediates p202 expression in breast cancer cells. To test the efficiency and to monitor the expression of p202 protein by Ad-p202 infection, we infected MDA-MB-468 breast cancer cells with either Ad-p202 or Ad-Luc followed by fluorescence microscopy and western blot analysis, respectively. As shown in Fig. 1*a*, Ad-p202 and Ad-Luc infection at MOI of 200 exhibited more than 90% infection efficiency as indicated by the GFP-positive cells shown in a representative field (Fig. 1*a*, right panels). Same cells are shown in phase contrast images (Fig. 1*a*, left panels). The mock-infected cells (control) showed no GFP expression. In addition to MDA-MB-468, we found that Ad-p202 could infect a panel of other human breast cancer cell lines (e.g., MDA-MB-453, MDA-MB-435, MDA-MB-231, and MCF-7), albeit, with various infection efficiency (data not shown). We chose MDA-MB-468 cell line for the subsequent studies because it is tumorigenic in mouse xenograft model and has relatively high infection efficiency by Ad-

p202. The expression of p202 protein in Ad-p202 infected cells was further analyzed by western blot using p202-specific antibody. Fig. 1*b* shows that, while the mock- and Ad-Luc-infected cells have no p202 expression, Ad-p202 infection efficiently directed p202 expression in MDA-MB-468 cells in a dose-dependent manner. These results clearly demonstrate that Ad-p202 infection adequately directs p202 expression in MDA-MB-468 cells.

Ad-p202 infection reduces breast cancer cell growth. Previously, we showed that p202-expressing MDA-MB-453, i.e., 453-p202, and MCF-7 stable breast cancer cell lines exhibited reduced cell growth rate (8). To assess the growth inhibitory effect of Ad-p202, we infected MDA-MB-468 cells with either Ad-p202 or Ad-Luc followed by *in vitro* growth assays such as MTT and ^{3}H-thymidine incorporation. As shown in Fig. 2, while the mock infection (control) and Ad-Luc infection have no growth inhibitory effect on MDA-MB-468 cells, Ad-202 infection significantly hampered cell growth (Fig. 2*a*) and DNA synthesis rates (Fig. 2*b*). This observation strongly indicates that Ad-p202 infection inhibits cell growth in breast cancer cells, and that is congruous to our previous findings using stable cancer cell lines (7, 8).

Ad-p202 infection induces apoptosis in breast cancer cells. Without stress signals, the p202-stable cancer cell lines do not exhibit apoptotic phenotype (7, 8). It is possible that p202 stable cell lines isolated from vigorous selection process may possess a physiologically tolerant level of p202. The fact that only a small number of p202 stable cell lines were obtained by colony-forming assay (7, 8) raises the possibility that p202

expression alone may induce apoptosis. To test that possibility, we infected MDA-MB-468 cells with Ad-p202 or Ad-Luc followed by flow cytometry analysis to detect apoptosis by measuring cell population in sub-G1 phase of cell cycle. As shown in Fig. 3*a*, although Ad-Luc infection induced a modest apoptosis, (compared lane 1 with lane 3), Ad-p202 infection (lane 5) caused significantly more apoptosis (>20%) than that of the mock (lane 1) and Ad-Luc (lane 3) infection. That observation was further confirmed by two other apoptosis assays: first, poly (ADP-ribose) polymerase (PARP) cleavage assay in which the full-length PARP (116 kD) is cleaved by caspases into a fragment of approximately 85 kD (Fig. 3*b*); and second, DNA fragmentation assay that is based on the activated endonucleases during apoptosis (Fig. 3*c*). Ad-p202 infection resulted in a marked increase of PARP cleavage product (85 kD) (Fig. 3*b*, lane 5 and Fig. 4*a*, lane 3) and an enhancement of DNA fragmentation (Fig. 3*c*, lane 5). In contrast, Ad-Luc infection yielded a minimum amount of 85 kD PARP cleavage product (Fig. 3*b*, lane 3 and Fig. 4*a*, lane 2) as well as a near basal level of DNA fragmentation (Fig. 3*c*, compare lane 1 and lane 3). It is possible that p202 may cooperate with viral proteins to trigger apoptosis. To test that possibility, we infected Ad-Luc either into the stable cell lines, 453-p202 or the control, 453-pcDNA3 (8), followed by flow cytometry analysis. We found that Ad-Luc infection did not enhance apoptosis in 453-p202 as compared with that in 453-pcDNA3 at comparable infection efficiency (data not shown). This result suggests that Ad-p202-induced apoptosis is not due to a cooperation between p202 and certain viral proteins. Together, our results strongly indicate that Ad-p202 infection induces apoptosis in MDA-MB-468 cells. Given that MDA-MB-468 cell line harbors

mutant p53 (14), Ad-p202-mediated apoptosis thus appears to be independent of p53 status.

Caspase-3 activation is critical for p202-mediated apoptosis. Since caspases are activated during apoptosis and have a variety of substrates including PARP (15), the cleavage of PARP in Ad-p202-infected cells suggests that the activation of caspase may be involved in Ad-p202-induced apoptosis. To test that hypothesis, we infected MDA-MB-468 cells with Ad-p202 or Ad-Luc in the presence or absence of a pan caspase inhibitor, Z-VAD. The intensity of PARP full-length and cleavage product bands on western blot were measured using NIH Image 1.62 software. The percentage of 85 kD product is calculated by setting the total intensity of both 116 kD and 85 kD bands in each lane at 100%. As shown in Fig. 4*a*, the addition of Z-VAD attenuates Ad-p202-induced apoptosis as indicated by the reduced (though not completely eliminated) level of PARP cleavage 85 kD product from 57.4% (lane 3) to 13.3% (lane 5), whereas Z-VAD has no effect on PARP cleavage in Ad-Luc-infected cells (lane 4). This result supports the idea that the activation of caspases is at least in part required for Ad-p202 to induce full apoptotic effect. Since PARP is also a substrate of caspase-3 that is considered to be a crucial enzyme commonly activated during apoptosis (15), we examined if the activation of caspase-3 plays a role in Ad-p202-induced apoptosis. To that end, we infected MDA-MB-468 cells with either Ad-p202 or Ad-Luc in the presence of a caspase-3 specific inhibitor, Z-DEVD-fmk (16). As shown in Fig.4*a*, the level of PARP cleavage product in Ad-p202-infected MDA-MB-468 cells is significantly reduced to 8.9% (lane 7) as compared with that without Z-DEVD-fmk (57.4%, lane 3). As a control,

no detectable PARP cleavage was observed in Ad-Luc-infected cells treated with Z-DEVD-fmk (lane 6). Thus, this result suggests that the activation of caspase-3 is critical for Ad-p202-mediated apoptosis. To further confirm that observation, we infected Ad-p202 or Ad-Luc into a caspase-3-null breast cancer cell line, MCF-7 (17) followed by flow cytometry analysis. We observed that, though with greater than 90% infection efficiency at MOI of 2000 based on GFP fluorescence microscopy (data not shown), Ad-p202 infection yielded near background level of apoptosis as that of the controls, i.e., mock and Ad-Luc infection (Fig. 4*b*). The inability of Ad-p202 to induce apoptosis in MCF-7 cells is not due to the lack of p202 expression since p202 protein was readily expressed as determined by western blot (Fig. 4*b*). Taken together, our data suggest that the activation of caspases, and caspase-3 in particular, is critical for Ad-p202 to exert full apoptotic effect.

Ad-p202 infection sensitizes breast cancer cells to TNF-α-induced apoptosis. We previously showed that the p202 stable breast cancer cell lines were sensitized to TNF-α-induced apoptosis (8). We tested if Ad-p202 infection could also sensitize breast cancer cells to TNF-α-induced apoptosis. Although MDA-MB-468 cells appear to be resistant to TNF-α (50 ng/ml)-induced apoptosis (Fig. 3*a*, lanes 1 and 2; Fig. 3*b*, lanes 1 and 2; and Fig. 3*c*, lanes 1 and 2), the combination of TNF-α and Ad-p202 induced a massive cell killing (Fig. 3*a*, lane 6; Fig. 3*b*, lane 6; and Fig. 3*c*, lane 6). Based on flow cytometry analysis data (Fig. 3*a*), we determined if the observed apoptotic effect of TNF-α and Ad-p202 combined treatment (lane 6) is synergistic using a formula $C < A \times B\% \times 70\%$ (18) (in which C is % of survival cells after combined treatment, and A and B are % of

survival cells after each treatment). In this case, C is 49.9% (Fig. 3*a*, lane 6), A is TNF-α treatment alone (95.5%, Fig. 3*a*, lane 2), and B is Ad-p202 infection alone (75%, Fig. 3*a*, lane 5). And the result, 49.9% < 50.1% (= 95.5% x 75% x 70%), suggests that the apoptotic effect of Ad-p202 and TNF-α combined treatment is indeed synergistic. In addition, the combined treatment of TNF-α and Ad-Luc infection did not cause a synergistic killing as compared with that of either treatment alone (Fig. 3*a*, lanes 2, 3, and 4; Fig. 3*b*, lanes 2, 3, and 4; Fig. 3*c*, lanes 2, 3, and 4), suggesting that such sensitization to TNF-α-induced apoptosis is specific to p202 expression. Since p202-mediated sensitization to TNF-α-induced apoptosis correlated with the inactivation of NF-κB, specifically, via the loss of NF-κB DNA binding activity (8), we then tested whether Ad-p202 infection affects TNF-α-induced NF-κB DNA binding activity. As shown in Fig 3*d*, we observed a complete abolishment of TNF-α-induced NF-κB DNA binding activity in Ad-p202-infected MDA-MB-468 cells (Fig. 3*d*, compare lanes 1, 3, 5 and 6). As controls, TNF-α-induced NF-κB DNA binding activity (lane 6) can be readily competed by cold wild type NF-κB DNA binding site (lane 7) but to a less extent by cold mutant probe (lane 8). Ad-Luc infection also reduces the TNF-α-induced NF-κB DNA binding activity somewhat but to a less extent than Ad-p202 (lanes 4 and 5). Together, our data suggest that Ad-p202 infection could sensitize otherwise resistant MDA-MB-468 cells to apoptosis induced by TNF-α, and that correlates with a loss of TNF-α-induced NF-κB DNA binding activity.

In this report, we showed that, like p202 stable breast cancer cell lines, Ad-p202 infection into MDA-MB-468 breast cancer cells resulted in growth inhibition and sensitization to

TNF-α-induced apoptosis. In addition, we demonstrated for the first time that Ad-p202 infection alone induces apoptosis. This process seems to require the activation of caspase-3 to achieve a full apoptotic effect. Our results thus raise the possibility of using Ad-p202-based gene therapy to treat breast cancer in mouse xenograft model. Moreover, our data also suggest that Ad-p202/TNF-α combined therapy may be a viable option to treat certain breast cancer cells that are resistant to TNF-α treatment. Experiments are underway to test the treatment efficacy of these approaches in animal models.

References

1. Landolfo, S., Gariglio, M., Gribaudo, G., and Lembo, D. The Ifi 200 genes: an emerging family of IFN-inducible genes, Biochimie. *80:* 721-728, 1998.
2. Johnstone, R. W. and Trapani, J. A. Transcription and growth regulatory functions of the HIN-200 family of proteins, Mol Cell Biol. *19:* 5833-5838, 1999.
3. Choubey, D. P202: an interferon-inducible negative regulator of cell growth, J Biol Regul Homeost Agents. *14:* 187-192, 2000.
4. Ferrantini, M. and Belardelli, F. Gene therapy of cancer with interferon: lessons from tumor models and perspectives for clinical applications, Semin Cancer Biol. *10:* 145-157, 2000.
5. Lembo, D., Angeretti, A., Benefazio, S., Hertel, L., Gariglio, M., Novelli, F., and Landolfo, S. Constitutive expression of the interferon-inducible protein p202 in NIH3T3 cells affects cell cycle progression., J. Biol. Regul. Homeost. Agents. *9:* 42-46, 1995.

6. Choubey, D., Li, S.-J., Datta, B., Gutterman, J. U., and Lengyel, P. Inhibition of E2F-mediated transcription by p202., EMBO J. *15:* 5668-5678, 1996.

7. Yan, D.-H., Wen, Y., Spohn, B., Choubey, D., Gutterman, J. U., and Hung, M.-C. Reduced growth rate and transformation phenotype of the prostate cancer cells by an interferon-inducible protein, p202, Oncogene. *18:* 807-811, 1999.

8. Wen, Y., Yan, D. H., Spohn, B., Deng, J., Lin, S. Y., and Hung, M. C. Tumor suppression and sensitization to tumor necrosis factor alpha-induced apoptosis by an interferon-inducible protein, p202, in breast cancer cells, Cancer Res. *60:* 42-46, 2000.

9. Beg, A. A. and Baltimore, D. An essential role for NF-kappaB in preventing TNF-alpha-induced cell death, Science. *274:* 782-784, 1996.

10. Van Antwerp, D. J., Martin, S. J., Kafri, T., Green, D. R., and Verma, I. M. Suppression of TNF-alpha-induced apoptosis by NF-kappaB, Science. *274:* 787-789, 1996.

11. Wang, C. Y., Mayo, M. W., and Baldwin, A. S., Jr. TNF- and cancer therapy-induced apoptosis: potentiation by inhibition of NF-kappaB, Science. *274:* 784-787, 1996.

12. He, T. C., Zhou, S., da Costa, L. T., Yu, J., Kinzler, K. W., and Vogelstein, B. A simplified system for generating recombinant adenoviruses, Proc Natl Acad Sci U S A. *95:* 2509-2514, 1998.

13. Shao, R., Karunagaran, D., Zhou, B. P., Li, K., Lo, S.-S., Deng, J., Chiao, P., Hung, M.-C. Inhibition of nuclear factor-kB activity is involved in E1A-mediated

sensitization of radiation-induced apoptosis., J. Bio. Chem. *272:* 32739-32742, 1997.

14. Hunt, K. K., Deng, J., Liu, T. J., Wilson-Heiner, M., Swisher, S. G., Clayman, G., and Hung, M. C. Adenovirus-mediated overexpression of the transcription factor E2F-1 induces apoptosis in human breast and ovarian carcinoma cell lines and does not require p53, Cancer Res. *57:* 4722-4726., 1997.

15. Thornberry, N. A. and Lazebnik, Y. Caspases: enemies within, Science. *281:* 1312-1316, 1998.

16. Pastorino, J. G., Chen, S. T., Tafani, M., Snyder, J. W., and Farber, J. L. The overexpression of Bax produces cell death upon induction of the mitochondrial permeability transition, J Biol Chem. *273:* 7770-7775, 1998.

17. Janicke, R. U., Sprengart, M. L., Wati, M. R., and Porter, A. G. Caspase-3 is required for DNA fragmentation and morphological changes associated with apoptosis, J Biol Chem. *273:* 9357-9360, 1998.

18. Hata, Y., Sandler, A., Loehrer, P. J., Sledge, G. W., Jr., and Weber, G. Synergism of taxol and gallium nitrate in human breast carcinoma cells: schedule dependency, Oncol Res. *6:* 19-24, 1994.

Figure Legends

Fig. 1. Ad-p202 construction, p202 expression, and infection efficiency. *a*. Ad-p202 was generated according to the protocol described previously (12). The pAdTrack-CMV vector contains two independent CMV promoter-driven transcription units, one for GFP and one for p202 cDNA. Human breast cancer cells, MDA-MB-468, were infected by Ad-Luc or Ad-p202 at MOI of 200. At 24-h post-infection, more than 90% cells were found to be GFP-positive as visualized by fluorescence microscopy (right panel), indicating the infection efficiency is more than 90%. Left panel: phase contrast microscopy. Control is the mock-infected cells. *b*. p202 protein is expressed in Ad-p202 infected cells. MDA-MB-468 cells infected with Ad-Luc or Ad-p202 for 72 h were analyzed for p202 protein expression by western blot. Control is the mock-infected cells. Actin protein was used as an equal loading control.

Fig. 2. Ad-p202 infection inhibits cell proliferation. MDA-MB-468 cells were infected with Ad-Luc or Ad-p202 at MOI of 200. Cell growth was monitored at the indicated post-infection time (3 - 5 days) by *a*, MTT assay, means ± SD (n = 3), or *b*, [^{3}H]-thymidine incorporation assay, data presented as means of quadruplicates.

Fig. 3. Ad-p202 infection induces apoptosis and sensitizes cells to apoptosis induced by TNF-α. MDA-MB-468 cells were infected with Ad-Luc or Ad-p202 at MOI of 200. At 24 h post-infection, TNF-α (50 ng/ml) was added to the medium and incubated for 48 h. *a*, At 72 h post-infection, apoptosis was monitored by flow cytometry analysis (done in triplets, Bars: SD). *b*, PARP cleavage assay: at 24 h post-infection, TNF-α (50 ng/ml)

was added to the medium and incubated for 24 h. Treated cells were harvested at 48 h post-infection, and *c*, DNA fragmentation assay: at 24 h post-infection, TNF-α (50 ng/ml) was added to the medium and incubated for 24 h. Treated cells were harvested at 48 h post-infection. The PARP protein (116 kD) was cleaved into 85 kD product in the event of apoptosis. *d*. Ad-p202 infection inhibits the TNF-α-induced NF-κB DNA binding activity. MDA-MB-468 cells were infected with Ad-p202 or Ad-Luc in the presence or absence of TNF-α (50 ng/ml) at 24 h post-infection for 30 minutes. The nuclear extracts were then isolated and incubated with a radioactive labeled oligonucleotide containing κB binding site (13). The excess cold wild type or mutant κB binding site were added to the incubation to demonstrate the specific NF-κB DNA binding activity. The NF-κB/DNA complex is indicated.

Fig. 4. The activation of caspases is critical for Ad-p202-mediated apoptosis. *a*. Z-VAD (100 μM) and Z-DEVD-fmk (80 μM) inhibit Ad-p202-mediated apoptosis in MDA-MB-468 cells. Western blot analysis of PARP cleavage and actin expression was performed at 48-h post-infection. The intensity of PARP full-length and cleavage product bands were measured using NIH Image 1.62 software. *b*. Ad-p202 infection fails to induce apoptosis in MCF-7 cells. Flow cytometry analysis was used to measure apoptotic cell population in mock- (control), Ad-p202- (MOI of 2000), or Ad-Luc- (MOI of 2000) infected MCF-7 cells at 72-h post-infection. The experiment was done in triplets. Bars: SD. p202 and actin protein expression was determined by western blot analysis.

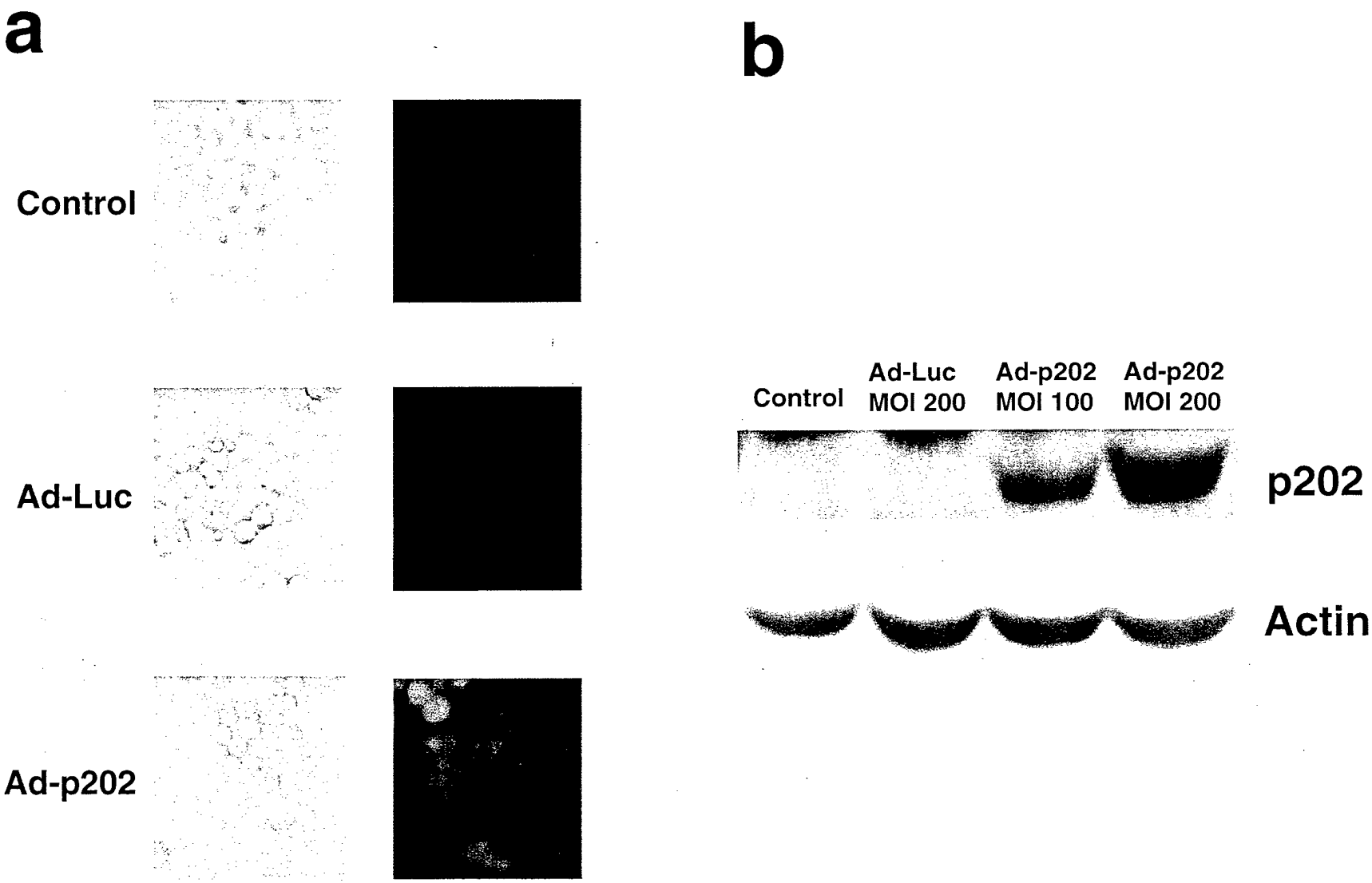
a
Control
Ad-Luc
Ad-p202
b
Control
Ad-Luc MOI 200
Ad-p202 MOI 100
Ad-p202 MOI 200
p202
Actin

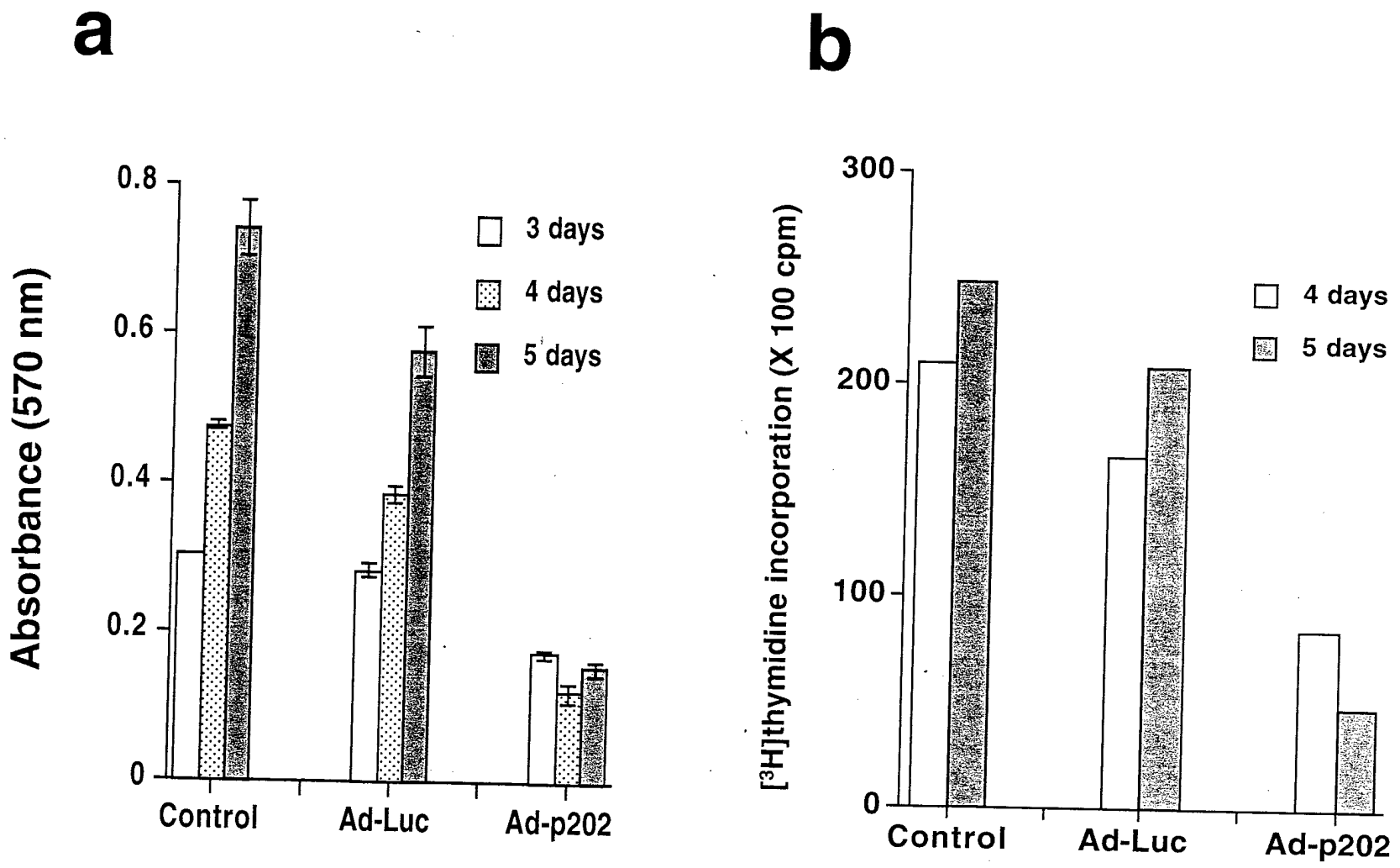
a
Absorbance (570 nm)
0.8
0.6
0.4
0.2
0
3 days
4 days
5 days
Control
Ad-Luc
Ad-p202
b
[3H]thymidine incorporation (X 100 cpm)
300
200
100
0
4 days
5 days
Control
Ad-Luc
Ad-p202

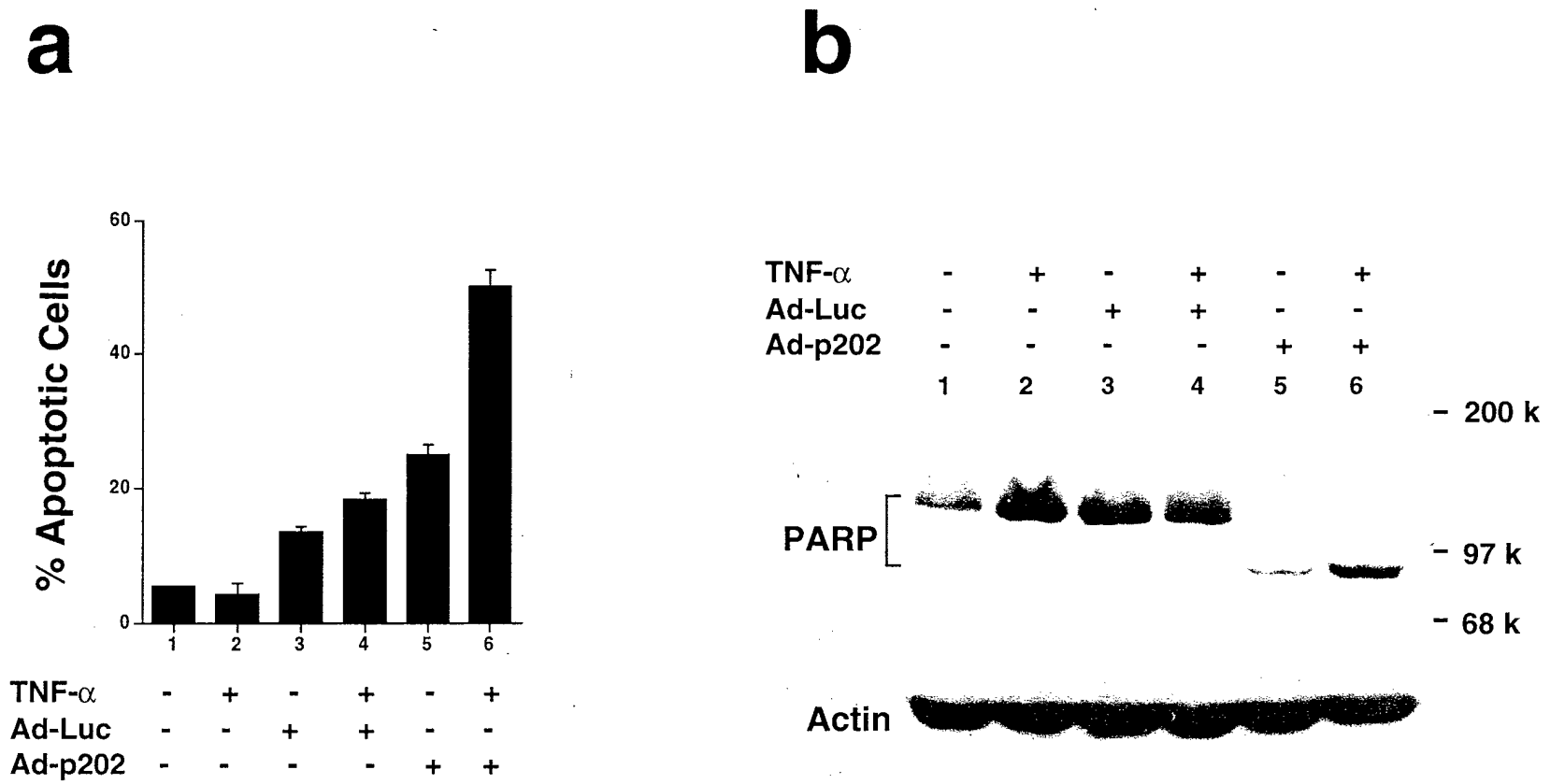
a
% Apoptotic Cells
60
40
20
0
1 2 3 4 5 6
TNF-α - + - + - +
Ad-Luc - - + + - -
Ad-p202 - - - - + +
b
TNF-α - + - + - +
Ad-Luc - - + + - -
Ad-p202 - - - - + +
1 2 3 4 5 6
200 k
PARP
97 k
68 k
Actin

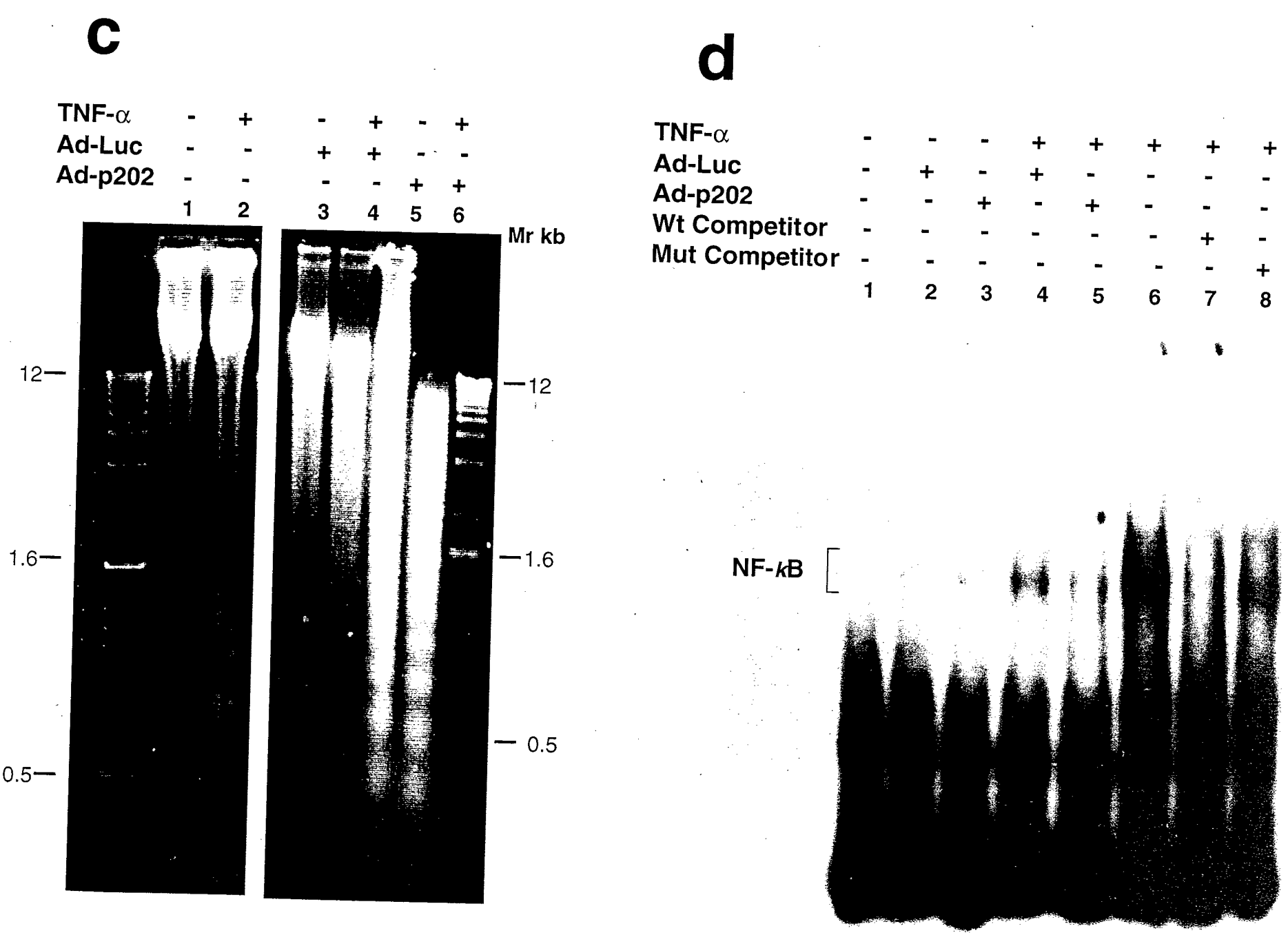
c
TNF-α - + - + - +
Ad-Luc - - + + - -
Ad-p202 - - - - + +
1 2 3 4 5 6
Mr kb
12
1.6
0.5
12
1.6
0.5
d
TNF-α - - - + + + + +
Ad-Luc - + - + - - - -
Ad-p202 - - + - + - - -
Wt Competitor - - - - - - + -
Mut Competitor - - - - - - - +
1 2 3 4 5 6 7 8
NF-kB

a

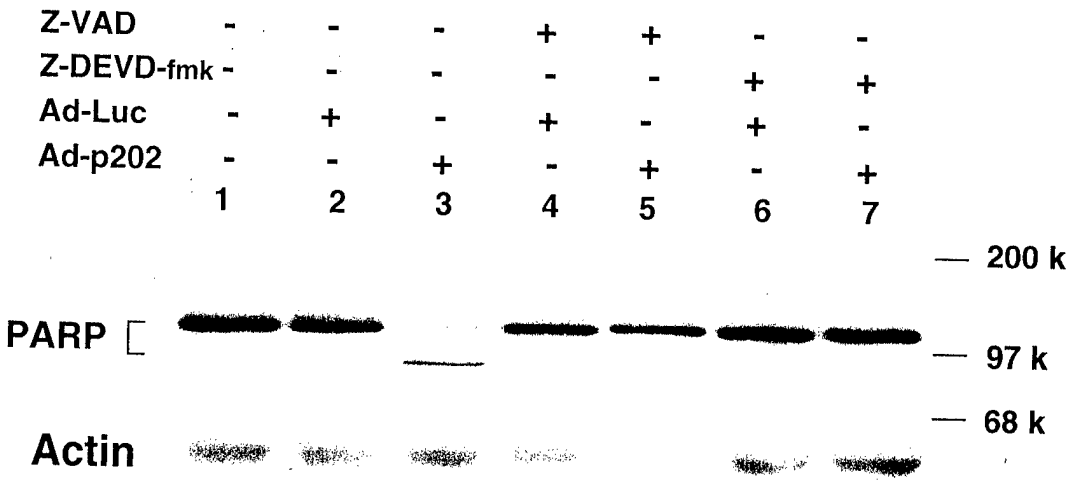
Z-VAD - - - + + - -
Z-DEVD-fmk - - - - - + +
Ad-Luc - + - + - + -
Ad-p202 - - + - + - +
1 2 3 4 5 6 7
200 k
PARP
97 k
68 k
Actin

b

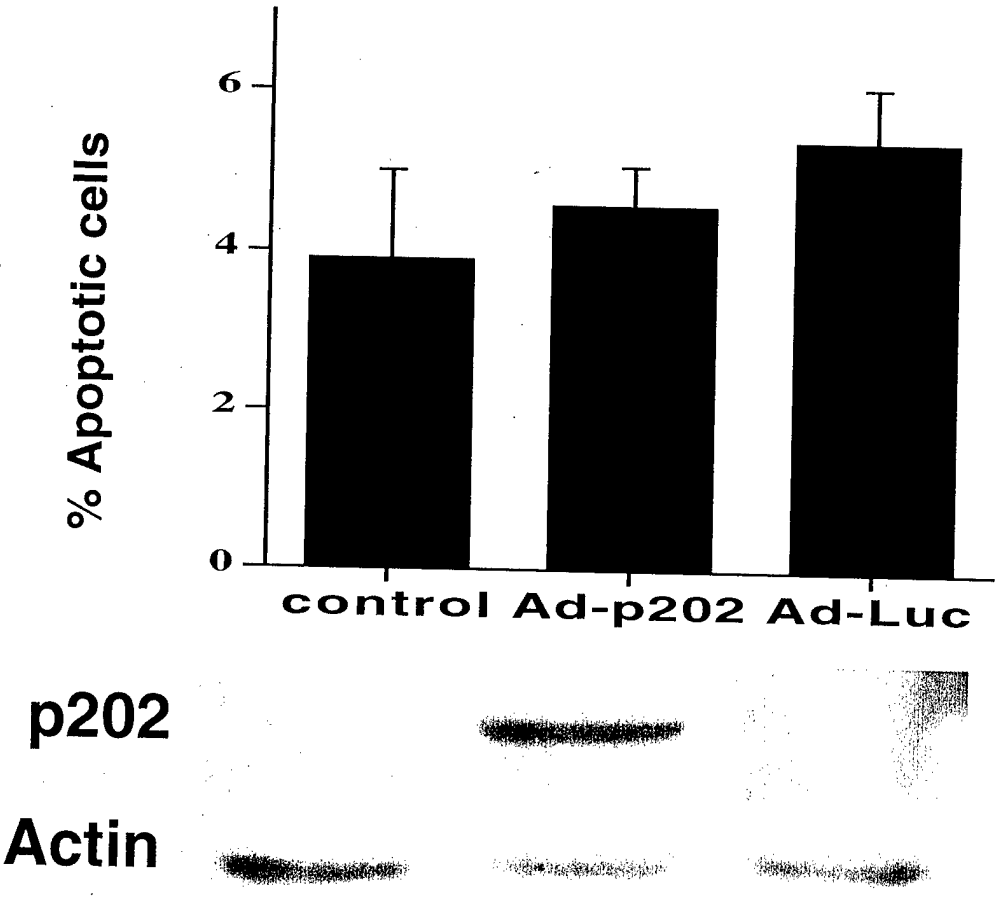
% Apoptotic cells
6
4
2
0
control Ad-p202 Ad-Luc
p202
Actin

vitro with the human wt-p53 cDNA by exposure to adenovirus-p53 (KATO-III/p53). Immunocytochemical staining and western blot analyses showed high effeciency and high level of wt-p53 and p21 protein expression, but no p53 and p21 was detected in parental (uninfected) cells or control cells infected with adenovirus-nLacZ (KATO-III/nLacZ). Overexpression of p53 alone indused growth arre t but could not promote DNA fragmentation in KATO-III cells. SB rapidly redused viability of KATO-III/p53 cells with DNA fragmentation. However SB did not damage parental KATO-III cells, nor KATO-III/nLacZ cells. Recently, it was reported that acetylation of lysine residues was an important post-translational modification to activate p53. Considering SB as a histone deacetylase inhibitor, we investigated whether SB induses acetylation of p53. Western blot analyses revealed that in , KATO-III/p53 cells, p53 was acetylated at Lys373 and Lys382 residues after treatment with SB. Based on these datas, we injected directly adenovirus-p53 into KATO-III tumors s.c. implanted into nu/nu mice and administrated SB i.p. This novel chemo-gene therapy indu ced massive apoptotic destruction of the tumors. In conclusion, it is suggested that SB could activate p53 by acetylation of lysine residues and induse apotosis in gastric cancer cells transduced wt-p53 gene in vitro and in vivo.

#3539 Exogenous Recombinant Adenoviral p53 Suppresses the Growth of HPV16 Mediated Human Cervical Cancer *in Vitro* and *in Vivo*. Woong Shick Ahn, Tae Hyung Kim, Min Suk Rho, Joon Mo Lee, Sung Eun Namkoong, Yong Seok Park, and Chong Kook Kim. *Catholic Research Institute of Medical Science, Research Institute of Cancer, The Catholic University of Korea, Seoul, South Korea, College of Pharmacy, Seoul National University, Seoul, South Korea, Dept. of Medical Technology, College of Health Science, Yonsei University, Wonju, South Korea, and Dept. of Obstetrics and Gynecology, Kangnam St.Mary's Hospital, The Catholic University of Korea, Seoul, South Korea.*

Human papilloma viruses (HPVs) bring about serious cervical cancer, and transforming oncogene of E6 is a critical factor in cervical carcinogenesis, which inactivates the tumor suppressor p53. Most of cancer cell lines have mutations in p53 gene, but not so much in cervical cancer cell lines. However the function of p53 is down regulated by E6 oncoprotein in cervical cancer cell lines transfected with HPV16, 18. We examined the growth inhibitory effect of overexpressed recombinant adenoviral p53 (AdCMVp53) on CaSki, SiHa, and HeLa, HeLaS3 *in vitro*, which are high risk virus HPV16 and HPV18 mediated tumor cell lines respectively, and C33A, HT3, which are p53 mutated tumor cell lines in cervix. Adenovirus-mediated p53 expression induced significant growth suppression in these six cervical cancer cell lines at cell count assay. On western analysis exogenously expressed p53 was increased transiently and decreased in CaSki, SiHa, and HeLa, HeLaS3, However in C33A, and HT3, p53 was not decreased, and maintained high expression level, because these cells were not infected with HPV. In RT-PCR analysis HPV16 type and 18 type E6 oncogene transcription was also strongly repressed in CaSki, SiHa, HeLa, and HeLaS3, when AdCMVp53 was expressed. We also examined the effects of exogenously expressed p53 as therapeutic gene on the suppression of cervical tumor in nude mice infected with CaSki, and SiHa cancer cell line. In tumor tissue of nude mice AdCMVp53 was significantly expressed on western analysis, and immunohistochemistry analysis. The growth of tumor is also suppressed for 6 days after AdCMVp53 was injected. These results suggest that the exogenously expressed p53 in tumor tissue of nude mice infected with SiHa or CaSki cell line strongly inhibits cancer proliferation.

#3540 Stimulation of the p53 Pathway with a Peptidic Inhibitor of the p53-hdm2 Interaction. Patrick Chene, Pascal Furet, and Carlos Garcia Echeverria. *Novartis, Basel, Switzerland.*

The hdm2 protein negatively regulates p53 tumour suppressor activity. Upon binding to p53, hdm2 stimulates p53 degradation and inhibits its transcriptional activity. The overexpression of the hdm2 protein observed in various tumours leads as a consequence to the inactivation of the p53 pathway. The synthesis of inhibitors of the p53-hdm2 interaction would therefore be very useful to activate the p53 pathway in such tumours. We have synthesised a very potent peptide that inhibits the p53-hdm2 interaction in vitro. This untagged peptide penetrates tumour cells and induces the accumulation of p53. The accumulation of p53 leads to its activation and two gene products transcriptionally regulated by p53, p21(Waf1/Cip1) and hdm2, are induced in the presence of the peptide. Moreover, in tumour cells that overexpress hdm2, the peptide induces cell death by apoptosis in a dose dependent manner. We also observe that this peptidic inhibitor induces more specifically the cell death of tumour cells than of normal cells. Therefore inhibitors of the p53-hdm2 interaction show a therapetic window. These inhibitors of the p53-hdm2 interaction are very attractive candidates for the activation of the p53 pathway in tumours expressing wild type p53.

#3541 Epidermal Growth Factor Receptor (HER-1) but not C-Erbb2 (HER-2) is Overexpressed in Human Intra-Hepatic Cholangiocarcinoma (ICC). Michelangelo Fiorentino, Annalisa Altimari, Elena Gabusi, Chiara Barozzi, Antonia D'Errico, and Walter Franco Grigioni. *University of Bologna, Bologna, Italy.*

Background. Cholangiocarcinomas of the intra-hepatic bile ducts are aggressive tumors whose prognosis mainly depends on the feasibility of a surgical resection in absence of other effective medical treatments. Novel anti-neoplastic agents like the specific inhibitors of the EGFR tyrosin kinase (EGFR-TKI) and the humanized anti p185HER-2 monoclonal antibody (Herceptin®) targeting HER-1 and HER-2 respectively are currently on trial in different human malignancies. We tested the expression of HER-1 by immunocytochemistry (IC) and HER-2 by IC (DAKO, HerceptestTM) and chromogenic in situ hybridization (CISH) on 48 paraffin embedded ICC samples. **Results.** HER-1 protein was found in 39/48 (81%) ICC being overexpressed (>50% stained cells) in 25/48 (52%) tumors. Almost all the hepatocytes of the normal surrounding liver tissue also strongly stained for HER-1. HerceptestTM revealed high expression of HER-2 (score 2+, 3+) in 2/48 (4%), low expression (score 1+) in 15/48 (31%) and no expression in 31/48 (65%) ICC. CISH confirmed HER-2 gene amplification (>4 spots) in the two ICC with scores 2+ and 3+. Statistical analysis failed to demonstrate significant associations between HER-1 and HER-2 expression and survival (log-rank test). **Conclusions.** 1) Most of ICC express high levels of HER-1 protein, thus disclosing the possibility of a treatment with EGFR-TKI for these tumors. 2) Based on our series, therapeutic strategies including the p185HER-2 monoclonal antibody (Herceptin®) might be appropriate only for few ICCs. 3) Expression of both HER-1 and HER-2 does not significantly influence survival of patients with ICC.

#3542 Role of PEA3 in Prostate Cancer. Kenji Sakata, Jane Barrett, Richard G. Tozer, and Gurmit Singh. *Hamilton Regional Cancer Centre, Hamilton, ON, Canada.*

The Ets family of transcription factors are not only involved in normal processes of growth and development but also have been implicated in various human malignancies. During the metastatic process, the expression of proteases such as the matrix metalloproteinase (MMP)s and uPA by the tumor cells is necessary. Ets proteins can bind to and activate the promoters of MMP-1, -3, -7, -9, -10, -13, TIMP-1 and uPA. The co-expression levels of Ets and MMP mRNA in human prostate cancer cell line PC-3 compared to the normal prostate epithelial cell strain PrEC has been analyzed by Northern blot. We found that Ets-1, Ets-2, PEA3, TIMP-1 and MMP-16 expression was higher in the PC-3 cell line versus PrEC. In this study, we focused on the relationships between the expression of PEA3 and some matrix degrading enzymes. To investigate the role of PEA3 in prostate cancer, a plasmid to express dominant-negative PEA3 was transfected into the PC-3 cell line and stable transfected PC-3 lines were obtained. A dominant-negative version of an Ets protein containing the DNA binding domain fused the drosophila Engrailed repressor functions by binding to and repressing transcription of Ets target genes. The expression of uPA, MMP-1, MMP-9 and TIMP-1 were compared in these cell lines (parental and transfected) by Northern blot, Western blot and gelatin or plasminogen zymography. (This work was supported by the Canadian Institutes of Health Research).

#3543 Antitumor Effects of PPAR−γ Ligand (Triglitazone) Against Anaplastic Thyroid Carcinoma in Vitro. Hayashi Nobuyasu, Nakamori Shoji, Okami Jiro, Nagano Hiroaki, Dono Keizo, Sakon Masato, Hiraoka Nobuaki, and Monden Morito. *Osaka University, Osaka, Japan.*

(Background) Anaplastic thyroid carcinoma (ATC) is the one of the most aggressive and malignant neoplasm in human. Several treatment modalities combining surgery, radiotherapy and cytotoxic drugs have been suggested to improve the progression of anaplastic thyroid carcinoma. It still seems to be resistant to nearly all anti neoplastic chemotherapy and radiotherapy. PPAR-gamma, a member of the nuclear receptor superfamily, functions as a master regulator of adipogenesis. Recently, several reports suggested that PPAR−γ ligands modulate the differentiation and the proliferation of both normal cells and tumor cells. Moreover, some studies have shown that ligands of PPAR−γ can induced terminal differentiation of several tumor cells, such as liposarcoma, breast cancer and colon cancer cells. These finding suggested that ligands of PPAR−γ might modulate the malignant potential of the poor prognostic neoplasm, anaplastic thyroid tumor. Here, we evaluated the effects of PPAR−γ ligands on anaplastic thyroid tumor cells in vitro. (Methods) Five human ATC cell lines (IAA, K-119, MSA, KOA-2 and ROA) were examined the expression of PPAR−γ by semi-quantitative RT-PCR. The effects of Triglitazone (TZD) on the proliferation and the motility of these cells were examined by 6-well proliferation assay, and scratched and boyden chamber method. The effects on the expression of thyroglobulin, oncofetal fibronectin and E-cadherin of these cells were also examined by RT-PCR, as differentiation markers. (Results) All five ATC cell lines expressed PPAR−γ abundantly. TZD inhibited the proliferation of these cells by 30 to 40% in dose dependent manners. TZD also inhibited the motility of these cells by 20 to 50%. Expression levels of the differentiation markers of these cells were not effected by the exposures of TZD. (Conclusion) PPAR−γ ligands may be useful therapeutic agents for anaplastic thyroid carcinoma, and by combining other therapy, might improve the prognosis of this carcinoma.

#3544 Modulation of Apoptotic Threshold: Enhanced Anti-Tumor Therapy Through Down-Regulate AKT and Up-Regulate p38 by Adenovirus E1A in Human Breast Cancer Cells. Yong Liau, Yi-yu Zou, Wei-ya Xia, Wei-Ping Lee, and Mien-Chie Hung. *Department of Molecular & Cellular Oncology, The University of Texas M.D. Anderson Cancer Center, Houston, TX, and The University of Texas M.D. Anderson Cancer Center, Houston, TX.*

Chemotherapeutic drug resistance is a major clinical problem and a source of treatment failure in cancer patients. We have previously shown that gene transfer of the adenovirus 5 E1A sensitized Her-2/neu-overexpressing human breast cancer cells to the chemotherapeutic agent paclitaxel (Taxol) by downregulating

the expression of Her-2/neu. To test whether E1A mediated Taxol sensitization involves different mechanisms other than down-regulation of HER-2/neu, we established stable cell lines expressing high level of wild type E1A proteins in HER-2/neu low level expressing human breast cancer cell lines: MDA-MB-231 and MCF-7, which are reported to harbor Akt overexpression. Both in vivo and in vitro studies showed that introduction of E1A significantly increased cells' sensitivity to Taxol cytotoxicity and dramatically enhanced tumor regression and prolonged survival in mice compared with that in Taxol or E1A alone treated controls. To understand the potential mechanism underlying E1A sensitization to Taxol cytotoxicity in this context, we screened a few cell signaling molecules that are known to be critical in signaling cells either to go apoptosis or against cell death. We found that downregulate Akt, a key player in cell survival signaling, and/or up-regulate p38, an important molecule in signaling cells to commit apoptosis, is required for E1A sensitization to Taxol induced apoptosis. Blocking p38 activity, by either chemical inhibitor SB203580 or genetic approach using an inducible dominant negative p38 mutant, and introducing constitutively active Akt did partially abrogate E1A ability to sensitize cells to Taxol cytotoxicity in E1A expressing MDA-MB-231 cells. Moreover, introducing p38 or blocking Akt activity in MDA-MB-231 cells also enhanced sensitivity to Taxol induced apoptosis. Although physical association between Akt and p38 was not detected by immunoprecipation, cross regulations between these two pathways were observed. This is the first report to show that E1A mediated chemosensitization was achieved by modulating apoptotic threshold through down-regulation Akt and up-regulate p38 activity in breast cancer cells. These results suggest a powerful strategy for the adjuvant chemotherapy of human breast cancer by combination of E1A gene therapy with chemotherapy.

#3545 p53 Status Determines Nuclear Factor-κB Response in Triptolide-Induced Apoptosis in Gastric Cancer. XH Jiang, SK Lam, MCM Lin, CH Cho, KC Lai, HF Kung, D. Yang, and Benjamin CY Wong. *University of Hong Kong, Pokfulam, Hong Kong.*

Triptolide, a major component in the extract of Chinese herbal plant Tripterygium wilfordii Hook f (TWHf), has potential anti-neoplastic effect. We investigated the potential role of triptolide in the treatment of gastric cancer cells. Two gastric cancer cell lines, MKN-28 (mutant p53) and AGS (wild-type p53), were compared as to growth inhibition, apoptosis, cell cycle phase distribution, apoptosis-related gene expressions and activation of NF-κB in response to triptolide treatment. We reported that in gastric cancer cells, Triptolide inhibited cell growth and induced apoptosis in a dose-dependent manner, whereas AGS cells with wild type p53 were more sensitive after treatment, associated with overexpression of p53, p21 and bax. Down-regulation of p53 suppressed triptolide induced apoptosis in AGS cells. Moreover, Triptolide inhibited NF-κB activation in AGS cells with wild-type p53 but increased NF-κB activation in MKN-28 with mutant p53. These results demonstrated the anti-neoplastic effect of Triptolide in gastric cancer through induction of apoptosis, mediated by different effect on NF-κB activation depending on the p53 status.

#3546 Adenoviral-mediated Gene Therapy for Treatment of Benign Prostate Hyperplasia (BPH) Using Tumor Suppressor Genes. Mitchell S. Steiner, Guimin Chang, and Yi Lu. *GTx, Inc., Memphis, TN, and University of Tennessee, Memphis, Memphis, TN.*

Benign enlargement of the prostate, BPH, is the most commonly occurring benign disease in men older than 50 years of age. Up to 25% of these men will eventually require treatment for symptomatic relief of clinical BPH. Understanding molecular events responsible for BPH will allow the design of more specific therapies. To determine whether the exogenous expression of the negative growth regulators will inhibit prostate growth, recombinant adenoviral vectors that express p16, p53, or TGFβ1 were used to transduce an established human BPH cell line, BPH-1. Adenoviral gene transfer resulting in the exogenous expression of p16, p53, or TGFβ1, all suppressed cell growth and induced apoptosis in BPH-1 cells. These results suggest that gene therapy of these negative growth regulator genes may induce apoptosis and may potentially be employed to treat BPH.

#3547 Manipulation of Differentially Expressed Genes Such as Bcl-2 Leads to Increased Killing of B Chronic Lymphocytic Leukemia. Shantaram S. Joshi, Peng Wang, John E. Dickinson, Uyen E. Vu, and Z. Steven Pavletic. *University of Nebraska Medical Center, Omaha, NE.*

B Chronic Lympocytic Leukemia (B-CLL) cells are known to have defective cellular apoptosis machinery and are resistant to immune effector cell mediated killing. Manipulations of differentially expressed certain key cellular genes in B-CLL may lead to their increased killing. Therefore, in this study we have investigated differentially expressed cell cycle/apoptosis associated genes in the WSU-CLL cell line and fresh leukemic cells obtained from B-CLL patients, before initiation of treatment, using cDNA microarray techniques and RT-PCR techniques. The results were compared to gene expression patterns of other B cell or myeloid tumor cells. The cell cycle/apoptosis associated differentially expressed genes on B-CLL cells include over expression of Bcl-2, DAD-1, Cyclin-D3 and cyclin dependent Kinase-4 inhibitor and lower expression of Bax and CDC25B. One of the over expressing genes, Bcl-2 expression was down regulated using 2.5 5.0 mM concentration of Bcl-2 antisense phosphorothioate oligonucleotides. The decrease in Bcl-2 expression was confirmed by RT-PCR analysis and then used for cytotoxicity studies. The Bcl-2 down regulated CLL cells were significantly ($p<0.01$) more susceptible to blood derived lymphokine activated killer cell mediated cytotoxicity. Bcl-2 down regulated CLL cells were also significantly ($p<.001$) more susceptible to Fludarabine, a known chemotherapeutic agent used for treating CLL patients. Thus our results showed that certain key apoptosis/cell cycle associated genes are differentially expressed in B-CLL cells and manipulations of some of these genes in B-CLL cells increase their susceptibility for killing by cytotoxic effector cells and cancer chemotherapeutic agents. These results warrant further preclinical studies to develop treatment modalities with this approach for B-CLL.

#3548 Wild-Type p53 Is not Required for the Level of Taxol-induced Apoptosis, but Mutant p53s Differentially Regulate G2/M Arrest and Apoptosis under Isogenic Condition in Lung Cancer Cells. Gokul C. Das, Rafael Gallardo, and Charles Haas. *UT Health Center at Tyler, Tyler, TX.*

Taxol has a broad spectrum of anticancer activity, but the effective dose, schedule, molecular basis of cytotoxicity and their dependence on the genetic background in tumor cells are still not well understood. Although p53 plays a key role in apoptosis and is the preferred mode of cell death by the anticancer agents, studies examining p53's role in chemosensitivity has yielded conflicting results due to the additional changes in cancer cells. Here, we examined the role of the wild-type p53 and its hot-spot mutants in taxol-induced apoptosis under isogenic conditions developed by stably expressing these genes in the p53 null background of H 1299 cells. First, we show by DNA content analysis that in two lung cancer cell lines, A 549 (p53,+/+) and H 1299 (p53,-/-), taxol progressively induced G2/M arrest in a time and concentration dependent manner. Apoptosis maximized at about 25 nM in both cell lines and was about 20% higher in H 1299 cells, implicating that taxol can induce G2/M and apoptosis independent of the wild-type p53. G2/M arrest, however, occurred at a lower concentration and at a faster rate in A 549 cells than in H 1299 cell line. In other established cell lines with mutant p53, taxol exhibited a differential response, one (H 226) being partially resistant to taxol and the others (H 441 and H 596) while sensitive to taxol were prone to the development of polyploidy. We show that the level of apoptosis in several clones of isogenic cell lines expressing wild-type p53 was the same as in parental H 1299 cells. The level of apoptosis was, however, reduced differentially in cells expressing mutants 143, 175 and 273. We conclude that the wild-type p53 does not make a significant difference in the level of apoptosis, but mutant p53 has a differential effect. Repeated use of low concentration of taxol and identification of targets downstream to bypass the effect of mutant p53 are of therapeutic significance.

#3549 Down-Regulation of Bcl-2 and Rb Are Associated with $P16^{Ink4}$-mediated Apoptosis in Non Small Cell Lung Cancer Cells (NSCLS). Kou Katsuda, Masafumi Kataoka, Takahiro Itoshima, Jianghua Shao, Toshihiko Waku, Futoshi Uno, Spitz Francis, Guido Schumacher, Dao Nguyen, Jack Roth, Richard Cristiano, Toshiyoshi Fujiwara, and Noriaki Tanaka. *Campus Virchow-Klinikum, Berlin, Germany, National Cancer Institute, Bethesda, MD, Okayama University Medical School, Okayama, Japan, Shiga University of Medical Science, Otsu, Japan, University of Pennsylvania, Philadelphia, PA, and University of Texas, Houston, TX.*

Alterations in $p16^{INK4}$ gene expression have been observed in numerous tumor cell lines and in many fresh tumors. Rb-positive NSCLC express little or no p16 while Rb-negative NSCLC express abundant p16. As a result, inactivation of either p16 or Rb appear to be critical steps in the pathway leading to a malignant phenotype in vivo. The p53-mediated check of DNA damage can be mediated by the transcriptional activation of p21, which inhibits cyclin dependent kinase-mediated Rb phosphorylation, leading cells to an arrest in the G_1 phase and thus giving the cell time to repair DNA-damage. p53 can also activate the expression of Bax (a cell death inducer) and mediate supression of Bcl-2 (a cell death inhibitor), leading to cellular apoptosis. It is still unclear as to whether p16 is capable of contributing to the apoptotic pathway. We have attempted define what this interaction may be. Adenovirally introduction of p16 (Adv/p16) in A549 cells (p16-, p53 wild type, Rb+) mediated dephosphorylation of Retinoblastoma (Rb) protein and G_0-G_1 arrest, followed by remarkable apoptosis on five days after infection, as compared in H1299 cells (p16-, p53 delated, Rb+) mediated G_0-G_1 arrest, but could not find apoptosis. An additional infection with Adv/p53 in H1299 cells induced apoptosis. In order to confirm the relationship of p53 to p16-mediated apoptosis 7 human NSCLC cell lines including two with wild type p53, two with mutant p53 and two with deleted p53 were treated with Adv/p16 and then were analyzed by the TUNEL assay. This assay indicated that p16 was only able to induce apoptosis in cells containing wild-type p53 and that this occurred only on the fifth day after Adv/p16 infection. Analysis of the blots in A549 cells infected with Adv/p16 indicated that dephosphorylated Rb and bcl-2 protein level was greatly diminished after infection, while E2F-1 expression was not affected. MDM2 expression increased on day 2 and diminished after day 6 and p60, the cleavage product of MDM2, gradually increased on day 2. These studies suggested that Adv/p16 mediates apoptosis in cells containing functional p53 but not in p53 null cells. Down-regulation of Rb, bcl-2 and MDM2 may be associated with the apoptosis mediated by $p16^{INK4}$. Furthermore, combination of Adv/p16 and Adv/p53 may be more effective for gene therapy for lung cancers that do not express either wild type p53 nor p16.

Keystone Symposia on Molecular + Cellular Biology

Heregulin β1-activated erbB receptor signaling and Human Breast Cancer Cell Aggregation, Invasion and Metastasis

Ming Tan, Kristine Klos, Rebecca Grijalva, and Dihua Yu, Department of Surgical Oncology and The Breast Cancer Basic Research Program, The University of Texas M. D. Anderson Cancer Center, Houston, Texas 77030

The aberrant expression of erbB family receptor tyrosine kinases is frequently observed in human malignant diseases. The role of erbB receptors in human cancer progression may involve signal transduction pathways initiated by ligand binding. Heregulin (HRG) can bind to erbB3 and erbB4, inducing erbB3 and erbB4 heterodimerization with erbB2, receptor tyrosine phosphorylation, and downstream signaling.

Homophilic adhesion (cell aggregation) may affect tumor cell invasive and metastatic potential. We found that HRG–β1 can enhance aggregation of MCF-7 and SKBR3 human breast cancer cells. While investigating the downstream signals involved in HRG-increased cell aggregation, we observed that HRG induced tyrosine phosphorylation of erbB2 and erbB3 receptor heterodimers and increased the association of the dimerized receptors with the 85-KDa subunit of phosphatidylinositol 3-kinase (PI3K). HRG also increased the kinase activities of extracellular signal-regulated protein kinase (ERK) and PI3K in these cells. By using the MAPK/ERK kinase 1 (MEK1) inhibitor PD98059 and PI3K inhibitors wortmannin and LY294002, we found that blocking the MEK1-ERK pathway had no effect on HRG-enhanced cell aggregation; however, blocking the PI3K pathway greatly inhibited HRG-mediated cell aggregation. This result indicates that HRG-activated PI3K is required for enhancing breast cancer cell aggregation. Since aggregation can contribute to invasion/metastasis phenotype of cancer cells, our results have provided one mechanism by which HRG-activated signaling of erbB receptors may-affect invasive/metastatic properties of breast cancer cells.

ErbB2 is the preferred binding partner of erbB receptor family members. It plays a very important role in erbB receptor signaling. To understand the role of erbB2 in HRG initiated signal transduction, we transfected MDA-MB-435 human breast cancer cells with a panel of erbB2 mutants. The preliminary results suggest that the structural integrity of erbB2 receptor is required for HRG signaling and HRG-enhanced breast cancer cell invasion and metastasis.

* Supported by the US Army Breast Cancer Research Program

Ming Tan, Phone: 713-794-1233, Code of Meeting: B1, Poster session Number: 1.

kinase, and the Stat1 and Stat3 transcription factors. IL-6 treatment also led to activation of the mitogen-activated protein kinase (MAPK) and the phosphatidylinositol 3'-kinase (PI3K) pathways and inhibition of both pathways reversed IL-6- and OSM-stimulated migration. Cross-talk between cytokine receptors and members of the ErbB family of receptor tyrosine kinases is becoming increasingly relevant. Thus, we have examined the interaction of these receptors in T47D cells. Down-regulation of ErbB receptor activity, through the use of specific pharmacological inhibitors or dominant negative receptor constructs, revealed that IL-6-induced MAPK activation was largely dependent on EGF receptor activity, but not on ErbB2 activity. Using a monoclonal antibody, which interferes with EGF receptor-ligand interaction, we have shown that, in T47D cells, IL-6 cooperates with an EGF receptor autocrine activity loop for signaling through the MAPK and PI3K pathways and for cell migration. This cooperation involves recruitment of the tyrosine phosphatase SHP-2 and the multisubstrate docking molecule Gab1 to the gp130/EGF receptor complex. Thus, in T47D breast carcinoma cells, IL-6 acts in synergy with EGF receptor autocrine activity to signal through the MAPK/PI3K pathways. While expression of dominant negative Stat3 did not affect cell migration, it prevented IL-6-induced growth inhibition. We are currently investigating the mechanism by which IL6-induced Stat3 activation results in decreased cell proliferation.

#4514 Tumor-Stromal-Endothelial Cell Interactions May Provide a Second-Generation Vaccine for Prostate Cancer. Joanne Haley, Eamon Lane, and Darren Stevenson. *Onyvax Ltd, London, UK.*

First generation whole cell cancer vaccines rely on the use of single, or multiple types, of tumor cells grown in a static two-dimensional environment to provide antigenic determinants for the host immune system. This method of culturing cells may not mimic the in vivo situation with regards to gene expression and indeed antigen presentation. Using co-culture techniques we have shown through microarray analysis and RT-PCR studies that gene expression can be altered and prostate specific antigens up-regulated. Culturing human prostate cell line DU145 on a basal layer of normal human prostatic stromal fibroblasts (NHPSF) or normal human bone stromal fibroblasts (NHBSF) leads to a large number of genes being down-regulated (e.g. CD58 and TIMP1) and a smaller number up-regulated (e.g. cytokeratin 19 and retinoic acid receptor alpha). ONYCAP-1, ONYCAP-23, P4E6 and SHMAC-4 human prostate cell lines were investigated for specific prostate and metastasis antigens. PSA mRNA expression was up-regulated in all four tumor lines, whereas the androgen receptor, MMP-9 and the hyaluronic acid receptor were up-regulated in ONYCAP-23 during co-culture with NHBSF. The phenotypic enhancement of the cell lines described above represent a shift towards a more in vivo phenotype. To investigate this further, a co-culture approach was applied in the Dunning rat model of prostate cancer. Two-dimensional co-cultures of allogeneic rat prostate tumor cells in combination with rat bone marrow stromal and/or rat prostate endothelial cells resulted in increased vaccine efficacy in both the therapy and protection models of prostate cancer. Tumors in situ are complex structures comprising not only the tumor cells but also associated stroma and endothelium. These studies have highlighted that tumor-host cell interactions do modify tumor antigenic presentation and by in vitro emulation of these interactions we may develop a more effective (second-generation) whole cell prostate cancer vaccine.

#4515 The Focal Adhesion Kinase Regulates Glioma Cell Survival and Migration by Integrating Growth Factor and Integrin Signalling Pathways. Graham J. Jones, Joel Machado, and Adrian Merlo. *University Hospital Basel, Basel, Switzerland.*

Glioblastomas, the leading cause of brain tumor related deaths in humans, are highly resistant to chemo- and radiotherapy. Infiltration of normal brain by tumor cells proceeds along the extracellular matrix (ECM) of white matter tracts and of blood vessels. Cell motility and survival is regulated by integrin receptor activation and the focal adhesion complex, which includes the focal adhesion kinase (FAK). To investigate whether the inhibition of FAK might provide the basis of an anti-invasive therapy, the focal adhesion targeting domain (FAT) of FAK was stably expressed in human glioblastoma cell lines. The LN-401 and LN-229 cell lines are deficient for p53, p16 and p14ARF, while only LN-229 cells express a functional PTEN protein. The FAT domain competed with FAK for localisation to focal adhesions and inhibited FAK phosphorylation. Of note, FAK phosphorylation was not regulated by PTEN. The inhibition of FAK was associated with a decrease in invasion and migration, together with an increase in apoptosis as measured by caspase-3 activity. In FAT-expressing cells, phosphorylation of the EGF receptor, which is frequently amplified or mutated in glioblastomas, was also inhibited in a fibronectin adhesion assay. Furthermore, by using the specific EGF receptor inhibitor PD153035, apoptosis was significantly enhanced in a dose dependent manner in FAT-expressing cells. This work shows that FAK integrates both growth factor and integrin signalling in glioma cells and defines FAK as an attractive target for the development of anti-invasive therapies.

#4516 Activation of Focal Adhesion Kinase Signaling by TNFα in Human Breast Cancer Cells. Li-Hui Xu, Xihui Yang, Albert S. Baldwin, and William G. Cance. *University of North Carolina at Chapel Hill, Chapel Hill, NC.*

The Focal Adhesion Kinase (FAK) is a cytoplasmic protein tyrosine kinase that is involved in cellular adhesion, migration, and cell survival. Our recent studies have shown that FAK acts as an anchorage-independent survival signal in human breast cancer cells and that downregulation of FAK causes transformation-associated apoptosis via death receptor related signaling pathway(s). To further investigate the potential linkage of FAK and TNF-induced signal transduction, we treated BT474 human breast cancer cells with human recombinant TNFα. We have demonstrated that TNFα treatment enhanced cellular spreading that was accompanied by increased expression of $p125^{FAK}$ at focal adhesions as well as increased tyrosine phosphorylation of $p125^{FAK}$ in a dose and time-dependent manner. TNFα treatment also induced nuclear translocation of NF-kB p65 in BT474 cells as demonstrated by gel shift assay. Additionally, treatment of BT474 cells with the Src-family kinase inhibitor PP2 completely abrogated tyrosine phosphorylation of $p125^{FAK}$ induced by TNFα, but had no effect on nuclear translocation of p65. Furthermore, pretreatment of BT474 cells with TNFα caused significant reduction of cellular detachment induced by downregulation of FAK using adenoviral transduction of FAK-CD. Taken together, these results suggest a potential interaction between TNF receptor mediated signal transduction and FAK signaling pathways in human breast cancer cells. Supported by NIH grant CA65910.

#4517 Activation of AKT Is Required for HER-2/neu-Mediated Anchorage-Independent Growth. Binhua Peter Zhou and Mien-Chie Hung. *The UT M.D. Anderson Cancer Center, Houston, TX.*

Overexpression and activation of HER-2/neu, a proto-oncogene, correlate with poor survival of breast and ovarian cancer and induce chemo-resistance to anti-cancer drugs and anchorage-independent growth. The mechanism of HER-2/neu-induced anchorage-independent growth is unknown. We recently have demonstrated that HER-2/neu activates PI-3k/Akt pathway without extracellular stimulation. Here we showed that blockage of Akt pathway by dominant-negative Akt (DN-Akt) completely suppressed the HER-2/neu-induced anchorage-independent growth in both HER-2/neu transformed NIH3T3 and MDA-MB453 cells. This suppression of anchorage-independent growth correlated with the induction of anoikis in these cells. Furthermore we found that overexpression of HER-2/neu associated and activated focal-adhesion kinase (FAK) in anchorage-independent manner. Inhibition of Akt pathway by DN-Akt suppressed the activation of FAK and HER-2/neu tyrosine-phosphorylation in these cells. Together, these results demonstrated a critical role for Akt in HER-2/neu-mediated anchorage-independent growth and indicate that inhibition of Akt pathway may provide a significant tool in cancer therapy.

#4518 Mechanisms of Cell Death during Anoikis in LNCaP and PC-3 Prostate Carcinoma Cells. Victor Bondar and David Mcconkey. *M.D. Anderson Cancer Center, Houston, TX.*

Normal epithelial cells routinely undergo apoptosis in the absence of adhesive interactions with extracellular matrix (ECM), a form of cell death known as anoikis. Dependence on adhesion to ECM is often lost in transformed cells, although the cells still retain some requirement for cell-matrix and cell-cell interactions in order to survive. Therefore, the degree of anoikis resistance may vary in non-metastatic and metastatic cancer cells. Bcl-2 oncoprotein overexpression has been correlated with the progression and metastases of prostate cancer, as well as the generation of apoptosis- and therapy resistant prostate cancer cell clones. To investigate these relationships further we studied anoikis in suspension cultures of PC-3 and LNCaP prostate carcinoma cells selected for different metastatic properties in vivo. As predicted, non-metastatic PC-3P cells were significantly more sensitive to anoikis than the metastatic PC-3 variants (PC-3M, PC-3M-PRO-4 and PC-3M-LN-4). However, the metastatic LNCaP subclone (LN-4) was even more sensitive to anoikis than the non-metastatic (PRO-5) one. Expression of Bcl-2 was higher in metastatic PC-3 and LNCaP subclones compared to isogenic non-metastatic cells, whereas the levels of other pro- and anti-apoptotic Bcl-2 family members were similar, and these levels were not affected by anoikis. Bcl-2 protein overexpression did not protect either PC-3P or LNCaP-PRO-5 cells from anoikis, even though it rendered them resistant to thapsigargin and blocked cytochrome C release. Lack of effects of Bcl-2 suppression and Cytochrome C release on DNA fragmentation suggested a novel apoptotic pathway in our models of anoikis. Caspase activation was observed during anoikis in LNCaP-PRO-5 cells, and contributed to the cell death. We found no evidence for caspase activation during anoikis in LNCaP-LN-4 cells. Using a large panel of protease inhibitors we found no evidence of any protease involvement, with or without DNAse activity, in LNCaP-LN-4 cell death during anoikis. Therefore, the DNA fragmentation seen in LNCaP-LN-4 cells is probably due to activation of a DNAse other then DFF-40, which is classically associated with apoptosis due to caspase activation. Identification of such enzyme(s) should prove invaluable in understanding pathways of anoikis and metastatic tumor progression.

#4519 Resistance to Anoikis in Human Melanoma Cells Is Associated with G1 Arrest. Vivi Ann Flørenes, Maria Rosa Bani, Shan Man, Janusz Rak, Cappucine Sheehan, and Robert S. Kerbel. *Division of Cancer Biology Research, Sunnybrook and Women's Health Science Centres, Toronto, Canada, Mario Negri Institute for Pharmacological Research, Bergamo, Italy, and The Norwegian Radium Hospital, Oslo, Norway.*

Most mammalian cells are dependent on adhesion to extracelluar matrix for continued growth and survival. Upon detachment from the substratum, anchorage dependent cells either become arrested in G1 phase of the cell cycle or they trigger an apoptotic death program referred to as anoikis. In vitro, loss of anchor-